Provenance of suspended sediment in subglacial drainage systems

Darrel A. Swift

A thesis submitted for the degree of Doctor of Philosophy

February 2002

Department of Geography and Topographic Science
Faculty of Physical Sciences
University of Glasgow

ProQuest LLC.
789 East Eisenhower Parkway
P.O. Box 1346
Ann Arbor, MI 48106 – 1346

This thesis is the result of my own unaided work and presents as original nothing that is the result of work undertaken in collaboration with others.

Dedicated to the memory of my father,
Michael Swift.

Abstract

The importance of subglacial sediment transport by fluvial processes has long been recognised, such that suspended sediment loads in proglacial streams have commonly been used to calculate glacier erosion rates. However, glaciers of similar type, bedrock lithology and location demonstrate large variations in sediment yield that cannot be adequately explained by estimates of glacier erosional potential. It is likely that seasonal and annual variations in suspended sediment yield that have complicated estimates of subglacial erosion reflect changes in the efficiency of subglacial fluvial processes. Such processes are important because the efficiency of basal sediment evacuation likely plays a critical role in maintaining glacier erosion rates and may explain large differences in rates and styles of glacier erosion and ice marginal sedimentation.

Previous studies have failed to reliably link variations in proglacial suspended sediment transport with subglacial processes because: 1) independent observations of the dynamic nature of the glacial and fluvioglacial systems have rarely been obtained; and 2) suspended sediment quality has been infrequently used to infer sediment provenance. In this study, variation in proglacial suspended sediment transport and quality is investigated at Haut Glacier d'Arolla, Switzerland during the 1998 and 1999 melt seasons. The study was supported by a NERC project that provided data on ice motion and catchment hydroclimatological conditions against which variation in suspended sediment concentration and quality could be rigorously interpreted.

Suspended sediment transport from the western subglacial catchment during the 1998 melt season demonstrates changes in both sediment availability and the efficiency of suspended sediment evacuation that are controlled by the evolution of glacial meltwater sources and pathways. Strong relationships between discharge and suspended sediment concentration for hydrologically defined sub-periods of the melt season demonstrate the importance of flow capacity in controlling suspended sediment concentration. Early in the season, relationships demonstrate relatively high sediment availability at low discharges and an approximately linear relationship between suspended sediment concentration and discharge. Increased flow through the distributed system due to rising supraglacial meltwater inputs are associated with periods of rapid forward glacier motion followed by episodes of channelisation. However, changes in suspended sediment concentration are commensurate with increased discharge, and early season 'spring events' result in the evacuation of only a small proportion of the annual sediment load.

Later in the season, non-linear relationships between discharge and suspended sediment concentration reflect the rapid increase in flow velocity with discharge in hydraulically efficient, channelised subglacial drainage systems (Alley et al., 1997). Sediment availability during development of the channelised system is initially limited due to the concentration of supraglacially-derived meltwaters into channels located along preferential drainage axes. However, sediment availability increases during the melt season as the rate of extension of the channelised system declines. Increasing

overpressurisation of channels due to the increasing peakedness of supraglacial runoff likely increases sediment availability by: 1) extra channel flow excursions at peak discharges over wider areas of the glacier bed; 2) the enhanced deformation of high-pressure subglacial sediments towards low-pressure channels; or 3) the winnowing of fines from sediments near to channels as bulk discharge declines (Hubbard et al., 1995). The net effect is such that suspended sediment evacuation demonstrates a 125× increase for only a 7.5× increase in discharge between periods representative of flow through predominantly distributed and channelised subglacial drainage configurations.

Suspended sediment particle size during the 1998 melt season demonstrates variation in the finer fractions that likely reflects spatial variation in the access of meltwater to subglacial sediments. Suspended and *in situ* sediment size distributions are characterised by two principal modes that likely represent rock particles (~ 500–2000 μm) and their constituent mineral grains (~ 5–50 μm). Hubbard et al. (1995) have suggested that finer distributions will occur in basal sediments distal to subglacial channels due to a winnowing effect associated with the diurnally reversing hydraulic gradient. The in-phase flushing of fines with discharge in the proglacial stream is observed early in the melt season when supraglacial meltwaters are known to contribute to a predominantly distributed subglacial drainage system. Fines also suggest changes in sediment availability to be associated with increased flow through 'new' areas of the distributed system as the spatial pattern of supraglacial runoff evolves. During the period of predominantly channelised drainage, relationships between size distribution parameters and discharge suggest high sediment availability is maintained by a combination of increased access to basal sediments due to extra-channel flow excursions and both the deformation of basal sediments and winnowing of fines towards low-pressure channels as bulk discharge declines.

A number of alternative provenancing techniques were used during the 1998 and 1999 melt seasons. Changing sediment sources during the melt seasons were investigated using mineral (XRD) and geochemical (stable oxygen isotope) tracers, and the contribution of potentially large extraglacial sediment sources were investigated using suspended sediment radionuclide and luminescence signatures. However, field data has so far demonstrated poor potential and it is suggested that further work is required before these techniques will provide reliable indicators of suspended sediment provenance.

Field data demonstrates that subglacial drainage configuration exerts a critical control on the rates and mechanisms of basal sediment evacuation. The style of subglacial drainage system is believed to impact significantly upon: a) rates of subglacial erosion and sediment production; b) the nature of debris transport and the proportion of sediment in glacial versus fluvioglacial pathways; and c) rates and styles of proglacial sedimentation. Channelised drainage configurations are predicted to encourage subglacial erosion by the efficient evacuation of basal sediments, resulting in high sediment yields and the fluvial transport of sediment to depositional environments that may be very distal to the ice-margin. Thus, consideration of the potential coupling between glacial and fluvioglacial processes may ultimately provide new frameworks for the understanding of rates and processes of glacial erosion, sediment transfer and deposition, and the complex geomorphology of ice-marginal environments.

Acknowledgements

I gratefully acknowledge the support of the University of Glasgow, The Carnegie Trust for the Universities of Scotland and the British Geomorphological Research Group.

I would like to express a sincere thankyou to my supervisors, Peter Nienow and Trevor Hoey, without whose insight, guidance and support this work could not have been accomplished. Research in Switzerland was made possible by a NERC research grant to members of the Arolla Glaciology Project, and I would like to express my sincere thanks to Doug Mair, Bryn Hubbard, Ian Willis, and to everyone else who assisted with data collection in the field. Thanks are due in particular to Doug for providing the ice motion data, Ian for the discharge and meteorological data, Ian Cochrane for collecting samples for luminescence analysis during 2000, and Sam Waples for collecting data on proglacial suspended sediment dynamics that was subsequently not used in this thesis. Logistics in Arolla were aided by Grande Dixence S.A. and P. and B. Bournissen, and I am very grateful to Yvonne Bams for being so welcoming and for providing words of support during a difficult time.

For the analysis of sediment radionuclide, stable isotope and luminescence properties that provide the backbone of Chapter 6, I am extremely grateful to Gus MacKenzie, Tony Fallick and David Sanderson at SUERC, who also provided valuable discussion of the results. Thanks too to Anne Sommerville, who helped with sample preparation during luminescence analysis and provided some important background information. I must also thank Bill Higgison at the Division of Earth Sciences, University of Glasgow for preparing samples for XRD and their subsequent analysis, and Robert McDonald, also at the Division of Earth Sciences, for providing access to and instruction on the SEM. Preparations for the field in both 1998 and 1999 were ably assisted by Peter Chung at the Department of Geography and Topographic Science.

Sincere thanks are also due to Nick Spedding for providing valuable insight and discussion on the geomorphic implications of suspended sediment evacuation, and to Peter Knight and Andy Russell for stimulating my interest in glaciology whilst an undergraduate at the University of Keele. Thanks also to all my friends in Glasgow, and abroad, who have helped to make these past few years so extremely enjoyable. Here's to many more, and with a considerable weight off my mind!

Finally, huge thanks to my mum for her unwavering support, for providing a wonderful home to return to away from Glasgow, and for not asking too many questions!

Contents

1. Introduction

2. Field site and methods

3. Meteorological, glacier-hydrological and glacier dynamics

4. Sediment provenancing: suspended sediment transport

5. Sediment provenancing: suspended sediment particle size

6. Sediment provenancing: alternative techniques

7. Summary, glaciological implications and conclusions

1.

Introduction

1.1 INTRODUCTION

This thesis is concerned with the mechanisms of suspended sediment evacuation by subglacial drainage systems. Sediment flux from subglacial drainage systems is observed to dominate the sediment budget of many glaciers. This chapter highlights the importance of understanding the mechanisms of sediment evacuation by subglacial meltwaters and reviews current knowledge in this field. The potential of suspended sediment characteristics to elucidate the mechanisms of basal sediment evacuation is discussed and a framework for the investigation of suspended sediment provenance from subglacial drainage systems is outlined. Central to this framework is the acquisition of independent evidence of the dynamic nature of the glacial and fluvioglacial systems.

Chapter 2 introduces the field site and methods before considering the reliability and representivity of the suspended sediment monitoring programme and laboratory methods. Chapter 3 uses meteorological, proglacial streamflow and ice motion data to obtain independent evidence of the sources and routing of meltwater in the glacial system. These observations provide independent evidence of the dynamic nature of the glacial and fluvioglacial systems against which variation in suspended sediment provenance can be interpreted and tested. Chapters 4 to 6 deal with issues of sediment provenance as indicated by suspended sediment concentration, particle size and both geological and environmental tracers. Chapter 7 concludes the thesis, providing a

summary of the mechanisms responsible for suspended sediment evacuation at Haut Glacier d'Arolla and the glaciological implications of the work for present understanding of glacial geomorphic processes and future research.

1.2 GLACIAL EROSION AND SEDIMENT YIELD

1.2.1 The efficacy of glacial erosion

It is often assumed that glacial conditions result in accelerated rates of erosion (e.g. Isacks, 1992); however, rates of glacial denudation are difficult to estimate and hence the efficacy of glacial erosion is subject to some debate (Hay, 1998). In mountainous regions, the scouring, widening and deepening of valleys by glaciers suggests that areas that have been heavily glaciated have experienced high erosion rates during relatively short periods of time (Isacks, 1992). However, using fluvial sediment yields from a variety of glaciated catchments, Hallet et al. (1996) and Gurnell et al. (1996) have suggested that mechanical denudation rates vary by 4 to 5 orders of magnitude. Hallet et al. (1996) found that rates varied from 0.01 mm $year^{-1}$ for both polar and thin temperate glaciers on crystalline bedrock, to 0.1 mm $year^{-1}$ for temperate glaciers also on crystalline bedrock in Norway. For small temperate glaciers in the Swiss Alps, mechanical denudation rates increased to 1.0 mm $year^{-1}$, and reached 10–100 mm $year^{-1}$ for large, fast-moving temperate glaciers in the tectonically active mountain ranges of southeast Alaska. Controversy also surrounds the effectiveness of ice sheets as erosional agents. Analysis of offshore sediment masses or comparison with modern glacial denudation rates (e.g. White, 1972; Laine, 1980) contradicts studies of terrestrial sediments that indicate low rates of mechanical denudation beneath the Laurentide ice sheet (Flint, 1971). Nevertheless, mechanical denudation rates in the Laurentide region throughout the whole of the Quaternary period have been calculated to have been just 0.006 mm $year^{-1}$ (Bell and Laine, 1985), and even this figure may be greatly overestimated (Hay et al., 1989).

Despite uncertainties surrounding both modern and ancient rates of glacial denudation, the assumption that glaciers are very effective erosional agents is commonplace. For

example, Raymo et al. (1988) and Raymo and Ruddiman (1992) believe the efficiency of glacial erosion contributed importantly to the onset of the Ice Age. They hypothesised that accelerated tectonic activity during the Cenozoic, resulting in the uplift of vast mountain regions such as the Himalayas and Tibet, led to increased weathering that consumed CO_2 from the atmosphere and lowered global temperatures. Having made the assumption that uplift would result in glacier expansion, they believed that glacial erosion constituted the critical mechanism enabling chemical erosion rates to increase with elevation. Although weathering reactions are believed to proceed very slowly under glaciers (Gibbs and Kump, 1994; Kump and Alley, 1994), glacial abrasion produces an abundance of freshly comminuted mineral surfaces that are able to react with meltwater at the glacier bed. Thus, the theory presented by Raymo et al. (1988) and Raymo and Ruddiman (1992) has received some support from studies of weathering processes in alpine glaciated catchments, where chemical denudation rates have been shown to be in excess of the global average (Reynolds and Johnson, 1972; Eyles et al., 1982; Collins, 1983; Souchez and Lemmens, 1987; Sharp et al., 1995). Molnar and England (1990) have also assumed that glacial erosion is very efficient in order to support their argument *against* the evidence for tectonically driven accelerated uplift during the Cenozoic. In contrast to Raymo and Ruddiman (1990), they suggest that climatic changes during the Quaternary occurred first, leading to glacial expansion and increased rates of mechanical denudation, such that uplift occurred only as a result of isostatic adjustment in response to rapid glacial erosion.

An understanding of the efficacy of modern glacial erosion is central to discussions of glacial denudation and sedimentation worldwide, and is essential if controversial theories linking climate and topography over long timescales are to be critically evaluated. The efficiency of mechanical erosion in glaciated catchments is of primary interest since this far exceeds rates of chemical erosion (e.g. Sharp et al., 1995). Indeed, high chemical denudation rates in glaciated catchments have been suggested to result largely from the abundance of fresh mineral surfaces produced by mechanical weathering (Sharp et al., 1995; Hallet et al., 1996). Anderson et al. (1997) have argued differently, suggesting that chemical weathering is related to discharge flux rather than sediment production and is not unusually rapid in glaciated catchments unless glaciation increases run-off production. However, they suggest that because glacial sediment yields

are higher than fluvial sediment yields, and because the debris is fine-grained and freshly ground, the transport of glacial sediments by wind or water to environments more favourable to chemical weathering may still play a significant part in increasing global solute yields.

Few studies have attempted to compare rates of mechanical denudation in glaciated and non-glaciated basins. Sediment yields from twelve partially-glaciated catchments and one non-glaciated catchment in Alaska indicated that extensively glaciated basins produce yields about one order of magnitude higher than for glacier-free basins (Guymon, 1974). In contrast, a study of sediment yields from twelve catchments in the Southern Alps, New Zealand, of which only one was extensively glaciated, concluded that mechanical denudation was not influenced by the extent of glacierisation (Hicks et al., 1990). Responding to Hicks et al.'s (1990) study, Harbor and Warburton (1993) argued that percentage glacier cover could not provide an adequate surrogate measure of glacial erosional intensity and that there is compelling evidence for relatively high rates of glacial denudation in mountainous environments. However, Harbor and Warburton also added that the accurate estimation of the relative rates of glacial and non-glacial processes could not be achieved by comparing present day sediment yields. Several key reasons were cited: 1) appropriate surrogate measures of glacial erosional intensity are not available; 2) the complicating effects of sediment storage and paraglacial sedimentation; and 3) the difficulty of obtaining representative sediment yields due to the intrinsic variability of sediment output from glaciated basins.

Nevertheless, Gurnell et al. (1996) and Hallet et al. (1996) have suggested that if the contrast between sediment output from glaciated and non-glaciated basins is sufficiently large, systematic differences should emerge despite these confounding effects. Plotting mechanical denudation rates from published literature against basin size for 51 glaciated catchments, Hallet et al. (1996) found that sediment yields from glaciated basins formed a population 'distinct and essentially non-overlapping' with non- and partially-glaciated basins. Expanding on an earlier study (Gurnell, 1987a), Gurnell et al. (1996) presented data from 73 glaciated catchments throughout the world. Gurnell et al. found that as a function of catchment area, sediment yields from glaciated catchments plotted above the relationship derived by Walling and Kleo (1979) from their global suspended sediment

database. Both studies concluded that as a function of basin area, mechanical denudation in glaciated catchments is essentially unsurpassed.

Despite the apparent difficulties, a number of studies have also attempted to identify a relationship between glacierisation and erosional intensity. Gurnell (1987a) and Gurnell et al. (1996) found negative but non-significant relationships between sediment yield and both catchment size and the size of glaciated area. Furthermore, there were no clear systematic differences between sediment yield from the temperate, subarctic and arctic catchments. Nevertheless, Hallet et al. (1996) found that in contrast to their non- and partially-glaciated counterparts, mechanical denudation rates in glaciated basins increased with basin size. This pattern was believed to indicate an increase in erosional capacity due to increasing ice flux from small to large, fast moving glaciers. However, a re-analysis of their data suggests that basin size or ice flux may represent very poor indicators of erosional capacity. Figure 1.1 demonstrates that Hallet et al.'s correlation is mainly a function of the different characteristics of individual regions, with typically small basin areas in Svalbard and Norway having low sediment yields, larger basins in

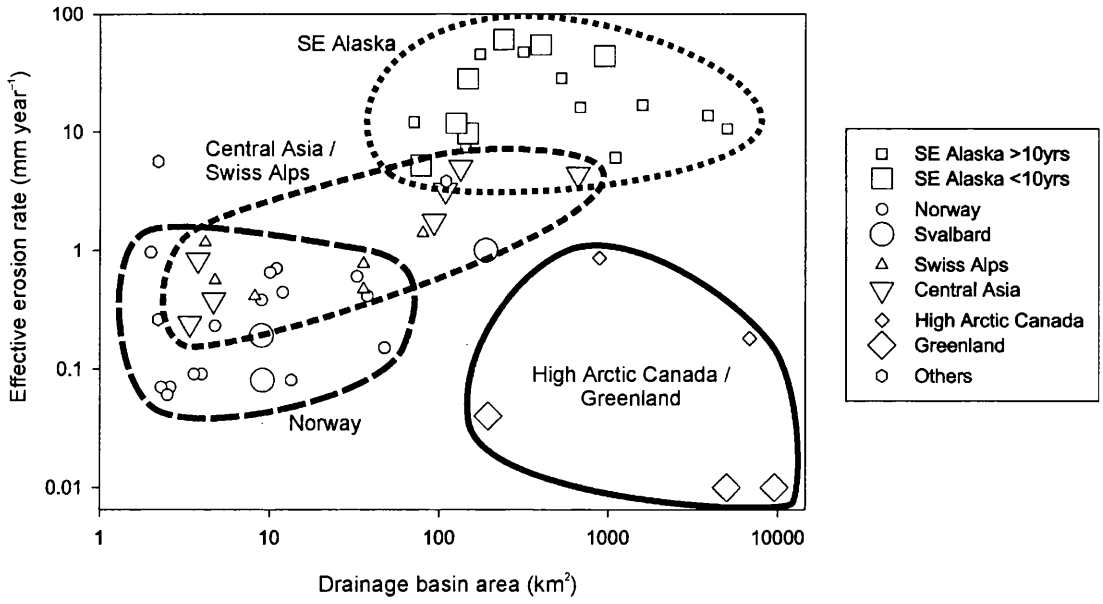

Figure 1.1 Effective erosion (mechanical denudation) rates calculated from suspended sediment yield (t km^{-2} $year^{-1}$) versus basin size for glaciated basins in various regions. Modified from Hallet et al. (1996).

Table 1.1 Regression relationships applied to log-transformed values of effective erosion rate and basin area for various regions (data from Hallet et al.,1996).

Region	n	a	b	t	p	r^2
SE Alaska	17	1.23	0.01	0.09	0.93	0.00
Norway	15	–0.98	0.36	1.48	0.16	0.08
Swiss Alps	6	–0.27	0.11	0.55	0.62	0.00
Central Asia	7	–0.66	0.52	5.14	0.00	0.81

n: number of basins; a: regression intercept; b: regression slope; t, p: t and p statistics associated with the regression slope.

Alaska having high sediment yields, and basins in Asia and the Swiss Alps falling in between. Also plotted is Hallet et al.'s information from high arctic glaciers in Canada and Greenland that were excluded from their original diagram and fall well outside of the relationship between basin area and rate of mechanical denudation. Clearly, other mechanisms must be responsible for these first-order differences in effective erosion; for example, regional differences in tectonic setting, subglacial lithology, climate, or sediment availability due to stage in the paraglacial cycle.

The large dataset presented by Hallet et al. (1996) therefore suggests that systematic variations in glacial mechanical denudation rates may exist due to continental-scale factors. However, Figure 1.1 reveals high variability in rates of mechanical denudation within individual regions that are independent of basin size. For the major regions represented ($n \geq 6$), rates of mechanical denudation show no correlation with basin area (Table 1.1); the relationship for central Asia is spurious as it is based on two separate groups of glaciers (Figure 1.1). It is clear that basin area, as a surrogate measure for ice flux, fails to explain both global and regional variations in glacial erosional intensity. Since these estimates of mechanical denudation are derived from catchment sediment yields, they are a function of both sediment production and transport processes within glaciated and partially-glaciated catchments. It is through a consideration of the factors that influence sediment production and transport in the subglacial environment that controls on the efficacy of glacial mechanical denudation are likely to be found.

1.2.2 Controls on glacial mechanical erosion and sediment yield

The principal mechanisms of glacial mechanical erosion are quarrying, abrasion, and erosion by subglacial streams. Quarrying is often considered to be the most important process of glacial erosion (e.g. Iverson, 1995; Hallet, 1996), and occurs through the fracturing or crushing of bedrock and the entrainment of bedrock fragments by ice. The mechanisms of bedrock fracturing beneath glaciers are not well understood, and some authors have emphasised the importance of pre-glacial weathering (Sugden and John, 1976; Addison, 1981; Lliboutry, 1994). Nevertheless, mechanisms believed to lead to bedrock fracturing or the propagation of small, pre-existing micro-fractures include: 1) pressure release due to unloading of bedrock as a result of erosion (Bennett and Glasser, 1996); 2) fluctuating patterns of basal ice and water pressure that impose stress gradients on bedrock and also result in localised basal freezing (Robin, 1976; Addison, 1981; Iken and Röthlisberger, 1981; Hallet, 1996); and 3) fluctuations in basal water pressure that enhance stress gradients at the glacier bed (Röthlisberger and Iken, 1981; Iverson, 1991). Rock fragments may then become entrained due to localised basal freezing, and the process may be enhanced if fluctuations in basal water pressure cause 'jacking' as a result of the opening of basal cavities (Robin, 1976; Röthlisberger and Iken, 1981).

Rock fragments that become entrained within the ice and maintain contact with the glacier bed result in abrasion. The rate of abrasion is dependent upon: 1) glacier sliding velocity; 2) the contact pressure between rock fragments and the glacier bed; and 3) the rate of supply and concentration of debris within basal ice (Sugden and John, 1976; Boutlon, 1978; Hallet, 1979b). However, abrasion is also influenced by the rate of removal of debris from the ice-bed interface (Riley, 1982). Abrasion is sometimes considered to be secondary to quarrying since the presence of rock fragments in basal ice is an essential pre-requisite (Lliboutry, 1994), although in mountain environments rock fragments may also be obtained by debris falling into the accumulation area from surrounding rock walls.

Meltwater will also perform mechanical erosion, and subglacial streams fed by sediment-poor surface melt should have exceptionally high erosive capacity (Alley et al., 1997). Though the rate of abrasion is strongly dependent upon the concentration of sediment in the water, erosion will be greatest over bedrock due to the largely unsatisfied

transport capacity (Howard et al., 1994). The low water pressures and high flow velocities characteristic of channelised subglacial drainage systems are also conducive to cavitation (Alley et al., 1997).

It is clear from a simple description of the basic erosional processes that the highest rates of mechanical denudation should occur under glaciers where: 1) bedrock is weak and highly fractured; 2) the bed is at pressure melting point; 3) rates of basal sliding are high; 4) subglacial water pressures are high and fluctuating; and 5) significant quantities of surface meltwater reach the glacier bed. Although large inputs of surface meltwater typically form low-pressure subglacial channels, these have been shown to co-exist with high pressure, distributed drainage systems fed solely by basal melt (Alley, 1992; Hubbard et al., 1995). In addition, strong diurnal fluctuations in water pressure within the channelised system may be transmitted to the distributed system and across wide areas of the glacier bed (Hubbard et al., 1995).

Evidence of regional variation in these characteristics may assist in explaining the variations in glacial erosional capacity evident in the data compiled by Hallet et al. (1996). Elverhøi et al. (1998) consider basal melting to be an essential pre-requisite for erosion to take place, and where basal melting occurs, glaciers with the steepest balance gradients due to high rates of accumulation will possess the highest basal shear stresses and sliding rates. Thus, rates of mechanical denudation are low in high arctic areas such as Svalbard, Greenland and high arctic Canada, where balance gradients are low and the thermal structure commonly prevents meltwater reaching the glacier bed. In Norway, the Swiss Alps and central Asia, balance gradients are higher and the thermal structure enables meltwater to reach the bed in large quantities. In Switzerland and central Asia, however, bedrock is more easily erodible and erosion rates therefore generally outstrip those of Norway. Finally, rates of mechanical denudation are expected to be highest in Alaska, where balance gradients are even higher and bedrock is very susceptible to erosion (Hallet et al., 1996).

Consideration of the mechanisms of glacial erosion identifies controls on mechanical denudation at a global scale but cannot account for large within-region variability. Catchment sediment yields need to be considered in detail and as the product of an

integrated sediment production-transport system. Following Fenn's (1987) approach, but considering only the subglacial environment, the various sediment production (p) and transport (t) processes can be represented as

$$\Sigma S_p = G_p + F_p \;\; ; \;\; \Sigma S_t = G_t + F_t \qquad (1.1,\ 1.2)$$

where ΣS denotes total sediment volumes, and G and F denote, respectively, glacial and fluvial processes. When estimating mechanical denudation rates, most studies implicitly assume steady-state where catchment sediment yields are directly representative of current rates of subglacial erosion, or

$$\Sigma S_t = \Sigma S_p \qquad (1.3)$$

However, the subglacial sediment production-transport system is likely to incorporate lags and sediment stores: not all sediments produced in a given time span are removed concurrently, and not all materials delivered to the ice margin over a given period are necessarily produced contemporaneously.

Harbor and Warburton (1993) have argued that large errors will exist in any estimate of sediment yield from glacierised catchments if the role of sediment storage is not first quantified using a sediment budget approach. A number of studies have used sediment budgets to study storage in the proglacial zone (Warburton, 1990) and in ice-marginal moraines (Small, 1987); however, the large proportion of glaciers that rest on soft sediments demonstrates that subglacial sediment storage is also important. Storage in the subglacial environment can be represented as

$$\Delta S_s = G_p + F_p - G_t - F_t \qquad (1.4)$$

where S_s represents sediment storage and t represents total sediment volumes delivered to the ice margin. Similar models of the glacial sediment system have been used to predict which glaciers erode their beds and which rest on soft sediment, but these have achieved only limited success (Maisch, 1999). Not surprisingly, the inaccessibility of the subglacial environment and the lack of adequate physically-based models of glacial erosion (Lawson, 1993; Alley et al., 1997) means estimation of the terms G_p and F_p is

extremely difficult and that quantification of changes in subglacial sediment storage is impossible to achieve.

Uncertainties regarding the origin of sediments exported from the subglacial environment confounds reliable estimates of mechanical denudation rates. For example, the high seasonal and annual variability in suspended sediment evacuation (e.g. Bogen, 1989, 1995, 1996) suggests difficulties in obtaining representative suspended sediment yields. However, the efficiency of sediment evacuation may also be important in determining glacial sediment yields, such that it is necessary to understand the mechanisms of sediment transport and storage in order to comprehend differences in mechanical denudation rates between glaciers. Processes of glacial erosion are largely dependent upon the efficient removal of subglacial debris (Riley, 1982; cf. Rea, 1996); hence, the quantity and distribution of sediment stored subglacially is likely to have a significant impact upon mechanical denudation rates. Where the products of glacial erosion are efficiently transported to the ice margin, increased ice-bedrock interaction will be encouraged and mechanical denudation rates will potentially be high.

The storage of sediment beneath glaciers in the form of soft-sediment layers has been predicted to render quarrying ineffective (Hallet, 1996) and will stifle abrasion by decreasing ice-bedrock interaction. It has been suggested that erosion by deforming sediment layers is also generally insignificant (Cuffey and Alley, 1996). Some areas of relatively sediment-free bedrock must exist for deforming layers to be sustained, but over the remainder of the bed, rates of mechanical denudation will be much reduced. Even bedrock erosion by subglacial meltwaters will be negated to some extent since the ready availability of subglacial sediments will result in greater satisfaction of transport capacity and reduced erosive potential. Thus, the contrasts in rates of mechanical denudation between glaciers resting on hard rock beds and those resting upon soft-sediments are likely to be great. Furthermore, the importance of sediment evacuation suggests that at a regional scale, mechanical denudation rates will strongly reflect the efficiency of sediment transport processes and not be confined to a narrow range predicted by the combination or efficiency of sediment production processes that regional characteristics prescribe.

For many temperate glaciers and ice caps, diverse data and theoretical analyses demonstrate the predominance of fluvial sediment transport over all other subglacial processes (Hallet et al., 1996; Alley et al., 1997). Basal sediment evacuation by meltwater has often been observed to dominate glacial sediment budgets, such that the majority of sediment delivered to the ice margin is entrained and transported by the subglacial drainage system (Hagen et al., 1983; Evenson and Clinch, 1987; Gustavson and Boothroyd, 1987; Kirkbride, 1995). If transport by glacial processes is very minor with respect to fluvial transport, Equation 1.4 effectively reduces to

$$\Delta S_s = G_p + F_p - F_t \qquad (1.5)$$

and it is the efficiency of subglacial fluvial sediment transport that plays a critical role in determining changes in subglacial sediment storage. In doing so, the efficiency of fluvial sediment transport processes is likely to modulate rates of mechanical denudation and sediment yield, and the thickness and spatial persistence of a deformable substrate may have significant implications for the mechanisms of glacier flow (Murray, 1997). High seasonal and annual variability in fluvial sediment yield observed at many glaciers suggests that the efficiency of subglacial fluvial processes is subject to large spatial and temporal variation. The inherent variability of such processes needs to be understood since they present important procedural difficulties for the estimation of mechanical denudation rates (Harbor and Warburton, 1993). More importantly, however, the critical role of sediment evacuation in controlling rates of mechanical denudation suggests that spatial and temporal variability in the efficiency of fluvial sediment transport may account for large within-region variability in rates of mechanical denudation. As a result, an understanding of the mechanisms responsible for sediment evacuation by subglacial drainage systems is critical.

1.3 SUSPENDED SEDIMENT EVACUATION BY SUBGLACIAL DRAINAGE

1.3.1 Introduction

Investigations of sediment evacuation by subglacial drainage systems at temperate, alpine glaciers have generally monitored suspended sediment and, to a lesser extent, bedload

transport in proglacial streams (see, for example, Gurnell (1987a, 1995) and Gomez (1987) for reviews of research in Alpine environments). Such studies have been conducted because the high sediment loads of subglacial streams present major difficulties for the management and use of meltwater (e.g. Østrem, 1975; Bezinge et al., 1987; Bogen, 1989), but also because the suspended sediment load can be used to make inferences about subglacial processes (e.g. Gurnell et al., 1992a; Clifford et al., 1995b; Hodgkins, 1996; Willis et al., 1996; Hodson and Ferguson, 1999). The inaccessibility of the subglacial environment means the character of the subglacial drainage system and the processes of sediment entrainment by subglacial meltwater cannot be directly observed. However, due to rapid transit through the subglacial drainage system (cf. Muste and Patel, 1997; Bogen, 1989), variation in suspended sediment at the glacier snout should reflect spatial and temporal variation in the processes of sediment entrainment.

The previous section recognised large regional variability in sediment yield from glaciated catchments and suggested that this may be due to differences in climate and lithology. These factors control sediment yield at regional scales because they dictate the amount of basal melting, rate of glacier flow, magnitude of surface runoff and the susceptibility of bedrock to erosion. However, it was suggested that significant within-region variability might arise from the efficiency of sediment evacuation by subglacial fluvial processes. At individual glaciers, studies of suspended sediment evacuation have revealed large variability over a wide range of scales (e.g. Bogen, 1988, 1996; Collins, 1990; Clifford et al., 1995b), suggesting spatial and temporal variability in the efficiency of sediment evacuation by subglacial meltwater. If the efficiency of sediment evacuation depends upon the ability of meltwater to access and entrain basal sediments, it follows that the morphology of the subglacial drainage system is critical. Previous studies have therefore attempted to identify the mechanisms responsible for sediment entrainment by linking variability in suspended sediment evacuation to subglacial fluvial processes operating at a variety of temporal scales.

1.3.2 Annual controls on sediment evacuation

Few studies have suggested processes that control variation in sediment evacuation at annual scales. Gurnell (1995) found some correspondence between annual catchment

discharge and total sediment yield for the Tsidjiore Nouve and Bas Arolla glaciers, Switzerland. If the quantity of basal sediment evacuated by subglacial meltwaters is limited by discharge (as suggested by Lawson, 1993), then annual discharge from the subglacial drainage system should be a good indicator of sediment transport. However, Bogen (1989) found very poor correlation between annual discharge and suspended sediment transport at Nigardsbreen, Norway. The highest suspended sediment transport rates occurred during years with several flash-flood events, whereas high rates of bedload transport appeared to require years with sustained high discharge. The different response of suspended load and bedload transport to variations in discharge was related to the relatively slow movement of bedload through the subglacial drainage system (days or weeks) compared to suspended material (a few hours). Exceptions to this pattern (i.e. low bedload transport despite sustained high discharge) did suggest that sediment availability might constitute an annual-scale control on sediment transport, and Bogen suggested that this was dependent upon the rate of glacial erosion.

Bogen emphasised the importance of sediment availability in a later paper (Bogen, 1996) that presented data from a larger sample of Norwegian glaciers and again demonstrated very poor relationships between annual suspended sediment yield and discharge. At Øvre Beiarbre, single years with exceptionally high suspended sediment evacuation were followed by periods of low yield lasting for 2 years or longer. This pattern was believed to indicate increased sediment availability in some years due to changes in the position of the subglacial drainage system: during some winters, the closure of subglacial channels may result in a complete shift in the position of the drainage system between one melt season and the next. It was suggested that a similar mechanism might control sediment availability at Nigardsbreen and Engabreen, although here the deformation of debris-rich ice into conduits was expected to have taken place throughout the year due to higher rates of glacier flow and frequent fluctuations in conduit discharge. Gurnell (1995) has also demonstrated some correspondence between sediment yield and glacier 'activity' at Tsidjiore Nouve. Annual sediment yield appeared to be related to the annual rate of glacier advance, and Gurnell suggested that high rates of glacier movement would cause continual adjustment in the subglacial drainage system. However, these studies suggest that variations in sediment yield are only crudely related to processes operating at annual time scales. Instead, annual variations in sediment yield may be largely

determined by the frequency of processes operating at seasonal time-scales or shorter (such as flash-floods or drainage system adjustments).

1.3.3 Seasonal controls on sediment evacuation

Suspended sediment transport in subglacial streams has been widely observed to fluctuate on a seasonal basis, and largely reflects the increased availability of meltwater during the melt season (Collins, 1990; Gurnell, 1987b, 1995). During winter, little or no surface melt reaches the glacier bed and drainage is predominantly distributed, being characterised by widespread access to basal sediments but low discharges (derived solely from basal melt) and flow velocities (cf. Richards et al., 1996; Nienow et al., 1998). Collins (1989) has suggested that the distributed system reaches its maximum spatial extent early in the melt season as snowmelt from the glacier surface begins to reach the bed via moulins and crevasses. Subsequent increases in supraglacial meltwater inputs result in the development of a channelised drainage network characterised by high discharges and flow velocities (cf. Richards et al, 1996; Nienow et al., 1998).

High suspended sediment concentration at the beginning of the melt season (i.e. increased suspended sediment transport relative to discharge) has been related to high sediment availability due to both the accumulation of sediment during winter (Collins, 1989, 1990; Leistøl, 1967; Vatne et al., 1992; Hooke et al, 1985) and the distributed system having widespread access to basal sediments (Collins, 1989; Hooke et al, 1985). However, following an early high, suspended sediment concentration has been widely observed to decrease during the melt season (Østrem, 1975; Bogen, 1995; Collins, 1990; Hammer and Smith, 1983; Leistøl, 1967; Hooke et al., 1985). This has been related to decreased sediment availability due to depletion of the subglacial sediment store (Østrem et al, 1986; Hooke et al., 1985) or relatively immobile channelised flowpaths having limited access to sediment sources (Collins, 1989, 1990; Gurnell, 1987b; Gurnell et al., 1992a). Gurnell et al. (1992a) identified decreasing suspended sediment availability following the development of a channelised drainage system at Haut Glacier d'Arolla, Switzerland. Gurnell et al. (1992a) suggested that sediment sources would effectively 'migrate' up-glacier as sediment sources near to stable, downglacier channels were exhausted. Total sediment availability would therefore decrease, and concentrations were

believed to decline further due to the increasing dilution of available sediment by rising discharges. It has also been suggested that the development of a low-pressure channelised system may cause a reduction in sediment availability since bed separation will be lower and less extensive (Hooke et al, 1985) and reduced basal sliding will decrease rates of mechanical erosion (Iverson, 1990, 1991; Willis, 1995).

Increasing suspended sediment concentration from subglacial drainage systems throughout a single melt season has rarely been observed. Gurnell (1995) demonstrated that hourly suspended sediment concentration and daily load increased throughout the 1989 melt season at Haut Glacier d'Arolla despite mean hourly discharge peaking mid-season. Gurnell suggested that expansion of the channelised network might enable streams to tap sediment sources across an increasingly wide area of the glacier bed. Due to suggested instabilities, the smallest channels or even the distributed drainage system were believed to be the predominant source of suspended sediments in the subglacial drainage system. Clifford et al. (1995b) also identified increasing suspended sediment concentration at Haut Glacier d'Arolla during the 1990 melt season. Suspended sediment concentrations were lower than expected during the mid-part of the melt season but were significantly higher towards the end of the monitored period. This pattern was again related to the seasonal development of a channelised drainage system, although changing characteristics of flow within the system were thought to be responsible for the unusual pattern of events. Low sediment concentrations observed during the mid-part of the melt season were believed to result from the drainage system extending upglacier via conduits predominantly at atmospheric pressure. Later in the season, the drainage system had reached its maximum extent but conduits were often surcharged and therefore able to transport higher suspended sediment concentrations. However, Clifford et al. (1995b) did not suggest how sediments are delivered to channels in order to maintain increasing sediment availability during the melt season.

A number of studies have also observed increasing suspended sediment concentration throughout the melt season at high-arctic polythermal glaciers (e.g. Hodson et al., 1998; Repp, 1988; Bogen, 1991). Gurnell et al. (1994) suggested that ground thaw may increase sediment availability during the melt season since much runoff is ice-marginal. Vatne et al. (1995) envisaged processes similar to those beneath temperate glaciers,

suggesting that steady deformation of high-pressure subglacial till into low-pressure channels might limit the exhaustion of sediment from stable drainage pathways. However, Vatne et al. again emphasised the intrinsic instability of many smaller tributary channels within the channelised network that are able to access sediments from a wide area of the glacier bed. Such observations of increasing suspended sediment concentration highlight the importance of a spatially extensive channelised drainage network, but suggest that it is processes operating at very short time scales are responsible for variability in suspended sediment evacuation.

1.3.4 Sub-seasonal controls on sediment evacuation

Sub-seasonal variations in suspended sediment evacuation are commonly related to drainage system instabilities. Large sediment flushes have been related to changes in drainage system configuration, particularly early in the melt season. At Gornergletscher in the Swiss Alps, Collins (1989, 1990) has related exceptionally high sediment transport over just a few days in the early melt season to large-scale re-organisation of the subglacial drainage system. Collins suggested that re-organisation from a distributed cavity system to a network of channels increases sediment transport as threads of flowing water change course and coalesce, integrating previously isolated areas of basal sediment with meltwater flow. These events take place during periods of glacier surface uplift and enhanced basal sliding, termed 'spring events' (Röthlisberger and Lang, 1987). Sediment evacuation during similar events has also been related to rapid channel inception. Such events are characterised by the storage of water at the glacier bed due to surface meltwater inputs exceeding the capacity of the distributed system. During the period of water storage, high suspended sediment concentrations have been taken to indicate that channels are being formed forcefully (Anderson et al., 1999), and the events may culminate in the rapid release of stored water and an associated pulse in suspended sediment that may reflect rapid channel formation (Warburton and Fenn, 1994; Anderson et al., 1999). However, Raymond et al. (1995) observed coupled ice-motion/turbidity events at two Alaskan Glaciers, many of which were not associated with any before-to-after changes in glacial or fluvioglacial dynamics. Events were associated with short-term injections of meltwater into the distributed system, resulting in the increased flow of meltwater through the system and the mobilisation of basal sediments. At one glacier,

events were linked to the sudden drainage of an ice-marginal lake, whilst events occurred at both glaciers during weather-induced glacier-wide inputs of melt water.

Collins (1989, 1990) has also suggested that variations in sediment flux at Gornergletscher are related to the temporary injection of meltwater from the channelised to the distributed system. Net flow of water into the distributed system will occur whenever meltwater inputs exceed the capacity of the existing channelised system; increases in suspended sediment concentration have therefore been related to intense rainfall events (Denner et al., 1999; Richards, 1984; Warburton and Fenn, 1994; Raymond et al., 1995), the release of ice-marginal or intra-glacial water stores (Beecroft, 1983; Gurnell, 1982; Collins, 1979b, 1986; Bjornsson, 1998), or the blocking of subglacial channels (Collins, 1990). Short-term increases in suspended sediment concentration have also been related to increased ice-bed separation and basal sliding associated with increased flow through the distributed system, indicating greater access of meltwater to basal sediments (Anderson et al., 1999; Hooke et al., 1985; Raymond and Malone, 1981; Raymond et al., 1995). At Variegated Glacier, Alaska, sediment flushes have been directly related to major changes in subglacial hydrology and enhanced basal motion during various surges and 'mini-surges' (Humphrey et al., 1986; Kamb and Engelhardt, 1987; Humphrey and Raymond, 1994).

At diurnal scales, variation in suspended sediment evacuation is closely related to diurnal variability in stream discharge (Gurnell, 1987b; Willis et al., 1996; Clifford et al., 1995). Leistøl (1967) suggested that sediment transport was related to the area of the bed that became integrated with meltwater flow during the diurnal cycle. However, hysteresis in the relationship between discharge and suspended sediment concentration is commonly observed, such that concentrations are lower at equivalent discharges on the falling limb than during the initial rise in discharge (e.g. Østrem, 1975; Leistol, 1967; Collins, 1979b; Bogen, 1980; Hammer and Smith, 1983; Gurnell, 1982, 1987b; Willis et al., 1996). Leistøl (1967) suggested that lower concentrations occurred as discharge was falling because little sediment remained in the area swept by meltwater on the rising limb. Hysteresis has also been observed during single flood events and over a sequence of events if the discharges of latter events do not equal or exceed the magnitude of those

preceding them (e.g. Leistol, 1967; Østrem et al., 1967; Church, 1972; Collins, 1979b; Gurnell, 1982, 1987b; Richards, 1984; Schneider and Bronge, 1993, 1996).

However, many studies have identified short-term variations in suspended sediment evacuation that appear unrelated to changes in discharge. Hodson and Ferguson (1999) suggested that early-season fluctuations in suspended sediment concentration were related to the establishment of interconnectivity in the distributed drainage system. Similarly, sudden inputs of sediment are suggested to occur as areas of the glacier bed become more efficiently linked with the channelised system throughout the melt season (Collins, 1989, 1990; Gurnell et al., 1991, 1992a). At the very smallest scale, turbulence has been suggested to give rise to variability in suspended sediment concentration over durations of approximately 10 seconds (Clifford et al., 1995b). However, a number of other mechanisms have been suggested through which increases in sediment availability are unrelated to discharge. Firstly, pulses of sediment have been related to local drainage system re-organisation (or re-adjustment) prompted by high rates of basal sliding or the collapse of channel roofs (Hodson et al., 1997; Gurnell, 1982, 1995; Willis et al., 1996). Secondly, drainage elements may be unstable, such that short-term variations in sediment transport reflect channel migration, capture or drainage system rationalisation (Collins, 1979b; Gurnell and Warburton, 1990; Willis et al., 1996), or inherent instabilities in the distributed system or smallest elements of the channelised network (Collins, 1979b, 1989, 1990; Gurnell et al. 1992a; Vatne et al., 1995). Finally, suspended sediment concentration may reflect sediment contributions from processes such as the deformation of till or debris-rich ice into channels (Collins, 1979b; Vatne et al., 1995; Bogen, 1996) or the collapse of unstable channel-margins cut into soft sediments (Collins, 1979b; Clifford et al., 1995b).

1.3.5 Summary

Previous studies indicate that suspended sediment evacuation is largely dependent upon the increased availability of meltwater during the melt season. However, annual and seasonal variability in suspended sediment transport is only poorly related to discharge magnitude due to changes in sediment availability at sub-seasonal scales. Studies have generally emphasised a decline in sediment availability during the melt season,

especially in the channelised system. In addition, increases in sediment availability have been suggested to be dependent on drainage system instabilities that enable meltwaters to access new sediment sources. However, the mechanisms by which sediment is accessed and entrained during such instabilities are still poorly understood, and different studies have suggested different processes during essentially similar events.

Increased sediment availability during the early part of the melt season is generally related to increasing surface meltwater inputs, although three mechanisms have been suggested: 1) increased flow through the distributed system, causing widespread access of meltwater to basal sediments and associated ice-bed separation and basal sliding (e.g. Hooke et al., 1985); 2) rationalisation of drainage such that distributed flowpaths coalesce, integrating wide areas of the bed with meltwater flow (e.g. Collins, 1989, 1990); and 3) the inception of channelised drainage (e.g. Anderson et al., 1999). However, very few studies have succeeded in directly relating increased suspended sediment transport to changes in drainage system configuration (e.g. Humphrey et al., 1986) or ice motion (Willis et al., 1996).

Increased sediment availability within the channelised system has also been related to instabilities that enable meltwater to access new areas of stored sediment. These instabilities are: 1) rapid changes in discharge, prompting injection of meltwater into the distributed system (Collins, 1989, 1990); 2) instabilities in major flowpaths or the smallest elements of the channelised network and distributed system that are unrelated to discharge (e.g. Gurnell et al., 1992a; Vatne et al., 1995); and 3) bank collapse or the deformation of sediment or basal ice into channels (e.g. Collins, 1979b; Bogen, 1996). Where a consistent increase in sediment availability has been observed during the melt season, studies have suggested this is likely due to: 1) extension of the channelised network (e.g. Gurnell, 1995); and 2) the deformation of high pressure basal sediments towards low pressure channels (e.g. Vatne et al., 1995). However, direct or independent evidence to support such explanations is often lacking.

Sharp (1991) suggested that studies of meltwater quality had contributed little to the understanding of subglacial hydrology. The reasons why such studies have achieved such limited success appear to be equally relevant to suspended sediment studies today.

Many studies are still technology-led, employing turbidity sensors as a surrogate for suspended sediment concentration because the range and reliability of such sensors has improved dramatically (Clifford et al., 1995a), they are easy to deploy, and their cost has decreased (Lawler, 1991). Furthermore, suspended sediment studies have: 1) depended on sediment concentration and load without investigating other parameters (suspended sediment mineralogy or particle size may provide better information concerning sediment provenance (cf. Fenn and Gomez, 1989)); 2) failed to address issues fundamental to the interpretation of suspended sediment transport data (e.g. what are the main sediment sources in the subglacial environment); 3) employed weak and inappropriate interpretative procedures (e.g. descriptive rating curve and time series methods); and 4) failed to take independent measurements that allow testing of the interpretations proposed (e.g. dye tracing to establish drainage system character and development, or ice-motion surveys to indicate rates of basal sliding).

Most importantly, however, such studies have been designed and carried out without regard to the insights gained from theoretical analysis of sediment transport by subglacial drainage and from other methods of investigation. For example, theoretical analysis suggests that the hydraulic efficiency of subglacial drainage is a critical control on basal sediment evacuation (Alley et al., 1997; see Section 1.3, below). At many glaciers, dye tracing has shown the subglacial drainage system to evolve from a hydraulically inefficient, distributed subglacial drainage system to a hydraulically efficient, channelised system during the course of the melt season (e.g. Nienow et al., 1998). The configuration of the drainage system at any location in space or time will determine the capacity of meltwater flow and its access to basal sediments. If suspended sediment studies are to provide new insights into the nature of the subglacial drainage system and the mechanisms by which meltwater evacuates basal sediments, studies must seek to utilise independent knowledge gained from other methods of investigation. The potential of suspended sediment studies, in light of our current understanding of subglacial hydrology, is discussed below.

1.4 THE POTENTIAL OF SUSPENDED SEDIMENT TRANSPORT STUDIES

1.4.1 Introduction

An understanding of the nature and efficiency of subglacial fluvial processes is crucial if variations in suspended sediment evacuation and their implications for the basal sediment layer and rates of mechanical denudation are to be understood. This section summarises current understanding of the nature of temperate, alpine subglacial hydrology and its potential impact upon suspended sediment evacuation. In conclusion, a new framework for the investigation subglacial fluvial processes in temperate, alpine environments using proglacial suspended sediment characteristics is suggested.

1.4.2 Subglacial hydrology and implications for suspended sediment evacuation

1.4.2.1 Drainage system configuration

Subglacial drainage systems are recognised to consist of one or both of two qualitatively different flow systems, commonly termed *channelised* and *distributed* (Hooke, 1989; Hubbard and Nienow, 1997; Fountain and Walder, 1998). Channelised subglacial drainage forms where meltwater becomes concentrated in sufficient magnitudes (Kamb, 1987; Walder and Fowler, 1994; Hubbard and Nienow, 1997), commonly as a result of concentrated inputs of surface meltwater that access the glacier bed via moulins or crevasses (Nienow et al., 1998). These systems are composed of hydraulically efficient channels that carry large discharges at high velocity and cover only a small proportion of the glacier bed. Channelised systems form arborescent (or dendritic) networks, since their flowpaths are characterised by an inverse relationship between discharge and water pressure (Röthlisberger, 1972) that tends to concentrate discharge into just a few large channels. Such networks have been predicted theoretically (Röthlisberger, 1972; Shreve, 1972) and have been inferred from dye tracing studies, which have demonstrated flow velocities of 0.2–0.8 m s^{-1} (e.g. Stenborg, 1969; Lang et al., 1979; Burkishmer, 1983).

Distributed subglacial drainage systems are non-arborescent and composed of hydraulically resistive or restricted flowpaths that cover a large proportion of the glacier bed. A variety of forms of distributed drainage have been suggested, including sheet

(Weertman, 1972; Weertman, 1986) or cavity flow (Kamb and La Chapelle, 1964; Lliboutry, 1968; Walder, 1986) at the ice-bed interface, and porous flow (Alley et al., 1986) or a network of shallow canals (Walder and Fowler, 1994) either through or over areas of basal sediment. Flow velocities are low, typically in the region of 0.025 m s^{-1} (Kamb, 1987; Willis et al., 1990; Nienow et al., 1998), and hydraulically resistive flowpaths cause water pressures to scale with increasing discharge and hence prevent downstream collapse into a low-pressure, channelised system. Distributed systems will exist where surface meltwater inputs are absent and meltwater is derived solely from basal melting, or where surface meltwater inputs are present but not of sufficient magnitude or concentration to form channelised drainage (Nienow et al., 1998). Distributed systems will therefore be the predominant form of drainage during winter, and will persist between channelised flowpaths during the summer in order to transfer meltwater generated by basal melting (Nienow, 1993). A distributed configuration might also predominate where conditions of glacier flow prevent rationalisation of subglacial drainage into a channelised network (e.g. under high sliding velocities (cf. Walder, 1986; Kamb, 1987), icefalls (Gurnell, 1995) or in overdeepenings (Röthlisberger and Lang, 1987; Hooke and Pohjola, 1994; Fountain and Walder, 1998)).

With few exceptions, the mechanics of sediment entrainment and transport in subglacial drainage systems must mirror those of subaerial streams (Spedding, 1997). Sediment transport in subaerial systems is a complex set of physical process, but as a first approximation, its efficiency can be related to a balance between the competence and capacity of the water flow and the nature and availability of sediment. If sediment supply is not limiting, flow competence, defined as the largest clast a given flow is able to carry, increases with flow strength. Although best defined in terms of flow energy or boundary shear stress, surrogate parameters such as flow velocity or discharge often provide acceptable approximations. Flow capacity is the total quantity of sediment of the available sizes a given flow can carry, and is governed by the excess flow strength over that required for sediment entrainment. Since flow through channelised and distributed systems differs markedly in terms of hydraulic efficiency, the configuration of the subglacial drainage system is likely to be a critical control on the efficiency of basal sediment evacuation.

Distributed drainage systems are likely to access a large area of the glacier bed and may transport significant volumes of meltwater, but their hydraulic inefficiency may limit the mobilisation and transport of basal sediments (Willis et al., 1996). Low flow velocities and the restricted physical size of distributed flowpaths will result in limited transport capacity and flow competence that may restrict sediment transport to the finer fractions of available sediments (c.f. Vivian, 1975; Hallet, 1979a; Humphrey and Raymond, 1994). In contrast, Alley et al. (1997) demonstrate how sediment transport increases rapidly as non-linear functions of flow velocity and discharge under channelised drainage conditions. Field observations also suggest subglacial channels are often of sufficient size to enable the entrainment of all but the largest sizes of basal sediment given sufficient flow velocity. Alley et al. (1997: p. 1020) conclude that the combination of high water discharges driven by steep head gradients, and the large temporal variability of discharge derived from surface melt, make subglacial and proglacial streams "among the most efficient sediment-transport mechanisms on earth".

A number of studies have suggested that distributed and channelised systems may be coupled (Nienow, 1993; Fountain, 1994), and exchange of meltwaters between the two has been indirectly observed to mobilise suspended sediment (Hubbard et al., 1995; Stone and Clarke, 1996). In the distributed drainage system, changing hydraulic gradients due to local variations in basal water pressures will cause variations in meltwater flow velocity and direction that may mobilise basal sediments. At Trapridge Glacier, Yukon, Stone and Clarke (1996) observed diurnal oscillations in the turbidity and pressure of basal meltwater, and found that peak turbidity occurred a number of hours after the peak in water pressure. The turbidity pulse indicated that water velocity peaked when subglacial water pressures were declining, suggesting mobilisation of sediments by flows driven hydraulically towards a low-pressure subglacial channel fed by surface melt. Similar observations were made by Hubbard et al. (1995) at Haut Glacier d'Arolla, Switzerland, where water level variation and basal turbidity were recorded in a dense network of boreholes across a channelised subglacial flowpath. The channel was defined by an area of low minimum daily water levels and maximum diurnal water-level variability, but water pressure fluctuations also occurred over an extended area either side of the channel. Diurnal pressure waves were observed to propagate through the distributed system both to and from the channel, with the highest

turbidity events in the distributed system occurring as the net flow of meltwater was towards the channel. Hydraulic conductivites were found to be higher closer to the channel, indicating preferential eluviation of fine particles from basal sediments near the channel margins.

Sediment pulses associated with such flushes have not yet been identified in proglacial suspended sediment data; the above studies have suggested that the exchange of meltwater remains very slow and hence the sediment entrained by this process is likely to be small relative to other processes. For example, high water pressures in subglacial channels likely cause ice-bed separation, exposing greater areas of the bed to high-velocity meltwater flow; at lower pressures, returning flows from the distributed system may induce bank failure or cause the deformation of sediments into channels (Collins, 1979b; Walder and Fowler, 1994; Stone and Clark, 1996). However, the suggested preferential eluviation of fines near to channels may result in an observable enrichment of fines in sediment evacuated from the drainage system during periods of falling discharge. Suspended sediment may also be periodically enriched in fines if meltwaters access sediments previously distal to major channels; at other times, sediment transport may reflect the entrainment of relatively coarse sediments near to channel margins.

1.4.2.2 Evolution of subglacial drainage configuration

Where surface meltwaters access the glacier bed, temporal and spatial variations in surface melt may result in similar variations in the configuration of the subglacial drainage system. Distributed flowpaths are likely to form the predominant mode of drainage at the beginning of each melt season; channels are unlikely to persist from year-to-year, except where ice is very thin, since the suppression of surface melt at the end of each melt season allows channels to be closed by the inward creep of ice (Röthlisberger and Lang, 1987; Fountain and Walder, 1998). As the melt season begins, basally-derived meltwaters within the distributed system will be augmented by heavily-damped inputs of meltwater delivered from the supraglacial snowpack via moulins and crevasses. As the snowpack is removed, exposure of low-albedo glacier ice results in a marked increase in the quantity of surface meltwater delivered to the glacier bed and in the amplitude of daily run-off cycles (Nienow et al., 1998). Concentrated inputs of surface meltwater locally destabilise the distributed system (cf. Kamb, 1987; Walder and Fowler, 1994),

and major flow pathways evolve in the form of a discrete network of hydraulically efficient subglacial conduits (Nienow et al., 1998). Because the magnitude of surface meltwater inputs and the peakedness of their diurnal amplitude drive the development of the channelised system, the system expands upglacier as the glacier snowline retreats (Nienow et al., 1998).

The proportion of the bed integrated with meltwater flow also evolves spatially and temporally. Vertical ice motion indicates increased flow through the distributed system, and enhanced basal sliding may result from an associated reduction in basal friction (e.g. Iken et al., 1983). However, formation of a low-pressure channelised system concentrates the majority of glacier discharge into just a few large channels thereby terminating enhanced basal sliding. Coupled hydrological-ice motion events similar to these 'spring events' (Röthlisberger and Lang, 1987) occur at a variety of temporal scales (Willis, 1995). Diurnal variations in glacier motion appear to be linked to fluctuations in subglacial water pressures driven by the runoff cycles of surface melt, and in some cases the amplitude of diurnal motion variations have been observed to increase throughout the summer (Iken, 1974; Iken and Bindschadler, 1986). These patterns suggest that increased flow through the distributed system at various times during the melt season due to ablation, heavy rainfall or the release of ice-marginal or intraglacial meltwater stores is responsible for enhanced basal motion. Under certain conditions, the storage of meltwater in the distributed system may result in surge or 'mini-surge'-type behaviour (Raymond, 1987; Kamb, 1987; Raymond et al., 1995), and surge formation and termination scenarios have been found to be very similar to those for spring events.

Evolution of the distributed and channelised systems and the resulting ice-motion events are likely to exert a strong control upon basal sediment evacuation. During periods dominated by flow through a distributed system, water will have widespread access to basal sediments but the hydraulic inefficiency of the system may result in low rates of evacuation that will be limited to the finer sizes of available sediment (see Section 1.4.2.1). Early in the melt season or during surges or spring events, increased flow may occur through wide areas of the distributed system, but flow velocities and hence sediment evacuation should increase only slightly. However, sediment evacuation may be enhanced by: 1) increased basal motion due to ice-bed separation causing widespread

disturbance of the glacier bed, thereby reducing the energy required for the mobilisation of fine sediments; and 2) the formation of channelised flowpaths, since hydraulic gradients between incipient low-pressure channels and the surrounding distributed system means that flow velocities into and through the channelised system will be fast. Following spring event or surge termination, upglacier expansion of the channelised drainage system as the snowline retreats will result in high sediment evacuation and the transport of almost all available particle sizes. Efficient sediment evacuation by established conduits may exhaust local sediment supplies and shift sediment sources upglacier, although this effect may be offset by rationalisation of the channel network in order to achieve greater hydraulic efficiency (Shreve, 1972). Similarly, sediment exhaustion and reduced evacuation may occur once drainage system evolution is complete; however, sediment availability may be maintained by: 1) frequent hydraulically-induced ice motion events; or 2) a strong diurnally reversing hydraulic gradient resulting in the winnowing of fines during falling discharge.

1.4.3 A framework for suspended sediment studies

Suspended sediment studies have had difficulty relating variations in proglacial suspended sediment transport to subglacial fluvial processes because little synchronous information has been obtained to indicate the dynamic nature of both the glacial and fluvioglacial systems. In addition, characteristics of the suspended material have infrequently been used to infer sediment provenance (e.g. Humphrey and Raymond, 1994; Fenn and Gomez, 1989). If suspended sediment studies are to enhance understanding of subglacial processes, suspended sediment monitoring programmes should attempt to include factors which indicate subglacial drainage system development as well as potential indicators of suspended sediment provenance. Specifically, studies should seek to measure:

— Catchment hydroloclimatological characteristics: Characteristics such as air temperature, precipitation and catchment discharge indicate the magnitude and variability of run-off production within the catchment. Runoff drives evolution of the supraglacial and subglacial drainage systems and hence controls access of meltwater to basal sediments (e.g. Gurnell, 1995; Arnold et al., 1996; Richards, et al. 1996).

The shape of the proglacial hydrograph provides an indication of the proportion of flow routed through distributed and channelised drainage systems and the storage of water in each component (e.g. Röthlisberger and Lang, 1987; Gurnell, 1993, 1995; Richards et al., 1996). Evolution of proglacial hydrograph form can also be used as a proxy for drainage system development (e.g. Hannah et al., 1999, 2000).

— Subglacial drainage system development: Dye-tracing can be used to directly investigate drainage system development (e.g. Nienow et al., 1998) and may usefully indicate the basic structure of the channelised system (e.g. Sharp et al., 1993), but detailed studies are labour-intensive. Instead, electrical conductivity is able to provide a crude indication of the proportion of meltwater routed through distributed and channelised drainage components (Collins, 1979b; Gurnell and Fenn, 1984b) since high electrical conductivities may indicate the release of meltwater from long-term storage at the glacier bed (Fenn, 1987).

— Glacier motion: Glacier motion provides an indicator of subglacial drainage conditions since high forward velocities and temporary glacier uplift indicate periods of water storage due to increased flow through the distributed drainage system (e.g. Iken et al., 1983; Röthlisberger and Lang, 1987; Willis, 1995). Since increases in forward motion during such events result from enhanced basal sliding, rapid forward motion events will also indicate increased disturbance of the glacier bed.

— Suspended sediment size: The size of sediment evacuated from the subglacial drainage system provides a potential indicator of sediment provenance in glaciated catchments (e.g. Fenn and Gomez, 1989). Finer size distributions may reflect entrainment in low-velocity fluvial environments such as the distributed system (Humphrey and Raymond, 1994). Eluviation of fines from sediments near to channelised flowpaths (Hubbard et al., 1995) means that coarser size distributions may reflect erosion or contributions of sediment from sources near to channel margins. Alternatively, enrichment in fines might indicate hydraulically efficient drainage gaining access to sediments previously distal to channelised flowpaths.

— Suspended sediment mineralogy: Suspended sediment mineralogy also has the potential to indicate sediment provenance (Fenn and Gomez, 1989). Where

catchment geology (and the overlying till) is heterogeneous, suspended sediment mineralogy should reflect the spatial evolution of the subglacial drainage system as meltwater accesses sediments at different locations beneath the glacier. Changes in suspended sediment mineralogy may be particularly likely during the establishment of a channelised drainage system due to an upglacier migration of the predominant sediment sources (cf. Gurnell et al., 1992a).

— Characterisation of subglacial, englacial and extraglacial sediment sources: Basal sediment samples may provide useful information on the nature of *in situ* subglacial sediments for sediment provenancing techniques. Extraglacial and englacial sediment may also be an important source of sediment, although englacial concentrations are typically very low in temperate Alpine environments. Nevertheless, methods that discriminate between these components may be essential for the rigorous investigation of sediment provenance.

— Proglacial stream characteristics: The sediment transport characteristics of proglacial channels are likely to provide a good proxy for sediment transport within channelised subglacial systems (Alley et al., 1997). The characteristics of sediment transport within such channels also need to be investigated to ensure monitoring programmes are reliable and representative of actual suspended sediment characteristics (Gurnell et al., 1992b).

The above framework was adopted in this study, the design and implementation of which is outlined in the following chapter. Suspended sediment studies that incorporate as many of these independent measurements as is possible will undoubtedly be in a position to elucidate more rigorously the mechanisms responsible for sediment evacuation by subglacial meltwaters. Identification of these processes will lead to a greater understanding of the variability of sediment evacuation by subglacial meltwater and its potential importance for basal properties (through the thickness and spatial persistency of the basal sediment layer) and rates of mechanical glacial denudation.

2.

Field site and methods

2.1 FIELD SITE: HAUT GLACIER D'AROLLA

2.1.1 Introduction

Haut Glacier d'Arolla (Figure 2.1) is a small, temperate valley glacier located at the head of Val d'Herens, Valais, Switzerland. The main characteristics of the Haut Arolla catchment have been summarised variously by Gurnell et al. (1992a), Sharp et al. (1993) and Richards et al. (1996). The catchment has an area of 11.7 km^2, of which ~ 6 km^2 is covered by permanent snow and ice, and ranges in altitude from ~ 2600 m at the glacier snout to 3838 m at the highest point of the watershed. The ~ 4 km-long glacier has an altitudinal range of ~ 2600–3500 m and is nourished from a single firn basin and by a small tributary glacier (Glacier de la Vierge). A number of small cirque glaciers exist within the catchment but are no longer confluent with the main glacier (including Glacier de la Mitre, which was confluent during the early 1990s). In common with other glaciers within the region, the position of the glacier terminus has been receding since the mid-nineteenth century. This retreat, estimated to have been ~ 20 m $year^{-1}$ during the 1990s (P. Nienow, pers. comm.), has revealed some thick exposures of glacial sediment, predominantly above the glacier's eastern margin (Figures 2.2 and 2.3). During the melt season, cirque glaciers below Bouquetins contribute meltwater to the main glacier that has been observed to entrain large quantities of sediment from these extraglacial sources.

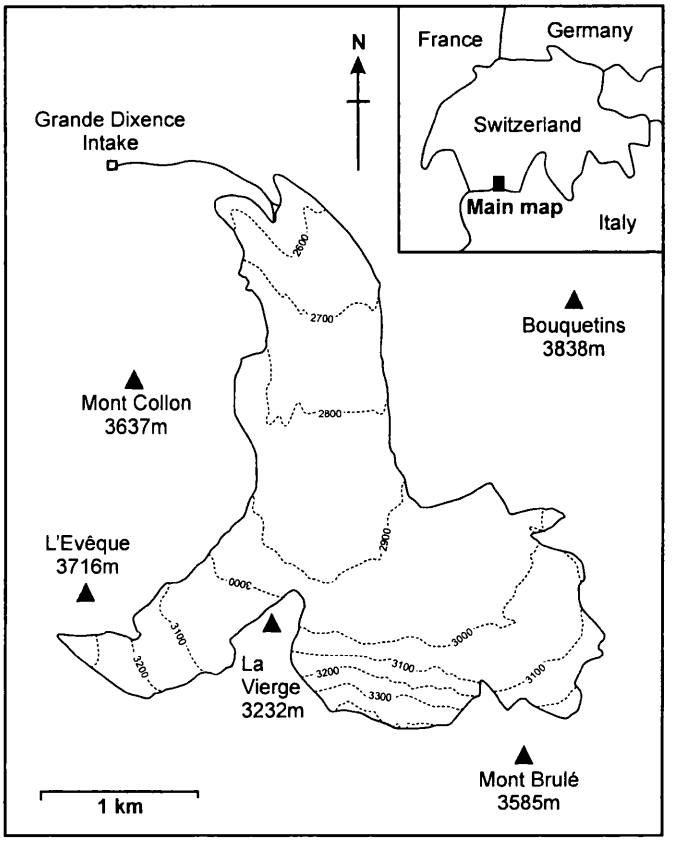

Figure 2.1 Haut Glacier d'Arolla (lat 46°0′N, long 7°30′E); inset shows the approximate area of the main map. Catchment discharge is measured at the Grande Dixence intake structure ~ 1.5 km from the glacier snout. Contours on the glacier surface are in metres.

Sharp et al. (1993) investigated the geometry, bed topography and drainage system structure of Haut Glacier d'Arolla during the 1989 and 1990 melt seasons. The glacier was shown to occupy a classic U-shaped valley and the valley floor to consist of three basins, the lowest of which appeared to be slightly overdeepened. Bed topography, together with ice-thickness, is predicted to exert the major control on the routing of subglacial drainage pathways (Shreve, 1972). Calculation of subglacial hydraulic potential, after Shreve (1972), revealed no significant 'valleys' in equipotential surfaces, suggesting that away from the valley walls there will be little tendency for subglacial drainage pathways to converge. However, the reconstructions of the subglacial drainage system indicated two preferential drainage axes (PDAs) beneath the glacier tongue. A PDA beneath the western glacier tongue originated from the principal tributary; whereas the eastern PDA drained the main accumulation area.

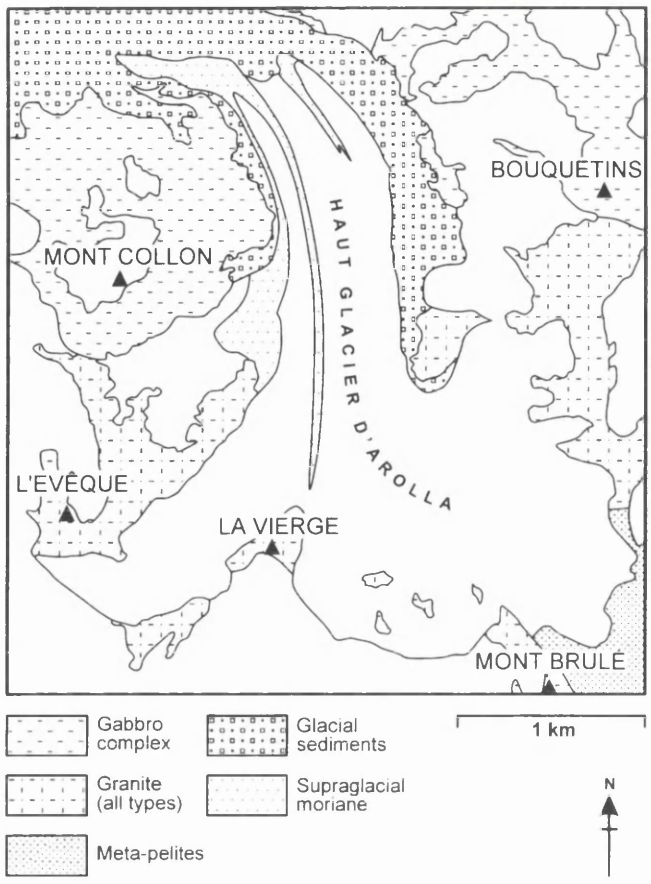

Figure 2.2 Generalised surficial geology of the Haut Arolla catchment (after Gurnell et al., 1992 and Goodsell, 1995). Unshaded areas indicate areas of permanent ice or snow.

This drainage reconstruction was broadly supported by observations in the field (Sharp et al., 1993). During 1989, the glacier was drained by five meltwater streams and marked variation in stream colour, due to differences in the composition of their suspended load, suggested the presence of two or more discrete glacial drainage catchments. However, dye-tracing revealed that the two western-most streams drained the majority of the glacierized area, including the main accumulation basin, the upper-eastern, central and western parts of the glacier tongue, and the principal tributary. These streams had a greenish-grey sediment and were estimated to have contributed up to 80 % of the total discharge during August. The eastern streams, which transported a brownish sediment, were found to drain only a small area of the eastern part of the glacier tongue, receiving a significant proportion of their discharge from the cirque basins below Bouquetins.

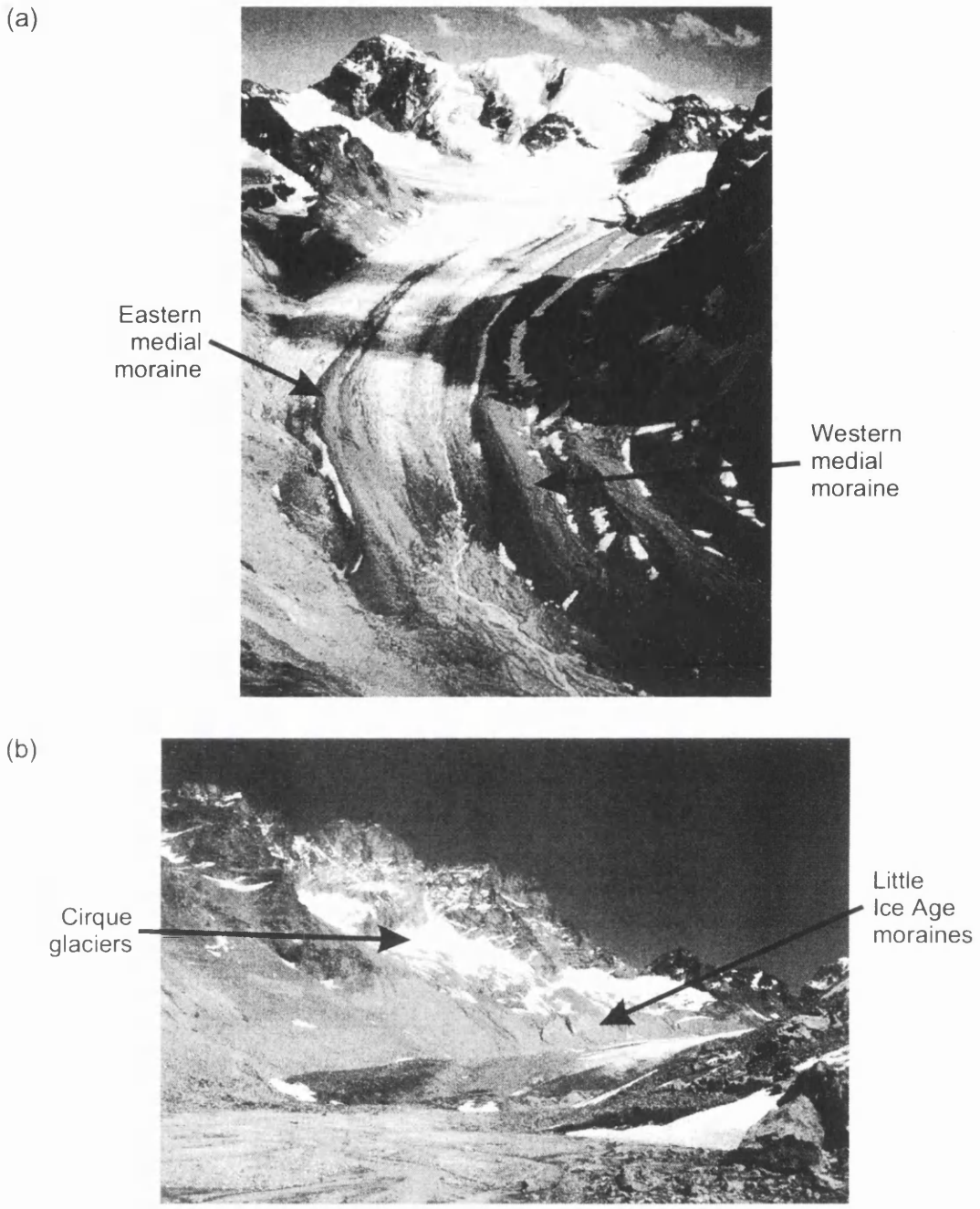

Figure 2.3 (a) Haut Glacier d'Arolla from the north. The western margin of the glacier has a thin mantle of supraglacial moraine derived from the adjacent slopes of Mont Collon and L'Evêque (Figure 2.2). The western medial moraine is also clearly visible, originating at the confluence of ice from the main accumulation area and the tributary glacier below La Vierge (Figures 2.1 and 2.2). The eastern medial moraine originates from the upper accumulation area but is traceable at the glacier surface for only 1–2 km from the snout. (b) Bouquetins and the eastern margin of the glacier snout viewed from the proglacial area. Large (~ 50 m high) Little Ice Age moraines are visible above the glacier's eastern margin that are dissected by streams originating from a number of cirque glaciers below the Bouquetins ridge (here shown under snow).

Ice-marginal observations (Hubbard, 1992) and borehole investigation (Copland et al., 1997a,b) suggest that the glacier rests on a mixed bed partly comprised of unconsolidated sediment, which bed penetrometry has revealed to be between 0.05 and 0.26 m thick (Hubbard and Nienow, 1997). Figure 2.2 shows the surficial distribution of the main rock and sediment types in the Haut Arolla catchment. The catchment geology is complex and represents various stages in the Alpine Orogeny (Goodsell, 1995). Meta-pelites that form part of the headwall in the southeast of the catchment and probably occur beneath part of the main accumulation area are typical of shallow marine deposits that were later buried. Granites that lie beneath the glacier accumulation area and upper tongue were then intruded before the area was subjected to intense tectonic activity. A gabbro complex was later emplaced (Dal Piaz et al., 1977) that now underlies the lower glacier tongue. Although the gabbroic rocks show great variability, it is unlikely that the geology beneath the lower part of the glacier is as complicated as some previous studies (e.g. Brown, 1991) have suggested (B. Goodsell, pers. comm; see Chapter 6). All lithologies in the catchment demonstrate a green (chloritic) schist facies metamorphic overprint (Dal Piaz et al., 1977).

Runoff from the Haut Arolla catchment is extracted by Grande Dixence S.A. at an intake structure ~ 1.5 km from the glacier snout (Figure 2.1). The intake structure integrates runoff from the various sources in the catchment (e.g. from snowmelt and the numerous ice-bodies), but measurements obtained from Grande Dixence SA have commonly been used as a surrogate for discharge from the main glacier (e.g. Tranter et al. 1993; Gurnell, 1993; Gurnell et al., 1992a, 1994; Brown et al., 1996; Richards et al., 1996; Nienow et al., 1998). Cross-correlation analysis of catchment discharge and river stage within 100 m of the glacier snout revealed no identifiable lags (Gurnell et al., 1992a). The error associated with discharge measurements obtained from Grande Dixence S.A. has been calculated to be ± 4 % (Brown and Tranter, 1990).

2.1.2 Subglacial drainage system evolution

Repeated observation over a number of melt seasons has shown that evolution of the subglacial drainage system occurs during the summer in response to concentrated inputs

of supraglacial meltwater via moulins and crevasses (Sharp et al., 1993; Richards et al., 1996; Nienow et al., 1998). During winter, surface ablation is negligible: high borehole water pressures (Hubbard et al., 1995; Gordon et al., 1998) and uniform, slow flow velocities determined from dye tracer studies (Sharp et al., 1993; Nienow et al., 1998) indicate the existence of a distributed drainage system. Distributed drainage through areas of unconsolidated sediment is believed to occur by porous flow and may be supplemented by flow at the ice-sediment interface (Alley et al., 1997; Walder and Fowler, 1994; Hubbard et al., 1995).

Towards the beginning of the melt season, surface meltwater inputs to the subglacial drainage system slowly increase as the supraglacial snowpack thins in response to rising air temperatures and solar insolation. An increase in horizontal ice-surface velocities (Nienow, 1996; Mair et al., 2001), similar to spring velocity events observed at other alpine glaciers (e.g. Iken and Bindschadler, 1986), reflects the initial disruption of the distributed system. Following this event, the removal of the supraglacial snowpack and the exposure of low-albedo glacier ice results in a marked increase in the quantity of surface meltwater delivered to the glacier bed and in the amplitude of daily runoff cycles (Arnold et al., 1998; Nienow et al., 1998). Concentrated inputs of surface meltwater locally destabilise the distributed system (cf. Kamb, 1987; Walder and Fowler, 1994), and major flowpaths evolve in the form of a discrete network of hydraulically efficient subglacial channels (Nienow et al., 1998). Locally, water levels in boreholes drilled to the glacier bed may show incoherent variation during drainage system destabilisation, but later show high, invariant levels where distributed drainage remains and significant diurnal variations near to channels fed by surface melt (Hubbard et al., 1995; Gordon et al., 1998). Similarly, flow velocities inferred from dye tracer investigations are an order of magnitude higher from moulins 'connected' to channelised flowpaths than those that are not (Nienow et al., 1998).

The channelised system migrates up-glacier as the supraglacial snowline retreats, growing in both extent (Nienow et al., 1998) and efficiency (cf. Shreve, 1972; Hock and Hooke, 1993). As a result, the temporal and spatial pattern of the up-glacier extension of the channelised system may vary from year to year. Assuming throughflow velocities in

Table 2.1 Development of the channelised drainage system during the 1990 melt season (based on data from Nienow, 1993)

Period	Description	r	x
JD 151–164	Early season: no channel development	0	700
JD 164–200	Rapid channelisation	60	2860
JD 200–222	Slow channelisation	20	3300
JD 222–239	Late season: extensive channelised system	0	3300

r: rate of upglacier extension of the channelised system (m d^{-1}); x: approximate position of the channel head from the glacier snout at the end of each period

excess of 0.5 m s^{-1} indicated fully channelised drainage, Nienow et al. (1998) calculated the approximate position of the head of the channelised component and its rate of upglacier extension during the 1990 season (Table 2.1). Channels were calculated to close during winter due to the deformation of ice and lack of wall melting generated by glacier runoff, although calculations indicated that channels may survive within the lower ~ 700 m of the glacier where the ice is less than 90 m thick. The head of the channelised network moved upglacier to a final distance of ~ 3400 m from the glacier snout, although the rate of upglacier extension declined with distance (Table 2.1). A distributed system remained the primary means of drainage in the upper 0.7 km of the glacier due to a residual firn aquifer that damps diurnal meltwater inputs to the glacier bed. The channelised system is predicted to close towards the end of the melt season as surface melt is suppressed (Sharp et al., 1993; Nienow et al., 1998).

Mair et al. (in press) found a different pattern of upglacier extension of the channelised system during the 1995 melt season. Assuming that throughflow velocities in excess of 0.4 m s^{-1} indicated flow through fully channelised flowpaths, the head of the channelised system was estimated to be about 1.1 km from the glacier snout on JD 191. Rapid headward extension then occurred until JD 220 at a rate of roughly 60 m d^{-1}. However, retreat of the snowline was atypically late during the 1995 melt season and was observed to lag behind the development of the channelised network. It was suggested that if a thick supraglacial snowpack exists well into the melt season, there may be time for the development of more efficient percolation of surface melt through the snowpack and of

more efficient supraglacial drainage at the snow-ice interface, such that diurnally-peaked inputs of surface melt are able to reach the subglacial drainage system.

The channelised drainage system covers only a small proportion of the glacier bed (Nienow et al., 1998); elsewhere, a residual distributed system feeds into and interacts with the network of channels. Borehole investigations have demonstrated coupling between low-pressure channels and the high-pressure distributed system (Hubbard et al. 1995; Gordon et al. 1998). During the summer, large areas of the glacier bed show significant diurnal variations in water pressures that indicate the presence of a major subglacial channel. Water pressures at the centre of this 'variable pressure axis' (VPA) vary from atmospheric pressure to pressures exceeding local ice-overburden. Minimum water levels increase in boreholes with distance from the centre of the VPA, whilst the amplitude of the diurnal oscillations decreases, until regions of high, stable water pressures characteristic of distributed flowpaths are reached. Variations in water pressure in the channelised system result from diurnal variations in surface melting; hence, net flow of water between the distributed and channelised systems reverses on a diurnal basis (see also Section 1.3.2.1).

The nature of flow within the channelised system has been investigated by Sharp et al. (1993). Following Hooke (1984), Sharp et al. (1993) calculated that flow in channels fed by surface melt at the height of the melt season would be at atmospheric pressure (or 'open'), except for a short distance upglacier of the slight overdeepening. However, drainage reconstructions (above) that assume full (or 'closed') flow conditions best described the major structural characteristics of the drainage system, suggesting that flow occurred under hydrostatic pressure throughout the summer. Three possible explanations were presented as to why open-flow channels, that should migrate easily, occupy positions predicted by closed-flow conditions: 1) channels develop under closed-flow conditions but are unable to migrate significant distances once open-flow conditions develop; 2) channel location is determined by the location of supraglacial meltwater inputs (both of which tend to coincide because valleys in subglacial hydraulic potential typically reflect valleys on the glacier surface); and 3) that channels may be

broad and low (Hock and Hooke, 1993) instead of semi-circular (as envisaged by Hooke, 1984), and thus open-flow conditions are over-predicted.

Richards et al. (1996) suggested that conduits are probably full during development and, as open flow conditions prevail, the rate of wall-melting is insufficient to enable them to migrate significant distances (Sharp et al., 1993). Studies of water chemistry at Haut Glacier d'Arolla have found that bulk runoff during the summer is also characteristic of rapid transit through ice-walled channels under open flow conditions (Tranter et al., 1993; Brown et al. 1994). However, investigation of the character of flow in subglacial channels by Nienow et al. (1996) has suggested that flow conditions at Haut Glacier d'Arolla cannot be classified as solely open or closed. Calculations based on relatively simple assumptions regarding the hydraulic geometry of subglacial channels should enable flow conditions to be estimated from the form of velocity-discharge relationships derived from dye-tracing experiments. Both clockwise and anticlockwise hysteresis was observed in velocity-discharge relationships suggesting that, because surface meltwater input at a particular moulin may vary out of phase with bulk runoff, discharge within tributary channels may be out of phase with major channels and moulins or sub/englacial channels may be experience hydraulic damming. Flow conditions might therefore be spatially and temporally variable throughout the channelised system. Resultant variations in subglacial water pressures suggest that basal sliding events at diurnal time scales may operate through extremely localised events.

2.1.3 Glacier dynamics

Surveying of stakes on the glacier surface and instrumentation of glacier boreholes at Haut Glacier d'Arolla has revealed that variations in basal sediment and hydrological properties influence the rates and mechanisms of glacier flow (Nienow, 1996; Harbor et al., 1997; Mair et al., 2001). Harbor et al. (1997) state that the spatial persistence, thickness and particle size of basal sediments is spatially variable. Bed penetrometer tests have supported Hubbard et al.'s (1995) assertion that basal sediments near channels had been winnowed of fine sediments. Penetration depths in the region of the suspected subglacial channel were typically only 25–50 % of those either side, suggesting either

Table 2.2 Phases of the melt season at Haut Glacier d'Arolla (Richards et al., 1996).

Period 1 (early to mid June)	Low air temperatures; low and invarient flows and suspended sediment concentrations; high solute concentrations; recession after period of melt during May; glacier surface snow–covered; no conduits; distributed drainage over glacier bed
Period 2a (mid to late June)	Gradual increase in discharge and appearance of clear diurnal discharge cycles reflecting increased levels of melt energy; decreasing solute concentrations, but larger diurnal variation of most solute species; suspended sediment concentrations relatively stable; glacier snow–covered; distributed drainage
Period 2b (early to mid July)	Higher suspended sediment concentrations with stronger diurnal cycles; low solute concentrations; higher mean discharges as lower albedo glacier ice exposed by snowline recession; continued development of diurnal discharge cycles as conduit growth occurs
Period 3 (mid July to early August)	Higher peak flows and lower minima suggest a well–developed conduit system; unstable solute and suspended sediment relationships with discharge as new sources are tapped; area of exposed ice increasing
Period 4 (early August onwards)	Strong diurnal discharge cycles continue, but with lower mean, maximum and minimum discharges; variable melt, especially when snowfall events increase albedo; a decline and stepped increase of sediment concentration may occur if the subglacial drainage reorganises intermittently, to release stored sediment until the supply becomes exhausted; maximum up–glacier retreat of snowline separating exposed glacier ice from the previous winter's snow cover

coarser sediments or a thinner sediment layer. Observations at the glacier margin also indicate variability in basal conditions, revealing striated and polished bedrock surfaces that protrude through layers of unconsolidated sediment. The bed is therefore likely to consist of a spatially variable sediment layer interspersed with bedrock bumps of a scale typically less than one ice thickness.

Hydrological non-uniformity occurs temporally and spatially during the melt season due to: 1) seasonal evolution of the subglacial drainage system (e.g. Mair et al., in press); and 2) the existence of large areas of the glacier bed that demonstrate high and diurnally

variable water pressures due to the presence of a subglacial channel (Hubbard et al., 1995; Gordon et al., 1998). An annual velocity profile across the glacier tongue demonstrated substantially higher rates of basal sliding in the area of the VPA during 1995 and 1996, although variability in basal motion was not observed at the glacier surface due to transverse ice-coupling effects that induced compensating deformation patterns in the overlying ice (Harbor et al. 1997). Observations at seasonal and short-term time scales during 1994 and 1995 show that summer glacier surface velocities are much greater than winter- and annually-averaged velocities. A large proportion of the summer motion in 1995 (14 %) occurred during a spring event and motion during the event was enhanced within the VPA. Harbor et al. (1997) suggested that locally high basal water pressures are responsible for high rates of basal motion within the VPA, and transverse coupling is believed to play an important role in increasing the summer velocity of ice in adjacent areas. Hydrological non-uniformity is therefore presumed to exert a major control on rates and processes of basal motion.

2.1.4 Meltwater run-off, storage and quality

Haut Glacier d'Arolla has a short melt season characteristic of many alpine glaciers, typically occurring from May–August inclusive (e.g. Gurnell et al., 1992a). Meltwater within the catchment is initially generated almost entirely by snow melt, but as the supraglacial snowpack is removed, an increasing quantity is derived by ice melt at the glacier surface. Towards the end of the season, the majority of runoff is derived from ice melt and snowmelt is virtually negligible. The routing of meltwater is complex and evolves throughout the melt season (Nienow et al., 1998; cf. Röthlisberger and Lang, 1987). Meltwater is initially delivered through the surface snowpack and via moulins and crevasses to a distributed subglacial drainage system. Flow through the snowpack and distributed subglacial drainage system is characterised by long residence times that damp surface meltwater inputs and glacier run-off. These systems are eventually replaced by the evolution of a well-structured supraglacial drainage network and channelised subglacial drainage system characterised by short residence times that rapidly transmit surface melt to the glacier snout. The co-evolution of the two systems thus increases the efficiency with which diurnal inputs of solar radiation are translated

Table 2.3 Regression relationships estimated between hourly suspended sediment concentration and discharge during previous melt seasons at Haut Glacier d'Arolla.

Dependent variable (lag)	Independent variable	Period	Start and end date	n	a	b	t_a	t_b	r^2
1989: Gurnell et al. 1992a									
$\log_{10}S$	$\log_{10}Q$	1	1 June–8 June	-	1.42	0.45	-	-	-
$\log_{10}S$	$\log_{10}Q$	2	9 June–15 June	-	0.92	0.53	-	-	-
$\log_{10}S$	$\log_{10}Q$	3	16 June–8 July	-	–3.95	1.98	-	-	-
$\log_{10}S$	$\log_{10}Q$	4	9 July–6 August	-	–1.69	1.32	-	-	-
$\log_{10}S$	$\log_{10}Q$	5	7 August–31 August	-	–1.13	1.23	-	-	-
1989: Gurnell et al. 1994									
$\log_{10}S$ (0)	$\log_{10}Q$	1	1 June–8 June	137	1.75	0.31	6.6	3.2	0.072
$\log_{10}S$ (0)	$\log_{10}Q$	2	9 June–15 June	116	–0.15	0.86	0.6	11.7	0.545
$\log_{10}S$ (0)	$\log_{10}Q$	3	16 June–8 July	506	–3.95	1.98	28.4	47.2	0.815
$\log_{10}S$ (–2)	$\log_{10}Q$	4	9 July–6 August	658	–0.87	1.09	5.2	22.9	0.445
$\log_{10}S$ (0)	$\log_{10}Q$	5	7 August–31 August	490	–1.07	1.21	7.3	29.2	0.443
1990: Gurnell et al. 1994									
$\log_{10}S$ (0)	$\log_{10}Q$	1	29 May–19 June	390	–1.16	1.10	6.8	18.6	0.471
$\log_{10}S$ (0)	$\log_{10}Q$	2	19 June–2 July	310	–5.21	2.39	30.0	46.4	0.875
$\log_{10}S$ (0)	$\log_{10}Q$	3	2 July–27 July	550	–0.27	0.95	1.9	23.0	0.490
$\log_{10}S$ (0)	$\log_{10}Q$	4	27 July–13 August	288	–0.87	1.18	3.8	18.4	0.541
$\log_{10}S$ (0)	$\log_{10}Q$	5	13 August–26 August	290	–0.27	1.07	1.1	32.8	0.789

S: suspended sediment concentration (mg l^{-1}), figures in parenthesis indicate lag in hours to obtain the best temporal match position (where applied); Q: discharge (l s^{-1}); a, b: regression intercept and slope, respectively; t_a, t_b: t-statistics associated with the regression intercept and slope, respectively.

into diurnal variations in surface melting and are then transmitted through the glacier drainage system to the proglacial stream (Gurnell et al., 1992a).

The characteristics of glacier run-off and meltwater quality follow a distinctive pattern throughout the melt season that is related variations in meteorological inputs that drive the retreat of the snowpack and the evolution of a channelised subglacial drainage system (Gurnell et al., 1992a; Richards et al., 1996). Richards et al. (1996) identified and qualitatively interpreted a number of phases during the melt season (Table 2.2). High solute concentrations occur during Period 1 since the majority of meltwater is routed

through a distributed subglacial drainage system characterised by prolonged meltwater-bedrock/sediment contact. These concentrations decline during Period 2a as increased levels of surface melt dilute meltwaters in the distributed system, and solute concentrations begin to exhibit diurnal variability due to diurnal variation in melt energy. Solute concentrations are lowest from Period 2b as the magnitude of surface melting continues to increase and establishment of the channelised drainage system begins. The growth of channelised flowpaths results in the increasing amplitude of diurnal discharge and solute cycles in the proglacial stream. Conversely, suspended sediment concentrations are lowest during Period 1 and gradually increase over Periods 2a–3 as growth of the channelised drainage system occurs. During period 4, suspended sediment concentrations may decline due to exhaustion of available sediment sources as the channelised drainage system reaches its maximum extent. However, concentration may exhibit sudden increases if subglacial drainage re-organises, thereby reaching new areas of stored sediment.

The seasonal decrease in suspended sediment concentration due to the exhaustion of available sediment supplies has been emphasised by Gurnell et al. (1992, 1994). Regression relationships were estimated between suspended sediment concentration and discharge for various periods of the melt season during 1989 and 1990 (Table 2.3). The steepest and strongest relationships occur early in the season (period 3 in 1989; period 2 in 1990), and therefore Gurnell et al. (1994) suggested that progressively lower suspended sediment concentrations must be associated with any given discharge later in the melt season. Gurnell et al. (1992a) also analysed data from the 1989 melt season using separate Transfer Function–Noise models for each of the 5 periods, suggesting that the decreasing 'moving average' parameter in the models for periods 3–5 reflected either a gradual exhaustion or progressive dilution of the available sediment by increasing discharge. However, these results contrast sharply with Clifford et al.'s (1995b) analysis of the 1990 data. Clifford et al. (1995b) estimated a simple bivariate power function between suspended sediment concentration and discharge for the whole melt season. Negative and positive residuals from the relationship indicate, respectively, lower and higher suspended sediment concentrations than expected for a given discharge. The residuals vary systematically throughout the melt season, being largely negative during

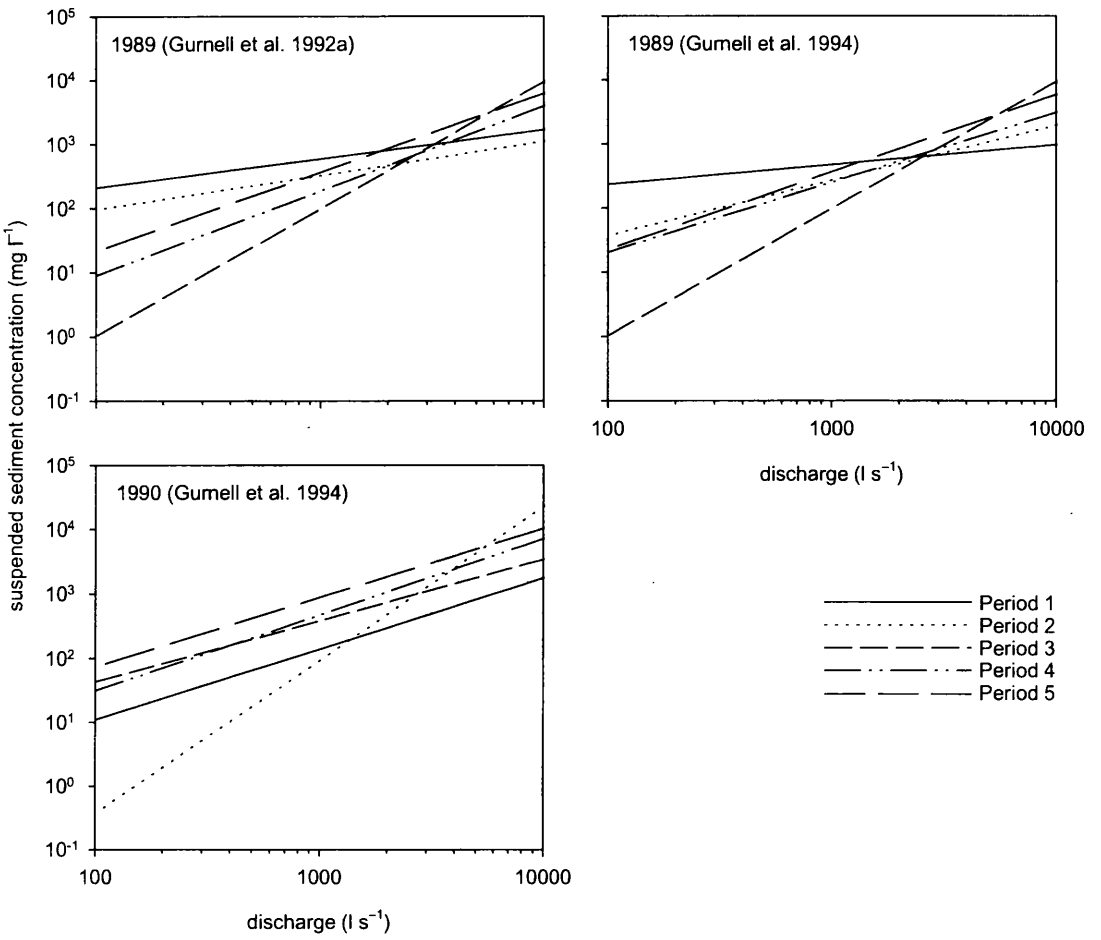

Figure 2.4 Regression relationships between discharge and suspended sediment concentration for various periods of the melt season at Haut Glacier d'Arolla during 1989 and 1990. Relationships are reconstructed from Gurnell et al. (1992a, 1994) for discharges typical of the Haut Arolla catchment; see Table 2.3 for definitive periods.

early July when conduits are forming (period 2 in Table 2.3) and remaining consistently positive throughout August. Furthermore, the residuals continued to increase throughout August, indicating higher than expected suspended sediment concentrations despite a gradual decline in discharge.

Re-plotting the regression relationships identified by Gurnell et al. (1992a, 1994), it can be shown that there is little evidence for the exhaustion of available sediment after the channelised system has become fully established (Figure 2.4). Gurnell et al (1992a, 1994) emphasised changes in the magnitude of the slope of the relationship when interpreting these results; however, it can be seen that changes in the relationship

Table 2.4 Monthly discharge and suspended sediment transport during the 1989 and 1990 melt seasons at Haut Glacier d'Arolla (Gurnell, 1995; Clifford et al., 1995b).

	Discharge ($m^3 s^{-1}$)				Suspended sediment concentration ($g l^{-1}$)				Load ($t d^{-1}$)
Period	*Min*	*Max*	*Median*	*Mean*	*Min*	*Max*	*Median*	*Mean*	*Mean*
1989: Gurnell, 1995									
June	-	-	-	1.37	-	-	-	0.390	55.5
July	-	-	-	3.40	-	-	-	1.061	358.6
August	-	-	-	2.93	-	-	-	1.628	560.5
1990: Clifford et. al., 1995b									
1 June–10 July	0.40	5.90	1.52	-	0.028	17.51	0.248	-	-
11 July–8 Aug	1.47	7.22	3.56	-	0.469	15.52	1.36	-	-
8 Aug–10 Sept	1.15	5.75	2.46	-	0.191	7.35	2.28	-	-

between suspended sediment concentration and discharge are described by changes in both the slope *and* intercept. Relationships with high slopes typically occur early in the season, but result in increased sediment availability relative to other periods only during exceptionally high discharges. Later in the season, typically during periods 3–5, the slopes are lower, but, due to changes in the intercept, relationships for period 5 plot above period 4 and occasionally period 3, demonstrating increasing sediment availability. Data from 1989 and 1990 summarised by Gurnell (1995) and Clifford et al. (1995b) also show increasing sediment availability later in the melt season, with mean or median suspended sediment concentration increasing even as discharge falls (Table 2.4).

2.2 MONITORING PROGRAMME AND INSTRUMENTATION

2.2.1 Introduction

Fieldwork was undertaken at Haut Glacier d'Arolla during the 1998 and 1999 melt seasons in order to investigate the mechanisms by which suspended sediment is evacuated by basal meltwater. It was therefore necessary to establish the nature and

variability of suspended sediment in the proglacial stream, as well as to obtain independent information on the dynamic nature of the glacial and fluvioglacial systems (see Section 1.3). A proglacial stream sediment monitoring programme was implemented during both seasons that comprised: 1) the continuous measurement of stream turbidity and suspended sediment concentration; and 2) the automated collection of stream samples for the analysis of sediment quality. Electrical conductivity in the proglacial stream was also monitored continuously in order to provide independent evidence of the dynamic nature of the subglacial drainage system.

The proglacial stream measurements complemented a two-year NERC-funded investigation into ice dynamics at Haut Glacier d'Arolla that provided additional measurements of glacier surface velocity and catchment hydrometeorological conditions (Willis et al., 1999). In addition to these measurements, P. Nienow (Geography, Glasgow University) undertook dye-tracer investigations of the subglacial drainage system during 1998. Details of the proglacial stream monitoring programme (sediment concentration and quality) and the additional measurements obtained throughout the seasons (electrical conductivity, glacier velocity, catchment hydrometeorology and dye-tracer investigations) are discussed below.

2.2.2 Proglacial stream monitoring programme

The aim of the proglacial stream monitoring programme was to obtain measurements of both suspended sediment concentration and quality throughout the melt season. Much work has been devoted to the reliability and representivity of sediment monitoring programmes in alluvial and glacial streams (e.g. Bogen et al., 1992; Gurnell, 1987). For long-term studies where frequent measurements are required, monitoring is usually conducted at a single location in the stream cross-section using turbidity sensors or automated samplers. Turbidity sensors may be deployed directly in the flow and provide a continuous, high-resolution proxy for suspended sediment concentration (e.g. Clifford et al., 1995b). Alternatively, automated samplers can be used to withdraw given volumes of water at specific time intervals for the analysis of sediment concentration and quality (e.g. Gurnell and Fenn, 1984a; Fenn and Gomez, 1989).

2.2.2.1 *Reliability of suspended sediment monitoring programmes*

The reliability of sediment monitoring programmes depends upon: 1) the extent to which at-a-point measurements of sediment concentration and quality reflect mean concentration and quality in the cross-section; 2) whether measurements taken at a cross-section are representative of sediment concentration and quality both up and downstream of that location; and 3) whether the frequency of the measurements/samples is sufficient to allow the investigation of variation in sediment concentration and quality at a resolution from which process-based inferences can be made.

At-a-point sampling

Under normal conditions of stream flow, suspended sediment size and concentration increase towards the centre of the flow and towards the bed. Consequently, it can be difficult to obtain measurements of mean sediment concentration and quality using at-a-point sampling without detailed knowledge of variability throughout the cross-section. In proglacial streams, the difficulties are expected to be greater since flow depth and velocity vary over short time scales due to diurnal variations in melt generation at the glacier surface. Variable discharge means the relative location of at-a-point measurements in the stream cross-section constantly changes, and high peak discharges and flow velocities provide a severe test of the equipment and its installation (cf. Gurnell et al., 1992b). However, extensive manual sampling of suspended sediment concentrations has generally found little systematic variation in suspended sediment concentration in proglacial stream cross-sections (cf. Fenn, 1983; Gurnell and Fenn, 1984a; Gurnell et al. 1992b). Fenn (1983) concluded that adequate estimates of mean suspended sediment concentration could be obtained by sampling near to the centre of the cross-section, although potential error remained high.

Gurnell et al. (1992b) evaluated the reliability of a sediment monitoring programme at Haut Glacier d'Arolla. Manual samples taken across a tributary of the main proglacial stream revealed a random variation in suspended sediment concentration and the degree of variability changed between days and stream cross-sections. Gurnell et al. (1992b) concluded that once away from shallow water near the stream banks, short-term, spatial

variation in suspended sediment concentration is essentially random. The turbulent nature of proglacial streams appears to distribute sediment concentration more evenly throughout the stream cross-section (Østrem, 1975; Bogen, 1992; Gurnell, 1987b); therefore at-a-point sampling at any one location should generally yield an unbiased estimate of suspended sediment concentration.

Upstream and downstream variation in suspended sediment transport

Gurnell et al. (1992b) found that over short distances variation in suspended sediment concentration both up and downstream of a monitored cross-section is also random. Østrem et al. (1971) also found no significant variation in suspended sediment concentration for samples collected near to the stream bank over a distances of ~ 75 m. However, in an analysis of fluvial sediment yields from 57 glaciated catchments, Gurnell (1987b) and Gurnell et al. (1996) found weak but significant, negative relationships between sediment yield and distance from the glacier snout, suggesting that proglacial areas act as a sink for fluvially-transported sediment. Boothroyd and Ashley (1975) also observed a decrease in suspended sediment concentration with distance from the glacier snout, but only after an initial increase that appeared to reflect downstream variation in flow velocity. However, many studies have observed contributions of sediment from proglacial sources (e.g. Bogen, 1980; Hammer and Smith, 1983; Richards, 1984) or consistent downstream increases in suspended sediment concentration (e.g. Fahnestock, 1963; Gurnell, 1982). The nature and origin of downstream variation in suspended sediment concentration clearly remains unresolved; however, the above discussion suggests that a monitoring site as close to the glacier snout as possible (cf. Gurnell et al., 1992b) and upstream of major proglacial sediment sources and/or sinks is crucial.

Temporal resolution of sampling programmes

Turbidity sensors can be used to obtain high-resolution records of suspended sediment concentration; however, where automated sampling is required, sampling frequency is an important consideration. Attempts to determine the appropriate temporal resolution for accurate measurements of suspended sediment concentration and quality have been limited. Gurnell (1987b) summarised the sampling frequencies employed in a range of

studies of suspended sediment concentration in proglacial streams. Sampling frequency is typically based on the perceived variability of the processes being monitored, but there are practical limitations too. It is extremely labour intensive to obtain good records of suspended sediment concentration for proglacial streams, and the highest resolution records thus far obtained comprise samples taken at hourly intervals.

Olive and Reiger (1988) examined the errors involved in estimating sediment load from measurements of discharge and suspended sediment concentration using simulated storm events and monitoring programmes with different sampling intervals. The duration of each event was 10 h, but otherwise the events were very similar in character to diurnal melt and storm-induced variations in discharge and suspended sediment concentration observed in proglacial streams. Two issues were investigated: 1) the magnitude of errors resulting from the time interval between samples; and 2) relative shifts in the timing of the events with respect to the sampling programme, since it is unlikely that samples will coincide with sediment peaks. For sampling programmes with intervals of 5–120 min in 5-minute increments, 50 determinations of sediment load were calculated for each storm event at randomised starting intervals between time t = 1 and 60 min. The mean and range of the 50 load determinations for each sampling programme were expressed as a percentage of the load determined using a 1-minute sampling interval. The results demonstrated relatively small errors in load estimation ($\pm < 2.5$ % of the 1-minute load) for sampling intervals of 30 min or less regardless of the starting time. A 30-minute interval represented 5 % of the duration of the event, and indicates that for proglacial streams where variability in suspended sediment concentration and quality is expected to be driven largely by diurnal events, hourly-sampling intervals should be adequate.

Olive and Reiger (1988) argued that such sampling frequencies are difficult to maintain and, in the case of suspended sediment concentration, better information could be obtained using continuous turbidity measurements. There is also the likelihood that a significant proportion of sediment evacuated may occur due to processes operating at sub-hourly scales. Clifford et al. (1995b) used continuous turbidity measurement to identify the scales of variation of suspended sediment concentration in the proglacial stream at Haut Glacier d'Arolla. A very limited dataset indicated rapid fluctuations in

turbidity at sub-hourly scales lasting a few tens of minutes that were attributed to channel-scale events (e.g. bank erosion), but these contributed only ~ 10 % of the seasonal variance in suspended sediment concentration. A further 1 % of the seasonal variance also originated at sub-hourly scales, and was attributed to stream turbulence and signal-noise. Gurnell and Warburton (1990) also examined sub-hourly events during a 22-day turbidity record from the proglacial stream of Glacier de Tsidjiore Nouve, Switzerland. 571 sediment pulses were observed that were of short duration but also relatively low magnitude. The sediment transported as a result of the pulses (i.e. transport over and above the background transport) was estimated to be only 10 % of the total sediment load. These results suggest that processes operating at sub-diurnal scales are unlikely to be a predominant control on suspended sediment evacuation.

2.2.2.2 Representivity of sediment monitoring programmes

Suspended sediment concentration can be highly variable at very short time scales and frequent measurements are desirable if not essential. Turbidity sensors provide a high resolution proxy for suspended sediment concentration. Modern sensors use infra-red light sources in order to avoid problems associated with noise from natural ambient light (cf. Gurnell et al., 1992a,b); however, the representivity of turbidity measurements are difficult to assess at the measurement frequencies involved. A practical way to do this is with the installation of a second sensor in the stream cross-section. Good correspondence between measurements from individual sensors should indicate high representivity of actual stream conditions.

Turbidity sensors are sensitive to variations in particle size and composition (Gippel, 1995; Clifford et al., 1995a), therefore sensor calibration is also required in order to establish a relationship between turbidity and suspended sediment concentration for individual catchments. Calibration may be undertaken in the laboratory using suspensions of known sediment concentration (cf. Clifford et. al., 1995a), but such procedures typically obtain only poor correlations (Gippel, 1989). It is likely to be particularly difficult to accurately simulate the particle composition, shape and size characteristics found in the field. Field calibration, using sediment concentrations determined from samples collected simultaneously at the same stream cross-section, has

generally provided the best relationships (Gippel, 1989). It is also likely that errors due to changing particle composition, shape and size characteristics will be minimal if the number of calibration samples is large and provide good temporal coverage of the monitored period.

Samples for suspended sediment quality can be collected quasi-continuously using an automated sampler and filtered in the field. The representivity of the filtration method is important and Gurnell (1987b) has reviewed some of the methods used in previous published studies. Relatively coarse papers were used at Glacier de Tsidjiore Nouve because: 1) filter papers clogged rapidly during filtration, such that the effective pore size was probably much smaller than the calibre of the paper would suggest; and 2) particle size data obtained for hourly samples collected over a diurnal period had shown that particles smaller than 8 μm in size constituted less than 5 % of the sediment volume. A later study by Fenn and Gomez (1990), also using 8 μm papers, showed that particles smaller than 8 μm constituted 25 % of the sediment volume. They observed that the main mode of suspended sediment was in the 2–120 μm range, demonstrating the capacity of the papers to retain far smaller particles than their initial pore size.

Gurnell et. al. (1992b) evaluated the effectiveness of 8 μm papers used at Haut Glacier d'Arolla by re-filtering samples through 0.45 μm papers. They found that the weight of sediment passing through the 8 μm papers was small with respect to the total weight of sediment in the samples (4 % for samples of ~ 0.4 g l^{-1}). However, a number of other studies have suggested that suspended sediment samples from glacial catchments comprise a large proportion of very fine sediments. At Nigardsbreen and Engabreen in Norway, sediment-size analysis using a Shimadzu centrifugal particle-sizer found that more than 6 % of suspended sediment by weight is finer than 2 μm (Bogen, 1992). Similarly, a composite analysis of 200 meltwater samples collected at Haut Glacier d'Arolla during 1996 and filtered using 0.45 μm papers indicated that ~ 10 % of sediment by weight was finer than 2 μm (unpublished data of A. Seagren, cited by Fisher and Hubbard, 1999). Analysis of till sediments has also suggested likely minimum sizes for the products of glacial erosion that depend upon the original sizes and shape of mineral grains within the rocks and the resistance of each mineral to

comminution during glacial transport (Dreimanis and Vagners, 1971). So-called 'terminal grades' for common minerals are 2–62 μm for calcite, 4–250 μm for quartz and 34–250 μm for feldspars (Vagners, 1969).

Samples obtained using automated samplers also need to be representative of suspended sediment concentration and quality throughout the flow. The Federal Interagency Sedimentation Project USDH48 (Federal Interagency Sedimentation Project, no date) is a manual sampler that collects a velocity-weighted water sample when lowered into the flow and raised again at a constant rate. Using the equal-width increment (EWI) method (Edwards and Glysson, 1988), the USDH48 can be used to obtain a velocity-weighted width and depth-integrated sample from the cross-section. Gurnell et. al. (1992b) used a USDH48 to assess the respresentativeness of automated samples obtained using an ISCO water sampler at Haut Glacier d'Arolla. Very good agreement was obtained between the sediment concentration of ISCO and USDH48 samples ($r^2 = 0.822$, $n = 51$), although the USDH48 was simply allowed to fill next to the ISCO intake hose as the ISCO was sampling. Stream width and depth-integrated samples are clearly required in order to assess the reliability of automated samples accurately. Cross and downstream variability of suspended sediment characteristics also require characterisation for individual basins.

2.2.2.3 Programme design, instrumentation and field equipment

The monitoring programme was designed with regard to the reliability and representivity of the measurements to be taken, the perceived scale of the processes being investigated, and the practical limitations of instrument installation, maintenance and data storage and/or sample processing in the field. Suspended sediment concentration was monitored in the stream using Partech IR40c infrared turbidity sensors, the characteristics of which have been described in detail by Clifford et. al. (1995a) and have been successfully used during previous melt seasons at Haut Glacier d'Arolla (Clifford et. al., 1995b). Water samples were collected using two ISCO vacuum-pump samplers (models 6700 and 2900) and filtered in the field. Large, 15 cm diameter Whatman 542 2.7 μm papers were chosen in order to maximise both particle retention and filtration speed. A quantitative, ashless grade of paper was chosen for ease and accuracy of sediment content in the laboratory (see

Section 2.3.1.1). The filtration method was designed around ~ 17 cm diameter Büchner funnels adapted using a custom-made gasket to reduce sample loss around and under the filter paper; however, laboratory testing suggested that a small proportion of sediment may bypass the paper by escaping under the gasket. Thus at least one sample per day was re-filtered through standard filtration equipment using 4.7 cm diameter 0.1 μm cellulose nitrate papers to assess the proportion of sediment lost. Standard manual vacuum pumps were used to increase filtration efficiency. Implementation of the programme is discussed in further detail for each melt season below, and the reliability and representivity of the programme are discussed in Section 2.3.2.

2.2.3 Implementation

During 1998 and 1999, the glacier was drained by two principal meltwater streams with distinct glacial sub-catchments (Figure 2.5). Dye-tracing investigations from moulins on the glacier surface were used to determine the boundary of the two sub-catchments during 1998 (Section 2.2.4.3; Figure 3.9). Monitoring was confined to a single sub-catchment during each season since sufficient equipment was not available to allow the monitoring of both sub-catchments simultaneously. In 1998, monitoring was concentrated on the western proglacial stream, which in previous years had been shown to drain the majority of the glaciated area (Sharp et al., 1993). The eastern proglacial stream, which drained the majority of the glaciated area during 1998 (Figure 3.9; Section 3.4.4), was monitored during the 1999 melt season. Monitoring of both sub-catchments from downstream of the confluence between the eastern and western proglacial streams was also impossible, since this would: 1) require a well-mixed sampling point downstream of the confluence, such that the gauging station could not be located near to the glacier snout; 2) integrate changes in suspended sediment concentration and quality from separate sub-catchments, thereby masking processes of sediment evacuation that may be temporally or spatially variable within each catchment; and 3) generate practical problems with regards to the maintenance and calibration of the gauging station due to high discharges and flow velocities.

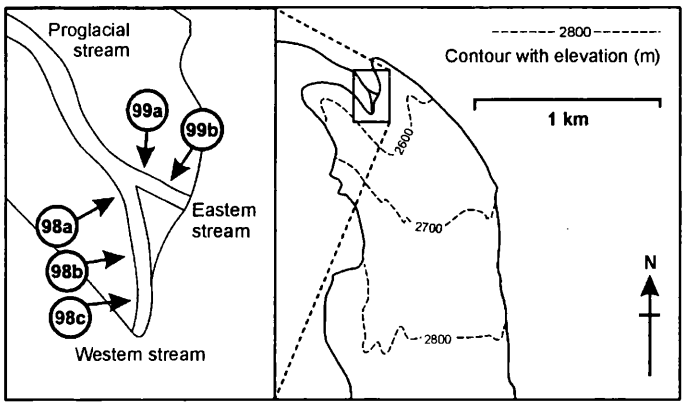

Figure 2.5 Detail of the proglacial area at Haut Glacier d'Arolla, showing the Eastern and Western proglacial streams and the position of the gauging stations during 1998 (98a–c) and 1999 (99a and 99b).

Monitoring was conducted from a fixed gauging station located near to the glacier snout in order to eliminate suspended sediment contributions from proglacial sources. A typical arrangement of sensors at the gauging site is shown in Figure 2.6. The sensors were positioned at roughly half the mean flow depth, as recommended for at-a-point measurements (Rooseboom and Annandale, 1981), although in practice such a position was difficult to maintain (see below). Care was taken to ensure that sensors were located away from the channel banks and within the main flow (cf. Gurnell et. al., 1992b), and that turbidity measurements were not influenced by excessive turbulence that may have introduced bubbles or large proportions of saltating material high into the flow.

2.2.3.1 1998 melt season

During 1998, monitoring began on Julian Day (JD) 135 (May 15th). Thick snow cover in the proglacial area required excavation of the western proglacial stream ~ 50m from the glacier snout in order to position the gauging station (gauging station 98a, Figure 2.4). The gauging station was subsequently moved to within ~ 40 and ~ 20m of the snout on JD 158 and 156 respectively (gauging stations 98b and c) as the proglacial snowcover retreated. Turbidity was monitored using a single sensor (T1) from JD 135 and from two sensors (T1 and T2) after JD 139. Turbidity was recorded separately for each sensor using a Campbell CR23x datalogger; measurements were taken every 10 seconds and averaged over 5-minute intervals. The sensors required frequent maintenance to remove

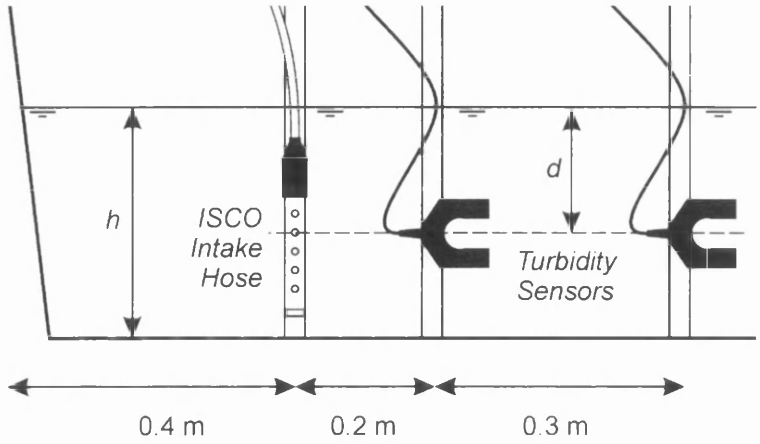

Figure 2.6 A typical arrangement of the turbidity sensors and Isco intake hose during the 1998 and 1999 melt seasons. The turbidity sensors were positioned at depth *d*, roughly equal to half the mean flow depth (*h*). Channel width was typically ~ 3–4 m.

saltating debris that became trapped between the sensor heads. Occasionally, the position of the sensors also had to be adjusted to take account of changes in bed elevation and mean daily flow depth. Sensor T2 failed on JD 187 and was replaced with a new sensor (T3) that operated during the period JD 216–217.

Automated sampling was initiated on JD 135. Since suspended sediment concentrations varied during the melt season, sample volumes were adjusted in order to obtain adequate sediment content whilst maintaining good temporal coverage and acceptable filtration times (Table 2.5). A number of significant gaps (> 12 h) occur during 1998, two of which were due to power failures and a third occurred when the intake hose became iced during cold weather. Sampling was also impaired if the intake hose became surrounded by sediment or large rocks, frozen or emerged above the water surface. Consequently, very small samples (typically < 200 ml) and samples with excessive quantities of sediment (usually when the intake hose had been found to be buried by rocks or sediment) were discarded. Only 35 % of days had complete temporal coverage at the desired interval due to loss of samples for reasons described above.

USDH48 samples were obtained daily for later assessment of sampling programme representivity. A width and depth-integrated sample was obtained immediately downstream of the gauging station whilst the ISCO was sampling. Normal practice is to

Table 2.5 Approximate volume and interval of samples collected for analysis of suspended sediment concentration and quality during 1998 and 1999.

Period (JD)	Volume (l)	Interval (h)	Notes
1998 Ablation Season			
135–136	4	4	
137–138	0.25	1	
139–140	-	-	Power failure
141–143	~ 1	~ 4	
144–147	~ 1	2	
148–149	-	-	Power failure
150–153	~ 1	2	
154–162	~ 0.8	1	
163	-	-	Hose iced
164–170	1	2	
171–208	0.9	1	
1999 Ablation Season			
169–175	5	6	
176–179	4	4	
180–185	2	2	
186–187	-	-	Spring flood event
188–204	2	2	

obtain a separate depth-integrated sample for each of 10 equal sections across the stream (cf. Edwards and Glysson, 1988); however, the ISCO sampled too rapidly and for consistency a single sample was obtained from 10 consecutive depth-integrations of 10 equal sections. Samples obtained using the USDH48 (full volume 470 ml) should be between 375 and 420 ml to be representative of mean suspended sediment characteristics (Federal Interagency Sedimentation Project, no date). In practice, it was difficult to obtain samples within this range in the turbulent, rapidly flowing proglacial stream, and hence only samples that were very low (< 350 ml) or almost full (> 460 ml) were discarded. A total of 52 USDH samples were obtained between JD 142 and 206 during 1998 at times ranging from 11:00 to 19:00, thus providing good seasonal coverage over a range of flow conditions.

ISCO and USDH samples were filtered in the field through 2.7 µm papers. Samples were screened for particles > 2 mm that may have biased measurements of sediment concentration and quality (cf. Fenn and Gomez, 1989) using a standard laboratory sieve. The filtrate from one sample per day (typically a USDH48 sample) was used to assess the representivity of the filtration method. This involved collecting any sediment remaining around the sides of the Büchner funnel and gasket and re-filtering using pre-weighed 0.1 µm papers.

2.2.3.2 1999 melt season

During 1999, monitoring began on JD168 (17th June) in the eastern proglacial stream. The gauging station was initially located within a well-defined channel ~ 20 m from the glacier snout (gauging station 99a) and moved to a more optimum location ~ 10 m from the snout on JD 186 (99b; Figure 2.4). Turbidity sensors T2 and T3 (see above) were installed on JD 168 and automated sampling was initiated on JD 169. As in 1998, the volume and frequency of sample collection was varied with respect to changing levels of suspended sediment in the eastern stream (Table 2.5). Automated sampling was used to obtain slightly larger samples than during 1998 of 2× 1 litre throughout most of the monitored period; one or both of the containers were filtered depending upon the sediment concentration. USDH48 samples were collected frequently as per the 1998 melt season. A total of 26 USDH48 samples were obtained; only one was discarded due to the volume being below 350 ml. A second automatic sampler was used to obtain composite daily samples from JD 171 to 205 for analysis of seasonal changes in sediment quality. Composite samples consisted of 120 ml samples collected every 3hrs from 00:00. All samples were filtered as per 1998.

Turbidity measurement and automated sampling suffered similar difficulties to those experienced during 1998, although some unique difficulties were experienced. From JD 181 to 189, frequent gaps occur in the turbidity records due to a faulty battery connected to a solar panel that resulted in the failure of the sensors at night. A logger failure later prevented the downloading of data from JD 191 to 195. Problems also occurred due to the dynamic nature of the eastern stream, which at different times occupied up to three channels as it flowed from the glacier snout. Following ~ JD 203, the stream once more

became entrenched in a single channel. High and variable discharge through the single channel prevented the collection of USDH48 samples and made the gauging station very difficult to maintain. Consequently, automatic sampling and turbidity measurement were stopped on JD 205 and 206, respectively, to avoid damage to and loss of equipment.

2.2.4 Additional measurements

2.2.4.1 Electrical conductivity

Electrical conductivity was used to provide independent evidence of the evolution of meltwater sources and pathways. Solute concentrations in basal ice and meltwater are high compared to supraglacial meltwater (Collins, 1979a), since solute concentration partly reflects the time and degree of contact between meltwater and sediment (Lemmens, 1978). Electrical conductivity has therefore been used to separate rapidly routed meltwater through channelised englacial and/or subglacial flowpaths from delayed flow through a distributed subglacial drainage system (Collins, 1979a; Gurnell and Fenn, 1984b). However, high solute concentrations may also be derived from snowmelt during snowpack elution as the supraglacial snowcover is removed (Fountain, 1996). Electrical conductivity does not appear to fluctuate greatly with distance from the glacier snout (Gurnell, 1985).

A Campbell Scientific 247 conductivity sensor was used during both field seasons. The sensor was mounted on the gauging station facing towards the flow such that the tube is flushed continuously. However, the relatively small tube (inner diameter ~ 5 mm) was frequently blocked by suspended sediment, necessitating frequent maintenance that was difficult without removing and re-fitting the sensor. Electrical conductivity was measured in the western proglacial stream during 1998 between JD 165 and 225 and in the eastern stream between JD 168 and 206 during 1999. Raw conductivity was sensed every 10 seconds and averaged at 5-minute intervals using a Campbell CR23x datalogger. 'Corrected' conductivity was also obtained by calculating errors due to ionisation and water temperature (Campbell Scientific, 1994-1996).

2.2.4.2 *Glacier velocity and catchment hydrometeorological conditions*

Glacier velocity and catchment meteorological conditions were monitored during the 1998 and 1999 melt seasons by members of the Arolla Glaciology Project (Willis et. al., 1999). Standard surveying methods were used to monitor glacier surface motion across a network of 33 stakes every 1–5 days during spring and summer in 1998 and 1999 (JDs 150–224 and 171–226, respectively). During 1998, meteorological conditions were obtained from the Bricola meteorological station approximately 8km NNE of Haut Glacier d'Arolla. The Bricola station (2415 m ASL) is the nearest source of meteorological data recorded at a similar altitude to the glacier, and should provide the best proxy for conditions in the Arolla catchment (I. Willis, pers. comm.). During 1999, meteorological data was monitored near to the intake structure operated by Grande Dixence S.A. (Figure 2.1) who provided catchment discharge during both melt seasons.

2.2.4.3 *Dye-tracer investigations*

During the 1998 melt season, a limited number of dye-traces were performed from moulins on the glacier surface by P. Nienow in order to confirm the structure and hydraulic configuration of the subglacial drainage system late in the melt season. Known quantities of rhodamine dye were injected into specific moulins and the two proglacial streams monitored by frequent manual sampling (< 5 minutes) of meltwater using a 0.5 l polypropelene bottle. Dye concentrations were measured for each sample immediately after collection by passing the samples through a fluorometer.

2.3 INITIAL DATA PREPARATION AND ANALYSIS

2.3.1 Data preparation

Suspended sediment samples and records of stream turbidity and electrical conductivity collected during the 1998 and 1999 melt seasons require pre-processing. Suspended sediment samples collected automatically and filtered in the field require determination of their suspended sediment content and preparation for analysis of sediment quality, whilst measurements of stream turbidity require calibration using known suspended

Table 2.6 Determination of change in sample weight during treatment at high temperature for proglacial and basal sediment samples from Haut Glacier d'Arolla.

Sample	Type	Weight[1]	Weight[2]	Difference	%
A	Kettle-hole deposits	5.1450	5.0475	–0.0975	1.90
B	Slackwater deposits	4.3708	4.3270	–0.0438	1.00
C	Slackwater deposits	4.6374	4.5823	–0.0551	1.19
D	Slackwater deposits	2.9740	2.9357	–0.0383	1.29
E	Basal melt-out till	4.1798	4.1352	–0.0446	1.07
				Mean	1.29

Weight[1] and Weight[2]: sample weight (minus weight of crucible) before and after ashing, respectively; Difference: change in sample weight; %: change in weight as a percentage of the original sample weight

sediment concentrations. Sampling programmes are likely to include errors due to highly variable flow conditions, icing and proglacial stream channel adjustments; hence, records must be carefully checked for anomalies. This section details preparation of the suspended sediment samples and stream turbidity and electrical conductivity records for further analysis. The reliability and representivity of suspended sediment samples and measurements of stream turbidity are discussed in Section 2.3.2.

2.3.1.1 Suspended sediment concentration and quality

Filtered samples were ashed at 900 °C for 30 min. To avoid loss of particles by ignition, papers were previously charred over a bunsen burner for ~ 20 min. The suitability of the ashing method was assessed using test samples, since treatment at high temperatures might be expected to cause physical alteration of sediments and loss of clay particulates. The effect of ashing was evaluated using sediments sampled from both proglacial backwater deposits and basal melt-out till at Haut Glacier d'Arolla. The samples were dried and sieved to exclude particles larger than 2 mm. Subsamples were prepared, placed into crucibles, weighed and then heated at 900 °C for 30 min. On weighing the subsamples after cooling, sample weight had fallen by 1–2 % (Table 2.6). The fall in weight could indicate the loss of sediment on exposure to high temperatures (the

sediments are unlikely to have contained organic matter) or the loss of moisture acquired from atmospheric sources during sample preparation.

To further test for physical changes to the sediment, two composite sediment samples were prepared for analysis under a scanning electron microscope (SEM). A single composite sample was obtained using equal quantities of samples A–E (Table 2.6) and split using a riffle box; half of the sample was then heated at 900 °C for 30 min. Samples of the normal and ashed sediments were mounted for analysis by pressing an adherent sample plate into the well-mixed sediment. The normal sample was found to be composed of a range of predominantly silt-sized grains (Figure 2.7, A) exhibiting a freshly ground appearance, together with a number of 'microparticles' (cf. Lamb, 1995) adhering to the larger grains (Figure 2.7, B to D). The samples are consistent with proglacial suspended sediment samples from Glacier de Tsidjiore Nouve (Fenn and Gomez, 1989) and subglacial sediments from Haut Glacier d'Arolla (Lamb, 1995). There were no discernible changes in the ashed sediment, with grains and adhering microparticles maintaining a freshly ground appearance (Figure 2.7, F–H).

Six subsamples of the normal and ashed composite sediment samples were also analysed using a Coulter LS230 particle size analyser with a sizing range of 0.04–2000 μm (for further details see Chapter 5). Size frequency distributions of one standard deviation about the mean of the six ashed and six normal samples are shown in Figure 2.8. Samples were dispersed using only water prior to analysis. The results demonstrate a consistently lower proportion of particles between 1 and 20 μm in the ashed samples and a generally higher proportion of particles larger than 200 μm. Care was taken to accurately subsample the normal and ashed composite samples using a riffle box and such consistent variation is unlikely to be due to the subsampling technique. The ashed sediment may have contained less moisture (it was noticeably freer-flowing) so that finer sediments were able to escape on air currents during the subsampling process. However, it is more likely that treatment at high temperature resulted in minor physical changes which bonded small particles to larger grains, requiring stronger methods of dispersal prior to particle size analysis (see Section 5).

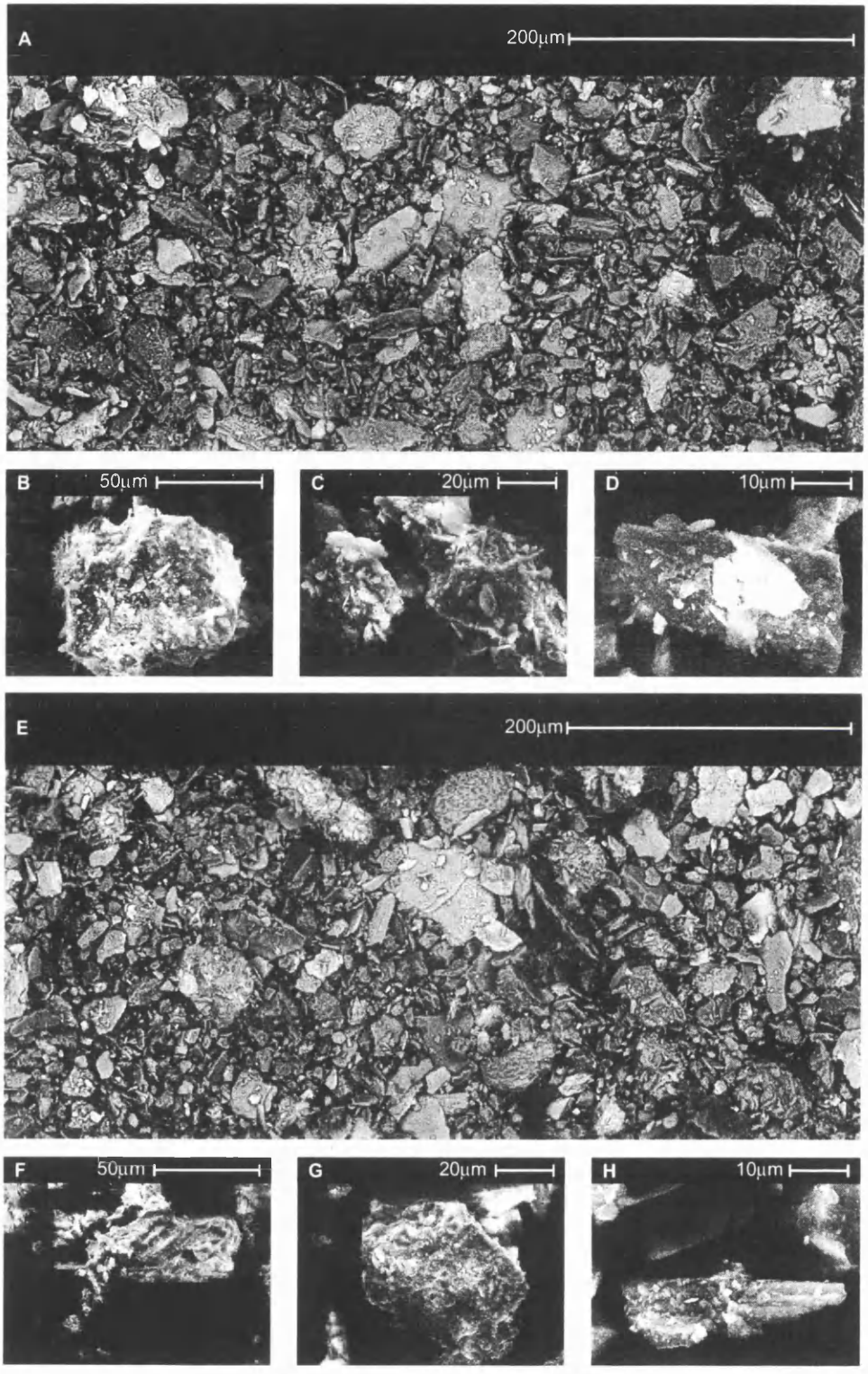

Figure 2.7 SEM images of normal proglacial sediment samples (A–D) and ashed proglacial sediment samples (E–H). Images C and H clearly show the presence of microparticles adhering to larger grains. Scale varies in each image.

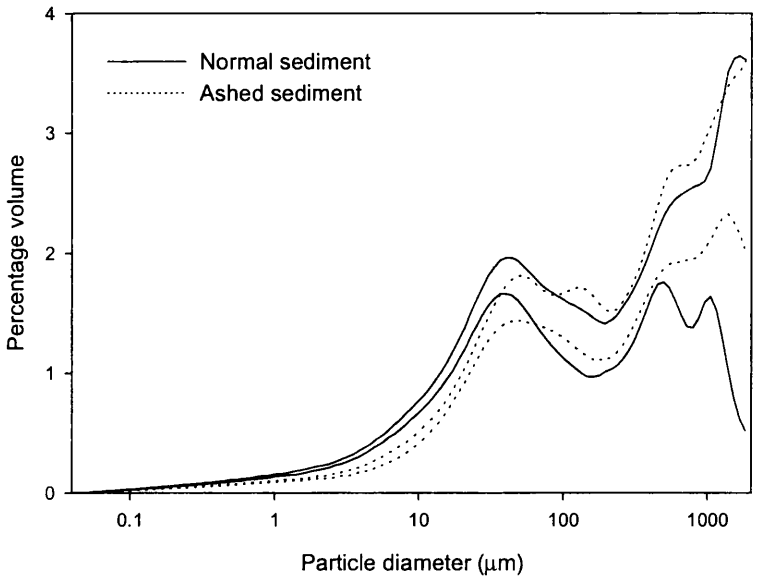

Figure 2.8 Size distributions of one standard deviation about the mean of six ashed and six normal composite proglacial sediment samples from Haut Glacier d'Arolla.

2.3.1.2 Stream turbidity

Output from the turbidity sensors is in the form of a voltage proportional to the level of suspended sediment. Raw sensor output for each of the melt seasons was plotted and carefully checked to remove periods of erroneous data. Data from during relocation or adjustment to the gauging station was removed. Sensors typically showed a high degree of covariance; hence further periods of data could be identified where the turbidity records departed significantly from one another. Such departures normally occurred when one sensor had become blocked by saltating debris, causing the sensor to 'sit' at maximum turbidity until the debris was removed, and could also be identified during periods when only a single sensor was operational. During 1998, the two records also show low levels of incoherent variation on JD 144 at 17:00–18:00 that is attributed to collapse of a snow bridge just upstream of the gauging station. However, this event was not observed, and snow and ice blocks observed to be caught in the gauging station on other occasions were never found to have noticeably influenced turbidity measurements.

The output ranges of individual sensors must be standardised before further analysis, typically by reporting the output as a percentage of the measured operating range. For

each sensor, the operating range was determined using minimum and maximum values from field data. During 1998, minimum values for sensor T2 occurred late in the season for short periods of time when the sensor was believed to have been above the level of the flow. Therefore, minimum output from sensors T1 and T2 was determined early in the season when proglacial stream waters were often visibly clear of suspended material. Subtle changes in the relationship of the output between the two sensors meant that minimum output was recorded on different days for each sensor. For sensor T2, values below the minimum deflection determined for water (indicating that the sensor was above the level of flow) were removed. Full-scale deflection was periodically reached for both sensors during the monitored period and therefore the maximum output could also be determined.

The 1999 field data were used to standardise the output range for sensor T3 and check the output range for sensor T2. The maximum output for T2 was identical to its value in 1998, although the minimum-recorded value (or offset) was somewhat higher. This was attributed to roughening of the sensor heads due to abrasion, which artificially scatters light from the sensor and influences the measurement of suspended sediment. Since the sensor had not been used between field seasons at Haut Glacier d'Arolla, the change in offset was determined to be 0.7 % of the operating range over ~ 75 days deployed in the proglacial stream. Changes in the operating range due to abrasion of the sensor heads were therefore small and have little influence on turbidity measurements, although it is recommended that the sensor range be standardised during each season.

Following removal of periods of unrepresentative data and standardisation of the operating range, the paired turbidity records in both seasons demonstrated a high degree of correlation (r = 0.994, n = 11382 and r = 0.989, n = 7376 for 1998 and 1999, respectively). The mean of the two records for each season was therefore used for further analysis. The resulting turbidity records from 1998 and 1999 had 7.2 % and 26 % of values missing, respectively.

Turbidity records for the monitored periods were calibrated using known suspended sediment concentrations obtained from automated sampling (above). Plots of standardised turbidity versus suspended sediment concentration deviate from log-

linearity due to saturation of the turbidity sensors at high suspended sediment concentrations. Stepwise regression techniques on log-transformed variables were used to identify relationships between the two series that provided a good statistical and visual fit to the measured data. For the 1998 data, a fourth-order polynomial of the form

$$\log_{10} SSC = -0.918 + 0.0717 \log_{10} T^2 + 0.279 \log T + 0.00662 \log_{10} T^6 + 0.000305 \log_{10} T^9 \quad (2.1)$$

was fitted to 1106 simultaneous measurements of turbidity (T) and suspended sediment concentration (SSC), where $r^2 = 0.702$ and p for all predictors ≤ 0.001. For 1999, a good fit was obtained for 200 simultaneous measurements of T and SSC from a second-order polynomial of the form

$$\log_{10} SSC = -1.06 + 0.704 \log_{10} T + 0.000213 \log_{10} T^{10} \quad (2.2)$$

for which $r^2 = 0.896$ and p for both predictors was ≤ 0.005. Calibration relationships are commonly defined using log-transformed variables; however Ferguson (1986; 1987) has noted that such techniques will result in the systematic underestimation of actual suspended sediment concentration when predicted logarithmic values are transformed back into standard arithmetic units. For the regression models derived above, the standard deviation of the residuals about the regression line indicate that calibrated values will be only ~ 80 % and 95 % of actual suspended sediment concentrations during 1998 and 1999, respectively (Ferguson, 1987; his Equation 10). Such underestimation cannot be readily corrected where the rating plot deviates significantly from log-linearity.

2.3.1.3 Electrical conductivity

Electrical conductivity records from 1998 and 1999 were checked against field notes to remove periods of unrepresentative data, commonly resulting from blockage of the sensor tube and relocation or adjustment to the gauging station. For the remainder of the monitored periods, the reliability of the records was more difficult to ascertain since no comparative measurements were obtained. Neither are the records calibrated; however,

relative variations in electrical conductivity throughout the monitored periods are likely to be sufficient to provide a qualitative interpretation of temporal changes in the sources and routing of meltwater.

2.3.2 Representivity and reliability of the stream monitoring programme

This section considers the representivity and reliability of measurements of suspended sediment concentration and quality obtained during the 1998 and 1999 melt seasons. Monitoring was conducted using automated equipment at a fixed location near to the glacier snout (Section 2.2.3). With regards to programme representivity, the turbidity series was calibrated in Section 2.3.1.2 using contemporaneous measurements of suspended sediment concentration that should provide the most reliable means of calibration (Gippel, 1989); whilst r for paired turbidity records from individual sensors was found to be ~ 0.99 for both melt seasons. However, samples obtained automatically must be checked for representivity using standard sampling equipment, such as the USDH48, and the effectiveness of the chosen filter papers requires investigation. Consequently, this section presents: 1) the representivity of automatically collected samples compared with width and depth integrated samples obtained using the USDH48; and 2) the proportion of sediment lost using 2.7 μm papers.

With regards to the reliability of at-a-point measurements, Section 2.2.2.1 identified three main issues: 1) the extent to which measurements are representative of mean suspended sediment characteristics across the stream cross section; 2) whether they are representative of suspended sediment characteristics up and downstream of that location; and 3) the frequency of sampling. Most studies suggest that suspended sediment is well-mixed across the stream section (e.g. Gurnell et al., 1992); however, few studies have analysed cross-stream variations in sediment quality. The extent to which suspended sediment characteristics vary with distance from the glacier is also poorly understood; suspended sediment concentration is commonly observed to show very different trends with distance downstream from different glaciers (e.g. Boothroyd and Ashley, 1975; Gurnell, 1982). The frequency of measurements for suspended sediment concentration has also been investigated, but again information on suspended

Table 2.7 Regression relationships between log-transformed suspended sediment concentration from the ISCO and USDH48 ($p \leq 0.001$ for all a and b coefficients).

Year	a	b	t_a	t_b	SE_a	SE_b	r^2
1998	0.142	0.869	5.09	21.16	0.028	0.041	0.897
1999	0.120	1.013	3.82	21.33	0.032	0.048	0.950

a, b: regression intercept and slope, respectively; t_a, t_b: t-statistics associated with the regression intercept and slope; SE_a, SE_b: standard error of the intercept and slope coefficients.

sediment quality is lacking. However, it would seem that hourly measurements are appropriate since the mechanisms that control suspended sediment evacuation likely operate at diurnal scales. As a result, the following reliability issues were also investigated due to a lack of current knowledge: 1) the extent to which suspended sediment concentration varies with distance from the glacier; and 2) the extent to which suspended sediment particle size varies across the stream section.

2.3.2.1 Representivity of automatically collected samples

Daily USDH48 samples were obtained during both field seasons in order to evaluate the representivity of automated sampling for obtaining measurements of both suspended sediment concentration and quality (Sections 2.2.3.1 and 2.2.3.2). Relationships between suspended sediment concentration from the ISCO samples versus samples collected contemporaneously using the USDH48 show generally good relationships with high r^2 values (Table 2.7; Figure 2.9). Slightly higher scatter is seen in the relationship for the longer 1998 melt season than during 1999. The intercepts for both relationships are significantly different from zero at the 95 % confidence level, and suggests that the ISCO underestimates suspended sediment concentration with respect to the USDH48. However, the slope of the relationship during 1998 is also significantly different from 1 and demonstrates that underestimation by the ISCO is progressively lower at higher suspended sediment concentrations (Table 2.7; Figure 2.9). During 1999, the slope of the relationship is not significantly different from 1.

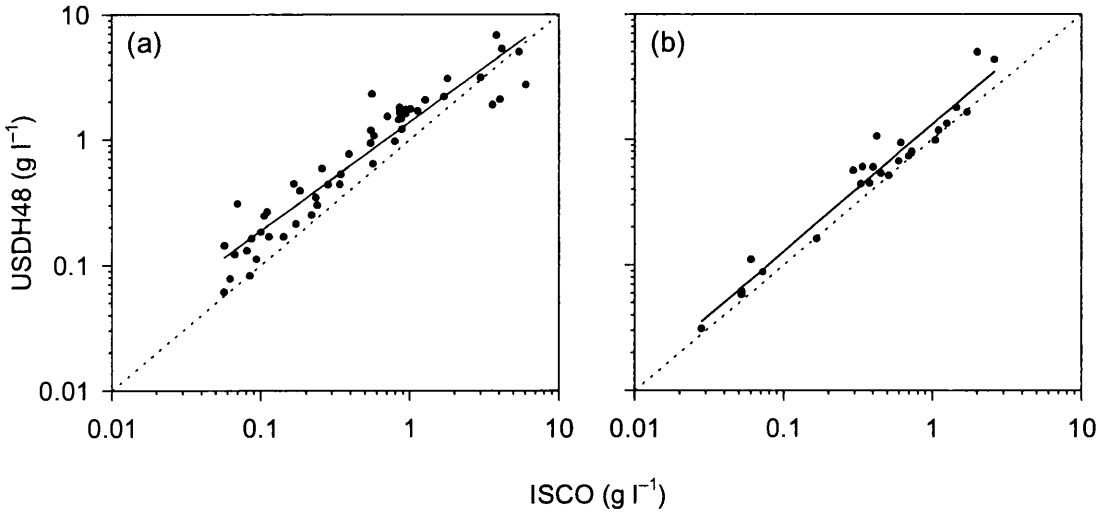

Figure 2.9 Relationships between log-transformed suspended sediment concentration from the ISCO and USDH48 (see Table 2.7).

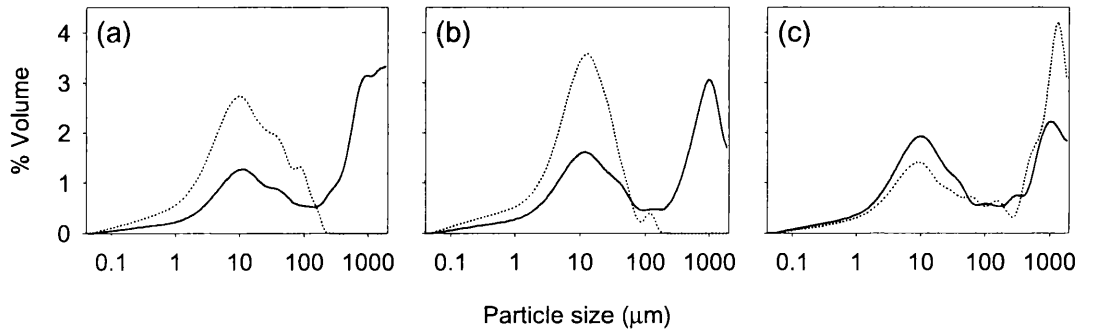

Figure 2.10 Size distributions for ISCO (solid lines) and USDH48 (dotted lines) samples obtained at (a) 15:00 JD 171, (b) 12:00 JD 187, (c) 18:00 JD 199.

Gurnell et al. (1992b) obtained an unbiased relationship between suspended sediment concentration determined by automatic sampling and a USDH48 at Haut Glacier d'Arolla. However, the USDH48 was simply allowed to fill next to the ISCO intake hose rather than providing a width and depth integrated sample. Fenn and Gomez (1989) suggested that a pump sampler used at Glacier de Tsidjiore Nouve was less effective at sampling coarser particles on account of USDH48 samples being slight coarser (~ 2 μm in the case of the median particle size). Particle size distributions for 11 USDH48 samples collected during 1998 were compared with contemporaneous ISCO samples to see if the underestimation of suspended sediment concentration was associated with a

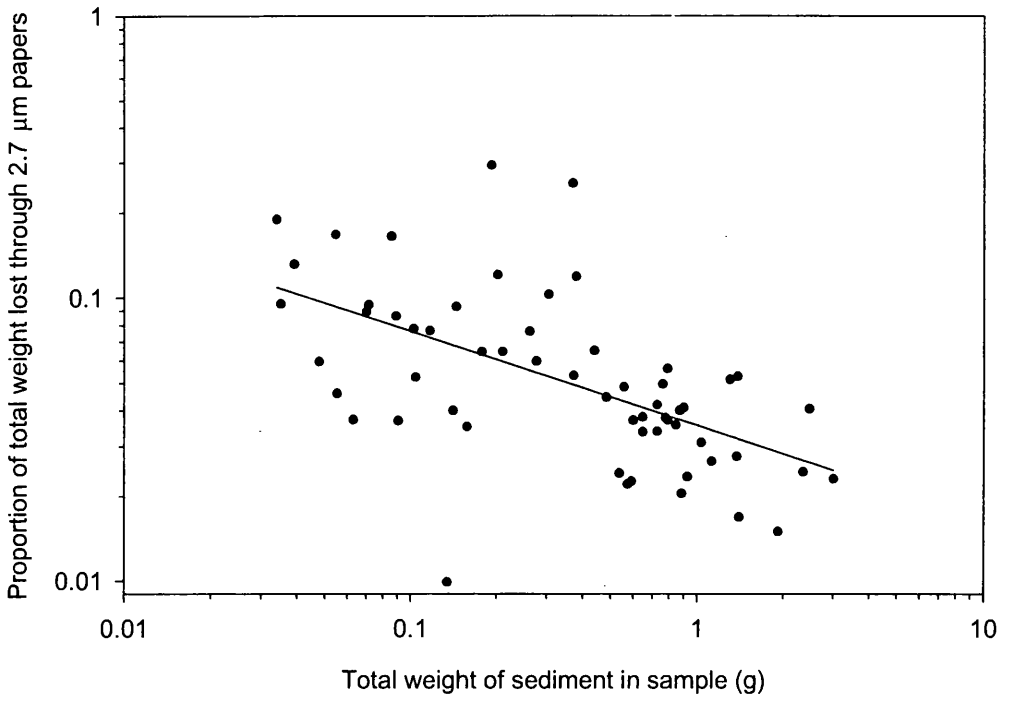

Figure 2.11 Proportion of sediment lost through the 2.7 µm papers by total sample weight. Line of best fit also shown.

difference in size distribution. In 10 samples, the USDH48 had sampled significantly more coarse sediment than the ISCO (Figure 2.10 a and b). The USDH48 is more likely to sample coarser particles if width and depth integrations are made that involve sampling from very close to the bed. Only in one sample was the ISCO observed to have sampled a greater proportion of coarse material than the USDH48 (Figure 2.10 c).

2.3.2.2 Proportion of sediment lost during filtering

Daily USDH48 samples were re-filtered through pre-weighed Whatman 0.1 µm cellulose nitrate papers in order to assess the proportion of sediment lost during filtering with large diameter 2.7 µm papers (see Sections 2.2.3.1 and 2.2.3.2). The 0.1 µm papers were dried in the lab and re-weighed, and the proportion of sediment lost through the 2.7 µm papers plotted against the total weight of sediment from both papers (Figure 2.11). A large proportion of sediment (~ 10 %) was lost through the 2.7 µm papers for samples of ~ 0.04 g; however, the proportion lost rapidly declined with increasing sample weight, such that less than 5 % was lost for samples greater than 0.5 g. Gurnell et al. (1992)

observed a similar pattern at Haut Glacier d'Arolla where samples were filtered through 8 μm papers and re-filtered at 0.45 μm (Section 2.2.2.2). Sample loss probably declined because sediment particles rapidly clogs pore spaces in the paper. Higher initial sample loss than that found by Gurnell et al. (1992b) likely results from the larger diameter of the papers, which resulted in a less rapid clogging of the pores.

2.3.2.3 Downstream variation in suspended sediment concentration

Downstream variation in suspended sediment concentration was investigated by comparing turbidity measured at distances of 50, 100, 150 and 200 m from that measured at a fixed gauging station very near the glacier snout (~ 20 m). The investigation was undertaken during 1998 on JD 225 in a single, unmixed reach of the western proglacial stream and at low suspended sediment concentrations to avoid problems due to turbidity sensor saturation. Dye tracing was used to determine the travel time of water and sediment from the gauging station to the downstream sensor to enable accurate comparison between the two records. Output from the downstream turbidity sensor (T3, see Section 2.3.1.2) was calibrated with that from the fixed turbidity sensor (T2); calibration was established from turbidity sensor output on JD 216–217 when the sensors were located ~ 1 m apart in the stream cross-section at the gauging station (r^2 = 0.995). The seasonal calibration relationship established for T1 and T2 from measured suspended sediment concentration during 1998 (Equation 2.1; Section 2.3.1.2) was applied to both sensors to convert the output to g l^{-1}.

Figure 2.12 shows the gauging station turbidity record and lagged downstream record for the four downstream sites. The results suggest that suspended sediment concentration declines with distance downstream despite mean flow velocities generally increasing. However, changes in concentration appear to be relatively small up to ~ 100 m downstream of the gauging station within which the stream occupied a single confined channel. Further downstream the channel began to braid, suggesting the potential for sediment deposition due to exchanges of discharge between different threads of flow. Importantly, however, short-term changes in suspended sediment concentration occur even 50 m downstream of the gauging station that are not reflected in the upstream suspended sediment concentration record. Differences between the records become more

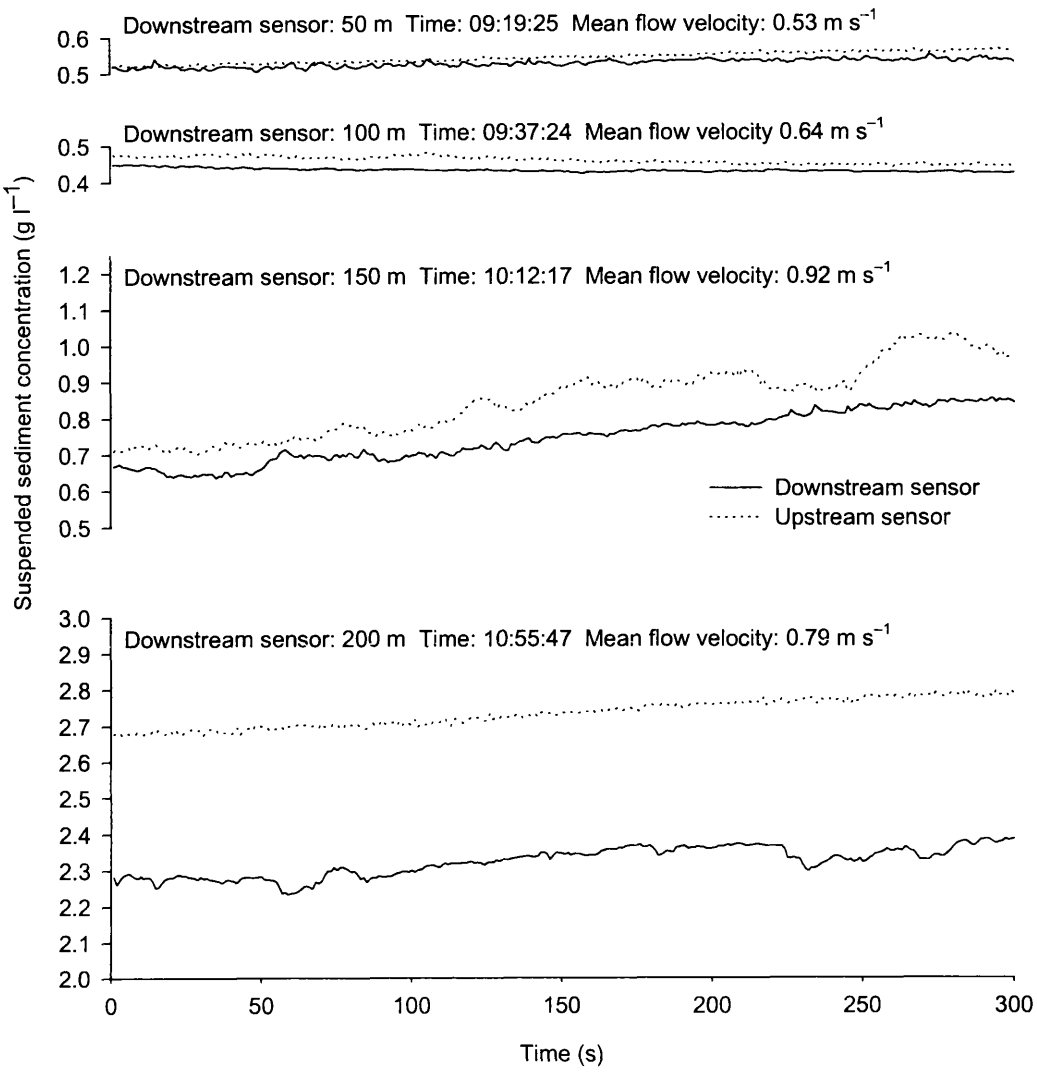

Figure 2.12 Suspended sediment concentration at progressive distances downstream from the gauging station on JD 225 1998.

exaggerated with distance downstream, suggesting there may be complex influences on long and short-term suspended sediment transport in the proglacial area.

2.3.2.4 Cross-stream variation in suspended sediment particle size

Cross-stream variation in suspended sediment particle size was investigated within a well-mixed distributary of the proglacial stream ~ 1 km from the glacier snout. Variation was investigated over two cross-sections roughly 3 m apart by collecting water samples at regular distances across the channel using a wide-necked 0.5 l polypropylene bottle.

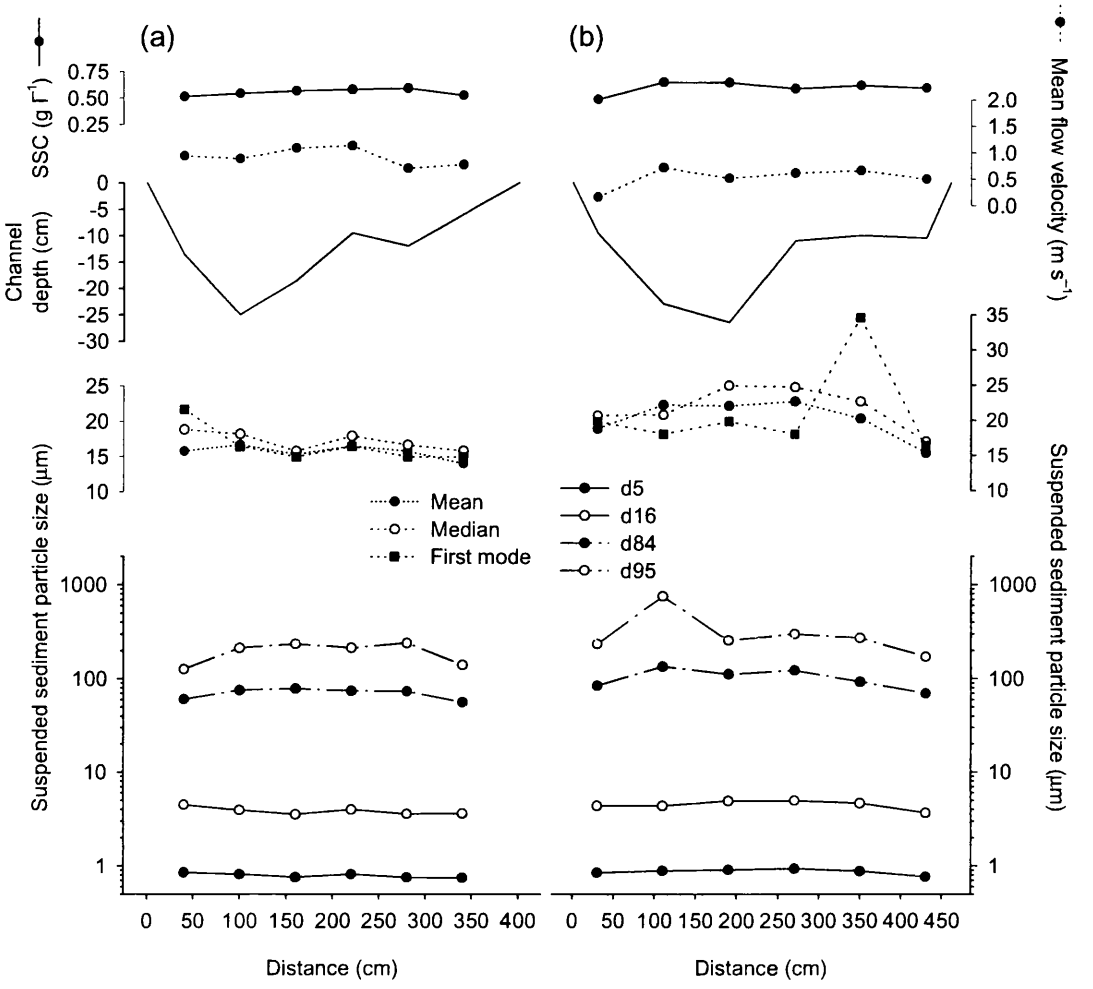

Figure 2.13 Cross-stream variation in suspended sediment concentration, mean flow velocity, channel profile and suspended sediment particle size parameters at two locations in a distributary of the main proglacial stream.

Samples were collected by lowering the bottle to a fixed distance (~ 5 cm) above the bed and opening the neck of the bottle for just enough time for the bottle to fill. Measurements of stream depth were obtained at each sampling location; mean flow velocity was calculated from a depth-integrated velocity record obtained using a current meter both before and after the collection of each sample. Samples were filtered through 2.7 µm papers and returned to the laboratory where suspended sediment concentration and particle size were determined.

Figure 2.13 shows the results from the upstream (a) and downstream (b) cross-sections. Suspended sediment concentration generally shows no systematic variation with flow

velocity or channel depth within and between cross-sections, although there is a tendency for concentration to be slightly lower near to the channel banks (cf. Gurnell et al., 1992b). Moment statistics demonstrate that particle size is also independent of flow velocity between cross-sections, with coarser distributions at the downstream cross-section where flow velocities are generally lower. Nevertheless, the proportion of coarse material in transport within each cross-section (as indicated by d_{84} and d_{95}) tends to increase away from the channel banks; the proportion of fines (as indicated by d_5 and d_{16}) appears to remain relatively stable. Variation in mean and median size distribution is also considerable at the downstream cross-section; however, distributions were polymodal and these parameters may be greatly affected by small changes in the number of just a few coarse particles (cf. Sambrook Smith et al., 1997). The first mode appears to be the most consistent size parameter (and has also been suggested to be the most reliable; see Chapter 5); however, occasionally much coarser first modes occur that most likely reflect natural time-dependent variations in suspended sediment size distribution.

2.3.2.5 Conclusion

Investigation of the cross-stream variability in suspended sediment concentration and particle size (above) suggests that in general sediment is well mixed across the flow. Relatively poor relationships between suspended sediment concentration and particle size from the ISCO with respect to the USDH48 probably result from the difficulty of using the USDH48 to obtain truly representative width and depth integrated samples in fast flowing proglacial streams. In general, a sampling position located as near to the glacier snout as possible and away from the channel banks will likely to result in unbiased estimates of suspended sediment character.

3.

Meteorological, glacier-hydrological and glacial dynamics

3.1 INTRODUCTION

This chapter uses meteorological, glacier-hydrological and ice motion data to investigate glacial and fluvioglacial dynamics during the 1998 and 1999 melt seasons. Previous investigations of suspended sediment transport in proglacial streams have generally suggested that sediment evacuation is largely dependent upon the increased availability of meltwater during the melt season (Section 1.2). Emphasis has also been placed on the importance of drainage system instabilities in controlling basal sediment evacuation at sub-seasonal scales that contribute to overall seasonal and annual variability. However, it was suggested in Section 1.3 that previous studies had failed to reliably link sediment transport to subglacial processes because independent measurements of the dynamic nature of the glacial and fluvioglacial systems had not been obtained. Section 1.4 considered the likely importance of drainage system configuration and its temporal and spatial evolution in controlling access to basal sediments and determining sediment transport capacity, as well as the potential importance of ice dynamics. It is against a background of detailed knowledge of the seasonal spatial and temporal evolution of the glacier drainage system and ice dynamics that variation in suspended sediment characteristics must be interpreted if the mechanisms of suspended sediment evacuation by subglacial meltwaters are to be rigorously identified.

3.2 METEOROLOGICAL INPUTS AND PROGLACIAL STREAMFLOW

3.2.1 Introduction

In this section, lags between meteorological inputs and proglacial streamflow are used to infer changes in the sources and routing of meltwater through the glacier system during the 1998 and 1999 melt seasons. Proglacial hydrograph form has the potential to provide important information about the general movement of meltwater through the glacier system (cf. Meier and Tangborn, 1961; Matthews, 1963; Elliston, 1973). Hydrograph form is a product of both spatial and temporal variation in the climatic processes and glacier surface characteristics (e.g. albedo) that generate surface melt and the routing of meltwater through the supraglacial, englacial and subglacial drainage systems. Hence, proglacial streamflow has been related directly to meteorological variables thought to control surface melting in order to investigate the physical mechanisms that control the flow of meltwater through the glacier drainage system (e.g. Gurnell et al., 1991).

The sources and routing of meltwater evolve systematically during the melt season (Röthlisberger and Lang, 1987; Gurnell, 1995; Nienow et al., 1998). Many researchers have subdivided proglacial streamflow records in order to investigate changing relationships between periods when the hydrological system is assumed to be relatively stable (e.g. Stenborg, 1970; Elliston, 1973; Lang, 1973; Gurnell et. al, 1991). At Haut Glacier d'Arolla, Gurnell et al. (1991) divided the melt season into five 'hydrologically meaningful' sub-periods identified from trends in diurnal minimum and maximum discharges. Systematic changes in the relationships between meteorological, proglacial streamflow and water quality series were identified between sub-periods that reflected the evolution of melt sources from snowmelt to predominantly icemelt and the development of a hydraulically efficient, channelised subglacial drainage system.

3.2.2 Meteorological and streamflow variables

Figures 3.1 and 3.2 show meteorological and proglacial streamflow time series for the monitored periods of the 1998 and 1999 melt seasons, respectively. Air temperature, incident radiation and catchment discharge are shown as hourly mean values;

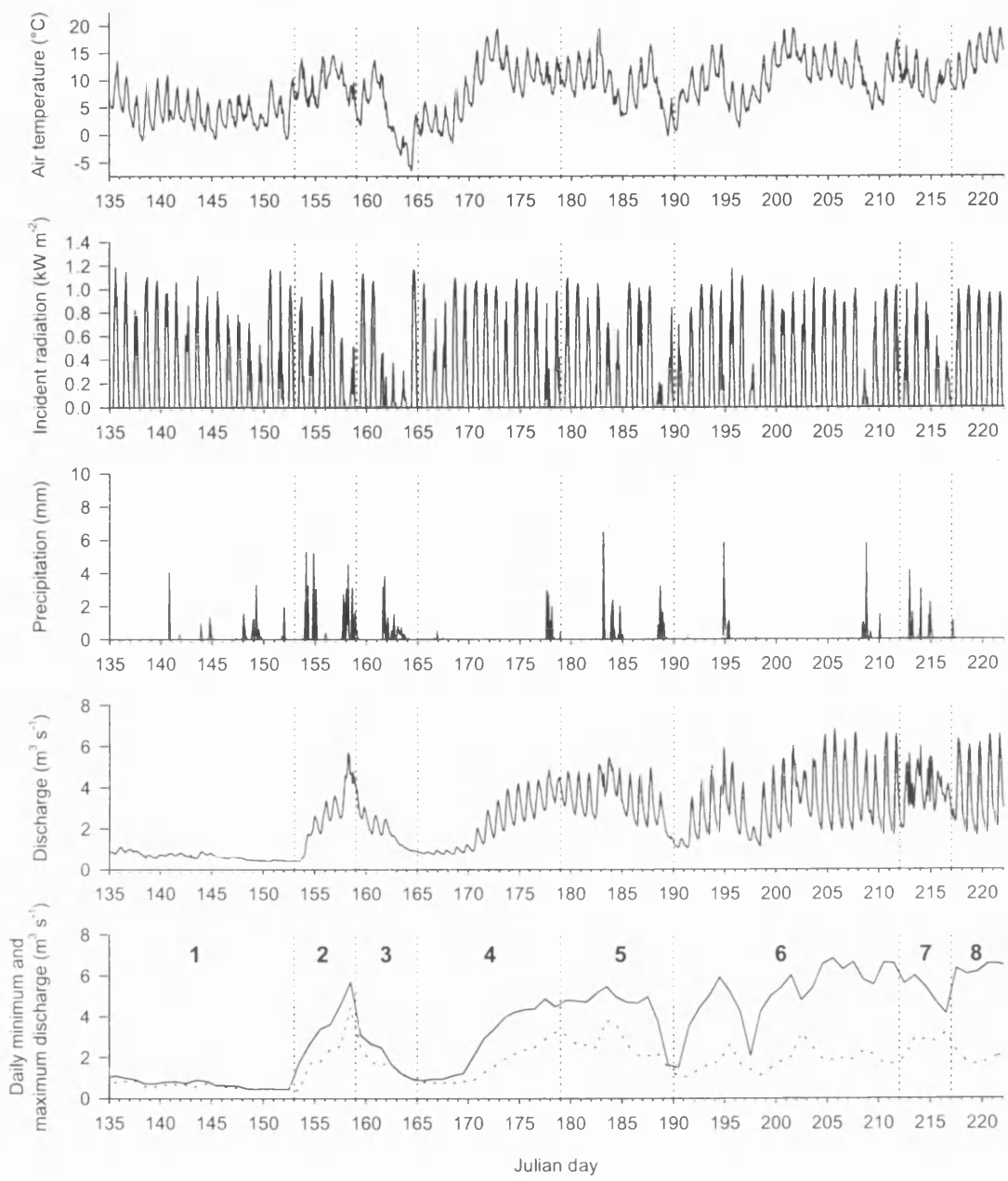

Figure 3.1 Meteorological and streamflow variables for the monitored period during 1998. Sub-periods 1–8 have been defined using trends in diurnal minimum and maximum discharge and are described in Table 3.1.

precipitation values are hourly totals. Meteorological data for 1998 was obtained from the Bricola meteorological station some 8km NNE of Haut Glacier d'Arolla. The timing and magnitude of precipitation events, the occurrence of frosts and periods of low incident radiation associated with cloud cover agreed well with field notes. The time

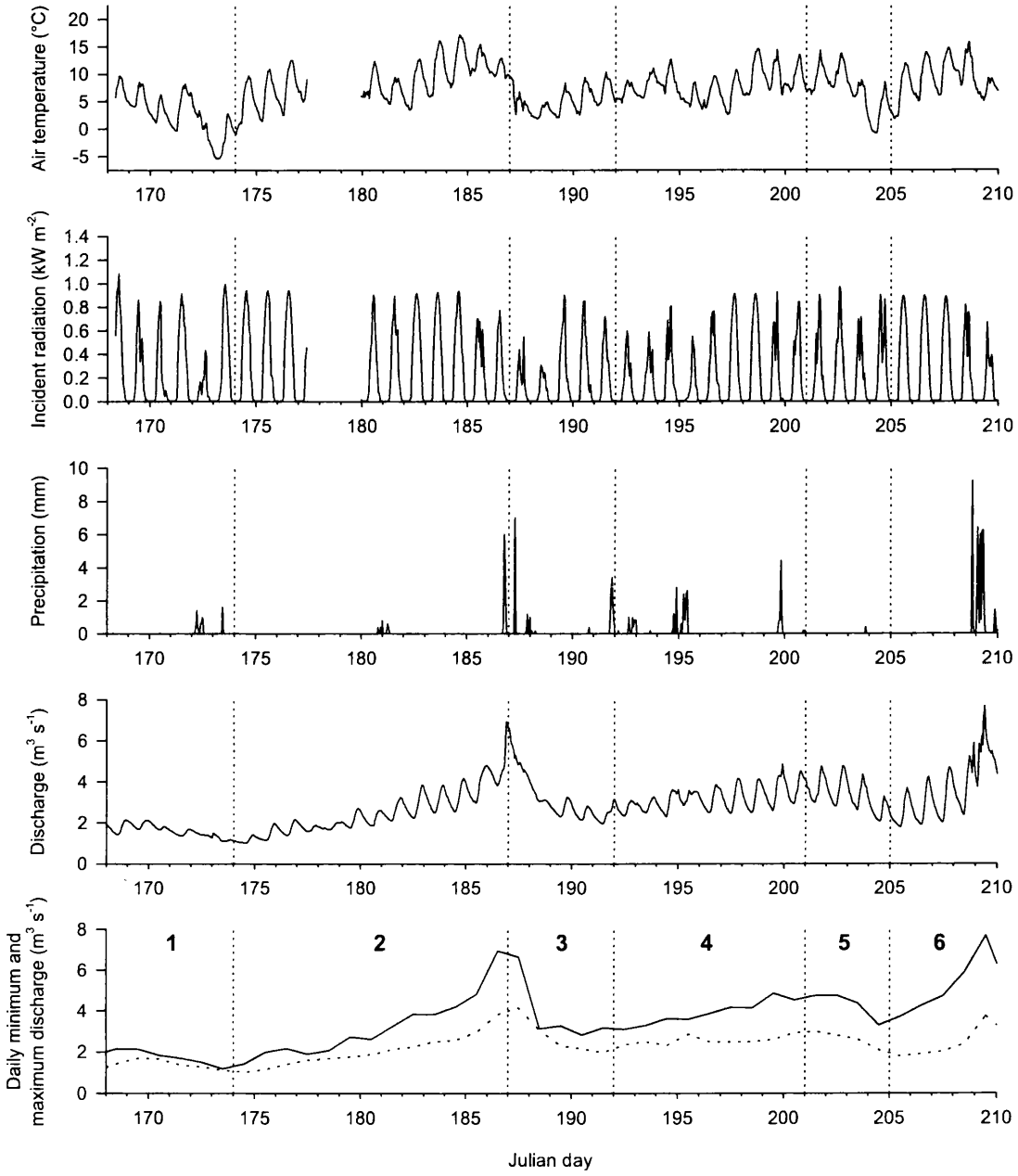

Figure 3.2 Meteorological and streamflow variables for the monitored period during 1999. Sub-periods 1–6 have been defined using trends diurnal minimum and maximum discharge and are described in Table 3.2.

series are complete with the exception of a short break in the meteorological series from JD 177–180 during 1999. Figures 3.1 and 3.2 also show various sub-periods of each melt season for which relationships between meteorological inputs and proglacial streamflow are investigated below.

Table 3.1 Sub-periods of the melt season for the monitored period during 1998.

Sub-period 1, JD 135–152 (mid to late May)
Low mean air temperatures; precipitation falls predominantly as snow; low mean discharge with weak, low-amplitude diurnal variation
Sub-period 2, JD 153–158 (early June)
Rising mean air temperatures; precipitation falls as rain; rising mean discharge with increasing baseflow and diurnal amplitude
Sub-period 3, JD 159–164 (early to mid-June)
Declining mean air temperatures; precipitation falls initially as rain (JD 161), turning to snow (JD 162–163); declining mean discharge, baseflow and amplitude
Sub-period 4, JD 165–178 (mid to late June)
Rising mean air temperatures; snow (JD 166), rain (JD 177–178); rising mean discharge, amplitude increases rapidly JD 170–172, increasing baseflow
Sub-period 5, JD 179–189 (late June to early July)
Stable mean air temperatures except during rainfall (JD 183–184); stable mean discharge but increasing diurnal amplitude due to declining baseflow; end of period: rain (JD 188) turns to snow (early JD 189); mean air temperatures rapidly decline
Sub-period 6, JD 190–211 (early to late July)
High mean air temperatures following JD 190 except JD 195–200 and 209–210; rainfall JD 194-195 and 208–209, light rain JD 194 and 197; mean discharge generally high with high diurnal amplitude
Sub-period 7, JD 212–216 (late July to early August)
High mean air temperatures; overcast, strong föhn; persistent drizzle/light rain, heavy rain during late afternoon/evenings; high mean discharge due to high baseflow; however, low amplitude, diurnal discharge pattern heavily modified by precipitation
Sub-period 8, JD 217–221 (early August)
High mean air temperatures; cloudless following light rain early JD 217; high mean discharge with low baseflow and high diurnal amplitude

3.2.3 Temporal patterns between meteorological and streamflow variables

Monitored periods of the 1998 and 1999 melt seasons were subdivided into 'hydrologically meaningful' sub-periods based on trends in the discharge series identified from daily minimum and maximum discharge (Figures 3.1 and 3.2; cf. Gurnell et al., 1991) and summarised in Tables 3.1 and 3.2.

Table 3.2 Phases of the melt season for the monitored period during 1999.

Sub-period 1, JD 168–173 (mid-June)
Low mean air temperatures; precipitation falls predominantly as snow; low discharge mean and weak, low-amplitude diurnal variation
Sub-period 2, JD 174–186 (mid-June to early July)
Rising mean air temperatures; light rain JD 180–181, strong föhn JD 184–186 and heavy rainfall JD 186; increasing discharge mean, baseflow and diurnal amplitude
Sub-period 3, JD 187–191 (early July)
Declining mean air temperatures; heavy rainfall early JD 187, light rain JD 187–188; declining discharge mean, low-amplitude diurnal variation
Sub-period 4, JD 192–200 (early to mid-July)
Rising mean air temperatures; precipitation falls as rain, light föhn JD 192–199; rising discharge mean and increasing diurnal amplitude
Sub-period 5, JD 201–204 (mid-July)
Initially stable mean air temperatures; no significant precipitation; stable discharge mean but increasing amplitude due to falling baseflow; end of period: declining mean air temperatures followed by frost JD 203–204; declining discharge mean and amplitude
Sub-period 6, JD 205–209 (mid to late July)
Rising mean air temperatures; rising discharge mean, amplitude and baseflow; end of period: heavy rainfall JD 208–209 resulting in significant modification to discharge pattern

During 1998, eight hydrologically distinct sub-periods have been identified. Within individual sub-periods, meteorological and proglacial streamflow variables commonly exhibit consistent trends. Notably, trends in the discharge series correspond to those of the air temperature series and, to a lesser extent, incident radiation values (Figure 3.1; Table 3.1). The influence of precipitation, either as rain or snowfall, is also apparent during a number of periods: in sub-period 2, discharge rises abruptly due to heavy rainfall despite only moderate air temperatures and incident radiation values (Figure 3.1); however, in sub-period 7, moderate rainfall mainly in the late afternoon and evenings maintains high mean discharge but with lower amplitude diurnal variation. Correspondence between meteorological variables should, of course, be expected: air temperatures are generally dependent upon incident radiation, and both these variables tend to decrease during periods of precipitation when there is significant cloud cover. In

sub-period 3, for example, proglacial discharge declines rapidly due to a combination of falling air temperatures, falling incident radiation and snowfall (Figure 3.1).

During the monitored period in 1999, six sub-periods were identified that demonstrate distinctive hydrological variation that is commonly consistent with meteorological variables (Figure 3.2; Table 3.2). Again, trends in the air temperature series are most closely associated with those of discharge for individual sub-periods. The influence of precipitation events is also apparent: heavy rainfall causes high peak discharges towards the end of sub-periods 2 and 6 despite low air temperature and incident radiation due to cloud cover (Figure 3.2).

Cross-correlation analysis was applied to pairs of meteorological variables and catchment discharge in order to identify changing lags and levels of correlation during each melt season (Table 3.3). Best-fit relationships were estimated for each subperiod by lagging the input series (incident radiation, air temperature and precipitation) against the output series (catchment discharge). Best-fit relationships were also estimated between the factors responsible for generating surface melt (incident radiation and air temperature). The response of air temperature to incident radiation is maintained at a relatively constant lag throughout each monitored period and levels of correlation are generally high (Table 3.3); however, discharge shows a changing response to incident radiation and air temperature as each melt season progresses (Figure 3.3).

During 1998, lags between discharge and incident radiation and air temperature are initially large but fall rapidly following sub-period 3 (Figure 3.3). Levels of correlation also vary, with predominantly higher values occurring later in the season (Table 3.3). In addition, there are differences in levels of correlation for functions estimated using the different meteorological input series. During sub-periods 1, 3, 4 and 5, correlations between discharge and air temperature are higher than for discharge and incident radiation (Table 3.3); however, this pattern is gradually reversed during sub-periods 6 to 8. Similar relationships between incident radiation, air temperature and discharge are evident during 1999 (Table 3.3; Figure 3.3); however, lags between these variables remain higher than for similar time periods during 1998 (Figure 3.3). With the exception

Table 3.3 Cross-correlation functions between pairs of meteorological variables and catchment discharge for phases of the 1998 and 1999 melt seasons.

1998 ablation season		Lag (h); r values in parenthesis			
Input series	Ouput series	Period 1	2	3	4
Incident radiation	Air temperature	+2 (0.790)	+1 (0.671)	+4 (0.420)	+2 (0.442)
Incident radiation	$\log_{10}$Discharge	+10 (0.248)	+11 (0.186)	+12 (0.521)	+6 (0.223)
Air temperature	$\log_{10}$Discharge	+8 (0.380)	+10 (0.187)	+7 (0.726)	+4 (0.797)
Precipitation	$\log_{10}$Discharge	NCD	+2 (0.198)	+2 (0.100)	+1 (0.188)
		5	6	7	8
Incident radiation	Air temperature	+2 (0.621)	+2 (0.539)	0 (0.643)	+2 (0.686)
Incident radiation	$\log_{10}$Discharge	+3 (0.506)	+3 (0.680)	+2 (0.446)	+2 (0.902)
Air temperature	$\log_{10}$Discharge	+2 (0.659)	+1 (0.680)	+4 (0.159)	0 (0.673)
Precipitation	$\log_{10}$Discharge	0 (0.174)	+1 (0.146)	0 (0.378)	NSP
1999 ablation season					
Input series	Ouput series	Period 1	2	3	4
Incident radiation	Air temperature	+2 (0.510)	+2 (0.636)	+2 (0.631)	+2 (0.751)
Incident radiation	$\log_{10}$Discharge	+13 (0.384)	+8 (0.234)	+7 (0.065)	+6 (0.736)
Air temperature	$\log_{10}$Discharge	+9 (0.849)	+6 (0.724)	+6 (0.116)	+4 (0.689)
Precipitation	$\log_{10}$Discharge	NCD	+2 (0.231)	NCD	+2 (0.118)
		5	6		
Incident radiation	Air temperature	+1 (0.487)	+2 (0.735)		
Incident radiation	$\log_{10}$Discharge	+6 (0.590)	+6 (0.389)		
Air temperature	$\log_{10}$Discharge	+3 (0.866)	+4 (0.453)		
Precipitation	$\log_{10}$Discharge	NSP	+2 (0.424)		

NCD: best-fit position not clearly defined; *NSP*: no significant precipitation during period

of sub-period 4, correlations between discharge and air temperature also remain higher than for incident radiation (Table 3.3).

The response of discharge to precipitation shows no significant variation throughout both monitored seasons (Table 3.3). Lags are typically small and suggest that discharge commonly responds faster to precipitation events than variations in incident radiation or air temperature; however, levels of correlation are low.

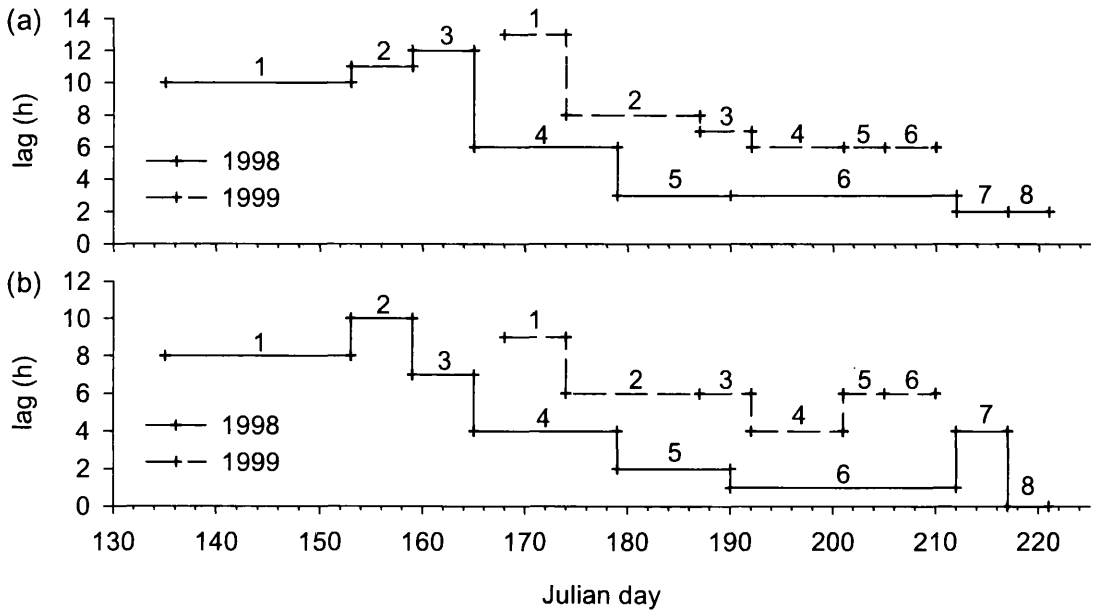

Figure 3.3 Seasonal variation in lags between (a) incident radiation and proglacial streamflow and (b) air temperature and streamflow during monitored periods of the 1998 and 1999 melt seasons (see Table 3.3).

3.2.4 Interpretation, discussion and conclusions

Lags between discharge and meteorological inputs decrease as the melt season progresses, reflecting increasing efficiency in both the translation of energy inputs into surface melt and the transfer of supraglacial runoff to the proglacial stream (Figure 3.3; Gurnell et al., 1991, 1992a). Initially during both seasons, the catchment is snow covered and lags between discharge and both incident radiation and air temperature are large (Table 3.3). Long residence times of meltwater in the catchment result from the slow percolation of surface runoff through the snowpack (Fountain, 1996) and, where melt occurs from snow overlying the glacier, flow through a distributed subglacial drainage system due to the closure of channelised drainage pathways over winter (Nienow et al., 1998). High-albedo snow reflects incident radiation and results in low levels of correlation between discharge and incident radiation. Instead, catchment runoff is more strongly related to air temperature, which is a better measure of advective warming of the supraglacial snowpack (Gurnell et al., 1991, 1992a).

During 1998, lags between discharge and meteorological variables begin to fall rapidly following sub-period 3, although correlations remain highest between discharge and air temperature until the beginning of sub-period 6, reflecting the predominance of runoff from snowmelt (Table 3.3; Figure 3.3). Reduced lags result from thinning of the supraglacial snowpack and its eventual removal, resulting in more efficient supraglacial drainage and the exposure of low-albedo glacier ice that is more susceptible than snow to melt induced by variation in incident radiation. The development of hydraulically efficient, channelised drainage due to the exposure of high albedo glacier ice (Nienow et al., 1998) will also cause lags to decline. By sub-period 8, the snowline had retreated to the upper accumulation area and low-albedo glacier ice was exposed across the majority of the glacier. Short lags and high correlations between discharge and incident radiation reflect the predominance of ice melt and the efficient translation of melt to the proglacial stream through a channelised subglacial drainage system.

During 1999, monitoring began much later in than during the 1998 melt season due to the delayed removal of snow from the glacier surface. Significant thinning of the snowpack had occurred before monitoring was initiated; however, lags between discharge and meteorological variables during sub-period 1 are comparable with sub-periods 1–3 in 1998 (Table 3.3; Figure 3.3). Lags decline following sub-period 1 (Figure 3.3), but remain in excess of those during 1998, suggesting the less efficient translation of surface energy inputs into melting and routing of meltwater through the glacier drainage system. Higher levels of correlation between discharge and air temperature than incident radiation towards the end of the monitored period (Table 3.3.) also suggest that a large proportion of runoff is still derived from snowmelt. Thus, the efficiency of the glacial drainage system during the monitored period in 1999 is unlikely to have reached that attained during 1998.

Precipitation has an interesting effect on relationships between discharge and meteorological variables during the 1998 melt season. Sub-period 2 experiences significant rainfall and levels of correlation between discharge and other meteorological variables are significantly reduced (Table 3.3). However, the lag of the best-fit position is unusually low and levels of correlation are little higher than for sub-periods 3 to 6. It is likely that low lags reflect rapid surface runoff from non-glaciated areas of the

catchment, and longer residence times of rainwater within the glacial system result in low levels of correlation between discharge and meteorological variables. A similar response to rainfall is evident in sub-period 7, where lags are even lower and levels of correlation between discharge and precipitation are slightly higher (Table 3.3). This pattern is presumably due to the increased efficiency of runoff in glaciated and non-glaciated areas due to the removal of the catchment snowcover and more rapid routing of meltwater through the glacial system.

Precipitation events do not occur with the same frequency and magnitude during 1999 as during 1998, and no sub-periods are rainfall dominated (Table 3.2). However, as with 1998, best-fit positions between discharge and precipitation remain relatively low throughout the season and the highest levels of correlation occur towards the end of the monitored period, indicating the increasing efficiency of runoff as the catchment snowcover is removed (Table 3.3).

3.3 EVOLUTION OF PROGLACIAL HYDROGRAPH FORM

3.3.1 Introduction

This section uses statistical analysis to classify diurnal hydrograph form in a way that can be used as a proxy for the evolution of the sources and routing of meltwater throughout the melt season. In Section 3.2, cross-correlation functions were estimated between proglacial streamflow and meteorological variables for sub-periods of each melt season in order to isolate the physical mechanisms that control glacier runoff. However, there is more information within the proglacial streamflow record than can be obtained using simple cross-correlation analysis. Proglacial streamflow time series typically consist of marked diurnal variations superimposed on a slowly varying baseflow component (Paterson, 1994). The diurnal component represents rapidly routed melt from the ablation area; strongly peaked diurnal components, typical of peak melt season runoff, represent predominantly ice melt that reaches the glacier bed via moulins and a hydraulically efficient, channelised subglacial drainage system to the glacier snout. The baseflow component may represent: 1) melt from snow and firn that is delayed during

travel through the supraglacial snowpack; 2) long-residence time meltwater that has travelled through a distributed subglacial drainage system; 3) the release of meltwater from storage; or 4) groundwater. Recently, principal component and cluster analyses techniques have been utilised to investigate seasonal evolution in hydrograph form (Hannah et al., 1999, 2000). This section adapts the methodology introduced by Hannah et al. (1999) in order to investigate seasonal evolution of the sources and routing of meltwater routing at Haut Glacier d'Arolla during the 1998 and 1999 melt seasons.

3.3.2 Method

Classification of diurnal hydrograph form was achieved by Hannah et al. (1999, 2000) using a three-stage procedure that deals separately with hydrograph 'shape' and 'magnitude' before combining the two to provide a composite hydrograph-classification index. Using streamflow data from Haut Glacier d'Arolla during the 1989 melt season, Hannah et al. (2000) identified five hydrograph shape classes and three magnitude classes which, using a process of cross-tabulation, resulted in the identification of nine principal hydrograph types. Temporal sequencing of the hydrograph types was shown to aid investigation of the changing hydrological functioning of the glacier basin.

Hannah et al.'s (2000) methodology has been adapted to provide a simplified classification of hydrograph types that exhibit a measurable diurnal component. Such hydrographs provide a reliable source of information on the sources and routing of meltwater since their form represents: 1) the volume of meltwater derived from rapidly routed snow and ice melt in the ablation area and its proportion to other meltwater sources (indicated by the magnitude of the baseflow component); and 2) the rapidity with which icemelt is transmitted through the hydrological system. The methodology excludes days with significant rainfall input and/or inherited hydrograph characteristics (for example, large recession limbs) that alter the form of the diurnal component.

3.3.2.1 Classification of hydrograph shape

Hydrograph shape was classified using principal component analysis (PCA) and hierarchical cluster analysis (HCA). Prior to analysis, the streamflow data was separated into individual diurnal periods to form a matrix of N days (cases) by n discharge

measurements (variables). PCA was used to reduce the number of variables by extracting a smaller number of principal components (PCs) that represent a very large proportion of the variability of the original dataset. PCA 'plots' the original variables in multidimensional space and computes a linear function (the first PC) that captures the maximum possible variance of the original dataset. Consecutive PCs are computed to maximise the variance of the original dataset not captured by the previous component (hence consecutive PCs are uncorrelated). Variance maximising rotation (varimax) of the original variable space was used during PC extraction in order to maximise the variability captured by each PC whilst minimising the variance around it.

Plots of the PC *loadings* (the correlations between the variables and each PC) were used as the basis for interpreting each PC. In the case of hydrograph analysis, the loading plots can be used to identify the basic underlying variability of hydrograph shape. Cases (days) were then grouped using HCA into classes with similar hydrograph forms using their PC *scores* (the regression values of individual cases with each PC). HCA is an agglomerative cluster analysis method that starts with individual cases and, in very small steps, progressively lowers the threshold at which two or more cases are judged to be dissimilar. Cases with similar PC scores are progressively linked to form clusters of increasingly dissimilar cases until all the cases occupy a single cluster. The process is represented graphically as a vertical icicle or cluster plot; a cutoff point is selected at a distance along the vertical axis to retain a physically interpretable number of clusters.

Streamflow during successive melt seasons at the same catchment should be controlled by the same physical mechanisms and diurnal hydrographs should therefore exhibit the same underlying variability. Thus, streamflow data provided by Grande Dixence SA from the 1998 and 1999 melt seasons at Haut Glacier d'Arolla (Figure 3.4 a) were combined into a single matrix. The streamflow data were split into diurnal hydrographs consisting of 24 hourly discharge measurements from 07:00 each day (07:00 being the typical time of minimum discharge, although the time of minimum discharge was observed to evolve systematically during each melt season). To ensure that hydrographs were classified by shape alone, their magnitudes were standardised using z-scores prior to analysis. The resultant matrix consisted of 310 cases (diurnal periods) and 24 variables (hourly discharge values).

Analysis of PC eigenvalues was used to retain an appropriate number of PCs. The eigenvalue is the variance extracted by each PC, and a plot of the eigenvalues (the scree plot) shows a steeply decreasing trend for the first few PCs (Figure 3.4 b). According to Cattell (1966), the point at which the continuous drop in eigenvalues begins to level off suggests the cutoff, after which only random noise is being extracted by additional PCs. The scree plot suggests retention of three PCs, which cumulatively explain 91.4 % of the variance of the original dataset. The form of each case (i.e. hydrograph) is described by 3 PC scores obtained from the correlation of the case with each PC. The loadings plot for the three PCs (Figure 3.4 c) suggests the following physical interpretations: PC1 very late-peaked hydrograph component; PC2 peaked hydrograph component; PC3 late-peaked hydrograph component.

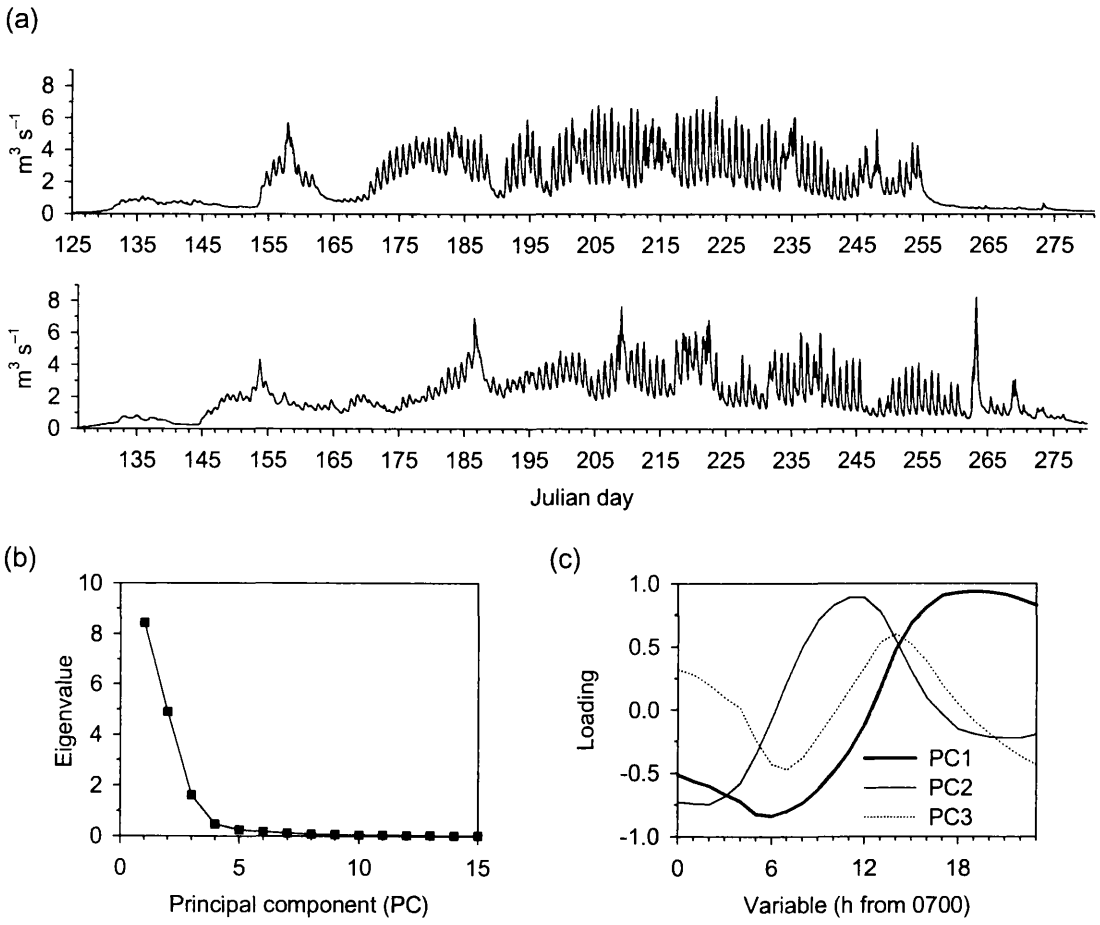

Figure 3.4 (a) catchment discharge during the 1998 and 1999 melt seasons. (b) scree plot of eigenvalues for extracted PCs and (c) loadings plot for PCs 1–3.

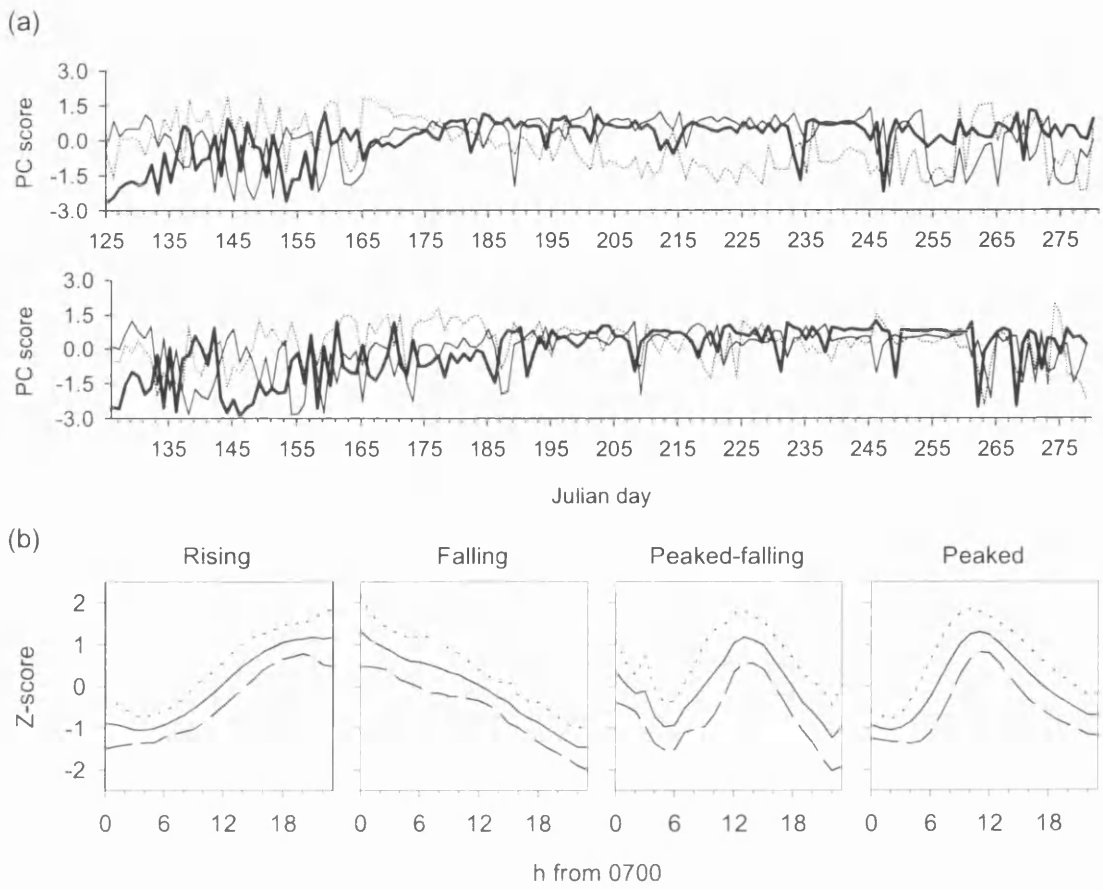

Figure 3.5 (a) PC scores during the 1998 and 1999 melt seasons for PCs 1–3 (see Figure 3.4 (c) for key to PCs). (b) Representative hydrograph shapes for the four clusters plotted using the mean z-score of each variable (hourly discharge measurement) for all cases in each cluster. Dashed lines show the standard deviation of each variable about the mean.

PC scores for cases during 1998 follow a distinctive pattern (Figure 3.5 a) that corresponds with trends in the discharge series identified in Section 3.2 (Figure 3.1 and Table 3.1). There is little consistency in PC scores during sub-periods 1–3. Following JD 165 (the beginning of sub-period 4), however, cases initially exhibit a high positive PC3 (late-peaked) score that gradually declines as discharge mean and amplitude increase. High positive scores for an individual PC suggest that a plot of the PC loadings (Figure 3.4 b) will closely approximate the shape of that particular case. Peak negative values for PC3 occur at ~ JD 225 when hydrographs were at their most peaked. In contrast, PC1 (very late-peaked) and PC2 (peaked) scores show increasing trends from low negative values at the beginning of sub-period 4 to high positive values at the beginning of sub-period 5. PC1 scores predominate during sub-period 5 and PC2 scores during sub-

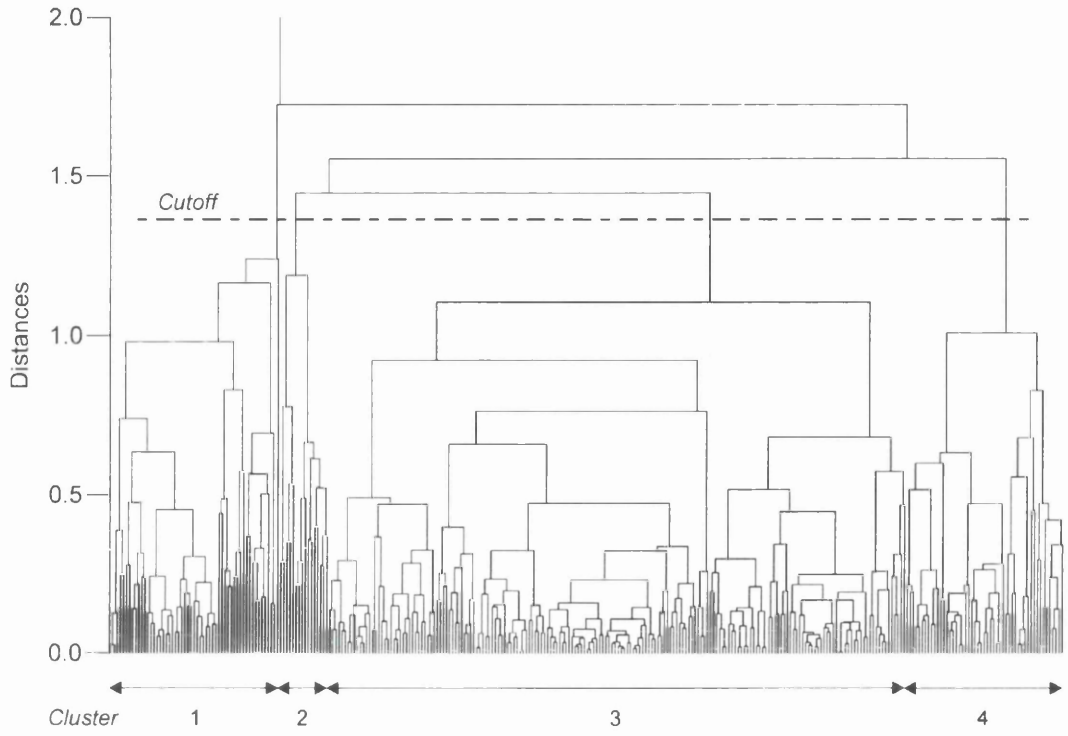

Figure 3.6 HCA vertical icicle plot. Individual cases along the horizontal axis are joined at increasing distances along the vertical axis. The clusters were interpreted as follows: (1) falling; (2) peaked-falling; (3) peaked; and (4) rising (see text and Figure 3.5 b).

periods 6–8. The pattern breaks down only as mean daily discharge begins to decrease following JD 225 (Figure 3.4 a). A similar, although less distinct pattern is evident during 1999, with PC3 scores being consistently high-positive during the first major rise in discharge during sub-period 2 (Figure 3.2 and Table 3.2), and cases showing high PC1 and PC2 scores throughout the remainder of the season.

HCA was used to cluster individual cases based on their PC scores. The average linkage rule was found to produce the most physically interpretable clusters compared to the alternative centroid, Ward's, single and complete linkage procedures (cf. Hannah et al., 1999, 2000; Kalkstein et al., 1987). The rule calculates the distance between two clusters as the average distance between all pairs of cases in the clusters and is generally very efficient when the cases form naturally distinct 'clumps' (StatSoft, 1995). Euclidean distances were specified in the joining processes since these are a measure of the actual geometric distance between cases in space (StatSoft, 1995).

The vertical icicle plot in Figure 3.6 shows the joining process. Selecting a cutoff point at linkage distance 1.4 on the vertical axis retains four distinct clusters, suggesting that hydrograph shapes group naturally into four main types. Representative hydrograph shapes are plotted for each cluster (Figure 3.5 b) and are interpreted as follows:

— Rising hydrograph. This cluster contains 21 cases during 1998 and 30 cases during 1999. The shape indicates a rise in discharge during the diurnal period with no clear evidence of a diurnal peak.

— Falling (or recessional) hydrograph. This cluster contains 27 cases from 1998 and 28 cases from 1999. The shape indicates a gradual fall in discharge with no superimposed diurnal peak.

— Peaked-falling hydrograph. This cluster contains 11 cases from 1998 and 5 cases from 1999. The shape indicates a fall in discharge or recession limb inherited from a previous hydrograph with a superimposed diurnal peak.

— Peaked hydrograph. This cluster contains 97 cases from 1998 and 91 cases from 1999; it is therefore the most common hydrograph type during both melt seasons. The shape is characteristic of a rapidly routed diurnal signal superimposed upon a stable baseflow component.

Cases in the peaked hydrograph cluster were retained for further analysis. Further classification of these cases using HCA of PC scores produced a poorly structured vertical icicle plot from which it was difficult to identify an appropriate number of clusters. Therefore, peaked hydrograph days were further classified on the basis of their magnitude characteristics.

3.3.2.2 Classification of hydrograph magnitude

The magnitude of peaked hydrograph days (Figure 3.5 b) was classified using HCA of hydrograph magnitude indices estimated from the hourly discharge observations during each diurnal period (i.e. 24 observations from 07:00). The indices describe the principal features of hydrograph magnitude as described below:

— Diurnal streamflow mean (Q_{mean}). This index includes the mean of all streamflow within the catchment derived from ice melt, snow melt, long-residence time meltwater/groundwater and meltwater released from storage.

— Diurnal streamflow standard deviation (Q_{std}). This index provides an indication of the variability of flow about the mean.

— Diurnal minimum flow (or baseflow; Q_b). This is the minimum streamflow recorded during each diurnal period, and represents long-residence time meltwater/groundwater and meltwater released from storage.

— Diurnal maximum flow (or peakflow; Q_p). This is the maximum streamflow recorded during each diurnal period, and represents the maximum contribution of meltwater from all sources.

— Diurnal streamflow range (Q_{range}). This is the maximum amplitude of flow during the diurnal period, calculated as the difference between diurnal maximum (Q_p) and minimum (Q_b) flows. It typically expresses the magnitude of the superimposed diurnal signal due to rapidly routed snow and ice melt from the ablation area.

— Diurnal standardised streamflow range ($Q_{strange}$). This index gives the diurnal streamflow range as a proportion of the diurnal minimum flow, or the approximate ratio of rapidly-routed to long-residence time meltwater, i.e.

$$Q_{strange} = \frac{(Q_p - Q_b)}{Q_b} \tag{3.1}$$

All indices were calculated using units of $m^3\ s^{-1}$. Similar indices were used by Hannah et al. (1999, 2000); however, time-to-peak discharge has not been included since this index for the efficiency of the routing of meltwater through the glacier is not a measure of hydrograph magnitude. In addition, diurnal maximum discharge is included here in order to emphasise the magnitude of the diurnal peak.

Prior to analysis, observations for each of the indices were standardised using z-scores to remove major variations in magnitude between individual variables that might unduly

Table 3.4 Magnitude clusters for peaked hydrograph cases, showing mean and standard deviation (in parentheses) of magnitude variables used for HCA and basic cluster shape variables calculated from the original dataset.

Composite classification (n)	Magnitude variables ($m^3 s^{-1}$)						Shape variables	
	Q_{mean}	Q_{stdev}	Q_b	Q_p	Q_{range}	$Q_{strange}$	Q_b	Q_p
Low-peaked (74)	1.439 (0.648)	0.310 (0.242)	1.072 (0.469)	1.981 (1.004)	0.909 (0.726)	0.835 (0.675)	11:15 (01:42)	19:16 (02:19)
Medium-peaked (65)	3.443 (0.490)	0.755 (0.266)	2.554 (0.442)	4.748 (0.793)	2.195 (0.766)	0.895 (0.380)	10:01 (01:21)	18:24 (02:18)
High-peaked (49)	2.911 (0.704)	1.217 (0.275)	1.555 (0.381)	5.180 (1.069)	3.626 (0.766)	2.404 (0.477)	10:03 (01:11)	17:28 (01:21)

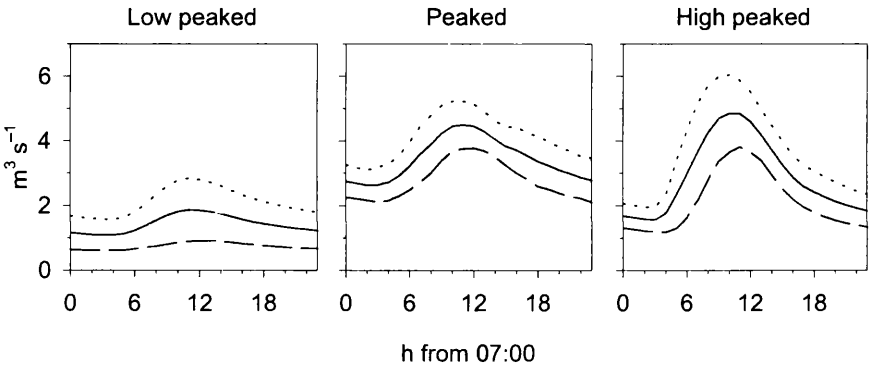

Figure 3.7 Representative hydrograph forms for magnitude clusters of peaked hydrograph cases obtained from the mean of each hourly discharge measurement for all

bias or influence the HCA process (cf. Hannah et al., 1999, 2000). HCA was performed from a matrix of 310 cases (diurnal periods) and 6 variables (the magnitude indices) and analysis of the vertical icicle plot resulted in the identification of three peaked hydrograph magnitude classes. The form of each cluster was interpreted from summary statistics based on mean values of non-standardised data for each of the indices used in the HCA process (Table 3.4). Basic 'shape' variables for each cluster calculated from the original data are shown for comparison; these variables were not used in the HCA process and are merely used to aid interpretation of the clusters. Representative hydrograph forms for the three clusters are plotted in Figure 3.7 and the clusters are interpreted as follows:

— Low-peaked hydrographs. This cluster contains 36 cases during 1998 and 38 cases during 1999 with the lowest mean magnitude variables. Mean $Q_{strange}$, the ratio of the magnitude of Q_p to Q_b, is below 1. Peak discharge occurs on average at around 19:00 with a mean rise to peak discharge of 8 h.

— Medium-peaked hydrographs. This cluster contains 29 cases during 1998 and 36 cases during 1999. Cases in this cluster have the highest mean Q_{mean} and Q_b. Mean Q_{range} and Q_{std} and Q_p are approximately twice those of the low peaked class; mean $Q_{strange}$ remains below 1. Peak discharge occurs ~ 50 min earlier on average than for the low-peaked class, although the mean rise to peak discharge is slightly longer.

— High-peaked hydrographs. This cluster contains 32 cases during 1998 and 17 cases during 1999. Cases in this cluster have the highest mean Q_{range}, Q_{std} and Q_p. Mean Q_{mean} and Q_b are slightly lower than for the medium-peaked class but higher than for the low-peaked class. Mean $Q_{strange}$ is greater than 2. The mean time of peak discharge occurs ~ 60 min earlier than the medium-peaked class, and the mean rise to peak discharge is the lowest of all three classes at 7 h 25 min.

3.3.3 Temporal sequencing of hydrograph classes

The temporal distributions of hydrograph shape and peaked hydrograph magnitude classes are shown in Figure 3.8 for the monitored periods of the 1998 and 1999 melt seasons. The diagram also indicates the subperiods of each melt season described in Section 3.2 (Tables 3.1 and 3.2).

3.3.3.1 Hydrograph shape classes

During 1998, hydrograph shape classes do not form a consistent pattern until the beginning of sub-period 4 (Figure 3.8 a). Prior to sub-period 4, peaked hydrograph cases are uncommon and there is a mixture of hydrograph forms. Sub-period 1 includes many rising, peaked-falling and falling days that occur without pattern. Sub-period 2 includes mainly rising hydrographs, whereas sub-period 3 is a combination of peaked and falling cases. The beginning of sub-period 4 is marked by a single peaked-falling hydrograph;

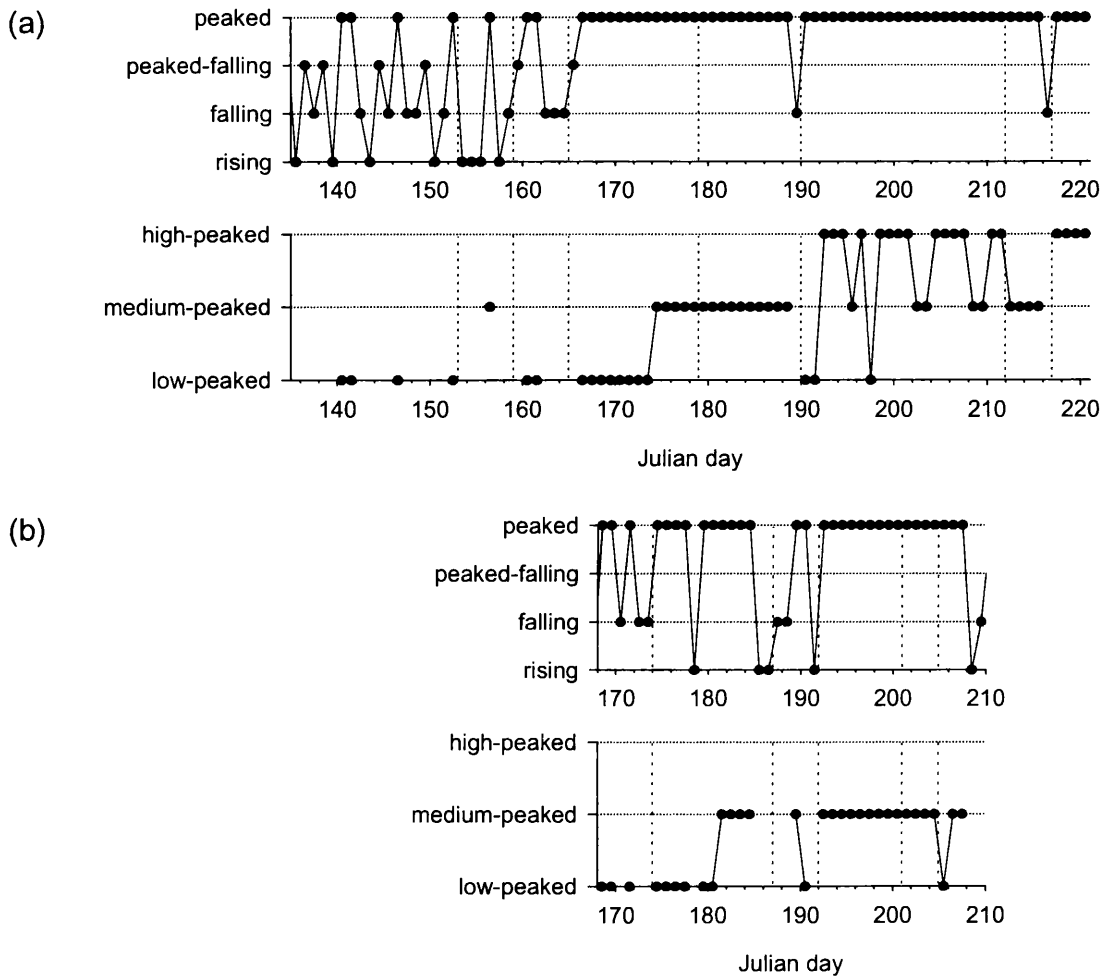

Figure 3.8 The distribution of hydrograph shape and peaked hydrograph magnitude classes during the 1998 (a) and 1999 (b) monitored periods (see Figure 3.6 for representative hydrograph forms).

following this, peaked cases predominate for the remainder of the monitored period. Isolated falling hydrograph shapes mark the end of sub-periods 5 and 7.

During 1999 (Figure 3.8 b), peaked hydrograph cases occur throughout the monitored period but temporal patterns in the distribution of shape classes are not clearly defined. Sub-period 1 includes a number of falling hydrographs; sub-periods 2, 4, 5 and 6 are dominated by peaked hydrograph forms, although the end of sub-periods 2 and 6 are marked by successively rising and falling hydrograph classes; and sub-period 3 shows a mixture of falling and peaked hydrographs. Peaked-falling hydrograph shapes do not occur within the monitored period.

3.3.3.2 Peaked hydrograph magnitude classes

There are clear patterns in the distribution of hydrograph types during 1998 (Figure 3.8 a): 1) predominantly low-peaked classes occur during sub-periods 1 to 3; 2) there is a transition between low-peaked and medium-peaked classes on JD 175 during sub-period 4; 3) high-peaked classes occur from the start of sub-period 6 and predominate for the remainder of the monitored period, except during sub-period 7 when medium-peaked classes occur. A broadly similar pattern is evident during 1999 (Figure 3.8 b), with the transition between low-peaked and medium-peaked hydrograph types occurring during sub-period 2, approximately 6 days later than in 1998. However, high-peaked hydrograph types do not occur during the monitored period, with medium-peaked forms predominating throughout sub-periods 4 to 6.

3.3.4 Interpretation, discussion and conclusions

The temporal distribution of peaked-hydrograph forms indicates the contribution of meltwater to the proglacial stream derived from rapidly routed snow and ice melt in the ablation area. During 1998, the majority of peaked forms occur after JD 165, indicating the onset of retreat of the supraglacial snowpack and exposure of low-albedo glacier ice on the glacier tongue (Figure 3.8 a). Prior to this, peaked hydrograph forms are rare and low in magnitude. During sub-period 1, the variety of hydrograph types probably reflects slow transit times of meltwater to the glacier snout as indicated by large lags between meteorological inputs and streamflow (Table 3.3), resulting in a high number of diurnal hydrographs with very late-peaking (rising) or inherited (falling and peaked-falling) characteristics.

During sub-period 2, significant diurnal variations in streamflow superimposed on a high baseflow are evident from discharge records (Figure 3.1), but hydrographs are classed predominantly as rising, indicating very late peaks in discharge due to a still inefficient drainage system (Figure 3.8 a). A number of peaked hydrographs occur during sub-period 3 following the peak in discharge towards the end of sub-period 2. Sub-period 3 shows a slight reduction in the lag between air temperature and streamflow (Table 3.3), suggesting efficient routing of snowmelt in the days following the rainfall-induced discharge peak. However, most hydrographs show falling or peaked-falling

characteristics (Figure 3.8 a) as discharge recedes and snowfall and freezing temperatures suppress surface melting (Table 3.1; Figure 3.1).

The distribution of peaked hydrograph magnitude classes following JD 165 reflects both the exposure of increasing areas of low-albedo glacier ice, providing greater volumes of peaked meltwater inputs to the glacier drainage system, and the increasing efficiency of meltwater flowpaths. Hydrograph forms evolve from low-peaked through medium-peaked to high-peaked classes from JD 165 (Figure 3.8 a), demonstrating an increasing diurnal amplitude, earlier time of peak discharge and visually steeper rising and falling limbs (Table 3.4; Figure 3.7). Evolution from low-peaked to high-peaked forms occurs as lags between meteorological variables and proglacial streamflow fall rapidly during sub-periods 4 and 5 (Table 3.3). High-peaked forms occur during sub-period 6 from JD 193 and during sub-period 8 (Figure 3.8 a), suggesting the contribution of icemelt from large areas of the ablation area routed through an efficient, channelised drainage system. During sub-period 7, medium-peaked forms predominate, due to rainfall in the late afternoon and evenings and cloud cover throughout the day reducing the amplitude of diurnal runoff (Table 3.1; Figure 3.1).

Changing baseflow magnitudes are also evident within the three peaked-hydrograph classes. The magnitude of the baseflow component remains higher than the diurnal signal during low-peaked and medium-peaked hydrograph cases (Figure 3.7), suggesting that meltwater is being released from storage or a large proportion of runoff is being routed slowly through the supraglacial snowpack and/or distributed subglacial drainage system. Evolution of subglacial drainage at Haut Glacier d'Arolla has previously been associated with negative water balances caused by the release of meltwater 'stored' in a distributed subglacial drainage system early in the melt season (Richards et. al, 1996). As the supraglacial snowpack thins and retreats, flow is released from storage by an expanding channelised subglacial drainage network and supraglacial meltwaters are routed more rapidly to the glacier snout. High peaked forms during sub-period 6 (Figure 3.8 a) demonstrate efficient routing of surface meltwater sources and low flow through distributed supraglacial or subglacial systems, suggesting that the majority of the glacier is drained by a hydraulically efficient, channelised subglacial drainage system.

During 1999, peaked hydrograph forms are common after JD 176, indicating retreat of the supraglacial snowpack and contributions of meltwater from ice melt during sub-period 2 (Figure 3.8 b). Rising hydrographs towards the end of sub-period 2 occur during strong föhn followed by high levels of precipitation that are likely to have resulted in high rates of surface melting (Table 3.2). High baseflow suggests large volumes of melt are slowly routed through a supraglacial snowpack or inefficient subglacial drainage system, indicated by large lags between meteorological variables and streamflow (Table 3.3). A number of hydrographs during sub-period 3 are classified as falling (Figure 3.8 b), reflecting the decline in discharge following the end of sub-period 2, although peaked hydrographs quickly return as incident radiation values and mean air temperatures increase once more (Table 3.2). A similar pattern in hydrograph form occurs towards the end of sub-period 6 (Figure 3.8 b); however, hydrographs are heavily modified by rainfall (Figure 3.2; Table 3.2) and the classification is likely to be unreliable.

The transition between low-peaked and medium-peaked hydrograph magnitude classes occurs later in 1999 than during 1998, and medium-peaked forms predominate throughout the remainder of the monitored period (Figure 3.8). Significant contributions of rapidly routed snow and ice melt from the ablation area therefore occur later in 1999, with a correspondingly later evolution of the subglacial drainage system. Medium-peaked hydrograph forms predominate throughout the remainder of the monitored period during 1999 (Figure 3.8 b), indicating a large proportion of meltwater routed through distributed supraglacial or subglacial drainage systems due to the delayed removal of the glacier surface snowcover.

3.4 ICE MOTION, DRAINAGE STRUCTURE AND WATER QUALITY

3.4.1 Introduction

This section uses glacier surface velocity, the results of dye-tracer studies and proglacial electrical conductivity time series in order to further investigate the structure and evolution of the subglacial drainage system during the 1998 and 1999 melt seasons. In Section 1.4 it was suggested that ice motion is a valuable indicator of subglacial drainage

system development and high horizontal ice velocities may result in the more efficient evacuation of basal sediments due to increased disturbance of the glacier bed. Dye tracing can be used to directly investigate or confirm drainage system structure and configuration, whilst electrical conductivity provides an approximation of the proportion of flow routed through distributed and channelised drainage components.

3.4.2 Glacier dynamics

3.4.2.1 Introduction

Glacier motion responds to variations in meltwater storage at the glacier bed. Subglacial water pressure plays a critical role in variations in ice motion since high basal water pressures lead to bed separation, reducing basal friction and promoting enhanced basal motion (Iken and Bindschadler, 1986; Kamb and Engelhardt, 1987; Hooke et al., 1989; Iverson et al., 1995). If flow through the distributed system increases rapidly, the widespread increase in subglacial water pressures may result in glacier surface uplift and rapid horizontal motion.

Subglacial water pressures are expected to vary both spatially and temporally. Spatial variations can occur due to the location and magnitude of surface meltwater inputs via moulins or crevasses and the location of major drainage elements, since water pressure in subglacial channels may vary from atmospheric to hydrostatic. Such channels have been shown to influence basal water pressures up to 70 m laterally from the channel (Hubbard et. al, 1995). Temporal variations result from variation in the magnitude of subglacial discharge due to changes in surface meltwater inputs and the morphology of the subglacial drainage system. Variations in basal water pressure are likely to cause spatial and temporal variations in basal drag (Fischer et al., 1999) and hence basal motion. This motion creates longitudinal stress gradients in the overlying ice, spreading the influence of local variations in basal water pressure over areas equivalent to several ice thicknesses (Mair et al., 2001; in press). Thus, the surface expression of glacier motion is the integration of many local variations in basal motion over a wide area.

At Haut Glacier d'Arolla, short-term variation in horizontal and vertical ice motion has been related to increased flow through the distributed system during sustained periods of

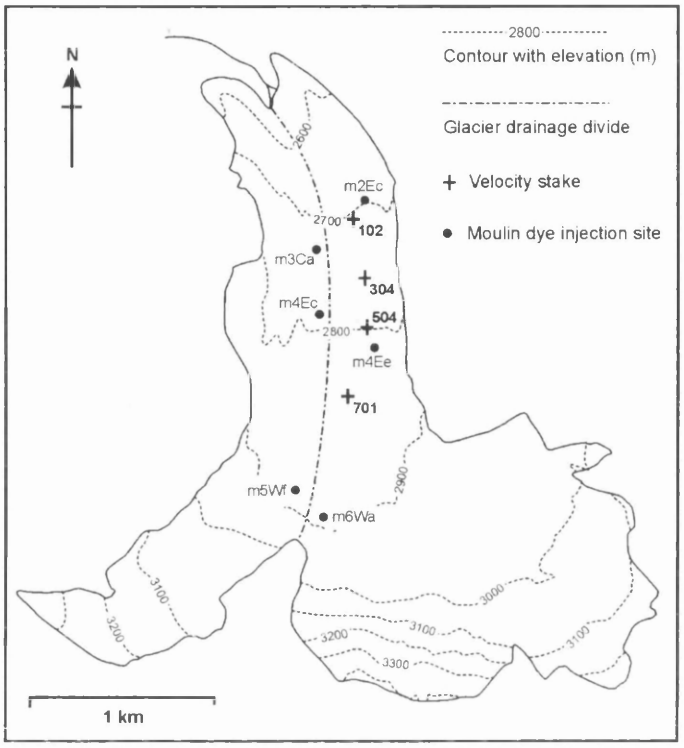

Figure 3.9 Haut Glacier d'Arolla, showing the location of velocity stakes and dye injection sites during the 1998 and 1999 melt seasons. The approximate location of the glacier drainage divide is also indicated (see Section 3.4.4).

rising supraglacial meltwater inputs (Mair et. al, 2001; in press). Early in the 1994 melt season when the glacier was still snow covered, a rapid increase in horizontal motion occurred during a föhn-induced period of high air temperatures, rainfall and wind. The event was characterised by high, temporally and spatially variable horizontal velocities, positive vertical glacier motion, and the removal of all areas of very high basal drag. This suggests that high snow melt delivered significant surface meltwater via moulins and crevasses to a distributed drainage system, resulting in a widespread increase in basal water pressures and consequent ice-bed separation. Separation initially occurred along a preferential subglacial drainage axis and propagated across a large area of the glacier bed, either due to direct propagation of water pressures or bridging effects (horizontal stress gradients that support areas of ice adjacent to where separation is occurring). Peak uplift occurred 3 days before the peak in proglacial discharge, suggesting that the drainage system had become increasingly hydraulically efficient towards the end of the event or that water pressures had decreased as separation became

more widespread. The end of the event coincided with a decline in air temperature and water pressures rapidly decreased in the area around the preferential drainage axis. Water pressure fell less rapidly in other areas, causing velocities to decline more slowly.

Glacier motion at Haut Glacier d'Arolla is also sensitive to the morphology of the subglacial drainage system (Mair et al., in press), which evolves from a hydraulically inefficient, distributed system to a hydraulically efficient, channelised system during each melt season (Richards et al., 1996; Nienow et al., 1998). Rapidly rising subglacial discharge near the start of the season is likely to cause high basal water pressures because surface inputs across the glacier are liable to contribute directly to the distributed system. Later in the melt season, channel formation within the lower tongue of the glacier reduces the ability of water pressures to rise: moulins tend to be located above preferential drainage axes and will thus contribute directly to low-pressure, channelised flowpaths. Variations in horizontal and vertical velocity due to rising surface meltwater inputs are therefore more likely to occur further upglacier later in the melt season, where channels are immature and many moulins remain unconnected to the still expanding channelised network. Towards the end of the melt season, when a mature channelised network has developed beneath a large proportion of the ablation area, rapid increases in surface meltwater inputs are unlikely to influence glacier motion since moulins connect directly to the channelised drainage network.

3.4.2.2 Sub-annual variations in glacier motion

Glacier horizontal (x) and vertical (z) velocities for the monitored periods during 1998 and 1999 are shown in Figures 3.10 to 3.13 together with catchment discharge and the various sub-periods of the melt seasons (Tables 3.1 and 3.2). Velocities were measured at four stakes along the glacier tongue east of the centreline (Figure 3.9).

1998 melt season

Two periods of rapid horizontal ice motion occured early in the 1998 melt season (Figure 3.10). A rapid, approximately five-fold increase in horizontal motion occured during sub-period 2 between JD 154 and 159. Horizontal velocities increased almost simultaneously at all four stakes from a pre-event velocity of ~ 0.02 m d^{-1}, although the

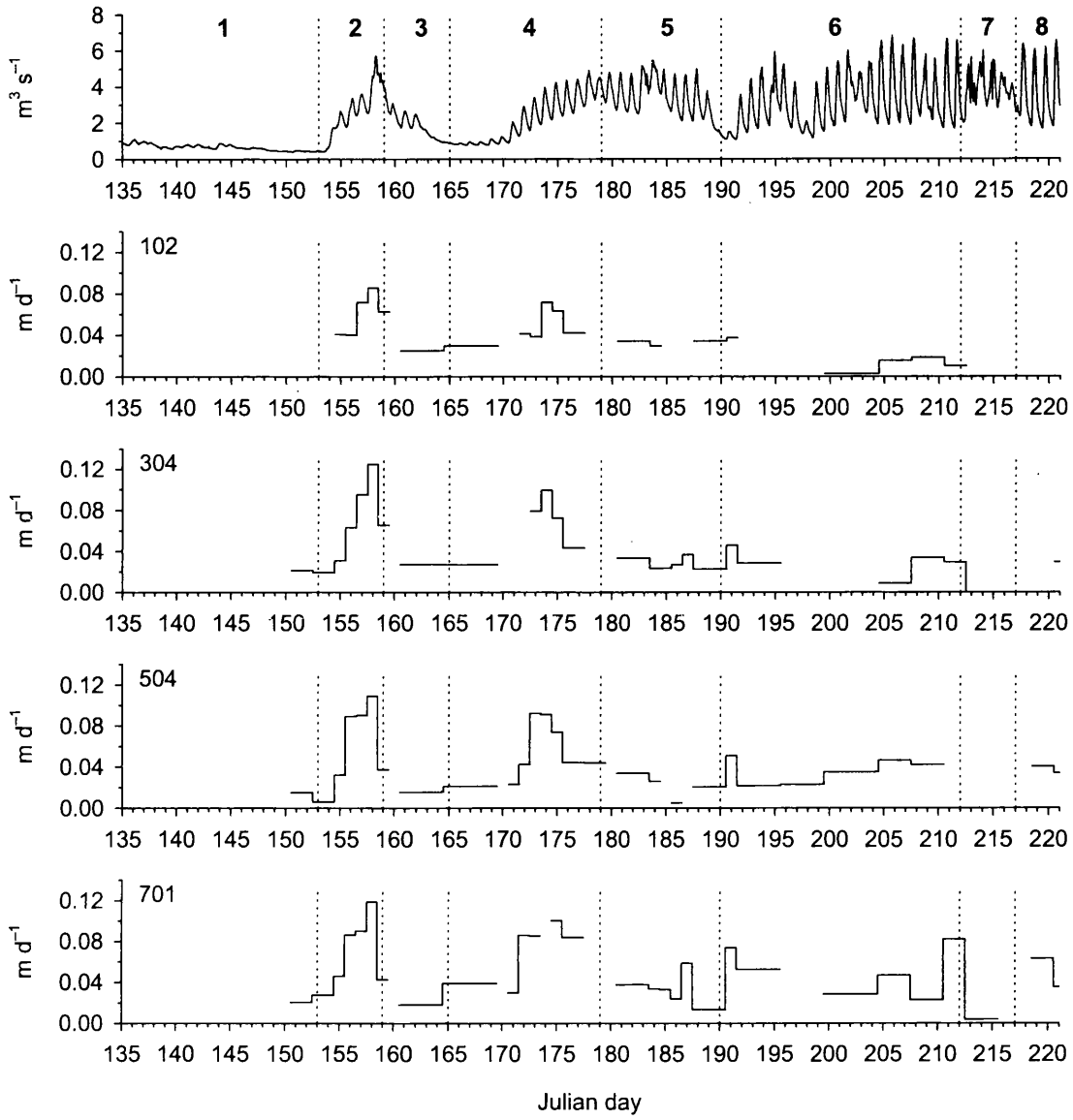

Figure 3.10 Catchment discharge and glacier *x*-velocities at stakes 102 to 701 during 1998.

initial increase was most rapid at upglacier stakes 504 and 701 (refer to Figure 3.9 for stake locations). Peak velocities were achieved on JD 157–158, although peak velocities at stake 102 (the farthermost downglacier stake) were only 80 % of their upglacier values (Figure 3.10). Vertical velocities peaked on JD 155–156 at the two upglacier stakes (504 and 701) and on 157-158 downglacier (stakes 304 and 102). Horizontal velocities declined rapidly on JD 158–159; by the beginning of sub-period 3, horizontal velocities had returned to pre-event levels.

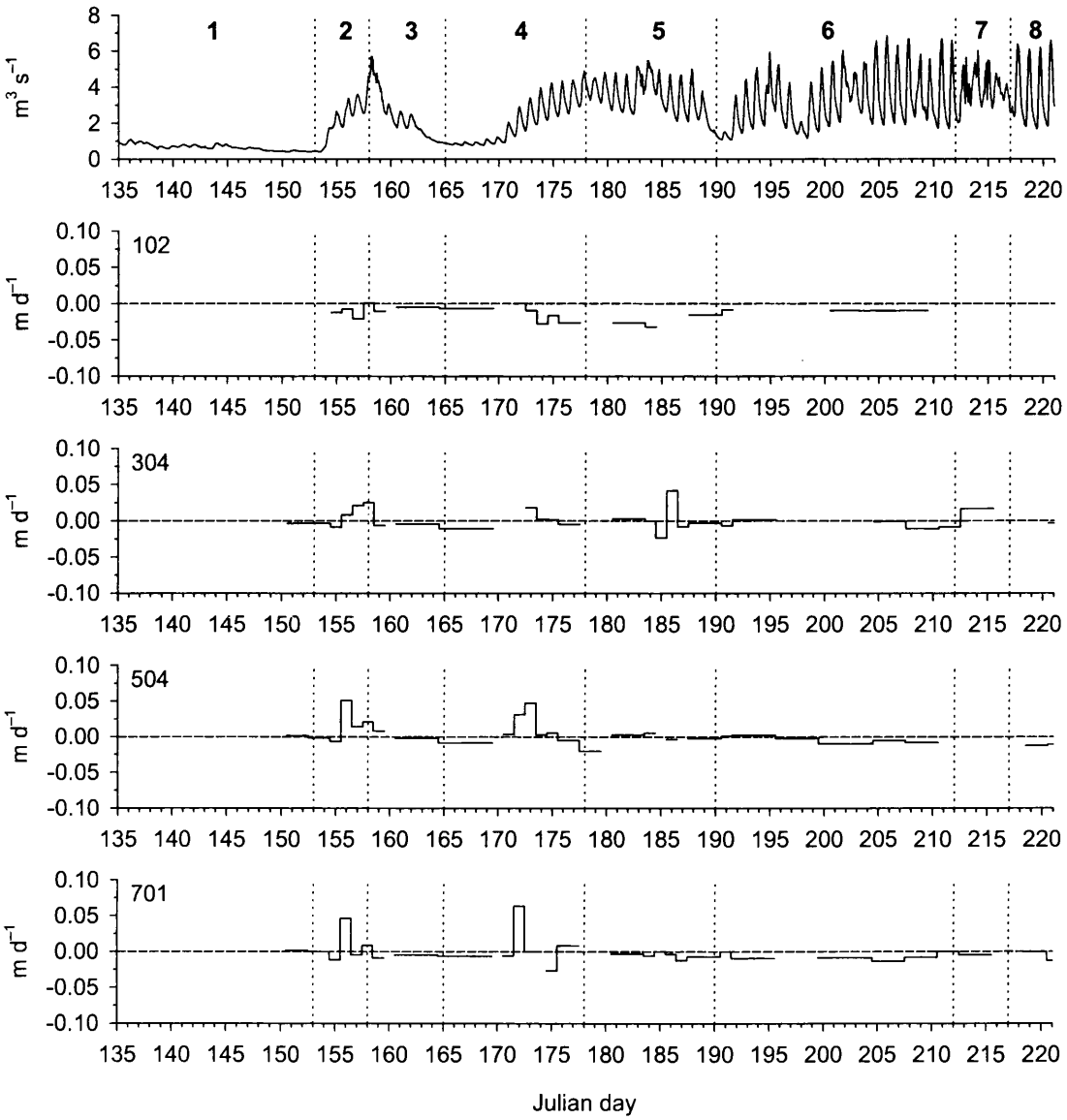

Figure 3.11 Catchment discharge and glacier *z*-velocities at stakes 102 to 701 during 1998.

The second rapid rise in horizontal velocity occurred during sub-period 4 between JD 171 and 175 (Figure 3.10). Horizontal velocities increased approximately four-fold from pre-event levels, but again peak velocities were lower downglacier. The initial magnitude of the increase also remained greatest upglacier and preceded uplift at the downglacier stakes. Peak horizontal velocities were also temporally variable, with peak velocity occurring on JD 172–173 at stake 504, on JD 173–174 at stakes 102 and 304, and on JD 174–175 at stake 701 (Figure 3.10). Peak vertical velocities followed a similar pattern, with peak vertical velocity occurring on JD 171–172 at stake 701 and progressively

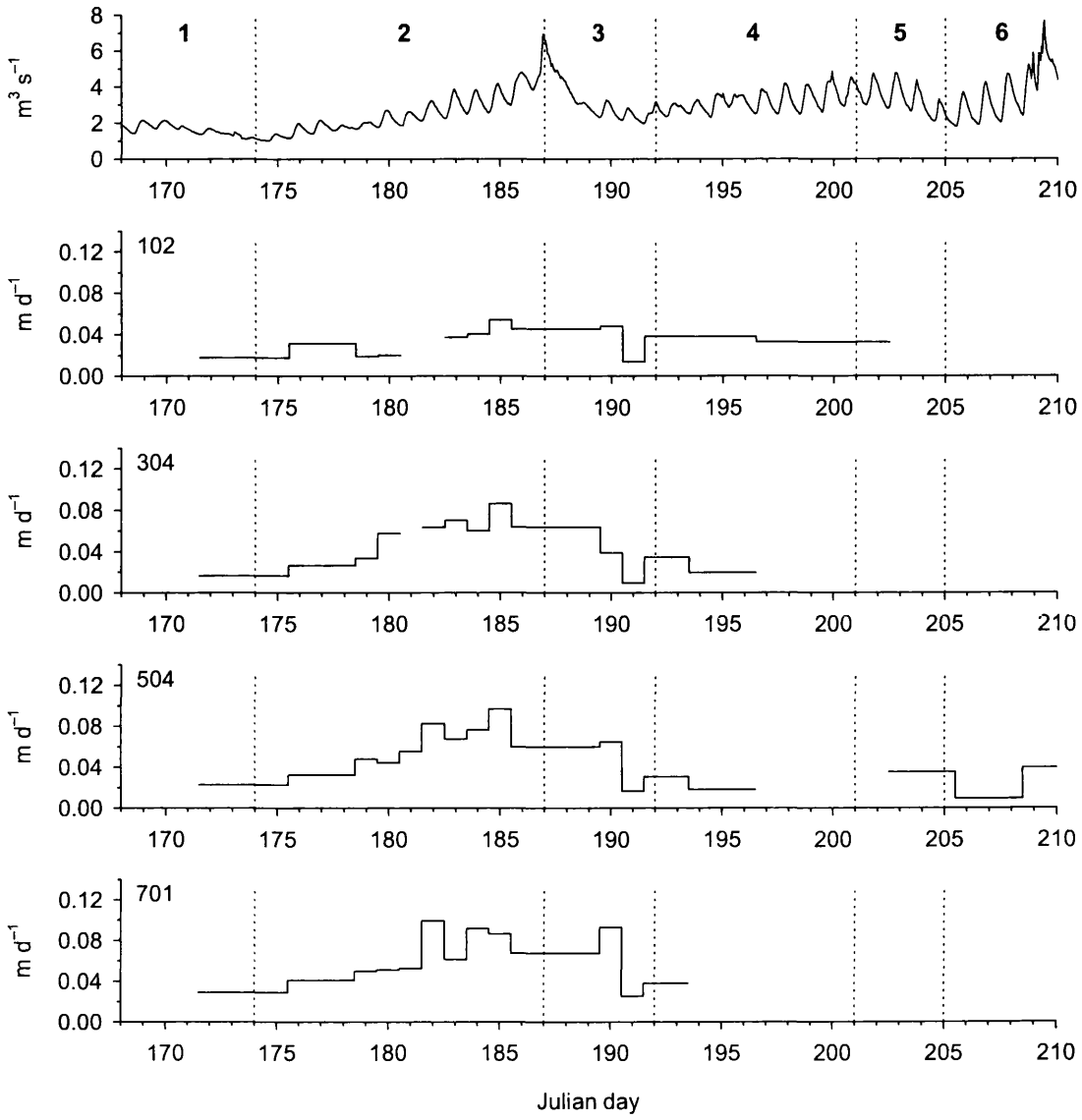

Figure 3.12 Catchment discharge and glacier x-velocities at stakes 102 to 701 during 1999.

lower magnitude peak velocities occurring downglacier at stakes 504 and 304 on JD 172–173 (Figure 3.11). At stake 102, vertical velocities remained negative throughout the event. Horizontal velocities begin to decrease on JD 174–175, but remained significantly above pre-event levels until approximately JD 185.

There is some evidence of a positive trend in horizontal motion at all stakes during sub-period 6 (Figure 3.10). The trend is clearest in upglacier at stakes 504 and 701, where late season velocities also appear highest. Stakes 304 and 701 suggest velocities fall to

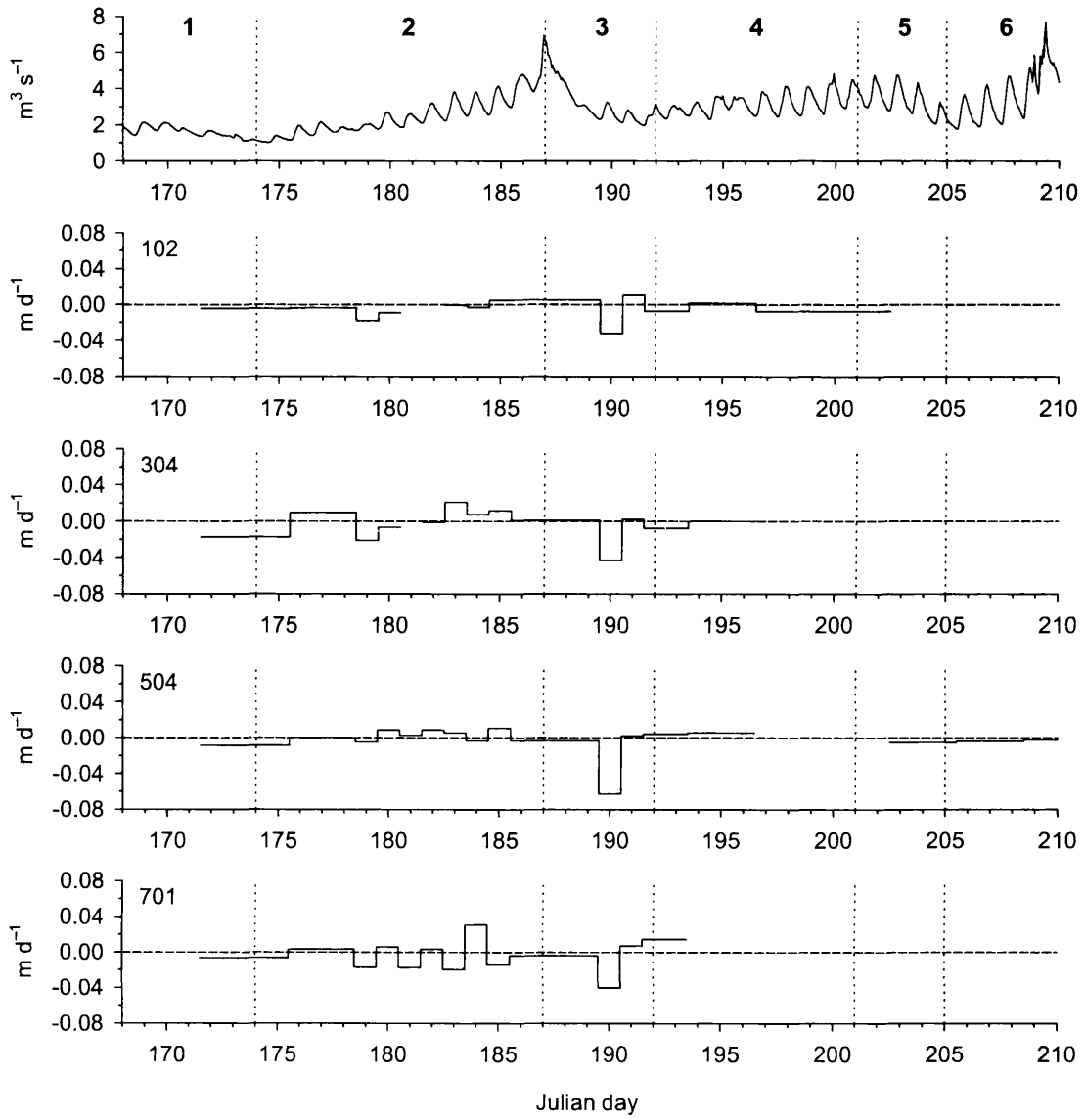

Figure 3.13 Catchment discharge and glacier *z*-velocities at stakes 102 to 701 during 1999.

zero across the glacier during sub-period 7, but there is evidence at stakes 304, 504 and 701 that velocities recovered during sub-period 8 (Figure 3.10).

1999 melt season

During 1999, one extended enhanced period of rapid glacier motion occurred early in the melt season during sub-period 2 between JD 175 and 191 (Figure 3.12). Prior to the event, horizontal velocities were ~ 0.02 m d^{-1}. Velocities peaked first at upglacier stake

701 on JD 181–182 with a secondary peak on JD 183–184. Peak velocities at stakes 102, 304 and 504 occurred on JD 184–185 (Figure 3.12). The magnitude of the increase in velocity from pre-event levels also increased with distance upglacier (Figure 3.12). Vertical velocities were mildly negative at all stakes prior to JD 175 and demonstrated low-magnitude and inconsistent variation during the event.

Horizontal velocities began to decline across the glacier on JD 185–186, but remained at approximately three times the pre-event level until JD 190 (Figure 3.13). Large negative vertical velocities occurred at all stakes on JD 189–190, following which all stakes demonstrated an abrupt decline in horizontal velocities.

3.4.2.3 Comparison with streamflow and meteorological variables

During 1998, the first rapid motion event occurred during sub-period 2, characterised by rapidly increasing catchment discharge following a period of low and constant catchment runoff (Figure 3.10). Sub-period 2 was characterised by high mean air temperatures and heavy rainfall after low mean air temperatures and snowfall during sub-period 1 (Figure 3.1; Table 3.1). Peak discharge was reached at approximately 00:00 on JD 158 during peak horizontal velocities (Figure 3.10). Peak vertical velocities occurred shortly after the initial rise in discharge and ~ 3 days before the discharge peak (Figure 3.11). Negative vertical velocities and a rapid decline in horizontal velocities coincided with the rapid fall in discharge on JD 158.

The second rapid motion event during 1998 occurred during sub-period 4, characterised by rising catchment discharge following low and constant runoff towards the end of sub-period 3 (Figure 3.10). Horizontal velocities were greatest during the initial discharge rise between JD 170 and 175, as baseflow and diurnal amplitude increased rapidly. Peak vertical velocities occurred very shortly after catchment discharge had begun to rise and 2–3 days before peak horizontal velocities (Figure 3.11). Sub-period 4 had rapidly rising mean air temperatures, especially during JD 170–175, after very low mean air temperatures and snowfall towards the end of sub-period 3 (Figure 3.1; Table 3.1). A significant reduction in velocity occurred as the rapid rise in diurnal amplitude ceased at about JD 175, but baseflow continued to climb (Figure 3.10). A further but slower

decline in velocity occurred during sub-period 5 as diurnal amplitude increases once more due to a declining baseflow.

The 1999 rapid motion event occurred during sub-period 2, a long period of rising catchment discharge with a slowly increasing diurnal amplitude following low magnitude and low amplitude catchment runoff during sub-period 1 (Figure 3.12). Mean air temperatures also rose following low air temperatures towards the end of sub-period 1 (Figures 3.1 and Table 3.2). Peak discharge was reached at approximately 00:00 on JD 187 following heavy rainfall (Figures 3.2 and 3.12); peaks in horizontal velocity occurred 2–3 days before the peak in discharge. Vertical velocities were temporally very variable, but typically peaked 2–4 days before the peak in discharge (Figure 3.13). Horizontal velocities remained high and stable throughout the rise and subsequent fall in discharge during sub-periods 2 and 3, receding gradually during sub-period 4 as catchment discharge and diurnal amplitude begins to rise once more (Figure 3.12).

The possible increasing trend in horizontal velocities towards the end of the monitored period during 1998 (Figure 3.10) occurred during periods characterised by high mean air temperatures and high-amplitude diurnal discharge variations (Figure 3.1; Table 3.1). Velocities appear to decline significantly during sub-period 7, where diurnal discharge amplitude was significantly reduced (Table 3.1; Figure 3.10).

3.4.2.4 Interpretation and discussion

Rapid motion events

Periods of rising catchment discharge during the 1998 and 1999 melt seasons are associated with horizontal ice velocities significantly higher than normal summer background levels. During 1998, the glacier was snow covered prior to and during the first rapid motion event: large lags between meteorological variables that control surface melting and proglacial streamflow during sub-periods 1–3 (Table 3.3; Figure 3.3) suggest that the glacier was underlain by a distributed subglacial drainage system. High mean air temperature and heavy rainfall was likely to have initiated rapid melting of the glacier snow cover and to have delivered significant inputs of surface melt to the glacier bed. High, spatially persistent horizontal velocities were likely to result from increased

basal motion due to rapidly increasing discharge through a distributed drainage system. Lower horizontal velocities near the glacier snout may have resulted from the presence of pre-existing channels (cf. Sharp et al., 1993; Nienow et al., 1998) and the proximity of upglacier areas to surface input points such as moulins (Mair et al., in press). Vertical ice velocities peaked very shortly after the initial rise in discharge; vertical and horizontal velocities rapidly returned to pre-event levels during an equally rapid decline in discharge. This suggests channelisation was able to rapidly release meltwater from temporary storage. It is possible that increased flow through the distributed system mainly occurred near to PDAs beneath the glacier tongue, since: 1) moulins on the glacier tongue tend to be located above PDAs (Sharp et al., 1993); 2) precipitation in the upper catchment may have occurred as snow; and 3) a thick supraglacial snowpack in the accumulation area may have delayed supraglacial runoff.

Peak horizontal velocities during the second event were generally of lower magnitude but show a more pronounced difference between upglacier and downglacier areas. Prior to the event, high lags between meteorological variables and streamflow suggest large areas of the glacier were still underlain by distributed drainage (Table 3.3; Figure 3.3). Rapidly increasing air temperatures during the event are likely to have resulted in significant inputs of surface meltwater from snowmelt that also exposed areas of low-albedo ice on the glacier tongue. The downglacier propagation and decrease in magnitude of horizontal ice velocities are likely to reflect the pattern of surface meltwater production and the spatial extent of an immature channelised system formed during the first event (cf. Mair et al., in press). Increasing baseflow after the event was probably due to increasing volumes of melt from upglacier areas routed through the supraglacial snowpack and distributed subglacial drainage system; however, horizontal velocities declined due to the extension and increase in efficiency of the channelised system releasing meltwater from 'storage' in the distributed system. A slow decline in horizontal velocities and baseflow during sub-period 5 suggests a decline in the proportion of melt routed through distributed supraglacial and subglacial drainage systems and an increasingly extensive and hydraulically efficient channelised system. Channel formation during the event is likely to have occurred under closed flow conditions during consistently high discharges; however, predominantly open flow conditions will occur during sub-period 5 as supraglacial runoff becomes increasingly peaked.

During 1999, peak horizontal ice velocities occurred 3 days before the peak in discharge. The glacier was snow covered prior to the event, and large lags between meteorological variables and proglacial streamflow again indicate the existence of a hydraulically inefficient, distributed subglacial drainage system (Table 3.3; Figure 3.4). Rising mean air temperatures and a strong föhn during sub-period 2 (Table 3.2) are likely to have resulted in the increasing contribution of supraglacial meltwater to a predominantly distributed subglacial drainage system. A similar downglacier decrease and propagation of horizontal ice velocities occurred during 1998. The relatively small amplitude variation in vertical velocities probably reflects a slow rise in discharge through the distributed system due to a slow increase in surface melting. Vertical and horizontal velocities did not return rapidly to pre-event levels, suggesting the slow extension and increase in efficiency of the channelised system following the event. However, velocities did gradually return to pre-event levels during sub-periods 3 and 4.

Vertical ice velocities during all events peak very shortly after the initial rise in discharge and before peak horizontal velocities, suggesting either: 1) the increasing efficiency of the drainage system during the events; or 2) declining water pressures due to increasingly widespread basal separation (cf. Mair et al., in press).

Other events

The slow trend of increasing horizontal velocities towards the end of 1998 is not related to increasing catchment discharge but occurs during periods of high diurnal discharge amplitude. Short lags between meteorological variables and proglacial streamflow during these periods (Table 3.3) suggest very efficient routing of meltwater through a channelised subglacial drainage system. Flow in the channels following the first event is likely to have been open for a large proportion of the diurnal cycle due to the increasing peakedness of supraglacial runoff; however, increasing peak discharge will have resulted in the increasing overpressurisation of channels for longer periods of the diurnal cycle. This effect may have been strengthened by a slight adjustment in channel size due to deformation of the overlying ice to reflect predominantly open conditions during the diurnal cycle. Meltwater was likely to have been forced from channels into the distributed system (Hubbard et al., 1995), reducing basal friction near to PDAs and

causing in a net daily increase in horizontal velocity (cf. Iken, 1974; Iken and Bindschadler, 1986; Willis, 1995).

3.4.2.5 Conclusions

Rapid motion events are precipitated by significant increases in surface melting early in the melt season when the subglacial drainage system is almost entirely or predominantly distributed. During 1998, the first event demonstrates a rapid response to increased supraglacial runoff, although the response is attenuated near to the snout due to pre-existing channelised drainage. Some channelisation appears to have occurred towards the end of the event, causing horizontal velocities to return rapidly to pre-event levels. The second event was attenuated with respect to the first and with increasing distance downglacier, probably due to channel formation along PDAs beneath the glacier tongue. A rapid, higher magnitude and temporally more persistent response occurred upglacier, probably due to increased flow through 'new' areas of the distributed system where channels were absent or immature. Declining horizontal velocities, despite increasing baseflow suggestive of increasing flow through a distributed drainage system, suggests the initially rapid expansion of the channelised system towards the end of sub-period 4. Gradually declining baseflow and horizontal velocities during sub-period 5 suggest the continued expansion or increase in efficiency of the channelised system up to approximately JD 190. During 1999, a single event shows a gradual response reflecting a steady rise in surface melting and an attenuated response with distance downglacier probably due to the presence of pre-existing channels. The gradual decrease in horizontal velocities to pre-event levels suggests a slow expansion and increase in the efficiency of the channelised system following the event.

The slow increase in horizontal velocities towards the end of the monitored period during 1998 suggests increased flow through the distributed system due to overpressurisation from increasingly peaked supraglacial runoff through efficient channelised drainage. Channels may also adjust in size to reflect predominantly open flow conditions, further increasing the magnitude of overpressurisation at peak discharge. The hydraulic gradient between the high-pressure distributed system and the low-pressure channel is reversed, resulting in basal separation near to channels and along preferential drainage axes that may influence velocity patterns across the glacier. The

response is likely to be dependent upon the magnitude and rapidity of surface runoff and will therefore increase throughout the season.

3.4.3 Electrical conductivity

3.4.3.1 Introduction

Stream conductivity can provide an independent record of the evolution of meltwater sources and pathways (see Section 2.1.4.1). Previous work at Haut Glacier d'Arolla has shown electrical conductivity to vary between 10 and 40 $\mu S\ cm^{-1}$ (Gurnell et al., 1992a; Richards et al., 1996). During the 1989 and 1990 melt seasons (Gurnell et al., 1992a), conductivity reached peaks of ~ 30–40 $\mu S\ cm^{-1}$ early in the season during periods of low and invariable discharge when runoff was suggested to have been generated solely by basal melting. Conductivity then fell rapidly to ~ 20 $\mu S\ cm^{-1}$ as air temperatures and discharge rose, suggesting the contribution of significant volumes of icemelt to glacier runoff. After this initial decline, mean conductivity during both seasons remained at ~ 20 $\mu S\ cm^{-1}$. Occasional increases in conductivity occurred during periods of low discharge associated with low or freezing temperatures and therefore the suppression of surface melting. Diurnal variations in conductivity increased as the amplitude of diurnal discharge variations increased, but bore an inverse relationship to discharge reflecting the mixing of rapidly routed icemelt with meltwater generated from basal sources.

3.4.3.2 Results

Electrical conductivity for the western proglacial stream during 1998 and eastern proglacial stream during 1999 is shown in Figure 3.12 and 3.13, respectively. 'Raw' conductivity not corrected for temperature or ionisation effects is presented since raw and corrected values did not differ significantly. During 1998, the conductivity probe was installed on JD 165. Conductivity exhibits a falling trend from JD 165–174 from a peak of ~ 35 $\mu S\ cm^{-1}$ (Figure 3.14). Following JD 174, mean conductivity remains between 10 and 15 $\mu S\ cm^{-1}$, except around JD 190 and JD 197 when mean conductivity reaches above 20 $\mu S\ cm^{-1}$. Despite an early-season peak in conductivity of ~ 27 $\mu S\ cm^{-1}$

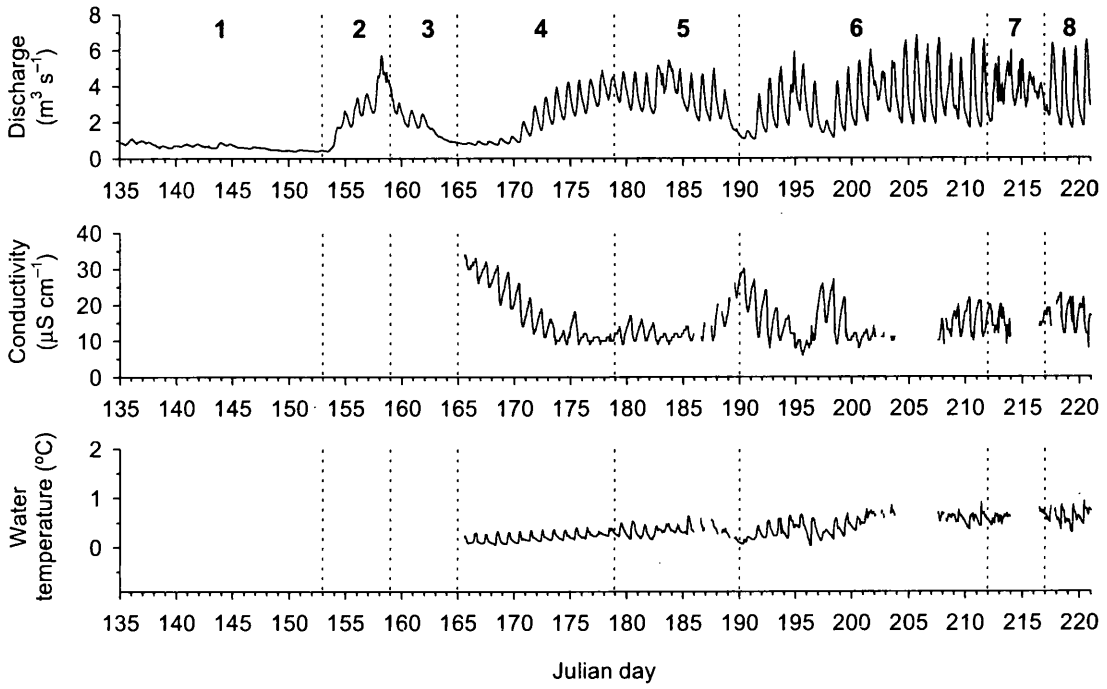

Figure 3.14 Catchment discharge, western proglacial stream conductivity and water temperature during the 1998 melt season.

between JD 173 and 175 during 1999, rapid variations often unrelated to discharge later in the season suggest that the conductivity sensor was operating poorly (Figure 3.15).

3.4.3.3 Interpretation and conclusions

Conductivity values during both seasons fell within the expected range for melted snow (2–42 µS cm^{-1}; Campbell-Scientific, 1994–1996) and from previous melt seasons (Gurnell et al., 1992; Richards et al., 1996). During 1998, conductivity fell rapidly from JD 165 to 174 during sub-period 4 as diurnal discharge amplitude increased, suggesting an increase in runoff from supraglacial sources and/or snowpack elution. Low mean conductivity with generally low levels of diurnal variability from JD 174 to 179 suggests the continuous mixing and dilution of basally-generated meltwater, likely due to increased flow through the distributed drainage system. Diurnal variability returned at the start of sub-period 5 as baseflow began to fall, suggesting meltwater was being routed more efficiently through a channelised system. Conductivity rose to reach a peak at the start of sub-period 6 as snowfall and low temperatures suppressed surface melting and basal meltwaters predominated, and the pattern is repeated around JD 197.

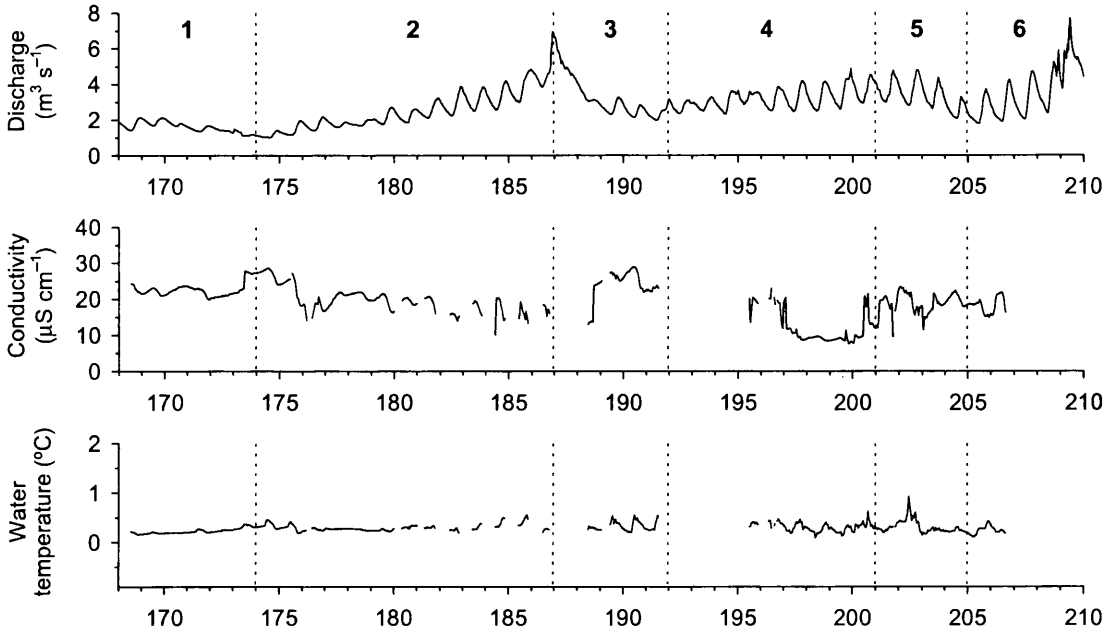

Figure 3.15 Catchment discharge, western proglacial stream conductivity and water temperature during the 1999 melt season.

During 1999, the early peak in conductivity was reached during a period of low discharge and freezing air temperatures (Table 3.2), indicating the complete suppression of surface melting. Falling conductivity during sub-period 2 occurs as discharge and air temperatures rise, again suggesting the contribution of surface melt to proglacial stream flow likely coupled with snowpack elution. High conductivities during sub-period 3 as discharge declined may indicate the predominance of meltwater released from basal storage following the spring event; however, subsequent variation in conductivity is considered to be unreliable.

3.4.4 Dye tracer investigation of the subglacial drainage system

3.4.4.1 Introduction

Dye-tracer investigations from moulins connected to the subglacial drainage system provide a means of directly investigating drainage system configuration (e.g. Nienow et al., 1998). Here, throughflow velocities of dye from given injection sites to the glacier snout are used to investigate the structure and spatial extent of the subglacial drainage

Table 3.5 Results of dye injections during the 1998 melt season. Detection indicates whether dye emerged in the eastern (E) or western (W) proglacial stream.

Moulin injection point	JD	I_t (hh:mm)	P_t (hh:mm)	Detection	x (m)	u (m s^{-1})
m3Ca	206	17:15	00:26	W	877	0.56
m3Ca	221	16:00	00:42	W	877	0.35
m4Ee	208	15:55	00:31	E	1551	0.83
m4Ee	217	18:05	00:34	E	1551	0.76
m3Cf	208	16:30	01:07	W	1293	0.32
m2Ec	208	14:15	*No Return*	-	799	-
m6Wa	209	15:25	01:03	E	2407	0.64
m5Wf	221	14:30	01:05	W	2227	0.57

I_t: time of dye injection; P_t: time of dye peak in the proglacial stream; x: distance from moulin to point at which dye was sampled from the proglacial streams; u mean dye travel velocity.

system during 1998. Throughflow velocities of greater than ~ 0.4 m s^{-1} indicate that a tracer has been routed entirely via a hydraulically efficient, channelised drainage system (Burkishmer, 1983). Previous investigations at Haut Glacier d'Arolla have shown flow velocities through distributed and channelised systems to be in the region of 0.025 and 0.7 m s^{-1}, respectively (Nienow et al., 1998).

3.4.4.2 Results

Table 3.5 shows the results of dye-tracing experiments from given injection points during the 1998 melt season (Figure 3.7). Moulins m3Ca, m3cf and m5Wf connected to the western glacial catchment, whereas dye was detected in the eastern proglacial stream from injections at moulins m4Ee and m6Wa. No return was observed from the single injection at moulin m2Ec. In the eastern catchment, flow velocities on JDs 208 and 217 (late sub-period 6 and early sub-period 8) at m4Ee ~ 1.5 km from the glacier snout are ~ 0.8 m s^{-1}. Flow velocity from m6Wa on JD 209 (late sub-period 6) ~ 2.5 km from the glacier snout is 0.64 m s^{-1}. In the western catchment, flow velocity from m3Ca on JD 206 (mid sub-period 6) ~ 0.9 km from the snout is 0.56 m s^{-1}; however, late in the monitored period on JD 221 (sub-period 8), flow velocity is < 0.4 m s^{-1}. At m3Cf, ~ 1.3 km from the snout, flow velocity on JD 208 is also < 0.4 m s^{-1}. However, flow velocity from m5Wf on JD 221 ~ 2.2 km from the snout is 0.57 m s^{-1}.

3.4.4.3 *Interpretation, discussion and conclusions*

The pattern of dye emergence during 1998 confirms the presence of two glacial sub-catchments; however, it suggests changes in the respective sizes of the western and eastern sub-catchments since detailed reconstructions were undertaken during 1989–1991 (Section 2.1.1; Sharp et al., 1993; Richards et al., 1996). Figure 3.9 indicates the approximate divide between the sub-catchments during 1998 based on the pattern of dye emergence (Table 3.5). The size and position of the sub-catchments compares well with drainage system reconstructions based on subglacial hydraulic potential (Section 1.1.2; Sharp et al., 1993), indicating a western sub-catchment draining the western glacier tongue and the principal tributary, and an eastern sub-catchment draining the eastern tongue and main accumulation area. Reconstructions based on dye tracing during 1989–1991, however, had indicated that the eastern sub-catchment drained only the lower eastern portion of the glacier tongue and that the western sub-catchment drained the western tongue, principal tributary and main accumulation area (Sharp et al., 1993).

During 1998, flow velocities from all but two injections indicate flow through hydraulically efficient subglacial channels. In the eastern catchment, flow velocity from m6Wa indicates that late in sub-period 6 the channelised system extended at least as far as the lower accumulation area. Flow velocity from m5Wf in the western sub-catchment demonstrates that by sub-period 8 the channelised system had extended up to and possibly beyond the confluence between the main glacier and principal tributary. This suggests the rate and pattern of drainage system evolution during 1998 was commensurate with that observed during previous melt seasons at Haut Glacier d'Arolla. During 1990 and 1991, dye injections at m5Wf and m5Ea (in the eastern catchment) then located ~ 2.5 km from the glacier snout indicated stable flow velocities indicative of channelised drainage from ~ JD 200 (Nienow et al., 1998). During 1990, the position of the channel head was inferred to have reached a position in the main accumulation area ~ 3.4 km from the snout by ~ JD 220 (Nienow et al., 1998).

Anomalous flow velocities are observed during two injections from m3Ca and m3Cf, respectively. Flow velocity from m3Ca was observed to decrease later in the season to values below 0.4 m s^{-1}. This result is likely caused by clockwise velocity hysteresis: strong clockwise velocity hysteresis has been observed from injections made at nearby

moulin m3Cb, resulting from flow through a tributary channel before joining a principal arterial channel (Nienow et al., 1996a). Clockwise hysteresis results in higher flow velocities during increasing bulk discharge and lower velocities after the discharge peak (Nienow et al., 1996a). The injection m3Ca from which the slower velocity was observed was made shortly after peak discharge, whereas the first injection was made during the bulk discharge peak. The other anomalous return was observed from m3Cf, from which flow velocities of < 0.18 m s^{-1} have consistently been observed during the height of the 1989–1991 melt seasons (Nienow et al., 1996b).

3.5 SUMMARY OF THE 1998 AND 1999 MELT SEASONS

This chapter began by emphasising the importance of obtaining independent evidence of the dynamic nature of the glacial and fluvioglacial systems if the mechanisms of sediment evacuation by subglacial meltwaters are to be rigorously identified. Sections 3.2 to 3.4 have investigated changes in ice motion and the hydrological functioning of the glacier basin related to the systematic evolution of meltwater sources and pathways. The major findings of the above analyses are summarised below and in Tables 3.6 and 3.7 for the 1998 and 1999 melt seasons.

3.5.1 Synthesis: 1998 melt season

The subperiods of the melt season identified and described in Section 3.2 (Table 3.1) are used as a basis for the summary and interpretation of seasonal evolution of the subglacial drainage during 1998 (Table 3.6).

— Sub-period 1. A period of low mean air temperature, occasional snowfall and low mean catchment discharge with weak, low-amplitude diurnal variability. Large lags between meteorological variables and proglacial discharge together with few peaked hydrograph forms suggest a predominantly distributed subglacial drainage system. Higher correlation between proglacial streamflow and air temperature than incident radiation suggests runoff was dominated by snowmelt. A residual channelised system likely existed along PDAs in the lower ~ 700 m of the glacier (Nienow et al., 1998).

Table 3.6 Glacial and fluvioglacial dynamics during the 1998 melt season.

Period 1, JD 135–152 (mid to late May)
Low discharge; snowmelt dominated; predominantly distributed drainage with residual channelised system (lower ~ 700 m)
Period 2, JD 153–158 (early June)
Rapidly increasing discharge mean; rapid ice motion event; snowmelt dominated; channelisation towards end of event in vicinity of PDAs along glacier tongue
Period 3, JD 159–164 (early to mid-June)
Discharge mean rapidly declining; snowmelt dominated; limited and/or immature channelised system beneath glacier tongue (lower ~ 2 km)
Period 4, JD 165–178 (mid to late June)
Rapidly increasing discharge mean; rapid ice motion event; snowmelt dominated but icemelt sources increasing; rapid channelisation towards end of event; rapid and increasing release of stored meltwater during channelisation; channels surcharged
Period 5, JD 179–189 (late June to early July)
Declining baseflow and increasing discharge amplitude; icemelt sources increasing; slower channelisation; declining rate of release of meltwater from storage; channels increasingly 'open' as baseflows decline
Period 6, JD 190–211 (early to late July)
Low baseflow, increasing amplitude; icemelt dominated, though sources still increasing; slow channelisation; channels predominantly 'open', but increasingly surcharged at peak melt as peak discharges increase; mean basal water pressures and horizontal motion increase
Period 7, JD 212–216 (late July to early August)
High baseflow, low diurnal amplitude due to rain and föhn; negligable rate of channelisation; channels 'open' or rarely surcharged; horizontal motion virtually negligible
Period 8, JD 217–221 (early August)
Low baseflow, high diurnal amplitude; icemelt dominated; mature channelised system; channels surcharged at peak melt; horizontal motion returns to pre-period 7 levels

— Sub-period 2. A period of rising mean air temperatures, frequent and heavy rainfall and steeply rising catchment discharge, baseflow and diurnal amplitude. Rapid horizontal ice velocities indicate increased flow through the distributed subglacial drainage system; velocities were attenuated near to the snout due to the presence of a residual channelised system. Long lags between proglacial streamflow and meteorological variables together with few peaked hydrographs suggest that the drainage system remained distributed throughout the event. The glacier remained

snow-covered with snowmelt the predominant source of supraglacial runoff; however, melt was strongly influenced by rainfall and correlations between proglacial streamflow and meteorological variables were low. Channelisation likely occurred towards the end of the event along PDAs beneath the glacier tongue, resulting in the release of stored meltwater and a rapid decline in forward glacier motion.

— Sub-period 3. A period of declining air temperature and precipitation that turned from rain to snow later in the sub-period. Mean discharge, baseflow and diurnal amplitude declined rapidly following the peak in discharge towards the end of sub-period 2. Long lags between streamflow and meteorological variables suggest distributed supraglacial and subglacial drainage systems remained. Higher correlations between proglacial streamflow and air temperature than incident radiation suggest snowmelt was the major source of catchment runoff; however, a number of peaked hydrographs suggest that some relatively efficient flowpaths also existed. It is possible that high rainfall during sub-period 2 resulted in the development of more hydraulically efficient percolation of meltwater through the snowpack and an efficient supraglacial drainage system beneath a saturated snow layer, particularly above the glacier tongue. These flowpaths are likely to have connected with the limited or immature channelised system formed during sub-period 2.

— Sub-period 4. A period of rising mean air temperature and increasing discharge mean, baseflow and diurnal amplitude. Lags between streamflow and meteorological variables fell sharply, indicating an increase in the efficiency of the translation of meteorological inputs into surface melt and its routing to the glacier snout. Predominantly peaked hydrographs suggest the contribution of rapidly routed icemelt from the ablation area; however, strong correlation between proglacial streamflow and air temperature as opposed to incident radiation suggest snowmelt remained the predominant source of glacier runoff. Stream conductivity was high towards the start of the sub-period but declined rapidly, indicating the dilution of long-residence time meltwaters by rapidly routed supraglacial runoff, likely coupled with snowpack elution. During the second half of the sub-period, rapid horizontal ice velocities occurred as proglacial discharge increased, indicating increased flow through the distributed system and enhanced basal separation. Horizontal velocities

attenuated downglacier, as in sub-period 2. Hydrograph forms evolved from low-peaked to medium-peaked during the rapid motion event, indicating an increase in discharge due to both increasing diurnal and baseflow components, and an increase in the rapidity with which runoff from snow and icemelt in the ablation area are transmitted to the glacier snout. Rapid channelisation occurred, particularly towards the end of the event, resulting in a decline in horizontal velocities despite increasing baseflow. Channels may have been surcharged since supraglacial runoff, augmented by the release of meltwater from storage, is likely to have increased faster than channel dimensions could adjust (Hooke et al., 1985).

— Sub-period 5. The first period of predominantly stable air temperature, which had a declining baseflow and increasing diurnal amplitude. Lags between proglacial streamflow and meteorological variables again fell sharply, indicating the exposure of larger areas of low-albedo glacier ice and the increasing efficiency of meltwater routing, although correlations between proglacial streamflow and meteorological variables indicate glacier runoff was still primarily due to snowmelt. Hydrograph forms during the sub-period demonstrated a still significant baseflow component; however, gradually declining baseflow demonstrated the continued retreat of the surface snowcover and expansion of the channelised system. Horizontal ice velocities also declined as meltwater was released from storage. Flow conditions in channels were likely to have been increasingly open due to declining baseflow and the increasing peakedness of diurnal runoff cycles.

— Sub-period 6. A period of high and predominantly stable air temperature; baseflow remained low whilst peak discharge slightly increased during the sub-period, resulting in a slowly increasing diurnal amplitude. Lags between proglacial streamflow and meteorological variables remained short, indicating efficient translation of meteorological inputs into surface melt and rapid routing of meltwater to the glacier snout. High-peaked hydrograph forms indicate a large proportion of discharge derived from rapidly routed ice melt, but peak discharges continued to increase as the snowline neared the upper accumulation area and supraglacial drainage became increasingly efficient. The channelised drainage network was thus likely to have extended beneath a large proportion of the glacier, with low or negligible rates of

channelisation. Channels likely remained predominantly 'open' due to low baseflow, and therefore may have closed slightly due to deformation of the overlying ice, but will have been increasingly surcharged during periods of peak melt due to the increasing peakedness of supraglacial runoff. This likely resulted in a strong lateral diurnally reversing hydraulic gradient that increased mean water pressures in the distributed system, with an associated increase in horizontal ice motion.

— Sub-period 7. A period of high air temperature, strong föhn and heavy rain in the afternoon and evenings. Discharge baseflow was high, although diurnal amplitudes were relatively low. Lags between proglacial stream flow and meteorological variables remained short and correlations were highest between proglacial streamflow and incident radiation, although runoff appeared to be significantly influenced by rainfall (medium-peaked hydrographs likely resulted from high baseflow and low diurnal peaks due to strong föhn and heavy late afternoon/evening rainfall). The rate of channelisation is expected to have been negligible, whilst horizontal ice motion fell to zero due to channels remain predominantly 'open'.

— Sub-period 8. A period of high air temperature, low discharge baseflow and high diurnal peaks, resulting in a high diurnal range. Lags between proglacial streamflow and meteorological variables remained short, and strong correlation between proglacial streamflow and incident radiation demonstrates ice melt was the predominant source of runoff. High-peaked hydrograph forms demonstrate high and rapidly routed runoff from icemelt through a channelised drainage system. High peak discharges are likely to have caused conduits to be highly pressurised during periods of peak melt; thus, horizontal motion returned to pre-sub-period 7 levels.

3.5.2 Synthesis: 1999 melt season

The subperiods of the melt season identified and described in Section 3.2 (Table 3.2) are used as a basis for the summary and interpretation of seasonal evolution of the subglacial drainage during 1999 (Table 3.7).

— Sub-period 1. A period of low mean air temperature, occasional snowfall with low catchment discharge and weak, low-amplitude diurnal variation. Long lags between

Table 3.7 Glacial and fluvioglacial dynamics during the 1999 melt season.

Period 1, JD 168–173 (mid-June)
Low discharge; snowmelt dominated; predominantly distributed drainage with residual channelised system (lower ~ 700 m)
Period 2, JD 174–186 (mid-June to early July)
Slowly rising discharge mean, baseflow and amplitude; rapid ice motion event; snowmelt dominated but icemelt sources increasing; channelisation towards end of event; initial storage followed by rapid and increasing release of meltwater during channelisation; channels surcharged
Period 3, JD 187–191 (early July)
Rapidly declining mean discharge; snowmelt dominated; limited and/or immature channelised system beneath glacier tongue (lower ~ 2 km); high, stable ice velocities due to storage of meltwater away from PDAs; channels 'open'
Period 4, JD 192–200 (early to mid-July)
Slowly rising discharge mean, amplitude and baseflow; snowmelt dominated but icemelt sources increasing; declining ice motion velocities due to release of meltwater from storage; slow channelisation; channels 'open' or rarely surcharged
Period 5, JD 201–204 (mid-July)
Declining discharge mean, baseflow and amplitude; remaining snowmelt dominated; limited and/or immature channelised system beneath glacier tongue (lower ~ 2 km); channels 'open'
Period 6, JD 205–209 (mid to late July)
Rising discharge mean, baseflow and amplitude; snowmelt dominated but icemelt sources increasing; low velocities; slow channelisation; channels 'open' or rarely surcharged

proglacial streamflow and meteorological variables and few peaked hydrograph forms suggest both inefficient translation of meteorological inputs into surface melt and of routing through the glacier drainage system. High correlation between proglacial streamflow and air temperature suggests the majority of catchment runoff was derived from snowmelt. A residual channelised system likely existed beneath the lower ~ 700 m of the glacier tongue.

— Sub-period 2. A period of slowly increasing mean air temperature, discharge mean, baseflow and diurnal amplitude. Lags between proglacial streamflow and meteorological variables fell slightly, indicating the more efficient translation of meteorological inputs into surface melt and routing through the glacier. Peaked

hydrograph forms were common, indicating the contribution of icemelt due to removal of the supraglacial snowpack, although strong correlation between proglacial streamflow and meteorological variables indicates runoff was strongly influenced by snowmelt. Electrical conductivity fell from high values at the end of sub-period 1 as surface melt was more rapidly routed to the snout. Horizontal ice velocities increase as flow through the distributed system is increased. Hydrograph forms evolved from low-peaked to medium-peaked during the rapid motion event, indicating a rise in catchment runoff due to both an increasing diurnal and baseflow component, and an increase in the rapidity with which runoff from icemelt in the ablation area is transmitted to the glacier snout. Channelisation likely occurred, particularly towards the end of the event, and resulted in a decline in horizontal velocities and the release of 'stored' meltwater.

— Sub-period 3. A period of declining air temperature and rapidly declining discharge, although baseflow remained high. Lags between proglacial streamflow and meteorological variables remained stable, but very poor correlation between streamflow and meteorological variables suggest little surface melting. High baseflow and high, stable horizontal velocities indicate the slow expansion and increase in efficiency of the channelised system. Channels are likely to have been 'open' as discharge fell.

— Sub-period 4. A period of slowly rising air temperatures, discharge mean, baseflow and diurnal amplitude. Lags between proglacial streamflow and meteorological variables fell slightly once more, indicating further increases in the efficiency of the translation of meteorological inputs into surface melt and its routing though the glacier. Medium-peaked hydrograph forms demonstrated still high baseflow, suggesting a large proportion of melt was still routed through distributed supraglacial and subglacial drainage systems. However, horizontal velocities gradually declined, indicating the continued expansion of the channelised system. Relatively low diurnal amplitudes and the slow removal of the supraglacial snowpack are likely to have resulted in only slow rates of channelisation. Channels were likely to have been surcharged, but supraglacial runoff is not peaked enough to have promoted spatially extreme high basal water pressures.

— Sub-period 5. A period of stable then declining air temperature; discharge mean declined along with baseflow and diurnal amplitude. Lags between proglacial streamflow and meteorological variables remained stable but relatively high, and strong correlation between proglacial streamflow and air temperature demonstrate the still large contribution to runoff from snowmelt. A limited and/or immature channelised system is therefore likely to have existed only beneath the glacier tongue. Channels are likely to have remained 'open' during falling discharge.

— Sub-period 6. A period of increasing air temperature, rising discharge mean, baseflow and amplitude. Lags between proglacial streamflow and meteorological variables remained stable but relatively long, and correlation remained highest between discharge and air temperature as opposed to incident radiation. Medium-peaked hydrographs indicate high proportions of long-residence time meltwaters and low proportions of icemelt, although icemelt sources were likely to have been slowly increasing. Gradual channelisation likely occurred with the slow retreat of the snowpack, and channels may occasionally have been surcharged.

3.6 CONCLUSIONS

- During both melt seasons, evolution of the subglacial drainage system, from a distributed to a channelised configuration, occurred systematically with the evolution of meltwater sources.

- During 1998, rapid channelisation occurred during the second event as the snowpack was rapidly removed to form an extensive system by the beginning of sub-period 6. Thereafter, only marginal increases in efficiency occurred, although increasingly peaked runoff likely resulted in a strong diurnally reversing hydraulic gradient (Hubbard et al., 1995) and increasing horizontal ice motion (Willis, 1995).

- During 1999, slow removal of the supraglacial snowpack resulted in the retarded evolution of meltwater sources and the subglacial drainage system, such that an extensive, efficient channelised system is unlikely to have existed by the end of the monitored period.

4.

Sediment provenancing: suspended sediment transport

4.1 INTRODUCTION

4.1.1 Aims and rationale

In this chapter, records of proglacial suspended sediment transport from the 1998 and 1999 melt seasons are used to investigate the mechanisms of suspended sediment evacuation by the subglacial drainage system. Previous studies have generally implied that sediment evacuation is largely dependent upon an early melt season increase in discharge (Section 1.2). High sediment availability coupled with high discharge are believed to result in high suspended sediment concentrations, and very efficient sediment evacuation may occur during spring events where: 1) ice-bed separation allows wider access of meltwater to the glacier bed; 2) basal sliding disturbs basal sediments; and 3) channels may be formed forcefully under high pressures. Studies have also emphasised the decline in suspended sediment concentration later in the season due to exhaustion of sediment sources near to subglacial channels and/or the dilution of available sediments by increasing discharge. However, Section 1.2 considered that such studies have largely failed to reliably link variation in suspended sediment concentration to processes operating in the subglacial environment and have therefore contributed little to our understanding of subglacial hydrology. In this chapter, variation in suspended sediment

transport is interpreted against a detailed knowledge of the dynamic nature of the glacial and fluvioglacial systems in order to identify more rigorously the mechanisms of sediment evacuation by subglacial meltwater.

4.1.2 Investigating relationships between sediment transport and discharge

Suspended sediment transport from subglacial drainage systems is commonly presented as either suspended sediment concentration or load. Studies that have investigated the mechanisms of subglacial sediment evacuation by fluvioglacial processes have generally employed records of suspended sediment concentration, since the concentration of sediment is suggestive of the efficiency of the drainage system at accessing and entraining basal sediments irrespective of discharge. For geomorphological purposes, such as the calculation of catchment sediment yields or denudation rates (cf. Hallet et al., 1996), suspended sediment transport is commonly presented as suspended sediment load (i.e. the weight of sediment transported by the proglacial stream per unit of time). Analysis of suspended sediment transport in the context of the investigation of the mechanisms of suspended sediment evacuation by subglacial drainage is discussed below.

4.1.2.1 Suspended sediment concentration

Variation in suspended sediment concentration has typically been related to variation in proglacial discharge, since the latter provides a crude indicator of subglacial hydrological conditions (e.g. flow capacity). The development of 'ordinary' linear rating curves is by far the most common means of investigating such relationships, due to the simplicity of their construction and interpretation (Hodgkins, 1999). Analysis commonly involves the logarithmic transformation of both variables in order to linearize the relationship and stabilise variance in the individual series (Gurnell et al., 1994; Willis et al., 1996). r^2 values for log-transformed data are often high, suggesting that flow capacity is a key control on suspended sediment entrainment and transport. However, it is important to note that: 1) high r^2 values should not be unexpected where n (the number of observations) is large; and 2) rating curves developed for one season's data are rarely found to be applicable outside that season (Fenn, 1989). Furthermore, the relationship

between suspended sediment concentration and discharge during individual melt seasons has been found to evolve (Gurnell et al., 1992a, 1994; Østrem, 1975).

The method of subdividing individual melt seasons based on the systematic evolution of meltwater sources and pathways, demonstrated in Chapter 3, has also been applied to the analysis of relationships between suspended sediment concentration and discharge. Changing relationships between suspended sediment concentration and discharge are reflected in the changing form of the linear rating curve. Changes in r^2 may also occur, suggesting changing dependence of suspended sediment concentration on discharge as the melt season progresses. Albeit erroneously, Gurnell et al. (1992a, 1994) used the changing slope of rating curves developed for various subperiods of the 1989 and 1990 melt seasons to make inferences about the changing availability of basal sediment at Haut Glacier d'Arolla (see Section 2.1.4). Hodson et al. (1998) used the technique more reliably at Austre Broggerbreen, Svalbard by plotting the regression relationships over the range of discharges recorded during individual subperiods of the melt season. By identifying statistically significant changes in the form of the rating curves, temporal trends in the relationship between suspended sediment concentration and discharge were reflected in changes in both regression intercept and slope.

Relationships between suspended sediment concentration and discharge for an individual melt season generally exhibit low r^2 values indicative of high scatter, suggesting that 'seasonal' ordinary rating curves are inappropriate. Fenn et al. (1985) considered such scatter to be the result of 5 separate effects: 1) seasonal variations in sediment availability, as represented by early season flushing and late season exhaustion effects; 2) diurnal variations in sediment availability, especially the hysteresis effect related to diurnal flow cycles (but also exhaustion over a number of days following recent high flows, e.g. Clifford et al., 1995b); 3) transient flushes of sediment that are independent of discharge and therefore generated by some other means; 4) sediment sources and sinks in the proglacial region; and 5) sediment supplied by rainfall-induced events. It may be possible to isolate seasonal variations in sediment availability by developing relationships for subperiods of the melt season, such that ordinary rating curves for individual subperiods should demonstrate improved r^2 values with respect to the seasonal rating curve. However, diurnal hysteresis effects are more difficult to account

for, since in effect there are two values of suspended sediment concentration for each value of discharge in a given diurnal flow cycle.

To investigate the effect of diurnal hysteresis, Collins (1979b) estimated separate relationships for periods of rising and falling discharge during diurnal flow cycles at Gornergletscher, Switzerland. Different relationships were found for rising and falling limbs; however, there appears to have been little consistency in the form of relationships for rising and falling limbs respectively, and r^2 values were rarely better than a single relationship estimated for the whole season. More commonly, hysteresis effects have been accounted for by lagging the suspended sediment series in order to maximise r^2 (e.g. Gurnell and Fenn, 1984a; Fenn et al., 1985; Gurnell et al., 1994). Such methods have indicated that for temperate alpine glaciers, suspended sediment concentration precedes discharge by ~ 1–2 hours. However, coefficients of determination may increase only marginally (e.g. Gurnell and Fenn, 1984a; Fenn et al., 1985), suggesting that lagging poorly accounts for the hysteresis effect or that a large proportion of the scatter is from other sources.

A different approach has been to eliminate temporal variations in sediment availability by fitting rating curves to suspended sediment concentration and discharge after first differencing the series; i.e. by replacing variable x_t by Δx_t, where $\Delta x_t = x_t - x_{t-1}$ (e.g. Gurnell and Fenn, 1984a; Gurnell et al., 1992; Willis et al., 1996). First differencing generates a stationary time series where rate of change of suspended sediment concentration is related directly to rate of change of discharge. However, r^2 values for such relationships are generally very poor ($r^2 < 0.1$; Gurnell and Fenn, 1984a; Willis et al., 1996). Lagging the suspended sediment concentration series only marginally improves r^2; however, it demonstrates that rates of change of suspended sediment concentration still precede rates of change of discharge and therefore some form of hysteresis remains.

Despite eliminating temporal changes in sediment availability, it is not unusual for a large proportion of the variance in the suspended sediment concentration series to remain unexplained (e.g. Gurnell et al., 1992a). However, it is inappropriate to assume *a priori* that suspended sediment concentrations are controlled solely by flow capacity, and

instead multivariate rating curves that include variables other than discharge may account for some of the scatter (e.g. Willis et al., 1996; Hodson and Ferguson, 1999). These additional variables are intended to represent seasonal and diurnal trends in suspended sediment availability, and variations in sediment supply due to rainfall, to which a suggestion of some process significance may be ascribed. Diurnal hysteresis is commonly represented using the variable 'rate of change of discharge', which is obtained by first differencing the raw (Richards, 1984; Willis et al., 1996) or log-transformed (Hodson and Ferguson, 1999) discharge series. Using stepwise or best subsets regression, an appropriate multivariate rating curve is identified using only the variables that are statistically significant, typically at $p < 0.05$ (Hodson and Ferguson, 1999). Such techniques have mostly been applied to high-arctic glaciers without subdivision of the melt season into hydrologically 'stable' periods. These models have had mixed success, achieving only modest r^2 values (~ 0.5) whilst the residual series remain highly autocorrelated (e.g. Willis et al., 1996; Hodson and Ferguson, 1999; Hodgkins, 1999).

Analysis of the residual series is a common method of evaluating the performance of ordinary and multivariate rating curves. r^2 values indicate the proportion of the variance in the dependent series explained by the independent variables; however, some of the variance in the output series may be due to random processes, such as sampling error or bank collapse within subglacial channels, and therefore r^2 values of 1 may be impossible to achieve. The presence of autocorrelation in the residual series indicates pattern in the dependent series that the rating curve has failed to account for. Two forms of autocorrelation can be identified depending on its source (Fenn et al., 1985). 'Quasi-autocorrelation' results from: 1) the inappropriate specification of the regression model, for example applying a linear rating curve to non-linear data; 2) omitting relevant explanatory variables; or 3) failing to identify lags or changes in response between the dependant and independant variables. 'True-autocorrelation' is due to an inherent dependence in the dependent series such that values in the series are not independent of each other but instead depend upon both previous values and upon present and previous random disturbances. True-autocorrelation is likely to exist in suspended sediment time series if basal sediment sources are accessed discretely and quasi-randomly, increasing sediment availability over several successive measurements (Willis et al., 1996; Hodson

and Ferguson, 1999). However, true-autocorrelation should also be expected due to the settling velocity of fine particles being lower than their entrainment velocity, meaning that sediment is likely to remain in transport even if discharge falls (Richards, 1982; Willis et al., 1996).

High autocorrelation in the residual series from bivariate rating curves was successfully removed by Gurnell and Fenn (1984a) using first differencing; however, they argued that such methods produce rating curves that are remote from the original data and, as a result, are difficult to interpret. As noted above, introducing additional explanatory variables to create multivariate rating curves can also fail to remove all of the autocorrelation. As a result, auto-regressive moving average (ARIMA) models have been applied that aim to characterise the internal dependence in the residual series (e.g. Gurnell et al., 1992a; Willis et al., 1996). However, Hodson and Ferguson (1999) have argued that ARIMA parameters are difficult to interpret physically when the models are applied to residual series. As shown in Section 2.1.4, Gurnell et al. (1992) inferred seasonal exhaustion of suspended sediment at Haut Glacier d'Arolla during 1989 from the moving average component of their ARIMA models, whilst sediment load data (Gurnell et al., 1995b; see also Table 2.4) and the form of bivariate rating curves (Gurnell et al., 1994; see also Figure 2.3) do not support this conclusion. Instead, Hodson and Ferguson (1999) found that simply including the previous value of suspended sediment concentration in the original multivariate rating curve satisfactorily removed almost all the residual autocorrelation.

An assumption of all regression and time series (e.g. ARIMA) techniques is that a successful model will remove all residual autocorrelation: in effect, the autocorrelation pattern will resemble 'white noise' (e.g. Willis et al., 1996). It could be argued that, in pursuit of this aim, many studies have resorted to complex rating curve/time series models in which the physical meaning of many of the explanatory variables is of secondary importance. Moreover, the variance in the residual series, which is held to be truly random and somehow, therefore, unimportant, is rarely subject to scrutiny. However, using a simple and physically comprehensible ordinary rating curve for the entire melt season at Haut Glacier d'Arolla, Clifford et al. (1995b) demonstrated that the residual series from a very simple model can be very revealing of important systematic

trends and processes. Clearly, there is value in some of the more complicated regression techniques, enabling the isolation of sediment availability factors, changing relationships between variables over time and additional important explanatory variables. However, care must be taken such that models do not become over-specified and explanatory variables are introduced only with a sound physical basis for doing so. Confidence limits (cf. Hodson and Ferguson, 1999) should be applied to autocorrelation patterns to test for significance in the remaining pattern before further investigation is undertaken. Attention should also be paid to time series plots of the residuals, even when remaining autocorrelation has been eliminated, as this may still be revealing of very important processes. For example, Willis et al. (1996) linked large positive residuals, which represent short-term sediment flushes, to glacier dynamics at Midtdalsbreen, Norway. A degree of correlation was found between sediment flushes and glacier motion peaks, suggesting sudden reorganisation of subglacial drainage associated with enhanced forward glacier motion. Such detailed information, however, is rarely available, and, when the remaining variance is small (i.e. r^2 is large), sampling errors are likely to obscure any meaningful pattern.

4.1.2.2 Suspended sediment load

Rating curves have also been used to investigate the relationship between suspended sediment load and discharge, although such relationships are somewhat spurious since discharge is incorporated into both variables. More usefully, annual suspended sediment loads have been used to estimate subglacial erosion rates (e.g. Hallet et al., 1996). By converting loads into spatially-averaged rates of sediment evacuation (or yields) and assuming a homogeneous bedrock density, a rough estimate of the rate of mechanical catchment denudation can be made.

Emphasis is generally placed on annual yields that are commonly found to be very variable even for glaciers of similar type, bedrock lithology and location (see Section 1.1). A more profitable approach might be to examine how yields vary at seasonal or sub-seasonal scales, and how this may be related to glacial or glacier-hydrological processes. An understanding of variation in sediment load at sub-seasonal scales may explain why annual yields are highly variable and hence little progress has been made in

understanding the efficiency of glacier erosion. An enhanced understanding of this problem is likely to have significant geomorphological implications.

4.2 SUSPENDED SEDIMENT TRANSPORT

4.2.1 Introduction

This section presents the results of the suspended sediment monitoring programme during the 1998 and 1999 melt seasons. The discharge record for both seasons represents runoff from the entire catchment; hence, suspended sediment load was calculated for the glacier as a whole using suspended sediment concentration from either the eastern or western glacial sub-catchment. The methods used and likely errors associated with the calculations are discussed below. An initial description of sediment concentration and evacuation is followed by analysis of their relationship with catchment discharge using ordinary linear regression. This approach aims to determine the suitability of seasonal ordinary rating curves and the importance of discharge for the evacuation of basal sediment from the subglacial drainage system.

4.2.2 Data preparation

Suspended sediment concentration and load are shown in Figures 4.1 and 4.2 for the monitored periods of the 1998 and 1999 melt seasons, respectively. The diagrams also show catchment discharge and indicate the various subperiods of each melt season described in Section 3 (Tables 3.1 and 3.2).

4.2.2.1 Suspended sediment concentration

Suspended sediment concentration was monitored using a combination of continuous turbidity measurement and automated pump sampling (Section 2.2). The calibrated 5 minute-averaged turbidity series (Figures 4.1 and 4.2) provides greater temporal coverage of each melt season due to frequent gaps in the automated sampling record. Analysis of turbidity records for individual sensors located ~ 0.3 m apart in the flow suggests measurements are representative of mean suspended sediment concentrations in

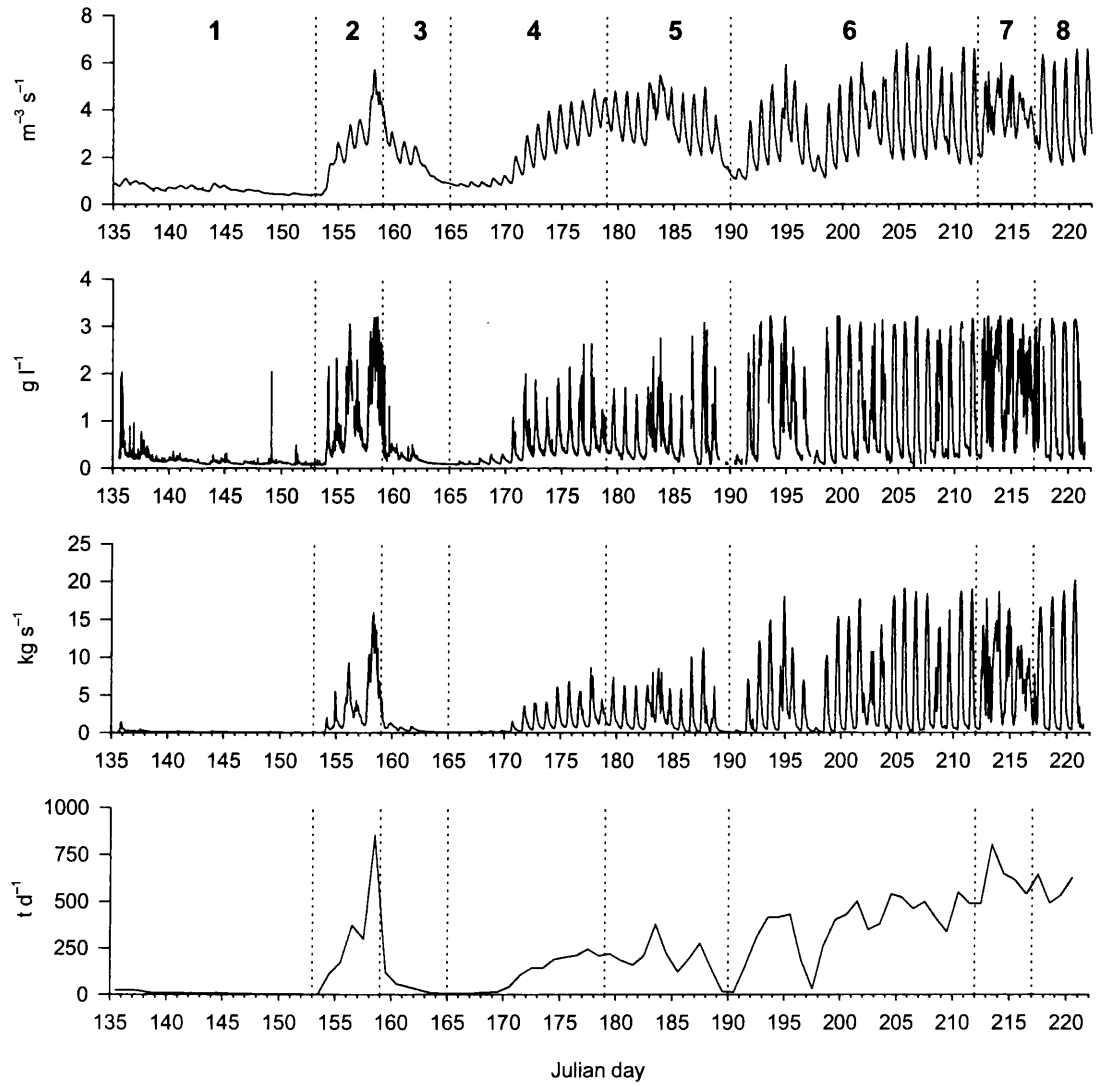

Figure 4.1 Catchment discharge, calibrated turbidity, hourly mean suspended sediment load and daily total catchment suspended sediment load during the 1998 melt season.

the stream cross-section (see Section 2.3.1.2). Field calibration of the turbidity series resulted in good relationships between turbidity and suspended sediment concentration, although the calibrated series are likely to slightly underestimate actual suspended sediment concentrations by ~ 15–20 % (Section 2.3.1.2).

4.2.2.2 Suspended sediment load

Suspended sediment load is calculated using hourly instantaneous measurements of suspended sediment concentration and discharge (cf. Collins, 1989). At Haut Glacier

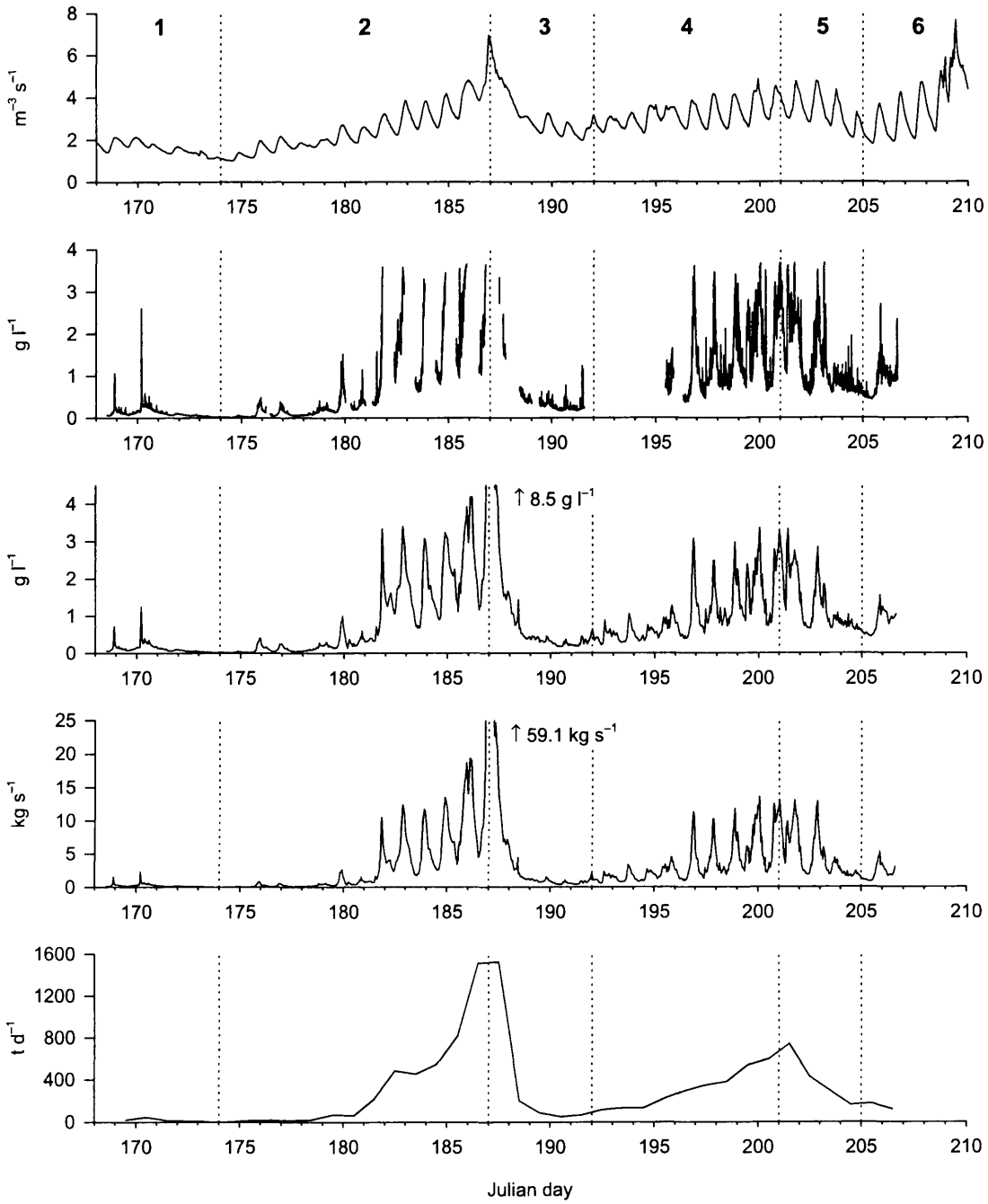

Figure 4.2 Catchment discharge, calibrated turbidity, cross-interpolated hourly suspended sediment concentration, hourly mean suspended sediment load and daily total catchment suspended sediment load during the 1999 melt season.

d'Arolla, catchment discharge is recorded as hourly mean values; therefore hourly mean suspended sediment load (kg s^{-1}) was obtained from catchment discharge (m^3 s^{-1}) and hourly-averaged calibrated turbidity (g l^{-1}). Hourly total suspended sediment load (kg h^{-}

^{1}) was obtained by integrating hourly mean suspended sediment load over time. Hourly totals were then summed into daily totals (t d^{-1}) for the monitored periods. Because a complete, unbroken turbidity series was not available for each of the monitored periods, missing values were interpolated in order to avoid significant error in the calculation of daily suspended sediment loads. The interpolation methods used for each season are described below.

1998 melt season

During the 1998 melt season, suspended sediment loads were obtained from the hourly-averaged turbidity series from the western proglacial stream. The hourly-averaged series provided good coverage of the monitored period, with just 5.3 % of values missing and only 6 gaps greater than 6 h. Gaps significantly shorter than the wavelength of diurnal variations in turbidity (i.e. < 6 h) and were interpolated linearly. Major gaps on JD 185–186 and 192–193 were interpolated using ordinary rating curves derived from values of discharge and turbidity during adjacent periods of rising and falling discharge (Table 4.1). Values interpolated using separate rating curves for rising and falling limbs from adjacent hydrological periods (Table 4.1) provide a better fit with measured data than values derived from seasonal rating curves (Figure 4.3 a). Remaining gaps on JD 189–

Table 4.1 Ordinary rating curves for discharge (independent variable) versus turbidity (dependent variable) used to model missing turbidity values during 1998.

Gap / Rating curve	n	a	b	t_a	t_b	p_a	p_b	r^2
Gap 1: JD 185 2300 – JD 186 1200								
Rising (JD 185 1000 – JD 185 1800)	9	–2.45	3.85	–13.69	11.74	< 0.001	< 0.001	0.945
Falling (JD 185 1900 – JD 185 2200)	4	–2.08	2.71	–5.98	4.7	0.027	0.042	0.876
Gap 2: JD 192 1900 – JD 193 1000								
Falling (JD 191 1900 – JD 192 0800)	10	–1.15	2.63	–10.13	10.94	< 0.001	< 0.001	0.930
Rising (JD 192 0900 – JD 192 1800)	13	–1.02	1.82	–18.53	11.34	< 0.001	< 0.001	0.914

n: number of cases; a, b: regression intercept and slope, respectively; t_a,t_b; t-statistics associated with the regression intercept and slope, respectively; p_a, p_b; p-statistics associated with the regression intercept and slope, respectively

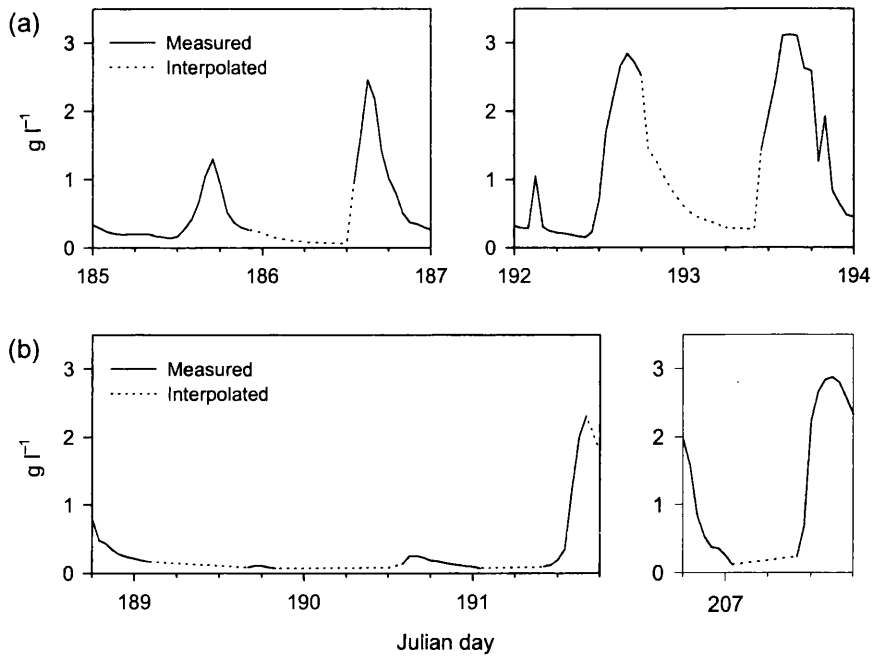

Figure 4.3 Missing values during the 1998 melt season modelled using (a) linear rating curves for rising and falling discharge values and (b) linear interpolation.

192 and JD 207 resulted from the turbidity sensor being above the water level during periods of very low flow (see Section 2.1.1.2). Due to the unusually low flow conditions, rating curves estimated for these periods resulted in the significant overestimation of suspended sediment concentration, and satisfactory modelling of missing values was achieved using linear interpolation (Figure 4.3 b).

1999 melt season

The hourly-averaged turbidity series for the eastern proglacial stream demonstrates poor temporal coverage, with 26 % of values missing and a large number of gaps < 6 h. The size of a number of gaps relative to the wavelength of typical diurnal variations in turbidity presents particular problems. During these parts of the monitored period, there is insufficient data to accurately model missing values from rating curves, and linear interpolation of missing values is likely to result in significant errors. Instead, 'cross-interpolation' of the turbidity and suspended sediment concentration series obtained from automated sampling was used to model missing values in one time series using contemporaneous variation within another. An equation was developed to linearly

interpolate missing values in the turbidity series whilst adjusting values for contemporaneous variation in the suspended sediment concentration series. As the net variation in both series may differ slightly over the interpolated period, the equation subtracts the gradient of the net variation in suspended sediment concentration over the interpolated period. Thus, for missing values of turbidity (T) between measured values at time $t = 0$ and $t = x$,

$$T_{t+j} = T_t + G_T - G_{SSC} + \left[SSC_{t+j} - SSC_t\right] \qquad [j = 1 \ldots (n-2)] \qquad (4.1)$$

where SSC is suspended sediment concentration, and G_T and G_{SSC} are the gradient of T and SSC, respectively, over the same period, defined as

$$G_{SSC} = \frac{SSC_{t_x} - SSC_{t_0}}{n+1} \qquad (4.2)$$

and

$$G_T = \frac{T_{t_x} - T_{t_0}}{n+1} \qquad (4.3)$$

Linear interpolation was used to increase the resolution of the suspended sediment concentration series to match that of the turbidity series and to interpolate small gaps of less than 6 h. The series provided good coverage during periods of missing data and demonstrated a good match with turbidity for values below 3 g l^{-1}. However, variation in suspended sediment concentration above this threshold is often significantly greater than for the turbidity record, and the magnitude of the discrepancy varies throughout the monitored period. Such discrepancies occur during periods when suspended sediment samples are suspected to have been contaminated by bedload. The turbidity series was therefore used to calibrate the suspended sediment concentration series prior to cross-interpolation. Using standard regression techniques, the following relationship was obtained from 222 simultaneous measurements of suspended sediment concentration (SSC) and turbidity (T)

$$\log_{10} T = 0.106 + 0.756 \log_{10} SSC - 0.204 \log_{10} SSC^2 \qquad (4.4)$$

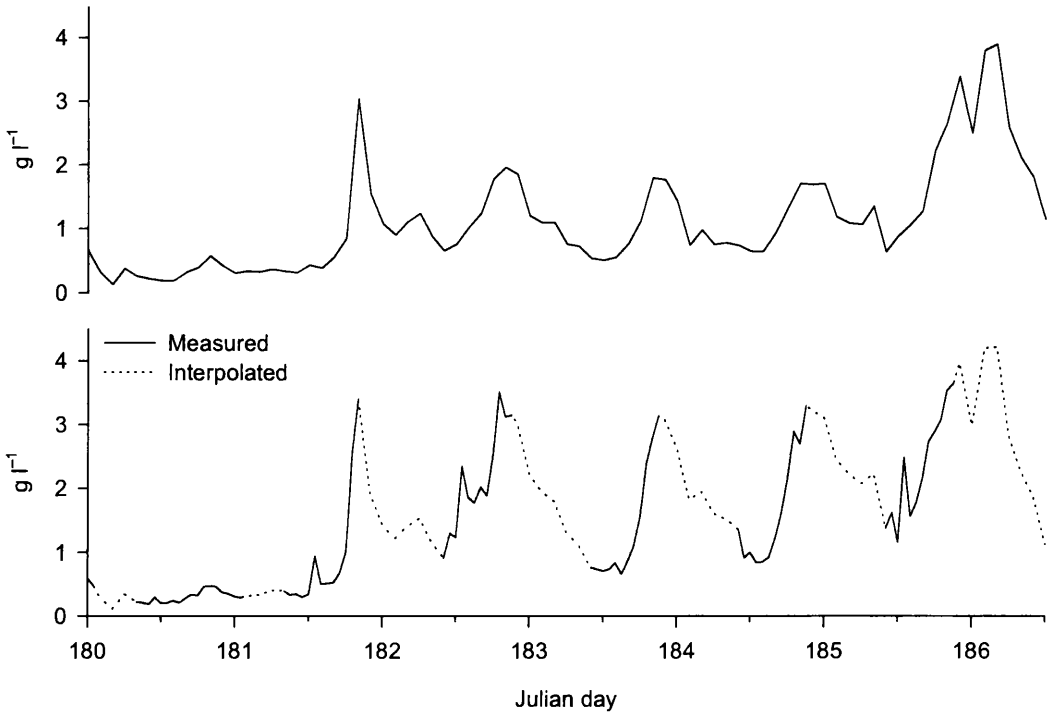

Figure 4.4 Cross-interpolated turbidity series (below) from the calibrated suspended sediment concentration series (above) during part of the 1999 melt season.

Table 4.2 Turbidity rating curves used to interpolate missing values from JD 186 21:00 – 187 10:00. For all rating curves, $p < 0.001$ for both predictors.

Rating curve		n	a	b	t_a	t_b	r^2	SSC_p
JD 186 0000 – 186 1900	falling	11	0.543	0.205	28.66	5.13	0.731	5.83
	rising	10	0.578	0.223	59.88	6.99	0.842	
JD 181 1100 – 186 1000	(all)	120	–0.818	2.06	–11.66	15.17	0.656	8.16
JD 181 1100 – 186 1000	rising	57	–0.941	2.22	–7.81	9.52	0.615	8.52
	falling	63	–0.679	1.86	–12.36	17.53	0.832	

n: number of cases; a, b: regression intercept and slope, respectively; t_a,t_b: t-statistics associated with the regression intercept and slope; SSC_p: modelled peak suspended sediment concentration

for which $r^2 = 0.916$ and p was < 0.001 for all predictors except the intercept ($p = 0.355$). Figure 4.4 shows the results of cross-interpolation for a short period of the monitored period during which just below 50 % of turbidity values are missing.

One remaining gap in the turbidity series of 14 h during peak discharge over JD 186 21:00 h – 187 10:00 was modelled using separate rating curves estimated for rising and falling discharge during the previous 5 days (Table 4.2). Rating curves estimated for rising and falling discharge on JD 185–186 immediately before the event demonstrated an exceptionally poor fit with the measured data. Composite curves representing periods of rising and falling discharge during the period of increasing diurnal discharge amplitude over the 5 days prior to the event provided a better fit despite their lower statistical significance.

Errors associated with the calculation of catchment sediment load

Calculated suspended sediment load during both melt seasons are unlikely to be directly comparable. Calculation of suspended sediment load during 1998 and 1999 assumes that measurements of suspended sediment concentration from either glacial sub-catchment are representative of suspended sediment concentration from both sub-catchments. However, the generally non-linear relationship between sediment transport and discharge (Alley et al., 1997) predicts that suspended sediment load will be higher from the larger eastern sub-catchment due to consistently higher discharges. Sediment is also contributed to the eastern sub-catchment from marginal streams below Bouquetins (Figures 2.1 and 2.3), the concentration of which is unknown but is suspected to be high.

Suspended sediment loads during 1998 will be significantly underestimated, especially during the height of the melt season. Here, loads will be significantly underestimated due to: 1) higher peak discharges in the eastern sub-catchment, resulting in higher suspended sediment concentrations than those measured in the western sub-catchment; 2) systematic underestimation of suspended sediment concentration due to calibration of the turbidity series; and 3) saturation of turbidity sensors at high suspended sediment concentrations during high discharges. During 1999, suspended sediment loads are likely to be significantly overestimated due to the larger size of the eastern sub-catchment and significant contributions of extraglacial sediment. Again, errors will be greatest during the height of the melt season due to higher peak discharges in the eastern sub-catchment with respect to the western sub-catchment, and consistently high runoff from cirque glaciers below Bouquetins.

Table 4.3 Summary of catchment discharge and suspended sediment transport during monitored periods of the 1998 and 1999 melt seasons.

Period	Q_{mean} ($m^3 s^{-1}$)	SSC_{mean} ($g l^{-1}$)	HML_{mean} ($kg s^{-1}$)	DCQ_{mean} ($m^3 d^{-1}$)	DCL_{mean} ($t d^{-1}$)
1998 melt season					
1	0.647	0.166	0.120	55000	9.2
2	2.566	0.988	3.477	224000	302.9
3	1.877	0.229	0.537	16000	44.0
4	2.137	0.421	1.265	185000	109.7
5	3.414	0.621	2.233	294000	192.4
6	3.150	1.079	4.249	272000	367.2
7	3.816	1.689	7.151	330000	619.2
8	3.433	1.257	6.050	307000	573.5
1999 melt season					
1	1.610	0.127	0.223	130000	15.5
2	2.492	0.911	3.622	243000	443.0
3	3.194	0.601	4.852	235000	104.9
4	3.191	1.010	3.503	286000	376.8
5	3.353	1.354	4.851	262000	266.9
6	2.421	0.823	2.097	218000	175.3

Q: hourly mean catchment discharge; *SSC*: suspended sediment concentration; *HML*: hourly mean suspended sediment load; *DCQ*: daily catchment discharge; *DCL*: daily catchment suspended sediment load

4.2.2.3 Summary of results

Suspended sediment transport for monitored periods of the 1998 and 1999 melt seasons is shown in Figures 4.1 and 4.2 summarised in Table 4.3. Catchment suspended sediment load is unlikely to be directly comparable between seasons due to the errors discussed above; however, it is possible to consider the pattern of suspended sediment transport and its relationship to catchment discharge within each melt season.

During 1998 (Figure 4.1 and Table 4.3), mean catchment discharge (*Q*), suspended sediment concentration (*SSC*) and daily catchment suspended sediment load (*DCL*) are initially low. Mean *Q*, *SSC* and *DCL* demonstrate an initial peak during period 2,

following which mean *SSC* and *DCL* decline rapidly whilst mean *Q* remains significantly higher than values prior to period 2. Throughout the remainder of the season, variation in mean *SSC* and *DCL* generally follows that of mean *Q* and *DCQ*, respectively, suggesting that flow competence and capacity are important controls on sediment evacuation. Highest mean *SSC* and *DCL* coincides with the highest mean *Q* and *DCQ* during period 7. However, during periods 5, 6 and 9, mean *DCL* continues to increase despite relatively stable mean *DCQ*, suggesting increasing sediment availability. Errors in the calculation of catchment suspended sediment load during 1998 suggest mean *DCL* is likely to be greatly underestimated towards the monitored period, and therefore the pattern of increasing suspended sediment transport will likely have been much greater than observed.

Mean *SSC* and *DCL* during 1999 (Table 4.3) exhibit a more complicated pattern that partly reflects the subdivision of the melt season (Figure 4.2). Mean *SSC* exhibits two main peaks during periods 2 and 5; however, mean *DCL* peaks during periods 2 and 4, coinciding with peaks in mean *Q*. Clearly, since discharge is included in both variables, *DCL* might be expected to exhibit a closer relationship with mean *Q* than *SSC*. The weak relationship between mean *SSC* and *Q* suggests that other processes may have influenced measurements of suspended sediment transport during the 1999 melt season (at least within the eastern glacial catchment).

4.2.3 Relationships between suspended sediment transport and discharge

Patterns of suspended sediment transport at Haut Glacier d'Arolla during the 1998 and 1999 melt seasons suggest links between suspended sediment transport and discharge. Here, the nature of the relationship between suspended sediment transport and discharge is described using ordinary linear regression in order to investigate the importance of discharge for sediment evacuation by the subglacial drainage system.

4.2.3.1 Suspended sediment concentration

Scatter plots of catchment discharge versus suspended sediment concentration are shown in Figure 4.5 for the monitored periods of the 1998 and 1999 melt seasons. The suspended sediment concentration series shown are interpolated hourly mean suspended

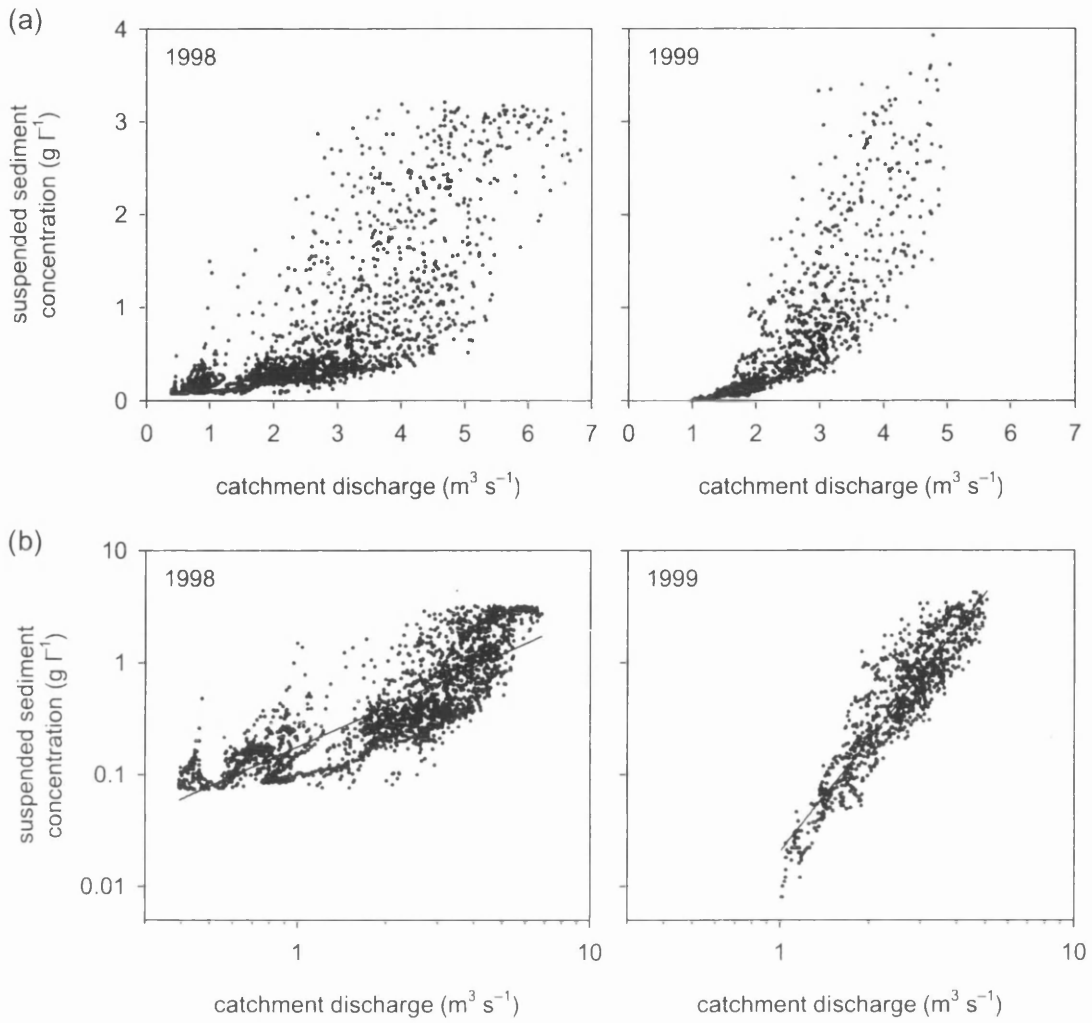

Figure 4.5 (a) scatter plots of suspended sediment concentration versus catchment discharge for the 1998 and 1999 melt seasons. (b) log-log scatter plots showing lines of best fit from the regression relationships given in Table 4.4.

sediment concentration for 1998 and cross-interpolated hourly suspended sediment concentration for 1999. Values during the large gap from JD 186 21:00 h – 187 10:00 during 1999 that were modelled from a discharge versus suspended sediment concentration rating curve are excluded so as not to arbitrarily increase the significance of the seasonal ordinary rating curve.

Relationships between discharge and suspended sediment concentration are positive but non-linear and subject to considerable scatter (Figure 5.4 a). A log-log transformation of the data (cf. Fenn et al., 1985) results in the variables being more linearly and

Table 4.4 Seasonal ordinary rating curves between catchment discharge and suspended sediment transport variables for the 1998 and 1999 melt seasons.

Independent variable	Dependent variable (lag in h)	n	a	b	p_a	p_b	r^2
1998 melt season							
log$Q$	logSSC	2061	–0.762	1.185	< 0.001	< 0.001	0.680
log$Q$	logSSC (–1)	2060	–0.769	1.195	< 0.001	< 0.001	0.697
$\log Q_t - \log Q_{t-1}$	$\log SSC_t - \log SSC_{t-1}$	2060	–0.001	2.344	0.796	< 0.001	0.405
log$Q$	logHML	2061	–0.762	2.184	< 0.001	< 0.001	0.879
log$Q$	logHML (–1)	2060	–0.766	2.194	< 0.001	< 0.001	0.886
logDCQ	logDCL	85	–10.05	2.292	< 0.001	< 0.001	0.926
1999 melt season							
log$Q$	logSSC	901	–1.679	3.296	< 0.001	< 0.001	0.837
$\log Q_t - \log Q_{t-1}$	$\log SSC_t - \log SSC_{t-1}$	899	0.001	1.336	0.791	< 0.001	0.061
$\log Q_t - \log Q_{t-1}$	$\log SSC_t - \log SSC_{t-1}$ (+1)	897	0.001	1.591	0.738	< 0.001	0.085
log$Q$	logHML	915	–1.672	4.274	< 0.001	< 0.001	0.903
logDCQ	logDCL	37	–21.36	4.381	< 0.001	< 0.001	0.940

n: number of observations; a, b: regression intercept and slope, respectively; p_a, p_b: p-values associated with the regression intercept and slope, respectively; refer to Table 4.3 for meaning of Q, *SSC*, *MHL*, *DCQ* and *DCL*

homoscedastically distributed (Figure 5.4 b) and suggests clear differences between the monitored periods. The most prominent feature is a shallower gradient in the relationship between suspended sediment concentration and discharge during 1998. An initial attempt to describe the relationship during each melt season was made by fitting ordinary rating curves to the transformed data of the form

$$\log SSC = a + b \log Q \qquad (4.5)$$

where *SSC* and Q are suspended sediment concentration and catchment discharge, respectively. The line of best fit is shown for each season is shown in Figure 4.5 (b).

The slope and intercept of resulting equations (Table 4.4) confirm the perceived differences in the form of the relationship between the two seasons. Such differences are likely to reflect: 1) monitoring during each melt season having taken place in streams

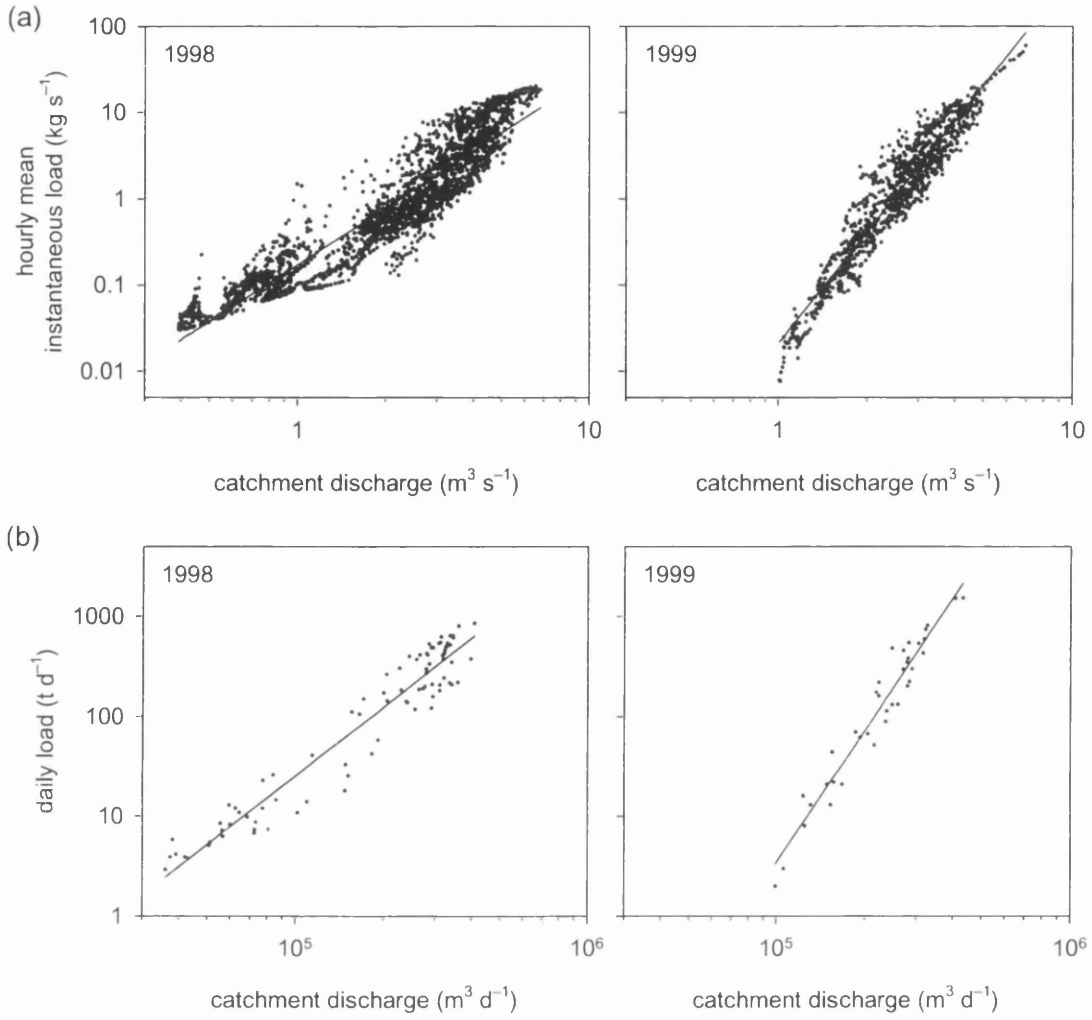

Figure 4.6 Log-log scatter plots of (a) hourly mean instantaneous suspended sediment load and (b) daily total suspended sediment load against catchment discharge for the monitored periods of the 1998 and 1999 melt seasons. Lines of best fit are also shown from the regression relationships given in Table 4.4.

draining separate glacial catchments, which may have naturally differing relationships between suspended sediment transport and discharge; and 2) the occurrence, as is common, of unique relationships between suspended sediment concentration and discharge for separate melt seasons (e.g. Fenn, 1989). It is important to note that the shallower gradient of the relationship during 1998 is associated with a lower r^2 value, indicating a weaker relationship between suspended sediment concentration and discharge during 1999.

4.2.3.2 *Suspended sediment evacuation*

Log-log scatter plots of discharge versus hourly mean suspended sediment load are shown in Figure 4.6 (a). Best-fit relationships demonstrate significantly higher r^2 values than for discharge versus suspended sediment concentration (Table 4.4) due to the inclusion of discharge in both variables. Log-log scatter plots of daily catchment discharge versus suspended sediment load (Figure 4.6 b) demonstrate an even stronger relationship between discharge and suspended sediment evacuation (Table 4.4). Higher r^2 values for daily total discharge versus sediment load are not unexpected, since much scatter in the suspended sediment series at diurnal or sub-diurnal scales will be eliminated. For example, scatter resulting from diurnal hysteresis, where sediment concentration is greater than expected during rising discharge and lower than expected as discharge falls, will essentially be removed. However, considerable scatter exists between daily catchment discharge and suspended sediment load during 1998 remains and the distribution appears less homoscedastic compared with 1999, indicating a more complex relationship between suspended sediment transport and discharge.

4.2.4 Evaluation of seasonal linear regression techniques

4.2.4.2 *Suspended sediment concentration*

The suitability of seasonal ordinary rating curves for the 1998 and 1999 melt seasons have been evaluated using residual autocorrelation analysis and visual inspection of the residual series. Residuals from both equations exhibit serial and diurnal autocorrelation which is significant at 95 % confidence (Figure 4.7 a). For autocorrelation analysis, 95% confidence limits are given by twice the standard error (S.E.) of r_k, where

$$S.E.(r_k) = [1 + 2(r_1^2 + r_2^2 + \ldots\ldots r_q^2)]^{0.5}(n)^{-0.5} \qquad (4.6)$$

in which r_k is the coefficient of determination at lag k, $k = q + 1$, and n is the total number of observations. Whilst true-autocorrelation is not unexpected, following Fenn et al. (1985), the following quasi-autocorrelation effects were also considered as possible causes of autocorrelation in the residuals: 1) non-linearity in the dataset; 2) the exclusion

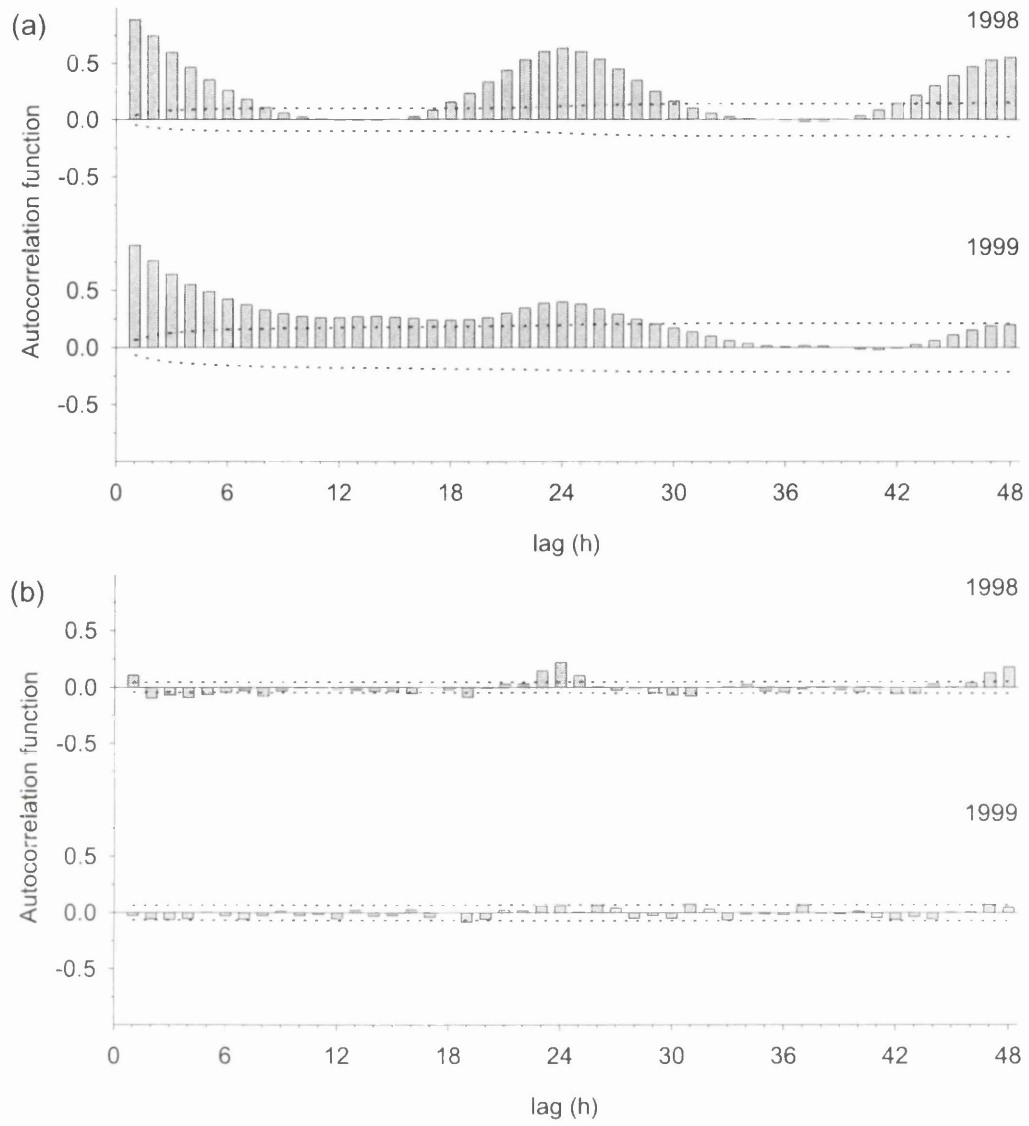

Figure 4.7 Residual autocorrelation plots from (a) seasonal linear regression and (b) seasonal linear regression after first differencing. Dotted lines are 95% confidence limits.

of other significant independent variables; and 3) the existence of lags between the independent and dependent variables.

1. *Linearity problems*. Fenn et al. (1985) recommend using a Box-Cox procedure to identify the most appropriate transformation of the raw variables in order to achieve as near normally, linearly, and homoscedastically distributed bivariate data as possible. However, log-log transformations are widely considered to be the most appropriate transformation for discharge and suspended sediment concentration data.

Visual inspection of the transformed scatter plots does suggest linearity problems in the 1998 data, namely due to an apparent clustering and attenuation of suspended sediment values at very low and very high values (Figure 4.5 b); however, high serial autocorrelation is also evident during 1999. Non-linearity in the 1998 data is possibly associated with the greater range of catchment discharge during the monitored period: the apparent clustering and attenuation of the suspended sediment concentration data at high values is likely to have resulted from saturation of the turbidity sensors since higher values of suspended sediment are likely to be associated with the higher discharges. Measured suspended sediment concentrations around peak discharge later in the melt season will be much lower than those predicted by the rating curve, resulting in diurnal residual autocorrelation. Apparent clustering and attenuation at low concentration values (Figure 4.5 b) suggests the turbidity sensors were insensitive to variation in very low suspended sediment concentrations. That lower concentrations appear to have been measured in 1999 than 1998 (Figure 4.5 b) likely reflects differences in the form of the calibration relationships applied in Section 2.3.

2. *Exclusion of other explanatory variables.* For both seasons, it is very unlikely that suspended sediment concentration was controlled solely by discharge. Hence, the inclusion of other explanatory variables in a multiple regression model may remove some of the autocorrelation in the residuals. The higher scatter during 1998 is clearly suggestive of a complex relationship between suspended sediment concentration and discharge. However, primary consideration must be given to the suitability of discharge as a surrogate for flow capacity. Separate 'clouds' of points in Figure 4.5 (b) suggests distinct populations in the 1998 dataset reflecting changing relationships between suspended sediment concentration and discharge. In particular, there appear to be at least two separate populations at flows lower than 1 m^3 s^{-1} that clearly influence the slope of the regression line and are responsible for much of the residual scatter. The existence of sub-seasonal variation in the relationship between discharge and suspended sediment concentration may suggest changes in subglacial hydraulic efficiency, possibly due to changes in drainage system morphology (Section 1.3), thereby invalidating seasonal ordinary rating curves.

3. *Autocorrelation resulting from lags in the dependent and independent variables, or hysteretic effects at diurnal and seasonal time scales.* Studies have commonly found values of suspended sediment concentration to precede those of discharge. Fenn et al. (1985) identified lags between the suspended sediment concentration and discharge series at a seasonal scale that suggested suspended sediment transport generally preceded discharge by 1 h. This effect was tested for the 1998 and 1999 data using cross correlation analysis of the log-transformed series. The best match position between the two series during the 1998 was found by lagging the suspended sediment concentration series by –1, such that Q_t was related to SSC_{t-1}, where Q and SSC are discharge and suspended sediment concentration, respectively. No lagging of the suspended sediment series was found to be necessary during 1999. The new rating curve for 1998 (Table 4.4) had slope and intercept terms significantly different from zero, but r^2 was only marginally improved. Moreover, there was no improvement in the autocorrelation pattern from the residual series.

Serial autocorrelation in the residual series is an indication that ordinary seasonal rating curves poorly describe the relationship between suspended sediment concentration and discharge. The above discussion suggests that residual autocorrelation in the 1998 and 1999 datasets is likely a combination of both true- and quasi-autocorrelation. Removing quasi-autocorrelation may significantly improve the performance of ordinary rating curves; however, accounting for quasi-autocorrelation is likely to be very difficult if there is systematic evolution of meltwater sources and pathways. For example, autocorrelation in the residual series resulting from lags between variables is likely to be very difficult to isolate if, as is likely at glaciers where discharge shows a strong diurnal signal, response lags at seasonal scales are mainly a product of diurnal hysteresis.

Fenn et al. (1985) investigated diurnal hysteresis using flow-based sub-periods of the melt season such as rising and falling discharge limbs. However, hysteresis effects will evolve with the sources and routing of meltwater during the melt season, for example the influence of diurnal hysteresis will change as the proportion of discharge derived from surface melting increases. Cross-correlation analysis of seasonal data, or the analysis of sub-sets of the data defined purely on flow-based periods such as rising or falling limbs, are unlikely to rigorously identify changing responses between variables. Fenn et al.

(1985) also considered longer-term hysteresis, suggesting a possible relationship to sediment availability factors, and therefore attempted to improve the performance of ordinary rating curves by dividing the season into climate-based and flow-based sub-periods, such as periods before and after an early season flush event. Once again, however, these factors are likely to evolve with the systematic evolution of the sources and routing of meltwater, since sediment availability will also be influenced by drainage system morphology.

In summary, evolution of the sources and routing of meltwater in the glacial system will most likely influence the access of meltwater to basal sediments and the mechanisms of sediment evacuation. As a result, quasi- and possibly true-autocorrelation effects are also likely to evolve throughout the melt season, seriously reducing the performance of seasonal linear regression techniques. Changing relationships between discharge and suspended sediment concentration at sub-seasonal scales will also invalidate seasonal ordinary rating curves. The ordinary rating curve approach is likely to succeed in isolating long-term sediment availability effects and reliably identifying changing responses between variables only where the evolution of meltwater sources and pathways is negligible.

The possibility of changing relationships between discharge and suspended sediment concentration can most easily be explored by visually examining the residual series. Plotting the residuals from the seasonal rating curve (Figure 4.8) shows systematic variations at diurnal and sub-seasonal scales. During both seasons, diurnal variation in the residuals evolves throughout the monitored period to form a regular, diurnally oscillating cycle. Residual variation is clearly more randomly distributed about the regression line early in the melt season, although during 1999 the diurnal pattern is never smooth. Diurnal variations are indeed superimposed upon longer-term, sub-seasonal trends that largely correspond to the phases of the melt seasons discussed in Section 3.2 (Tables 3.1 and 3.2; see below).

One way of removing much of the autocorrelation from seasonal ordinary rating curves is to fit seasonal rating curves to the log-transformed data series after first differencing (Gurnell and Fenn, 1984a; Willis et al., 1996). First differencing removes the trends from

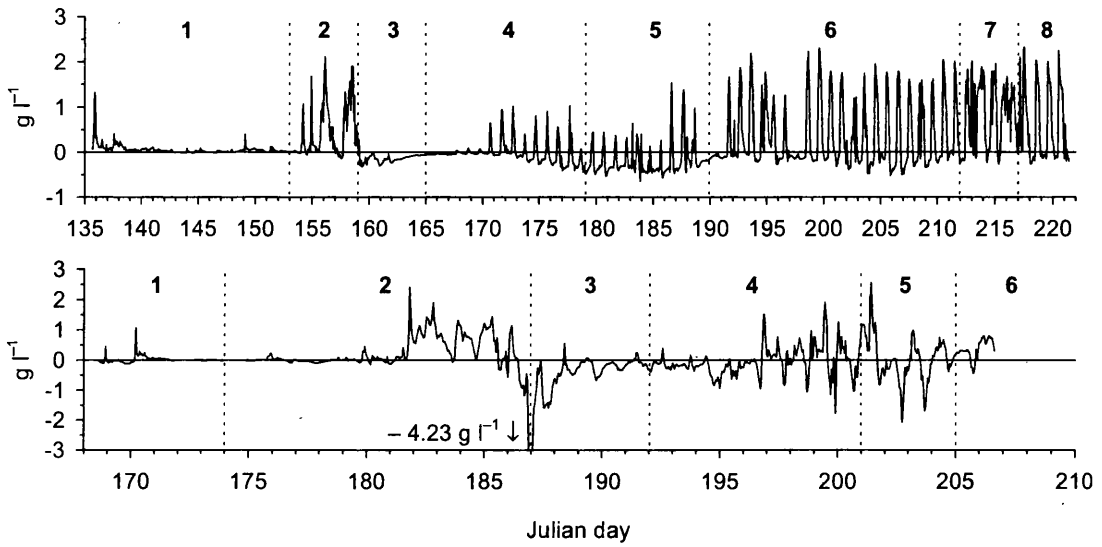

Figure 4.8 Time series plot of residuals from seasonal linear regression models for the 1998 (top) and 1999 (bottom) melt seasons.

the two series, and a scatter plot of first differenced variables directly relates rate of change of suspended sediment concentration to rate of change of discharge. Regression equations on first differenced variables (Figure 4.7; Table 4.4) had mixed success. This approach was most successful for the 1999 dataset, which demonstrated no autocorrelation in the residual series (Figure 4.7 b); however, the model explained only 7% of the variance, showing that rates of change during 1999 were not significantly correlated. Cross-correlation analysis showed that changes in discharge preceded changes in suspended sediment by 1 h, although r^2 was not greatly improved.

Regression on first differenced variables from the 1998 melt season showed that rates of change exhibited relatively high correlation ($r^2 = 0.405$; Table 4.4); results reported from other glaciers show that r^2 values for regression on first differenced variables are typically very low (Gurnell and Fenn, 1984a; Willis et al., 1996). However, residual autocorrelation analysis (Figure 4.7 b) demonstrates autocorrelation at short lags with a diurnal wavelength. This pattern is suggestive of diurnal hysteresis effects, although cross-correlation analysis failed to find a better match position between the two series. Interpretation of residual variation from regression on first differenced variables is difficult since the resulting series is far removed from the original variables (cf. Gurnell and Fenn, 1984a), hence direct visual comparison was made between time series plots of

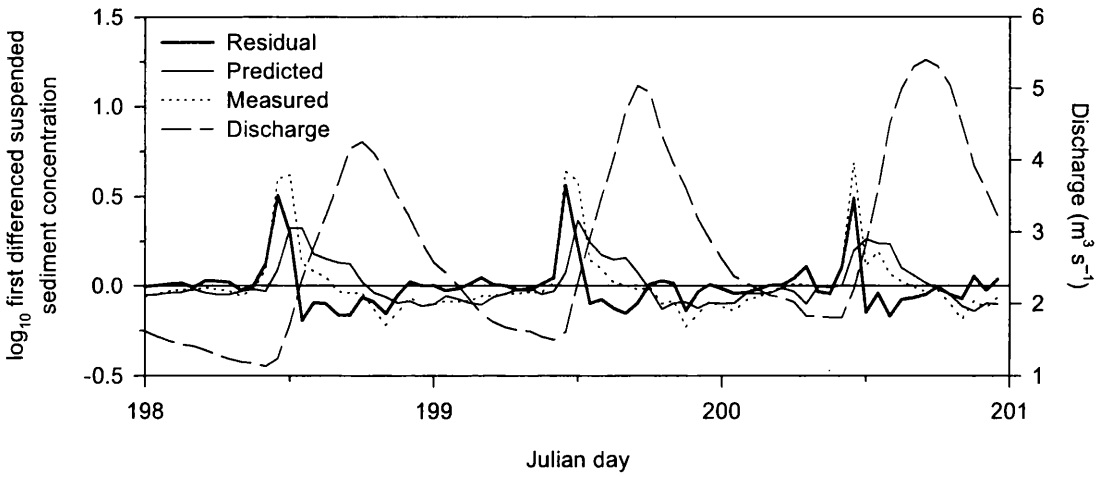

Figure 4.9 Large positive residuals with a ~ 24 h periodicity due to hysteresis between rate of change of log-transformed discharge and suspended sediment concentration.

the predicted, residual and first differenced suspended sediment concentration series. The plots demonstrate that from JD 170, there is a relatively simple hysteresis effect whereby the rate of change of suspended sediment concentration precedes the rate of change of discharge by approximately one hour (e.g. Figure 4.9). This simple effect appears to have been hidden in seasonal analysis of potential lags between the two series because, as predicted above, the effect evolves throughout the melt season.

4.2.4.3 Suspended sediment evacuation

Rating curves obtained for daily total suspended sediment evacuation against daily total discharge were also evaluated using residual autocorrelation analysis. Residuals from the relationship between hourly discharge and mean suspended sediment load should largely reflect both diurnal and sub-seasonal trends already identified from hourly suspended sediment concentration data. However, residuals from the relationship between daily total load and discharge are also likely to be revealing of longer-term, sub-seasonal trends related to the systematic evolution of meltwater sources and pathways. In particular, the 1998 dataset appears to cluster into low and high values (Figure 4.6 b) that may indicate the presence of two separate populations.

Residual autocorrelation diagrams (Figure 4.10 a) confirm the presence of serial autocorrelation in the residuals from the 1998 melt season. Serial autocorrelation also

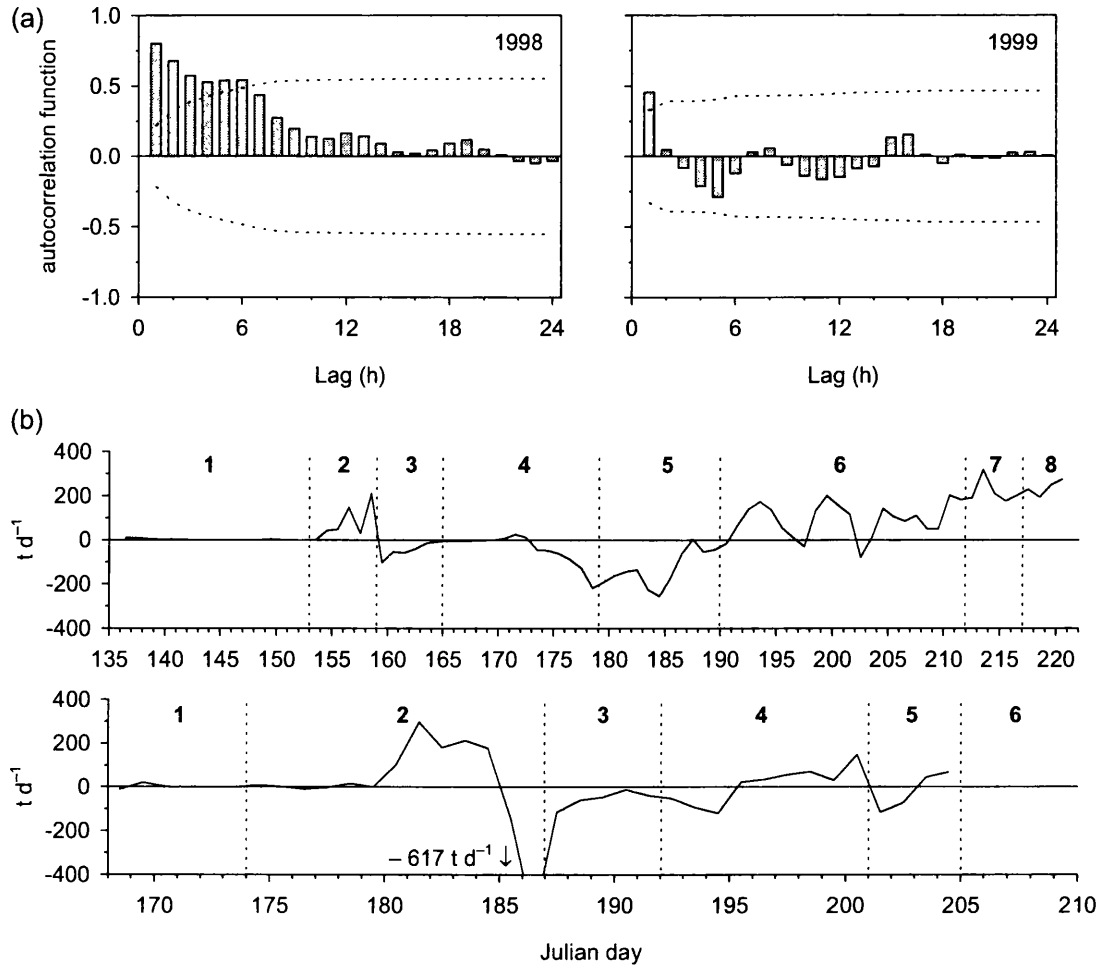

Figure 4.10 (a) Residual autocorrelation plots for seasonal relationships between daily suspended sediment load and catchment discharge for the 1998 and 1999 melt seasons. Dotted lines indicate 95% confidence limits. (b) Time series of the residuals.

exists during 1999 but at very short lags, indicating that the residuals are more randomly distributed around the regression line and that large, systematic variations are absent. This interpretation is confirmed by visual analysis of time series plots of the residual series (Figure 4.10 b). Systematic trends are clearly evident during 1998, which broadly coincide with the phases of the melt season identified in Section 3.2 (Table 3.1). A brief period of positive residuals, indicating that suspended sediment evacuation is slightly underestimated by the rating curve occurs during period 2, followed by an abrupt switch to negative residuals at the beginning of period 3, indicating lower than expected suspended sediment evacuation. During period 4, the residuals rapidly fall once more, and early in period 5 actual suspended sediment evacuation is strongly overestimated.

The remainder of the season demonstrates a consistently increasing trend in the residuals, such that by period 8 suspended sediment evacuation is ~ 200 t d^{-1} greater than predicted using the seasonal rating curve.

During 1999, shorter time-scale, less systematic variation is evident (Figure 4.10 b) that shows only slight agreement with the phases of the melt season identified in Section 3.2 (Table 3.2). Suspended sediment load is most strongly underestimated during the latter half of period 2, followed by an abrupt switch to very high negative residuals. Peak negative residuals are reached on JD 186, indicating that the rating curve underestimates suspended sediment evacuation by ~ 600 t d^{-1}. Importantly, this event coincides with the period of values originally interpolated from rating curves, which are likely to have presented conservative estimates of suspended sediment concentration.

4.2.5 Conclusions

Suspended sediment transport at Haut Glacier d'Arolla demonstrates a positive relationship with discharge at seasonal scales. However, seasonal ordinary rating curves perform poorly due to the likely existence of changing relationships between discharge and suspended sediment transport at sub-seasonal scales. These relationships are likely to reflect the evolution of the sources and routing of meltwater that control access to basal sediments and the mechanisms of sediment evacuation. Regression on first differenced variables helps to remove pattern in the residual series, but a high proportion of the variance in the dependent series remains unexplained (Table 4.4) and problems may persist due to the evolution of lags between variables. As a result, where evolution of meltwater sources and pathways occurs, seasonal ordinary rating curves of discharge versus suspended sediment concentration are unlikely to aid the rigorous investigation of the mechanisms of suspended sediment evacuation.

Improvements in the performance of ordinary rating curves are likely to result from the division of melt seasons into sub-periods concordant with the systematic evolution of meltwater sources and pathways. This method has the potential to isolate and identify sub-seasonal changes in the relationship between suspended sediment transport and discharge that are linked to the availability of sediment and changes in drainage system

morphology. Changing lags or leads between variables are also likely to be more rigorously identified and eliminated. Such an approach will result in quasi-stationary sub-periods for which relationships between discharge and suspended sediment transport can be estimated with greater confidence. Changes in the form of such relationships between periods may be indicative of the influence of evolution in drainage system morphology, whereas the importance of discharge during the melt season, indicated by the strength of such relationships, may suggest the existence of other important controlling factors.

4.3 SUB-SEASONAL LINEAR REGRESSION ANALYSIS

4.3.3 Introduction and methods

In this section, ordinary rating curves are fitted to discharge versus suspended sediment concentration for sub-periods of the 1998 and 1999 melt seasons. Analysis of sub-periods of the melt season during which the glacier drainage system is assumed to be relatively 'stable' should: 1) isolate major changes in sediment availability throughout the melt season associated with changes in how meltwater accesses basal sediments; 2) enable the more rigorous determination of the relationship between discharge and suspended sediment concentration; and 3) identify changes in the importance of discharge for suspended sediment evacuation during the melt season. The hydrological bases for the division of the melt season into the sub-periods used are given in Tables 3.1 and 3.2. The evolution of meltwater sources and pathways throughout these periods are summarised in Tables 3.6 and 3.7.

For each sub-period, cross-correlation analysis was used to lag the suspended sediment series to its best match position with discharge in order to identify and account for diurnal hysteresis effects. Ordinary rating curves fitted to lagged data are evaluated using the significance of their slope and intercept values and the strength of r^2, and the residual series tested for autocorrelation. Changes in the form of the rating curves are used to investigate the changing relationship between discharge and suspended sediment concentration during each melt season.

Due to the strong relationship between first differenced variables during the 1998 melt season, regression on log-transformed first differenced variables (ΔQ and ΔSSC) was also performed for each of the individual periods. Because regression on first differenced variables relates rate of change of suspended sediment concentration to rate of change of discharge, the strength of the relationship between the two variables might be expected to change throughout the melt season depending on the mechanisms of sediment evacuation. First-differenced variables were obtained from the log-transformed suspended sediment concentration and discharge series and the first-differenced suspended sediment series was lagged to its best match position. The first differenced models were evaluated as for the ordinary rating curves; analysis of changes in the form of the relationship, however, is limited to changes in regression slope since first differencing generates a stationary time series and therefore regression intercepts are not expected to be significantly different from zero.

4.3.4 Ordinary linear regression

4.3.4.2 1998 melt season

Table 4.5 summarises the ordinary rating curves developed for individual sub-periods of the 1998 melt season (the seasonal ordinary rating curve is shown for comparison; see Section 4.2.3.1). Rating curves for individual periods of the 1998 melt season had intercept and slope values that were significantly different from zero. Notably, the slope coefficient for each of the sub-seasonal rating curves is higher in magnitude than the seasonal model, further emphasising the inappropriateness of seasonal rating curves where controlling conditions vary. With the exception of subperiod 1, the rating curves also demonstrated improved r^2 values over the seasonal rating curve. Small improvements in r^2 were also made for subperiods 4–6 by lagging the suspended sediment series, such that relationships were fitted to values of $\log Q_t$ against $\log SSC_{t-1}$.

Regression relationships for each subperiod are plotted over the range of discharge values observed (Figure 4.11). Changes in the form of the relationship between sub-periods are evident due to differences in both model intercept and slope (Table 4.5). In particular, there is good evidence in the changes in model slope for at least two separate

Table 4.5 Ordinary rating curves for log-transformed discharge versus suspended sediment concentration for sub-periods of the 1998 and 1999 melt seasons after lagging the suspended sediment series to its best match position (p for all coefficients < 0.001).

Sub-period (lag in h)	n	a	b	t_a	t_b	SE_a	SE_b	r^2
1998 melt season								
All data (–1)	2060	–0.769	1.195	–101.7	68.84	0.008	0.017	0.697
1	417	–0.575	1.322	–39.58	21.27	0.015	0.062	0.520
2	144	–0.643	1.375	–30.63	29.73	0.021	0.046	0.861
3	144	–1.047	1.355	–81.45	31.30	0.013	0.043	0.873
4 (–1)	335	–0.860	1.283	–78.69	43.40	0.011	0.030	0.849
5 (–1)	263	–1.622	2.370	–36.36	28.20	0.045	0.084	0.752
6 (–1)	527	–1.227	2.182	–60.36	53.31	0.020	0.041	0.844
7	120	–1.469	2.857	–21.81	24.11	0.068	0.119	0.830
8	108	–1.138	2.152	–21.99	21.98	0.052	0.098	0.818
1999 melt season								
All data	915	–1.672	3.274	–83.06	70.81	0.020	0.046	0.846
1 (+3)	128	–1.750	3.567	–37.88	16.77	0.046	0.213	0.688
2	312	–1.836	3.840	–69.08	58.05	0.027	0.066	0.915
3	120	–1.758	3.107	–35.00	30.95	0.050	0.100	0.889
4 (+1)	215	–1.458	2.759	–17.72	16.90	0.084	0.167	0.751
5	96	–0.715	1.520	–6.79	7.56	0.105	0.201	0.371
6 (+2)	38	–0.551	1.203	–7.16	5.97	0.077	0.202	0.483

n: number of observations; a, b: intercept and slope coefficients, respectively; t_a, t_b: t-statistics for intercept and slope coefficients, respectively; SE_a, SE_b: standard error of intercept and slope coefficients, respectively

groups, comprised of sub-periods 1–4 and sub-periods 5, 6 and 8, respectively. Models within these two groups demonstrate reasonably consistent slope, indicating that within each group suspended sediment concentration responds similarly to changes in discharge. Variation in model intercept also occurs (Table 4.5) that may indicate changes in sediment availability. For example, for two models with similar slopes, a decrease in intercept for the second model indicates consistently lower suspended sediment concentrations for any given value of discharge with respect to the first. The steeper slope of period 7 suggests it may form a third separate and distinct group.

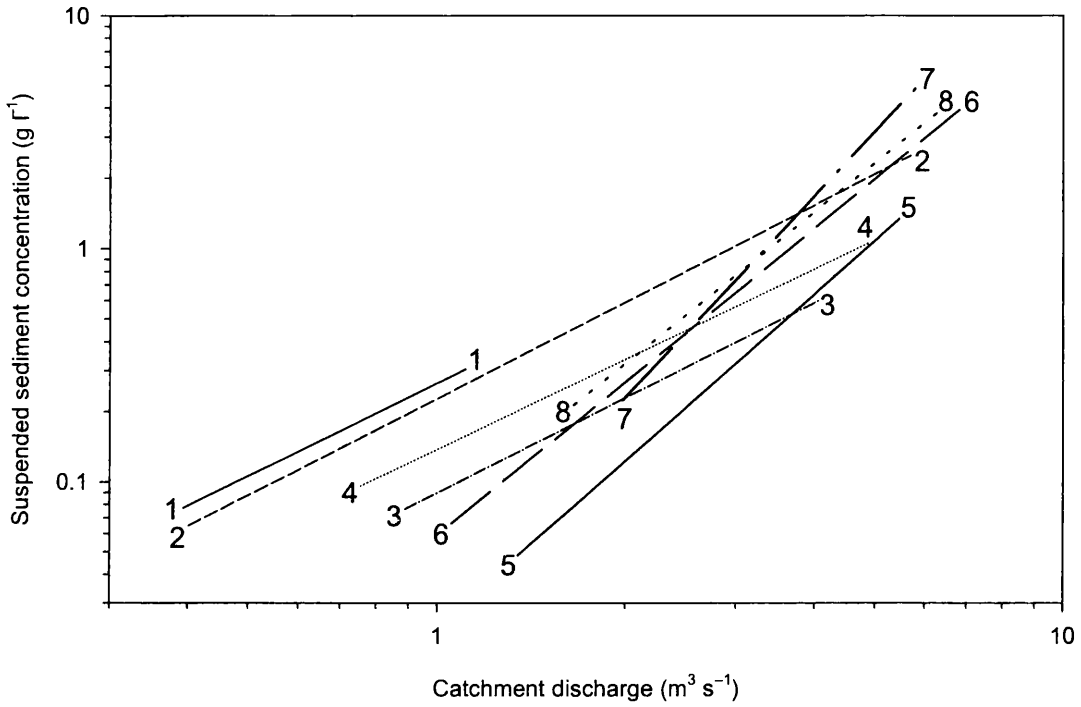

Figure 4.11 Ordinary rating curves for sub-periods of the 1998 melt season (Table 4.5) plotted over the range of discharge recorded within each sub-period.

Rating curve slope and intercept coefficients were analysed to identify statistically significant changes in the relationship between discharge and suspended sediment concentration between sub-periods. For any two sub-periods, a statistically significant change in the relationship is indicated where the 95% confidence limits (calculated as ± 2 S.E.) for either model slope or intercept do not overlap. For model slope, Figure 4.12 (a) demonstrates 3 statistically different but internally consistent groups: group A) sub-periods 1–4; group B) sub-periods 5, 6 and 8; and group C) sub-period 7. Analysis of model intercepts (Figure 4.12 b) demonstrates that within group A, confidence limits for the sub-periods 1 and 2 are not statistically different; however, relationships are statistically different for sub-periods 3 and 4. Within group B, the intercept for sub-period 5 is statistically different from sub-periods 6 and 8; the relationship between discharge and suspended sediment concentration is not statistically different between sub-periods 6 and 8.

Statistically significant relationships have been found that generally explain a high proportion of the variance in the suspended sediment series (Table 4.5) However,

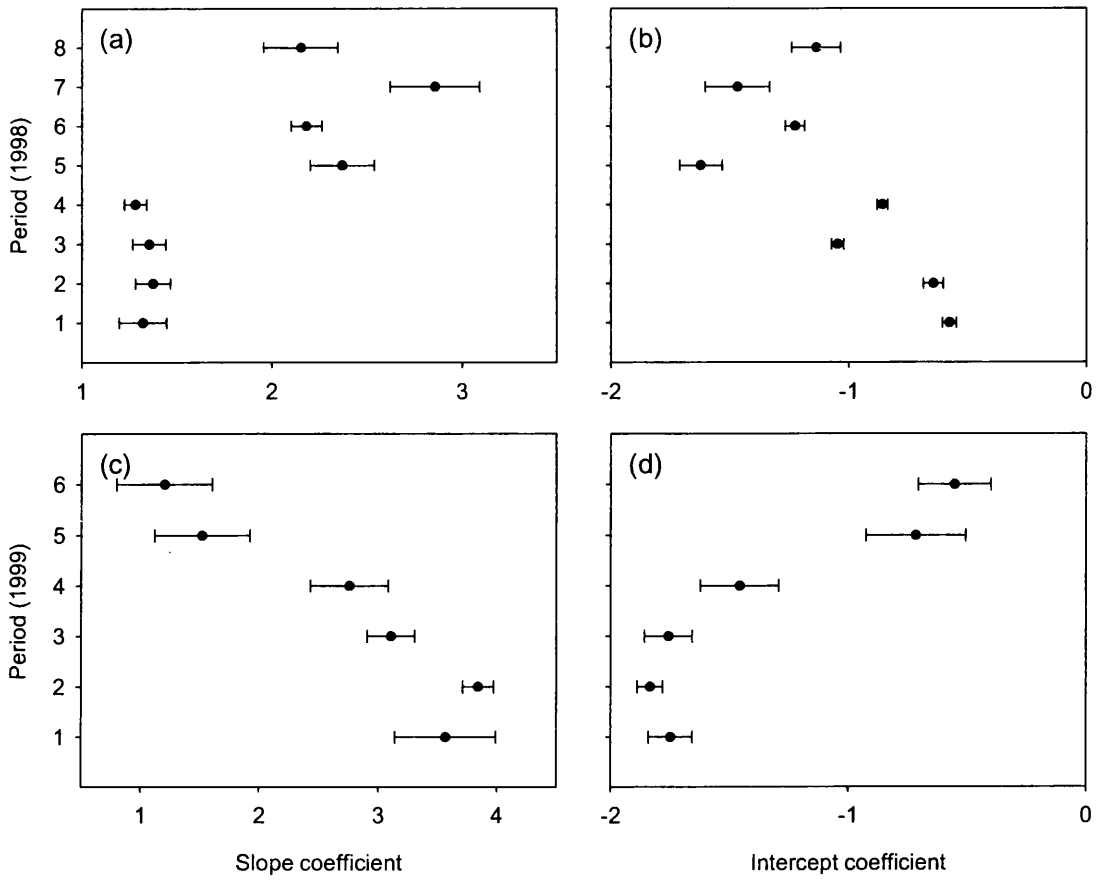

Figure 4.12 (a) slope and (b) intercept coefficients relating to ordinary rating curves between log-transformed discharge and suspended sediment concentration for sub-periods of the 1998 melt season (Table 4.5); (c) and (d) show the same for 1999 melt season (Table 4.5). Error bars represent 95% confidence limits.

autocorrelation analysis demonstrates systematic variation in the residual series that indicates poor model performance (Figure 4.13). Serial autocorrelation persists for all sub-periods, although the wavelength decreases during the season. Sub-periods 4, 5 and 6 also show evidence of a diurnal autocorrelation pattern (sub-period 8 shows a similar pattern but it is not significant). Model performance is best for sub-period 7, where serial autocorrelation is significant only at lag 1.

4.3.4.3 1999 melt season

Rating curves for sub-periods of the 1999 melt season had intercept and slope values that were again significantly different from zero (Table 4.5); however, only two of the six periods demonstrate improved r^2 values relative to the seasonal rating curve. The high r^2

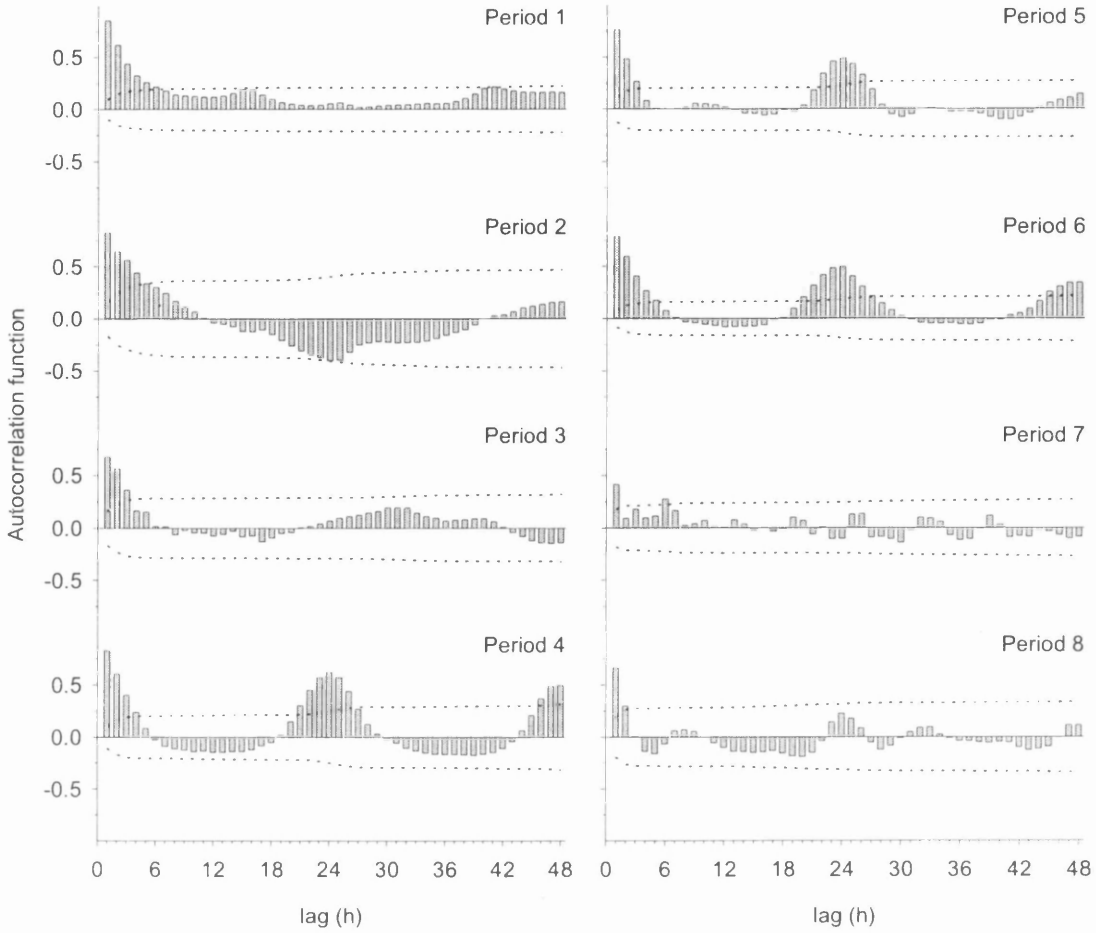

Figure 4.13 Residual autocorrelation diagrams from ordinary rating curves for sub-periods of the 1998 melt season (Table 4.5). Dotted lines show 95% confidence limits.

value for the seasonal rating curve is probably due to the large sample size, but is also likely to reflect the less-scattered nature of the seasonal data. Small improvements in r^2 were obtained for periods 1, 4 and 6 by lagging the suspended sediment concentration series. However, cross-correlation analysis showed that for these periods discharge preceded suspended sediment concentration by 1–3 hours, indicating the presence of anti-clockwise hysteresis, as opposed to the more common clockwise hysteresis evident during 1998 (above).

The form of the models (Figure 4.14) demonstrates that the steepest relationships occur early in the monitored period and are generally associated with the highest coefficients of determination. Towards the end of the season, periods 5 and 6 show shallower relationships between suspended sediment concentration and discharge and the models

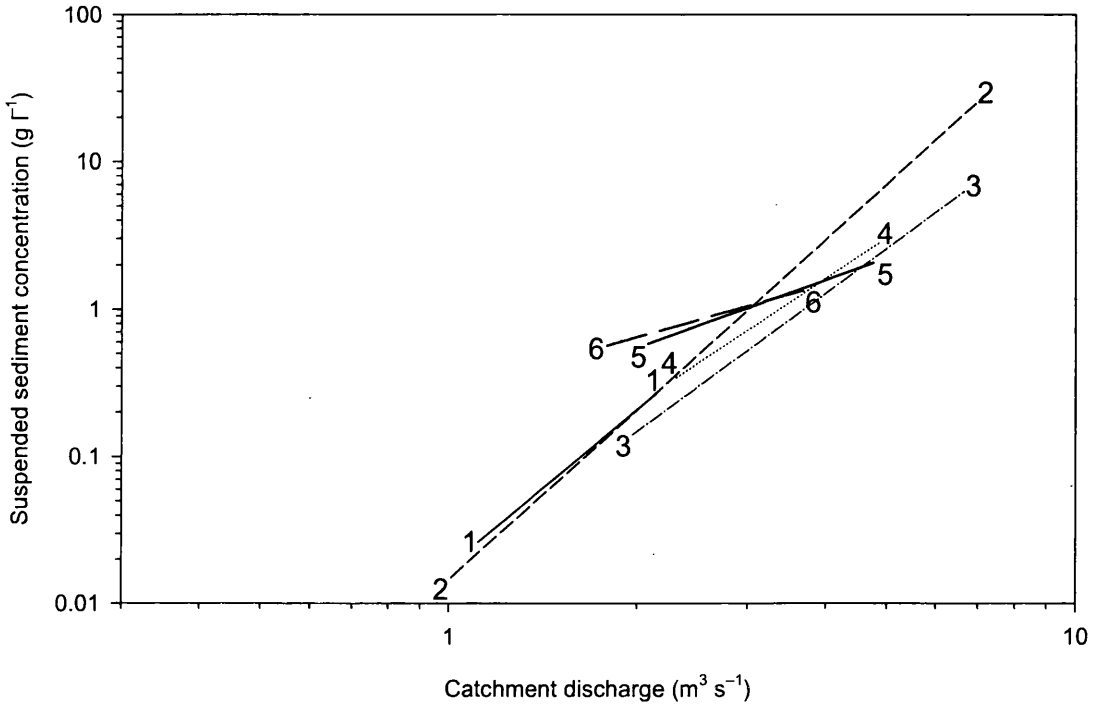

Figure 4.14 Regression relationships for sub-periods of the 1999 melt season (Table 4.5) plotted over the range of discharge recorded within each sub-period.

explain a low proportion of the variance in the suspended sediment series. Identifying statistically significant changes in the form of the relationship between sub-periods, regression slopes fall into two main groups: group A) sub-periods 1–4; and group B) sub-periods 5 and 6 (Table 4.5; Figure 4.12 c and d). Analysis of the model intercepts shows that in group A only sub-period 4 is statistically unique, whilst none of the intercepts for the regression relationships in group B are statistically different. Residual autocorrelation analysis (Figure 4.15) demonstrates that serial autocorrelation is a feature of each of the periods; there are complex additional autocorrelation patterns in many of the periods, but these are not significant.

4.3.5 Regression on first-differenced variables

4.3.5.2 1998 melt season

Ordinary rating curves for first differenced variables for sub-periods of the 1998 melt season are shown in Table 4.6. As expected, intercept values for the rating curves were

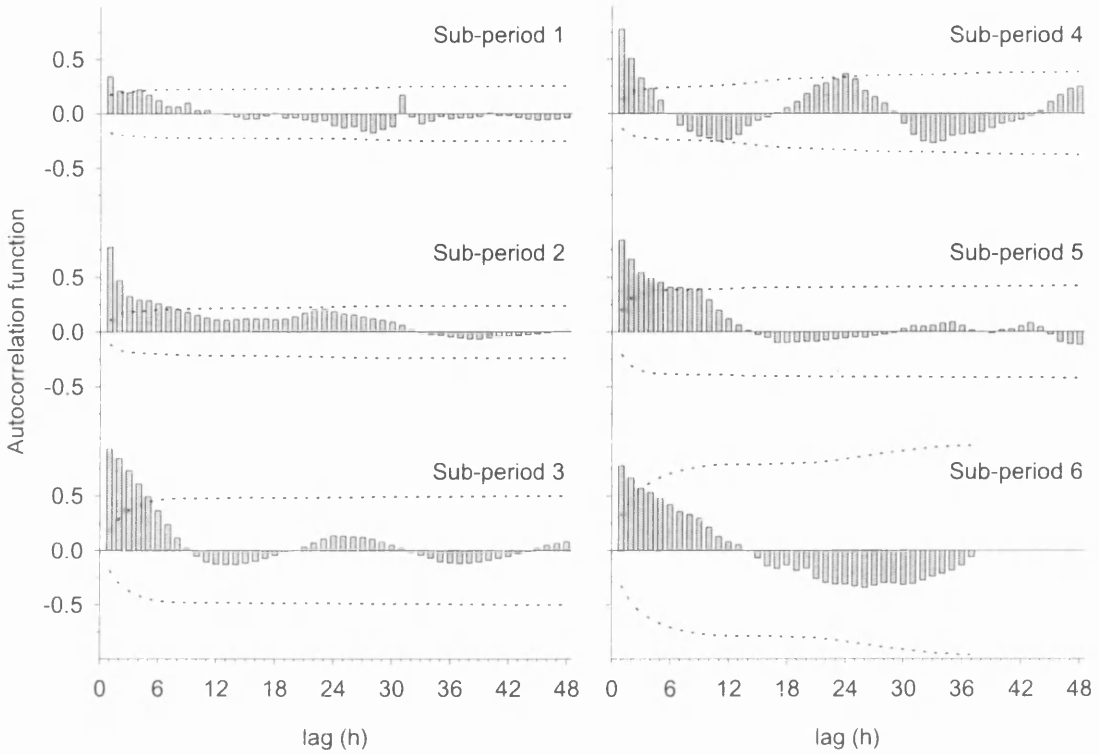

Figure 4.15 Residuals autocorrelation diagrams from ordinary rating curves for sub-periods of the 1999 melt season (Table 4.5). Dotted lines indicate 95% confidence limits.

not significantly different from zero; however, model slopes were significant at $p \leq 0.001$. r^2 values exhibit a generally increasing trend throughout the season, with the relationships during periods 4, 6, 7, and 8 showing improved r^2 relative to the seasonal relationship. For periods 1, 3, 4, and 6, best match positions were found by lagging the suspended sediment concentration series by 1 h, indicating that rate of change of suspended sediment concentration preceded the rate of change of discharge.

Due to the stationary nature of the data series, the regression intercept is close to zero for all periods. Model slope is lowest during periods 1 and 3, with the steepest relationship between rate of change of suspended sediment concentration and discharge occurring during period 5. Analysis of confidence limits for model slope coefficients reveals few clear patterns (Figure 4.17 a). The slope of the relationship during period 1 is statistically different from relationships during the latter part of the monitored period (with the exception of sub-period 7), although there is no clear evidence of any distinctive groups. Serial autocorrelation in the residual series is completely removed; however, diurnal

Table 4.6 Ordinary rating curves for first differenced log-transformed discharge versus suspended sediment concentration during 1998 and 1999 after lagging the first-differenced suspended sediment series to its best match position. For all curves, p_a is never significant; p_b is significant at < 0.05 except for sub-period 3 during 1999.

Sub-period (lag in h)	n	a	b	t_a	t_b	SE_a	SE_b	r^2
1998 melt season								
All data	2060	–0.001	2.34	–0.26	37.43	0.002	0.063	0.405
1 (–1)	415	0.000	1.09	–0.13	3.38	0.003	0.322	0.025
2	144	–0.009	2.62	–1.19	7.81	0.008	0.335	0.296
3 (–1)	143	–0.001	1.56	–0.17	5.30	0.004	0.295	0.160
4 (–1)	335	–0.003	2.64	–0.91	18.04	0.003	0.146	0.493
5	264	0.003	3.36	0.40	12.99	0.007	0.258	0.389
6 (–1)	527	0.000	2.47	0.03	25.24	0.005	0.098	0.547
7	120	0.002	2.06	0.14	9.96	0.011	0.207	0.452
8	108	–0.003	2.39	–0.2	9.40	0.015	0.254	0.450
1999 melt season								
All data (+1)	897	0.001	1.59	0.33	9.17	0.003	0.174	0.085
1 (+2)	128	–0.001	1.93	–0.09	2.21	0.011	0.871	0.030
2 (+1)	308	0.001	3.04	0.18	10.46	0.005	0.290	0.261
3	109	–0.006	1.13	–0.73	1.92	0.008	0.588	0.024
4 (+2)	214	0.002	1.68	0.37	5.07	0.006	0.332	0.104
5 (+1)	95	–0.006	1.02	–0.62	2.78	0.009	0.368	0.067
6 (+2)	38	0.010	1.12	0.01	0.28	0.007	0.283	0.281

n: number of observations; a, b: intercept and slope coefficients, respectively; t_a, t_b: t-statistics for intercept and slope coefficients, respectively; SE_a, SE_b: standard error of intercept and slope coefficients, respectively

autocorrelation remains during sub-period 4 (Figure 4.18), potentially indicating the evolution of lags between series.

4.3.5.3 1999 melt season

Ordinary rating curves for first differenced variables for sub-periods of the monitored period during 1999 (Table 4.6) contrast with those from 1998. The seasonal rating curve has previously indicated a poor relationship between rate of change of discharge and rate of change of suspended sediment concentration. Although a number of sub-periods show

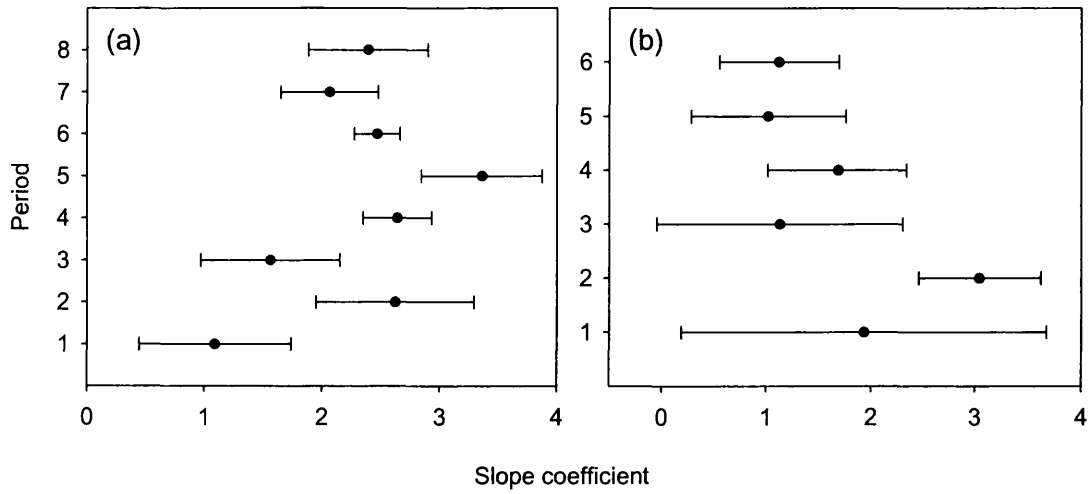

Figure 4.17 Slope coefficients with 95% confidence limits for ordinary rating curves between first differenced discharge and suspended sediment concentration during sub-periods of the (a) 1998 and (b) 1999 melt seasons (Table 4.6).

improved r^2 values, there is no clear pattern in model form or r^2 values. In addition, best match positions between the two variables were often found by backwards lagging the suspended sediment concentration series (e.g. $\log\Delta Q$ against $\log\Delta SSC_{t+1}$), demonstrating that rate of change of suspended sediment concentration typically the followed rate of change of discharge by 1–2 h.

Confidence limits show no clear pattern in model slope (Figure 4.17 b); however, residual autocorrelation analysis demonstrates no pattern in the residual series (Figure 4.19). Nevertheless, r^2 values are very poor for all sub-periods during 1999, and therefore the absence of pattern in the residual series does not indicate good model performance.

4.3.6 Interpretation, discussion and conclusions

4.3.6.2 1998 melt season

For periods 2–8, ordinary rating curves on log-transformed variables demonstrate improved r^2 values over the seasonal rating curve. During period 1, r^2 is relatively low and indicates a weak relationship between discharge and suspended sediment concentration (Table 4.5). Subsequent relationships are stronger, although in general

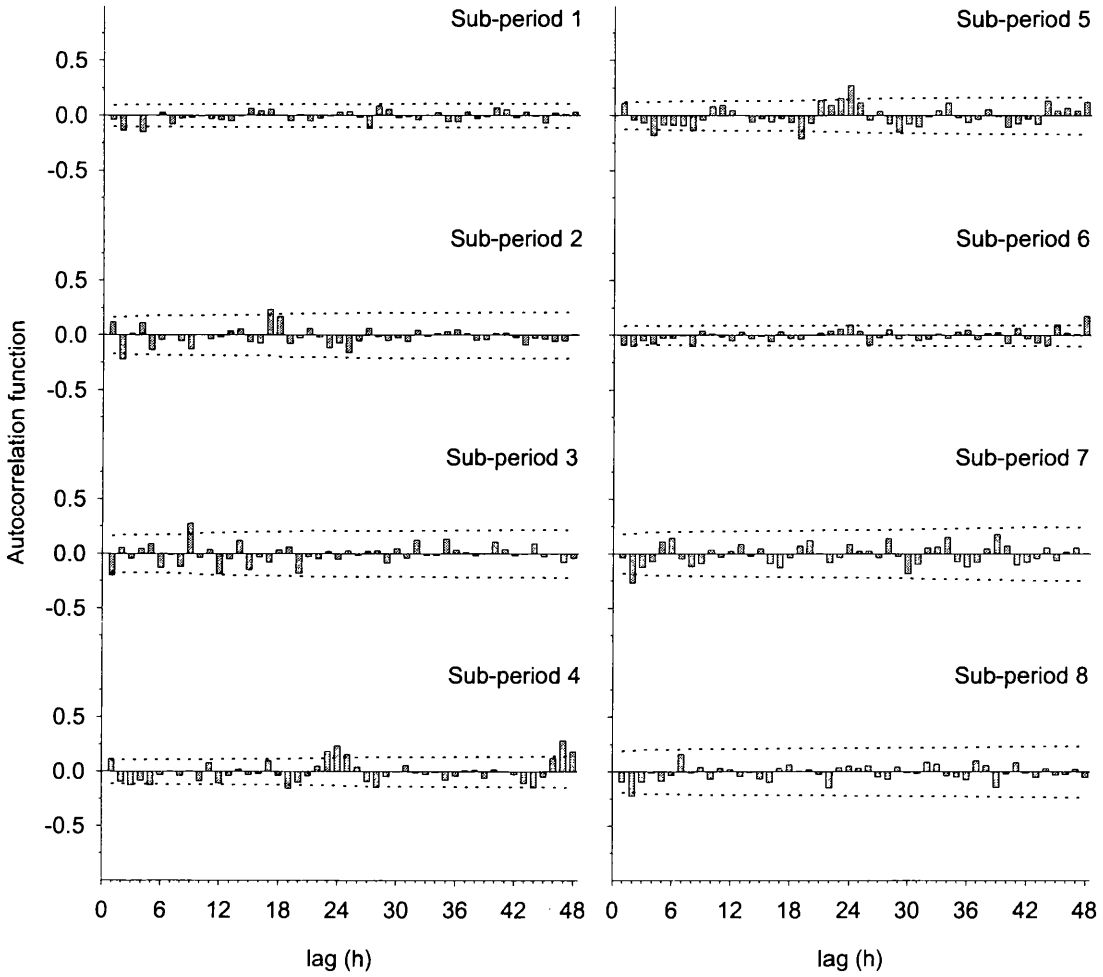

Figure 4.18 Residual autocorrelation diagrams for ordinary rating curves between first differenced variables for sub-periods of the 1998 melt season (Table 4.6).

there is a slight seasonal decrease in r^2 following period 3. Improved r^2 values are likely to result from the elimination of scatter due to the existence of different populations in the dataset and changing lags between variables. The slight decline in r^2 after period 3 may indicate the increasing importance of additional controlling variables.

Analysis of the form of the models indicates three groups of sub-periods characterised by statistically significant changes in the slope of the relationship between discharge and suspended sediment concentration: group A) periods 1–4; group B) periods 5, 6 and 8; and group C) period 7 (Table 4.5; Figure 4.12 a). There is strong evidence therefore for seasonal evolution in the form of the relationship between discharge and suspended sediment concentration. Differences in the slope of the relationship can be interpreted in

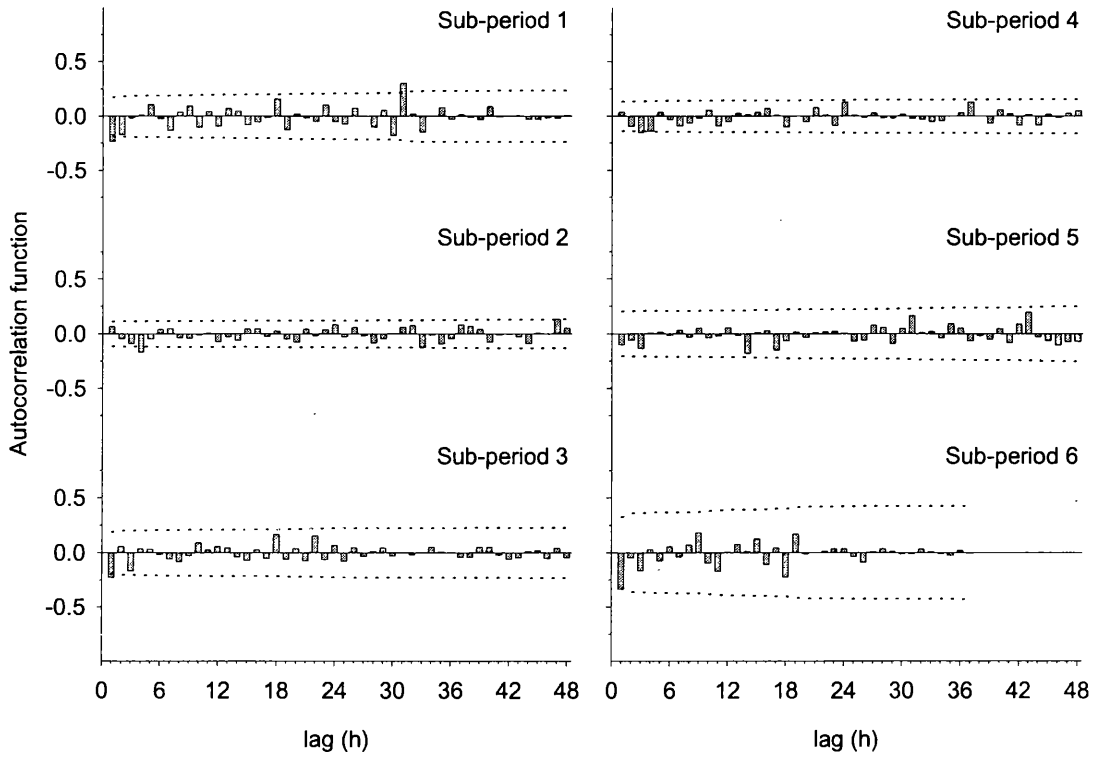

Figure 4.19 Residual autocorrelation diagrams for ordinary rating curves between first differenced variables for sub-periods of the 1999 melt season (Table 4.6).

terms of drainage system hydraulic efficiency: a consistently steeper relationship suggesting increased hydraulic efficiency exists during the second half of the monitored period that steepens further during sub-period 7. During sub-periods within group A, logSSC $\propto$ ~1.3log$Q$, whereas for periods in group B logSSC $\propto$ ~2.2log$Q$ (Table 4.5). Hence, a marked and consistent increase in sediment transport efficiency occurs during the melt season that may be associated with a change in drainage system morphology.

Changes in the model intercept within groups A and B suggest changes in sediment availability (Table 4.5; Figure 4.12 b). Within group A, sediment availability decreases from sub-periods 1 and 2 to sub-period 3 before recovering slightly between sub-periods 3 and 4. Within group B, sediment availability increases between sub-periods 5 and 6 and appears to remain stable between sub-periods 6 and 8. Considering both model intercept *and* slope, trends in the relationship between discharge and suspended sediment concentration can be identified over the monitored period (Figure 4.11). Early in the season, sub-periods 1 and 2 demonstrate a consistent relationship between discharge and

suspended sediment concentration and suspended sediment concentrations are higher at discharges below ~ 4 $m^3 s^{-1}$ than at any time during the monitored period. Sediment availability falls slightly during sub-period 3, such that suspended sediment concentrations are much lower for any given discharge, but recovers during sub-period 4. However, a significant change occurs between sub-periods 4 and 5. During sub-period 5, the relationship between discharge and suspended sediment concentration steepens significantly, but suspended sediment concentration is the lowest for any given discharge throughout the monitored period. Sediment availability then increases such that during sub-periods 6 and 8, suspended sediment concentrations remain relatively low at discharges below ~ 4 $m^3 s^{-1}$ but are higher at discharges over ~ 4 $m^3 s^{-1}$ than at any other time throughout the monitored period.

Analysis of the residuals from the sub-periods shows that autocorrelation persists in all periods with the possible exception of period 7 (Figure 4.13). This suggests that most of the models perform relatively poorly; however, many explain a high proportion of the variance within each sub-period, and any residual pattern must represent a very small proportion of the original variance. A large proportion of the remaining variance is likely to be due to measurement error and, as a result, it may be very difficult to improve the model's performance. In other words, for many of the sub-periods, even if it is possible to identify additional controlling variables and therefore remove some of the remaining scatter, their influence on sediment transport must be minor.

However, determining the causes of residual autocorrelation are important if sediment transport processes are to be fully understood. In particular, establishing whether pattern in the residuals is due to true-autocorrelation rather than quasi-autocorrelation has significant process implications. Obvious causes of quasi-autocorrelation have been considered previously, namely: 1) non-linearity in the dataset; 2) lags or hysteresis between variables; and 3) missing explanatory variables. Scatter plots for each of the sub-periods suggests linearity problems during sub-periods 6–8 due to apparent attenuation and clustering of suspended sediment concentrations at high values (Figure 4.20). This effect is attributed to saturation of the turbidity sensors, and although non-linear calibration curves were used, its influence cannot be completely removed.

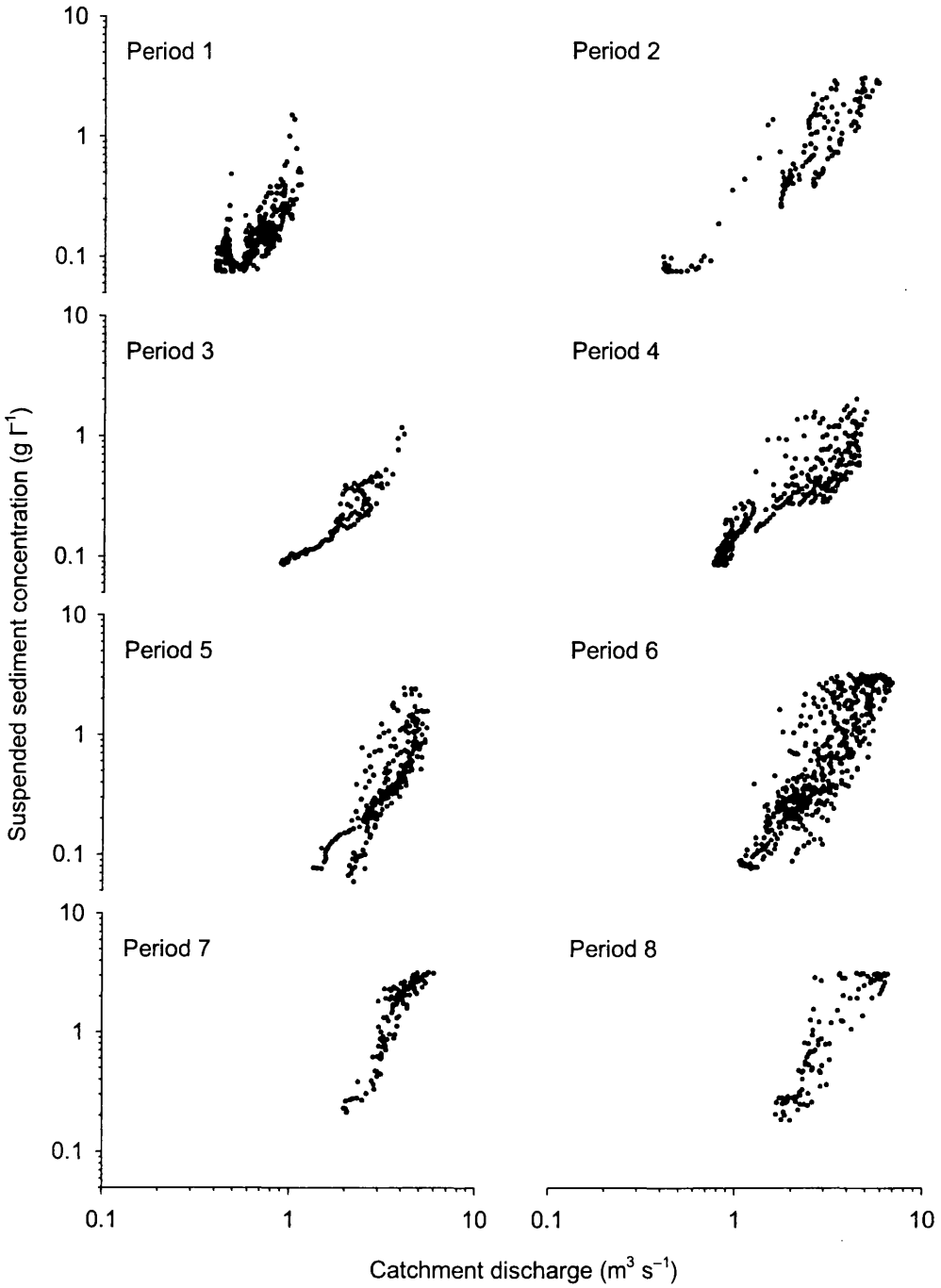

Figure 4.20 Log-log scatter plots of discharge versus suspended sediment concentration

Nevertheless, autocorrelation persists in periods where no saturation is evident, and other sources of residual autocorrelation must exist.

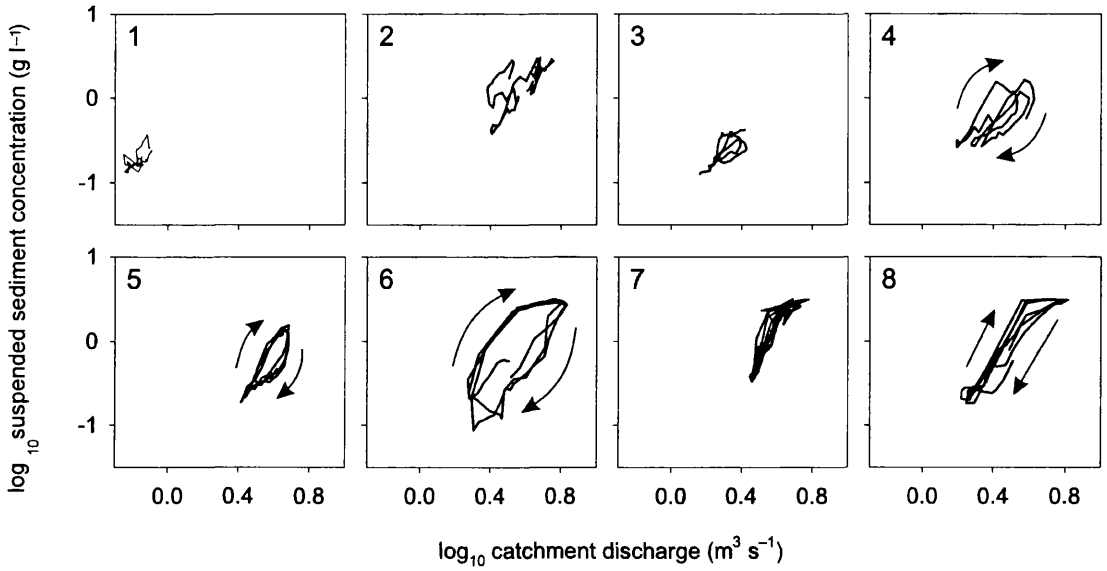

Figure 4.21 Hysteresis plots of log-transformed discharge versus suspended sediment concentration for representative days from sub-periods 1–8 of the 1998 melt season. Sub-periods 1, 2, 3 and 7 show complicated clockwise and anticlockwise patterns.

Subdividing the time series into shorter periods is unlikely to render the series completely stationary, and lagging variables to their best match position may poorly characterise diurnal hysteresis effects if the form of the hysteresis evolves particularly rapidly. Fitting rating curves to first differenced variables in order to generate a completely stationary data set did not reveal any significant seasonal trends in the form of the relationship between rate of change of discharge and rate of change of suspended sediment concentration; however, a seasonally increasing trend is evident in r^2. This trend demonstrates that rates of change of discharge are significantly better correlated with rates of change of suspended sediment concentration towards the end of the monitored period, and the increase in r^2 accompanies the slight decline in r^2 for ordinary rating curves following sub-period 3.

It is possible, therefore, that the rate of change of discharge may explain some of the residual variation from the ordinary rating curves. Rate of change of discharge has previously been used to model diurnal hysteresis in multiple regression analysis (e.g. Willis et al., 1996), since the variable is positive during rising discharges (where hysteresis results in positive suspended sediment residuals) and negative on falling discharges (when suspended sediment residuals are also negative). Hysteresis plots of

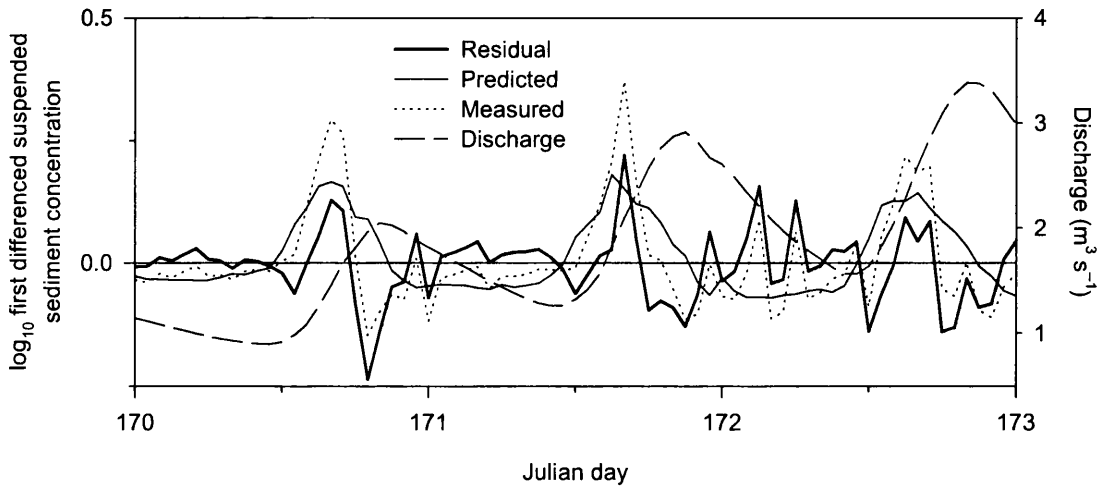

Figure 4.22 Positive residuals with a ~24 hour periodicity from an ordinary rating curve between rate of change of log-transformed discharge and suspended sediment concentration. The rating curve underestimates high values of rate of change of suspended sediment concentration during rising discharge during rapid evolution of lags between the independent and dependent variables.

log-transformed data for representative days during each of the sub-periods show the evolution of hysteresis throughout the melt season (Figure 4.21). Strong hysteresis is evident for all periods in group B except sub-period 8, where the absence of an identifiable lag between the variables suggests that the effect may have been hidden by other variation within the series. For the first differenced variables, lagging was also necessary for some sub-periods in order to obtain a best match position between the two variables, such that rate of change of suspended sediment concentration was found to precede rate of change of discharge. However, residual autocorrelation was still not completely removed from sub-period 4. Visual inspection of the residuals during sub-period 4 (Figure 4.22) suggests that rate of change of discharge under-predicts rate of change of suspended sediment concentration during periods of rising discharge, likely due to rapidly changing relationships between variables.

Further division of the season into smaller sub-periods in order to take account of such rapidly evolving relationships and remaining non-stationarity due to changes in sediment availability is undesirable on account of the processing time involved and the increasingly subjective nature of the divisions of the monitored period into smaller sub-periods. Smaller sub-periods will also result in a decrease in n, such that results may

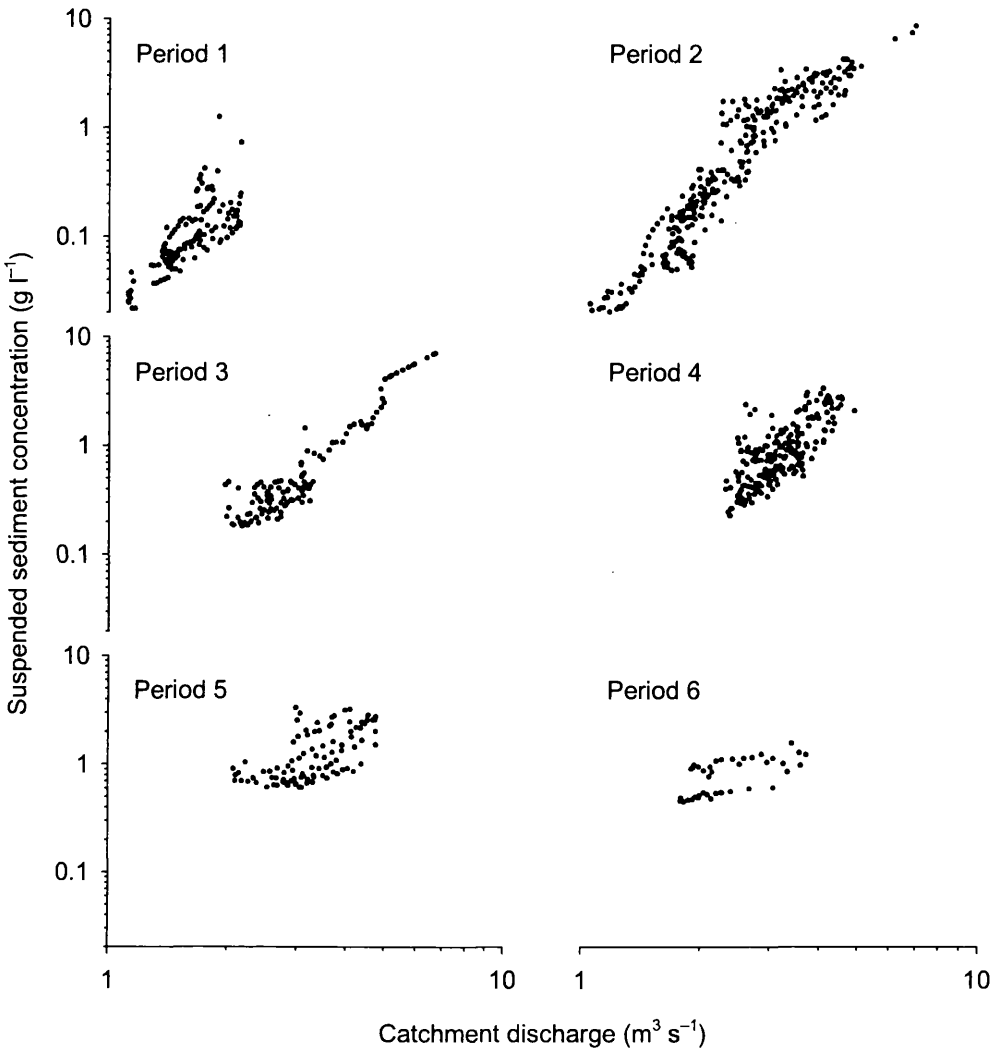

Figure 4.23 Log-log scatter plots between discharge and suspended sediment concentration for sub-periods of the monitored period during 1998.

become more difficult to interpret. Instead, multivariate techniques can be used to improve model performance through the identification of additional explanatory variables that reduce autocorrelation in the residual series. Such an approach may succeed in identifying physical processes additional to discharge that are responsible for the evacuation of suspended sediment from the subglacial drainage system.

4.3.6.3 1999 melt season

Ordinary rating curves for sub-periods of the monitored period during 1999 result in few improvements in r^2 over the seasonal rating curve (Table 4.5). Moreover, despite high r^2

values during sub-periods 1–4, r^2 is very low towards the end of the monitored period. This pattern is also reflected in the form of relationships between discharge and suspended sediment concentration, with shallower relationships during sub-periods 5 and 6 (group B; Figure 4.14). The season is also distinct from the 1998 melt season in that for a number of sub-periods discharge precedes suspended sediment concentration, resulting in anti-clockwise hysteresis (Table 4.5) that is uncommon in fluvial environments. Similarly, ordinary rating curves for first differenced variables suggests that for many of the periods, rate of change of suspended sediment concentration follows rate of change of discharge (Table 4.6). As the eastern catchment is much larger than the western and therefore contributes the majority of glacier runoff, it is unlikely that the effect is due to processes in the eastern catchment being out of phase with bulk catchment discharge.

Autocorrelation analysis demonstrates that despite lagging the series to obtain best match positions significant pattern remains in the residual series. This, combined with low r^2 values for the later periods, indicates very poor model performance. First differencing succeeds in removing all residual autocorrelation; however, r^2 values are very low. The characteristics of the 1999 melt season, therefore, appear very unusual compared with those of the 1998 season and of most temperate and even many polythermal glaciers (e.g. Gurnell et al., 1992a, 1994). Of the quasi-autocorrelation effects that may contribute to poor model performance: 1) scatter plots suggest non-linearity in the dataset is unlikely (Figure 4.23); and 2) lags and hysteresis are accounted for by obtaining best-match positions between variables. As a result, the presence of missing explanatory variables seems a likely source of the residual scatter, suggesting that there are physical processes other than discharge that control sediment transport. In line with decreasing r^2 values towards the end of the monitored period, these additional mechanisms must increase in importance throughout the melt season.

A particularly unusual characteristic of the dataset during 1999 is the way discharge (and rate of change of discharge) is observed to precede suspended sediment concentration or rate of change of suspended sediment concentration. Visual analysis of the time series clearly shows that for sub-periods 4, 5 and 6, higher suspended sediment concentrations occur on the falling limbs of each diurnal cycle (Figure 4.24). In most fluvial

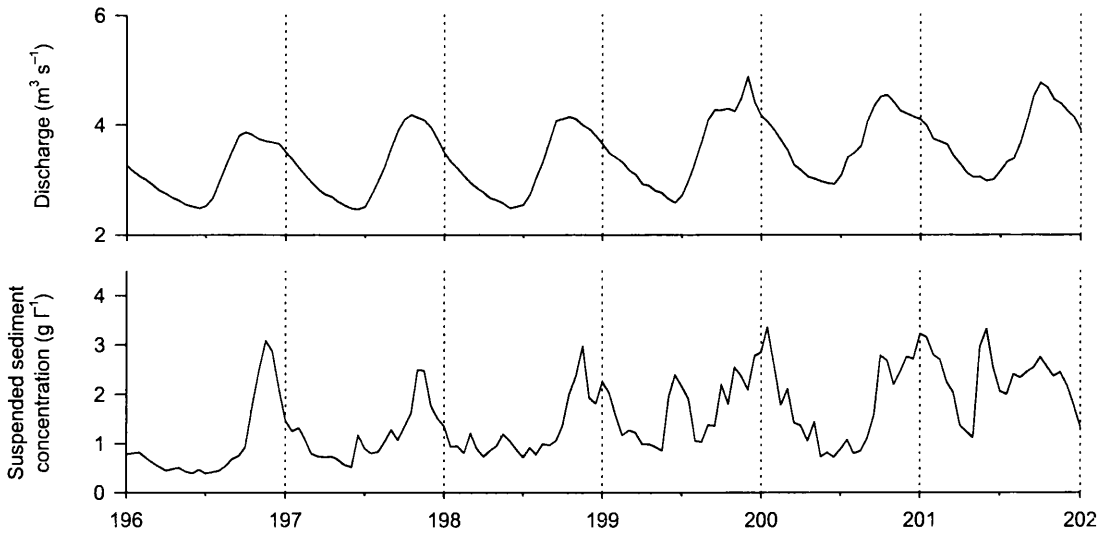

Figure 4.24 Peaks in suspended sediment concentration in the eastern catchment during 1998 occurring after peak catchment discharge.

environments, the entrainment and transport of sediment is largely controlled by flow capacity (see Section 1.3.2.1) and is typically characterised by clockwise hysteresis between discharge and suspended sediment transport (Bogen, 1981). It is difficult to envisage subglacial processes that may be responsible for the transport of greater sediment concentrations as discharge (and thus flow capacity) is falling.

A far simpler explanation is the contribution of additional sediment sources from outside the subglacial catchment, namely in marginal streams draining from small cirque glaciers below Bouquetins (cf. Figures 2.1 and 2.3). Discharge from these streams is unlikely to represent a significant proportion of the catchment discharge; however, they are observed to carry high concentrations of extraglacial sediments obtained from the steep valley sides that are thickly plastered with unconsolidated glacial sediment. Seasonally, flow in these streams is observed to lag behind discharge from the main glacier due to the high altitude of the cirque basins (~ 3000–3300 m) and thus a more persistent snow cover. Their altitude and westerly facing aspect also means that on a diurnal basis, melting occurs later and continues even as melting on the main glacier declines due to shading from adjacent peaks. Field observations suggest high suspended sediment concentrations in these marginal streams during and particularly towards the

end of the monitored period during 1999, with peak suspended sediment concentrations during the late afternoon. Consequently, extraglacial sources of sediment are believed to have had a major contribution to sediment transport in the eastern proglacial stream later in the melt season, and their contamination of the glacial signature is likely to present severe difficulties for provenancing suspended sediment from the subglacial drainage system.

4.4 SUB-SEASONAL MULTIPLE REGRESSION ANALYSIS

4.4.1 Introduction and method

In this section, multiple regression analysis is used to improve the performance of ordinary rating curves established for sub-periods of the 1998 melt season (see Section 4.3). Multiple regression can improve understanding of sediment entrainment by the identification of variables other than discharge that are significant in explaining suspended sediment transport and for which some form of process significance can be ascribed. For example, Willis et al. (1996) included variables designed to simulate short (diurnal), medium and long-term suspended sediment availability at Mitdtalsbreen, Norway. Variables found to be significant in explaining variation in suspended sediment concentration, in addition to discharge, were *rate of change of discharge* and *days since discharge was equalled or exceeded.* Hodson and Ferguson (1999) empolyed a similar approach, although long-term sediment availability was simulated using a cumulative discharge index (as opposed to Willis et al. (1996)'s *days since the beginning of summer*), which Ferguson (1984, 1987) had previously found to be a good surrogate for sediment exhaustion in the Hunza River, Karakoram.

Both these studies found that multiple regression techniques explained significantly more of the total variance in the suspended sediment series than discharge alone; however, autocorrelation in the residual series remained. Using an ARIMA model, Willis et al. (1996) modelled residuals from a 2 hourly sediment series and suggested that rates of change of suspended sediment concentration were also influenced by random changes in suspended sediment concentration 2 hours (i.e. SSC_{t-1}), 24 and 48 hours previously. However, it is often difficult to place physical interpretations on parameters from

ARIMA models of the residual series (see Section 4.1.2.1). Instead, Hodson and Ferguson (1999) have favoured a simpler approach involving the production of new multiple regression models that included previous values of suspended sediment concentration at time *t–n*. These variables were intended to simulate changes in sediment availability due to subglacial processes, and successfully removed the remaining pattern in the residual series.

Here, multiple regression analysis is performed for sub-periods of the 1998 melt season in order to identify additional significant variables that control suspended sediment transport for which some process significance can be ascribed. Multiple regression analysis was not performed for sub-periods of the 1999 melt season due to the possible contamination of the subglacial signature due to likely significant extraglacial sediment contributions (see Section 4.3). There is some advantage in applying multiple regression techniques to sub-periods rather than the whole melt season, since it is likely to enable the identification of the changing importance of different variables as the season progresses. Note, however, that for ordinary rating curves developed in Section 4.3, the residual variance for many of the sub-periods was small and therefore a large proportion may reside in measurement errors.

Following Willis et al. (1996) and Hodson and Ferguson (1999), the variables used in the multiple regression analysis (in addition to discharge) and the reason for their inclusion are given below.

— *Hours since period began* (*h*). This variable represents longer-term changes in sediment availability during an individual sub-period. This variable is essentially the same as Willis et al. (1996)'s *days since the beginning of summer*, for which Hodson and Ferguson (1999) substituted cumulative discharge.

— *Days since discharge was equalled or exceeded* (Q_d). This variable represents medium-term sediment supply variations; for example, the extent to which recent flows have exhausted subglacial sediment sources (Willis et al., 1996). Hodson and Ferguson (1999) used the same variable, although changes during the previous three hours were excluded such that the variable did not drop to zero during large events when the rise in discharge was temporally arrested. Here, Q_d was calculated for the

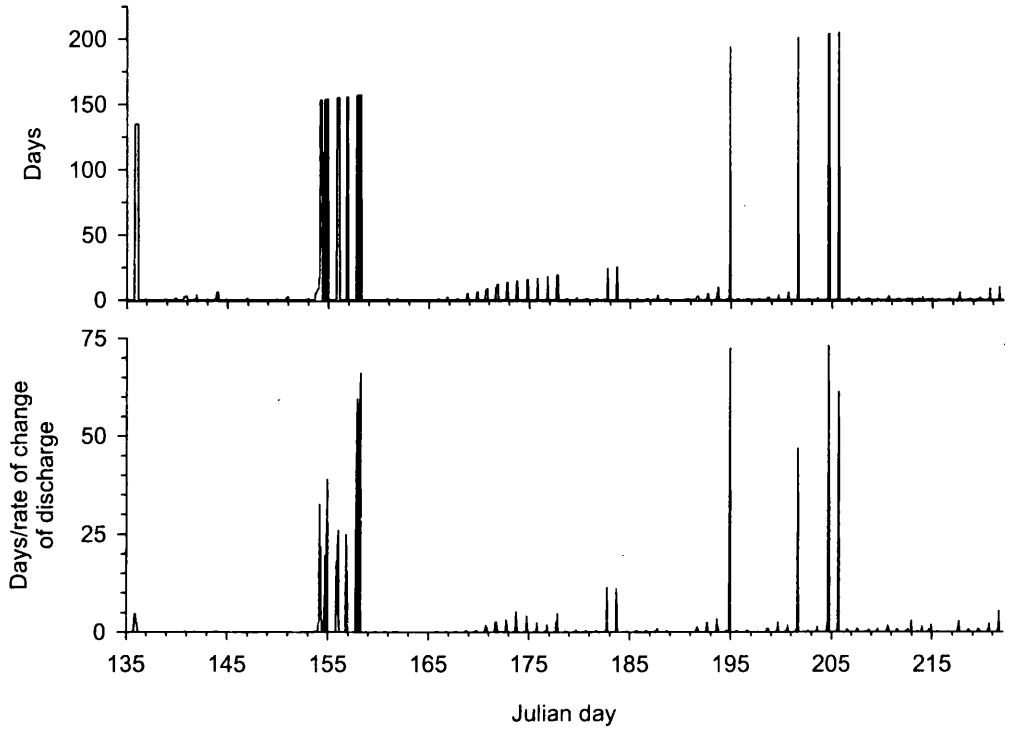

Figure 4.25 *Days since discharge last equalled or exceeded* (top) and *days since discharge last equalled or exceeded* multiplied by rate of change of discharge (below).

entire melt season from 01:00 on JD 1. However, Figure 4.25 shows that large values of Q_d often occur in response to very marginal increases in discharge, most notably when a value of discharge had not previously been exceeded during the season. A partial solution to this problem was found by multiplying values of Q_d by the rate of change of discharge (in $m^3 s^{-1}$) during the preceding hour (i.e. $Q_t - Q_{t-1}$, where Q_t represents catchment discharge), such that values of Q_d took into account the magnitude by which recent flows were being exceeded (Figure 4.25).

— *Rate of change of discharge* ($\Delta \log Q$). This variable was calculated by first differencing the log-transformed catchment discharge series. The variable represents flushing and exhaustion of sediment on the rising and falling limbs during diurnal cycles (Willis et al., 1996; Hodson and Ferguson, 1999), and has been identified by ordinary linear regression techniques as being a potentially significant explanatory variable in the 1998 dataset (see above).

— *Rainfall in the preceding 1, 2, 3, 4 and 6 h, and at lags 1 to 3 h* ($\Sigma R1$ to $\Sigma R6_{t-3}$, respectively). Rainfall in the preceding 1, 2, 3, 4, and 5 h was identified by Willis et al. (1996) as a potential control on suspended sediment transport since runoff during rainstorms is likely to have traversed the valley sides and proglacial zone from which sediments can be easily entrained. At Haut Glacier d'Arolla, suspended sediment monitoring took place very close to the glacier snout in order to minimise contributions from proglacial sources; however, some rainfall on extraglacial areas will enter the glacial drainage system via marginal streams that become subglacial before reaching the glacier snout. Since rain falling in extraglacial locations may be very much delayed in reaching the glacial drainage system, lagged rainfall variables were also used in the multivariate analysis.

Histograms were used to check for normality in each of these additional independent variables. Only $\Delta \log Q$ was found to be normally distributed; however, where n is large, non-normality in the distribution of the independent variables is unlikely to have a significant effect on the reliability of the multivariate models (StatSoft, 1995).

For each sub-period, stepwise regression techniques were used in order to find the simplest and most efficient multiple regression model based on the prescribed independent variables. The F-statistic in the stepwise procedure was set to 4.0, such that explanatory variables whose t-statistic was ≤ 2, and were therefore not significant at $p \leq 0.05$, were excluded from the final equation. The explanatory power of the multiple regression models were evaluated using their coefficient of determination, and the significance of individual explanatory variables assessed using the proportion of variance in the dependent series they explain, the magnitude of their slope coefficient and its significance (i.e. p-statistic). Finally, the residual series was checked using autocorrelation analysis in order to identify any remaining systematic variation that the multiple regression model had failed to explain.

4.4.2 Multiple regression results

Initial multiple regression equations for each of the sub-periods of the 1998 melt season are shown in Table 4.7. This approach resulted in improved R^2 values for each of the

Table 4.7 Multiple regression models for sub-periods of the 1998 melt season. Figures in parenthesis beneath each coefficient indicate the coefficient *p*-statistic followed by the proportion of variance explained (b-coefficients only). See text for abbreviations.

Sub-period and equation		R^2
1	$\log SSC = \underset{(<0.001)}{-0.604} \underset{(<0.001;0.569)}{-0.000923\,h} \underset{(<0.001;0.117)}{+0.148\,Q_d} \underset{(0.006;0.006)}{+0.294\log Q}$	0.690
2	$\log SSC = \underset{(<0.001)}{-0.564} \underset{(<0.001;0.861)}{+1.63\log Q} \underset{(<0.001;0.014)}{+0.0351\,\Sigma R2_{t-1}} \underset{(0.004;0.005)}{-0.0023\,h} \underset{(0.033;0.004)}{-0.00936\,\Sigma R6_{t-3}}$	0.881
3	$\log SSC = \underset{(<0.001)}{-0.699} \underset{(<0.001;0.873)}{+0.678\log Q} \underset{(<0.001;0.009)}{-0.00285\,h} \underset{(0.010;0.007)}{+0.0149\,\Sigma R4} \underset{(0.046;0.003)}{+0.718\,Q_d}$	0.889
4	$\log SSC = \underset{(<0.001)}{-0.761} \underset{(<0.001;0.824)}{+1.59\log Q} \underset{(<0.001;0.079)}{+4.23\,\Delta\log Q} \underset{(<0.001;0.016)}{-0.00114\,h} \underset{(<0.001;0.004)}{+0.0427\,Q_d}$	0.923
5	$\log SSC = \underset{(<0.001)}{-1.72} \underset{(<0.001;0.711)}{+2.36\log Q} \underset{(<0.001;0.086)}{+4.2\,\Delta\log Q} \underset{(<0.001;0.022)}{+0.076\,h} \underset{(0.007;0.005)}{+0.0446\,\Sigma R1_{t-1}}$	0.821
6	$\log SSC = \underset{(<0.001)}{-1.08} \underset{(<0.001;0.753)}{+2.07\log Q} \underset{(<0.001;0.118)}{+3.32\,\Delta\log Q} \underset{(<0.001;0.013)}{-0.00384\,h} \underset{(<0.001;0.004)}{+0.0375\,\Sigma R2_{t-2}}$	0.886
7	$\log SSC = \underset{(<0.001)}{-1.48} \underset{(<0.001;0.831)}{+2.74\log Q} \underset{(0.007;0.009)}{+0.000965\,h} \underset{(0.002;0.010)}{+0.0645\,\Sigma R1_{t-2}} \underset{(0.034;0.006)}{-0.014\,\Sigma R6_{t-3}}$	0.851
8	$\log SSC = \underset{(<0.001)}{-1.17} \underset{(<0.001;0.820)}{+2.16\log Q} \underset{(<0.001;0.029)}{+0.609\,\Sigma R2_{t-1}} \underset{(<0.001;0.019)}{+0.906\,\Delta\log Q} \underset{(<0.001;0.013)}{+0.248\,\Sigma R6_{t-3}} \underset{(0.015;0.007)}{-0.286\,\Sigma R6_{t-2}}$	0.883

models; however, some unusual characteristics in the form of the models were noted for sub-periods 1–4. In sub-period 1, log$Q$ is unexpectedly usurped by h, whilst the b-coefficient of log$Q$ is markedly different from that obtained using simple linear regression modelling. Although log$Q$ remains the primary explanatory variable, radically different b-coefficients from those obtained using linear regression models also occur for log$Q$ during sub-periods 2–4. Since linear models have demonstrated that log$Q$ explains the majority of the variance in the suspended sediment concentration series, the inclusion of additional explanatory variables should result in only minor adjustments to the slope of log$Q$. A process of trial and error revealed the cause of these radical changes to be the inclusion of variable h.

This type of effect is a known symptom of multicollinearity, where individual variables are strongly correlated with each other and, whilst R^2 values and predictions from models with inter-correlated variables are reliable, the partitioning out of the individual

Table 4.8 Multiple regression models for sub-periods of the 1998 melt season after removing variable h from the list of possible independent predictors.

Sub-period and equation	R^2
1 $\log SSC = \underset{(<0.001)}{-0.62} \underset{(<0.001;0.520)}{-1.191 \log Q} \underset{(<0.001;0.109)}{+0.148 Q_d} \underset{(0.004;0.007)}{+0.0159 \Sigma R6_{t-3}}$	0.635
2 $\log SSC = \underset{(<0.001)}{-0.662} \underset{(<0.001;0.862)}{+1.31 \log Q} \underset{(0.005;0.014)}{+0.0277 \Sigma R2_{t-1}} \underset{(0.028;0.004)}{+0.00278 Q_d}$	0.877
3 $\log SSC = \underset{(<0.001)}{-1.04} \underset{(<0.001;0.873)}{+1.36 \log Q} \underset{(0.003;0.004)}{-0.0205 \Sigma R6_{t-3}} \underset{(0.031;0.004)}{+0.0254 \Sigma R3_{t-3}}$	0.879
4 $\log SSC = \underset{(<0.001)}{-0.859} \underset{(<0.001;0.824)}{+1.20 \log Q} \underset{(<0.001;0.079)}{+4.12 \Delta \log Q} \underset{(<0.001;0.010)}{+0.0637 Q_d}$	0.913
5 $\log SSC = \underset{(<0.001)}{-1.50} \underset{(<0.001;0.711)}{+2.13 \log Q} \underset{(<0.001;0.086)}{+4.39 \Delta \log Q} \underset{(<0.001;0.009)}{+0.0352 \Sigma R2_{t-1}}$	0.804
6 $\log SSC = \underset{(<0.001)}{-1.12} \underset{(<0.001;0.753)}{+1.94 \log Q} \underset{(<0.001;0.118)}{+3.41 \Delta \log Q} \underset{(<0.001;0.005)}{+0.0413 \Sigma R2_{t-2}}$	0.874
7 $\log SSC = \underset{(<0.001)}{-1.46} \underset{(<0.001;0.831)}{+2.81 \log Q} \underset{(0.007;0.008)}{+0.0581 \Sigma R1_{t-2}} \underset{(0.018;0.008)}{-0.016 \Sigma R6_{t-3}}$	0.843
8 $\log SSC = \underset{(<0.001)}{-1.17} \underset{(<0.001;0.820)}{+2.16 \log Q} \underset{(<0.001;0.029)}{+0.609 \Sigma R2_{t-1}} \underset{(<0.001;0.019)}{+0.906 \Delta \log Q} \underset{(<0.001;0.013)}{+0.248 \Sigma R6_{t-3}} \underset{(0.015;0.007)}{-0.286 \Sigma R6_{t-2}}$	0.883

effects of the independent variables is not (Statsoft, 1995; Rogerson, 2001). Examining correlation coefficients between independent variables for the 8 sub-periods, h and log$Q$ were found to be highly correlated for sub-periods 1–4, demonstrating r values of between 0.85–0.94. These values demonstrate high levels of inter-correlation between variables; for the remaining sub-periods, r values were below 0.5. Most statistical packages check for correlation between variables when performing multiple regression; however, the version of Minitab used here (Release 9.2) outputs a warning only if r^2 for any two variables is greater than 0.990 (Minitab Inc., 1993).

Variable h appears to be highly correlated with log$Q$ for sub-periods 1–4 due to subdivision of the melt season being based primarily on trends in minimum and maximum discharge; hence, early in the season when there are marked trends in these variables, h shows strong positive or negative association with daily mean flows. New multiple regression equations produced without variable h (cf. Rogerson, 2001) demonstrate only minor reductions in R^2 (Table 4.8). In addition to this, relationships

Table 4.9 Ordinary rating curves between h and suspended sediment concentration residuals from the multiple regression models presented in Table 4.8. Values in parenthesis indicate the significance level of the intercept and slope coefficients.

Sub-period	Equation	R^2
1	$\log SSCresids = \underset{(<0.001)}{0.0439} - \underset{(<0.001)}{0.000212}\ h$	0.039
2	$\log SSCresids = \underset{(0.383)}{0.0244} - \underset{(0.313)}{0.000342}\ h$	0.000
3	$\log SSCresids = \underset{(0.510)}{0.0097} - \underset{(0.446)}{0.000136}\ h$	0.000
4	$\log SSCresids = \underset{(0.068)}{0.0221} - \underset{(0.035)}{0.000132}\ h$	0.010
5	$\log SSCresids = \underset{(<0.001)}{-0.0718} + \underset{(<0.001)}{0.000546}\ h$	0.060
6	$\log SSCresids = \underset{(<0.001)}{0.0826} - \underset{(<0.001)}{0.000313}\ h$	0.078
7	$\log SSCresids = \underset{(0.024)}{-0.0529} + \underset{(0.009)}{0.000889}\ h$	0.048
8	$\log SSCresids = \underset{(0.736)}{0.0047} + \underset{(0.031)}{0.0696}\ h$	0.034

between the residuals from the new multiple regression equations and variable h are poor (Table 4.9), with slope coefficients typically << 0.1 and intercept coefficients either approaching or not significantly different from zero.

After removing h, the multiple regression equations (Table 4.8) show log$Q$ to be the most important explanatory variable for all sub-periods. In addition, b-coefficients for log$Q$ demonstrate only minor differences with respect to those calculated using ordinary rating curves. In addition to discharge, the variables found to be significant in explaining suspended sediment concentration were *days since discharge was equalled or exceeded*, *rate of change of discharge*, and *rainfall* (over a variety of time periods and lags). As expected, the variables found to be significant in explaining suspended sediment evacuation varied during the melt season, and individual variables account for different proportions of the total variance during different sub-periods. Log$Q$ is especially dominant during sub-periods 2, 3 and 7, where the additional independent variables account for less than 2% of the total variance in the suspended sediment series. During

the remaining sub-periods, the additional variables account for between 6.8 and 12.3% of the total variance in the suspended sediment series.

4.4.3 Residual analysis

Multiple regression analysis resulted in occasionally significant increases in the coefficient of determination for each of the sub-periods; however, good model performance is best indicated by the absence of pattern in the residuals. Compared with the results from the lagged, linear regression models (above), there is a substantial reduction in autocorrelation for many of the sub-periods (Figure 4.26). In particular, the magnitude of the diurnal wavelength within the patterns has been much reduced for sub-periods 4–6, such that for sub-period 4 it is no longer significant. Serial autocorrelation, however, remains a significant feature for all sub-periods.

Poor performance of the multivariate models again raises the question of whether residual autocorrelation persists due to quasi-autocorrelation or true-autocorrelation effects. Having performed multivariate analysis, previous authors have successfully modelled the residuals using auto-regressive models or by including lagged suspended sediment concentration series in new multiple regression models. Both approaches tacitly assume the presence of true-autocorrelation in the suspended sediment time series, since they effectively relate present values of suspended sediment concentration to those at time $t–n$, where t is the sampling interval and n is typically found to be 1. These 'last resort' approaches are acceptable if both a satisfactory physical interpretation can be placed upon the model parameters and any still remaining autocorrelation can be satisfactorily explained.

Here, new multiple regression models are constructed following Hodson and Ferguson (1999) that incorporate lagged values of suspended sediment concentration in order to account for the serial autocorrelation in the time series (Table 4.10). The residual series from the multiple regression models was first analysed using stepwise regression of 24 variables of lagged SSC (i.e. SSC_{t-1} to SSC_{t-24}), in order to identify those parameters that best describe the residual autocorrelation. The most significant parameter was then entered into a new multiple regression model along with the significant independent

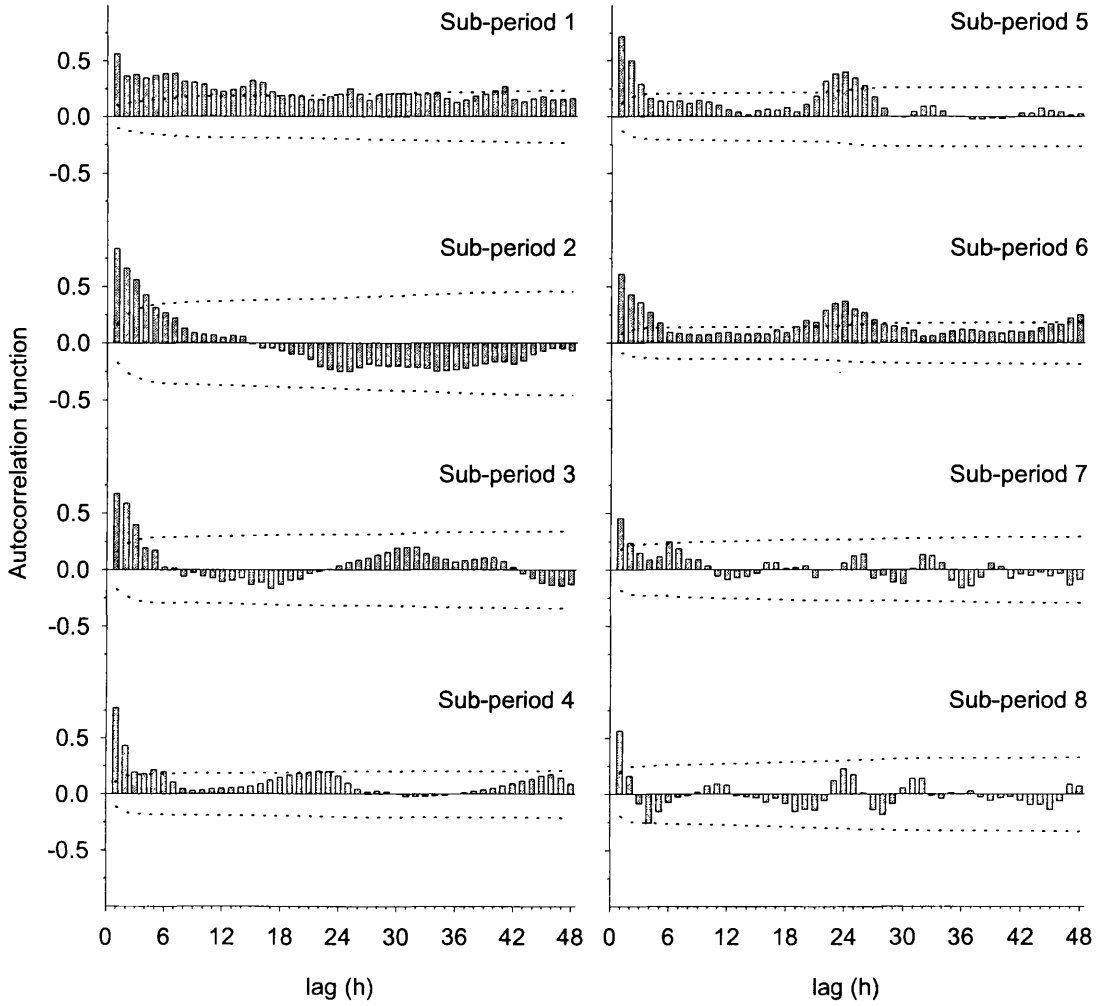

Figure 4.26 Residual autocorrelation diagrams from multiple regression models for sub-periods of the 1998 melt season (Table 4.6).

variables from the original multiple regression model (Table 4.8). Stepwise regression was again used to identify the best set of predictors, and the residuals checked to establish if the remaining autocorrelation had been successfully removed. If pattern in the residuals remained, the next most significant lagged value of SSC was added to the multiple regression model and the process repeated.

Figure 4.27 shows autocorrelation patterns for the residual series from the new multiple regression models (Table 4.10). For sub-periods 1–7, stepwise regression of variables SSC_{t-1} to SSC_{t-24} and residuals from the original multiple regression model demonstrated SSC_{t-1} to be the most important predictor, the addition of which successfully removed the

Table 4.10 Multiple regression models incorporating lagged values of log*SSC* to remove serial autocorrelation patterns in the residual series. Values in parenthesis: see Table 4.7.

Sub-period and equation	R^2
1 $\log SSC = -0.109_{(<0.001)} + 0.831_{(<0.001;0.889)} \log SSC_{t-1} + 0.0357_{(<0.001;0.004)} Q_d + 0.186_{(<0.001;0.005)} \log Q$	0.897
2 $\log SSC = -0.130_{(<0.001)} + 0.797_{(<0.001;0.955)} \log SSC_{t-1} + 0.00215_{(0.002;0.005)} Q_d + 0.227_{(<0.001;0.003)} \log Q + 0.0128_{(0.020;0.001)} \Sigma R2_{t-1}$	0.963
3 $\log SSC = -0.218_{(<0.001)} + 0.788_{(<0.001;0.956)} \log SSC_{t-1} + 0.268_{(<0.001;0.004)} \log Q - 0.00045_{(0.025;0.001)} \Sigma R6_{t-3}$	0.961
4 $\log SSC = -0.174_{(<0.001)} + 0.792_{(<0.001;0.954)} \log SSC_{t-1} + 3.17_{(<0.001;0.023)} \Delta \log Q + 0.240_{(<0.001;0.005)} \log Q - 0.0119_{(0.020;<0.001)} Q_d$	0.982
5 $\log SSC = -0.327_{(<0.001)} + 0.741_{(<0.001;0.856)} \log SSC_{t-1} + 3.67_{(<0.001;0.067)} \Delta \log Q + 0.439_{(<0.001;0.006)} \log Q$	0.929
6 $\log SSC = -0.227_{(<0.001)} + 0.739_{(<0.001;0.884)} \log SSC_{t-1} + 2.68_{(<0.001;0.067)} \Delta \log Q + 0.357_{(<0.001;0.003)} \log Q + 0.0179_{(0.002;<0.001)} \Sigma R2_{t-2}$	0.953
7 $\log SSC = -0.941_{(<0.001)} + 1.82_{(<0.001;0.831)} \log Q + 0.392_{(<0.001;0.045)} \log SSC_{t-1} - 0.0159_{(0.007;0.008)} \Sigma R6_{t-3}$	0.881
8 $\log SSC = -0.535_{(<0.001)} + 0.978_{(<0.001;0.820)} \log Q + 0.471_{(<0.001;0.029)} \Sigma R2_{t-1} + 1.64_{(<0.001;0.019)} \Delta \log Q + 0.525_{(<0.001;0.041)} \log SSC_{t-1} + 0.401_{(<0.001;0.004)} \Sigma R6_{t-3} - 0.371_{(<0.001;0.011)} \Sigma R6_{t-2}$	0.920

residual autocorrelation in all sub-periods except sub-period 6 (Figure 4.27). Here, autocorrelation with a wavelength of 24 *h* remains; however, the next most significant variable, SSC_{t-24}, was not significant at $p < 0.05$ and thus true-autocorrelation could not satisfactorily explain the diurnal autocorrelation pattern. For sub-period 8, SSC_{t-15} was identified as explaining the largest proportion of the variance in the residual series. However, SSC_{t-15} is unlikely to have any process significance, and addition of this variable to the mutliple regression equation increased the amplitude of the residual pattern. Instead, entering SSC_{t-1} again resulted in a significant decline in residual autocorrelation (Figure 4.27).

The new multiple regression models for sub-periods 1–6 show that the variable SSC_{t-1} becomes the most important predictor, generally at the expense of log$Q$ (Table 4.10). Hodson and Ferguson (1999) observed the same effect, suggesting that SSC_{t-n} is bound to usurp log$Q$ in terms of predictive power because the general level of suspended sediment concentration depends at least partially upon the level of discharge. Hence,

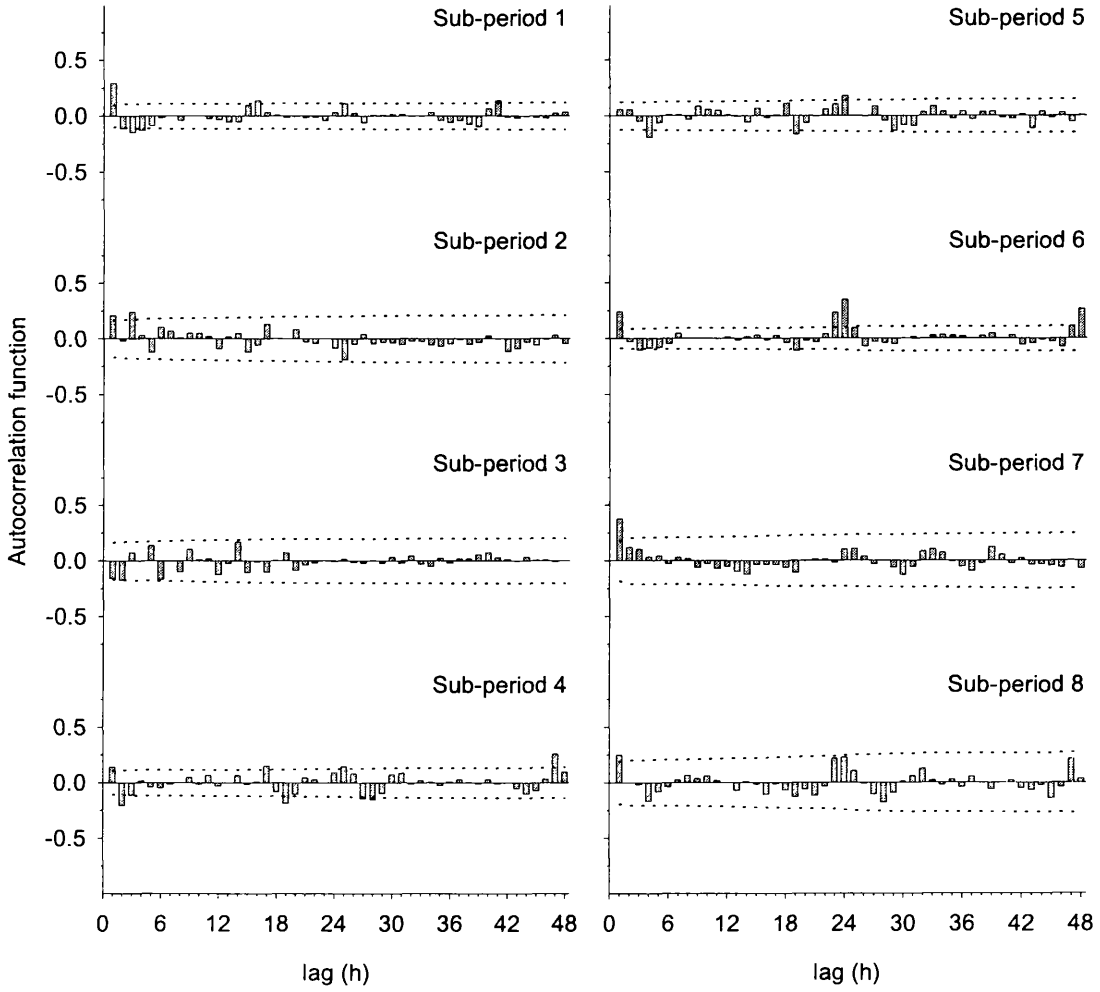

Figure 4.27 Residual autocorrelation diagrams from multiple regression models for sub-periods of the 1998 melt season incorporating lagged values of suspended sediment concentration (see Table 4.10).

during sub-periods 1 and 3 discharge drops out of the new model completely, and in the remaining sub-periods explains less than 1 % of the total variance.

The significant improvement in the performance of the multiple regression models suggests that true-autocorrelation is an inherent feature of the suspended sediment concentration series throughout the melt season. However, there is remaining pattern in the residuals from sub-period 6. Plotting the residuals through time demonstrates that for sub-period 6 there are large, systematic deviations in the residual series with a wavelength of approximately 24 h, the magnitude of which increases with time (Figure 4.28). Pattern with a diurnal wavelength is also evident during sub-period 8, although it

is not statistically significant (cf. Figure 4.27). Figure 4.29 relates the daily mean residual pattern to the mean discharge cycle for each sub-period. Sub-periods 1–3 show no clear pattern in the residual series, whereas sub-periods 4, 5 and 7 show a classic hysteresis pattern (although again not significant), with positive residuals as discharge rises followed by negative residuals during peak discharge and as discharge falls. Sub-sub-periods 6 and 8, however, show initially positive but then strongly negative residuals as discharge rises, roughly coinciding with the timing of peak suspended sediment concentrations. Residuals are then positive once again as discharge falls.

This effect is believed to be due to the increasing saturation of the turbidity sensors at peak suspended sediment concentrations as the season progresses: during sub-period 6, the effect is mainly seen as an increasing underestimation of suspended sediment concentrations at peak turbidity (Figure 4.28). During sub-period 8, the mean residual variation is large (Figure 4.28) but is not significant in autocorrelation plots (Figure 4.27) since n is small. It is here, however, that turbidity saturation has possibly the greatest effect on the form of the linear and multivariate models: in order that the residuals are evenly distributed around the main regression line, consistently lower measured peak suspended sediment concentrations have likely resulted in a lowering of the model intercept. The effect is such that the model for sub-period 8 underestimates concentrations either side of the overestimated suspended sediment peak.

4.4.4 Interpretation and conclusions

The results of the multivariate analysis demonstrate that suspended sediment concentration was primarily influenced by discharge, emphasising the importance of flow capacity for sediment entrainment and transport. However, variables other than discharge are significant in explaining suspended sediment concentration, and the specific combination and individual importance of the controlling variables changes throughout the melt season. The proportion of the variance explained, and the magnitude of the slope coefficient, is important in identifying the variables that have a significant impact upon suspended sediment transport.

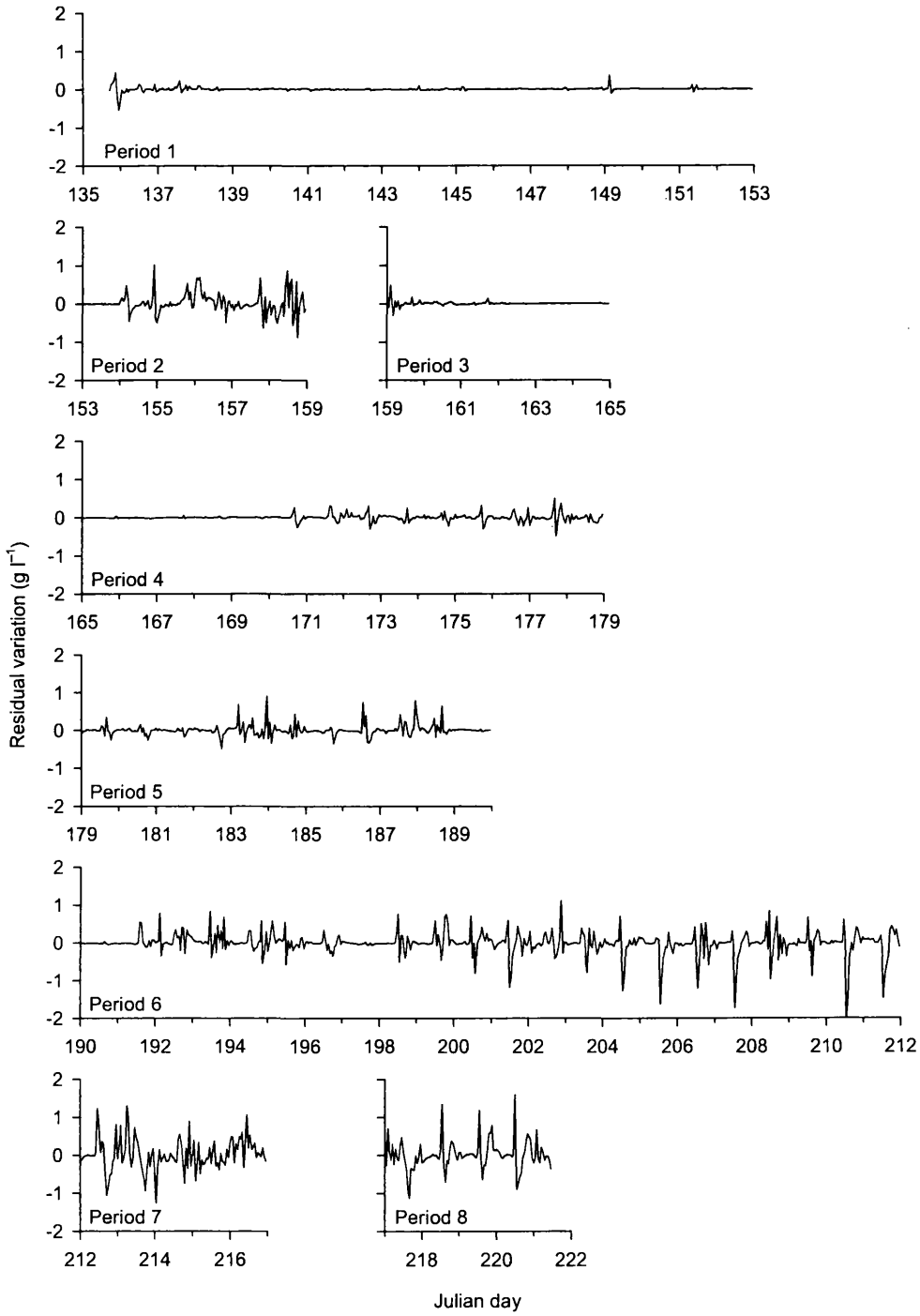

Figure 4.28 Time series plots of the residuals from the multiple regression models given in Table 4.10 for sub-periods 1–8 during the 1998 melt season.

Of the variables found to be significant during the 1998 melt season, rainfall variables typically explained a low proportion of the variance since rainfall events were rare

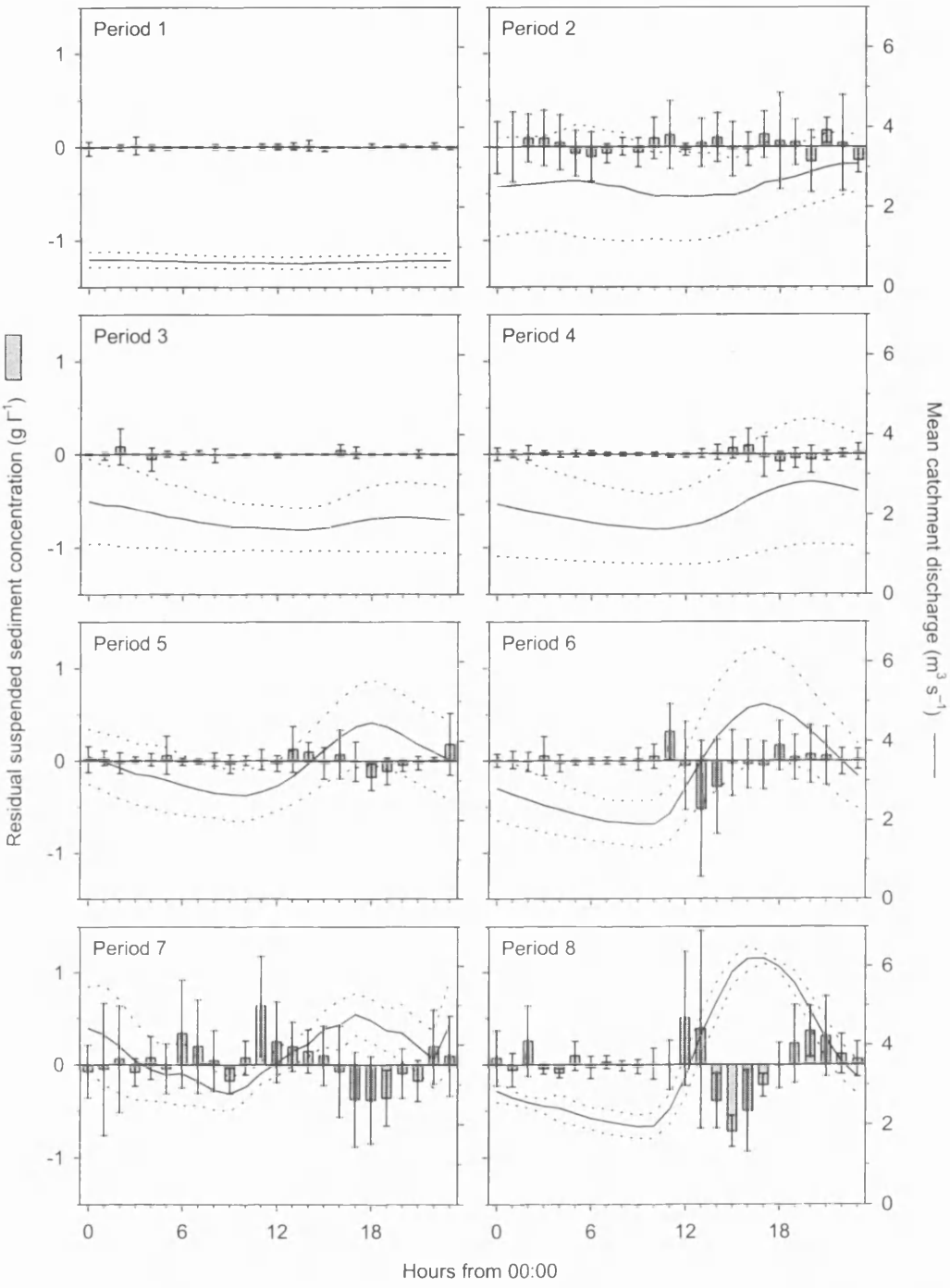

Figure 4.29 Hourly mean residual suspended sediment variation for sub-periods 1–8 of the 1998 melt season. Error bars represent one standard deviation about the mean. Dotted lines show one standard deviation about hourly mean discharge during each sub-period.

within most sub-periods. During sub-period 1, rainfall during the last 6 h with a lag of 3 h contributed to almost 1% of the variance in the suspended sediment series (Table 4.8),

although precipitation during this sub-period fell exclusively as snow (Table 3.1). During sub-periods 2, 3 and 5–8, precipitation fell predominantly as rain and was positively associated with sediment transport, often over short periods and with short lags that probably reflect the mean time with which overland flows traversed extraglacial areas to reach the glacial drainage system. Interestingly, rainfall variables that are negatively associated with sediment transport also occurred during sub-periods 3, 7 and 8. These variables were mainly rainfall over long periods (6 h) with long lags (2–3 h), suggesting that over these time scales extraglacial sediment sources were being exhausted. However, with the exception of sub-period 8, rainfall variables typically had low slope coefficients, suggesting that even during the heaviest, catchment-wide rainfall, the contribution of sediment from extraglacial areas was minor. For sub-period 8, the unusual significance of the rainfall variables, which also demonstrate $\Sigma R6_{t-3}$ to be positively correlated with sediment transport whilst $\Sigma R6_{t-2}$ is negative, is probably spurious. The sub-period was predominantly rain-free but also very short; since n is small, some rainfall occurring at the start of the sub-period (due to the somewhat arbitrary location of the boundary between sub-periods 7 and 8 at 00:00 on JD 217) likely had a large influence on the multiple regression model.

Analysis of the explanatory power of variable h on residuals from each multivariate equation shows that for all sub-periods the relationship was very weak (Table 4.9), indicating that changes in sediment availability were successfully isolated by dividing the melt season into smaller, hydrologically-defined sub-periods (Table 3.1). Variables that are clearly important from the multivariate equations are Q_d and $\Delta \log Q$. Variable Q_d explained a sizeable proportion of the variance during sub-period 1, demonstrating that increases in discharge above recent values were important for accessing and entraining basal sediments; $\Delta \log Q$ is important during sub-periods 4–6 and 8, indicating the presence of hysteresis. Notably, $\Delta \log Q$ explained an increasing proportion of the variance through sub-periods 4–6. The relative insignificance of $\Delta \log Q$ during sub-period 8 was probably due to large measurement errors resulting from saturation of the turbidity sensors.

As expected, true-autocorrelation has been shown to persist throughout the melt season, indicated by the general significance of variable SSC_{t-1}. However, in removing the

remaining serial autocorrelation, analysis of the final residual series has also enabled some insight into the cause of the remaining unexplained variance in the suspended sediment series. The residuals from sub-periods 1–3 demonstrate no identifiable mean daily pattern, although there are temporal trends (Figure 4.28). During sub-periods 1 and 3, the magnitude of the residuals is low; however, sub-period 2 shows high residual variation that exhibits increasing amplitude as the sub-period progresses. Throughout the remainder of the season, hysteresis effects dominate residual variation, although during sub-period 8 this is masked by the influence of turbidity sensor saturation on the multiple regression model. This is also likely to have contributed to the increasing amplitude in the residual series as the season progressed, although sub-period 7 is markedly different, exhibiting high-amplitude and closely-spaced residual variation.

4.5 RELATIONSHIPS BETWEEN SUSPENDED SEDIMENT TRANSPORT, GLACIAL AND FLUVIOGLACIAL DYNAMICS DURING 1998

4.5.1 Introduction

Ordinary rating curve and multiple regression techniques have demonstrated that for individual sub-periods of the 1998 melt season, suspended sediment concentration is strongly related to discharge. However, the form of this relationship changes throughout the season, suggesting changes occur in the mechanisms by which basal sediments are evacuated from the subglacial drainage system. In this section, relationships between discharge and suspended sediment transport during the 1998 melt season are interpreted against knowledge of the dynamic nature of the glacial and fluvioglacial systems in order to elucidate the mechanisms responsible for sediment evacuation by subglacial meltwater. Analysis of the 1999 melt season suggested that late in the monitored period suspended sediment transport was likely to have reflected significant extraglacial sediment inputs; therefore potential to obtain information about the entrainment of sediment by subglacial meltwaters is likely to be very limited, and the 1999 season is not considered below.

4.5.2 Summary of glacial and fluvioglacial dynamics during 1998

Analysis of proglacial streamflow, water quality and ice motion data indicated a systematic evolution of meltwater sources and pathways within the monitored period of the 1998 melt season (Table 3.6). During sub-periods 1 to 4, a predominantly distributed subglacial drainage system persisted, fed by basal meltwaters and highly-damped inputs of surface melt routed initially through the supraglacial snowpack. Consequently, during sub-periods 2 and 4, rapid increases in surface melting were associated with two 'spring events' caused by increased discharge through the distributed system and associated high basal water pressures. During sub-period 2, melting was initiated by a combination of rising air temperatures and heavy rainfall; however, increased flow through the distributed system is likely to have been greatest beneath the glacier tongue. Hence, channelisation was likely to have been limited, being confined to PDAs along the lower glacier tongue, but still resulted in the release of 'stored' meltwater. During sub-period 4, melting occurred due to high incident radiation, resulting in the widespread increase in flow through the distributed system. Rapid channelisation is likely to have occurred towards the end of the event, causing in the decline in horizontal ice motion despite rising flow through the distributed system. Flow through these incipient channels most likely occurred under closed conditions.

During sub-periods 5–8, supraglacially derived meltwaters were increasingly routed through a channelised subglacial drainage system (Table 3.6). During sub-period 5, rapid channelisation probably continued as the snowline retreated (cf. Table 2.1), resulting in the increasing amplitude of glacier runoff as both ice melt sources increased and the proportion of melt routed through distributed supraglacial and subglacial drainage declined. During sub-periods 5 and 6, the increasing peakedness of supraglacial runoff likely resulted in channels being open for an increasing proportion of the diurnal cycle but increasingly surcharged at peak flows, resulting in high basal water pressures and thus local ice-bed separation. Channelisation was likely complete by the end of sub-period 6 and overpressurisation during peak discharges continued during sub-period 8. Sub-period 7, however, was quite distinct, since the diurnal pattern of surface melt was heavily modified by föhn and rain. Hence, channels are expected to have been 'open' and rarely overpressurised, with correspondingly low horizontal ice motion.

4.5.3 Suspended sediment concentration

4.5.3.2 Controls on suspended sediment entrainment

For individual sub-periods of the melt season, ordinary rating curves demonstrate that suspended sediment transport is closely related to discharge. However, there are marked differences in the relationship between discharge and suspended sediment concentration that correspond to periods of predominantly distributed and channelised drainage (Section 4.3, Table 4.11). During sub-periods 1–4 when the subglacial drainage system is predominantly distributed, the relationship is $\log SSC \propto \sim 1.25 \log Q$, whereas for sub-periods 5, 6 and 8 following initial channelisation, $\log SSC \propto \sim 2.1 \log Q$. Sub-period 7 shows an even stronger relationship, with $\log SSC \propto \sim 2.8 \log Q$. Multiple regression (Section 4.4) confirms that additional independent variables explain little of the variance in the suspended sediment series, and result in only minor changes to the relationship between suspended sediment concentration and discharge.

During periods of distributed and channelised drainage, there are also statistically significant changes in the intercept of ordinary rating curves for the individual sub-periods (Section 4.3). During the period of distributed drainage, there is evidence for high sediment availability during sub-periods 1 and 2 (the first spring event), decreased sediment availability during sub-period 3, and a slight recovery in sediment availability during sub-period 4 (the second spring event). During the period of channelised drainage, there is evidence of initially low but increasing sediment availability as the season progressed. The actual increase in availability between sub-periods 6 and 8 is certain to have been greater than indicated due to the influence of turbidity sensor saturation on the form of the ordinary rating curves (see Section 4.4). These broad changes in sediment availability are clearly evident in time series plots of the residuals from seasonal ordinary rating curves for catchment discharge and suspended sediment concentration or daily suspended sediment load (Figures 4.8 and 4.10 b).

During the change from distributed to channelised drainage, it is the combination of changes in both intercept and slope of the relationship between discharge and suspended sediment concentration that are most significant (Section 4.3; Figure 4.11). These changes demonstrate that following initial channelisation towards the end of sub-period

4 and the beginning of sub-period 5, sediment availability fell such that flows across the measured range of discharge during sub-period 5 were less efficient at entraining basal sediments than equivalent flows during any previous sub-period (Figure 4.11). Later in the season, sediment availability increased, such that during sub-period 8, flows over ~ 4 m^3 s^{-1} were more efficient at accessing and entraining sediments than during any previous sub-period. This probably explains the much higher daily suspended sediment loads towards the end of the monitored sub-period than predicted from daily catchment discharge (Figure 4.10 b).

From multiple regression models, the explanatory strength of the individual independent variables during the season also demonstrate variations that correspond to systematic changes in meltwater sources and pathways (Table 4.8). During sub-period 1, when flow through the distributed system was low and dominated by snowmelt, discharge accounts for a relatively low proportion of the variance in the suspended sediment transport series and the variable *days since discharge was equalled or exceeded* accounted for an additional ~ 11 %. In addition to this, much of the variance during sub-period 1 remains unexplained. However, during the first spring event (sub-period 2) and immediately afterwards (sub-period 3), suspended sediment concentration is strongly forced by discharge, explaining a large proportion of the variance in the suspended sediment concentration series, with additional independent variables being largely unimportant.

During the remainder of the season, *rate of change of discharge* becomes increasingly important as an explanatory variable; other statistically significant explanatory variables are relatively unimportant (Table 4.8). (During sub-period 8, turbidity sensor saturation is the probable reason for the absence of identifiable lags between suspended sediment and discharge, and thus the poor performance of *rate of change of discharge*, which mimics diurnal hysteresis, in the multivariate models.) An exception to this rule is sub-period 7, during which variables other than discharge explain little of the variance in the suspended sediment series. As with sub-period 2, during which additional variables are also largely unimportant and discharge is the only significant predictor, sub-period 7 shows unexplained high amplitude residual variation.

4.5.3.3 Interpretation and discussion

The close relationship of suspended sediment concentration with discharge for sub-periods of the 1998 melt season suggests flow capacity is the predominant control on sediment transport. However, changes in: 1) the slope of the relationship between discharge and suspended sediment concentration; 2) sediment availability as determined from changes in the intercept of the same relationship; and 3) additional significant explanatory variables suggest that the mechanisms of sediment evacuation are strongly influenced by seasonal evolution of meltwater sources and pathways.

The relationship between suspended sediment concentration and discharge during the period of predominantly distributed drainage is shallower than during the period of predominantly channelised drainage, suggesting that flow capacity increases more rapidly with discharge under channelised conditions. This is consistent with expectations from flow in distributed systems, where flow velocity increases proportionally with discharge (e.g. Kamb, 1987), and in channelised systems, where flow velocity, and hence flow capacity, is expected to increase non-linearly (Alley et al., 1997). Thus, under channelised conditions, suspended sediment concentration in the proglacial stream is expected to outstrip suspended sediment concentrations during periods of predominantly distributed drainage. However, suspended sediment concentrations decline as the channelised system becomes established, such that during sub-period 5 entrainment efficiency is at its lowest. This trend is even more surprising since incipient subglacial channels, characterised by steep hydraulic gradients at channel heads, are expected to result in the efficient removal of large quantities of basal sediment (Section 1.3.2.2). Following sub-period 5, sediment availability increases, despite a decline in the rate of channelisation. These patterns are indicative of changes in basal sediment availability, key controls on which are likely to be: 1) the spatial persistency of the drainage system; 2) the initial distribution of basal sediments; and 3) the rate at which basal sediments are delivered to it.

High sediment availability early in the season during the period of distributed drainage is likely to have been due to the accumulation of erosion products during winter (cf. Hooke et al., 1985). The significance of *days since discharge equalled or exceeded* as an explanatory variable suggests increases in discharge through the system above recent

levels are important for accessing basal sediments. These slight increases may reflect the establishment of interconnectivity in the distributed system as new connections are opened very early in the season and small volumes of stored water are periodically released (cf. Hodson et al., 1997; Hodson and Ferguson, 1999). Alternatively, small increases in discharge above previous values may result in increased flow through areas of the distributed system with an associated increase in capacity that may entrain sediments (cf. Stone and Clark, 1996). The large proportion of unexplained variance in the suspended sediment series during this sub-period suggests increases in suspended sediment concentration that are unrelated to changes in discharge are common.

High sediment availability is maintained during the first spring event (sub-period 2), despite a significant increase in discharge through the distributed system that might be expected to exhaust available sediment sources. It is possible that rapid horizontal ice motion plays an important role in maintaining sediment availability, either due to increased subglacial erosion (e.g. Humphrey and Raymond, 1994) or continued disturbance of basal sediments (e.g. Humphrey et al., 1986). High amplitude residual variation occurs during this sub-period, and large positive residuals are frequently associated with rapid motion events as measured by a significant number of englacial and subglacial sensors and linked to high basal water pressures (Figure 4.27, Table 4.10; D. Mair, pers. comm.). During the peak in discharge towards the end of the sub-period, the residual series also demonstrates rapid increases in suspended sediment concentration followed by short periods of exhaustion that may be associated with sudden episodes of channelisation.

Sediment availability decreases markedly during sub-period 3 relative to sub-periods 1 and 2, even though discharges are often higher than during sub-period 1 (Figure 4.11). This suggests exhaustion of available sediment sources as opposed to a reduction in the spatial extent of the distributed system. Sediment availability increases again during sub-period 4, which includes the second spring event. However, whilst the residual series indicates increased sediment availability throughout the sub-period, (Figure 4.28) increased forward glacier motion is limited to the latter half of the period and channelisation is expected only to occur following peak ice velocities on ~ JD 175. Increased flow through the distributed system during the first spring event is likely to

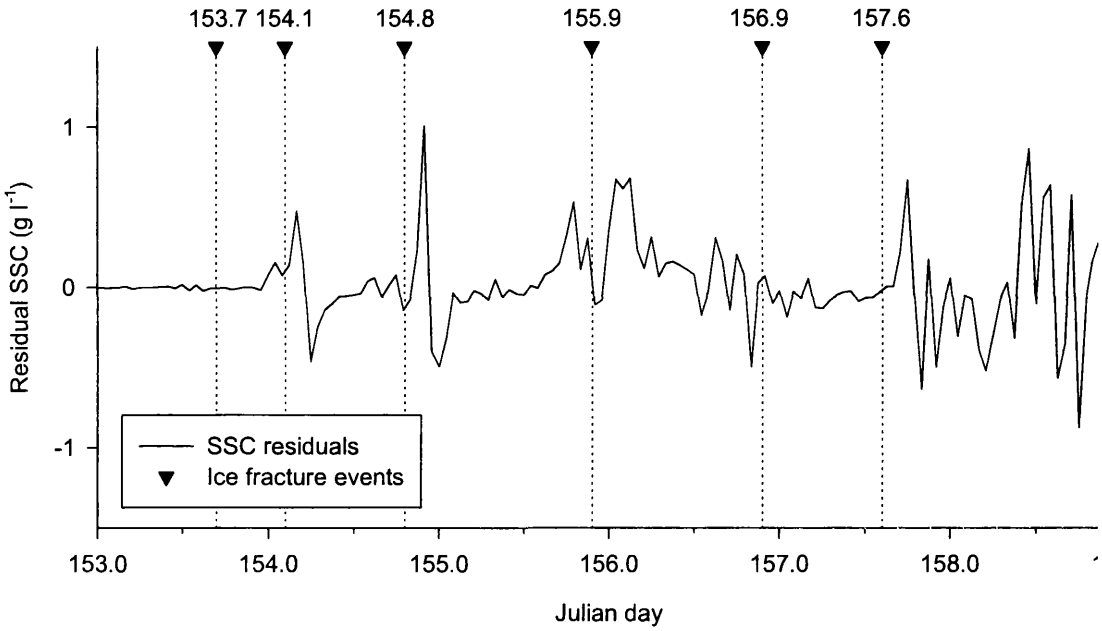

Figure 4.27 Time series plot of residual suspended sediment concentration (SSC) during sub-period 2. Dotted lines show the timing of ice-fracture events (see Table 4.10).

Table 4.10 Ice fracture/rapid motion events during the 1998 melt season measured by englacial tilt cells (*EGT*), basal tilt cells (*BT*), ploughmeters (*PL*) and basal water pressure sensors (*Pw*) at sites 1–5 (D. Mair, pers. com.)

Julian day	*EGT*	*BT*	*PL*	*Pw*
153.7	1, 3	4, 5	–	–
154.1	1, 3, 4, 5	4, 5	–	1, 5: steep rise @ ~154.0
154.8	1, 4, 5	4, 5	1	–
155.9	1, 3, 5	–	1	1, 5: major broad peaks
156.9	3	4	–	1: minor peak @ 156.6
157.6	3, 4, 5	4, 5	1	1: minor peak @ 157.3

have occurred beneath the glacier tongue but not more widely, possibly due to a thick supraglacial snowpack and precipitation in the form of snow in the upper catchment (Section 3.4.2.4). During the second event, rapid thinning and removal of the surface snowpack due to high air temperatures is likely to have resulted in supraglacial melt accessing the subglacial drainage system more widely, increasing flow through new areas of the distributed system and hence increasing sediment availability.

The abrupt decrease in sediment availability during sub-period 5 (Figure 4.11) occured during a further period of channelisation that commenced towards the end of sub-period 4. The greatest disparity in sediment availability was at low flows, suggesting that channelisation resulted in flows becoming confined to preferential drainage axes (PDAs) beneath which basal sediments were relatively thin or became armoured. Previous work has suggested that PDAs form in similar locations during consecutive seasons (Sharp et al., 1993) and that the basal sediment layer in these locations may be particularly thin or spatially inextensive (Harbor et al., 1997). This might also explain why periods during which channelisation is expected to occur, such as the latter half of sub-period 4, are not characterised by large suspended sediment concentration residuals (Figure 4.28).

Also associated with the change to channelised conditions is the increasing importance of *rate of change of discharge* as an explanatory variable, suggesting sediment entrainment by flow through channels is characterised by strong diurnal hysteresis effects. Previous research (e.g. Liestøl, 1967) has suggested hysteresis effects occur due to flow in channels 'spreading out' as discharge rises, thereby accessing areas of the bed that have been replenished with basal sediment since the last high flows; flows on the falling limb, however, cover the same area and sediment availability is greatly reduced. However, velocity hysteresis (Richards, 1982; Nienow et al., 1996), whereby velocity is greater on the rising limb of a flood wave due to a higher hydraulic gradient, may also contribute towards suspended sediment hysteresis. Proglacial hydrographs clearly suggest higher hydraulic gradients during rising limbs (see Section 3.3), suggesting flow capacity will be larger than on the falling limb. This is particularly important, as it means that even if sediment availability increases on the falling limb (e.g. due to bank collapse in unconsolidated sediment), there will be a tendency for sediment to remain within the channel to be evacuated on the rising limb of the next flow event.

Significantly, sediment availability within the channelised system increases as the melt season progresses. Suggested mechanisms that have been postulated to increase the availability of basal sediment to subglacial channels include: 1) the deformation of till (e.g. Boulton and Hindmarsh, 1987; Alley, 1992; Walder and Fowler, 1994; Collins, 1996) or basal ice (e.g. Röthlisberger, 1972; Hooke, 1984; Shreve, 1985; Hooke et al., 1990, Bogen, 1996) into channelised flowpaths; 2) the glacial transport of till or basal ice

to flowpaths transverse to glacier flow (e.g. Spedding, 1997); 3) conduit migration to previously isolated basal areas, or the glacial transport of flowpaths to areas of higher sediment availability (e.g. Collins, 1979b; Hooke, 1984; Gurnell et al., 1988); and 4) extra-channel flow excursions (e.g. Collins, 1979a; Hubbard et al., 1995).

Processes involving deformation of basal ice and the glacial transport of sediment to flowpaths (or vice versa) are unlikely to significantly enhance sediment availability because they operate relatively slowly and PDAs appear largely to be orientated parallel to ice flow. Channel migration is also unlikely, since PDAs have been found to occupy similar positions between melt seasons (Sharp et al., 1993), and the location of channels is primarily determined by the distribution of moulins or crevasses, the position of which rarely changes during a melt season. Instead, deformation of till or extra-flowpath excursions due to a diurnally reversing lateral subglacial hydraulic gradient are most likely to provide channels with access to basal sediments. Previous work has shown that changes in water pressure within channels can influence areas of the bed over a lateral distance of ~ 70 m (Hubbard et al. 1995). The overpressurisation of channels later in the season due to the increasing amplitude of supraglacial runoff is likely to strengthen oscillations in the diurnally reversing gradient. This suggests three key mechanisms by which basal sediments are accessed by largely immobile subglacial channels:

1. Increasingly high water pressures within channels at peak diurnal discharge result in local ice-bed separation, enabling extra-channel flow excursions over wider areas and hydraulically efficient flows to reach basal sediments increasingly distal to subglacial channels (cf. Liestøl, 1967).

2. Increasingly high water pressures within channels influence increasingly extensive areas of the distributed system, encouraging basal sediments to deform towards channels as water pressures in the channels decrease (cf. Vatne et al., 1995).

3. Flows returning from the high pressure distributed system as water pressure in the channels decreases causes the winnowing of fines from basal sediments. Hubbard et al. (1995) have observed the mobilisation of sediment in the distributed system due to the diurnally reversing gradient but the extent to which this contributes to basal sediment evacuation is unknown.

High sediment availability and a steep relationship between discharge and suspended sediment concentration is also maintained during sub-period 7, where the amplitude of diurnal runoff cycles is markedly reduced. Sub-period 7 is characterised by a föhn wind and heavy late-afternoon rainfall; very low horizontal ice velocities indicate predominantly open flow conditions within subglacial channels and the likely reduced efficiency of the diurnally reversing hydraulic gradient. The predominant sources of sediment are therefore likely to be extraglacial areas of the catchment where the winter snow cover has been removed, exposing large areas of extraglacial sediment to entrainment by rainfall. The multiple regression model for sub-period 7 suggests suspended sediment concentrations were only weakly determined by rainfall; however, low relationships might occur due to extraglacial sediment transport by mass movement processes such as debris flows, as is likely in unconsolidated sediments. Strong relationships with discharge probably reflect the influence of flow capacity on sediment transport once sediment is delivered to the subglacial drainage system.

4.5.4 Suspended sediment load

Daily suspended sediment load appears to vary systematically with discharge during the 1998 melt season (Figure 4.1; Table 4.3). Loads during the period of predominantly distributed drainage are generally low (< 100 t d^{-1}) except where flow through the distributed system is greatly increased (i.e. during sub-periods 2 and 4). Peak suspended sediment evacuation is achieved during the peak in discharge of the first spring event (sub-period 2), reaching ~ 850 t d^{-1} on JD 185 (Figure 4.1). However, total suspended sediment evacuation during the event is < 2000 t d^{-1}. Using the seasonal rating curve for daily discharge versus suspended sediment load (Table 4.4), predicted annual suspended sediment evacuation during 1998 was ~ 25,000 t, suggesting that < 10 % of the annual suspended sediment load was transported during the first spring event. Suspended sediment transport during the second spring event, during which rapid channelisation is expected to have occurred, was even lower (Figure 4.1; Table 4.3).

During the period of predominantly channelised subglacial drainage, suspended sediment load increased steadily from ~ 200 t d^{-1} during sub-period 5 to ~ 500 t d^{-1} during sub-period 8 (Figure 4.1; Table 4.3) despite relatively stable daily mean and daily

Table 4.11 Linear regression relationships between log-transformed daily discharge variables and daily catchment suspended sediment load.

Independent variable	Dependent variable	a	b	t_a	t_b	p_a	p_b	r^2
By julian day								
logDQ	log$DSSL$	−11.3	2.53	−14.47	17.34	<0.001	<0.001	0.857
logQ_{range}	log$DSSL$	1.91	1.21	64.22	20.57	<0.001	<0.001	0.894
logΔQ	log$DSSL$	1.28	1.25	20.78	17.72	<0.001	<0.001	0.862
By diurnal event								
logDQ	log$DSSL$	−11.3	2.52	−16.07	19.24	<0.001	<0.001	0.881
logQ_{range}	log$DSSL$	1.88	1.27	73.93	25.35	<0.001	<0.001	0.928
logΔQ	log$DSSL$	1.25	1.27	17.81	15.83	<0.001	<0.001	0.833

logDQ: daily catchment discharge; logDCL: daily catchment suspended sediment load; logQ_{range}: daily catchment discharge amplitude; logΔQ_{range}: daily catchment discharge amplitude divided by discharge time to peak

total discharge (Table 4.3). This pattern reflects the increase in sediment availability demonstrated by changing relationships between discharge and suspended sediment concentration (Figure 4.11). Table 4.11 demonstrates that suspended sediment evacuation is best modelled using the amplitude of the diurnal discharge cycle, confirming the likely importance of overpressurisation or strength of the diurnally reversing hydraulic gradient for maintaining access to basal suspended sediments (cf. Section 4.5.3.4). The table shows ordinary rating curves fitted to log-transformed discharge parameters and daily suspended sediment load from sub-periods 4, 5, 6 and 8. The independent variables comprise catchment discharge (logDL), daily discharge amplitude (logQ_{range}) and daily discharge amplitude divided by time to peak discharge (logΔQ_{range}), since the rapidity of the rise to peak discharge likely results in higher pressures in subglacial channels and a further strengthening of the diurnally reversing gradient. Rating curves are initially estimated for variables calculated 'daily' (i.e. by julian day). However, due to slight changes in hydrograph form throughout the melt season, variables were also calculated by 'diurnal event', where events are defined as the period of minimum-to-minimum discharge on consecutive days. For logDL and logQ_{range}, r^2 values are slightly better for variables calculated by 'diurnal event', and logQ_{range} explains a slightly higher

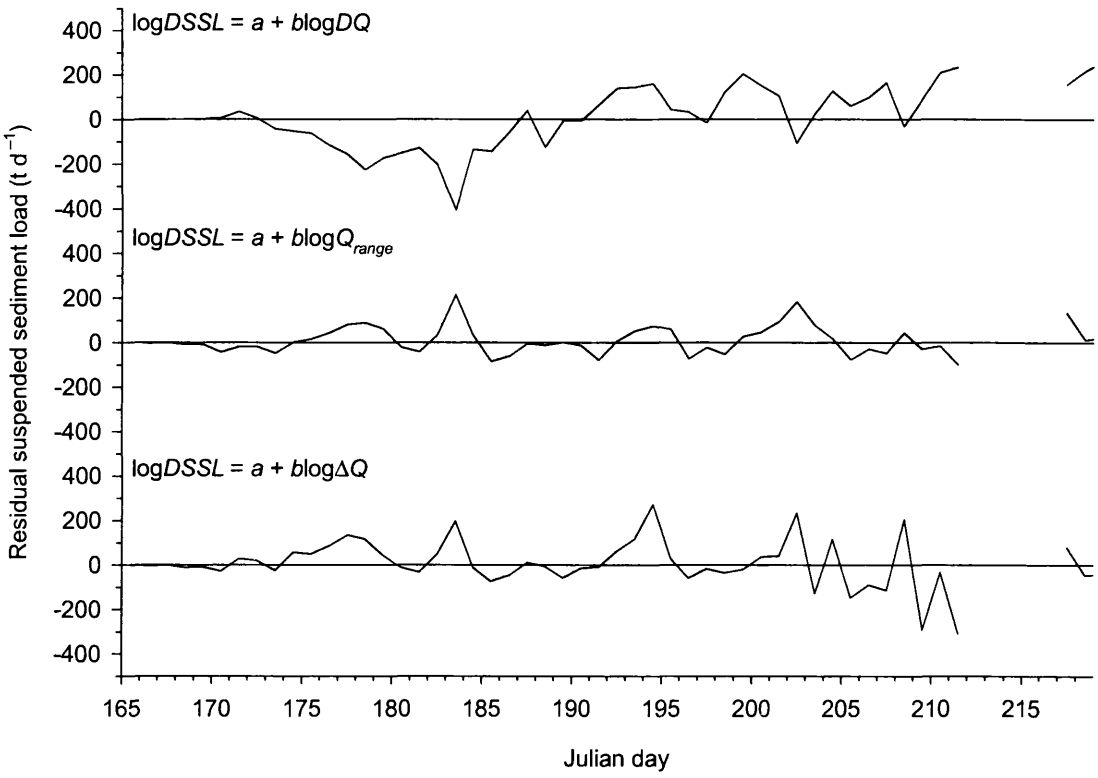

Figure 4.28 Time series plots of residuals from rating curves shown in Table 4.11

proportion of the variance in the suspended sediment load series. Time series plots of the residuals demonstrate that $\log Q_{range}$ predicts suspended sediment load more accurately than $\log DL$ and $\log \Delta Q_{range}$ (Figure 4.28).

Suspended sediment evacuation was therefore significantly influenced by subglacial drainage configuration, demonstrating a non-linear increase with respect to discharge between periods representative of predominantly distributed and channelised subglacial drainage conditions. Accurate values of sediment evacuation from a predominantly distributed system are most likely to be obtained during sub-period 1. Initially, flow through the distributed system (and hence suspended sediment load) is overestimated due to snowmelt from the proglacial area; however, towards the end of the sub-period 1 the proglacial snowcover had significantly thinned. Between JD 148 and 153, mean discharge and suspended sediment load are 0.4×10^5 m^3 d^{-1} and 4.0 t d^{-1}, respectively (Figure 4.1), equating to a spatially-averaged basal suspended sediment yield of 0.6 g m^{-2} d^{-1}. During sub-period 8, which is characteristic of a mature, channelised subglacial

drainage system, mean discharge is approximately 3×10^5 m^3 d^{-1} and suspended sediment loads are commonly in excess of 500 t d^{-1} (Figure 4.1), equivalent to the evacuation of 79.4 g m^{-2} d^{-1} from the glacier sole. These values indicate a 125× increase in suspended sediment evacuation for only a 7.5× increase in discharge.

Non-linear increases in suspended sediment transport with respect to discharge are typical of many fluvial environments. For flow in subglacial channels, Alley et al. (1997) have shown $S \propto Q^2$, where S is the total bedload capacity and Q is discharge, and that similar relationships apply for suspended sediment load. However, if $S \propto Q^2$, an increase in discharge of 7.5× predicts an increase in sediment transport of only 56×, a figure much lower than that demonstrated during 1998. Crucially, the cross-sectional area of the drainage system has been shown to decrease during establishment of the channelised drainage system (Nienow et al. 1998). Under such conditions, because $Q = w.h.v$, where w, h and v are flow width, depth and velocity, respectively, S will be proportional to at least v^2. Dye-tracing studies at Haut Glacier d'Arolla (Nienow et al., 1998) show flow velocities in the order of 0.025 m s^{-1} within the distributed system, whilst the channelised system is characterised by flow velocities of 0.3–0.7 m s^{-1}. Assuming a value of 0.4 m s^{-1} is representative of mean flow velocity within the channelised system, a 15-fold increase in flow velocity during 1998 predicts at least a 200-fold increase in suspended sediment transport.

This predicted rate of increase in sediment evacuation is higher than that observed from field data. However, due to the errors discussed in Section 4.2.2.2, the rate of increase is likely to have been far greater than measured, since suspended sediment load is expected to have been significantly underestimated towards the height of the melt season. In addition, bedload transport has not been taken into account. Bedload transport at a variety of temperate glaciers has been shown to be between 30 and 60 % of the total sediment load (Gurnell, 1987a). Bedload transport from the distributed subglacial drainage system is likely to have been almost negligible due to the low flow velocities and the restricted physical size of distributed flowpaths. In contrast, rates of bedload transport under a mature, channelised drainage system are likely to have been in the same order as those suggested by Gurnell (1987a). Assuming bedload contributed just one-third of the total sediment flux at Haut Glacier d'Arolla during the height of the melt

season, total sediment load is likely to have reached upwards of 750 t d^{-1} and resulted in a greater-than 180-fold increase in total sediment evacuation. Since suspended sediment concentration may have been significantly underestimated, total sediment loads may have reached far in excess of this figure due to the sensitive dependence of S upon v.

4.6 CONCLUSIONS

- Suspended sediment evacuation is primarily dependent upon the configuration of the subglacial drainage system. Sediment evacuation under distributed drainage configurations is typically low, probably because flow velocity (and hence sediment transport capacity) is low and increases linearly with discharge. Higher flow velocities (that increase non-linearly with discharge) are likely to be responsible for the increased capacity of the channelised drainage system to entrain and transport basal sediments.

- Distributed systems may evacuate large volumes of sediment if flow through the system is increased (for example during spring events). However, high discharges through the distributed system at Haut Glacier d'Arolla are not sustained and result in the evacuation of only a small proportion of the annual sediment yield. In general, high discharges through distributed systems are unlikely to be sustained since theoretical analyses have shown that such systems are prone to collapse if water pressure exceeds a critical value (Kamb, 1987; Walder and Fowler, 1994).

- The efficiency of sediment evacuation is not observed to increase during spring events, despite the likelihood of enhanced disturbance of basal sediments and rapid channelisation. Nevertheless, links are suggested between high residual suspended sediment concentrations in the proglacial stream and sudden ice motion events or 'quakes' and sudden periods of channel formation.

- Changes in suspended sediment availability may occur during the melt season due to the exhaustion of available sediments. A slight 'recovery' in suspended sediment availability over sub-period 4 during the 1998 melt season likely reflects increased flow through 'new' areas of the distributed system where exhaustion had not yet

occurred. Low sediment availability during periods of channelisation is probably due to flowpaths becoming confined to PDAs where basal sediments are thin, spatially inextensive or armoured.

- Throughout the period of predominantly channelised drainage, sediment availability increases, such that the mature, channelised subglacial drainage system results in the very efficient evacuation of basal sediments. This is contrary to many previous studies that have largely emphasised the exhaustion of available sediment sources during the melt season, based on the assumption that flow through stable channels accesses only a small proportion of the glacier bed (e.g. Collins, 1989, 1990; Gurnell et al., 1992a).

- Basal sediment evacuation under channelised conditions is thought to be critically linked to the operation of a diurnally reversing hydraulic gradient that operates transverse to channels. Three key mechanisms are envisaged by which basal sediments may be accessed by largely immobile subglacial channels: 1) increasingly high water pressures within channels during diurnal discharge peaks result in local ice-bed separation and extra-channel flow excursions over increasingly wide areas of the bed; 2) increasingly high water pressures within channels influence increasingly extensive areas of the distributed system, enabling basal sediments to deform towards channels as water pressure in the channels declines; and 3) flows returning from the high pressure distributed system winnow fines from basal sediments as water pressures in the channelised system decline.

- The mobilisation of fine sediments within the distributed system near to subglacial channels is likely to have implications for the particle size signature of suspended sediments evacuated from the subglacial drainage system (Section 1.3). The following chapter aims to investigate the particle size signature of suspended sediments from the subglacial drainage system at Haut Glacier d'Arolla in order to elucidate more rigorously the processes responsible for suspended sediment evacuation.

5.

Sediment provenancing: suspended sediment particle size

5.1 INTRODUCTION

5.1.1 Aims and rationale

This chapter uses proglacial suspended sediment particle size during the 1998 melt season to investigate further the mechanisms responsible for suspended sediment evacuation from the subglacial drainage system. Sections 1.2 and 1.3 suggested that studies must acquire independent data on the dynamic nature of the glacier and glacier hydrological systems if the mechanisms responsible for sediment evacuation by subglacial meltwater are to be rigorously identified. However, studies should also include indicators of sediment provenance that have the potential to identify changes in suspended sediment source. Suspended sediment particle size is important in this respect for two reasons. Firstly, particle size must reflect drainage system morphology at the point where sediments are being entrained, since flow capacity is largely determined by hydraulic efficiency. Thus, under distributed drainage conditions, entrainment should be limited to the finer fractions of available sediments. The occurrence of coarser or more complete size distributions may therefore indicate increased availability of larger particles (perhaps due to basal disturbance during high horizontal ice motion) or an increase in hydraulic efficiency (e.g. due to channelisation). Secondly, systematic spatial

variations in the particle size of basal sediment have been suggested to occur, resulting from the eluviation of fines from sediments near to major subglacial channels (Hubbard et al., 1995). Under channelised conditions, the size distribution of suspended sediments should be relatively coarse unless meltwaters are able to access sediments previously distal to channel margins (e.g. by channel migration). Once again, however, rigorous interpretation of the particle size characteristics of suspended sediment from the subglacial drainage system requires independent knowledge of glacier and glacier hydrological dynamics.

Chapter 4 has demonstrated a significant change in the relationship between discharge and suspended sediment concentration during 1998 associated with the reorganisation of the subglacial drainage system. Variation in suspended sediment particle size has the potential to provide important information about subglacial hydrological conditions and the mechanisms of sediment evacuation within periods of distributed and channelised drainage. Especially important are the mechanisms responsible for increasing sediment availability during the period of channelised subglacial drainage. Likely mechanisms are suggested to be: 1) extra-channel flow excursions due to the increasing overpressurisation of channels later in the season, resulting in local basal separation and the integration of hydraulically efficient meltwater flow with progressively wider areas of the bed; 2) an increasingly strong diurnally-reversing lateral hydraulic gradient that encourages high-pressure basal sediments to deform towards low-pressure channels; and 3) the winnowing of fines from sediments near to channels as bulk discharge declines.

Assuming the presence of systematic spatial variations in the size distribution of basal sediments due to the diurnally reversing hydraulic gradient, suspended sediment particle size suggests the potential to investigate the mechanisms likely associated with increasing sediment availability during the period of channelised drainage. Under mechanism (1), high proportions of fines are expected at high discharges as flows access sediments distal to channels by the active erosion of channel banks. Under mechanisms (2) and (3), the highest proportion of fines will occur during periods of falling discharge; however, mechanism (2) may also be associated with a higher proportion of coarse material during periods of declining discharge due to passive bank collapse as sediments deform towards channels.

5.1.2 Suspended sediment particle size as an indicator of sediment provenance

5.1.2.1 Lessons from non-glaciated catchments

Suspended sediment particle size is not a widely used tracer in fluvial environments, since it is dependent upon a large number of independent variables and thus varies markedly (Kurashige and Fusejima, 1997). In a small non-glaciated catchment, Udelhoven and Gasparini (1997) summarised the main factors influencing particle size distribution as: 1) mixing of solids of different origins (Santiago et. al., 1992); 2) sorting of suspended solids according to spatial transport energy variations (Walling and Moorhead, 1987, 1989); 3) spatial and temporal change of selective resuspension and sedimentation (Walling, 1983); 4) flocculation and dispersion (Droppo and Ongley, 1989; Eisma, 1993; Droppo and Stone, 1994); and 5) the biogenic alteration of solids and autochthonous formation of organic particles (Droppo and Ongley, 1989; Schallenberg and Kalef, 1993). Similar generalised controls affect particle-size distributions from glacial and subglacial catchments. The contribution of organic particles (e.g. from algae and organic debris blown onto the glacier surface) is likely to be small, although little is known about the extent to which subglacial biota cause the physical alteration of sediments (Sharp et al., 1999).

Traditionally, studies that have utilised the particle-size distribution of suspended sediment have relied upon simple statistical parameters such as mean size, standard deviation, sorting, and skewness (Kurashige and Fusejima, 1997). However, size-distributions may be polymodal due to the combination of many different sediment sources, such that standard moment statistics are of limited value in characterising and describing changes in particle size distribution. For example, for bimodal sediments, the median diameter (d_{50}) may lie in the gap between modes where little sediment is actually present; moreover, it may be very unstable, switching rapidly between modes with only minor changes in the distribution (Sambrook Smith et. al., 1997). Size distributions in glacial sediments have been shown to be bimodal due to an apparently abrupt transition from rock particles to their mineral constituents, which themselves may occupy distinct log-normal distributions (Dreimanis and Vagners, 1971).

Kurashige and Fusejima (1997) used whole size distributions from suspended sediment samples to trace sediment sources in a non-glaciated catchment. They cite previous studies that have attempted to stratify whole distributions into separate log-normal sub-distributions in order to compare them; however, such studies have been unable to use the technique successfully as a tracer. Instead, Kurashige and Fusejima used inferential statistics to assess the similarity between whole particle-size distributions. The technique was found to be successful only when: 1) the number of major sources were limited to two; and 2) the grain size distributions of the two sources were known and were found to be statistically different.

Polymodal size distributions are common in fluvially-deposited sediments due to the range of sediment sources and flow conditions. Using multivariate analysis, Brown (1985) successfully discriminated between different sedimentary units within non-glaciated catchments. Multivariate analysis enables sediment in each particle-size class or range in a given distribution to be considered a unique attribute of that particular sample (Kloven, 1966). Cluster analysis (cf. Section 3.3) was used to divide vertical sections through flooplain deposits into units of similar particle size characteristics. Nevertheless, the mode was found to be the most useful and sensitive parameter in the interpretation of floodplain sediments, and to be of great practical value where size-distributions were non-normal and, as result, moment statistics may have been unreliable. The number of modes was also found to be useful in suggesting the minimum number of separate log-normal sub-distributions within the sample, although the causes of polymodality in sedimentary environments may be many.

5.1.2.2 Glaciated catchments

Few studies have utilised suspended sediment particle size distribution as an indicator of sediment provenance from glaciated or subglacial catchments. Early studies (e.g. Rainwater and Guy, 1961; Fahnestock, 1963; Church, 1972; Guymon, 1974; Fenn, 1983; Richards, 1984) typically employed relatively small numbers of samples that prohibited rigorous investigation of relationships with discharge or identification of sediment sources. Rainwater and Guy (1961) demonstrated that diurnal trends in particle size followed trends in proglacial discharge due to varying proportions of coarser particles

that presumably reflect variations in transport capacity (Gurnell, 1987b). However, Rainwater and Guy (1961) sampled ~ 250 m from the glacier snout and Karlsen (1991) suggested that processes operating proglacially might have obscured any subglacial signature. However, Fenn (1983) also demonstrated a clear link between discharge and the concentration greater than 8 μm for daily suspended sediment samples collected 280 m from the snout of Glacier de Tsidjiore Nouve, and found evidence of the increased transport of coarser fractions during rising discharge.

Fenn and Gomez (1989) later analysed 1440 hourly proglacial stream samples from Glacier de Tsidjiore Nouve. Suspended sediment size distributions were typically unimodal and in the silt size range, with a mean median grain size of 14.6 (± 2.3) μm. In general, the distributions were found to closely resemble those associated with the abrasive wear of debris by Gaudin (1926) and Haldorsen (1981), which supports the assertion that such sediments had a subglacial origin. Although changes in median size and sorting coefficient were found to occur broadly in phase with changes in discharge, grain size parameters were characterised by erratic, hourly-scale fluctuations as well as subseasonal trends, the magnitude of which demonstrated little correspondence with subseasonal fluctuations in discharge. This rapid variability in particle-size parameters was held to arise due to: 1) the unsteadiness of hydraulic conditions in steep, step-pool streams; and 2) the unsteadiness of sediment supply in active glacier basins. The latter effect was considered to be largely controlled by the sources and pathways of runoff within the basin that control access to sediment sources with differing particle size characteristics.

Generally, particle size at Glacier de Tsidjiore Nouve during normal diurnal runoff events, whether due to snow or ice melt, demonstrated clockwise hysteresis resulting from the increased transport of coarser fractions during rising flows. This was considered to result from the deposition of coarse material within channel margins that become isolated from flow as stage falls and are then re-entrained as stage increases (cf. Richards, 1984). Analysis of particle size trends during sub-periods characterised by particular meltwater sources or runoff characteristics further succeeded in relating changes in particle size to processes operating in the proglacial zone. For example, snow melt and heavy rainfall were considered to result in coarser distributions due to the entrainment of sediments from non-glaciated areas. Particle size was least variable

during a spring event, during which the rationalisation of the subglacial drainage system and evacuation of significant quantities of basal sediment have been demonstrated (see also Gurnell and Fenn, 1984b). Fenn and Gomez (1989) attribute this apparent homogeneity to subglacial processes favouring the development of a distinctive 'terminal grade' determined by sediment mineralogy (cf. Dreimanis and Vagners, 1971).

Karlsen (1991) demonstrated the occurrence of statistically different sediment populations during a single melt season that likely represented individual subglacial sediment sources. Samples were obtained from two short periods of the melt season at Austre Okstindbreen, Norway, before and after a major flood event. Statistically different populations were found between the two periods for a variety of size distribution parameters. Since discharge was not statistically different, Karlsen suggested changes in the size distribution must be controlled by mechanisms other than hydraulic ones. However, the mechanisms Karlsen suggests are primarily hydraulically controlled, namely: 1) the slumping of unstable channel banks (Collins, 1979b) composed of poorly sorted sediments; and 2) the temporary deposition and erosion of sediments at the channel bed during falling and rising flows (Bogen, 1980). Furthermore, these mechanisms likely control variation in suspended sediment size distribution only at the diurnal scale; the presence of distinct populations over significantly longer periods suggests a more permanent change in the mechanisms by which suspended sediments are evacuated. Karlsen concluded that the two populations likely represent access of meltwater to two discrete sediment sources resulting from an unspecified change in the main drainage system during the mid-season storm event. However, independent investigation of the structure of the subglacial drainage system was not undertaken, and it is impossible to determine whether this represents: 1) a physical shift in the position of subglacial channels; or 2) a change in the hydraulic mechanisms by which subglacial sediments are accessed and entrained.

Thayyen et al. (1999) have studied suspended sediment particle size at Dokriana Glacier, India in order to elucidate the processes governing suspended sediment evacuation. Coarser, bimodal distributions similar to those of supraglacial sediments occurred during periods of high intensity rainfall. Similar distributions were also observed during an early-season melt-driven flood event that resulted in the evacuation of a significant

volume of subglacial sediment. Coarser particles were therefore suggested to be preferentially evacuated from the distributed subglacial drainage system due to their low entrainment velocities. Later diurnal variations are interpreted as evidence of a diurnally reversing hydraulic gradient (cf. Hubbard et. al., 1995). Two distinct peaks in diurnal suspended sediment concentration occurred 'up to 27 July' that were associated with particular size distributions (although results are presented for 27 July only). The first peak during rising discharge was associated with an increased proportion of fine and medium sands that is again suggested to indicate the preferential erosion of coarse particles from the distributed system. The second peak during peak discharge was associated with a larger contribution of fine and medium silt, and is suggested to be the period of peak translatory flow, thus transporting the most fines to the glacier snout. However, net flow in the distributed system will be away from major channels during rising and peak discharge, such that it is impossible for sediments eroded in these locations to be transported to the glacier snout. Logic suggests that the most fines should be contributed from the distributed system as bulk discharge declines.

5.1.3 A summary: the way forward

Previous studies have demonstrated many difficulties in utilising suspended sediment particle size as an indicator of sediment provenance. Work in non-glaciated catchments suggests that the factors influencing suspended sediment particle size are many; hence, recognising the particle size signature of various sediment sources is likely to be very difficult. Studies in non-glaciated catchments have also highlighted problems resulting from bimodal distributions when using moment statistics. Studies based on the whole sample distribution are likely to be the most reliable, although this requires efficient interpretative methods that are able to compare distributions from a large number of samples.

In glaciated catchments, many studies have suffered for reasons similar to those that have hampered investigations of suspended sediment concentration (see Section 1.3). Early studies are limited primarily by small sample sizes; however, later studies are characterised by: 1) often weak or inappropriate interpretative procedures (e.g. the dependence on moment statistics and simple correlations between discharge and particle

size); 2) a disregard for or poor understanding of insights gained from experimental observation and theoretical consideration of the nature of the fluvioglacial system (e.g. sampling too far from the glacier snout (cf. Section 2.3.2); poor knowledge of drainage system morphology or evolution and its impact on subglacial processes); 3) poor characterisation of probable sediment sources (e.g. sampling or theoretical consideration of likely sediment sources and size distributions rarely undertaken); and 4) a lack of independent measurements that allow testing of the theories proposed (e.g. knowledge of the dynamic nature of the subglacial and fluvioglacial systems).

In glacial streams with high turbulence and diurnal discharge amplitudes, sediment sorting due to temporal variations in stream transport capacity and within-channel selective resuspension and sedimentation are likely to be great. For example, Bogen (1980) has demonstrated that size fractions greater than ~ 16 μm are very sensitive to changes in flow velocity; below 16 μm velocities must fall to less than 0.08 m s^{-1} for sedimentation to take place. Thus, finer particles are steadily evacuated from the system, whereas progressively coarser particles likely move only at progressively higher flows for progressively shorter periods and in higher concentrations. Erosion of the channel floor or the re-integration of marginal channel areas during rising flows (cf. Richards, 1984) will access and entrain predominantly coarse sediments and further concentrate them in the flow. This concentration of coarser particles during rising flows is likely to be increased further by velocity hysteresis (Richards, 1982), which may be very strong within subglacial channels under closed flow conditions (cf. Nienow et al., 1996).

In this study, variation in suspended sediment particle size is rigorously interpreted against knowledge of the dynamic nature of the subglacial and fluvioglacial systems. Sediment sources and size distributions have been characterised theoretically (Section 5.1), and a sampling location chosen that is very close to the glacier snout (Section 2.2.3). However, if sediment provenance is to be reliably identified from proglacial particle size variation, a large number of samples may be required in order to overcome problems resulting from local hydraulic effects. In such circumstances, the investigation of simple relationships between discharge and particle size parameters is likely to provide the most useful initial description of the data. These relationships are estimated for appropriate sub-periods of the melt season due to seasonal evolution of the sources

and routing of meltwater (cf. Section 4). Nevertheless, analysis techniques that utilise whole sample distributions and are likely more powerful are also investigated, and the analysis of probable sediment sources is undertaken in order to provide a framework for the interpretation of the results and to aid testing of the hypotheses proposed.

5.2 PARTICLE SIZE ANALYSIS

5.2.1 Introduction

There are many problems associated with the characterisation of particle size for samples of geological material. Importantly, particles are typically irregular and possess no single characteristic linear dimension by which their size can be defined. The available methods characterise a particle's size using different dimensional properties (e.g. projected area, volume, axis lengths, settling velocity or size of the smallest hole through which it will pass), which, except in the case of spheres, are not equivalent (McCave and Syvitski, 1991; Matthews, 1991). Matthews (1991) has also demonstrated that particle shape and density variations within samples interact with different techniques to create consistent biases in particle size estimates. Different techniques are therefore rarely comparable, and even well established sizing techniques are inherently biased.

McCave and Syvitski (1991) note that geological samples tend not to fall into narrow size ranges and are often polymodal, requiring techniques with large measurement ranges and high resolution. Many methods require the joining of size distributions for different size fractions, which is inherently difficult (see Matthews, 1991). McCave and Syvitski (1991) also note that for many studies large numbers of samples mean that the speed of sample preparation, processing and analysis becomes important. Some modern techniques, such as laser diffraction, possess the ability to process samples at rates of up to ten per hour; however, it is commonly sample preparation and not analysis time that is the rate-determining step.

Importantly, McCave and Syvitski (1991) note that regardless of technique, accuracy is very difficult to assess due to irregularities in sample shape and density. Precision is more

easily determined by systematic analysis of a few samples and should always be reported (although precisions are often presented for different statistical parameters and therefore preclude comparison between techniques). McCave and Syvitski (1991) also stress that care should also be taken when interpreting results, particularly where data analysis is automated. Spurious precision may arise if curve-fitting programs output results at a greater resolution than the technique is able to determine, or distribution parameters may be derived after fitting potentially inappropriate (e.g. log-normal) size-distribution models. Automation also makes it easier to derive moment statistics or other parameters that for certain distributions are invalid (as noted above). McCave and Syvitski (1991) conclude that for geological samples, a straightforward modal decomposition of the frequency curve may be the clearest and most revealing method of analysis.

Providing the aim is not to duplicate or compare results with those obtained by previous analysis, there appears to be little to commend one technique over another. However, recent advances in laser diffractometry do offer advantages for the analysis of geological samples. Importantly, the principal of particle sizing by laser diffraction means that it is one of the few methods that obtain size results based on some measure of particle volume, which is the only adequate representation of the three-dimensional size of a particle (Matthews, 1991). The technique uses the principle that a particle in the path of a laser beam scatters the light forward in the form of a unique pattern from which its diameter can be calculated. If the particle is passed in suspension through the beam repeatedly, it will be randomly orientated and the average diffraction pattern will indicate a diameter close to the particle's true nominal diameter (the diameter of a sphere of equivalent volume; Wadell, 1932).

Most laser diffraction apparatus now have the ability to size wide ranges in a single measurement and are vastly less labour-intensive than classical methods of analysis (Buurman et. al., 1997). In a relatively recent review of this field, Agrawal et. al. (1991) highlighted a number of specific problems that have now largely been solved: there is no longer a need for separate analyses using different focusing lenses to make full use of the sizing range, thus avoiding problems associated with the joining of separate size distributions; apparatus now have up to 126 detectors, giving far greater precision and greatly enhancing the resolution of polymodal distributions; improvements in software

allow the determination of particle distribution using more advanced optical theory, enabling accurate distributions to be obtained down to 0.4 μm; and additional methods have been incorporated to extend the range to even finer particles.

5.2.2 The Coulter LS230

In this study, a Coulter LS230 laser diffractometer was used for particle size analysis due to its wide sizing range, rapid processing capability and ability to produce accurate and highly precise distributions that are more detailed than those obtained from sieving and sedimentation (Buurman et. al., 1991). The theory of laser diffraction is treated in detail by Agrawal et. al. (1991). Here, the general method and characteristics of the LS230 are outlined, and the reliability of the LS230 evaluated using relevant previous studies followed by testing using samples collected in the field.

5.2.2.1 Sizing method and general characteristics

The LS230 obtains the size distribution of a sample by analysis of the forward diffraction pattern produced when its constituent particles are passed through a beam of monochromatic laser light (λ = 750 nm). The scattering of light by spheres (particles) at small angles is considered equivalent to diffraction by apertures of an equivalent diameter. For a single particle of a given size, the pattern and intensity of forward scattered light is unique and can be predicted. The pattern and intensity of the forward scattered light for many particles of differing sizes is the product of many individual diffraction patterns. The forward-diffracted light is focussed onto a range of detectors using a Fourier lens; thus, particle position within the beam is unimportant, and a steady stream of particles will generate a stable diffraction pattern. This pattern is used to back calculate the sizes of all particles in the sample.

Reverse Fourier optics are utilised in the LS230, resulting in a longer focal length that reduces the scattering angle and achieves an operating range of 0.4–2000 μm in a single measurement. The angular scattering pattern is resolved using 126 detectors to achieve high resolution. However, accuracy is also dependent upon the appropriateness of the optical model (the theory describing the diffraction of light by small particles) used to

back calculate sample size distribution. Two optical models are available: Fraunhofer, which assumes that there is only diffraction and no refraction of light by particles; and Mie, which fully describes: 1) diffraction; 2) deflection at the particle surface; and 3) refraction (i.e. absorption) of light passing through the particle. Fraunhofer is applicable only to particles that are large relative to the wavelength of the light source: for particles whose diameter is below ~ 10λ (~ 7 μm for the LS230), light is not diffracted in the correct manner, and Fraunhofer becomes increasingly poor as particle diameter decreases (Bayvell and Jones, 1981; de Boer, 1987). However, Beckman Coulter have recently suggested that Fraunhofer is accurate down to ~ 1 μm (Munt, 1995).

Using Mie theory, accurate results can be obtained down to particle diameters of 0.4 μm. However, the theory requires accurate knowledge of the sample's refractive index and absorptive characteristics (the degree to which light is attenuated as it passes through a particle of a given material). For geological samples, a refractive index of ~ 1.56 is commonly assumed, since refractive indices for common minerals and clays fall into a narrow range within which differences in the refractive index have a negligible effect on the calculations (Loizeau et. al., 1994; Buurman et. al., 1997). Coefficients describing the absorption of light of a given wavelength by soils and other geological samples are more difficult to obtain. Coefficients for quartz and kaolin clay are suggested by Coulter to be ~ 0.01 (Hoff and Bott, 1990); however, since absorption is largely depend upon the colour of the material, coefficients for geological samples are likely to be very variable.

The choice of optical model for geological samples poses some difficulty. Burmann et. al. (1997) demonstrated that subtle changes in the absorption coefficient could result in large changes in measured size distribution, whereas Loizeau et. al. (1994) ignored the absorption coefficient on the grounds that absorption is negligible for small translucent particles. Elsewhere (Bueselinck et. al., 1998), Fraunhofer has been used in preference to Mie on account of Loizeau et. al. (1994) having shown it to detect a significantly larger proportion of clay. Hoff and Bott (1990) conclude that although Mie will be more accurate in all cases and that Fraunhofer is likely to result in some systematic error at small sizes, Fraunhofer will still provide a precise, relative measure of particle size that is extremely reproducible and sensitive to small differences in size distribution.

For particles smaller than 0.4 μm, a second optical system is applied that measures the differential scattering of light caused by the oscillation of electrons under horizontally and vertically polarised light. PIDS (Polarisation Intensity Differential Scatter) extends the measurement range to 0.04 μm, but again requires information on the absorptive coefficient of the material at the three additional wavelengths of light used: 450 nm; 600 nm; and 900 nm. Buurman et. al. (1997) found that entering an absorptive coefficient of 0.2 for each wavelength increased the reported volume of the sample below ~ 1 μm. However, as suitable data are not available, there was no physical basis for the value of the chosen coefficient and the results are inconclusive.

A variable speed fluid module continuously circulates the sample through the laser beam and from a sample vessel. Fluid is usually drawn from the mains water supply to both rinse and fill the module. Since the LS230 requires a specific range of suspension density, the amount of dry sample required lies within a narrow range. The degree of diffraction is defined as the 'obscuration' of the laser light by the sample, and should be in the range 8–12%. For samples that contain mostly very fine particles in the range at which PIDS analysis is required, a second obscuration value for the PIDS system should be in the range 45–55% and the level of laser obscuration disregarded. For all other samples, it is the first obscuration value that is of primary importance, since the PIDS system has an obscuration tolerance of up to 85% (Beckman Coulter, pers. comm.).

The LS230 is controlled from a PC running specialist software provided by Beckman Coulter (version 3.01). The raw diffraction data for both optical systems is saved and, if requested, the calculated sample size distribution is also retained. Using the chosen optical model, the software calculates and seamlessly integrates the data from both optical systems to give an operating range of 0.04–2000 μm in 116 fractions, geometrically increasing from 0.04 μm with an incremental multiplier of 1.098. The raw data is also saved and can be reanalysed using a different optical model at any later date.

5.2.2.2 Reliability and representativeness

The reliability and representativeness of the laser diffraction technique used in the LS series has been evaluated for geological samples by Loizeau et. al. (1994) and Buurman

et. al. (1997), the latter using an LS230 also equipped with PIDS. Reproducibility was assessed by Loizeau et. al. (1994) by repeat analysis of a natural lacustrine sample with the particle size range 1–100 μm. Variability (defined as the coefficient of variance) for skewness based on 10 measurements was 9.2 %; for all other statistical moments (mean, sorting and kurtosis) variability was at or below 0.3 %. By comparison, variability was an order of magnitude higher for 10 subsamples of the same material. Reproducibility also depends on how consistently laser beam alignment is maintained; to this end, the LS series aligns individual detectors based on the pattern of scattered light from a sheet steel reticule with a single 600 μm hole moved into the path of the beam. Realignment is rapid (~ 1 minute) and is repeated every 2 hours.

Accuracy was tested by Loizeau et. al. (1994) using latex sphere standards. Different standards (2.72 μm, 10.5 μm and 78.3 μm) were added progressively such that any modifications to the size distribution with increasing particle size would be apparent. Accuracy was determined to be fair, with deviation from the nominal diameter of the latex spheres being ~ 2 % for both fine and coarse particles. No modifications associated with increasing particle size appear to have been observed. Loizeau et. al. (1994) also assessed the LS100's ability to accurately determine the amount of clay (< 2 μm). Whilst the amount of sand was found to be well correlated with results obtained by sieving, the proportion of clay with respect to that determined from settling was not. Clay content determination is likely to have been significantly improved by the addition of the PIDS system on the LS230.

Buurman et. al. (1997) attempted to assess the reliability of the optical model for sample size determination, as noted above. Using Mie theory, they suggested that the chosen refractive index had little effect on the calculations, although sensitivity to different absorption coefficients appeared to be high. No comparison was made with the results obtained using Fraunhofer. Correlation with the pipette-clay technique found that the clay content of the sample remained systematically lower using the LS230; however, providing samples are of a similar origin and measured using similar apparatus settings with the same optical model, it was suggested that subtle changes in the distribution at small sizes should be detected. The effect of suspension density on size distribution was

also investigated, since obtaining the correct PIDS obscuration (~ 50 %) typically resulted in low laser obscurations (~ 2 %) and the non-detection of particles coarser than ~ 4 μm. At correct laser obscurations (~ 10 %), for which PIDS obscuration was clearly too high (> 90 %), information about the fine fractions appears to be lost. Beckman Coulter have since indicated (above) that PIDS obscurations of up to 85 % are permissible; however, due regard must be paid to the particular characteristics of the sample in order to achieve a reliable size determination.

5.2.2.3 Sample preparation and analysis

Reliability and accuracy depend not just on machine characteristics but also upon adequate sample preparation. For many studies utilising suspended sediment size distributions, flocs may comprise a significant proportion of the total volume of sediment in transport and effective particle size is important. For the majority of geological studies, however, full disaggregation without the breakage of individual mineral crystals or rock fragments to reveal the true size distribution is required.

Reported methods of sample preparation vary and are greatly dependent upon individual sample characteristics. Loizeau et. al. (1994) state that for natural samples (probably lacustrine sediments), normal sample preparation involves resuspension in 10 ml of deionised water followed by ultrasonic dispersion (exact method not specified) for 5 minutes. For soils, more complicated preparation is necessary, involving a number of washes to remove organic matter followed by overnight shaking using dispersing agents, ultrasound or even boiling (e.g. Muggler et. al., 1997; Bueselinck et. al., 1998).

Chappell (1998) systematically investigated methods of dispersing sandy soils for analysis using Malvern 2600 laser diffractometer. Monitoring the level of laser obscuration over time as a surrogate for sample dispersal, the effects of different pretreatments were tested. Chappell (1998) demonstrated that Calgon (sodium hexametaphosphate and sodium carbonate) was particularly effective for dispersing sediments, and dispersal was greater if samples were prepared ~ 24 hours prior to analysis. Dispersal was further increased using ultrasound; however, there was evidence that sonication could lead to the breakage of individual particles and, over periods

greater than 10 min, flocculation also tended to occur. As prior preparation using Calgon also considerably increased the preparation time, Chappell (1998) concluded that preparation in pure tapwater followed by 3 min of sonication was probably most appropriate for the particular sample characteristics.

5.2.3 Evaluation of the LS230 for glacial sediments

Laser diffraction apparatus have not been evaluated using a wide range of sediment types, and no information exists on the appropriateness of the technique for the sizing of glacial sediments. For glaciofluvial suspended sediments, the origin of the source materials in terms of the geology from which they are derived and the mechanisms of subglacial chemical and physical weathering that lead to their formation likely result in particular sediment characteristics. Sediment composition, size, shape and colour likely vary according to geology and weathering regime. The characteristics of sediment entrainment and transport by subglacial meltwaters, which is likely to be size selective (see Section 1.3), may also lead to unique size distribution characteristics.

It is therefore necessary to consider the appropriateness of the laser diffraction technique in any area where it has not already been successfully applied. Here, results are presented from initial tests using the LS230 aimed at establishing the most reliable sample analysis procedure. Samples from the Haut Arolla catchment, mostly comprising fine proglacial backwater deposits, are then used to find the most appropriate method of sample dispersion. Finally, the proglacial samples are used to assess the precision and accuracy of the LS230 in order to characterise the reliability of the laser diffraction technique for the analysis of fluvioglacial suspended sediments.

5.2.3.1 Sample analysis

Using the variable speed fluid module, sample should be loaded into the sample vessel until optimum laser obscuration is reached before a size determination run can be taken. Geological samples with typically wide size-ranges need to be wetted in a small sample container before being poured into the sample vessel to avoid small particles floating on the surface of the fluid. Sterilised, 60 ml containers were used and samples dispersed

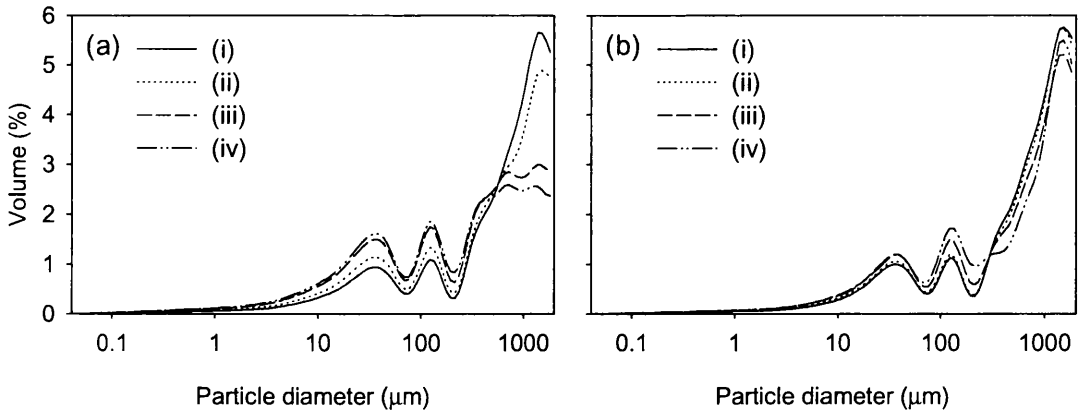

Figure 5.1 Modification of sample size distribution during sample extraction from the fluid module by (a) draining and (b) using a ladle. (i) represents the original sample distribution; (ii)–(iv) show the distribution after successive extractions of ~ 300 ml.

with ~ 40 ml of fluid. This method presents two main difficulties: 1) pouring of a sample into the vessel will generally introduce air bubbles and result in inaccurate size determinations; and 2) the whole sample must be added to ensure representativeness, which may result in laser obscurations outwith recommended ranges.

Bubbles were avoided by stopping the pump during sample loading and restarted ~ 30 s later in order to check the obscuration. Due to the narrow range of recommended obscurations, sample weight must also be within a fairly narrow range. Relatively small suspended sediment samples that include large proportions of fine material may still produce excessive obscurations but these cannot be reliably subsampled in order to overcome the problem. In contrast, several very small samples may need to be added cumulatively to produce the minimum required obscuration, resulting in a loss of temporal accuracy. However, by lowering the fluid in the sample vessel almost to the base, small samples were more concentrated within the fluid and adequate obscurations could be obtained. For large samples, following Buurman et. al. (1997), sample was extracted from the vessel and the remaining sample diluted by adding new fluid and repeating if necessary. Opening the drain valve is an unreliable method of sample extraction since coarse particles are lost preferentially (Figure 5.1 a). Instead, sample was extracted with the pump working at full speed using a ladle to make deep

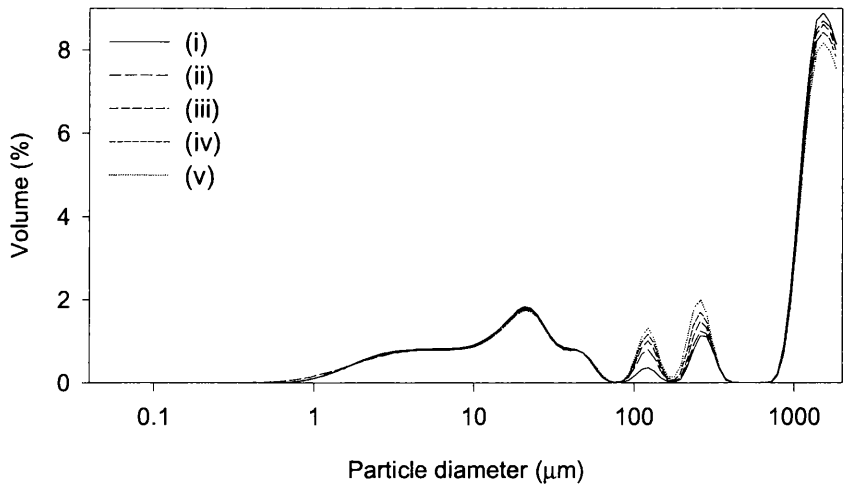

Figure 5.2 Bubble formation in the fluid module for tap water circulated at a typical pump speed. (i)–(v) are successive size determinations of the natural background signal of the water with an interval of ~ 2 min.

integrations of the sample vessel. This method was found to perform significantly better (Figure 5.1 b).

Bubble formation during sample analysis was another common problem. Due to the high demand for suspension fluid (1.7 l for each analysis and ~ 10× this to flush the fluid module between samples), it is common to connect the LS series directly to the mains water supply (Loizeau et. al., 1994). However, containment under pressure means that tap water is likely to degass as it circulates in the fluid module. Although a background reading of the suspension fluid to eliminate the effect of impurities is taken before each sample is added, bubble formation during the analysis may alter the measured size distribution. Loizeau et. al. (1994) noted that bubble diameters typically varied between 150 and 500 μm; this can be demonstrated by running a series of size determinations on the scattering pattern caused solely by the suspension fluid (Figure 5.2). The need to process a large number of samples necessitates connection to the mains water supply and makes storage of water before analysis to induce degassing impractical.

Bubble formation increased during cold weather, likely due to a greater temperature gradient between mains tap water and the laboratory. However, bubble formation was minimised by: 1) running samples in rapid succession, since the constant addition of

fresh water to the fluid module kept internal components cooler; 2) avoiding running the pump at excessive speeds and turning it off when not needed to avoid undue heating of the pump components; and 3) checking for bubbles in the sample vessel immediately prior to sample loading. If bubbles were present, the apparatus was flushed for up to an hour in order to cool internal components. At least two size determinations were made for each sample, since the presence of bubbles could be identified from in an increase in measured sample volume over time together with systematic changes in size distribution. Bubble formation can be severely aggravated by the use of the fluid module's internal sonication system and was therefore not employed during any of the sample analyses.

5.2.3.2 Sample preparation

Inadequate preparation typically leads to unstable sample size distributions due to the formation of flocs or breakage of flocs or aggregates during analysis. Laser obscuration provides a surrogate measure of sample dispersal within the apparatus and is useful for identifying the most appropriate dispersal technique (Chappel, 1998). Monitoring obscuration through time, and dividing by the initial obscuration value, a dispersion coefficient was obtained that enabled comparison between different samples (Cf. Chappel, 1998). Subsamples of a composite proglacial sediment sample (samples A–E, sieved to < 2 mm; Table 2.4) were dispersed in sterilised 60 ml containers using 40 ml of a) tap water; b) dilute Calgon (approximately 5% in tap water); and c) dilute Calgon ~ 24 h before analysis. Calgon is a commonly used dispersing agent prepared in the lab to the British Standard of 35 g sodium hexametaphosphate and 7 g sodium carbonate to 1 l of distilled water (Head, 1980). A sample dispersed with 60 ml of 5 % Calgon solution gives a Calgon concentration of ~ 0.02 % in the fluid module. Samples were shaken after addition of the dispersant and again immediately prior to addition to the fluid module.

Initial PIDS obscuration for all three samples was in direct proportion to the dry sample weight. Figure 5.3 (a) shows that PIDS obscuration increased gradually for all samples over time, with some evidence of sample stability having been reached after 8–12 minutes. Initial laser obscuration showed no systematic variation with sample weight; variation through time also shows no systematic trend (Figure 5.3 b), although trends are difficult to follow due to lack of precision in the reporting of the obscuration value (the

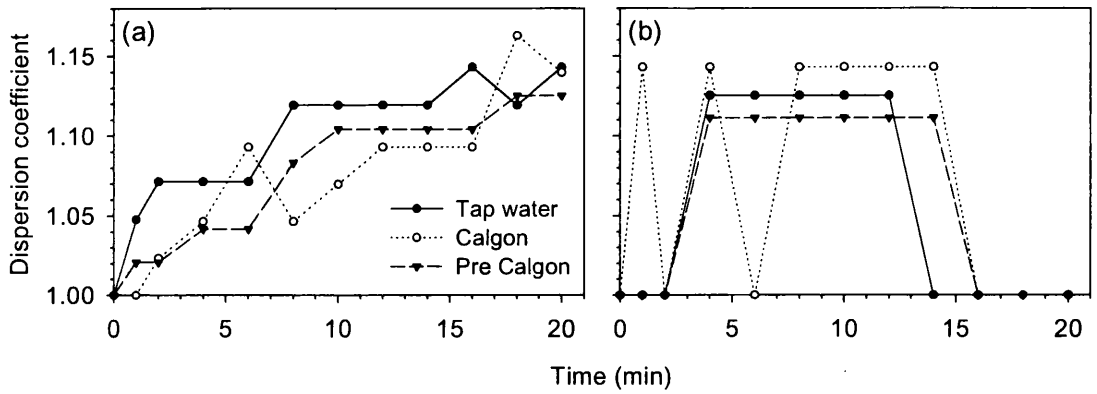

Figure 5.3 Dispersion curves for proglacial sediments determined using (a) PIDS and (b) laser obscuration. The Pre Calgon sample was prepared ~ 24 h before analysis.

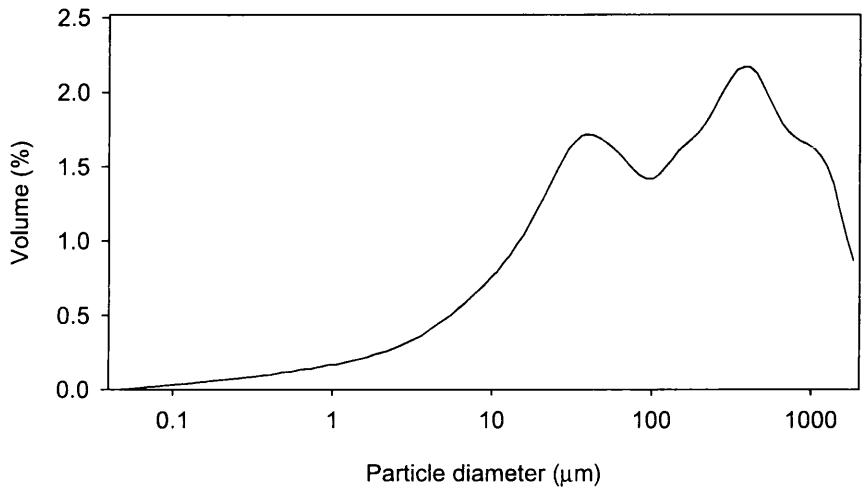

Figure 5.4 A composite proglacial sediment sample dispersed using tap water.

value is given in whole figures only). PIDS obscuration may therefore be a better indicator of sample dispersal, although the size distribution of a typical subsample of composite proglacial sediment suggests that an exceptionally small minority of particles lie in the 0.04–0.4 μm range (Figure 5.4).

These results indicate that for fine proglacial sediments from the Haut Arolla catchment, tap water is an effective dispersant and the addition of Calgon does little to improve dispersal. However, Calgon is designed to eliminate the surface charge that causes particles to flocculate; stronger bonds are likely to form between particles where they

Table 5.1 Effectiveness of sonication for sample dispersal using ashed proglacial sample C.

Subsample	Sonication (min)	Obscuration (%)			
		Type	Mode	Mean	SD
1	0	Laser	7.0	7.0	0.67
		PIDS	44	43.4	0.70
2	1	Laser	9.0	9.4	0.52
		PIDS	49	49.4	0.52
3	2	Laser	10	9.5	0.53
		PIDS	50	50	0.00
4	5	Laser	10	9.9	0.32
		PIDS	51	51	0.00
5	10	Laser	10	10	0.00
		PIDS	51	51	0.00
6	15	Laser	10	9.7	0.48
		PIDS	52	51.8	0.42

have been ashed. Mechanical action such as shaking or sonication can break such bonds without breaking rock particles or mineral fragments. For test samples of proglacial sediment filtered through 2.7 μm papers and ashed at 900 °C for 30 min, flakes of particles were often observed during sample preparation that could not be satisfactorily be disaggregated by shaking. A number of subsamples of ashed proglacial sample C were analysed after treatment in an ultrasonic bath. Six subsamples of near-identical weight were prepared in sterilised 60 ml containers with 40 ml of a 5 % Calgon solution to guard against flocculation during analysis. The subsamples were shaken well before being sonicated for 0, 1, 2, 5, 10 and 15 minutes. After addition to the fluid module, laser and PIDS obscurations were measured at 30 s intervals over a period of 5 min to check for sample stability before a size determination run was taken.

After addition to the fluid module, samples exhibited good stability as measured by laser and PIDS obscuration values (Table 5.1); however, the sample with no sonication shows the highest standard deviation, and standard deviation generally decreases with increasing exposure to ultrasonic sound. Mean dispersion coefficients calculated for laser

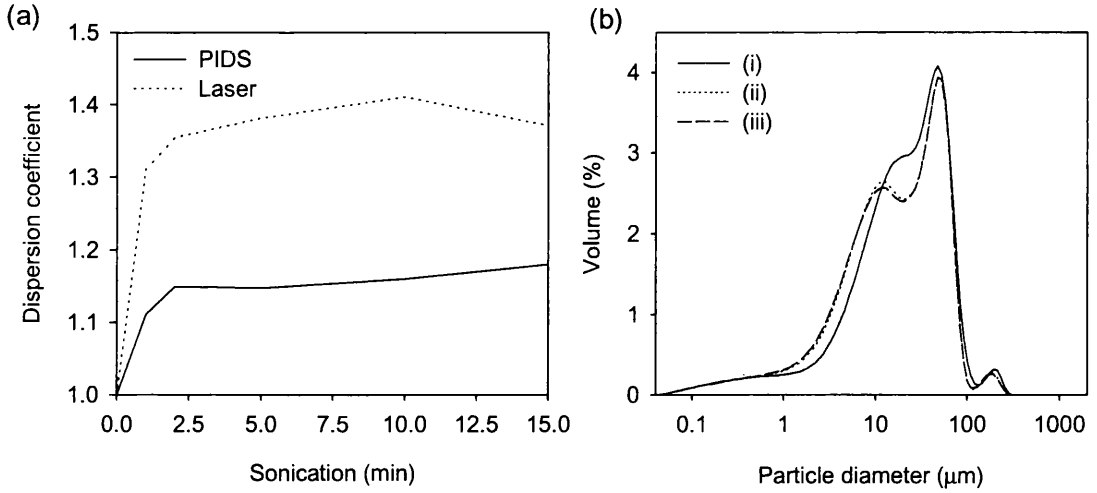

Figure 5.5 (a) Effectiveness of sonciation for dispersal of ashed sample C measured using PIDS and laser obscuration. (b) size determinations of sample C (i) prior to sonication and after 2 (ii) and 15 (iii) minutes of exposure to ultrasound.

and PIDS obscurations for each subsample were normalised with respect to dry sample weight (Figure 5.5 a). For particles to which both the PIDS and laser systems are sensitive, dispersion rapidly increases with exposure to ultrasonic sound up to a certain exposure period. The change in size distribution between samples sonicated for 0 and 2 min (Figure 5.5 b) indicates that sonication for at least 2 min is recommended for ashed proglacial sediment samples. It has been noted elsewhere (Chappell, 1998) that ultrasound may cause the breakage of individual clasts or mineral fragments; however, the change in size distribution between the sample sonicated for 2 min and the sample sonicated for 15 min is negligible (Figure 5.5 b).

5.2.3.3 Precision and accuracy

Precision

The precision of the laser diffraction method employed by the LS230 was evaluated using repeat analysis of subsamples of the composite proglacial sediment sample from the Haut Arolla catchment. Three subsamples of known weight were prepared and precision was tested at a) low; b) recommended; and c) high laser obscuration (Table 5.2). Table 5.2 shows the coefficient of variation for 6 statistical parameters from 10

Table 5.2 Coefficient of variation for size distribution parameters from 10 repeat size determinations of three subsamples of proglacial sediment at 1) low, 2) recommended and 3) high obscuration. Values in parenthesis give Laser/PIDS obscuration.

Statistic	Low (4/26)	Recommended (8/48)	High (20/80)
Mean	3.91	2.27	4.99
Median	4.74	2.91	4.42
Mode	2.84	0.00	7.45
Standard deviation	1.21	0.81	1.90
Skewness	–1.61	–1.60	–3.40
Kurtosis	18.82	7.45	13.45

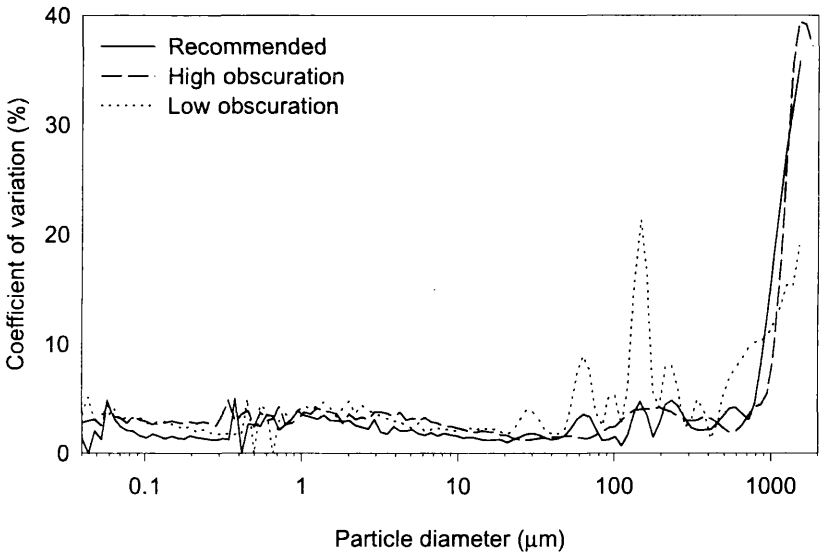

Figure 5.6 LS230 reproducibility by particle diameter for proglacial sediments.

repeat size determinations of each subsample. At recommended obscuration values, precision is good: the mode is reported consistently, standard deviation is also very reproducible (cv < 1 %) and mean, median and skewness show fair reproducibility (< 3 %); kurtosis, which is very sensitive to outliers, is poor (7.5 %).

Higher precisions were reported by Loizeau et. al. (1994) for the LS230 using a fine (~ 1–100 µm) lacustrine sample. Particle size for the composite proglacial sample ranges

from ~ 0.04–2000 μm and the distribution is polymodal. Coarser grains are fewer in number and the resulting diffraction pattern may be inconsistent between measurement runs, causing moment statistics (especially skewness) to be less reproducible. Using the coefficient of variation for the volume of sediment in each size fraction, reproducibility diminishes rapidly at grain sizes greater than ~ 800 μm (Figure 5.6). In general, precision for both statistical parameters (Table 5.2) and individual size fractions (Figure 5.6) diminishes outwith the recommended obscuration limits.

Accuracy

The accuracy of results for geological samples is difficult to assess due to the lack of geological standards; results are also presented in greater detail than can be obtained using other available techniques (e.g. sieving or settling). Nevertheless, accuracy appears to vary with the degree of laser obscuration: mean size distributions for the 10 analyses of each of the three samples used above show systematic variation in size distribution with obscuration (Figure 5.7). Two prominent modes are evident in all three samples; however, the size distribution at low obscuration suggests the presence of many more modes and suggests software difficulties when processing relatively weak diffraction pattern. At high obscurations, detail is lost and the 'trough' between the two modes is slightly inverted, possibly due to multiple scattering in dense particle suspensions.

The ability of the LS230 to accurately detect and resolve multimodal sediment distributions was assessed using specific size fractions of the composite proglacial sediment sample. Three separate size fractions were obtained by sieving and added cumulatively to the fluid module (Table 5.3); a size determination run was performed after the addition of each fraction. No modification to the distribution of the finer fractions was observed with increasing particle size (Table 5.3; Figure 5.8 a), although the second and third modes were slightly coarser than the upper sieve aperture-size for each fraction. This is presumably since non-spherical particles can pass into smaller sieve fractions than if they were perfect spheres (Matthews, 1991). However, using the cumulative weight of the samples to convert the raw volume percentage results to actual weight distributions, important differences are noted (Figure 5.8 b). Conversion of the results into actual weight distributions is desirable since the concentration of certain size

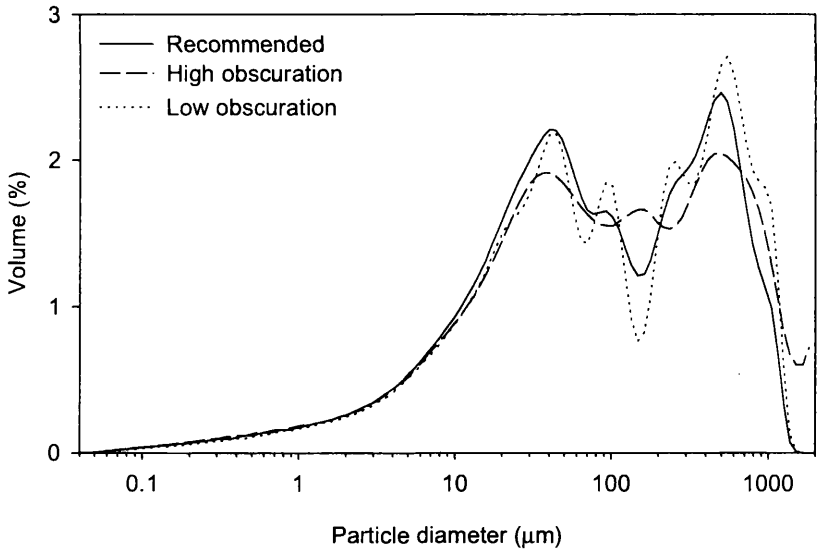

Figure 5.7 Mean size distribution for proglacial sediment samples described in Table 5.2.

Table 5.3 Accuracy of LS230 for cumulatively added fractions of proglacial sediment. Note that estimated sample volume as reported by the LS230 has no units.

Fraction (μm)	Weight (g)	Cumulative weight (g)	Obscuration (Laser/PIDS)	Cumulative volume	1st mode (μm)	2nd mode (μm)	3rd mode (μm)
< 63	0.60	0.60	10/47	6.66×10^{11}	45.75	–	
180–250	0.56	1.16	10/50	1.10×10^{12}	45.75	269.2	–
500–710	0.50	1.66	10/53	2.18×10^{12}	45.75	269.2	751.1

fractions within the flow can also be obtained where volume percentage results are potentially misleading.

Figure 5.8 (b) shows that addition of the second size fraction causes the estimated weight of the < 63 μm fraction to increase, whereas, on addition of the third size fraction, the estimated weight of both finer fractions is greatly decreased. Conversion of volume percentage results into actual weight distributions assumes a consistent particle density with particle size; the above results suggest that the second size fraction has a higher density than the first, such that the weight of the first fraction increases, whilst the third fraction has a much lower density than both the finer fractions and accounts for too much of the weight of the total size distribution. Particle density varies with particle size as a

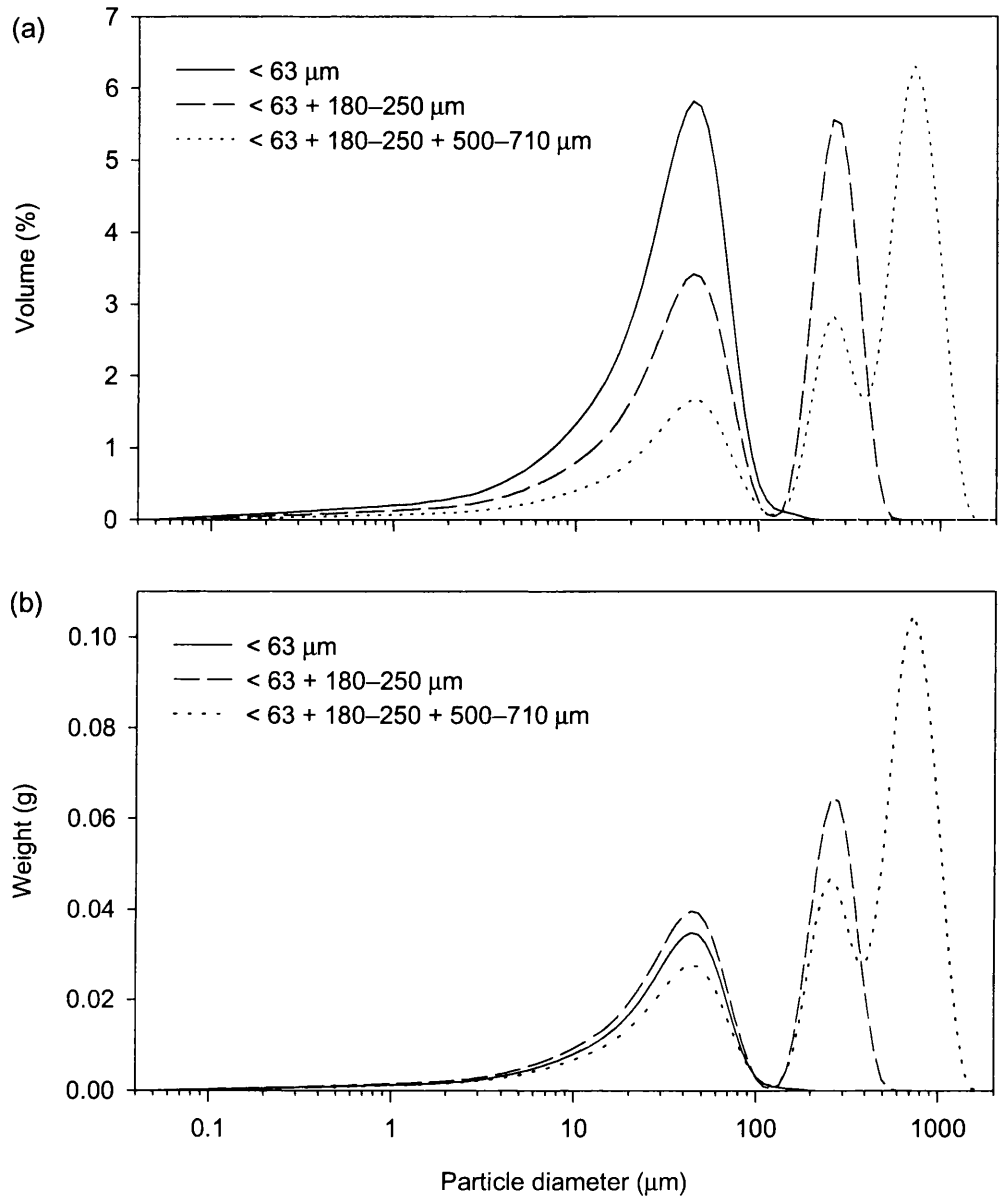

Figure 5.8 (a) volume percentage and (b) calculated weight distributions for samples described in Table 5.3.

result of mineral size. Rubey (1993) found that heavy minerals tend to be found in finer sieve classes, creating a density-related bias that artificially shifts the size distribution towards the finer sizes (Matthews, 1991).

The magnitude of the density-related bias in sediments from the Haut Arolla catchment was investigated using proglacial sediment samples A–D (cf. Table 2.4). Samples were

Table 5.4 Calculation of relative densities for specific size fractions of proglacial sample A. Density is reported relative to the mean density of the < 63 μm fraction. Note that volume and density do not have standard units.

	< 63 μm fraction (g)	Volume < 63 μm fraction	Density < 63 μm fraction	Added fraction (μm)	Added fraction (g)	Volume both fractions	Added fraction		
							Volume	Density	Relative density
1	0.4670	0.6289	0.7426	63–90	0.4205	1.0500	0.4211	0.9986	1.3812
2	0.4751	0.6487	0.7324	90–125	0.4499	0.9103	0.2616	1.7198	2.3787
3	0.4666	0.6396	0.7295	125–180	0.4464	0.9583	0.3187	1.4007	1.9373
4	0.4470	0.6047	0.7392	180–250	0.4176	0.9355	0.3308	1.2624	1.7461
5	0.4955	0.6734	0.7358	250–355	0.4168	1.0490	0.3756	1.1097	1.5348
6	0.4170	0.5728	0.7280	355–500	0.4538	1.0990	0.5262	0.8624	1.1928
7	0.4477	0.6243	0.7171	500–710	0.4199	1.3344	0.7101	0.5913	0.8179
8	0.4353	0.6091	0.7147	710–1000	0.4311	1.8260	1.2169	0.3543	0.4900
9	0.4675	0.6641	0.7040	1000–1400	0.3752	1.9890	1.3249	0.2832	0.3917
10	0.4515	0.6578	0.6864	1400–2000	0.3173	1.1210	0.4632	0.6850	0.9474

dry sieved into 11 size fractions (Table 5.4); a quantity of < 63 mm sediment was added to the fluid module and a size determination run was taken before a second, coarser fraction was added to the same suspension and a second sizing run performed. The density was then determined for both fractions. Table 5.4 shows the results of 10 tests conducted for sample A; because sample volume determined by the LS230 is unitless, the density variation has been converted into a relative density coefficient assuming that the mean density of the < 63 μm fraction from all of the tests is 1. Relative density varies relatively consistently with particle size for samples A–D (Figure 5.9); density peaks in the 90–500 μm range and declines with increasing particle size. The small increase in density in the 1400–2000 μm range is probably due to a large proportion of particles whose true nominal diameter is much larger, having passed through the 2000 μm sieve. Such particles will scatter light beyond the measurement range and will therefore not be included in the estimation of sample volume, resulting in relative density being overestimated.

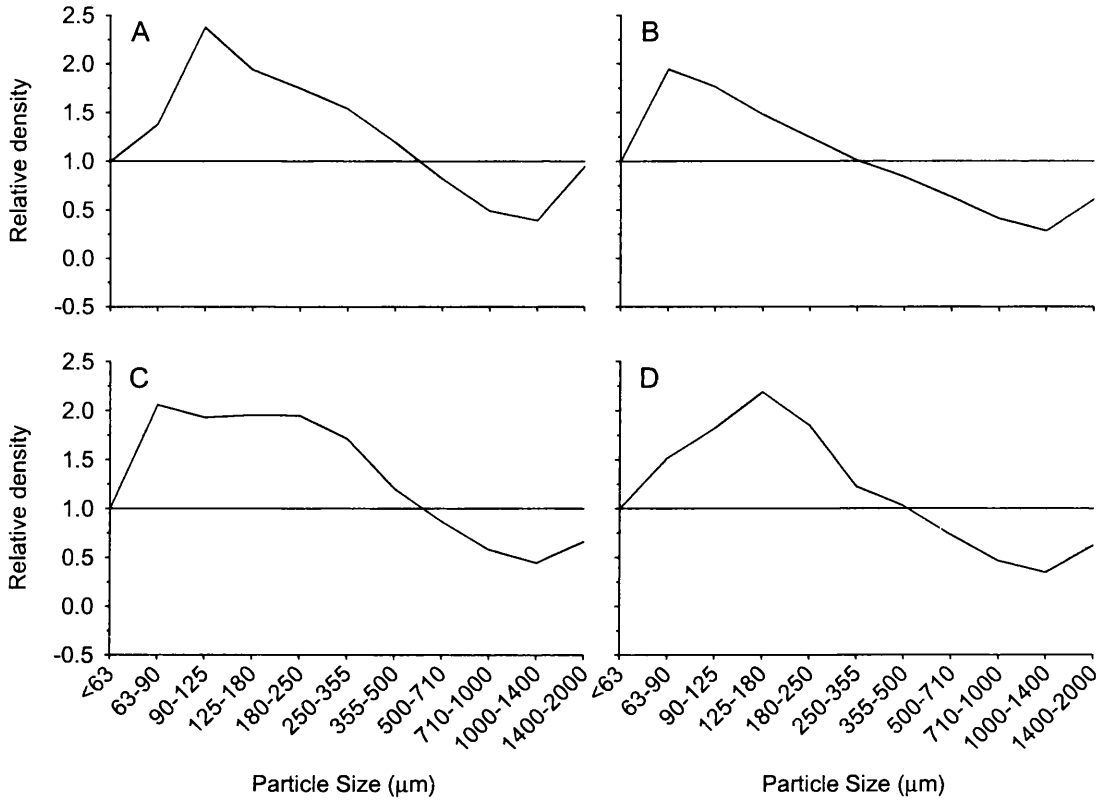

Figure 5.9 Relative density variation for size fractions of proglacial samples A–D.

The variation in relative density is large, with the 90–125 µm fraction being up to four times denser than the 1000–1400 µm fraction. Densities of common rock-forming minerals usually fall into a very narrow range (typically 2.2–2.8 g cm^{-3}); suspended sediment from the Haut Arolla catchment analysed using x-ray diffraction (Section 6) indicates the presence of hematite (density ~ 5.1 g cm^{-3}), but the difference in density between pure quartz and pure hematite is only a factor of two. It is therefore likely that other sample properties contribute to the apparent change in density. Particle refractive index and/or absorptive capacity are unlikely to contribute to the effect since particles larger than ~ 7.5 µm are opaque and Fraunhofer should be an accurate approximation of the scattering of light. Using the full Mie theory with particle refractive index and absorption coefficient set at realistic values, the size distributions shown in Figure 5.8 (b) are unchanged above ~ 10 µm, with Fraunhofer having slightly overestimated the proportion of sediments finer than this. The effect is more likely to be related to particle

shape: larger particles in the 1000–2000 μm range are often well-rounded; whilst smaller particles appear plate or rod-like under a scanning electron microscope (Figure 2.7 a–h).

5.2.3.4 Summary

The advantages of using the LS230 to size sediment samples from the Haut Arolla catchment are its wide sizing range, comparatively high resolution, and ability to perform size analyses on a wide range of dry sediment weights (typically ~ 0.1–1 g). For accurate size determinations, sample concentration within the fluid module should be kept within recommended obscuration ranges. In such circumstances, the LS230 is able to resolve polymodal sediment distributions with high resolution and accuracy. However, it is important to note that for the geological samples tested here, the reported volume of sediment in specific size ranges may be in error. Such errors are likely due to particle shape effects, which, if they remain consistent throughout the catchment, are likely to cause systematic shifts in sediment distributions or the innaccurate reporting of the prevalence of individual modes. Combined with variations in absolute particle density, this problem prohibits the conversion of volume percentage results into more useful actual weight distributions. Despite the consistency of the apparent shape/density effect, so far it has not been possible to characterise the nature of the effect for particles below 63 μm, and it is unlikely that sufficiently accurate and representative size fractions could be prepared in order to do so. If sediment sources or mineralogy are expected to vary between samples, such a calibration would also be very unreliable. Beckman Coulter recognise such problems but suggest that for most applications relative, rather than absolute, measurements are sufficient, and have strongly advised against attempting calibration of the LS230 (S. Munt, pers. comm.; Munt, 1995).

These difficulties mean that for geological samples where the mineral content or particle shape is expected to vary as a function of particle size or throughout time, volume results reported from laser diffraction apparatus and moment statistics derived therefrom should be treated with caution. Despite advances in laser diffraction, McCave and Syvitski's (1991) recommendation that sample modal decomposition is the most revealing form of analysis remains just as applicable today. Nevertheless, there is the possibility that with

sufficiently large sample numbers and the use of appropriate analysis techniques, systematic trends in size distribution parameters may still be identified.

5.3 CATCHMENT SUSPENDED AND *IN SITU* SEDIMENT SIZE

5.3.1 Introduction

This section presents suspended and *in situ* sediment size distributions in order to: 1) characterise sediment variability within the Haut Arolla catchment; and 2) identify trends or relationships in and between suspended and potential sediment sources. Only suspended samples from the western sub-catchment collected during the 1998 melt season are considered here; suspended sediment evacuation from the eastern sub-catchment is thought to have been strongly influenced by extraglacial sediment contributions and, as a result, is unlikely to accurately reflect subglacial processes (see Section 4). Sample preparation and analysis is outlined briefly before the general particle size characteristics of the sediments are considered.

5.3.2 Sample preparation and analysis

5.3.2.1 Suspended sediment samples

Ashing of the filtered samples collected in the field is detailed in Section 2.1.1.1; afterwards, samples were stored in sterile 60 ml plastic containers. Prior to analysis using the LS230, samples were re-suspended using ~ 40 ml of 5 % Calgon solution and sonicated for ~ 10 min to ensure particles were adequately disaggregated. Dry sample weights ranged from 0.01–12.3 g (median 0.198 g); by lowering the water level in the fluid module before adding the sample and then extracting and diluting as necessary, satisfactory laser obscurations were obtained for samples in the range of ~ 0.1–1 g. Samples larger than 1 g required a lengthy extraction/dilution procedure in the fluid module. Many larger samples, reflecting higher suspended sediment concentrations, occurred later in the season and contained significant amounts of coarse sand. Analysing these samples presented practical difficulties, and the volume of material in the range

Table 5.5 Mean change in various size distribution parameters for extracted portions of 23 samples with respect to those for the original samples.

	First mode	Mean	Median	SD	Skewness	Kurtosis
Original sample (μm)	14.86	204.20	322.53	6.50	–1.00	3.43
Change (μm)	0.07	76.82	121.93	0.10	–0.29	2.08

1000–2000 μm tended to mask variation in the finer sizes. As a result, processing of samples from the 1998 melt season was stopped at 12:00 JD 201. Of the 974 samples analysed, ~ 100 of these were combined on account of the laser obscuration being too low and 175 required extraction/dilution due to obscurations being too high.

Extracted portions of 23 of the samples that required dilution were analysed to assess the likely error involved in this technique (Table 5.5). For the extracted samples, mean and median are generally coarser due to coarse particles being preferentially removed during extraction (Section 5.2.3.1). Skewness and kurtosis, which are strongly influenced by outlying values, also show large variation between initial and extracted samples. However, deviation in first mode and standard deviation from the initial sample statistics is typically small. Moment statistics for the extracted samples should therefore be treated with caution, and for all samples a break down of the modal structure may be the most reliable approach to analysis.

Time series plots of size distribution parameters were checked against field notes. This resulted in rejection of six samples with uncharacteristically coarse first modes collected during periods when the ISCO hose was subject to icing, and two samples during periods when the hose was thought to have been partially blocked. As a result, a total of 872 individual size distributions were obtained, providing good coverage of the period between JD 135–201.

5.3.2.2 In situ sediment samples

Sediments sampled from the proglacial area (samples A–E) were obtained to evaluate the LS230 since they were assumed to be similar in size distribution to suspended sediment from the subglacial drainage system. A sample of basal sediment (sample E)

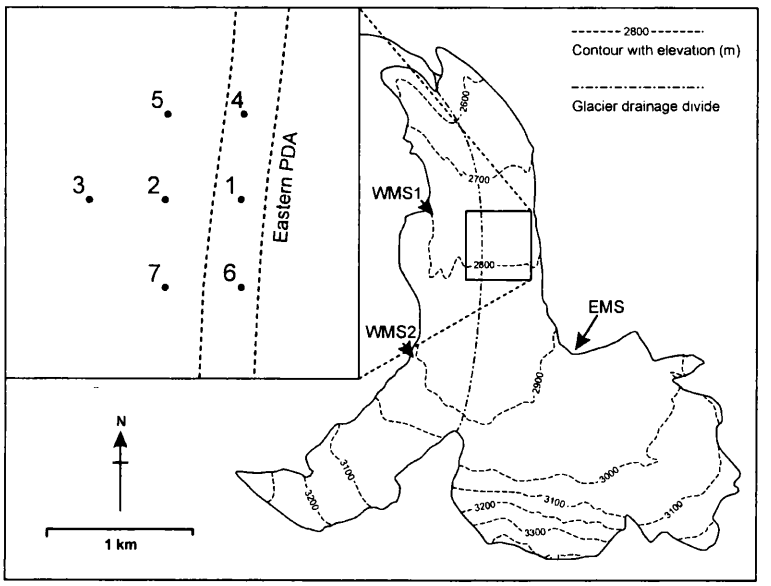

Figure 5.10 Haut Glacier d'Arolla showing the location of drill sites 1–7. The approximate positions of the eastern PDA (see Sharp et al., 1993) and locations of the western (WMS) and eastern (EMS) marginal stream samples are also shown.

was taken to provide an indication of the subglacial sediment distribution. This had a clayey consistency and contained many clasts > 2 mm, and was found melting out from beneath the glacier margin between the two major outlet streams. These samples were dried and dry sieved to remove particles greater than 2 mm before being subsampled using a riffle box to obtain quantities suitable for particle size analysis. Samples A–C had 0–4 % of particles larger than 2 mm; samples D and E had 20 % and 14 % of particles larger than 2 mm, respectively. Subsamples of between 0.4–0.8 g were prepared and analysed as for the suspended sediment samples (above).

Sediments were also sampled from the base of boreholes drilled to the bed of the glacier. Eleven samples were collected during late May/early June, 1998 ~ 1 km from the glacier snout and above the eastern PDA. Drilling using hot water under high-pressure will cause strong turbulence at the base of boreholes that is likely to suspend basal sediments; hence, samples were obtained immediately after drilling using a manually triggered Nielsen water sampler (Nielsen, 1995) lowered to the borehole base. Samples were taken from separate holes drilled at 5 of the 7 drilling sites during late May (Figure 5.10); sampling was not attempted at site 1, and at site 3 the ice thickness was too great to

enable sampling. Samples were stored in plastic bottles and returned to the laboratory before being filtered through 0.1 μm papers.

Waters at the base of boreholes had sediment concentrations after drilling in the range 0.3–47.5 g l^{-1}. However, the pattern of sediment concentration does not reliably indicate any spatial pattern in basal sediment abundance. Concentrations were very variable even for boreholes ~ 1 m apart, and is most likely to reflect the time allowed for sediments to settle out of suspension before the sample was taken. The borehole sediments were removed from the papers using a scalpel and placed into sterile containers; samples were dry-split as required before being re-suspended (as above) and sonciated for 5–15 minutes prior to analysis using the LS230. None of the samples contained sediments larger than 2 mm.

Further suspended sediment samples were obtained manually from ice marginal streams during late August 1998 (Figure 5.10). On the western side of the glacier tongue, one major stream emerges submarginally from beneath the tributary glacier before flowing along the glacier margin through deeply-incised glacial sediments and disappearing subglacially ~ 1 km from the snout. This stream almost certainly contributes to the western proglacial stream. Samples were collected using wide-necked 0.5 l plastic bottles from where the stream emerges and a few hundred metres before it enters the subglacial drainage system. Samples were filtered through 0.01 μm papers and prepared and analysed as above; two samples taken near the tributary glacier had sediment concentrations of 5.5–7.8 g l^{-1}, whereas two obtained in the gully had concentrations of 16–17 g l^{-1}. A fifth sample from a marginal stream on the eastern side of the glacier in the main accumulation basin had a sediment concentration of 4.0 g l^{-1}.

5.3.3 General suspended and source sediment characteristics

5.3.3.1 Suspended sediments

Figure 5.11 shows the mean size distribution of all 872 suspended sediment samples from the western glacial catchment during 1998. The distribution is approximately log-normal with a major mode in the 5–50 μm range; a second, minor mode is indicated

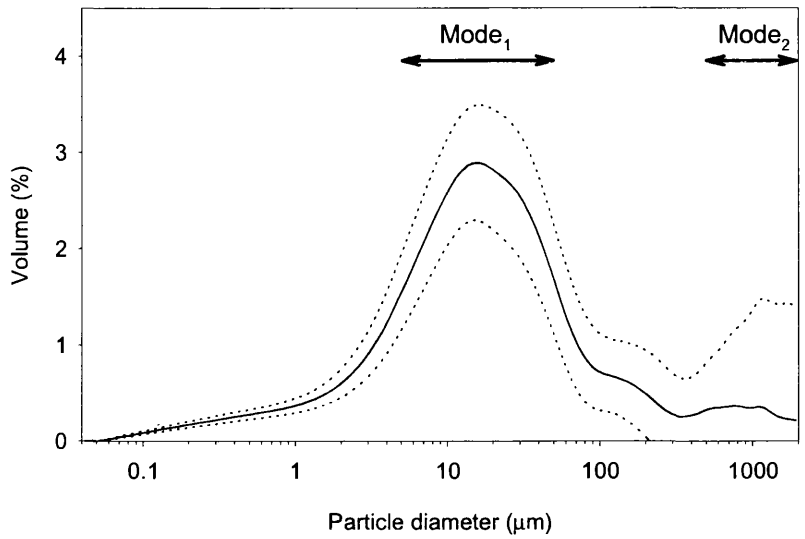

Figure 5.11 Seasonal mean suspended sediment size distribution; dotted lines indicate one standard deviation about the mean. $Mode_1$ and $Mode_2$ indicate the first and secondary modes referred to in the text.

Table 5.6 Size distribution statistics for suspended sediment samples during 1998. All values (except skewness and kurtosis) are in μm.

Sub-period	Mean	Median	First Mode	SD	Skewness	Kurtosis
All data	17.5	17.33	15.65	5.68	–0.01	0.84
1	17.30	17.69	14.26	4.94	–0.42	0.63
2	16.34	16.78	14.26	5.20	–0.32	0.50
3	12.97	14.61	15.65	4.32	–0.58	1.10
4	13.50	15.31	17.18	4.62	–0.39	1.29
5	15.16	17.30	18.86	4.61	–0.53	1.12
6	33.23	24.01	15.65	8.90	0.10	–0.42

between 500–2000 μm. Only a small proportion of sediment is below 2 μm, indicating a dearth of clay-sized minerals. Standard deviation limits about the mean distribution also show low temporal variability in the clay fraction. In contrast, variability is high about the peak of the 'first' mode, suggesting its position may be subject to frequent shifts in location. Variability generally declines either side of the main mode, but increases markedly above 100 μm to a maximum in the 1000–2000 μm range. The distribution suggests that suspended sediments are characterised by a fine, well-sorted mode between

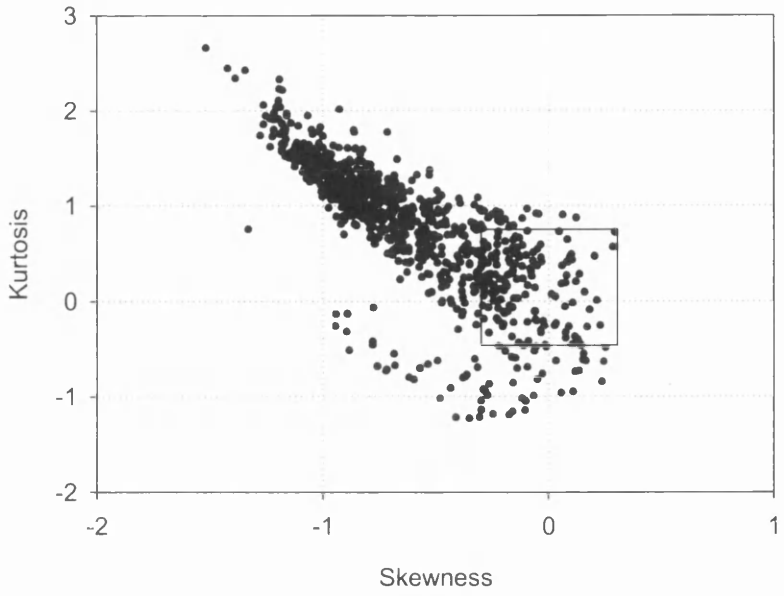

Figure 5.12 Normality of suspended sediment size distributions. The box bounds the area within which there is less than 1 % chance that samples are non-normal (after Rice and Church, 1998).

5–50 μm; larger particles are less common but when present they form a distinctive secondary mode in the 500–2000 μm range.

Size statistics for the seasonal mean suspended distribution are shown in Table 5.6. The distribution is approximately log-normal, although slightly leptokurtic (a mesokurtic distribution has a kurtosis of 0). The main mode is centred on 15.7 μm, whereas the mean and median lie at ~ 17 μm, indicating a slight negative (fine) skew. Individual samples were checked for log-normality by plotting sample skewness against kurtosis (cf. Rice and Church, 1998). Most distributions are negatively skewed and leptokurtic (Figure 5.12); for greater clarity, seven very highly skewed and leptokurtic samples from JD 193 are not shown. These samples have a dominant mode in the 1000–2000 μm range, raising the possibility that bed material had also been sampled. Despite pre-analysis sieving, these samples also had a large proportion of particles with a true nominal diameter exceeding the range of the LS230, effectively curtailing the distribution and accentuating skewness.

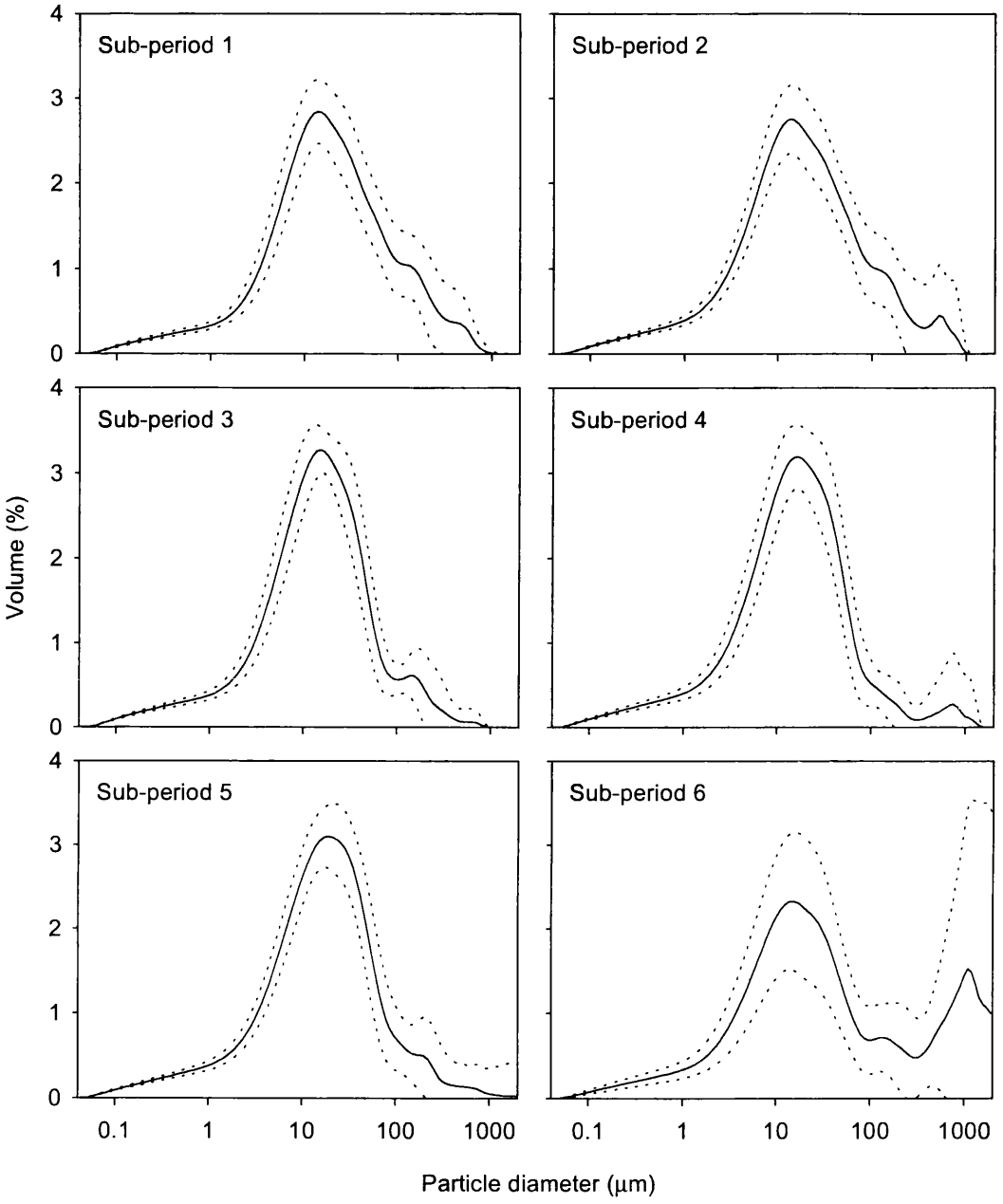

Figure 5.13 Mean size distributions for sub-periods of 1998 (cf. Figure 5.11).

Table 5.6 and Figure 5.13 show the mean size distributions and distribution statistics for samples during sub-periods 1–6 of the monitored period. The distributions show some evidence of evolution throughout the melt season, demonstrating a consistent coarsening of the main mode during sub-periods 2–5 (Table 5.6). The shape of the distribution also changes: during sub-periods 1–3, mean, median and standard deviation decrease as the

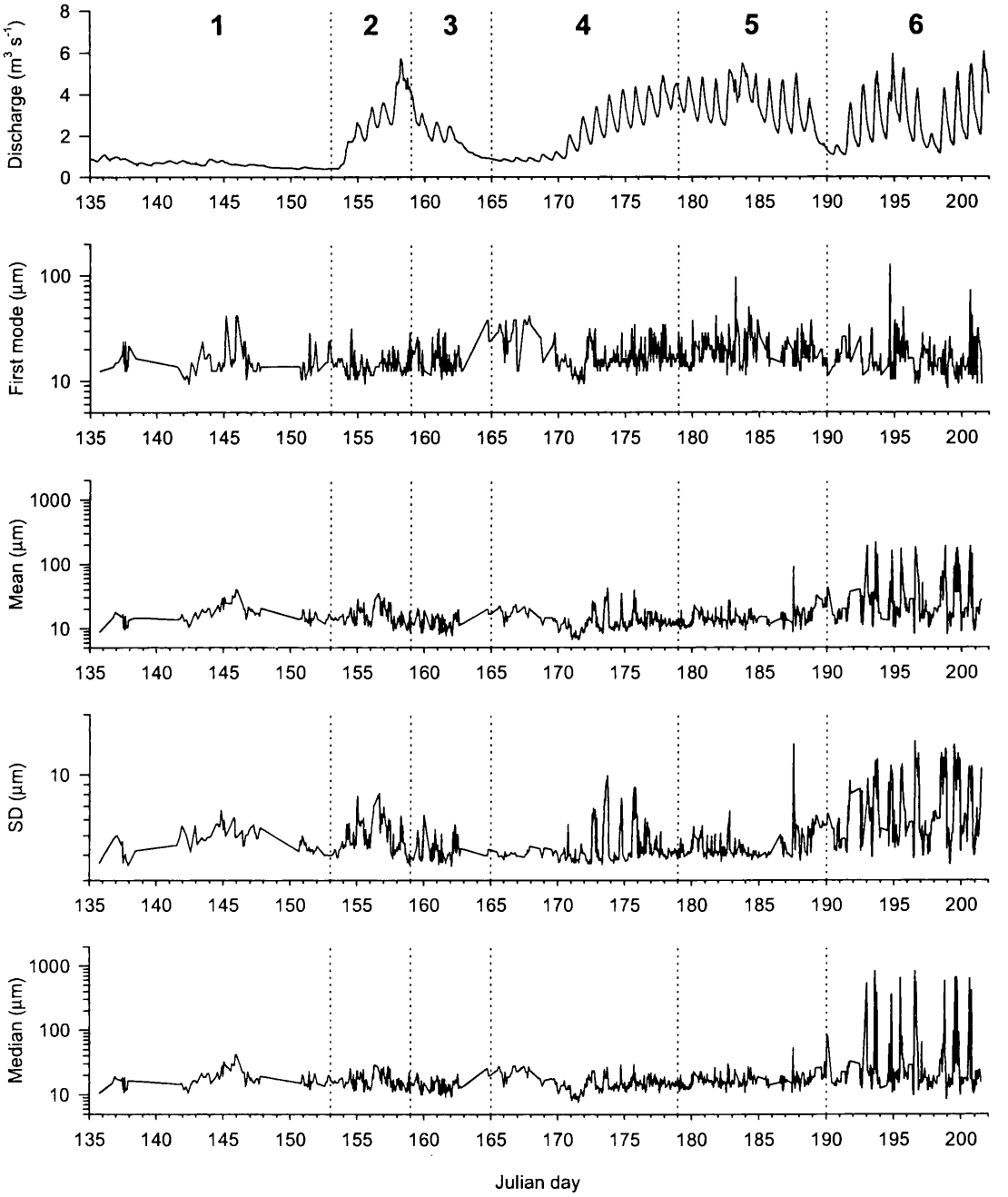

Figure 5.14 Time series of suspended sediment size distribution parameters and discharge. The various sub-periods of the 1998 melt season are also shown (Table 3.1).

volume of coarse material falls and sorting improves. The main mode remains much better sorted during sub-periods 4 and 5, but mean, median and standard deviation increase once more as a 'tail' of coarse particles becomes evident (Table 5.6; Figure

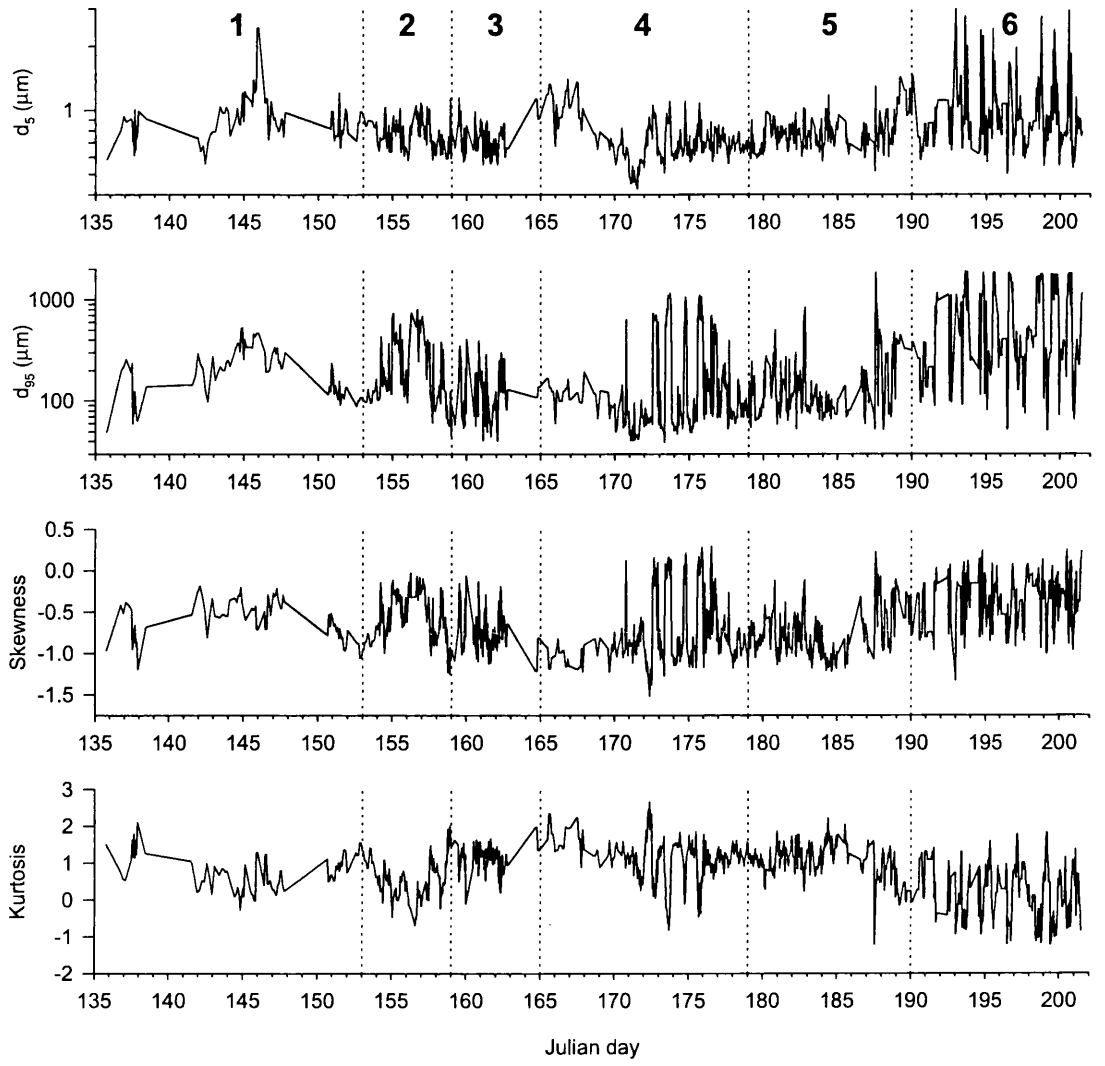

Figure 5.15 Time series of suspended sediment size distribution parameters (see Figure 5.14).

5.13). A very large increase in the volume of coarse material occurs during sub-period 6 due to the appearance of a strong secondary mode in the 500–2000 µm range, and moment statistics are affected accordingly; however, there is also a slight fining of the main mode (Table 5.6). Secondary modes occupying distinct size ranges are evident in many of the other sub-periods, but these are typically minor features (Figure 5.13).

Time series of size distribution statistics during 1998 are shown in Figures 5.14 and 5.15. For clarity, the seven samples on JD 193 that demonstrated high non-lognormality suggestive of contamination by bedload have been removed and gaps in the record are

linearly interpolated. Measures of central tendency and sorting are shown in Figure 5.14, together with catchment discharge. The modal position of the 'first' mode is shown in preference to the sample mode, since the latter is frequently subject to rapid shifts in location resulting from an occasionally dominant secondary mode. Sorting is indicated by the standard deviation. The d_5 and d_{95} percentiles (Figure 5.15) illustrate variation in the finest and coarsest components of the distributions. Sample skewness and kurtosis are both approximately normally distributed (Figure 5.15); other size distribution parameters are log-normally distributed and are represented on a logarithmic scale.

Temporal variation in suspended sediment size distributions is characterised by erratic, hourly-scale fluctuations that are not evident in the discharge series (Figures 5.14 and 5.15). Rapid, high-magnitude variability occurs in the coarser fractions, indicated by d_{95}, which varies from ~ 40–2000 μm (Figure 5.15). Variation in d_5, mean and sorting largely reflect variation in d_{95}, although there are a few trends in d_5 that appear independent of changes in the volume of the coarse material in transport (Figures 5.14 and 5.15). Similar variability occurs in the median size but is more marked towards the end of the monitored period, indicating that d_{50} becomes unstable where samples are polymodal (Figure 5.13). However, erratic variation is also evident in the first mode, the position of which is independent of changes throughout the rest of the distribution (Figure 5.14). Nevertheless, despite showing a number of high peaks between 60–140 μm on JD 154, 184 and 194, first mode is very stable, varying between ~ 10–40 μm.

5.3.3.2 In situ sediments

Proglacial sediments exhibit great differences in size distribution (Figure 5.16 a; Table 5.7) since they may not represent single deposition events under steady flow regimes. With the exception of sample C, the first mode is typically much coarser than that of the suspended samples (Figure 5.13; Table 5.6). This is likely to reflect the fact that water must be flowing very slowly for the finest size fractions to be deposited (Bogen, 1981). Sample E, however, shares many characteristics of the suspended samples, with a first mode centred on 10.3 μm and another principal mode in the 500–2000 μm range and centred on 1314 μm (Figure 5.16 a; Table 5.7). The location from which this sample was taken and its similarity to the seasonal mean suspended distribution, albeit with a greater

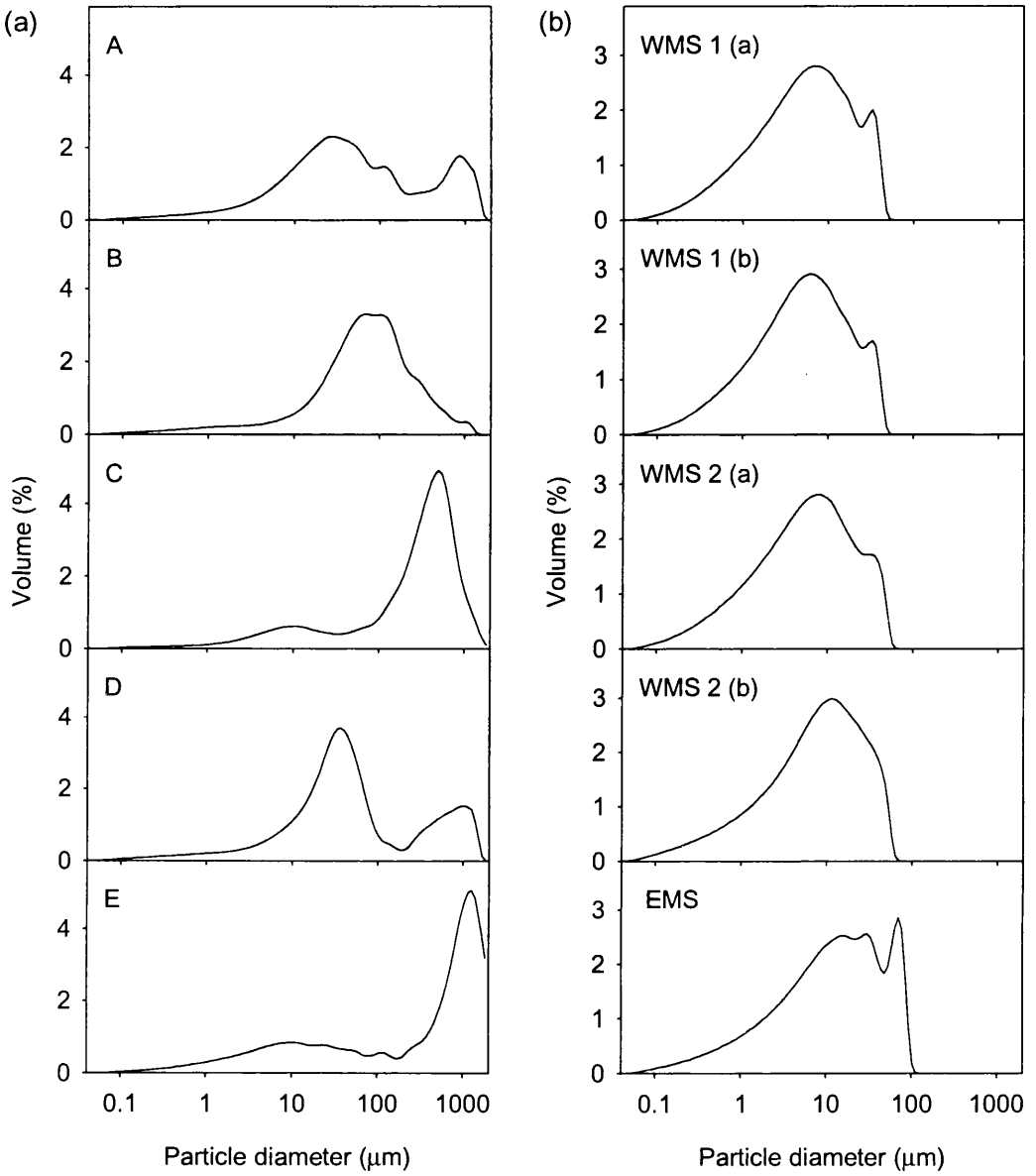

Figure 5.16 Size distributions for (a) proglacial and (b) marginal stream samples.

proportion of sediment in the secondary mode, suggests that it may be a good model for the general character of subglacial sediments.

Marginal stream samples (Figure 5.16 b; Table 5.7) also exhibit similar characteristics to the seasonal average suspended distribution; however, there are key differences. The modal distribution of samples from the western marginal stream ~ 1 km from the snout (WMS 1 a and b) is much finer (~ 7 μm) than the seasonal mean suspended distribution

Table 5.7 Particle size statistics for proglacial, marginal stream and subglacial sediment samples collected during 1998. All values (except skewness and kurtosis) are in μm.

Sample (Date)	Mean	Median	$Mode_1$	$Mode_2$	$Mode_3$	$Mode_4$	S.D.	Skew.	Kurt.
Proglacial A	50.6	43.7	28.7	116	905	–	6.96	–0.21	–0.14
Proglacial B	61.3	74.3	72.9	106	–	–	4.54	–1.20	2.48
Proglacial C	190	354	10.3	517	–	–	5.73	–1.59	2.11
Proglacial D	50.0	40.8	38.0	1091	–	–	6.43	–0.20	0.36
Proglacial E	174	609	10.3	23.8	116	1314	11.2	–0.94	–0.34
WMS 1a (JD 223)	4.96	5.76	7.78	34.6	–	–	3.78	–0.52	–0.24
WMS 1b (JD 223)	4.77	5.43	6.45	34.6	–	–	3.70	–0.49	–0.19
WMS 2a (JD 223)	5.24	6.12	8.54	34.6	–	–	3.92	–0.53	–0.19
WMS 2b (JD 223)	7.00	8.83	12.4	–	–	–	4.05	–0.76	0.17
EMS (JD 223)	10.8	13.6	16.4	34.5	73.0	–	4.43	–0.76	0.12
Site 2 (JD 142)	11.8	14.9	19.8	66.4	–	–	3.37	–1.27	2.10
Site 4 (JD 145)	7.41	9.04	12.4	–	–	–	3.73	–0.73	0.36
Site 4 (JD 145)	7.47	9.09	12.4	66.4	–	–	3.67	–0.74	0.35
Site 4 (JD 145)	8.89	10.8	13.6	66.4	–	–	4.11	–0.71	0.22
Site 4 (JD 146)	4.30	5.05	6.45	–	–	–	3.05	–0.59	–0.09
Site 5 (JD 146)	19.1	20.4	31.5	684	–	–	6.12	–0.03	0.29
Site 5 (JD 147)	11.3	13.1	14.9	72.9	–	–	4.07	–0.76	0.69
Site 5 (JD 147)	15.8	19.9	28.7	–	–	–	3.33	–1.35	2.44
Site 6 (JD 153)	9.40	11.7	14.9	72.9	–	–	3.78	–0.90	0.87
Site 6 (JD 153)	7.62	9.05	11.3	66.4	–	–	3.58	–0.74	0.56
Site 7 (JD 154)	10.9	13.1	19.8	45.8	–	–	3.06	–0.98	0.98

$Mode_{1-4}$: principal modes; S.D.: standard deviation; Skew.: skewness; Kurt.: kurtosis.

(~ 15.7 μm). Samples from the same stream nearer the tributary glacier (WMS 2 a and b) are slightly coarser but inconsistent (Figure 5.16 b; Table 5.7), probably due to the stream section being much steeper and highly turbulent; however, the main mode remains finer than for the seasonal mean suspended distribution (Table 5.6). A number of samples, including the sample from the eastern marginal stream (EMS, Figure 5.16 b; Table 5.7), also exhibit a minor second mode at ~ 34.6 μm that is not evident in the seasonal mean suspended distribution (Table 5.6). The EMS sample itself is slightly coarser than the WMS samples, having a 'first' mode centred on 16.4 μm, and exhibiting

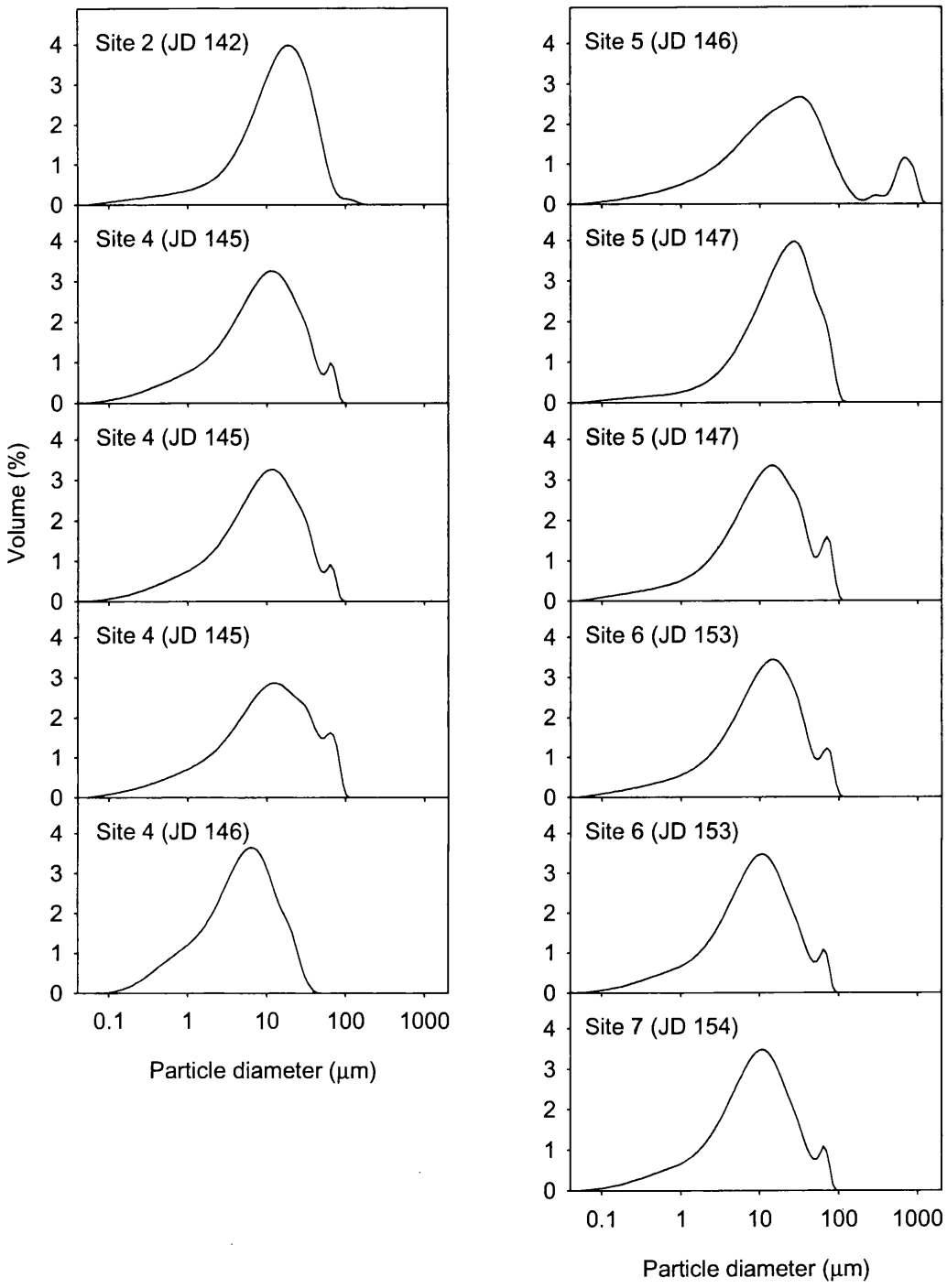

Figure 5.17 Size distributions for subglacial sediment samples.

a third mode at 73.0 μm (Figure 5.16; Table 5.7). None of the marginal stream samples contained particles significantly in excess of 100 μm.

Borehole samples (Figure 5.17; Table 5.7) are closer to the seasonal mean suspended distribution, having a dominant first mode that, for the majority of samples, lies in the range 12.4–19.8 μm. The sample taken at Site 5 on JD 146 also exhibits a second mode in the 500–2000 μm range, suggesting some non-suspended basal material may also have been sampled. More commonly, however, a very minor second mode is observed between 45.6–72.9 μm that is not observed in the seasonal mean suspended distribution (Figure 5.11). The first mode also varies more than in the seasonal mean suspended distribution, and mean and median values are typically much finer, mainly due to the absence of particles coarser than ~ 100 μm, but also due to noticeably larger volumes of fines (Figure 5.17; Table 5.7). There is some spatial pattern to the size distribution of basal sediments as determined from the borehole samples: samples from sites 2, 5 and 7, between the VPA and the glacier centreline (Figure 5.10) have relatively coarse first modes (14.9–31.5 μm) and mean and median values are in the range 10.9–20.4 μm. Samples at sites 4 and 6 in the region of the VPA are generally finer, having first modes in the range 6.45–14.9 μm and mean and median values between 4.3–11.6 μm.

5.3.4 Discussion and conclusions

The size distributions of suspended sediments sampled from the western proglacial stream typically comprise of two distinctive modes: a prevalent first mode and an occasionally dominant, though often absent, second mode between 5–50 μm and 500–2000 μm, respectively (Figure 5.13). This distribution is characteristic of glacial sediments described by Dreimanis and Vagners (1971), where larger rock fragments and individual mineral grains occupy distinctive 'terminal' grades. Sediments sampled from the proglacial area show broadly similar characteristics (Figure 5.16 a; Table 5.7), but their first mode is consistently much coarser, probably reflecting the fact that the finest sediments remain in suspension since flow velocities are rarely low enough for their deposition to occur. Basal melt-out till demonstrates a very similar distribution to suspended sediments, suggesting a close relationship between the character of subglacial sediments and those exported from the subglacial drainage system.

Basal sediments obtained from boreholes in the region of the eastern PDA differ from suspended sediments due to the absence of a significant second mode (Figure 5.17; Table 5.7), most likely reflecting the inability of the sampling technique to collect large particles. However, the first mode, although reasonably similar to that observed in suspended sediments, is more variable and much finer. This may reflect local geological variations since suspended sediments were sampled from the western catchment, but also differences in mechanical or chemical weathering rates between the two glacial catchments. Although only a small number of samples were obtained, it appears that sediments are finer near to PDAs than elsewhere (Table 5.7; Figure 5.10). Hubbard et. al. (1995) demonstrated higher basal porosities near to PDAs late in the melt season, suggesting preferential winnowing of fines from sediments near to major subglacial conduits. In this study, borehole samples were collected before any channelisation had occurred. It is possible that during channel closure due to the suppression of supraglacial meltwater inputs at the end of each melt season, hydraulic gradients will continue to drive meltwaters from the distributed system towards low-pressure PDAs where fine sediments may be deposited. As a result, sediments near to and within PDAs in early spring may be significantly finer than those elsewhere. Generally thinner basal sediments near to PDAs may also result in the more efficient mechanical weathering of coarser particles.

The first mode of suspended sediments sampled from the western marginal stream, which flows through thick, formerly subglacial sediments, is also much finer than in those collected in the proglacial stream (Figure 5.16 b; Table 5.7). However, similar modes were not observed in the western proglacial stream, where contributions from both subglacial and marginal sources might be expected to give rise to bimodal distributions with modes centred on 7 μm and ~ 15 μm. This suggests that although suspended sediment concentrations in the marginal stream were observed to be high relative to those proglacially, the stream is likely to have contributed only a small proportion of the catchment runoff and sediment load. The distribution of the sample collected from the eastern marginal stream, which flows across extraglacial sediments near to the glacier margin is also different (Figure 5.16 b; Table 5.7); however, the first mode is only very slightly coarser than samples from the western proglacial stream.

Generally, proglacial suspended sediments appear to show some temporal variation characterised by an initial fining and increase in sorting of the first mode during sub-periods 1 to 3, followed by a decrease in sorting and an increase in coarse material during sub-periods 4 to 6 due to the occurrence of the 'second' mode (Figure 5.13; Table 5.6). However, time series plots of size distribution parameters show that suspended sediment particle size is characterised by erratic, hourly-scale variation (Figures 5.14 and 5.15). For moment statistics, such variability may largely be the product of significant variability in the volume of coarse material in transport; however, similar variation also occurs in the first mode. The range of variability in the position of the first mode suggests that sediments entrained by the western marginal stream do not influence suspended sediment size distributions in the western proglacial stream. Instead, the distribution of basal melt out till and sediments obtained from the base of boreholes (Figures 5.16 a and 5.17) suggests that subglacial sediments are the dominant source. Changes in the size distribution of sediments in the western proglacial stream indicated above might therefore reflect the contribution of different sediment sources beneath the glacier, which may yield important information on the mechanisms of basal sediments evacuation.

5.4 TEMPORAL VARIATION IN SUSPENDED SEDIMENT PARTICLE SIZE

5.4.1 Introduction

Temporal variation in suspended sediment size distribution during 1998 (Figures 5.14 and 5.15) is investigated to further constrain the provenance of suspended sediment from the subglacial drainage system. The large number of samples collected very near to the glacier snout and knowledge of the dynamic nature of the glacial and fluvioglacial systems throughout the monitored period is expected to obviate many of the problems encountered by previous studies (see Section 5.1.3); however, three major difficulties remain. Firstly, since the total concentration of suspended sediment in the proglacial stream varies, it would be preferable to analyse variation in the concentration of individual size fractions. However, errors in the sizing of glacial sediments using the Coulter LS230 prevent this, since volume percentage results cannot reliably be converted

into actual weight distributions (Section 5.2.3.3). Secondly, moment statistics may not be reliable indicators of true size variation where samples are polymodal and are unlikely to accurately represent changes in the finer fractions if variation is dominated by changes in the transport of very coarse particles (e.g. due to local variations in entrainment velocity). In such cases, variation in first mode is likely to provide the most reliable results, although statistical methods that utilise information in the whole distribution are also likely to provide potentially powerful forms of analysis. Thirdly, particle size distribution reflects a very complex set of physical processes and the contribution of many and varied sediment sources. The size distribution of samples obtained at the glacier snout represents a complex integration of these factors but also measurement errors (e.g. those arising from moment statistics). With these limitations in mind, temporal variation in suspended sediment size distribution is investigated using a variety of methods that aim to maximise the information that can be obtained from this complex data set.

5.4.2 Relationships between particle size and discharge

5.4.2.1 Introduction

Bulk discharge has been shown to largely control suspended sediment evacuation from the subglacial drainage system (Section 4). However, relationships evolve throughout the melt season, reflecting the evolution of meltwater sources and pathways. Hence, relationships between bulk discharge and various suspended sediment size distribution parameters were investigated for sub-periods of the melt season as defined in Chapter 3. Temporal variation in suspended sediment size distribution is subject to erratic, hourly-scale fluctuations (Figures 5.14 and 5.15) that make relationships between particle size and discharge difficult to identify. As a result, relationships between discharge and size distribution parameters were initially investigated using simple cross-correlation analysis and linear regression on size parameters lagged to their best-match position.

5.4.2.2 Results

Where good relationships exist between discharge and particle size parameters, cross-correlation plots are expected to show moderate to strong sinusoidal patterns with periodicities of ~ 24 h (i.e. one diurnal cycle). Cross-correlation plots for sub-periods 1–

Table 5.8 R^2 values for regression relationships between discharge and particle size parameters lagged to their best-match position. Lag indicated in square brackets; bold type indicates a negative relationship. Only relationships significant at $p < 0.05$ are shown; the significance of the slope of each relationship is given in parenthesis.

	Sub-period (n)					
	1 (88)	2 (117)	3 (79)	4 (243)	5 (215)	6 (225)
Mode$_1$	–	[+4] **0.026** (0.048)	[−12] **0.125** (0.001)	[+2] **0.074** (<0.001)	[−12] 0.103 (<0.001)	[−12] 0.028 (0.007)
Mean	–	–	[+1] **0.061** (0.015)	[−7] **0.034** (0.002)	[−3] **0.182** (<0.001)	[+2] 0.254 (<0.001)
SD	–	–	[+8] **0.059** (0.016)	[+3] 0.131 (<0.001)	[−7] **0.231** (<0.001)	[+2]0.329 (<0.001)
Median	–	[+4] **0.021** (0.064)	[+1] **0.079** (0.006)	[−5] **0.060** (<0.001)	[−3] **0.098** (<0.001)	[+2] 0.196 (<0.001)
d_5	–	[+4] **0.184** (<0.001)	[+1] **0.077** (0.007)	[−5] **0.114** (<0.001)	[+2] **0.266** (<0.001)	[+1] 0.125 (<0.001)
d_{95}	–	–	[+9] **0.062** (0.013)	[+3] 0.070 (<0.001)	[−8] **0.207** (<0.001)	[+2] 0.304 (<0.001)

6 during 1998 (Figure 5.18) show generally weak patterns, the significance of which were investigated using linear regression on discharge versus size distribution parameters lagged to their best-match position (Table 5.8). Particularly weak cross-correlation patterns are evident during sub-periods 1 and 2 (Figure 5.18), although for these sub-periods there is no strong diurnal pattern in the discharge series either (cf. Section 3.2). Significant relationships are not observed during sub-period 1. Generally weak relationships also exist during sub-period 2; however, d_5 is negatively correlated at a best-match position of lag + 4 h and is significant at $p \leq 0.05$. A similar, significant relationship is also evident for median and first mode, suggesting that finer distributions are most prevalent during sub-period 2 at ~ 4 h prior to peak discharge.

The strength of cross-correlation plots generally improves throughout the remaining sub-periods (Figure 5.18), with best-match relationships between discharge and all size parameters being significant at $p \leq 0.05$ (Table 5.8). During sub-period 3, sorting and d_{95} are negatively correlated at best-match positions of lag + 8 and + 9 h, respectively, suggesting distributions are coarsest during periods of falling and low discharge (Table 5.8). For d_5, mean and median, best-match positions occur at a lag of + 1 h and are

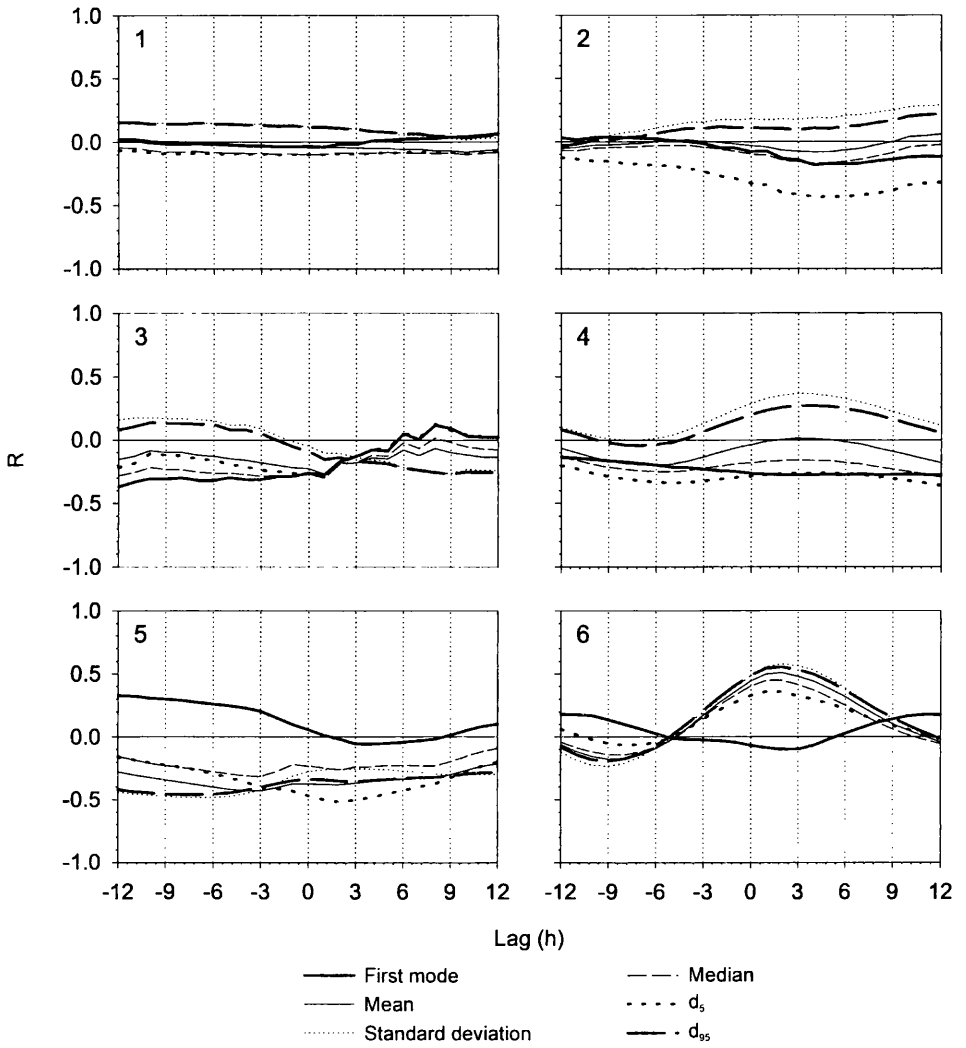

Figure 5.18 Cross-correlation plots between discharge and suspended sediment size distribution parameters.

negatively correlated with discharge, suggesting that fines are most prevalent ~ 1 h before the discharge peak. First mode, however, exhibits negative correlation at a best-match position of lag – 12 h, although the cross-correlation plot is weak (Figure 5.18) and first mode is generally equally negatively correlated at lags of + 1 h to – 12 h.

During sub-period 4, sorting and d_{95} show positive correlation with discharge at best-match positions of lag + 3 h, suggesting the proportion of coarse material is highest on the rising limb (Table 5.8). With the exception of first mode, other variables are negatively correlated at best-match positions of lag – 5 to – 7 h, when relationships

between discharge and both sorting and d_{95} are weakest (Table 5.8; Figure 5.18), suggesting that size distributions are finer during falling discharge. The relationship between discharge and first mode is negatively correlated at a best-match position of lag + 2 h (Table 5.8); nevertheless, the very weak pattern in the cross-correlation plot suggests that it is unlikely to be reliable (Figure 5.18).

Sub-period 5 exhibits relatively high correlations between discharge and particle size parameters (Table 5.8), although cross-correlation patterns are notably weak (Figure 5.18). However, d_5 shows significant negative correlation at a best-match position of lag + 2 h (Table 5.8), suggesting that fines peak some 2 h before discharge. First mode varies in a similar fashion, showing positive correlation at a best-match position of lag – 12 h and thus varying out of phase with discharge (Table 5.8; Figure 5.18); highest negative correlations, indicating the greatest proportion of fines, precede discharge by ~ 3 h (Figure 5.18). Remaining parameters show negative correlation at best-match positions between lag – 3 and – 9 h (Table 5.8), although cross-correlation patterns are weak (Figure 5.18). Patterns during sub-period 6 are very similar to those during sub-period 4 (Table 5.8; Figure 5.18), although relationships between discharge and mean, median, sorting, d_5 and d_{95} are stronger and show closer correspondence to each other, being strongly positively correlated with discharge at a lag of ~ + 2 h. First mode, however, continues to exhibit a weak, out of phase relationship with discharge, and with highest negative correlation again preceding discharge by ~ 3 h (Table 5.8; Figure 5.18).

5.4.2.3 Discussion and interpretation

Cross-correlation plots and regression on lagged size parameters demonstrate changing relationships between suspended sediment size distribution and discharge (Table 5.8; Figure 5.18). Notably, during sub-periods 2, 3 and 5, negative relationships between discharge and d_5 at best-match positions of lag + 1 h to + 4 h suggests fines are 'flushed' from the subglacial drainage system during periods of rising bulk discharge. However, during sub-periods 4 and 6, distributions containing the greatest proportion of fine sediments are found during falling discharge due to positive relationships for d_5 at similar lags. Fines are likely to be flushed in-phase with rising discharge if contributions of supraglacial melt are routed through a predominantly distributed subglacial drainage

system, creating a hydraulic pressure gradient towards pre-existing channels beneath the lower glacier tongue that is in phase with bulk discharge.

Generally, the transport of coarse particles is expected to scale with discharge; however, during sub-period 3, negative correlations for d_{95} and sorting at best-match positions of lag + 8 h and + 9 h indicate the largest proportions of coarse particles during falling discharge. Bank collapse into channelised flowpaths under open flow conditions is likely to provide a broader assemblage of particles as discharge falls that require lower entrainment capacities. Flow in the immature channelised system beneath the lower glacier tongue is certain to occur under largely open conditions following high bulk discharges during sub-period 2 that are likely to have significantly enlarged channelised flowpaths.

During sub-period 4, negative correlations for d_5, median and mean at best-match positions of lag – 5 h to – 7 h suggests a pattern of finer distributions at falling discharges, likely resulting from the winnowing of fines from the distributed system under a diurnally reversing hydraulic gradient. However, the pattern of correlation between discharge and d_5, mean and median closely follows that of discharge and d_{95} (Table 5.8; Figure 5.18). The latter also exhibits the greatest amplitude of variation, suggesting that the proportion of coarse particles might cause bias in d_5, mean and median such that correlations for these parameters are spurious. That distributions are coarser on rising limbs rather than during falling discharge does, however, suggest that coarser particles are more efficiently accessed as discharge rises. This may reflect flow under closed or overpressurised conditions where velocity hysteresis is likely to favour the transport of coarser distributions as discharge rises. This pattern is not evident during sub-period 5 (Table 5.8; Figure 5.18) when flow in channels is expected to occur under largely open conditions (Table 3.6), but is exceptionally strong during sub-period 6 when overpressurised flow conditions are expected to be increasingly frequent (Table 3.6).

That fines precede discharge during sub-period 5 as in sub-period 2 (above) suggests flow conditions are largely open (cf. Table 3.6) and hydraulic gradients within the distributed system remain towards channels up to a few hours before the bulk discharge peak. This may represent meltwaters routed initially through a distributed system, flushing fines in phase with rising discharge, having been contributed through moulins or

crevasses that are poorly connected to the channelised system. Throughout both sub-periods 5 and 6, however, high negative correlations for first mode at ~ + 3 h shows the finest first modes precede peak discharges (Figure 5.18). Although very weak, this pattern suggests that meltwaters may be accessing sediments previously distal to major channels during rising and peak discharge due to the integration of hydraulically efficient flow with larger areas of the bed during periods of overpressurisation.

Although the relationships described above are significant at $p \leq 0.05$, coefficients of determination remain below 0.35 indicating generally high scatter (Table 5.8). Such scatter is due to rapid fluctuations in size distribution parameters evident in the raw series that are most likely to result from rapid changes in the velocity field at the sampling point. Highest correlations occur during sub-period 6 when size distribution parameters show high amplitude variation, which is likely to be due to higher flow velocities being able to entrain coarser particles. The large proportion of coarse particles during sub-periods 4 and 6 also appears to strongly determine variation in other size distribution parameters, resulting in somewhat spurious correlations with discharge.

The generally weak cross-correlation patterns suggest that poor relationships may result from changing relationships between discharge and size distribution parameters within individual sub-periods. Without residual analysis, such underlying trends may not be obvious using linear regression techniques (cf. Chapter 4). Analysis of the residual series from regression relationships generally relies on the calculation of autocorrelation plots, the results of which are likely to be spurious where large gaps in size distribution parameters have been linearly interpolated. Consequently, alternative approaches to the analysis of size distributions are required that are able to isolate and identify subtle trends in size distribution parameters and more accurately characterise size distributions.

5.4.3 Visual identification of temporal trends

5.4.3.1 Introduction

Weak relationships between discharge and particle size parameters are most obviously likely to result from the rapid, short-term fluctuations that dominate the size distribution

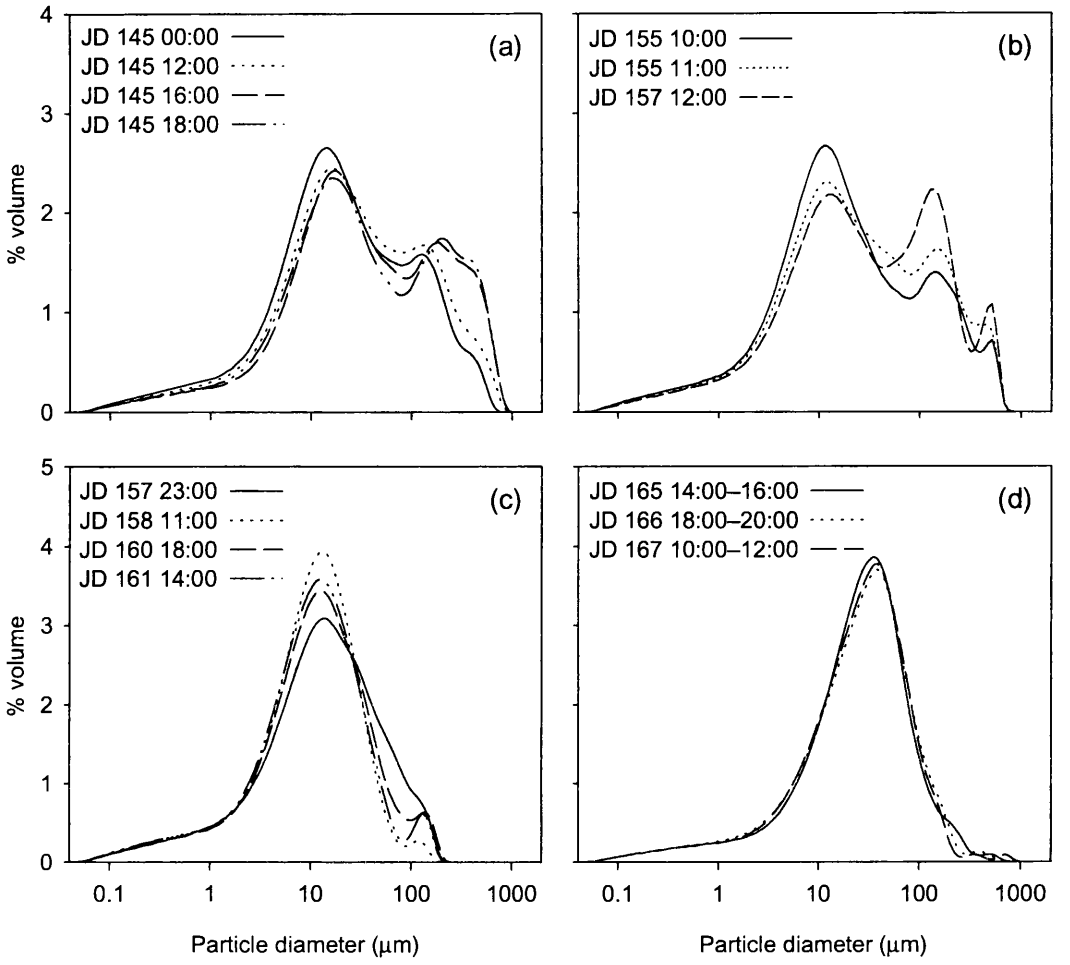

Figure 5.19 Example size distributions (see text for explanation). Some distributions represent combined samples (see Section 5.3.2.1).

series. However, these may also be indicative of changing relationships with discharge or other underlying trends that do not fit well with the hydrologically-based subdivision of the melt season. Here, techniques used to assess and improve the reliability of similar relationships between discharge and suspended sediment concentration (cf. Chapter 4) are difficult to apply due to the number of missing samples, high scatter and potentially large number of unknown variables that are likely to influence size distributions. Hence, a straightforward descriptive summary of variation in suspended sediment size distribution is interpreted against knowledge of the dynamic nature of the glacial and fluvioglacial systems discussed in Chapter 3.

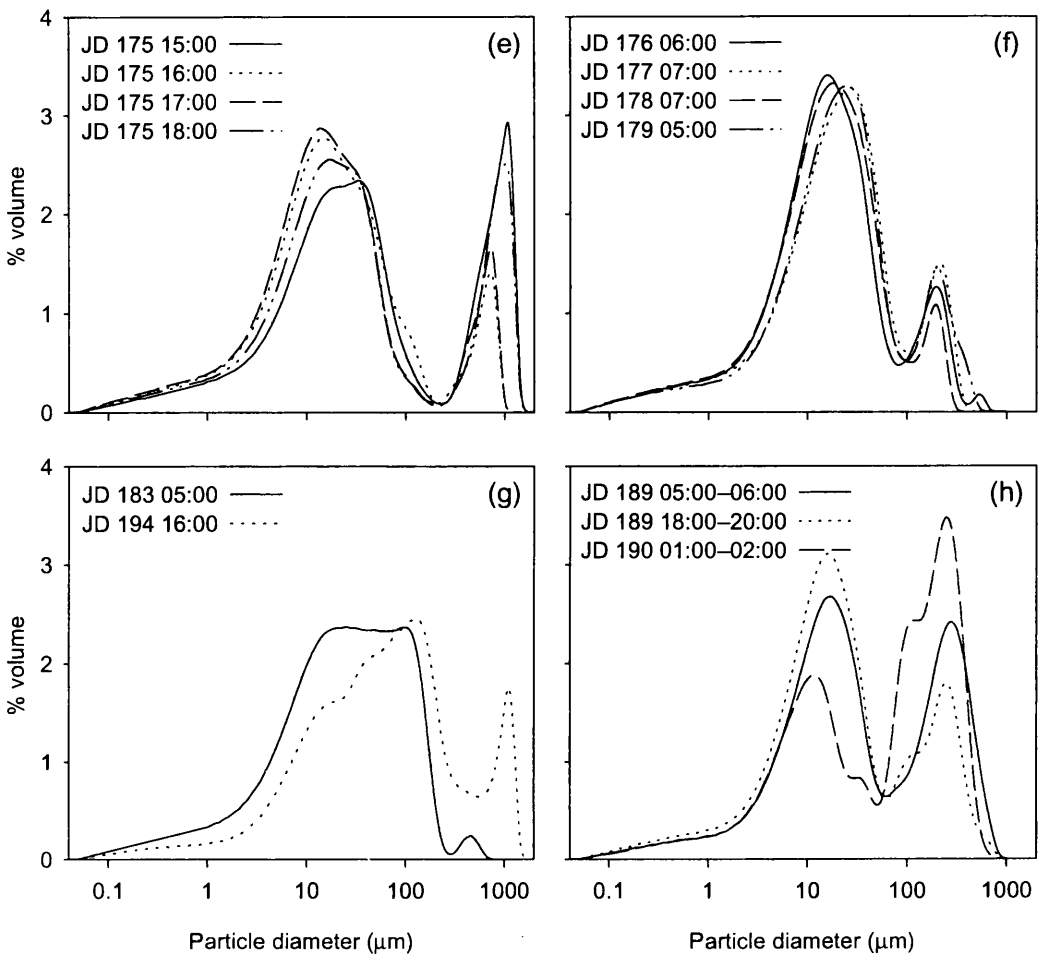

Figure 5.19 *continued.*

5.4.3.2 Sub-periods 1–3

Sub-periods 1–3 represent predominantly distributed subglacial drainage configurations and a rainfall-induced 'spring event' during sub-period 2. During sub-period 1, sample size distributions are relatively coarse (Figures 5.13– 5.15) and poorly sorted. However, despite a few samples on JD 145 that are bimodal with significant second modes at ~ 200 μm (Figure 5.19 a), sample first mode is not particularly coarse compared to values later in the season. Samples become finer towards the end of sub-period 1, noticeably due to a fall in the proportion of coarse material indicated by a decline in d_{95} (Figure 5.15). Over the same sub-period, d_5 also declines, suggesting an increase in the proportion of fines, and the trend of increasing fines continues throughout sub-period 2

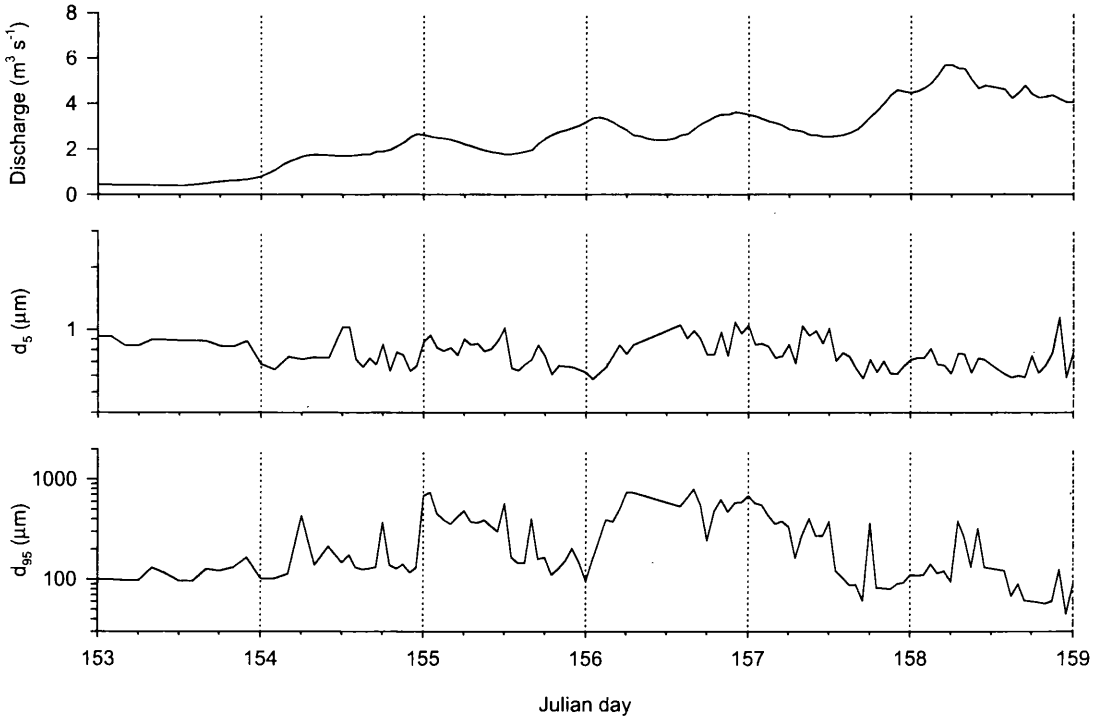

Figure 5.20 Variation in d_5 and d_{95} during the first spring event (sub-period 2).

and into sub-period 3 (Figure 5.15). It is possible that the decline in d_5 values is largely a product of the decline in d_{95}; however, the proportion of coarse material increases rapidly during sub-period 2, with d_{95} values in excess of 500 µm (Figure 5.15), and there is an associated decrease in sorting and an increase in sample median and mean.

Flushing of fines in advance of peak discharge during sub-period 2 is evident on JD 154–156 (Figure 5.20), with coarser, occasionally bimodal distributions during falling discharge (Figure 5.19 b); however, first mode remains relatively stable with no consistent trend throughout sub-periods 2 and 3 (Figure 5.14). Throughout the discharge cycle between JD 156 12:00 and JD 157 12:00, samples remain coarse and fine poor (notably, this cycle was not associated with an increase in suspended sediment concentration; Figure 4.1). However, d_5 and d_{95} decline rapidly as discharge rises on JD 157 (Figure 5.20), with sediments remaining largely fine and unimodal during the event peak. Samples remain relatively fine and unimodal throughout sub-period 3 (Figure 5.13 and 5.19 c), although d_{95} remains variable as a result of occasionally coarser, bimodal distributions during falling discharge.

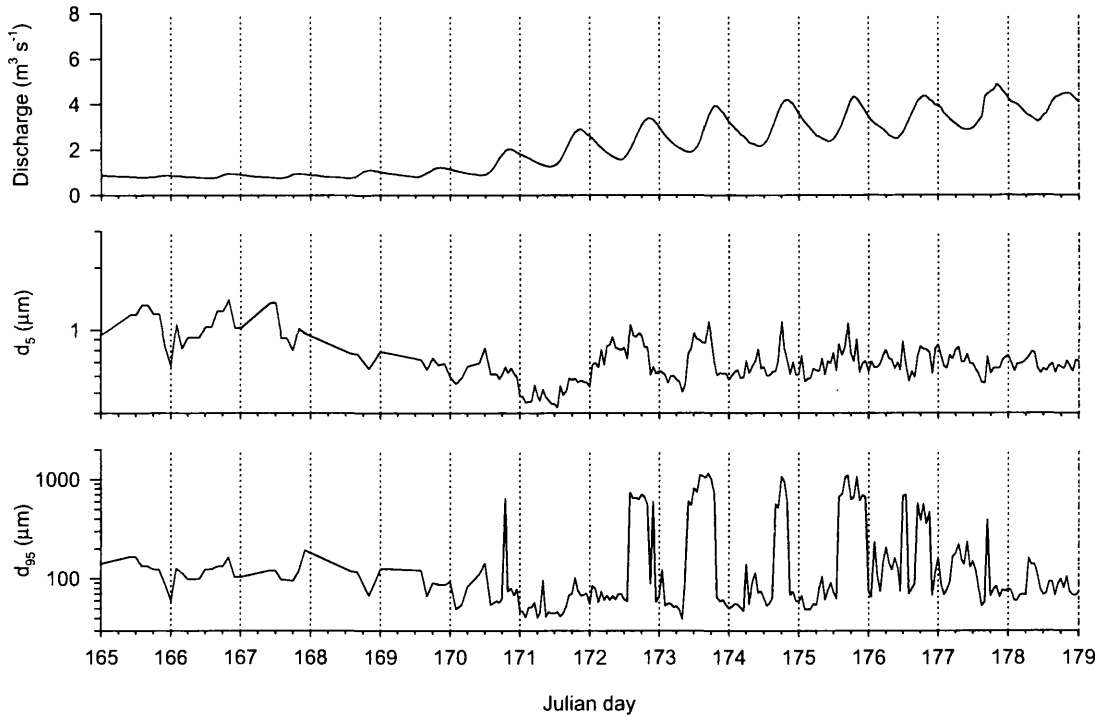

Figure 5.21 Variation in d_5 and d_{95} during sub-period 4.

5.4.3.3 Sub-periods 4–6

Sub-periods 4–6 include the transition from distributed to channelised drainage. Samples at the beginning of sub-period 4 are relatively fine poor, with high d_5 values despite a relatively low proportion of coarse particles (Figure 5.21); first mode is also uncharacteristically coarse (Figures 5.14 and 5.19 d). On JD 167, d_5 and first mode begin to decline rapidly (Figures 5.14 and 5.20), and there are small flushes of fines superimposed on this trend at peak discharges between JD 167–170 (Figure 5.21). Sample d_{95} also declines, and d_5 and mean both reach a seasonal minima on JD 171, suggesting a strong flush of finer sediments immediately following the first significant rise in discharge amplitude since sub-period 3 (Figure 5.21).

The proportion of fines declines rapidly between JD 171–172 (Figure 5.21) and there is a strong coarsening in both first mode (Figure 5.14) and, shortly afterward, d_{95} (Figure 5.21). Similarly, on JDs 173–175, there is a significant reduction in fines and increased transport of coarse particles during rising discharge (Figure 5.20). Around JD 175, the

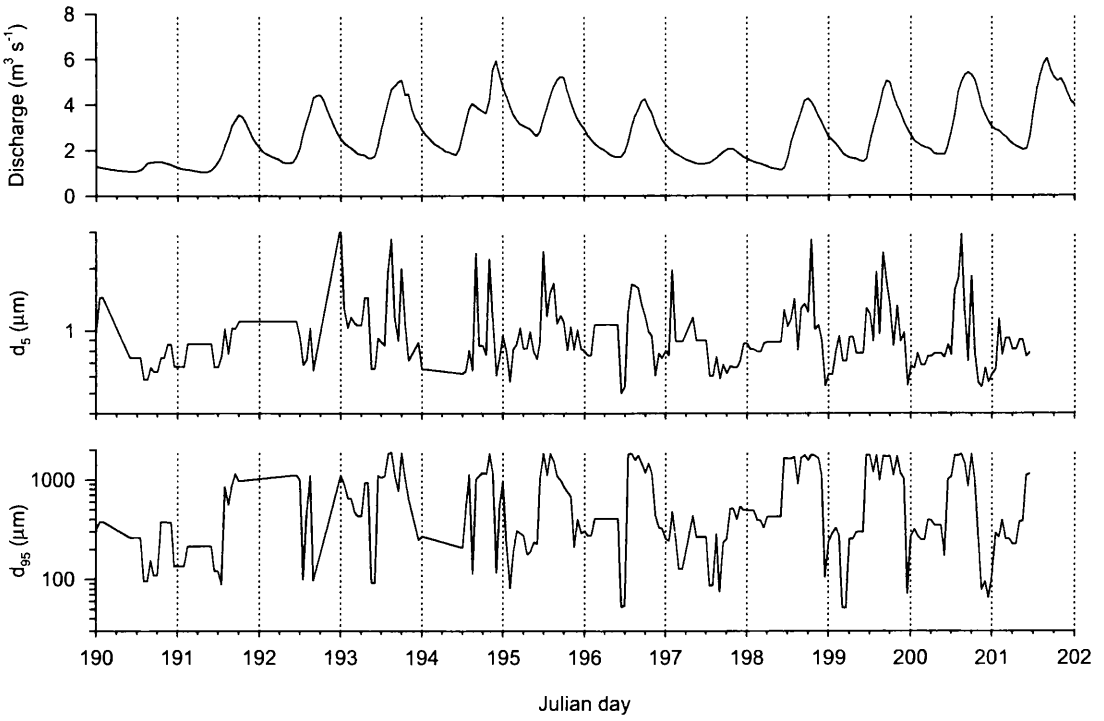

Figure 5.22 Variation in d_5 and d_{95} during sub-period 6.

coarsest distributions are bimodal with a significant proportion of particles greater than 1000 µm (Figure 5.19 e); this mode disappears on the falling limb, but is consistently replaced by another significant second mode at ~ 200–300 µm (Figure 5.19 f). This pattern continues to ~ JD 189, although there appears to be little consistent diurnal variation in particle size parameters (Figures 5.14 and 5.15). Whilst d_{95} exhibits a decline over ~ JD 175–189 (Figure 5.15), first mode exhibits a gradual but consistent coarsening (Figure 5.14). An atypically coarse first mode occurs during rainfall on JD 183 (Figure 5.19 g).

During the brief period of very low discharge on JD 189 and 190 that marks the boundary between sub-periods 5 and 6, distributions become consistently coarse once more, with d_5 values akin to those at the start of sub-period 4 and d_{95} in the region of 200 µm (Figure 5.15). Samples are also bimodal, with a significant second mode at ~ 200–300 µm (Figure 5.19 h). Distributions fine again as discharge recovers (Figure 5.15); however, the remainder of sub-period 6 is subject to rapid diurnal variations in all size parameters with the exception of first mode (Figures 5.14 and 5.15). Samples during

periods of rising discharge are bimodal, with a significant second mode in the 1000–2000 μm range, and d_{95} tends to be very high (Figure 5.22). d_5 varies consistantly with d_{95} (Figure 5.22), suggesting that it is largely influenced by the large volume of coarse material in transport. However, unusually low d_5 values, indicating short-lived flushes of very fine sediment, occur between 2 and 6 h after peak discharge on JD 198, 199 and 200 (Figure 5.22). The values are coupled with minima in the d_{95} series, but are very low with respect to d_5 values throughout the season as a whole (Figure 5.15). Throughout the same period, first mode shows little correspondence with discharge and exhibits a gradual decline (Figure 5.14), although a large shift in mode occurs on JD 194 during rainfall (Figure 5.19 g).

5.4.3.4 Discussion and interpretation

Periods of predominantly distributed drainage with negligible contributions from surface melt, such as sub-period 1 and the beginning of sub-period 4, exhibit generally fine-poor distributions (Figures 5.14 and 5.15). A similar pattern is evident around JD 190 (Figures 5.14 and 5.15), when a channelised system is certain to exist but low rates of supraglacial melting mean most runoff is contributed through the distributed system by basal melt and long-residence time meltwaters. This suggests that the majority of sediments evacuated during from the distributed system may be entrained within pre-existing or established channels. During periods of distributed drainage, melt is driven towards channels where flows will have greater capacity for entraining sediments, and are likely to rework sediments deposited during previous high-flow events. It is possible that sediments in pre-existing channels are fine poor since coarser sediments will have been preferentially deposited during the falling stage of previous events whilst fines remain in transport (cf. Bogen, 1981). Most sediment during periods of distributed drainage where supraglacial meltwater inputs are negligible may be entrained by flow through channels. The distributed system may therefore be much less efficient at evacuating basal sediments than the study of proglacial sediment transport suggests.

Distributions become noticeably finer during periods of predominantly distributed drainage prior to each of the spring events and at least a few days before the characteristic rapid increase in proglacial discharge (Figures 5.14 and 5.15). During sub-

period 4, this fining was initially associated with small flushes of fines at peak discharge (Figure 5.21), and occurs simultaneously with the decline in electrical conductivity (Figure 3.14). This suggests the increasing evacuation of fines from the distributed system, most likely due to flow through the system having been substantially increased. It is likely that small supraglacial meltwater inputs to the glacier bed occur at least a few days before each spring event that are not sufficient to promote spatially extreme high basal water pressures. Analysis of proglacial hydrograph form and electrical conductivity during sub-period 4 suggests that supraglacial melt accesses the basal drainage system after JD 165 (Chapter 3; Table 3.6). These inputs are likely to locally strengthen the hydraulic gradient between the distributed system and low-pressure channels, resulting in increased flow velocities towards channels and the increased evacuation of fines in phase with discharge.

In-phase flushing of fines also occurs during the first spring event as indicated by cross-correlation analysis of relationships between discharge and size distribution parameters (Section 5.4.2.3). Drainage likely remained predominantly distributed throughout the first event, with the possibility of substantial channelisation only as the event ended on JDs 158 and 159 (Table 3.6). However, there is no in-phase fining on the discharge cycle between JD 156 and 157 (Figure 5.20) when there is no diurnal peak in suspended sediment concentrations either (Figure 4.1). It is possible that both low proportions of fines and the absence of a suspended sediment peak reflect the exhaustion of entrainable sediments within the distributed system. Peak discharges over JD 156–157 only slightly exceed those on 155 (Figure 5.20), suggesting the area of the distributed system subject to increased flow remained stable and meltwaters were unable to access new areas of the glacier bed.

Coarser, bimodal distributions during the first spring event and within periods of declining discharge are likely to be accessed in the pre-existing channelised system, possibly as a result of bank collapse associated with falling stage under predominantly open flow conditions (cf. Section 5.4.3.2). Relatively fine distributions at the peak of the event (Figure 5.20) when channelisation is likely are difficult to interpret, since channelisation should result in higher flow velocities that enable a wider range of particle sizes to be entrained. However, it is possible that channelisation was confined to

PDAs where basal sediments appear to be finer than elsewhere (Section 5.3.3.2). Generally fine size distributions during sub-period 3 may result from the continued winnowing of fines by flow through the distributed network (Figures 5.14, 5.15 and 5.19 d). However, coarser bimodal distributions that are likely to reflect bank collapse are again evident during falling discharge (cf. Figure 5.19 b). The proportion of fines eventually declines significantly between JD 163 and 165 as discharge recedes due to a rapid decrease in surface melt (Figures 5.14 and 5.15).

During the second spring event, the absence of the flushing of fines in-phase with discharge is likely to be masked by variation due to rapid channelisation. However, following exhaustion during the first event, a flush of fines on JD 171 (Figure 5.21) during the period of high vertical ice motion (Figure 3.11) suggests an expansion in the area of the distributed system subject to increased flow velocities due to supraglacial meltwater inputs. Uplift is negligible after JD 171–172 (Figure 3.11) and the proportion of fines falls rapidly (Figure 5.21). Instead, size variation appears to be dominated by the transport of coarser particles during periods of rising discharge (Figure 5.21). High flow velocities under closed flow conditions (Table 3.6) are likely to be responsible for transporting a greater proportion of coarse material than hitherto possible that is accessed from the floor of pre-existing or incipient conduits. Strong velocity hysteresis under closed flow conditions is likely to further concentrate the transport of coarse materials to the rising stage of the hydrograph.

Very coarse distributions during periods of rising discharge gradually disappear after JD 175 (Figure 5.21) and distributions indicative of bank collapse are again evident (Figure 5.19 f). This pattern is consistent with channels becoming increasingly subject to open flow conditions (Table 3.6), possibly including a slight decrease in net flow velocity within arterial channels and a reduced velocity hysteresis effect, leading to coarser sediments being stored within the drainage system. Fines also gradually decrease during this period, as indicated by d_5 and first mode (Figure 5.13, 5.15 and 5.21), suggesting that the majority of flow is concentrated within channels that have limited access to fine sediments. However, cross-correlation analysis still identified the in-phase flushing of fines with discharge (Section 5.4.2.3), suggesting a number of moulins may still be unconnected to the channelised system.

The proportion of fines increases once more towards the end of the monitored period when overpressurised, closed flow conditions are again believed to exist. First mode, and to a certain extent d_5, begin to decline after ~ JD 185 (Figure 5.14 and 5.15), roughly coinciding with the transition to high-peaked hydrograph forms (Section 3.3.3). From JD 190, the pattern of particle size is dominated by variation in the coarse component once again, but significant flushes of fines are commonly observed during periods of falling discharge (Figure 5.22). Such a pattern is indicative of high velocities through an overpressurised channel system during rising and peak discharge that are responsible for mobilising coarse sediments from channel floors, high velocity hysteresis between rising and falling discharge periods, and a strong diurnally reversing hydraulic gradient responsible for the winnowing of fines from basal sediments as bulk discharge declines.

The winnowing of fines is likely to play only a minor role in increasing sediment availability. Cross-correlation analysis (Section 5.4.2.3) has shown the position of the first mode to vary out-of-phase with discharge during sub-period 6, suggesting winnowing evident in position of the d_5 percentile contributes only the very finest sediments that comprise a very small percentage of the proglacial suspended sediment load. Coarser sediments are likely to remain in channels to be evacuated by higher flow velocities during overpressurisation later in the season, but a mechanism must exist by which increasingly complete size distributions are delivered to the channelised system as the season progresses. Finer first modes at peak discharge suggest increasingly widespread local basal separation, enabling hydraulically efficient flows to access sediments previously distal to channels. However, evidence of the enhanced deformation of sediments towards channels during falling discharge is likely to be masked by low sediment transport capacities due to high velocity hysteresis. Hence, only the finest sediments are likely to be transported to the snout during falling discharge whilst coarser particles remain in channels to be entrained by higher velocity flows during the next rise in discharge.

5.4.4 Multivariate particle size analysis

5.4.4.1 Introduction

Previous analyses have simplified the form of suspended sediment size distributions using moment statistics; however, these parameters demonstrate a high degree of scatter, a large proportion of which may arise from the problems associated with moment statistics and their inappropriateness where samples are polymodal. Furthermore, Section 5.4.3 suggested that distinctive modes in addition to the normally prevalent first mode occur at certain times during the season that may have process significance. Large numbers of distributions cannot be classified qualitatively, therefore statistical techniques that use the whole sample distribution must be developed. These multivariate techniques should provide a more reliable, objective and quantitative basis for the identification and classification of size distribution types.

5.4.4.2 Method and results

Multivariate techniques identical to those applied in Section 3.3 for the classification of proglacial stream hydrographs are used to classify suspended sediment size distributions. Hydrograph classification employed a three-stage procedure that dealt separately with hydrograph shape and magnitude before combining the two into a single, composite index of hydrograph types. For suspended sediment particle size, the form of each distribution is presented as percentage volume by size-fraction, and therefore classification of distribution magnitude is not required.

Principal Component Analysis (PCA) was used to reduce the dimensionality of the data set before using Hierarchical Cluster Analysis (HCA) to cluster individual samples based on their Principal Component (PC) scores. PCA was performed on a matrix of 880 rows of samples (cases) and 116 columns of particle size data (variables); the latter representing the 116-fraction percentage volume output for each sample obtained using the LS230. PCs can be extracted from both the so-called *covariance* and *correlation* matrices of the given variables, the former being suitable where values are measured in the same units (Joliffe, 1984) and was therefore employed in Section 3.3. Where variables are in different units, the highest-variance variables will dominate the first few

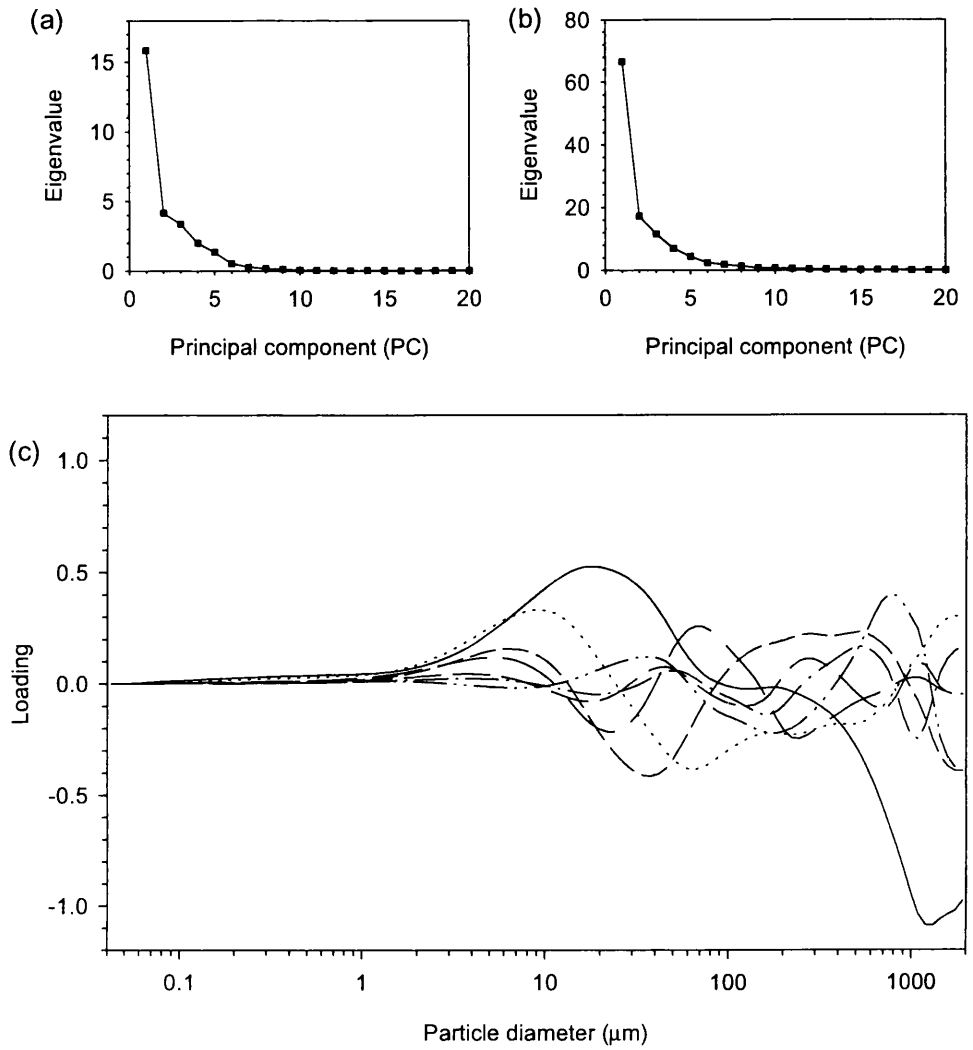

Figure 5.23 Scree plot of eigenvalues for PCs extracted from (a) covariance matrix and (b) correlation matrices. (c) loadings plot for PCs extracted from the covariance matrix (first PC indicated by the solid line).

PCs; using the correlation matrix, variables are standardised such that all variables are given equal weight (Joliffe, 1984). Here, HCA was performed on sample PC scores from both techniques, since it was unclear how very high variability in the coarsest fractions would affect the clustering result.

Figure 5.23 (a) and (b) shows the scree-plot of eigenvalues and cumulative percentage variance explained for PCs extracted from both the covariance and correlation matrices. Scree-plots are usually employed to select an appropriate number of PCs for further

analysis based on where the continuous drop in PC eigenvalues begins to level off (Cattell, 1996; cf. Section 3.3.2.1); however, the so-called 'cutoff' is unclear in each of the figures and therefore standard statistical retention criteria were employed (SPSS software, Version 11). Seven PCs were retained using the covariance matrix, explaining 98.0 % of the total variation in the original data set, and eight PCs using the correlation matrix, explaining 96.7 %. The high number of significant PCs indicates complex variation in the size distribution data set. A loadings plot for PCs extracted using the covariance matrix (Figure 5.23 c) shows the first PC to be strongly influenced by the prevalent first mode between 5–50 μm and occasionally dominant second mode between 500–2000 μm. Subsequent PCs vary in a complicated manner and are difficult to interpret.

HCA using Euclidean (geometric) distances was performed on sample PC scores separately for both sets of PCs. The aim of the clustering processes was to obtain a vertical icicle plot from which an interpretable number of clusters could be identified. Only Ward's linkage rule (Ward, 1963) succeeded in producing an ordered and easily interpretable plot, with other methods (including the more common average and complete linkage methods) producing 'stringy' plots with many outliers and few distinct clusters (Figure 5.24). Ward's method joins individual cases and clusters by merging those resulting in the smallest increase in the sum of squares between each case in the cluster and the cluster centre. Ward's method is unlikely to be robust with respect to outliers (e.g. samples having large relative distances) and is biased towards creating clusters of equal size (SAS Institute, 1990; Mojena, 1998). Nevertheless, the method appeared to perform well for both sets of PC scores, producing ordered icicle plots that did not appear overly biased towards clusters of equal size (Figure 5.25).

For the icicle plot of PC scores obtained from the correlation matrix, a cutoff point at a linkage distance of ~ 35 on the vertical axis was selected for initial analysis, retaining 6 clusters (Figure 5.25 a). Since they are joined last, the icicle plot indicates large differences between the shape of distributions in cluster 1 and clusters 2–6. However, overlaying samples for each cluster demonstrated that clusters 1 and 2 are in fact very similar, and visually appear far similar in terms of distribution shape than, for example, clusters 2 and 6 (Figure 5.26). In addition to this, high within-cluster variability was evident for the majority of clusters, suggesting that clustering of PC scores from the

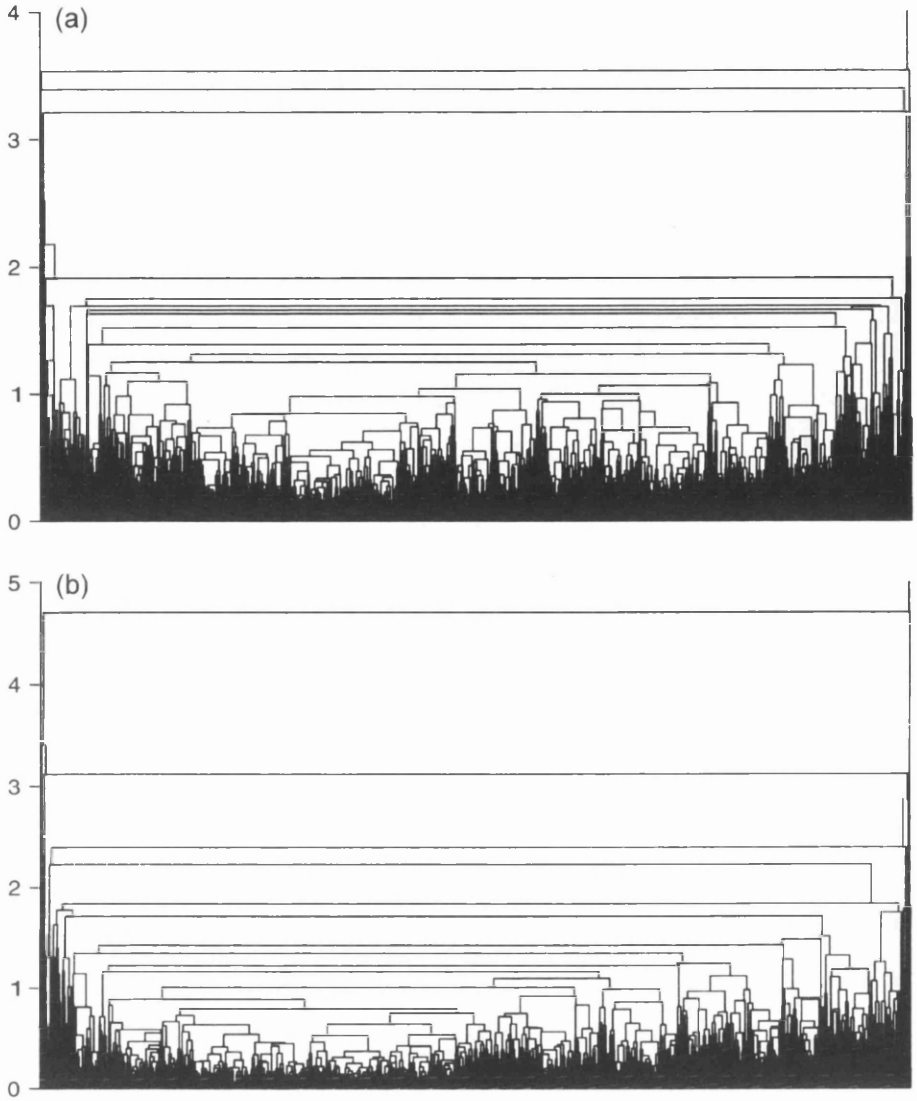

Figure 5.24 Clustering of PCs obtained from the (a) correlation and (b) covariance matrices using the average linkage rule (cf. Figure 3.6).

correlation matrix is not good at discriminating distribution shape. This probably results from standardisation of the variables causing the principal features of the distributions to assume low importance relative to subtle changes below 1 μm that are more likely to result from measurement error.

Clustering of PC scores obtained from the covariance matrix appeared to perform significantly better. Selecting a cutoff point at a distance of 25 along the vertical axis retained 9 clusters (Figure 5.25 b). The icicle plot reveals the size distributions to be

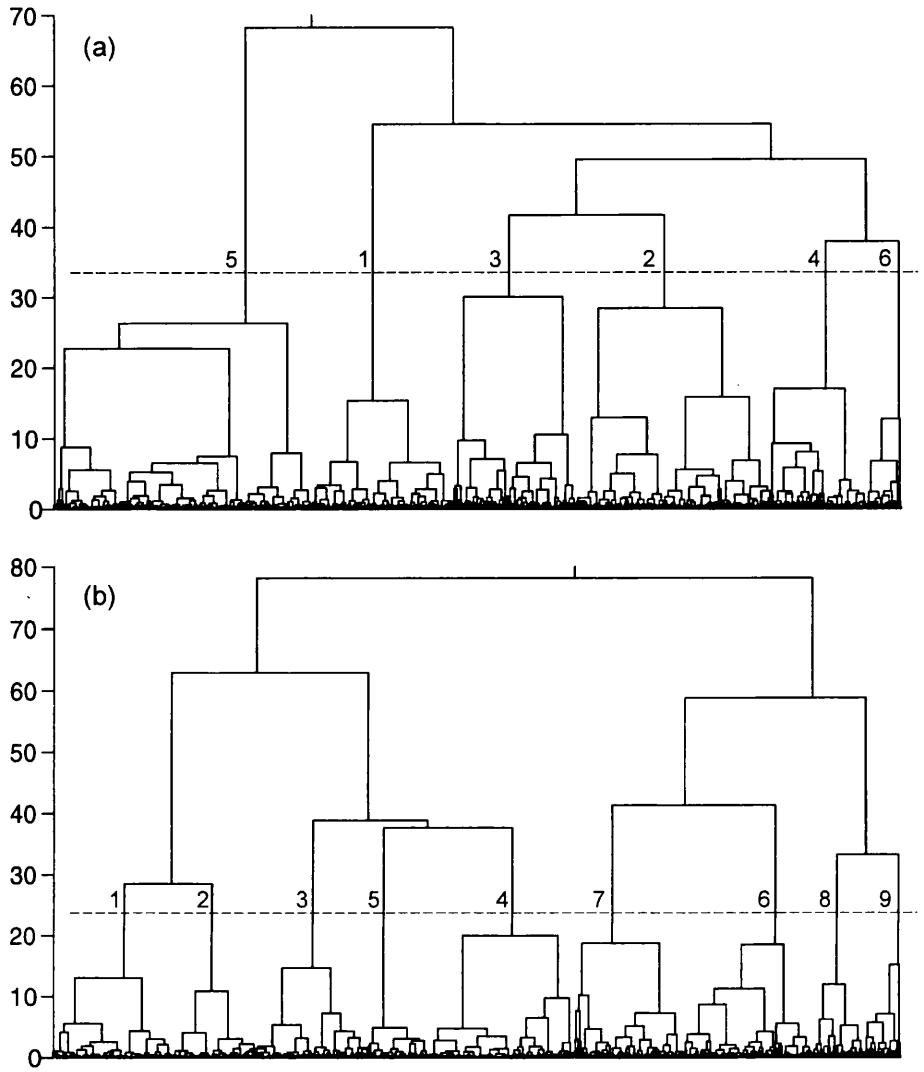

Figure 5.25 Clustering of PCs obtained from the (a) correlation and (b) covariance matrices using Ward's linkage rule. The cutoff and retained clusters are also indicated.

composed of two principal groups (Figures 5.25 b and 5.27): A) clusters 1–5, having a single mode in the 5–50 μm ranges; and B) clusters 6–9, with a significant second mode ranging from ~ 200–2000 μm. Size distributions in Group A generally show low-levels of within cluster variability and suggest the technique is very sensitive to subtle changes in distribution shape and particularly the position of the first mode. Clusters 1 and 2 contain fine, well-sorted distributions with a mean mode of 13.5 and 18.9 μm, respectively. Cluster 3 exhibits a shift in mean mode to 28.0 μm, with a negligible decrease in sorting. Clusters 4 and 5 exhibit almost identical mean modes to clusters 1

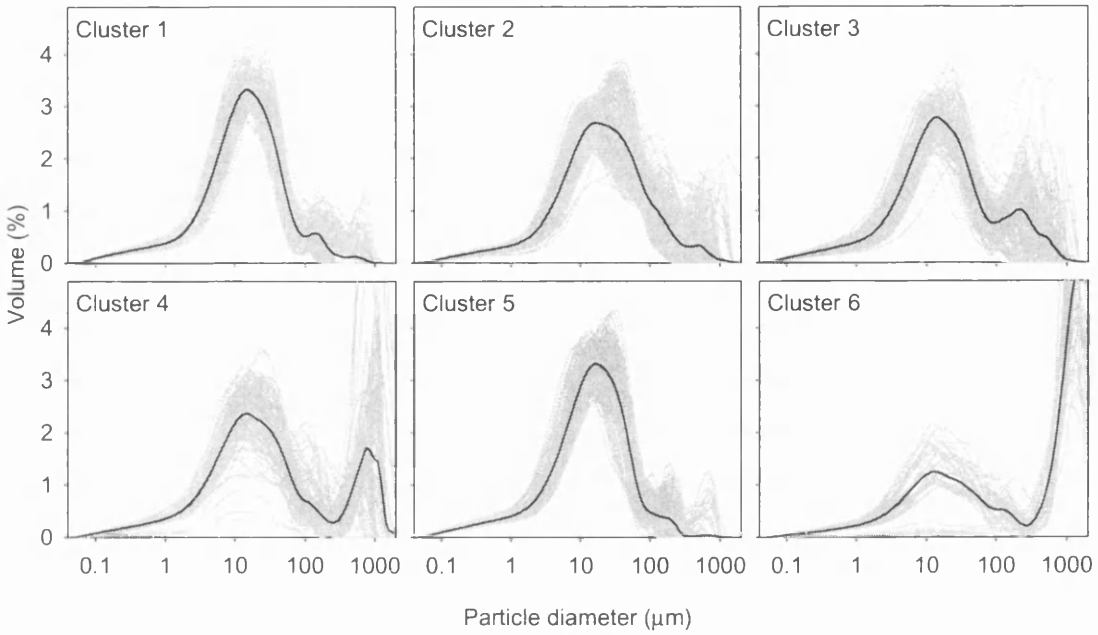

Figure 5.26 Size distributions for samples in clusters 1–6 obtained using Ward's linkage rule on PCs extracted from the correlation matrix (see Figure 5.25 a). The thick black line indicates the cluster mean size distribution.

and 2, respectively, but demonstrate a progressively higher proportion of material coarser than the mode.

High within-cluster variability, however, occurs within group B (Clusters 6–9; Figure 5.27). This appears to be largely due to: 1) occasionally large changes in the form of the lower magnitude mode, since distributions appear to have been clustered principally on the position of the highest magnitude mode; and 2) variation in the relative magnitude of the principal modes, despite a general trend showing the second mode to predominate as it becomes coarser. From (1), it follows that clusters 6–9 do not reliably demonstrate changes in the position of the first mode (Figure 5.27). In addition to this, less common distributions cluster poorly, suggesting that the technique does not in fact cope well with a small number of very different samples (or outliers). For example, occasional samples have more than two principal modes, and the unusual distributions during rainfall noted in Section 5.3 are included in cluster 8 rather than clustering separately (Figure 5.27). Nevertheless, cluster 6 (Figure 5.27) is characteristic of size distributions observed in

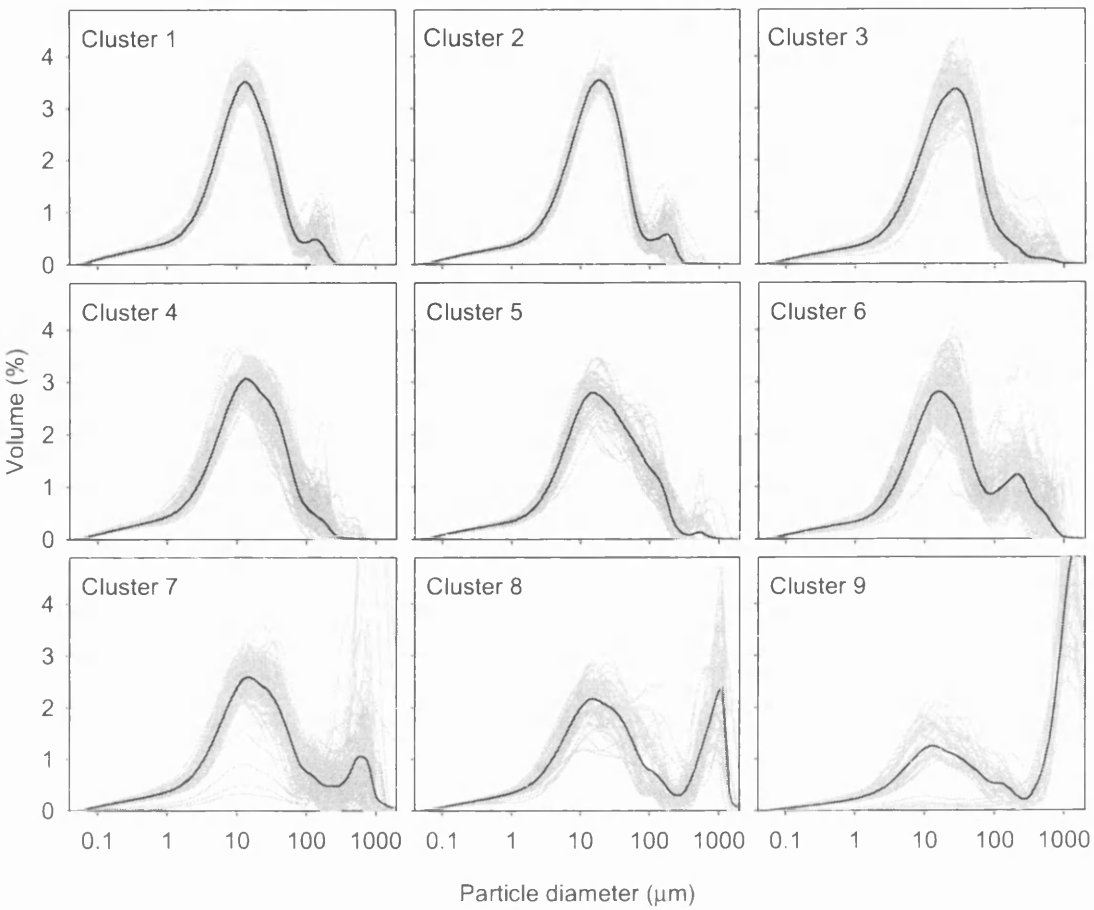

Figure 5.27 Size distributions for samples in clusters 1–9 obtained using Ward's linkage rule on PCs extracted from the covariance matrix (see Figure 5.25 b). The thick black line indicates the cluster mean size distribution.

Section 5.4.3 on the falling limbs of hydrographs that are suggested to arise from bank-collapse under open-channel flow.

These results suggest very complex variation in the size distribution dataset, resulting in many small clusters from generally more robust HCA techniques such as the average linkage method (Hannah et. al., 2000). Ward's method, using PCs extracted from the covariance matrix, produces the most easily interpretable icicle plot (Figure 5.25), but the underlying complexities of the size distribution data remain. Few new features of the data set have been identified; nevertheless, the technique identifies and discriminates between principal size distributions with relative accuracy, and temporal sequencing of

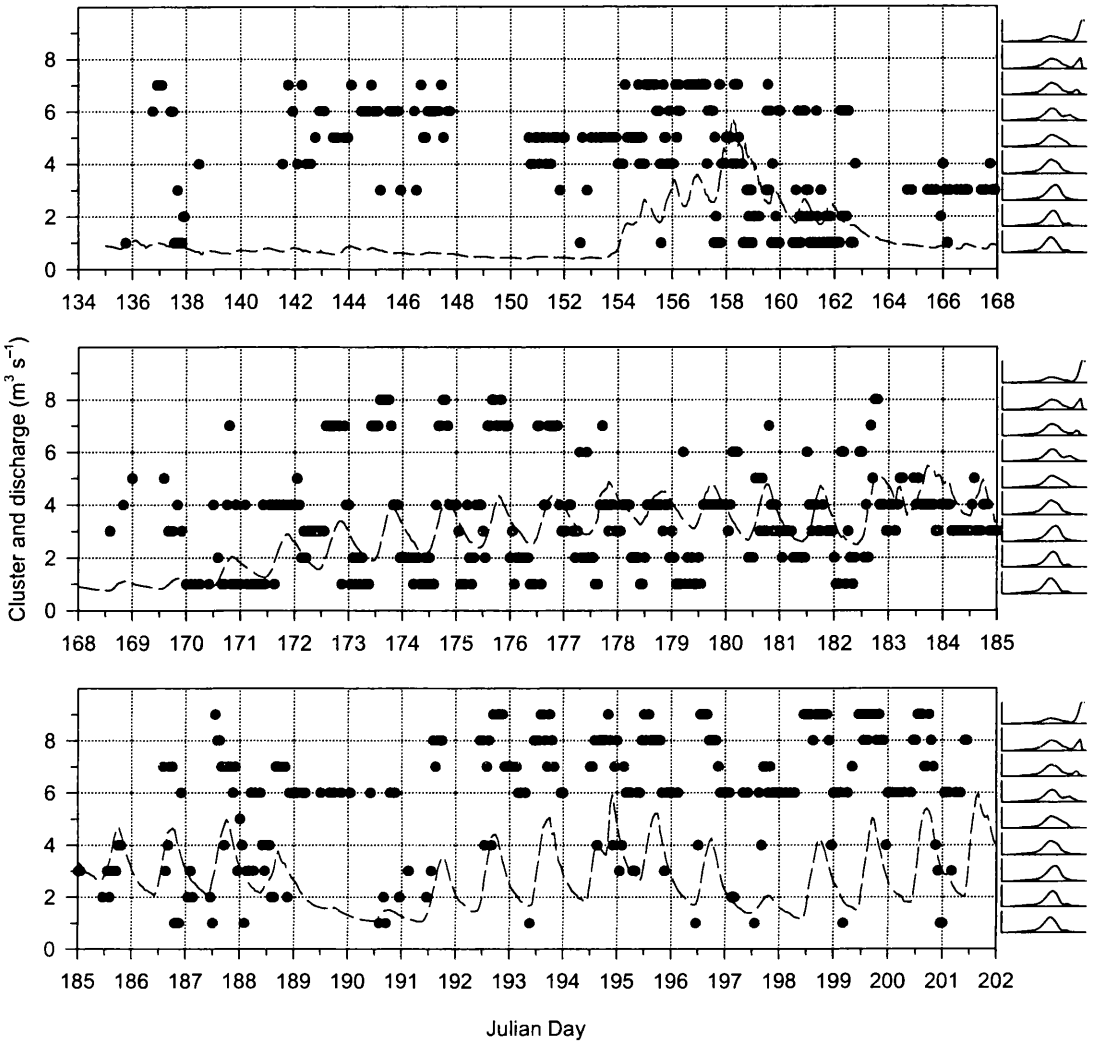

Figure 5.28 Temporal sequenced clusters obtained using Ward's linkage rule on PCs extracted from the covariance matrix (see Figures 5.25 b and 5.27). Cluster mean size distributions are shown on the right; discharge is included for reference.

distribution types can be used as a basis for a refined interpretation of temporal variation in particle size.

5.4.4.3 Temporal sequencing of distribution types

Temporal variation of size distribution type (Figure 5.28) shows patterns in distribution type that are difficult to reliably classify due to: 1) the complexity of distribution types in each cluster; 2) inadequacies in the clustering technique when dealing with outliers; and 3) a limited understanding of how distribution types relate to each other (for example, do

size distributions in cluster 4 (Figure 5.27) result from a combination of separate size distributions typified by clusters 1 and 3, or do they represent a unique sediment source?). However, the general pattern in size distribution type (Figure 5.28) is consistent with visual interpretation of temporal variation in size distribution parameters.

During sub-period 1, samples are relatively coarse and commonly bimodal, characterised by clusters 5-7, although clusters 4 and 5 predominate towards the end of the sub-period, reflecting a fining that is mainly due to a fall in the coarse component (Figure 5.28). At the beginning of sub-period 2, distributions tend strongly towards cluster 4 during rising discharge, with coarser, bimodal distributions predominating (cluster 7) during falling discharge. Coarser distributions persist during the diurnal discharge cycle of JD 156-157, before appearing to fine significantly from cluster 7 to cluster 1 during the peak of the event (Figure 5.28). Following the event, cluster 1 (the very finest cluster; Figure 5.27) predominates, especially at low discharge, and cluster 6, with a second mode suggestive of bank collapse (Section 5.3), occurs predominantly during falling discharges.

Samples exhibit a lack of coarse material and a very coarse first mode (cluster 3) at the beginning of sub-period 4 (Figure 5.28). However, there is evidence of fining (cluster 1) during JD 170-171.5, followed by coarsening of the first mode from cluster 4 to cluster 3 from JD 171.5 to 172 (Figure 5.28). Following this, coarse, bimodal samples (clusters 7 and 8) occur during rising and peak discharge, with progressively finer distributions as discharge falls (Figure 5.28). Coarse, bimodal clusters gradually become less common after JD 175, but the distinctive second mode at 200-300 μm (indicated by cluster 6) is actually observed to occur only three times between JD 175 and 180 (Figure 5.28). From JD 177, coarser unimodal distributions (cluster 4) occur during peak discharges.

The pattern between JD 179 and 182 is unclear; however, during a period of rainfall and low discharge amplitude from JD 182-184, distributions are unimodal and consistently coarse (clusters 3 and 4; Figure 5.28), a feature not readily evident from temporal plots of size parameters (Figures 5.14 and 5.15). Following this, as discharge amplitudes increase rapidly, coarse, bimodal distributions (cluster 7; Figure 5.28) are again evident at rising and peak discharge, with cluster 6 increasingly typifying distributions on falling

hydrograph limbs (Figure 5.28). As discharge declines rapidly between sub-periods 5 and 6, cluster 6 accounts for almost all sample size distributions, until discharge begins to increase rapidly once more on JD 191. From JD 192 to 201, discharge amplitudes are typically high, demonstrating increasingly coarse, bimodal distributions at rising and peak discharge (clusters 7 and 8) with cluster 6 predominating during falling limbs (Figure 5.28). Again, cluster 6 also predominates during a brief period of low discharge on JD 197-198. Fine, unimodal distributions are noticeably absent later in the monitored period; however, a number are found between JD 192 and 201 at times very close to minimum discharge.

5.4.4.4 Discussion and conclusions

Temporal sequencing of distribution forms generally confirms the patterns observed in Section 5.3. In particular, it highlights the increasing prevalence of the second mode towards the end of the season associated with greater discharge amplitudes, higher flow velocities and higher velocity hysteresis (Figure 5.28). Few very fine distributions appear to occur later in the season due to the occurrence of a significant second mode at most stages of the hydrograph, even at low discharges (Figure 5.28). This results in most distributions, irrespective of the form of their first mode, clustering in clusters 6-9 (Figure 5.27). This pattern is likely to result from generally higher flow velocities through an efficient channelised drainage system and an associated increase in sediment transport capacity across the diurnal cycle later in the season.

However, a number of other potentially important features are also highlighted. Firstly, cluster 6 is more prevalent during periods of low and falling discharge than previously identified (Figure 5.28), particularly during sub-periods 5 and 6 (JD 179 onwards) when flow conditions during these parts of the hydrograph are expected to be predominantly open (Table 3.6). Few distributions of type 6 occur during JD 175–182 (Figure 5.28) since flow conditions are likely to be closed (Table 3.6), although it is likely that some distributions with relatively small second modes in the 200–300 μm range have been classified into different clusters (Figure 5.27).

Secondly, there are distinct differences between periods of low discharge earlier in the season when drainage is predominantly distributed (JD 135–153 and 164–169; Figure 5.28). Here, size parameters show that samples are typically coarse relative to other times of the season, but this results from different distribution types (Figure 5.28). During sub-period 1, distributions are often bimodal, with cluster 6 being particularly prevalent, whereas during the beginning of sub-period 4, distributions are tightly unimodal but have a coarse first mode characterised by cluster 3 (Figure 5.28). During sub-period 1, it is likely that coarser sediments entrained from channel floors are supplemented by fines being slowly winnowed from the distributed system. After the evacuation of fine sediments during sub-period 3 following the spring event, very coarse unimodal distributions at the beginning of sub-period 4 (Figure 5.28) may result from the exhaustion of coarser sediments from the floors of pre-existing channels and of fines from the distributed system. Distributions may therefore represent coarser sediments just within the entrainment capacity of the distributed system rather than sediments entrained from channel floors. Prior to the second spring event, these distributions fine (Figure 5.28) due to surface meltwater beginning to access the distributed system in areas further upglacier where finer sediments have not been exhausted.

A similar pattern of coarse, unimodal distributions of cluster types 3 and 4 are observed during the period of rainfall on JD 182–184 (Figure 5.28). This period is characterised by high but low amplitude discharge, suggesting that the absence of fines may be related to the weak functioning of the diurnally reversing hydraulic gradient.

5.5 SUMMARY

This chapter has investigated the provenance of suspended sediment from the subglacial drainage system using bulk suspended sediment particle size properties. Previous studies have had difficulties relating variations in suspended sediment particle size to the mechanisms responsible for suspended sediment evacuation due to generally small sample numbers, weak interpretative procedures, and/or poor knowledge of the nature of the subglacial drainage system and likely catchment sediment sources. In addition, studies have failed to take independent measurements that might indicate the dynamic

nature of the glacial and fluvioglacial systems and, despite an appreciation of the complexity of factors that influence suspended sediment size, have not monitored suspended close to the subglacial portal.

In this study, a large number of samples have been utilised that were collected near to the glacier snout. The character and seasonal variability of suspended sediment size distributions have been investigated and compared with distributions from likely catchment sediment sources. This has revealed patterns in suspended sediment size distribution that are unlikely to reflect measurement or analysis error and are consistent with changes in the nature of the glacial and fluvioglacial systems (Chapter 3) and with suspended sediment transport (Chapter 4).

During periods of distributed drainage, changes in suspended sediment particle size typically demonstrate the flushing of fines in-phase with discharge that probably represents contributions of surface melt to areas of the bed that are poorly connected with the pre-existing or expanding channelised system (Section 5.4.2). This pattern is also evident during sub-period 5, where many moulins are expected to remain poorly connected to the channelised system and flow in channels is expected to be predominantly open (Table 3.6), resulting in a strengthening of the hydraulic gradient towards pre-existing channels during periods of rising surface melt. The exception to this pattern is sub-period 1, during which surface meltwater inputs are absent. Here, size distributions appear to reflect (fine) contributions from the distributed system but also coarser sediments (Figure 5.28), suggesting that the reworking of coarser sediments from the floors of pre-existing channels strongly influences suspended sediment size distributions and concentrations early in the meltseason.

Following the first spring event, surface meltwater inputs fall but fine size distributions still suggest that the distributed system is the predominant source of suspended sediment. However, distributions believed to arise from channel bank collapse also occur due to predominantly open flow conditions (Figure 5.28). Towards the end of sub-period 3 and during the beginning of sub-period 4, coarser, unimodal size distributions (Figure 5.28) probably reflect the exhaustion of fine sediments from the distributed system and very low discharges unable to entrain coarse sediments from channel floors.

Sub-period 4 shows complex variation in suspended sediment size distribution due to an increase in surface meltwater inputs to the distributed system followed by the establishment of the channelised drainage system (Figure 5.21). In phase flushing of fines is initially clear, suggesting increased flow through the distributed system in previously undisturbed areas of the bed (Figure 5.21). However, rapid channelisation during the second spring event characterised by pressurised flow through incipient channels results in the transport of larger proportions of coarse material at rising and peak discharges (Figure 5.21).

Throughout the remainder of the season, suspended sediment size distributions predominantly reflect conditions within the channelised system. Open channel conditions prevail during sub-period 5 and pressurised conditions are expected to be rare (Table 3.6), such that the proportion of coarse transported at rising and high discharges falls, but distributions associated with bank collapse appear to be common (Figure 5.28). Sample first mode also shows a gradual coarsening that probably reflects the reduced flow through the distributed system (Figure 5.14).

Size distributions during sub-period 6 show the increasing transport of coarse sediments at rising and peak discharges (Figures 5.22 and 5.28). This is consistent with increasingly pressurised flow conditions within the channelised system due to the increasingly efficient routing of meltwater resulting in the increasing peakedness of the diurnal hydrograph (Table 3.6). This effect may be compounded by adjustments in channel size in response to flow conditions being open for much of the diurnal cycle, such that pressurised conditions prevail at progressively lower flows around discharge peaks. Size distributions consistent with bank collapse remain common during falling limbs (Figure 5.28), suggesting open flow conditions following peak discharges. Low flows are occassionally associated with much greater proportions of fines than previously observed, and sample first mode shows evidence of the increasing abundance of fine sediments throughout the remainder of the monitored period (Figures 5.14 and 5.22).

The increasing coarseness of size distributions during sub-period 6 (Figure 5.28) is associated with the increasing overpressurisation of the channelised system at peak daily flows that has been suggested to largely control accesses to subglacial sediments later in the season (Chapter 4). This is thought to result in sediments increasingly distal to channels

being accessed due to increasingly pressurised conditions resulting in greater conduit flow excursions, or an increasingly efficient diurnally reversing hydraulic gradient resulting in sediment deformation towards conduits and/or the winnowing of fines as discharge falls. Bank collapse during falling discharge (Figure 5.28), the occasionally high proportion of fines at low flows (Figure 5.22) and a general fining in sample first mode (Figure 5.14) are suggestive of a strong diurnally reversing hydraulic gradient; however, relationships between sample first mode and discharge (Section 5.4.2) suggest the in-phase flushing of fines with peak discharge. It is most likely that both mechanisms are responsible to some extent, since access of flows at peak discharges to sediments previously distal to channels will be enhanced by the deformation of sediments towards channels as discharges declines.

5.6 CONCLUSIONS

- Considerable difficulties exist in the investigation of suspended sediment provenance using sediment size distributions: 1) size distributions are subject to rapid fluctuations reflecting the complex influences on particle size; 2) a large number of samples must be analysed if the mechanisms of sediment evacuation are to be rigorously identified; 3) the nature of geological samples suggests it is unlikely that truly representative size distributions can be obtained; 4) standard moment statistics can be unreliable where distributions are often bimodal, and large variability in the coarse fraction may mask subtle variation in the finer sizes; 5) errors in the laser diffraction method may severely complicate subsequent analysis and interpretation; and 6) potentially powerful multivariate techniques cope poorly with multimodal samples, since they tend to cluster samples based on the form of the dominant mode.

- Generally, sediment size distributions throughout the catchment appear to be controlled by the underlying geology, being mainly composed of two principal modes characteristic of Dremainis and Vagner's (1971) terminal grades. The first mode, likely comprised of individual mineral grains, is common to all catchment sediments.

- The first mode of sediments obtained from boreholes indicates that sediments near to or along PDAs may be much finer than those observed elsewhere. Having been

obtained early in the melt season, this might reflect the precipitation of fines from the distributed system or increased ice-sediment-bedrock interaction along PDAs over winter due to thinner basal sediments that reduces the prevalence of coarser particles. It is probable that fine sediments near to PDAs become depleted towards the end of the season due to channelisation along PDAs and the occurrence of a strong diurnally reversing hydraulic gradient.

- In suspended sediments exported from the subglacial drainage system, an increase in the proportion of fines appears to be associated with increased flow through the distributed system and may suggest the entrainment of very fine particles in sediments distal to major subglacial channels.

- During periods of distributed drainage, changes in suspended sediment particle size typically demonstrate the flushing of fines in-phase with discharge that probably represents contributions of surface melt to areas of the bed that are poorly connected with the pre-existing or expanding channelised system.

- During rainfall events, the first mode of suspended sediment from the subglacial drainage system is unusually coarse. This probably reflects the contribution of sediments derived from extraglacial areas where weathering processes are very different, probably due to the absence of glacial grinding processes.

- The greatest variability in the particle size of suspended sediment from the subglacial drainage system occurs in the second mode, the volume and mode of which generally increases throughout the melt season. This probably reflects the increasing capacity of flows through the hydraulically efficient channelised drainage system. Increasing diurnal variation in flow capacity also concentrates the transport of increasingly coarse particles at the peak of diurnal flows.

- Increasing sediment availability later in the melt season (Chapter 4) is likely to be dependent upon the operation of a diurnally reversing hydraulic gradient; however, analysis of suspended sediment particle size has not succeeded in rigorously identifying the exact mechanisms by which basal sediments are accessed and entrained.

6.

Suspended sediment provenance: additional techniques

6.1 INTRODUCTION

This chapter investigates additional techniques that can be used to further constrain the provenance of suspended sediment from the subglacial drainage system. In Chapter 1 it was suggested that many studies had previously failed to relate variations in suspended sediment concentration to subglacial processes due to poor knowledge of the dynamic nature of the glacial and fluvioglacial systems and because potentially useful indicators of suspended sediment provenance had been neglected. A new framework for suspended sediment studies was suggested (Section 1.3.3) including such indicators, specifically suspended sediment particle size (see Chapter 5), but also additional techniques that are likely to enable more rigorous characterisation of suspended sediment sources. Where catchment geology is heterogeneous, investigations of suspended sediment mineralogy or geochemistry should be useful, since they should provide information on the spatial evolution of the predominant sediment sources. In addition, methods must be developed that enable discrimination between subglacial and potentially large extraglacial sources, which may not be distinguishable by mineralogy or particle size.

The following four sections present pilot studies aimed at addressing these additional issues of sediment provenance. Their aim is principally to determine which methods

have the greatest potential for use in future research. Nevertheless, a few of the techniques have already provided unique information regarding sediment sources and the processes of basal sediment evacuation. However, the limited number of samples dictated by the preliminary nature of the studies, coupled with an occasionally incomplete knowledge of the catchment characteristics, that means these preliminary studies almost invariably raise more questions than answers.

Sediment mineralogy and geochemistry are used to investigate the evolution of catchment sediment sources using x-ray diffraction analyses and whole-sample stable oxygen isotope signatures. Analyses of sediment radionuclide and luminescence signatures are then considered as potential techniques for the discrimination of extraglacial and subglacial sediment sources. Sample preparation and analyses have been performed by members of the Department of Earth Sciences, University of Glasgow, and the Scottish Universities Environmental Research Centre (SUERC), East Kilbride, Scotland. Sample collection and interpretation is entirely the work of the author, except where indicated below.

6.2 SEDIMENT MINERALOGY

6.2.1 Introduction and method

The mineralogy of suspended and *in situ* subglacial sediments from Haut Glacier d'Arolla were analysed using x-ray diffraction (XRD) in order to: a) investigate possible changes in suspended sediments that reflect changes in sediment sources due to spatial evolution of the subglacial drainage network; b) characterise the mineralogy and likely spatial variability of subglacial sediments and their relationship to local subglacial bedrock; and c) determine the extent to which suspended sediments reflect basal sources. XRD is the most common determinative technique in mineralogy, providing a semi-quantitative characterisation of whole sample mineralogical composition (Zussman, 1977). This technique has previously been used in the investigation of sediment provenance within fluvial (e.g. Hillier, 2001) and fluvioglacial environments

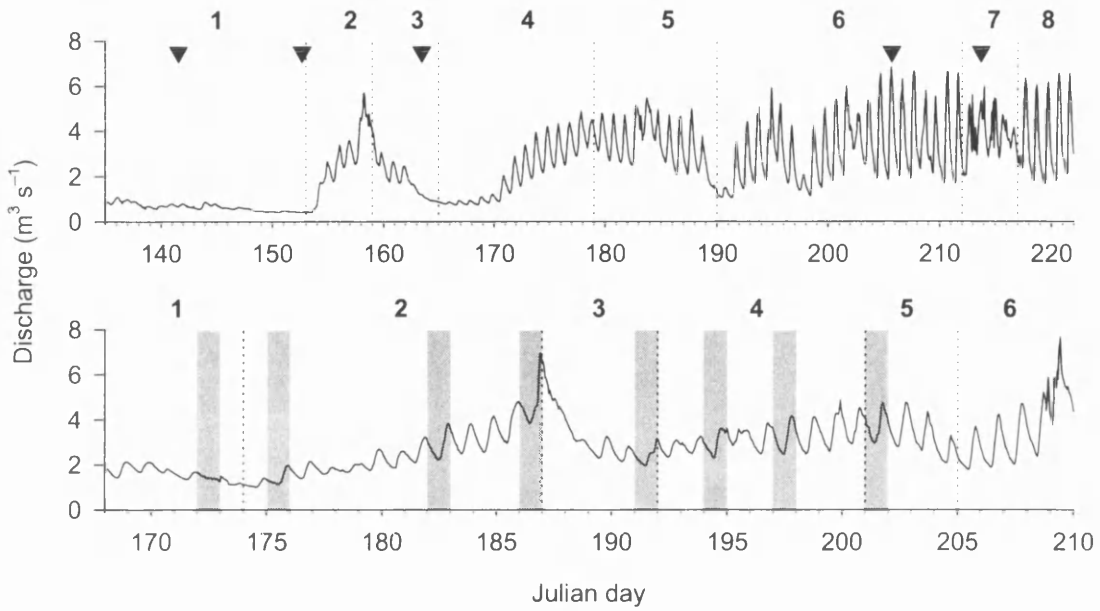

Figure 6.1 The timing of suspended sediment samples collected for XRD analysis. Triangles show the timing of samples collected during 1998 (top). During 1999 (bottom), daily-integrated samples were collected throughout the season (see text); shaded areas of the graph show the 8 days selected for analysis.

(e.g. Fenn and Gomez, 1989). Together with relatively simple sample preparation and short analysis times, this technique is ideally suited to both the characterisation of sediment sources and the investigation of changing sediment sources in small samples of proglacial suspended sediments over time.

Lamb (1997) has previously identified variations in suspended sediment mineralogy at Haut Glacier d'Arolla from two bulk stream samples collected on JD 195 and 247 during (although not explicitly stated) 1993 or 1994. Catchment geology at Haut Glacier d'Arolla is comprised mainly of a gabbro complex underlying the lower ~ 1 km of the glacier tongue and granites occupying the upper tongue and accumulation area (Section 2.1.1; Figure 2.2). Sediments derived from each of these principal units are likely to be mineralogically distinct; hence, spatial evolution of the subglacial drainage system (and therefore the predominant sediment sources) may be reflected in the mineralogy of sediments transported to the glacier snout. Meta-pelites in the upper accumulation area of the eastern catchment are also likely to be represented in proglacial samples, since

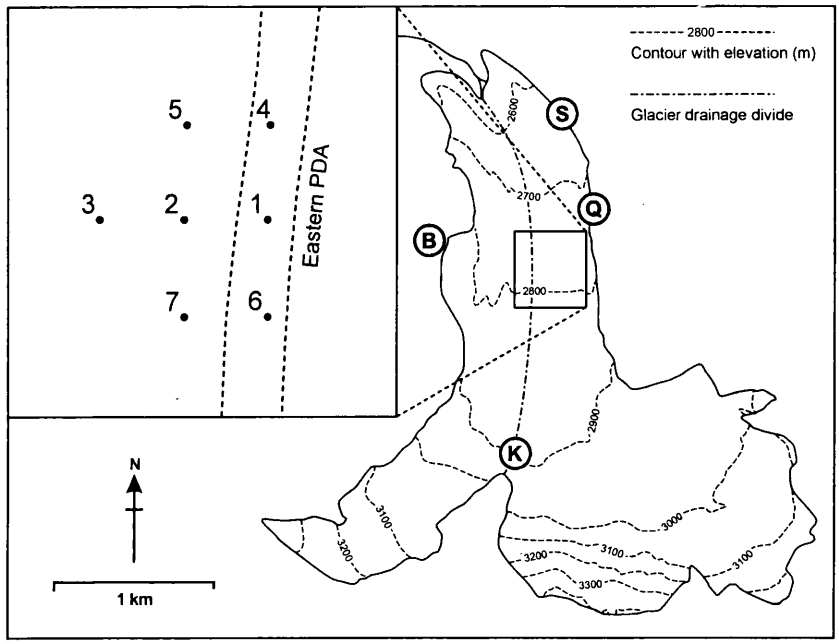

Figure 6.2 Haut Glacier d'Arolla, showing the approximate position of borehole sites 1–7 and the eastern PDA. The location of extraglacial sediment samples B, K, Q and S obtained for radionuclide analysis is also shown (see Section 6.3).

material derived from these can be traced throughout the catchment on account of their distinctive colour. Such materials are found in both the eastern medial moraine and can be traced throughout the proglacial area.

An initial investigation of suspended and *in situ* subglacial sediment mineralogy was conducted using samples collected during the 1998 melt season. Five USDH48 samples collected from the western proglacial stream were analysed, covering the full extent of the monitored period (Figure 6.1), together with 3 subglacial samples collected from the base of boreholes at sites 2, 5 and 7 (Figure 6.2). During 1999, daily-integrated suspended sediment samples were collected from the eastern proglacial stream with the aim of characterising changes in suspended sediment quality (see Section 2.1.1.2). Eight such samples were selected for analysis, providing good coverage of the monitored period (Figure 6.1). All samples were filtered in the field using 2.7 μm ashless papers. The papers were ashed in the laboratory as described in Section 2.3.1.1.

Fenn and Gomez (1989) used a single sample from the proglacial stream of Glacier de

Tsidjiore Nouve to show that suspended sediment mineralogy reflects bedrock characteristics, albeit with a comparative enrichment of quartz and a dearth of clay minerals. Loss of clay minerals is likely to occur during ashing of sediment-laden filter papers. To investigate the possibility of clay mineral loss, a sample of composite proglacial sediment (cf. Section 2.3.1.1) was also analysed before and after ashing. All sample preparation and analysis was undertaken by Mr Bill Higgison (Earth Sciences, Glasgow University), who also assisted with the mineralogical interpretation of the XRD peaks. Samples were prepared for XRD analysis by dry sub-sampling and grinding before being precipitated onto glass slides using an acetone solution.

6.2.2 Results and interpretation

Figure 6.3 shows XRD traces from suspended sediment samples collected during the 1998 season. The positions of significant peaks (those ~ 3× the standard deviation of the background; Zussman, 1977) are highlighted and labelled. Most peaks are common to all samples, and represent the presence of quartz, feldspar and mica. Potentially significant variations between samples is seen in only two peaks: one peak at ~ 37.2 °2θ, tentatively identified as siderite (iron carbonate), occurs solely on JD 141; another peak at ~ 24.6 °2θ, possibly tremolite, occurs throughout the season but shows marked variation in intensity.

Figure 6.4 shows the results of analyses for composite-proglacial and subglacial sediment samples. The pattern of peaks from Figure 6.3 has been overlaid; additional peaks, highlighted with bold lines and labels, are clearly evident in the proglacial sediments and borehole samples that were not subjected to ashing. These peaks indicate the presence of chlorite and possibly kaolin clay, and an enrichment of mica; the latter demonstrating a strong peak at ~ 31.7 °2θ previously hidden by the principal peak for quartz. These characteristics are not evident in the ashed proglacial sample, suggesting that these minerals were also likely to have been present in the suspended sediment samples prior to ashing.

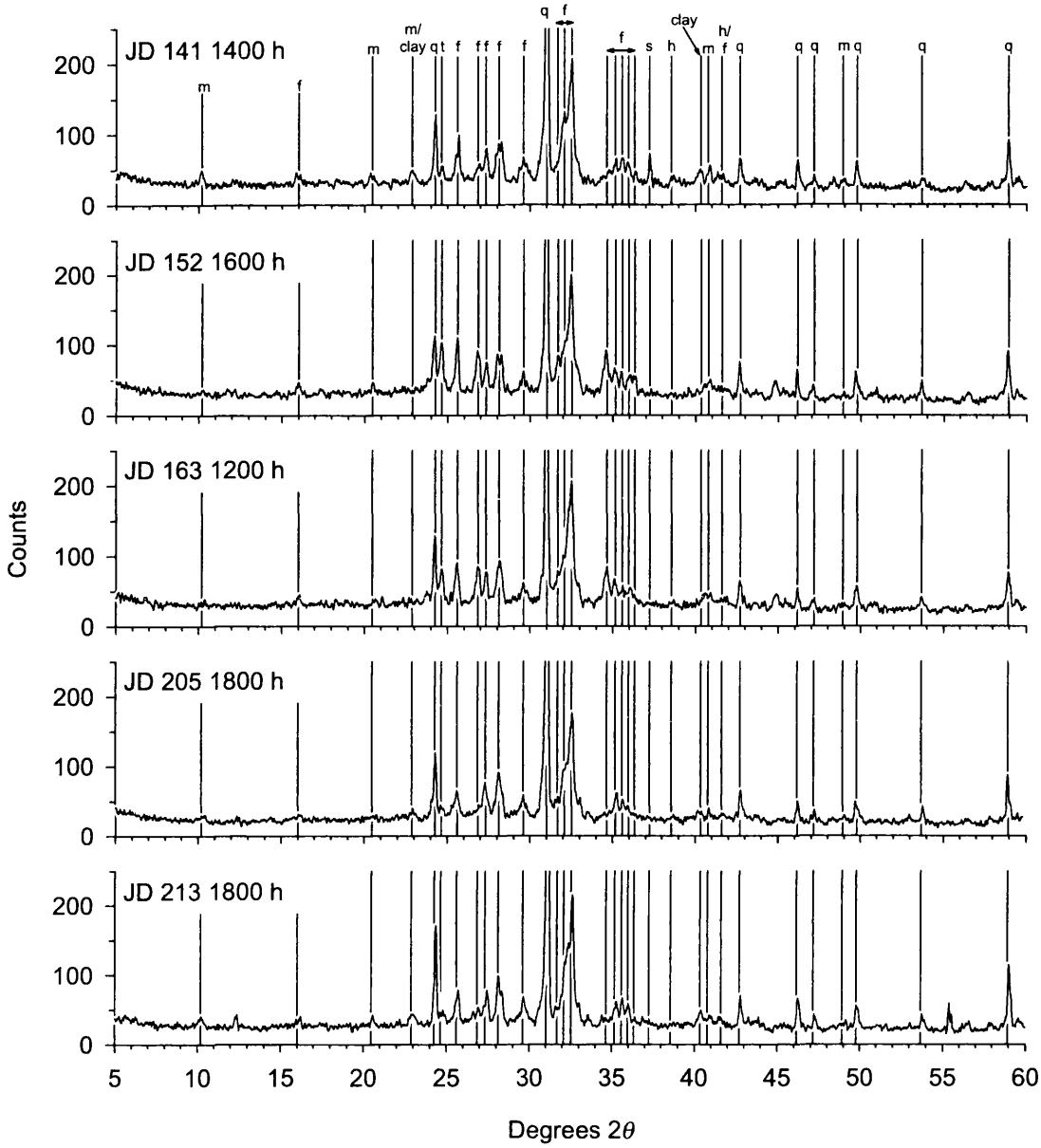

Figure 6.3 XRD traces for suspended sediment samples collected during the 1998 melt season. Peaks associated with the minerals quartz (q), feldspar (f), mica (m), hematite (h), siderite (s), tremolite (t) and clay are indicated.

Another additional peak occurs at borehole site 5 that is likely to be calcite (calcium carbonate). This single peak represents the only definitive evidence of mineralogical variation between borehole locations; however, variation in the magnitude of the chlorite/kaolin and mica peaks also suggests subtle mineralogical differences.

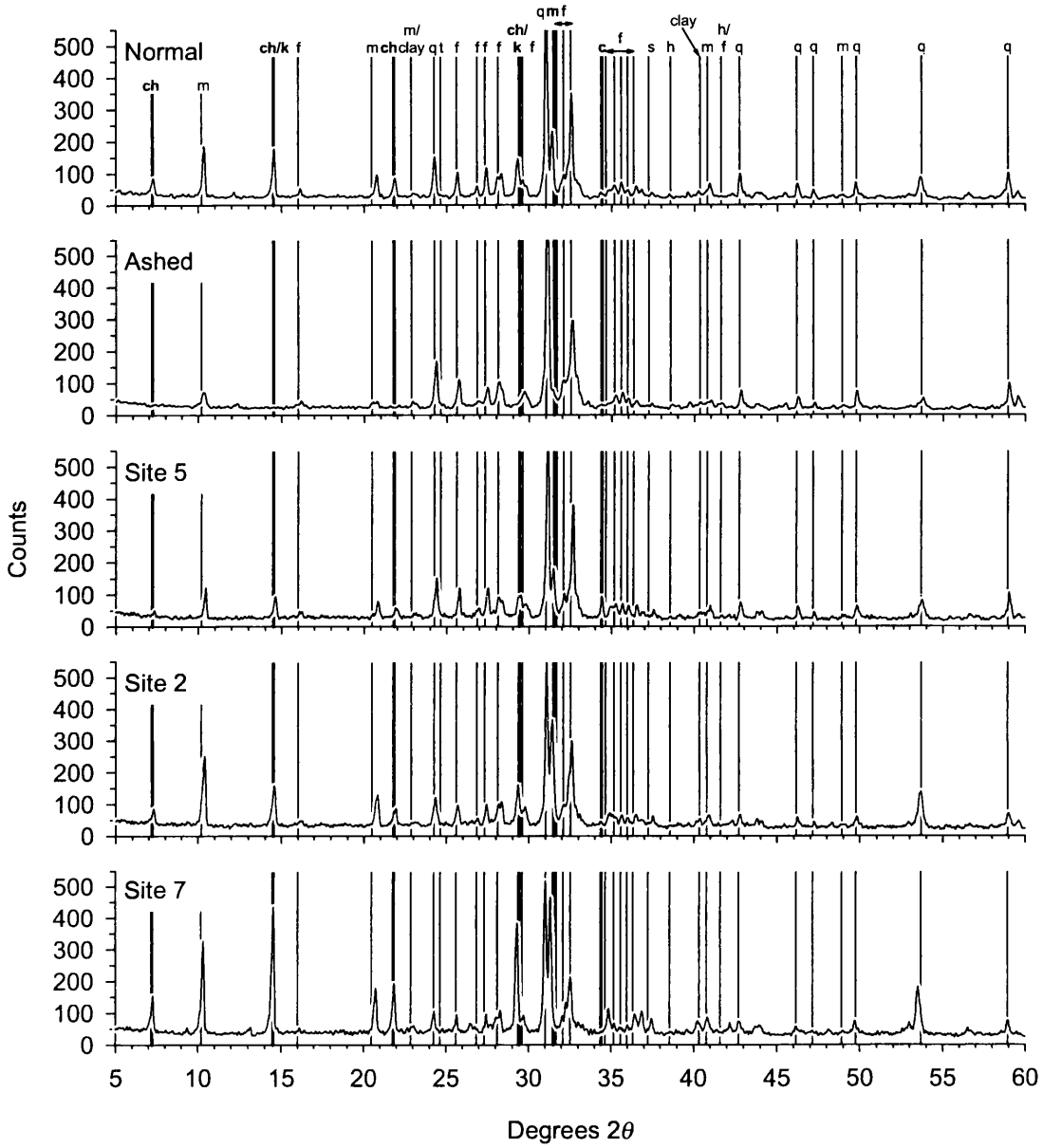

Figure 6.4 XRD traces for proglacial sediments (normal and ashed) and for subglacial sediments from borehole sites 2, 5 and 7 (see Figure 6.2). Peaks for various minerals are indicated (from Figure 6.3); peaks for chlorite (ch), kaolin clay (k) and calcite (c) are also present, together with another mica peak (indicated by thick lines; see text).

Quantitative analysis of sample mineralogy from XRD traces always present difficulties (Zussman, 1977); qualitatively, however, there is a clear increase in the magnitude of the chlorite/kaolin and mica peaks with distance upglacier.

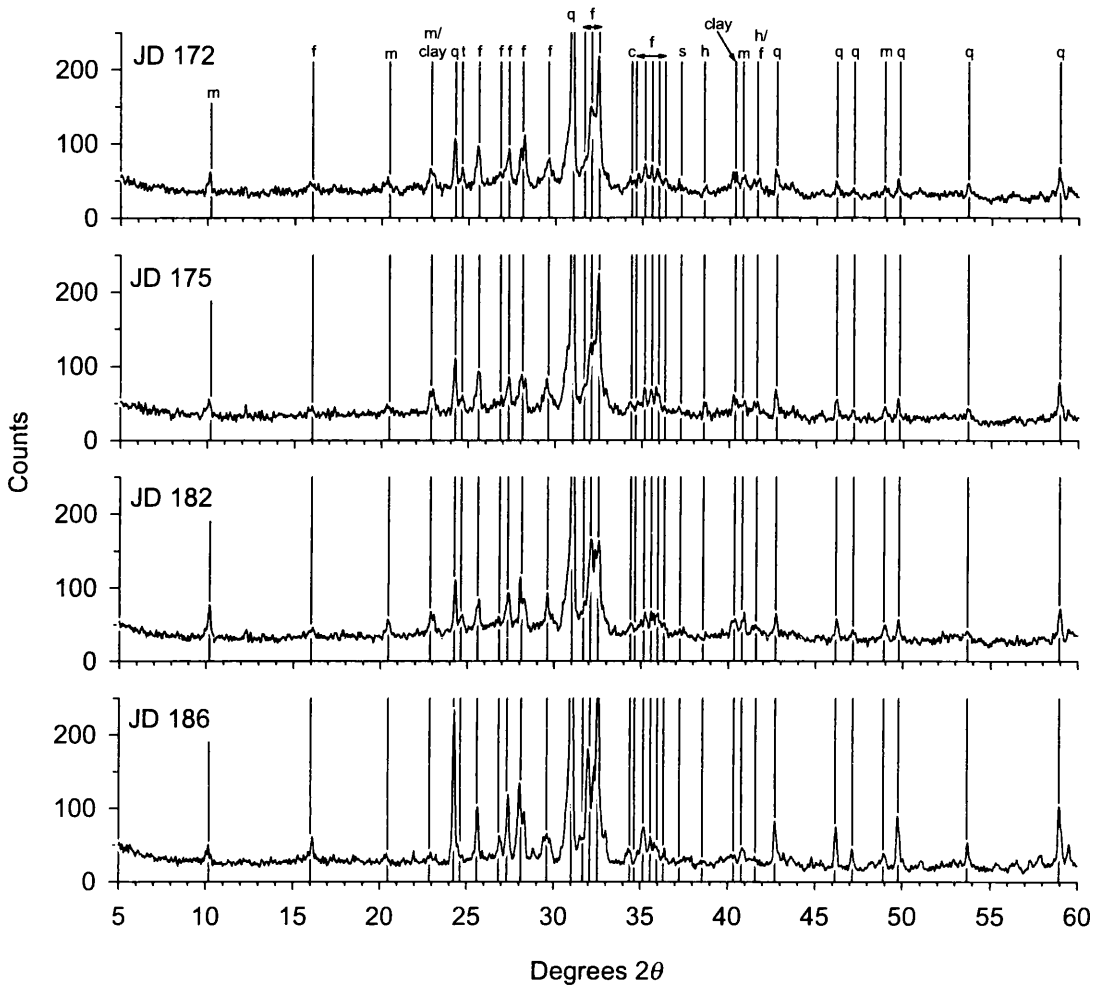

Figure 6.5 XRD traces for daily-integrated suspended sediment samples collected during 1999. Peaks for various minerals are indicated (from Figure 6.3); the peak for calcite is also shown (cf. Figure 6.4). *Continued over.*

XRD traces from integrated daily samples collected from the eastern catchment during 1999 are virtually indistinguishable from those collected from the western catchment in 1998 (Figure 6.5). However, a notable exception is calcite, which is present throughout the monitored period and is also observed in subglacial samples from the eastern catchment. The peak identified as tremolite is again evident, but shows only weak variation, demonstrating a weak peak in samples early in the monitored period (JD 172, 175 and 182) and being generally absent thereafter.

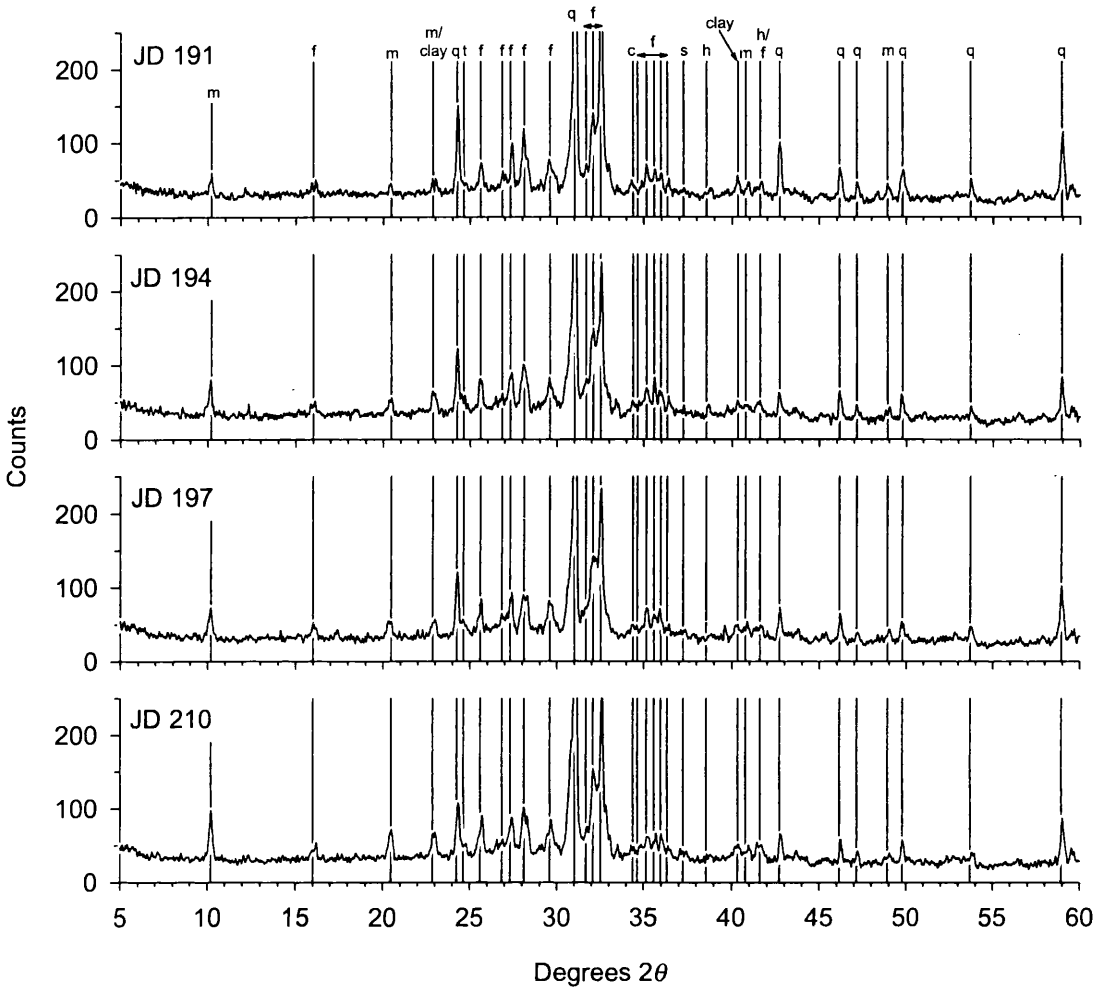

Figure 6.5 *continued.*

6.2.3 Discussion and conclusion

The mineralogy of the sediment samples is comparable to that obtained by Lamb (1997) and of bedrock and stream samples from the Tsidjiore Nouve catchment where the geology is Arolla Gneiss (Fenn and Gomez, 1989). The predominant minerals are the common rock-forming minerals muscovite mica, quartz and feldspar, which are to be found in all three rock types: igneous, metamorphic and sedimentary. Chlorite, which is characteristic of metamorphic rocks, is also common to both catchments. Metamorphic rocks exist beneath Haut Glacier d'Arolla principally in the form of meta-pelites in the upper accumulation area; however, the area has been subject to greenschist facies

regional metamorphism (Dal Piaz et al., 1977) that has given rise to the presence of chlorite in the granites and probably throughout the catchment.

The absence of chlorite and other clay minerals in the suspended sediment samples (Figures 6.3 and 6.5) is almost certainly due to ashing of the samples before analysis. The loss of clay-mica (illite), formed from microscopic, hydrated muscovite, during ashing is also likely to explain the lower proportion of mica. However, these minerals are relatively common throughout the catchment and are unlikely to indicate any spatial evolution of sediment sources. Nevertheless, the increasing enrichment of these minerals beneath the glacier in an upglacier direction warrants further investigation (Figure 6.4). It is possible that the pattern reflects an increasing proportion of sediment derived from siliclastic pelitic rocks transported from the upper accumulation area. Minerals derived from these rocks are likely to be less evident beneath the lower glacier tongue due to the greater likelihood of their evacuation by hydraulically efficient drainage with increasing distance downglacier. However, the distance between samples from sites 5 and 7 is only ~ 200 m. The pattern is therefore more likely to reflect local variation in subglacial weathering and fluvial processes, such as proximity to the PDA near to which fine sediments may be winnowed by the diurnally reversing hydraulic gradient.

Minerals observed in the suspended sediment samples that show significant variation throughout the monitored periods are siderite, calcite and tremolite. Siderite and calcite are carbonate minerals, whilst tremolite is a silicate mineral commonly derived from carbonate rocks. The only potential sources of carbonate rocks in the catchment are meta-pelites in the upper accumulation area of the eastern glacier catchment. Although these are predominantly siliclastic, it is possible they do contain carbonate rocks; that meta-pelite rocks obtained from the eastern supraglacial moraine contain carbonate has been proven by their reaction with acid (B. Goodsell, pers. comm). During 1998, siderite and tremolite generally occur early in the season before the development of a channelised drainage system during periods 4 and 5. A similar pattern in tremolite occurs during 1999, with tremolite peaks being strongest prior to the principal period of channelisation towards the end of period 2; calcite, on the other hand, is equally represented throughout.

These results suggest that sediments containing carbonate minerals, which are more prevalent towards the head of the catchment, are accessed early in the melt season. It is possible that during periods of distributed drainage sediments are accessed more evenly across the glacier bed, reflecting more accurately the relative proportions of the different underlying lithologies. However, it seems very unlikely that the distributed system beneath the main accumulation area would have the capacity to entrain and transport significant quantities of sediment early in the melt season. Logically, flow through the distributed system will increase towards the glacier snout due to the progressively larger upglacier contributing area; hence, transport capacities will be greatest beneath the glacier tongue. Clearly, significant quantities of sediment might be entrained from beneath the upper accumulation area if flow through the system were to be increased; however, significant inputs of surface melt are not likely to occur due to the persistence of the supraglacial snowpack in upglacier areas until relatively late in the melt season.

Another difficulty is that meta-pelites appear to be confined to the eastern catchment, on account of their occurrence both *in situ* and in the distribution of sediments derived therefrom. The existence of tremolite in the western catchment suggests previously unknown sources of carbonate rocks in the catchment, which needs to be more rigorously investigated. In particular, some previous work based on the 1:200,000 Geotechnishe Karte der Schweiz Blatt Nr 3 (see Brown, 1991) has accepted the presence of amphibolites beneath the lower glacier tongue (Brown, 1991; Foster et. al., 2000). If present, amphibole is likely to be an important source of tremolite and possibly other carbonate minerals; however, despite complex variability and evidence of metamorphism, the gabbro complex is thought unlikely to have undergone sufficient metamorphosis for amphibolite facies to have been formed (B. Goodsell, pers. comm).

In conclusion, XRD analysis of suspended sediments at Haut Glacier d'Arolla suggests few changes in mineralogy that might indicate the evolution of subglacial sediment sources. Suspended and *in situ* samples primarily consist of very common rock forming minerals that suggest little potential for identifying individual sediment sources. Variations are observed in a few carbonate minerals, but their provenance needs to be better constrained before they are able to serve as a useful tracer.

6.3 SEDIMENT GEOCHEMISTRY

6.3.1 Introduction and method

The geochemistry of suspended sediment samples collected during the 1999 melt season was analysed in order to assess its potential for inferring the spatial evolution of catchment sediment sources. Foster et. al. (2000) have demonstrated the potential to discriminate between the major rock types of the Haut Arolla catchment using the chemical properties (Na, K, Ca and Mg) of suspended sediment samples. However, Foster et al. (2000) compared only a few samples obtained at the height of the melt season from two locations: 1) the proglacial stream of a cirque glacier below Bouquetins, which was assumed to access sediments derived solely from amphibolite/gabbro in the lower portion of the catchment; and 2) the western proglacial stream of the main glacier, which was assumed to access sediment derived solely from granite in the upper western portion of the catchment.

In this study, whole-sample stable isotope analysis was used to investigate the oxygen-isotope ratio of suspended sediments. Analysis of the oxygen isotope content of a rock or sediment sample enables calculation of the $^{18}O/^{16}O$ ratio, where ^{18}O is a rare stable isotope of oxygen. This ratio varies for different rock types, principally due to their origin and thermal history (Taylor, 1974; Criss, 1995; Attendorn and Bowen, 1997). A dimensionless δ-value is used to represent the difference in isotopic composition of the sample from a standard, typically Vienna Standard Mean Ocean Water (V-SMOW; see Attendorn and Bowen, 1997). Basic igneous rocks, such as basalts and gabbros, have $\delta^{18}O$ values of ~ 5–7, whereas granites have values in the range ~ 7–14, making the Haut Arolla catchment an ideal location with which to assess the potential of the technique.

Seventeen daily-integrated suspended sediment samples collected during 1999 (Section 2.1.1.2) from the eastern glacial stream were analysed, providing good coverage of the monitored period (Figure 6.7). Samples identified for analysis were concentrated during periods of interest, such as the spring event during sub-period 2. The ashed samples were prepared for analysis by washing in HCl to remove carbonate minerals. Carbonate minerals demonstrate high $\delta^{18}O$ values of ~ 18–32 and are therefore likely to greatly

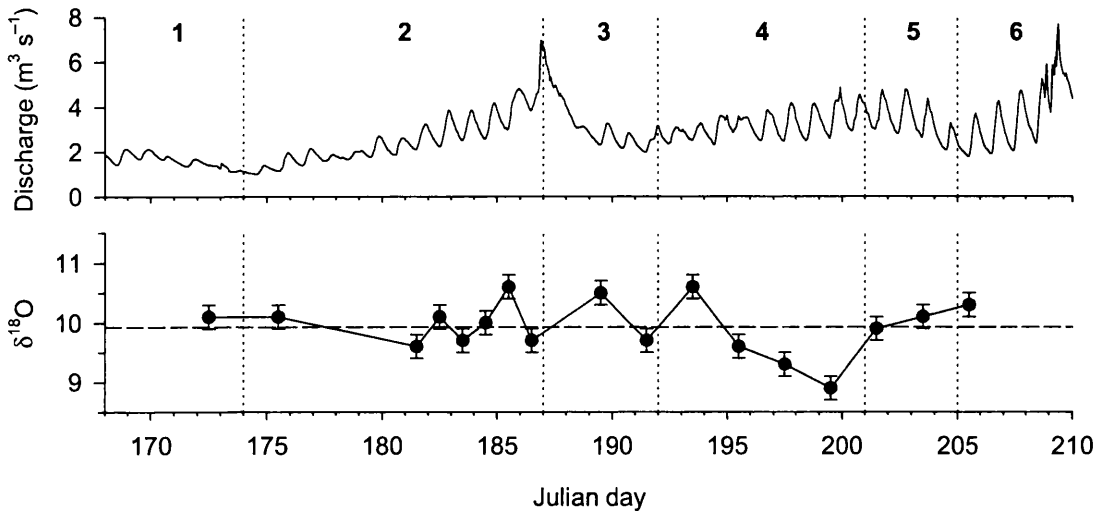

Figure 6.6 Suspended sediment $\delta^{18}O$ variation for samples collected during 1999 from the eastern proglacial stream. Dashed line indicates mean $\delta^{18}O$. Error bars show analytical precision.

complicate the $\delta^{18}O$ signature. Carbonates are most likely to occur in meta-pelites from the upper accumulation area; however, they may also occur in the gabbro complex beneath the lower glacier tongue (see Section 6.2.3). Analysis of sample isotopic ratio was performed at SUERC by A. E. Fallick. Oxygen was liberated from the samples using fluorine and the ratio of oxygen isotopes precisely determined using a mass spectrometer; δ-values were then determined using V-SMOW (above).

6.3.2 Results and interpretation

Figure 6.7 shows the variation in sample $\delta^{18}O$ throughout the monitored period. The samples demonstrate some geological variation, but this is small (~ 9–10.5) relative to the possible range of values suggested by catchment rock types (~ 5–14). Mean $\delta^{18}O$ for all samples is 9.9 (standard deviation 0.5), indicating a strong contribution from granitic bedrock in the upper catchment. Nevertheless, there is the suggestion of a temporal trend during period 4, with samples on JD 195, 197 and 199 demonstrating a slight decline in $\delta^{18}O$ values that may indicate a greater contribution of material derived from the gabbro complex beneath the lower glacier tongue.

6.3.3 Discussion and conclusion

The uniformity of the data does not suggest significant evolution of the predominant sediment sources during the monitored period. The signature would be expected to reflect predominantly gabbro sources early in the melt season during the initial increased flow through the distributed system and incipient channelisation beneath the glacier tongue. It is possible that sediments derived from granites predominate beneath the lower tongue, since ~ 60–70 % of the glacier by area is underlain by granitic rocks. There may also be selective transport of minerals by both glacial and fluvioglacial processes: quartz grains are likely to undergo lower rates of mechanical and chemical weathering beneath the glacier, such that they persist longer and are less likely to be entrained by subglacial meltwaters. However, this effect is likely to be very small.

The possible temporal trend during period 4 is intriguing but represents a very small change in $\delta^{18}O$. In addition, greater contributions of sediment from beneath the lower glacier tongue are not expected late in the melt season, and a significant decrease in $\delta^{18}O$ is not observed during sub-period 2 when channelisation was most likely to have been occurring (Section 3, Table 3.7). The most likely explanation for this signature is the influence of sediment contributed via the eastern marginal streams originating from cirque glaciers below Bouquetins. This strong signature has previously been observed in terms of the pattern of suspended sediment concentration from the eastern proglacial stream (see Section 4.3.5.2). However, the Bouquetins streams continue to contribute sediment to the eastern glacial catchment during sub-period 5, when $\delta^{18}O$ are observed to increase once more.

In conclusion, the catchment geology at Haut Glacier d'Arolla would be expected to offer great potential for the separation of sediment sources using the $\delta^{18}O$ signature of suspended sediments. However, the field data suggests no significant temporal trends, indicating a strong contribution from granites throughout the monitored period. It is possible that granite sediments predominate throughout the catchment due to the large upglacier contributing area that overlies granitic bedrock. Sediments may also be less likely to be evacuated by meltwater from beneath the lower glacier tongue due to

channels being predominantly at atmospheric pressure. In addition, erosion rates may also be lower beneath the lower glacier tongue due to thinner ice and lower velocities. Alternatively, the gabbro complex may be less extensive beneath the lower glacier than previously indicated, or $\delta^{18}O$ values may be higher than expected due to complex variation in rock types. These issues could be resolved using a more detailed study of the catchment geology and $\delta^{18}O$ values of *in situ* rock and sediment.

6.4 RADIONUCLIDE SIGNATURE

6.4.1 Introduction

Few studies have attempted to use radionuclides as indicators of sediment provenance in sediments exported from glaciated catchments, despite their clear potential to discriminate between sediments of subglacial and proglacial or extraglacial origin (Hasholt and Walling, 1992; Foster et. al., 2000). The study of fallout radionuclides has been largely applied to the dating of snow and ice layers in glaciers and ice sheets and of sediment layers in proglacial lakes, enabling changes in the rate of snow or sediment accumulation to be determined (Pinglot and Pourchet, 1995). However, fallout radionuclides have been shown to provide an effective means of investigating rates of sediment erosion, redistribution and deposition in non-glaciated catchments (e.g. Walling and Quine, 1992; Higgit, 1995). In addition, analysis of the radionuclide signature of suspended sediment in non-glaciated fluvial environments has enabled the investigation of both sediment sources and temporal changes in sediment provenance (e.g. He and Owens, 1995; Zhang and Zhang, 1995; Bonniwell, et. al. 1999).

The potential use of fallout radionuclides for determining sediment sources and transfer processes in glaciated basins has been demonstrated by Hasholt and Walling (1992). They used ^{137}Cs (a fallout radionuclide principally derived from nuclear testing) to investigate the provenance of suspended sediment in the proglacial stream of a glaciated catchment in Greenland, where the predominant sediment sources were glacial and proglacial. Hasholt and Walling reasoned that whilst proglacial sediments would have

been exposed to ^{137}Cs, glacial sediment sources would have been protected from fallout by ice. This was confirmed by the sampling and coring of proglacial sediments and the sampling of englacial debris bands exposed at the glacier surface. The present study, however, has highlighted the potential importance of extraglacial sediments derived from marginal areas of the catchment (e.g. the slopes below Bouquetins) and routed to the proglacial area via the subglacial stream.

Foster et. al. (2000) have outlined the potential of radionuclide analysis for discriminating between subglacial and extraglacial sediment sources at Haut Glacier d'Arolla. Due to their differing times and methods of deposition, and distinctive half-lives, Foster et. al. (2000) suggest that a combination of atmospherically-derived ^{210}Pb and ^{7}Be, in addition to ^{137}Cs, will enable the source and approximate residence time (or age) of sediments to be determined. In this study, the potential of this technique was investigated using sediments collected from the proglacial stream under varying catchment hydrological conditions, from the base of boreholes drilled to the glacier bed, and from various extraglacial and proglacial locations. In particular, samples of suspended sediment were obtained during periods of high solar insolation, characterised by strong glacial melt, or intense rainfall, characterised by high extraglacial runoff, when the proportion of extraglacial sediments is likely to be high. The majority of samples were analysed for both ^{137}Cs and ^{210}Pb; ^{7}Be analysis was not conducted since its short half-life (53.3 days) would have required analysis to be carried out in the field.

6.4.2 Method and results

An initial study undertaken using samples collected during the 1998 melt season comprised three samples from the base of boreholes at sites 4 and 5, four supraglacial/extraglacial samples (B, K, Q and S; Figure 6.3), and two suspended sediment samples from the western proglacial stream (Table 6.1). The stream samples were collected at high suspended sediment concentrations, the first during a period of high glacial melt (JD 208) and the second during a period of prolonged rainfall (JD 222). Stream and borehole samples were filtered using 2.7 μm papers and ashed in the laboratory at 350 °C to remove the majority of the paper without the loss of clay

Table 6.1 Summary of samples collected during the 1998 melt season for radionuclide analysis. See Figure 6.3 for location of samples B, K Q and S and drill sites 4 and 5.

Sample	Date	Description
B	JD 223	Debris flow from valley side
K	JD 223	Supraglacial sediment from medial moraine
Q	JD 223	Marginal moraine
S	JD 223	Fine slackwater sediments adjacent to marginal stream
BH1	JD 147	Subglacial sediment, borehole 15 (site 5)
BH2	JD 147	Subglacial sediment, borehole 15 (site 5)
BH3	JD 145	Subglacial sediment, borehole 13 (site 4)
Stream 1	JD 208 15:00	Western proglacial stream; rain
Stream 2	JD 222 15:00	Western proglacial stream; high melt

minerals to which radionuclides may be attached; extraglacial samples were sieved to remove particles larger than 2 mm.

Analysis of sample radionuclide signature was performed at SUERC by A. B. MacKenzie. For this initial study, ^{137}Cs alone was used in order to indicate exposure to atmospheric fallout. Subglacial sediments from the base of boreholes were tested since radionuclides in melt from ice and snow that finds its way to the subglacial environment may 'contaminate' basal sediments, reducing the potential to discriminate between extraglacial and subglacial sources. It is also possible that extraglacial sediments may be temporarily stored beneath the glacier. The results demonstrated the presence of ^{137}Cs in samples B and S, with ^{137}Cs activities in the remaining samples being below the limit of detection. However, the results from the stream samples were inconclusive due to the relatively small amount of sediment obtained.

Samples collected during the 1999 season comprised 6 suspended sediment samples from the eastern proglacial stream and two 'soils' from the proglacial area (Table 6.2). Emphasis was placed on obtaining larger stream samples representing a wide range of catchment hydrological conditions. Soil samples (collected from a depth of ~ 2–3 cm) were obtained from above and below the 1850 (Little Ice Age maximum) moraine in

Table 6.2 ^{210}Pb (total, supported and unsupported) and ^{137}Cs activity in samples collected at Haut Glacier d'Arolla during the 1999 melt season.

Sample	Total ^{210}Pb (Bq kg^{-1})	Sup. ^{210}Pb (Bq kg^{-1})	Un. ^{210}Pb (Bq kg^{-1})	^{137}Cs (Bq kg^{-1})
JD 177 17:30 (30 min after rain)	386 ±168	74 ±4	312 ±168	–
JD 182 17:30	81 ±10	96 ±2	–	12.5 ±3
JD 200 18:30	65 ±8	91 ±4	–	20 ±3
JD 201 18:00	81 ±10	91 ±3	–	10 ±2
JD 209 12:00 (high SSC ~ 6 h after rain)	93 ±11	90 ±3	–	10 ±2
JD 212 18:00 (30 min after rain)	125 ±14	80 ±3	45 ±14	13 ±4
Soil A (below 1850 moraine) JD 215	162 ±7	78 ±1	84 ±6	148.5 ±6
Soil B (above 1850 moraine) JD 215	154 ±8	133 ±2	21 ±8	116.5 ±2.5

Uncertainties expressed as 1 σ within a 68% confidence limit

order to characterise sediment radionuclide exposure away from the rapidly eroding slopes surrounding the glacier. Sample preparation and analysis was conducted as for samples collected during 1998; however, samples were also analysed for the presence of ^{210}Pb. ^{210}Pb is likely to provide a better tracer in rapidly eroding glacial environments since it is continuously precipitated from the atmosphere (^{137}Cs fallout has declined rapidly since the period of nuclear weapons testing from 1955–1970, whilst fallout from Chernobyl during 1986 was relatively low over this part of Europe; Foster et. al., 2000). However, some ^{210}Pb is also produced *in situ* due to the decay of ^{226}Ra in sediment. As a result, total sample ^{210}Pb was separated into its *in situ* produced (supported) and atmospherically-derived (unsupported) components (see Bonniwell et al., 1999).

Table 6.2 shows the results of radionuclide analyses for samples collected during 1999. The radionuclide signature of soils A and B is typical for European soil (A. B. MacKenzie, pers. comm.); the soils demonstrate the presence of ^{137}Cs and atmospherically derived (unsupported) ^{210}Pb. For the stream samples, ^{137}Cs is evident in all samples except on JD 177; however, activities are consistently low and there is no pattern between ^{137}Cs activity and the occurrence of rainfall. Unsupported ^{210}Pb, however, is only present in samples obtained shortly after rainfall; the sample on JD 209

taken ~ 6 h after rainfall and samples taken on days dominated by glacial melt show no activity. However, there are three important features of the ^{210}Pb results that are distinctly unusual: 1) unsupported ^{210}Pb activities are very high relative to soils from stable situations in the catchment; 2) the highest unsupported ^{210}Pb activity occurs very early in the melt season when the glacier and the surrounding catchment are snow-covered and the potential for rainfall to mobilise extraglacial sediment is likely to be very limited; and 3) for a number of samples, especially the sample on JD 182, supported ^{210}Pb exceeds the total measured ^{210}Pb.

6.4.3 Discussion and conclusion

Samples collected from extraglacial areas during 1998 suggest that ^{137}Cs is not present in many of the extraglacial deposits. ^{137}Cs precipitated mainly between 1955–1970 is likely to have undergone relatively rapid removal due to high erosion rates on steep extraglacial surfaces. Used independently, ^{137}Cs is unlikely to reliably indicate the contribution of extraglacial sediments to the subglacial drainage system. Nevertheless, low ^{137}Cs activity is present in the majority of samples from the eastern subglacial catchment during 1999, although there is no correlation with precipitation events (Table 6.2). It is possible that this activity reflects the influence of marginal streams from Bouquetin remobilising valley-side sediments; however, activity is observed in the sample on JD 182 during sub-period 2 when extraglacial areas were snow-covered and the Bouquetin streams were not active (Table 6.2). In addition, these highly active streams are likely to have exhausted sediments tagged with ^{137}Cs. A more likely source of ^{137}Cs is melt from ice layers accumulated during periods of ^{137}Cs fallout. Ice retains ^{137}Cs precipitated in snow (e.g. fallout from Chernobyl is a useful reference marker for glaciers in the French Alps; Pourchet et. al., 1998). Consequently, it may become attached to basal sediments entrained by melt reaching the glacier bed.

^{210}Pb is likely to be a better tracer due to constant precipitation from the atmosphere. High unsupported ^{210}Pb activities are observed shortly after rainfall in the eastern proglacial stream; however, activity on JD 177 is unusually high and occurs when large areas of the catchment remain snow-covered (Table 6.2). It is possible that high

activities on JD 177 represent the rapid rainfall-induced melting of surface snow layers that have been exposed to fallout for many months. In the absence of melting and percolation, snow acts as a 'closed system' for ^{210}Pb (Picciotto and Crozaz, 1967), therefore significant accumulations of radionuclides may occur in snow over the winter that will be rapidly sorbed onto sediments during periods of melt (Cooper et. al., 1991). However, significant thinning of the catchment snowcover prior to JD 177 would have resulted in the slow concentration of ^{210}Pb in extraglacial sediments beneath. Early season rainfall may access and directly entrain sediments from only limited areas of snow-free extraglacial sediment, but such areas will have high ^{210}Pb concentrations. Unsupported ^{210}Pb activities on JD 212 when the catchment snowcover had been largely removed are in keeping with activities from proglacial soils (Table 6.2).

Nijampurker et. al. (1985) observed ^{210}Pb in snout water at Changme-Khangpu Glacier, Sikkim; ^{210}Pb ages were younger than mean ages within ice, suggesting a large contribution from recent precipitation. However, unsupported ^{210}Pb is absent during periods of icemelt when a similar signature to that of ^{137}Cs might be expected (Table 6.2). Supported ^{210}Pb is determined by sealing the samples to contain ^{222}Rn (gas), a daughter product of ^{226}Ra, that decays to ^{210}Pb via ^{214}Bi. After 3–4 weeks, which is long with respect to the half-life of ^{222}Rn and ^{214}Bi, measurement of sample ^{214}Bi activity enables quantification of ^{226}Ra activity in the sediment (see Bonniwell et. al., 1999). Since unsupported ^{210}Pb is determined by subtracting calculated supported ^{210}Pb from total ^{210}Pb, a small unsupported ^{210}Pb signature will be masked if the supported ^{210}Pb content is overestimated. This is possible if a quantity of the gaseous ^{226}Ra is able to escape, such that the measured ^{214}Bi activity in sealed samples is likely to indicate only the maximum possible supported ^{210}Pb (Bonniwell et. al., 1999). Consequently, supported ^{210}Pb may exceed total ^{210}Pb, with the possibility that a small, unsupported ^{210}Pb component will be hidden.

In conclusion, radionuclides offer some potential for the discrimination of extraglacial and subglacial sediment sources; however, at present the potential is severely limited by complications arising from the retention of radionuclides within snow and ice. Further research is required on the distribution and behaviour of radionuclides within catchment

snow, ice and sediment sources. In addition, the behaviour of ^{210}Pb in the subglacial environment and its associated decay processes require further investigation to understand how and in what quantity gaseous ^{222}Rn may escape. The use of ^{7}Be, with a much shorter half-life than ^{137}Cs and ^{210}Pb, may result in a better discrimination of sediment sources if its shorter half-life means its retention in snow and ice is less significant. However, the use of ^{7}Be may be impractical where its short half-life requires the analysis of samples in the field.

6.5 LUMINESCENCE SIGNATURE

6.5.1 Introduction

The luminescence signature of suspended sediments in the Haut Arolla catchment was investigated in order to assess its potential to discriminate between extraglacial and subglacial sediment sources. Luminescence dating of sediments is a widely employed, especially amongst Quaternary scientists, since it offers the potential to establish detailed chronologies of sediment deposition in a wide range of environments (Aitken, 1998). When naturally-occurring ionising radiation interacts with the crystal lattice of minerals (such as quartz or feldspar), electrons may be stripped from the outer shells of atoms and are attracted to defects in the lattice where they become trapped (Aitken, 1985, 1998). Electrons are only able to escape such traps on exposure to heat or light; in a sedimentary setting, the number of trapped electrons will increase over time (Aitken, 1998). Sediments collected in the field and stimulated by heat or light in the laboratory release the trapped electrons and when these recombine at luminescence centres a proportion of the energy of the electron is expelled as heat and/or light (Aitken, 1985, 1998). The total amount of light emitted (the luminscence) is proportional to the number of electrons, and allows the sediment to be dated (Berger, 1986; Aitken, 1998).

Obtaining accurate dates, however, relies on the complete removal of stored electrons by exposure to light (i.e. bleaching) during transport and deposition in order to 'reset' the luminscence signal (Berger, 1986; Aitken, 1998). In many environments, complete

resetting of the luminescence signal may not occur, the degree of bleaching being dependent upon the mode of sediment transport and deposition. For example, sediments evacuated from the subglacial environment by meltwater will initially have maximum luminescence ages, since they represent freshly eroded bedrock not previously exposed to light. The maximum opportunity for bleaching of these sediments will occur during transport through the proglacial area; however, the extent to which bleaching occurs will be dependent upon many factors. Gemmell (1988, 1994) has shown that variations in the thermoluminescence (TL) age of suspended sediment in proglacial streams may be a function of: 1) the TL age of the sediment at the time of entrainment; 2) the duration or distance of transport; 3) the concentration of sediment in the flow and the presence of floating debris or ice blocks, which reduces penetration of light into the water; and 4) ambient light levels (e.g. sediment may undergo transport and deposition entirely during the hours of darkness).

In modern fluvioglacial environments, the luminescence signature of suspended sediments passing a fixed location is likely to be a unique combination of the various sediment sources and their transport history, suggesting the technique can enable the provenance of suspended sediments to be constrained. Gemmell (1997) suggested links between the TL age of suspended sediment in the Dorra del Ferret River, Italy and episodes of erosion from subglacial (high TL ages) and proglacial (low TL ages) locations. Unfortunately, the redeposition and re-entrainment of sediment in the proglacial area, together with ambient light effects, is likely to result in a very complex signature that may preclude the reliable identification of sediment sources. In addition, Gemmell (1997) suggests transport over only short distances in proglacial streams is required to bleach sediments. However, the technique offers great potential for the discrimination of extraglacial and subglacial sediment sources if samples are obtained at or just within the glacier snout (i.e. the influence of proglacial factors are excluded). Extraglacial sediments routed through the subglacial drainage system should demonstrate a reasonable degree of bleaching due to transport via marginal streams during the day and/or having been eroded from surficial or stream-bank sources that have been exposed to light over many days, weeks or months. In contrast, subglacial

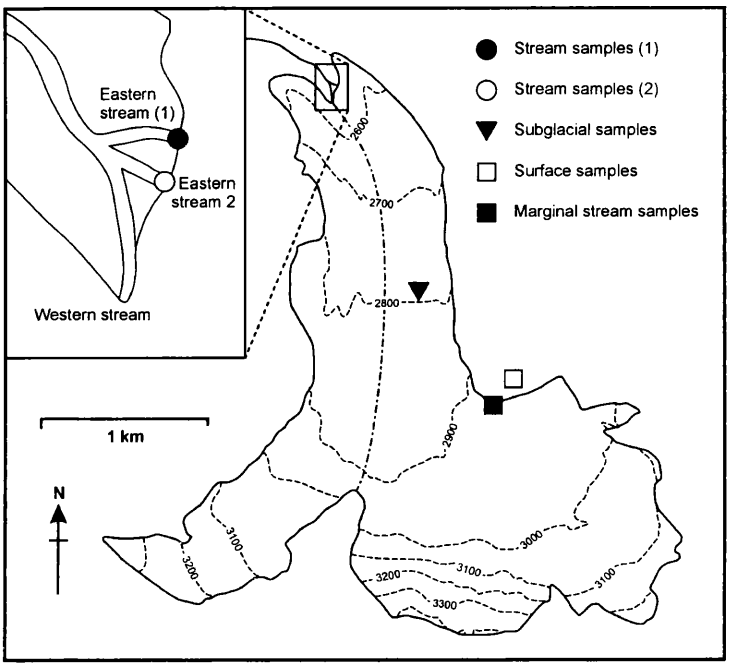

Figure 6.7 Location of proglacial, subglacial and extraglacial sediments sampled for luminescence analysis.

sediments will demonstrate no bleaching due to erosion and transport occurring entirely beneath ~ 100 m of ice.

6.5.2 Method and results

The potential for sediment luminescence signature to discriminate between extraglacial and subglacial sources was investigated using samples collected from the glacier margin and from the base of boreholes drilled to the glacier bed (Figure 6.7). Samples were also collected from two distributaries of the eastern proglacial stream (cf. Section 2.2.3.2) to ascertain the relative contribution of extraglacial and subglacial sources. Samples were collected by I. Cochrane (Geography, Glasgow Universiy) over 3 days during the 2000 melt season. Sampling was undertaken at ~ 00:00 in order to eliminate sediment bleaching during sample collection. Borehole samples were collected from the base of three boreholes using a Nielsen sampler (Nielsen, 1995) and placed directly into opaque polypropylene bottles; the same bottles were used to manually collect stream samples from the proglacial and marginal streams. Marginal stream samples were collected from

two tributaries of the eastern marginal stream in the accumulation area (Stream EMS; see Section 5.3.2.2) that likely feeds into the eastern glacial catchment. A single surface sample was scraped from sediments near to one of the marginal streams and sealed in an opaque 35 mm film canister.

Samples were prepared at SUERC with assistance from A. A. Sommerville (SUERC; Glasgow University) and I. Cochrane; D. C. W. Sanderson (SUERC) supervised their analysis. Preparation involved settling the samples in water for 5 minutes in order to retain the coarse fraction (prepared sample particle size was estimated to be between ~ 10–100 μm). Samples were then subjected to a 10 % HCl wash for 30 mins to remove carbonate sediments and washed 3 times in acetone. Two samples (1 original, 1 replicate) were prepared from each field sample in order to indicate the likely error due to unconstrained sample mineralogy and grain size. Samples were subjected to a standard multiple stimulation analysis (D. C. W. Sanderson, pers. comm.) using a Risø DA15 luminescence reader. The run involves a 220 °C preheat for 30 seconds to remove electrons trapped in shallow defects within the minerals. Samples were then analysed using Infra-Red Stimulated Luminescence (IRSL) for 60 seconds at 50 °C and at 60 % laser power. A post-IR Blue Optically Stimulated Luminescence (Blue OSL) run was then performed for 30 seconds at 125 °C and again at 60 % laser power. Finally, sample Thermoluminscence (TL) was analysed by raising the samples from room temperature to 500 °C at a heating rate of 5 ° s^{-1}. The run was then repeated after giving the samples a 50 Gy dose of β radiation in order to assess sample sensitivity to radiation dose. Results are presented as sample equivalent dose, which is obtained by dividing the natural by the 50 Gy response. The equivalent dose therefore gives the residual luminescence signal accounting for natural variations in sample sensitivity to radiation (for example, sample mineralogy or particle size).

Raw response curves for sample IRSL/OSL and TL signature are shown in Figure 6.8. Before calculating equivalent doses, the results for both the natural and 50 Gy response were simplified as per standard analysis procedure (D. C. W. Sanderson, pers. comm.). For IRSL/OSL, the curves were divided into 'fast' and 'slow' components (Figure 6.8 a) over which the response was summed after subtracting the mean background signal; for

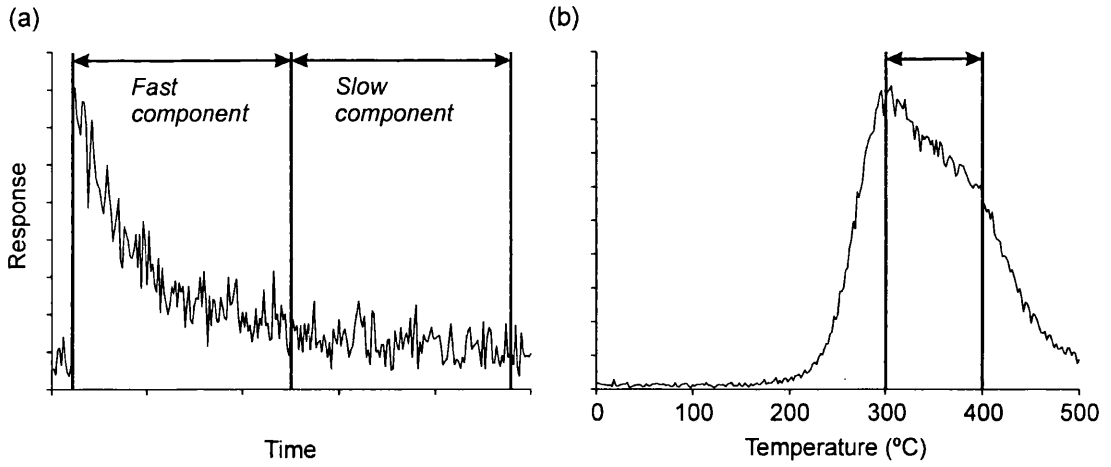

Figure 6.8 (a) A typical luminescence response stimulated by exposure to an infra-red (IRSL) or visible light source (OSL). The response can be divided into 'fast' and 'slow' (rate of luminescence decay) components, separated at time $t \times 0.5$. (b) A typical luminescence response stimulated by exposure to heat (TL). The response in the range 300–400 °C was used for analysis (see text).

TL, the response was summed over the range 300–400 °C (Figure 6.8 b). Concordance plots (original versus replicate samples) of the fast and slow components of the IRSL and post-IR Blue OSL signatures (in equivalent dose) are shown in Figure 6.9. The most striking feature of the dataset is that the subglacial samples have the lowest equivalent doses and are therefore consistently better bleached than any other sediments sampled from the catchment. Furthermore, equivalent doses of subglacial samples cluster tightly compared to other samples, suggesting that between sample differences and errors due to sample preparation are small. A similar pattern is evident for sample TL signature (Figure 6.10). Other than indicating low levels of bleaching, there is no consistent pattern of bleaching in and between proglacial stream, marginal stream and surface sediment samples.

6.5.3 Discussion and conclusion

The results show that surface sediments and sediments in meltwaters draining into and exiting from the glacier have widely-scattered but similar ranges of luminescence characteristics. Since the tributary stream and surface sediments were sampled in close

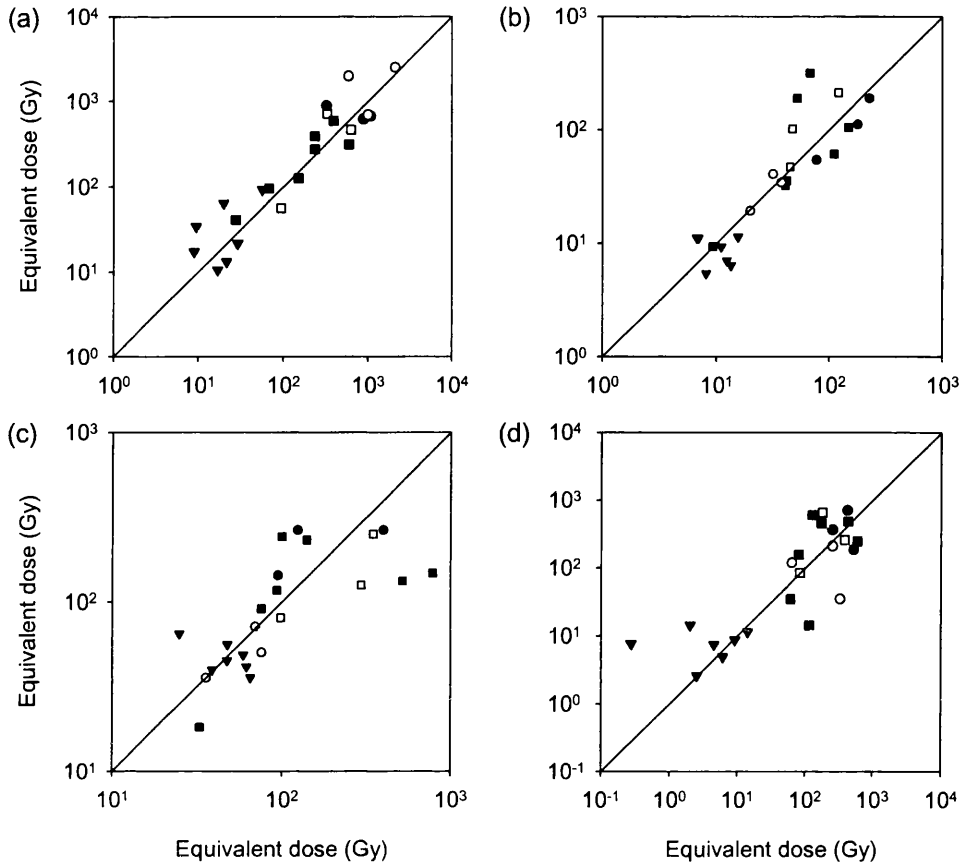

Figure 6.9 IRSL and OSL characteristics of subglacial, extraglacial and proglacial sediments collected during the 1999 melt season. (a) IRSL fast component, (b) IRSL slow component, (c) Blue OSL fast component, and (d) Blue OSL slow component. Triangles are used to represent subglacial samples; see Figure 6.7 for key to all symbols.

proximity to one another, this suggests that it may be difficult to use the luminescence signature to identify specific sediment sources. Nevertheless, it should generally still be possible to separate extraglacial from subglacial sources. The luminescence characteristics of subglacial sediments do occupy a very distinctive range; however, the samples indicate very high levels of bleaching relative to other samples from the catchment, which is inverse to the predicted relationship. This highly unusual result throws doubt not only on the ability of luminescence signatures to discriminate between extraglacial and subglacial sediments, but also on many widely-held assumptions regarding subglacial environments.

If likely sampling or measurement errors are addressed first, the necessary

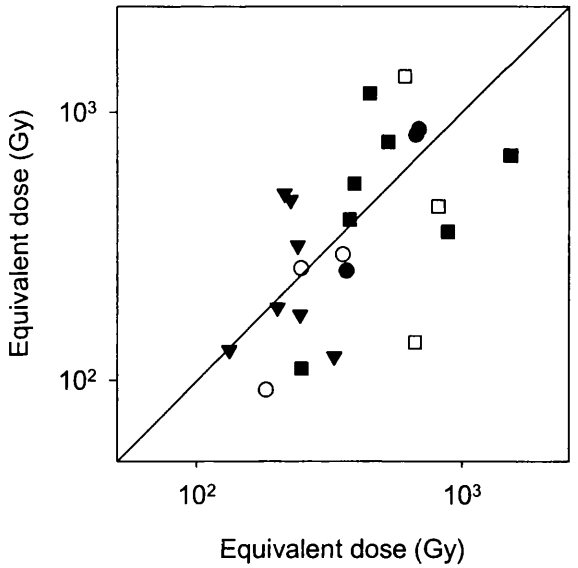

Figure 6.10 TL characteristics of subglacial, extraglacial and proglacial sediment samples collected during the 1999 melt season. Triangles are used to represent subglacial samples; see Figure 6.7 for key to all symbols.

contamination or bleaching of subglacial samples due to exposure to light or heat is thought extremely unlikely. Firstly, contamination of sediments at the base of boreholes by bleached supraglacial sediments is unlikely due to typically very low supraglacial sediment concentrations and the absence of any evidence of supraglacial meltwaters carrying sediments into open boreholes. That sufficient sediment could be transported into boreholes by wind is even more unlikely. Secondly, bleaching is very unlikely to have occurred due to exposure to light since all sampling was conducted at night. Samples may have been exposed to moonlight or light from head-torches for very short periods of time, but such sources are not sufficient to bleach sediments (D. C. W. Sanderson, pers. comm.). In addition, all samples were collected and stored in an identical manner, which cannot therefore account for the observed differences between subglacial and other samples from the catchment. Thirdly, heat from borehole drilling is unlikely to have been high enough to have bleached sediments, since water temperatures in excess of ~ 200 °C would have been necessary to remove the luminescence signature (D. C. W. Sanderson, pers. comm.). Sediments at the base of boreholes are very unlikely to have been exposed to temperatures exceeding 80 °C, and in reality, temperatures are

very unlikely to have exceeded 50 °C (B. Hubbard, pers. comm.).

Satisfactory glaciological interpretations for the observed bleaching in the subglacial sediments are also lacking. Firstly, it is possible that the sampled basal sediments represent previously exposed proglacial sediments that have been overridden; however, overriding in this region of Switzerland must have occurred during the onset of the last ice age. In addition, sediment residence times are likely to be in the order of only 500 years maximum given the thin basal sediment layer (~ 0.25 m) and the current rate of sediment evacuation (~ 1–2 mm $year^{-1}$; see Chapter 4; Gurnell, 1995). Secondly, it is highly unlikely that samples have become bleached through the ice, since the glacier is sufficiently thick in the region of the drill site (~ 100 m) to be considered opaque. Given reasonable sediment residence times on the order of 1–100 years at the ice-sediment interface, bleaching of sediment requires an attenuation of light through the glacier of no more than ~ 6–7 orders of magnitude compared with the surface energy input (P. Nienow, pers. comm.). However, ice is expected to be completely opaque, and extreme stability in the position of basal sediments is required. Thirdly, sediments may have been bleached by light entering the open boreholes, which were open for ~ 1 month prior to sampling. However, the boreholes are both narrow (~ 10 cm in diameter) and unlikely to be straight. If sediments were to remain at the base of the borehole for ~ 1 month, bleaching suggests attenuation of light down the borehole of no more than ~ 4 orders of magnitude (P. Nienow, pers. comm.). However, once again the base of boreholes are likely to remain completely opaque to light, and extreme stability of sediments beneath the hole during the height of the melt season is required.

The final possibility requires unexpected geological variations in the samples. It is possible that due to very different sample mineralogy, too much luminescence signal was liberated from the subglacial samples during the preheat (intended to only release electrons from shallow traps) rather than during the measurement (E. Rhodes, pers. comm.). The geology beneath the glacier is certainly variable; however, for the subglacial samples to be mineralogically distinct from proglacial and tributary stream samples suggests that at midnight on the days in question no sediment was accessed from the region of the drill site. This suggests that at the time of sampling, low flows

beneath the lower glacier tongue were confined to PDAs from which sediments had been largely swept clean.

In conclusion, theory suggests that suspended sediment luminescence signature has great potential to discriminate between subglacial and extraglacial sources. However, contrary to expectations, basal sediments sampled at Haut Glacier d'Arolla were more bleached relative to other catchment sediment sources. Satisfactory explanations for this result are still being investigated; however, it is clear that at the time of sampling, sediments from beneath the drill site were not being accessed in significant quantities by the subglacial stream. At present, it is thought very unlikely that basal sediments can be bleached by natural processes. However, if basal sediments beneath contemporary glaciers are found to be well bleached, it suggests many more glacial sediments in the Quaternary record could be very accurately dated.

6.6 CONCLUSIONS

- The mineralogy of both suspended and *in situ* sediments at Haut Glacier d'Arolla (as determined using XRD) predominantly reflects very common rock-forming minerals. Some variation is observed in the magnitude of a number of small mineralogical peaks, but the provenance of these minerals is not well constrained.

- Significant temporal variation in suspended sediment $\delta^{18}O$ signature was not observed during the monitored period of the 1999 melt season, suggesting that sediments derived from granitic rocks predominate beneath the glacier due to their large upglacier contributing area. If flow in channels occurs under mainly open conditions in the lower ~ 1–1.5 km of the glacier, where the underlying geology is gabbro, then sediments derived therefrom may not be accessed by the subglacial drainage system.

- The use of ^{137}Cs to indicate sediment provenance is likely to be limited due to rapid erosion rates in many glacial environments that have removed much of the sediment exposed during fallout from 1955–1970. However, combined with atmospherically-

derived radionuclides, the presence of ^{137}Cs may indicate the accessing of relatively 'old' sediment sources (Foster et al., 2000). It is likely to be difficult, however, to separate sources that are not tagged with ^{137}Cs simply because they are very recent from those that were formerly buried too deeply to have been exposed to fallout.

- ^{210}Pb and ^{7}Be likely provide the greatest potential for tracing sediment provenance due to constant precipitation from the atmosphere; however, more work must be done on how radionuclides behave in glaciated catchments before these techniques can be effectively applied. The behaviour of radionuclides in the subglacial environment also requires more detailed investigation, particularly the extent to which supported ^{210}Pb may be overestimated due to the gaseous loss of ^{222}Rn.

- Results from the analysis of sediment luminescence are contrary to expectations and confound explanation: subglacial sediments from Haut Glacier d'Arolla are well bleached with respect to other sediment sources, such that the discrimination of extraglacial and subglacial sediment contributions may be impossible. How basal sediments come to be bleached remains unclear; however, it suggests that sediments from the drill site ~ 1.5 km from the glacier snout were not being accessed by the subglacial stream at the time of sampling.

7.

Summary, glaciological implications and conclusions

7.1 INTRODUCTION

This thesis has investigated the provenance of suspended sediment at Haut Glacier d'Arolla in order to identify more rigorously the mechanisms of basal sediment evacuation by subglacial meltwater. The predominance of sediment transport by fluvial processes in the subglacial environment has long been recognised, to the extent that the suspended sediment yields of glacial meltwater streams have commonly been used to calculate glacier erosion rates (Chapter 1). However, glaciers of similar type, bedrock lithology and location show large variability in erosional efficiency that cannot be explained by erosional potential as defined by glacier size (e.g. Hallet et al., 1996). Studies of individual glaciers demonstrate that sediment yields tend to be highly variable at both seasonal and annual scales, presumably reflecting changes in the efficiency of subglacial fluvial processes. Such processes are important because the efficiency of basal sediment evacuation is likely to play a critical role in controlling rates of mechanical denudation. The potential coupling of fluvioglacial and glacial geomorphic processes has been largely ignored by the glacial literature, but may explain the large differences in mechanical denudation rates between glaciers of similar type, bedrock lithology and location (Swift et al., 2002).

The principal aim of the thesis has been to investigate the mechanisms responsible for sediment evacuation by subglacial drainage. Previous studies have failed to reliably link variations in suspended sediment transport with subglacial fluvial processes due to a lack of independent knowledge of the dynamic nature of the glacial and fluvioglacial systems. In addition, potential indicators of suspended sediment provenance, such as particle size, have rarely been employed. This study has used a variety of provenancing techniques that have been interpreted against knowledge of the behaviour of the glacial and fluvioglacial systems obtained from other investigative methods. This chapter summarises the principal conclusions of this research and discusses the glaciological implications through a consideration of potential coupling between fluvioglacial and glacial geomorphic processes. Finally, recommendations are given for future work that may improve our understanding of the mechanisms of basal sediment evacuation by subglacial drainage systems and the understanding of glacial geomorphic processes.

7.2 SUMMARY

The importance of flow capacity in entraining and transporting sediment has led previous studies of suspended sediment evacuation by subglacial drainage to suggest that annual discharge should be a good indicator of sediment yield (Lawson, 1993; Gurnell, 1995). However, Alley et al. (1997) have suggested that the hydraulic efficiency of meltwater flow, which to a certain extent is independent of discharge, is likely to be an important control. Field data from the 1998 melt season at Haut Glacier d'Arolla suggests that subglacial drainage system configuration critically impacts on rates of basal sediment evacuation. Suspended sediment loads demonstrate at least a 125× increase for only a 7.5× increase in daily discharge between periods representative of hydraulically inefficient, distributed and hydraulically efficient, channelised drainage configurations. Failure to appreciate changes in the hydraulic efficiency of subglacial drainage systems might explain why very poor relationships have often been observed between annual discharge and suspended sediment yield (e.g. Bogen, 1989).

Changes in the efficiency of sediment evacuation at Haut Glacier d'Arolla are reflected

in changes in the relationship between log-transformed discharge and suspended sediment concentration (Chapter 4). Variations in the slope of the relationships are due to changes in hydraulic efficiency associated with seasonal evolution of the subglacial drainage system. During periods of predominantly distributed drainage, $\log SSC \propto \sim 1.25 \log Q$, such that the efficiency of sediment transport increases roughly in proportion to discharge. Since transport capacity is primarily determined by flow velocity (Section 1.4.2.1), this likely reflects the fact that flow velocities scale linearly with discharge within distributed systems (Kamb, 1987). During periods of predominantly channelised drainage, $\log SSC \propto \sim 2.1 \log Q$, such that the efficiency of sediment transport rises rapidly with discharge. Flow velocity, and hence sediment transport capacity, has been predicted to increase rapidly with discharge in channelised systems (Alley et al., 1997).

Variations in the intercept of log-transformed relationships between discharge and suspended sediment concentration result from changes in sediment availability. During periods of distributed drainage, previous work has suggested that sediment availability may increase due to increased flow through the system as a result of rapidly rising surface melt water inputs (Section 1.3). Higher discharges result in higher basal water pressures leading to ice-bed separation, meltwater having widespread access to basal sediments and the disturbance of basal sediments due to high rates of basal sliding. At Haut Glacier d'Arolla, there is little evidence for the increased efficiency of sediment evacuation during 'spring events': ice-fractures and periods of channelisation appear to be associated with only short-lived suspended sediment concentration residuals (Chapter 4). Instead, sediment evacuation during the events has been shown to be commensurate with increased flow through the system. However, changes in sediment availability were observed due to the exhaustion of entrainable sediments following the first event and a slight recovery during the second event, which is likely to be due to increased flow through 'new' areas of the distributed system.

During the period of predominantly channelised drainage, the system is initially availability-limited, resulting in the lowest suspended sediment concentrations for any given discharge throughout the whole melt season. This probably reflects the concentration of supraglacially-derived meltwaters into hydraulically efficient channels

located along preferential drainage axes where sediments are thin, spatially limited or have quickly become armoured. Many studies have emphasised decreasing suspended sediment availability associated with channelised drainage systems due to their limited access to basal sediments (e.g. Gurnell et al., 1992a). Gurnell et al. (1992a) believe this to be the case at Haut Glacier d'Arolla, and suggested that late-season increases in sediment availability were the result of inherent instabilities in the smallest channels or in the distributed system. Later, Gurnell (1995) pointed to increasing monthly mean suspended sediment concentration at Haut Glacier d'Arolla despite declining discharge, suggesting that extension of the channelised network would allow access to sediment sources over an increasingly wide area of the bed. However, this implies that any decline in the rate of channel extension would result in gradual sediment exhaustion.

Field data from 1998 demonstrate that sediment availability continues to increase as extension of the channelised system slows, until the highest suspended sediment availability occurs under a mature, channelised drainage system during August (Chapter 4). Higher suspended sediment concentrations are observed for discharges above ~ 4 m^3 s^{-1} than at any other time during the season. Clifford et al. (1995b) suggest that high concentrations late in the season result from increasing sediment transport capacity in increasingly overpressurised channels; however, this does not explain how increasing volumes of transported sediment are accessed. Discussion of the likely factors that enhance the delivery of sediment to channels favours the operation of an increasingly strong diurnally-reversing lateral hydraulic gradient between channelised flowpaths and the distributed system (Chapter 4; Hubbard et al., 1995). As the translation of meteorological inputs into supraglacial runoff becomes increasingly efficient during the melt season, flow conditions in channels formed under closed conditions will be open for an increasing proportion of the diurnal cycle. This may cause channel sizes to decrease marginally due to ice deformation, causing only slight increases in the peakedness and magnitude of diurnal runoff cycles later in the season to result in the increasing overpressurisation of channels at peak discharges. This is likely to encourage a net flow of meltwater into the distributed system at peak discharges (Hubbard et al., 1995; Alley, 1998), causing local ice-bed separation that leads to increasing forward ice

velocities during the summer (Iken, 1974; Iken and Bindschadler, 1986; Willis, 1995; Alley, 1998). The increasingly efficient operation of the diurnally-reversing gradient is likely to lead to the enhanced availability of sediments via three principal mechanisms:

1. Increasing ice-bed separation will lead to extra-flowpath excursions over increasingly wide areas that are occupied by the distributed system at low flows (cf. Leistøl, 1967);

2. Net flow into the distributed system will raise the pore-water pressure within basal sediments, resulting in the deformation of sediments towards channels as discharges decline (Collins, 1979b; Walder and Fowler, 1994; Stone and Clark, 1996). Due to velocity-hysteresis effects (cf. Nienow et al., 1996), much sediment will remain in the channel to be evacuated during the next rise in discharge; and

3. Net flow from the distributed system following peak discharge results in the winnowing of fines from sediments near to channels (Hubbard et al., 1995).

Alley (1998) has suggested that because ice-bed separation near to channels decreases rapidly as bulk discharge falls, returning flows are impeded and higher water pressures are maintained in the distributed system long after peak discharge. The asymmetric form of diurnal borehole water pressure records at Haut Glacier d'Arolla suggests that a similar mechanism occurs where ice is underlain by basal sediment, likely due to the effect of channel-marginal effective pressures on sediment consolidation (Hubbard et al., 1995). This will increase the hydraulic gradient between the distributed system and the channel as bulk discharge falls, which may result in higher velocity flows towards channels that are capable of entraining high quantities of sediment or destabilising channel walls. Sustained higher pressures in the distributed system may also increase the potential for basal sediments to deform towards low-pressure channels.

The particle size of suspended and source sediments at Haut Glacier d'Arolla demonstrates two principal modes that are characteristic of glacial sediments (Dreimanis and Vagners, 1971). The larger mode (~ 500–2000 μm) is likely to represent rock particles and the finer mode (~ 5–50 μm) individual mineral grains (Chapter 5). Variation in the finer mode is

likely to reflect spatial variations in subglacial meltwater flow. Early in the melt season, flushes of fines are believed to represent increased flow through 'new' areas of the distributed system (e.g. Figure 5.21). When surface meltwater inputs are negligible, particle size suggests that much sediment may be entrained from the floors or banks of pre-existing channels; however, as supraglacial inputs increase, moulins connected to the distributed system result in the in-phase flushing of fines with discharge (Section 5.4.5). This in-phase flushing is observed when surface meltwaters are known to be accessing the distributed drainage system. The exhaustion of fines appears to occur following the first spring event (Figure 5.15) and is reflected in a decline in sediment availability indicated by relationships between discharge and suspended sediment concentration (Chapter 4). In-phase flushing is again observed prior to and during the second event (Figure 5.21), suggesting that flow is increasing through new areas of the distributed system, which is again supported by the increased availability of sediments indicated by relationships between discharge and suspended sediment concentration.

Since fine sediments are winnowed from channel margins during the melt season, increases in the proportion of fines may reflect: 1) extra conduit excursions at high discharges to access sediments previously distal to channels; 2) the deformation of sediments towards channels during falling bulk discharge; or 3) the winnowing of fines by returning meltwater flows. Suspended sediment first mode and d_5 both suggest that fines are least abundant following the second spring event when flow is confined to PDAs and occurs under largely open conditions (Figures 5.14 and 5.15). As the diurnally-reversing hydraulic gradient begins to strengthen, first mode gradually declines, indicating the contribution of finer sediments, and d_5 values indicate larger proportions of fines. However, analysis of the relationship between discharge and size distribution parameters indicates that first mode decreases in-phase with discharge (Section 5.4.5), suggesting that high flows are accessing sediments distal to channels (cf. Leistøl, 1967), whilst d_5 decreases out of phase, suggesting the deformation of sediments towards channels or the winnowing of fines by returning flows (Hubbard et al., 1995). These mechanisms are not mutually exclusive, however, and it is possible that late in the melt season more complete size distributions (indicated by finer positions of the first

mode) are accessed as discharge rises due to extra flowpath excursions, whilst greater proportions of fines (lower d_5 values) are delivered as bulk discharge declines. Unique sediment distributions during falling discharge (Figure 5.28) may reflect bank collapse due to destabilisation of channel banks by flows returning from the distributed system or from the deformation of high-pressure basal sediments towards channels.

The use of additional provenancing techniques in Chapter 6 mainly suggested that, during the height of the melt season, sediments may not be accessed from beneath the lower glacier tongue. Stable oxygen isotope ratios of suspended sediments suggest a predominance of sediments derived from granitic bedrock (i.e. from upglacier), even early in the melt season when increased flow through the distributed system and incipient channelisation is likely to be greatest beneath the lower glacier tongue. This suggests that highly efficient channels may not access sediments beneath the lower glacier tongue, such that sediments remain in glacial transport and that they predominantly reflect the upglacier geology. Suspended sediment luminescence signatures also suggests that sediment from beneath the drill site (~ 1 km from the snout) were not being accessed by meltwaters following peak discharge. This may suggest that sediments are predominantly accessed during rising and peak discharge, and that the winnowing of fines and deformation of sediments towards channels is negligible. However, it may also suggest inefficient operation of the diurnally reversing hydraulic gradient near to the glacier snout where channels will be predominantly at atmospheric pressure and may rarely be overpressurised (the glacier snout has retreated ~ 300–500 m since Hubbard et al. (1995) observed large diurnal water pressure variations beneath the drill site). Marginal streams from Bouquetins that enter the subglacial drainage system and cut across glacial sediment transport pathways are also likely to be at atmospheric pressure and may not have the capacity to remove significant quantities of sediment from glacial transport or the ice-bed interface.

The additional provenancing techniques discussed in Chapter 6 suggest varying potential for investigating the evolution of catchment sediment sources. Radionuclide studies offer good potential for the discrimination of extraglacial inputs, which are known to be significant in the eastern glacial catchment (Chapter 4); however, sediment

luminescence signatures suggest that subglacial sediments are well bleached and at present offers no potential for the discrimination of extraglacial and subglacial sources. XRD analysis also demonstrates little potential due to the predominance of minerals common to all rock types and, where variation in some mineral peaks is observed, the provenance of minerals in the catchment is poorly constrained.

7.3 GLACIOLOGICAL IMPLICATIONS

7.3.1 Controls on the variability of glacial erosion and sediment yield

In Chapter 1 it was demonstrated that the efficacy of glacial erosion is subject to great debate, and data from contemporary glaciers is commonly based on catchment fluvial sediment yields (e.g. Hallet et al., 1996) that are inherently variable. The results from Haut Glacier d'Arolla suggest that great variability in sediment yield from glaciers of similar type may be related to the hydraulic efficiency of the subglacial drainage system. Contrasting rates of sediment evacuation under different drainage configurations may produce variability in rates of subglacial erosion, since the removal of basal sediment will encourage ice-bedrock interaction. Abrasion of the glacier bed by rock particles within the basal ice layer plays the major role in bedrock erosion beneath temperate glaciers (Section 1.3), and the evacuation of eroded debris is critical in order to prevent basal sediment forming a protective layer over bedrock (cf. Riley, 1982; Rea, 1996). The build-up of sediment at the glacier bed is likely to render quarrying ineffective (Hallet, 1996) and stifle abrasion (Boutlon, 1974; Hallet, 1979b).

Consequently, there is likely to be a strong, non-linear dependence of subglacial erosion rates on the effectiveness of basal sediment evacuation. Assuming a bedrock density of 2.7 t m^{-3}, effective subglacial mechanical denudation rates can be calculated for the two drainage system configurations at Haut Glacier d'Arolla during 1998. Under distributed conditions where mean suspended sediment load was ~ 4 t d^{-1} (Chapter 4), annual yields were equivalent to the removal of a ~ 0.01 mm layer of subglacial bedrock. Under channelised conditions, evacuation rates of ~ 500 t d^{-1} (a conservative estimate given the

errors described in Section 4.2) could result in ~ 11 mm of subglacial erosion annually. Although the channelised system may predominate for only a small proportion of the year due to the limited length of the melt season, it is still likely to have a significant impact on sediment evacuation. An increase in the rate of suspended sediment evacuation to just 200 t d^{-1} over 20% of the year at Haut Glacier d'Arolla (the approximate period of channelised drainage during 1998) is sufficient to raise the effective rate of annual subglacial erosion by an order of magnitude. Field data suggests that actual mechanical denudation at Haut Glacier d'Arolla during 1998 was in the order of 1.5 mm (~ 25,000 t $year^{-1}$), a figure that compares favourably with estimates made during previous melt seasons (Gurnell, 1995).

Field data therefore suggest that a significant control on the variability of glacial erosion (and hence sediment yield) is the extent and efficiency of the channelised subglacial drainage network. Glacier-to-glacier variability in the extent of the channelised system is primarily dependent upon the availability, magnitude and distribution of surface meltwater inputs to the glacier bed (Nienow et al., 1998). These factors dictate if and where sufficient quantities of meltwater will become concentrated in order to produce subglacial water pressure perturbations sufficient to destabilise the distributed network. Subtle differences in glacier aspect, slope and altitudinal distribution will influence the availability, timing and magnitude of surface melt (Gurnell et al., 1988), but these variables will be largely dependent upon climatic regime and the presence of glacier surface input points such as moulins and crevasses (Nienow et al., 1998). Contributions of surface melt to the subglacial drainage system occur at a wide variety of glaciers, including some polythermal glaciers (Skidmore and Sharp, 1999; Nienow et al., submitted). The extent of the channelised drainage system is then a function of the distribution of these inputs, which will be sensitively dependent upon glacier surface morphology, the routing of supraglacial meltwater and the location of moulins and crevasses (Nienow et al., 1998). Glaciers without sufficient surface melting and/or available input points, such as many high-arctic glaciers or the interior of ice-sheets, are unlikely to develop channelised drainage. Channelised drainage may also be restricted if the input points are too numerous. A heavily crevassed glacier will deliver widely

distributed inputs of surface melt that may not be of sufficient magnitude to locally destabilise the distributed system (Nienow et al., 1998).

Where channelised drainage occurs, another key control on glacier-to-glacier variability in erosion and sediment yield will be the efficiency with which the channelised system accesses and entrains subglacial sediments. At Haut Glacier d'Arolla, consistently high sediment flux during late summer (see also Clifford et al., 1995b; Gurnell, 1995) indicates a highly efficient channelised configuration. However, theoretical work has suggested that under certain conditions drainage system efficiency and hence the rate of sediment evacuation may be restricted. High rates of basal sliding, for example, are likely to suppress the enlargement of incipient channels and prevent rationalisation by discouraging flowpath migration (Hooke, 1984; Walder, 1986; Kamb, 1987). Gurnell (1995) suggested lower sediment yields at Bas Glacier d'Arolla and Glacier de Tsidjiore Nouve with respect to neighbouring Haut Glacier d'Arolla were due to the presence of large ice-falls and therefore higher rates of basal sliding that discouraged the development of extensive, channelised drainage networks. It has also been shown that basal meltwaters rising from overdeepenings in the glacier bed may undergo supercooling, leading to ice growth plugging subglacial channels and eventually to englacial water flow (Strasser et al., 1996; Alley et al., 1998; Lawson et al., 1998).

For individual glaciers, changes in drainage system hydraulic efficiency may explain variability in glacial erosion and sediment yield at seasonal and annual scales. In some seasons, unusual or unseasonal events such as jökulhläups (Collins, 1979b; Walder and Costa, 1996; Björnsson, 1998) or periods of intense rainfall (Warburton and Fenn, 1994; Denner et al., 1999) may be solely or largely responsible for the development of a channelised subglacial network. Such events are likely to increase sediment evacuation for a short time-period due to destabilisation of the distributed system and the rapid growth of incipient subglacial channels. However, large events will cause high rates of melting of channel walls, such that channels will be large and subsequent flows will likely occur under predominantly open flow conditions. Less frequent overpressurisation and the reduced efficiency of the diurnally reversing hydraulic gradient will result in low rates of sediment evacuation.

More gradual processes may also affect the evacuation of basal sediments. Changes in glacier surface morphology are likely to slowly alter the routing of supraglacial meltwaters (Sugden and John, 1976), the distribution of surface input points, and the routing of channelised subglacial drainage pathways (Sharp et al., 1993). Input points may also be opened or closed by glacier flow due to the strong influence of crevasse distribution on their location (e.g. Holmlund, 1988; Seaberg et al., 1988). However, since the number and distribution of surface input points is unlikely to be highly variable at anything less than decadal scales, the primary factor in variability in glacier erosion and sediment yield is likely to be the extent and pattern of seasonal snowline retreat (Nienow et al., 1998). Snowline retreat is exceptionally important in determining the location and timing of peaked inputs of surface melt to the subglacial drainage system. Climatic variability, together with the influence of snow-drift and avalanching in mountainous environments, means that snowline retreat may be highly irregular both spatially and temporally, with significant implications for the extent, efficiency and temporal persistency of the channelised network.

7.3.2 A conceptual model of subglacial sediment evacuation and deposition

Figure 7.1 (a) presents a conceptual model of suspended sediment evacuation by channelised subglacial meltwater based on the summer configuration of the subglacial drainage system at Haut Glacier d'Arolla. The model conceptualises the spatial pattern of subglacial erosion and relative thickness of basal sediments, as well as the proportion of sediment in glacial versus fluvioglacial transport. Since sediment evacuation by channelised drainage is likely to dominate the annual sediment budget (Section 4.5.4), these patterns also apply at the annual scale.

The basic assumptions of the model are temperate climate, late melt season snowline position, homogeneous catchment geology (no spatial variation in the susceptibility of bedrock to erosion) and smooth basal topography with no icefalls, regels or significant overdeepenings, such that the formation of a mature, channelised drainage system is not impeded. The model divides the glacial laterally into four sections for ease of description; the sections are defined by changes in the peakedness and routing of

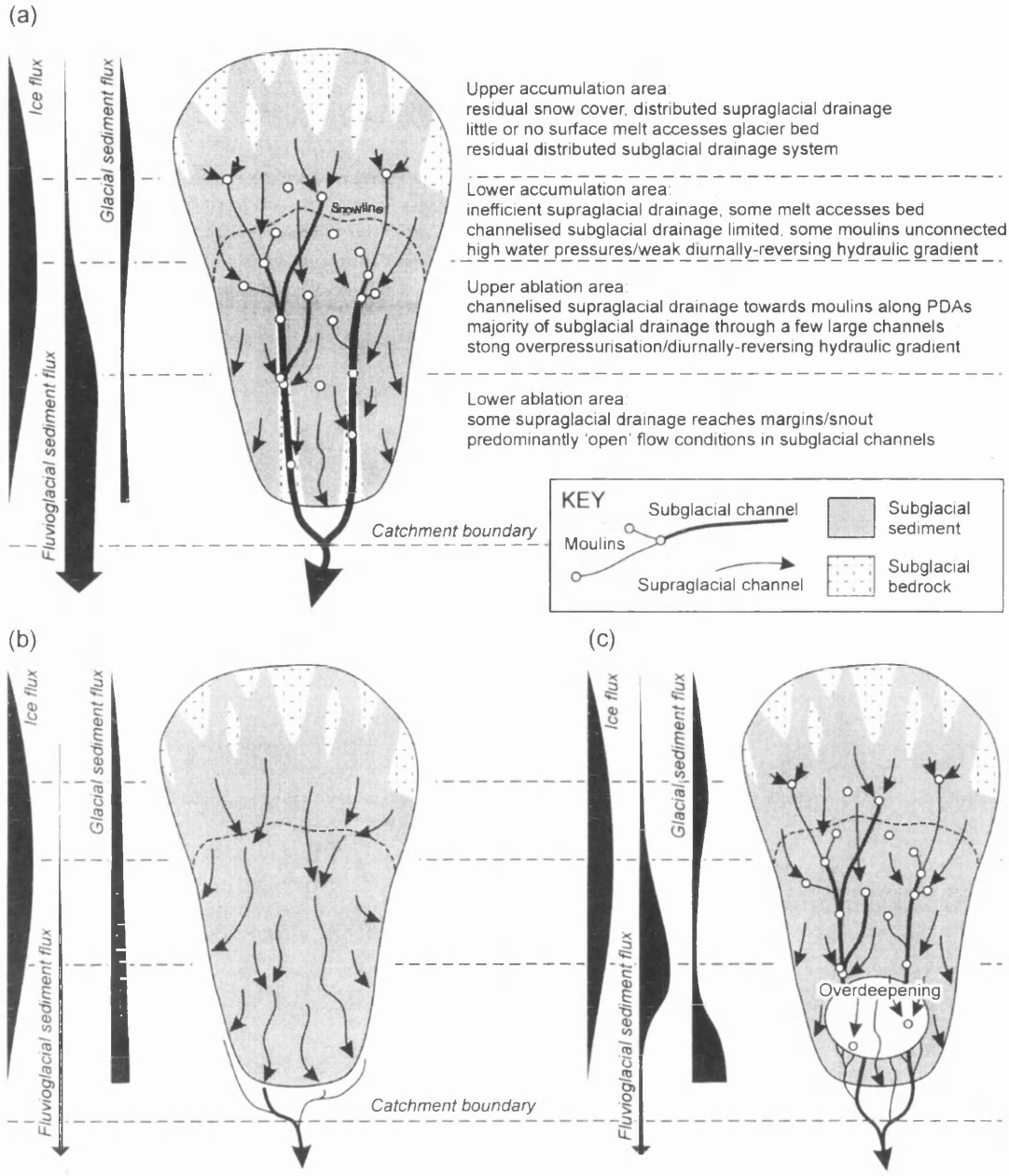

Figure 7.1 Suggested relationships between hydrology and sediment flux in glacial and fluvioglacial pathways for various glacier types if supraglacial sediment transport is negligible. (a) Conceptual model of hydrology and sediment flux for a glacier with a mature, channelised subglacial drainage system; (b) a distributed subglacial drainage system; and (c) a channelised subglacial drainage system with a terminal overdeepening.

supraglacial runoff. (The relative size of each section will vary depending on glacier length and the factors influencing the removal of the surface snowpack).

— Upper accumulation zone. In this zone, the supraglacial snowpack persists throughout the melt season; supraglacial runoff is low and derived mainly from snow melt. Supraglacial runoff is routed through the snowpack or a distributed supraglacial drainage system at the snow-ice interface; where supraglacial melt reaches the glacier bed, the amplitudes of diurnal runoff cycles are insufficient to perturb the distributed subglacial drainage system. Basal sediments are thin and patchy but basal sediment flux increases downglacier with the ice flux due to glacial erosion. Basal meltwaters are drained by a distributed drainage system that encourages sediment to be retained in glacial transport pathways; the fluvioglacial sediment flux is negligible.

— Lower accumulation zone. Thin residual supraglacial snowpack, surface melting increases due to greater advective warming of the snowpack at lower altitudes. Supraglacial runoff is still low and contributes to a distributed supraglacial drainage system. This system rationalises with distance downglacier and may feed into moulins connected to the glacier bed. Only a few streams will contribute peaked inputs of surface runoff sufficient to destabilise the distributed system; thus, many moulins (if at all present) will remain isolated from the channelised subglacial drainage system. Channels will be widely spaced and discharges will be relatively low, although water pressures within immature channels are likely to be high. Channels will begin to capture sediments from glacial transport but their influence will be small due to a weak or laterally inextensive diurnally reversing hydraulic gradient and relatively low flow velocities. Basal sediment flux will increase slowly as the basal sediment layer thickens and begins to hamper subglacial erosion rates.

— Upper ablation zone. In this zone, gradually more efficient supraglacial drainage contributes high magnitude, peaked surface runoff to the subglacial drainage system. The majority of moulins connect to the channelised system, which begins to rationalise along PDAs dictated by subglacial hydraulic potential (due to channel formation under closed flow conditions). Moulins may also be preferentially located above PDAs (Sharp et al., 1993), since subglacial hydraulic potential is partly determined by glacier surface morphology. Subglacially, flow occurs through a

small number of large channels that are hydraulically efficient. Supraglacial runoff is high, very peaked and contribute directly to PDAs, resulting in overpressurisation at peak discharges and a strong diurnally reversing hydraulic gradients. Meltwaters likely capture basal sediments from glacial transport through a combination of extra channel flow excursions over wide areas of the glacier bed and the deformation of sediments under high-pressure towards low-pressure channels as bulk discharge falls. The capture of basal sediment from glacial transport results in increased ice-bed interaction and sediment production may increase rapidly with the fluvioglacial sediment flux whilst the proportion of sediment in glacial transport declines.

— Lower ablation zone. Towards the glacier snout, supraglacial melting and runoff are very efficient, although some runoff reaches the ice margin or the snout rather than the subglacial drainage system. Subglacial drainage occurs through just a few large channels, but near the snout flow conditions are predominantly open, resulting in a weak or non-existent diurnally reversing gradient. Consequently, access to basal sediment sources is limited, and areas near to channels may be stripped of sediment; however, thin ice and lower flow velocities result in limited erosion in sediment-free areas. Largely unsatisfied transport capacity due to further inputs of surface melt means the fluvioglacial sediment flux is unlikely to be deposited; however, the proportion of sediment in basal transport may increase since the products of erosion are not captured by the channelised drainage system.

In summary, efficient evacuation of sediment by the channelised system causes high erosion rates, but sediment may be transport beyond the catchment boundary (Figure 7.1 a); relatively little sediment remains in basal transport, such that the volume of sediment directly deposited at the ice-margin is small in relation to overall sediment production. Sediment evacuation may be low if: 1) the development of a channelised system is restricted (e.g. by high rates of basal sliding); or 2) peaked supraglacial runoff that are responsible for the diurnally reversing gradient are absent. At Haut Glacier d'Arolla, the upper ablation area is large due to seasonal retreat of the snowline to the upper ~ 0.5 km of the accumulation basin. The likely result is that sediment evacuation also increases due to a larger area of the glacier bed subject to strong diurnally reversing gradients.

7.3.3 Controls on glacial sediment transport and geomorphology

7.3.3.1 Sediment transport pathways and ice-marginal deposition

The potential efficiency of sediment evacuation by channelised drainage systems suggests that drainage configuration may also exert a critical control upon sediment transport pathways. The nature of sediment transport and the proportion of sediment in glacial versus fluvioglacial transport pathways will be highly significant for rates and styles of ice-marginal sedimentation. Field data from Haut Glacier d'Arolla during the 1998 melt season emphasises the strong influence of subglacial meltwater in determining the mechanisms of sediment transport and deposition. Flow conditions characteristic of distributed systems will ensure that debris is retained at the glacier bed, leading to the occurrence of thicker and more spatially extensive basal sediments. At Haut Glacier d'Arolla, areas of basal sediment determined by borehole investigation (e.g. Copland, 1997a,b; Harbor et al., 1997) demonstrate the temporary storage of sediment in areas isolated from channelised flowpaths. Hence, sediment transport by glacial mechanisms is likely to predominate, leading to direct (or primary) forms of glacial sedimentation at the ice margin. Material will therefore be deposited locally, favouring the formation of ice-marginal moraines, and sediment will be available for reworking by other glacial and ice-marginal processes.

Under channelised drainage configurations, initial sediment exhaustion suggests that areas near to channelised flowpaths are rapidly stripped of unconsolidated sediment. In addition, high late season sediment availability suggests that sediments are delivered to channels from other areas of the bed, helping to keep the glacier bed relatively free of sediment. Hence, the existence of very efficient channelised drainage will lead to both an overall increase in glacial sediment production (due to enhanced ice-bed interaction) and to an increase in sediment transport by meltwater at the expense of alternative glacial transport mechanisms. Increased ice-bedrock interaction will also result in the enhanced abrasion of larger clasts, resulting in finer sediments that are more susceptible to evacuation by fluvial processes. In Chapter 5, it was noted that prior to channelisation, sediments sampled from boreholes drilled to the glacier bed above the eastern PDA

appear finer than those obtained elsewhere, possibly resulting from increased ice-bed contact in the region of the PDA during winter. Not only will vastly different ice-marginal landforms be produced, but unless significant sediment sinks occur within the proglacial area, such as proglacial lakes, much sediment will remain in fluvial transport and be deposited distal to the ice-margin. As a result, the rate of direct sedimentation at the ice-margin will be much reduced in favour of fluvioglacial deposition and the export of glacial debris beyond the catchment boundary.

7.3.3.2 Implications for ice-marginal geomorphology

This model of integrated glacial and fluvioglacial sediment transport suggests a new framework for the understanding of glacial geomorphic processes and complex ice-marginal environments. The efficacy of sediment evacuation by channelised drainage, the positive impact upon rates of glacial erosion and the potentially strong control on debris transport pathways highlights the fundamental importance of glacier hydrology for glacial geomorphic processes. The potential importance of the work of meltwater within glacial sediment budgets and the implications for rates and styles of ice-marginal deposition undermine traditional approaches to the understanding of ice-marginal geomorphology. For example, ice-marginal landsystem models have long-recognised the existence of subglacial fluvioglacial landforms (e.g. eskers), but appreciation of the role of meltwater has been largely limited to its influence on sediment transport, deposition and the re-working of sediments in the proglacial area (e.g. Benn and Evans, 1998).

Many existing classes of ice-marginal landsystems models are largely defined by the relative availability of supraglacial meltwater but do not explicitly deal with subglacial drainage. Ice-marginal landsystems are characterised by Benn and Evans (1998) as: a) *temperate*, where meltwater is present at the glacier surface and accesses the glacier bed; b) *sub-polar*, where glaciers are polythermal and where surface melting is present but does not reach the bed; and c) *polar-continental*, where glaciers may be polythermal but no surface melting occurs. *Glaciated valley* landsystems represent a special case of the *temperate* landsystem since the valley walls will provide both a significant proportion of glacial debris and a strong topographic control on sedimentation. Traditional

landsystems models also imply that *temperate* glaciers have the highest balance gradients, will posses the greatest erosional potential, and hence produce the largest moraines (cf. Andrews, 1972). However, the potential efficiency of channelised drainage suggests that the most erosive glaciers may not exhibit the highest rates of direct sedimentation at the ice-margin, since sediment is likely to be removed from glacial transport and deposited beyond the catchment boundary (Figure 7.1 a). Where efficient channelised drainage exists, it is possible that direct sedimentation will only predominate in the special case of *glaciated valley* glaciers where there is significant supraglacial debris transport. Instead the highest rates of direct sedimentation are likely to be produced at *temperate* glaciers where the efficiency of channelised flowpaths is sufficiently restricted or absent, or polythermal, *sub-polar* glaciers that lack surface meltwater inputs. The former will almost certainly posses the highest balance gradients, but the latter are likely to result in high rates of direct sedimentation due to a combination of distributed drainage in the up-glacier, wet-based zone and freeze-on of debris at the cold-based margin (Weertman, 1961; Boulton, 1967; Boulton, 1974; Kirkbride, 1995, pp. 283–284). Recent observations of surface meltwater inputs effecting seasonal reorganisation of subglacial drainage at a number of sub-polar glaciers (Vatne et al., 1995; Skidmore and Sharp, 1999; Nienow et al., submitted) also raises the possibility of considerable differences in ice-marginal geomorphology between glaciers of similar type as defined by the relative availability of meltwater.

There is evidence therefore to suggest a new framework for the understanding of rates and styles of glacial erosion, sediment transport and deposition based on the hydraulic efficiency of the subglacial drainage system and ultimately defined by the magnitude and distribution of surface meltwater inputs to the glacier bed:

1. *Glaciers with predominantly distributed subglacial drainage.* For these glaciers, rates of basal sediment evacuation by glacial meltwater will be relatively low (Figure 7.1 b). Accumulation of a thick and spatially extensive basal sediment layer will encourage sediment transport by alternative glacial mechanisms, possibly including subglacial sediment deformation, the formation of thick basal ice layers and the elevation of sediment to higher levels of debris transport. A thick basal

sediment layer will retard subglacial erosion and overall sediment production will diminish, but high rates of direct sedimentation at the ice-margin are likely to result in large proglacial moraines (Figure 7.1 b).

2. *Glaciers with predominantly channelised subglacial drainage.* Here, glaciers will demonstrate high rates of basal sediment evacuation by subglacial meltwater at the expense of alternative debris transport pathways (Figure 7.1 a; for example, sediment transport by subglacial sediment deformation will be spatially limited and sediment-rich basal ice may be destroyed). Where supraglacial debris transport is insignificant, sediment transport by glacial mechanisms will be low, resulting in low rates of direct sedimentation at the ice-margin (Figure 7.1 a). Proglacial moraines may be small or non-existent, but overall rates of sediment production will be high due to sustained ice-bedrock interaction.

3. *Glaciated valley glaciers.* These will remain a special case of type (2) where supraglacial debris transport represents a significant proportion of the total glacial debris flux, and where very thick and extensive glacier debris cover inhibits surface melting and thus restricts the efficiency of the subglacial drainage system. These will deliver a large amount of supraglacial debris to the ice margin, possibly resulting in the formation of very large moraines.

4. *Glaciers with terminal bedrock overdeepenings.* These may also represent a special case of type (2). For such glaciers, the existence of channelised drainage upglacier of the overdeepening will result in high rates of erosion with relatively little sediment transported by glacial mechanisms (Figure 7.1 c). Downglacier, the closure of subglacial conduits rising from an overdeepening, or a switch to englacial flow, is likely to return a large proportion of sediment to glacial transport (Kirkbride and Spedding, 1996; Lawson et al., 1998; Ensminger et al., 1999; Spedding, 2000). The situation means that glaciers with terminal overdeepenings have the potential to be both highly erosive and produce exceptionally large moraines.

7.4 CONCLUSIONS

This thesis has described an integrated approach to the investigation of the mechanisms of basal sediment evacuation by subglacial meltwaters. Central to this approach has been the supplementation of suspended sediment transport data with independent measurements of glacier and fluvioglacial dynamics and potential indicators of sediment provenance. Detailed analysis of suspended sediment transport using simple rating curve and multiple regression techniques was founded on a hydrologically-based subdivision of the periods of investigation (Chapters 3 and 4). This has enabled identification of reliable relationships between discharge and suspended sediment concentration that have indicated changes in hydraulic efficiency and sediment availability. Knowledge of the dynamic nature of the glacial and fluvioglacial systems has provided a basis for the rigorous interpretation of these results, and demonstrates that subglacial drainage system configuration is a critical control on the rates and mechanisms of sediment evacuation.

Suspended sediment particle size (Chapter 5) offers good potential for the further investigation of the mechanisms of sediment evacuation, but has presented numerous difficulties. A major difficulty lies in obtaining accurate size distributions: high resolution can be achieved using laser diffraction methods but investigation of the technique using geological materials suggests the results may be subject to significant error. The potential error means analysis is limited to the investigation of changes in particle size indicated by percentage volume distributions. The utilisation of a large number of samples has enabled the identification of systematic trends and relationships with discharge; however, these have not succeeded in reliably identifying the mechanisms fundamental to increasing suspended sediment availability during the period of predominantly channelised subglacial drainage. Importantly, suspended sediment size distributions are likely to represent an integrated signature of a large number of processes that operate at a variety of spatial and temporal scales. This complexity presents a major challenge if studies of suspended sediment particle size are to further knowledge of subglacial processes. Additional provenancing methods offer some potential (Chapter 6), but the limited nature of the pilot studies means further work is required before these techniques can be successfully utilised for the investigation of suspended sediment provenance.

Field data demonstrates that rates and mechanisms of basal sediment evacuation are largely controlled by the style of subglacial drainage (Chapter 4). Because sediment evacuation by subglacial meltwater is likely to exert a critical control on debris retention at the ice-bed interface, drainage system configuration will also play a significant role in the operation of many glacial geomorphic processes (this chapter). Specifically, the nature of subglacial drainage is predicted to significantly influence: 1) rates of subglacial erosion and debris production; 2) the nature of debris transport and proportion of sediment in debris transport pathways; and 3) rates and styles of proglacial sediment deposition. The potential coupling between glacial geomorphic processes and subglacial meltwater/drainage system configuration has been largely neglected by both the glacial hydrological and geomorphic literature, but may ultimately provide new frameworks for the understanding rates and processes of glacial erosion, sediment transfer and deposition, and the complex geomorphology of ice-marginal environments.

7.5 RECOMMENDATIONS FOR FURTHER RESEARCH

Whilst this study has advanced our understanding of the provenance of suspended sediment from subglacial drainage systems, a number of further investigations could provide further information on the mechanisms of sediment evacuation. In particular, three lines of future research are suggested as potentially providing the best opportunities for progress within this field.

7.5.1 Particle size analysis of suspended sediment *in situ*

A major limitation of investigations of proglacial suspended sediment particle size is the compromise between sampling frequency and the pore size of the chosen filter papers that largely determines sample filtering time in the field. Choosing filter papers with a smaller pore size in order to obtain more representative samples will often result in slower filtration and the ability to process fewer samples. The most detailed previous study has been by Fenn and Gomez (1989) who obtained hourly samples using 8 μm filter papers. This study utilised 2.7 μm papers in order to increase the

representativeness of the filtered samples; however, larger papers had to be used to maintain filtration speeds such that hourly sampling programmes could be sustained. Comparison with work by Gurnell et al. (1992a) suggests that larger papers are actually less representative since blocking of the filter papers by sediment is slower and a larger proportion of sediment is typically lost through the paper for samples < 0.5 g.

A potential solution is to use continuous *in situ* suspended sediment monitoring in glacial environments using portable laser diffraction apparatus such as the Par-Tec 200 (Phillips and Walling, 1995; Phillips, 1996; Phillips and Walling, 1998). Phillips and Walling (1998) have shown this device to perform well in comparison to a Coulter LS130 and to accurately distinguish relative changes in size distribution. Such devices offer the potential to measure samples that are *in situ* (which are more representative) and at greater temporal scales. Chapter 5 demonstrated numerous difficulties with the laser diffraction technique for investigating geological samples and for analysing and interpretating their results. However, with expected improvements in these techniques in the future, there will likely be great potential for obtaining further information on the mechanisms of sediment evacuation using *in situ* particle sizing.

7.5.2 Environmental and geochemical tracers

More detailed work on geochemical and environmental tracers in glaciated environments could provide excellent information regarding changes in suspended sediment provenance and the contribution of extraglacial sediments. Chapter 6 suggests there is great potential for using whole sample stable isotope signatures to investigate the evolution of catchment sediment sources on the grounds of its simplicity; however, glaciers with more favourable geology may need to be found, since sediments beneath Haut Glacier d'Arolla are thought to be dominated by granite derived from the upper catchment. Suspended sediment radionuclide and luminescence signatures also offer great potential for separating contributions from potentially large extraglacial sediment sources. Radionuclide studies at Haut Glacier d'Arolla suggest ^{210}Pb has the greatest potential in rapidly eroding glacial environments; ^{7}Be also likely has good potential if samples can be analysed in the field. Recent developments in gamma-ray spectrometry

mean radionuclide detection can now be applied *in situ* (e.g. Tyler, 1999) and techniques are being developed that allow the continuous measurement of radionuclide signature in natural waters (e.g. Murdock et al., 2001), raising the possibility of continuous measurement in proglacial streams in the future. However, it is clear from Chapter 6 that further work is first needed on the behaviour of radionuclides in glaciated catchments.

7.5.3 Alternative field sites

Studies of proglacial suspended sediment transport and quality that aim to isolate subglacial processes will benefit greatly from choosing glaciers that are suited to the application of particular provenancing techniques, as opposed to applying many techniques to a single glacier where they are unlikely to produce good results. Mineral and geochemical tracers are likely to be most successful in catchments with a variety of geological units that have unique mineral or geochemical signatures. At Haut Glacier d'Arolla, Chapter 6 has suggested that gabbro beneath the lower glacier tongue is unlikely to be extensive enough for the geochemical signature of basal sediments to be significantly different from those beneath the upper glacier. In addition, differences in the geochemical signature between the major rock types at this particular location have not been experimentally determined.

A significant problem at many glaciers is the likelihood of extraglacial sediment contributions masking subglacial variations in suspended sediment concentration and quality. It is unlikely that temperate glaciers can be found where extraglacial contributions are minimal. Future studies may therefore have to look to polythermal glaciers in order that extraglacial sediment contributions can be excluded. Supraglacial meltwater inputs and the seasonal development of channelised drainage have been observed at a number of polythermal glaciers where the ice margin is likely to remain frozen (e.g. Vatne et al., 1995; Skidmore and Sharp, 1999; Nienow et al., submitted). Providing glacier hydrology and ice dynamics are also well constrained, such glaciers present an ideal opportunity for more rigorous investigation of the mechanisms of suspended sediment evacuation by subglacial processes.

Addison, (1981). The contribution of discontinuous rock mass failure to glacier erosion. *Annals of Glaciology*, **2**, 3–10.

Agrawal, Y.C., McCave, I.N. and Riley, J.B., (1991). *Laser diffraction analysis.* In: J.P.M. Syvitski (Ed.), *Principles, methods, and application of particle size analysis.* Cambridge University Press, Cambridge, 119–128.

Aitken, M.J., (1985). *Thermoluminescence dating.* Academic Press, London.

Aitken, M.J., (1998). *An introduction to optical dating: The dating of quaternary sediments by the use of photon–stimulated luminescence.* Oxford University Press, New York.

Alley, R.B., (1992). How can low–pressure channels and deforming tills coexist subglacially? *Journal of Glaciology*, **38**, 200–207.

Alley, R.B., Blankenship, D.D., Bentley, C.R. and Rooney, S.T., (1986). Deformation of till beneath ice stream B, West Antarctica. *Nature*, **322**, 57–59.

Alley, R.B., Cuffey, K.M., Evenson, E.B., Strasser, J.C., Lawson, D.E. and Larson, G.J., (1997). How glaciers entrain and transport basal sediment: Physical constraints. *Quaternary Science Reviews*, **19**, 1017–1038.

Alley, R.B., Lawson, D.E., Evenson, E.B., Strasser, J.C. and Larson, G., (1998). Glaciohydraulic supercooling: a freeze–on mechanism to create stratified, debris-rich basal ice: II. Theory. *Journal of Glaciology*, **44**, 563–569.

Anderson, S.A., Fernald, K.M.H., Anderson, R.S. and Humphrey, N.F., (1999). Physical and chemical characterisation of a spring flood event, Bench Glacier, Alaska, USA: evidence for water storage. *Journal of Glaciology*, **45**, 177–189.

Anderson, S.P., Derver, J.I. and Humphrey, N.F., (1997). Chemical weathering in glacial environments. *Geology*, **25**, 399–402.

Andrews, J.T., (1972). Glacier power, mass balances, velocities and erosional potential. *Zietschrift fur Geomorphologie*, **13**, 1–17.

Arnold, N., Richards, K., Willis, I. and Sharp, M., (1998). Initial results from a distributed, physically based model of glacier hydrology. *Hydrological Processes*, **12**, 191–220.

Arnold, N.S., Willis, I.C., Sharp, M.J., Richards, K.S. and Lawson, W.J., (1996). A distributed surface energy–balance model for a small valley glacier. I. Development and testing for Haut Glacier d'Arolla, Valais, Switzerland. *Journal of Glaciology*, **42**, 77–89.

Attendorn, H.–G. and Bowen, R.N.C., (1997). *Radioactive and stable isotope geology.* Chapman and Hall, London.

Bayvel, L.P. and Jones, A.R., (1981). *Electromagnetic scattering and its applications*. Applied Science, London.

Beecroft, I., (1983). Sediment transport during an outburst from Glacier de Tsidjiore Nouve, Switzerland, 16–19 June, 1981. *Journal of Glaciology*, **29**, 185–190.

Bell, M. and Laine, E.P., (1985). Erosion of the Laurentide region of North America by glacial and glaciofluvial processes. *Quaternary Research*, **23**, 154–174.

Benn, D.I. and Evans, D.J.A., (1998). *Glaciers and Glaciation*. Arnold, London.

Berger, G.W., (1986). Dating quaternary deposits by luminescence – Recent advances. *Geoscience Canada*, **13**, 15–21.

Beuselinck, L., Govers, G., Posen, J., Degraer, G. and Froyen, L., (1998). Grain-size analysis by laser diffractometry: comparison with sieve-pipette method. *Catena*, **32**, 193–208.

Bezinge, A., (1987). *Glacial meltwater streams, hydrology and sediment transport: The case of the Grande Dixence hydroelectricity scheme*. In: A.M. Gurnell and M.J. Clark (Eds.), *Glacio–fluvial sediment transfer: An Alpine perspective*. Wiley, Chichester, 473–498.

Björnsson, H., (1998). Hydrological characteristics of the drainage system beneath a surging glacier. *Nature*, **395**, 771–774.

Bogen, J., (1980). The hysteresis effect of sediment transport systems. *Norsk Geogrrafisk Tidsskrift*, **34**, 45–54.

Bogen, J., (1988). *A monitoring programme of sediment transport in Norwegian rivers*. In: M.P. Bordas and D.E. Walling (Eds.), *Sediment Budgets*. IAHS Publication No. 174, 149–159.

Bogen, J., (1989). Glacial sediment production and development of hydro-electric power in glacierized areas. *Annals of Glaciology*, **13**, 6–11.

Bogen, J., (1991). *Erosion and sediment transport in Svalbard*. In: Y. Gjessing, J.O. Hagen, K.A. Hassel, K. Sand and B. Wold (Eds.), *Arctic hydrology: present and future tasks*. Norwegian National Committee for Hydrology, Oslo, 147–158.

Bogen, J., (1992). *Monitoring grain size of suspended sediments in rivers*. In: J. Bogen, D.E. Walling and T. Day (Eds.), *Erosion and sediment transport monitoring programmes in river basins*. IAHS Publication No. 210, 183–190.

Bogen, J., (1995). *Sediment transport and deposition in mountain rivers*. In: I.D.L. Foster, A.M. Gurnell and B.W. Webb (Eds.), *Sediment and water quality in river catchments*. Wiley, Chichester, 482–451.

Bogen, J., (1996). Erosion rates and sediment yields of glaciers. *Annals of Glaciology*, **22**, 48–52.

Bonniwell, E.C., Matisoff, G. and Whiting, P.J., (1999). Determining th times and distances of particle transit in a mountain stream using fallout radionuclides. *Geomorphology*, **27**, 75–92.

Boothroyd, J.C. and Ashley, G.M., (1975). *Process, bar morphology and sedimentary features on braided outwash fans, northeastern gulf of Alaska.* In: A.V. Jopling and B.C. MacDonald (Eds.), *Glaciofluvial and Glaciolacustrine Sedimentation.* Society of Economic Palaeontologists and Mineralogists Special Publication, 193–222.

Boulton, G.S., (1967). The development of a complex supraglacial moraine at the margin of Sorbreen, Ny Friesland, Vestspitzbergen. *Journal of Glaciology*, **6**, 717–736.

Boulton, G.S., (1974). *Processes and patterns of glacial erosion.* In: D.R. Coates (Ed.), *Glacial Geomorphology.* State University of New York, Binghampton, 41–87.

Boulton, G.S., (1978). Boulder shapes and grain–size distributions of debris as indicators of transport paths through a glacier and till genesis. *Sedimentology*, **25**, 773–779.

Boulton, G.S., (1996). Theory of glacial erosion, transport and deposition as a consequence of subglacial sediment deformation. *Journal of Glaciology*, **42**, 43–62.

Brown, A., (1985). Traditional and multivariate techniques in the interpretation of floodplain sediment grain size variations. *Earth Surface Processes and Landforms*, **10**, 281–291.

Brown, G.H., (1991). *Solute provenance and transport pathways in alpine glacial environments.* Unpublished PhD thesis, University of Southampton.

Brown, G.H., Sharp, M.J., Tranter, M., Gurnell, A.M. and Nienow, P.W., (1994). Impact of post-mixing chemical-reactions on the major ion chemistry of bulk meltwaters draining the Haut Glacier d'Arolla, Valais, Switzerland. *Hydrological Processes*, **8**, 465–480.

Burkishmer, M., (1983). Investigations of glacier hydrological systems using dye tracer techniques: Observations at Pasterzengletcher, Austria. *Journal of Glaciology*, **29**, 403–416.

Buurman, P., Pape, T. and Muggler, C.C., (1997). Laser-grain size determination in soil genetic studies: 1 Practical problems. *Soil Science*, **162**, 211–218.

Cattell, R.B., (1966). The scree test for the number of factors. *Multivariate Behavioural Research*, **1**, 245–276.

Chappell, A., (1998). Dispersing sandy soil for the measurement of particle size distributions using optical laser diffraction. *Catena*, **31**, 271–281.

Church, M. and Ryder, J.M., (1972). Paraglacial sedimentation: a consideration of fluvial processes conditioned by glaciation. *Geological Society of America Bulletin*, **83**, 3059–3072.

Clifford, N.J., Richards, K.S., Brown, R.A. and Lane, S.N., (1995a). Laboratory and field assessment of an infrared turbidity probe and its response to particle size and variation in suspended sediment concentration. *Hydrological Sciences Journal*, **40**, 771–791.

Clifford, N.J., Richards, K.S., Brown, R.A. and Lane, S.N., (1995b). Scales of variation of suspended sediment concentration and turbidity in a glacial meltwater stream. *Geografiska Annaler*, **77 A**, 45–65.

Collins, D.N., (1979a). Quantitative determination of the subglacial hydrology of two Alpine glaciers. *Journal of Glaciology*, **23**, 347–362.

Collins, D.N., (1979b). Sediment concentration in meltwaters as an indicator of erosion processes beneath an alpine glacier. *Journal of Glaciology*, **23**, 247–257.

Collins, D.N., (1983). *Solute yield from a glacierised high mountain basin.* In: B.W. Webb (Ed.), *Dissolved loads of rivers and surface water quantity/quality relationships*. IAHS Publication No., 41–49.

Collins, D.N., (1990). *Seasonal and annual variations of suspended sediment transport in meltwaters draining from an Alpine glacier.* In: H. Lang and A. Musy (Eds.), *Hydrology in Mountainous Regions 1: Hydrological Measurements; the Water Cycle*. IAHS Publication No. 193, 439–446.

Cooper, L.W., Cook, R.B., Grebmeier, J.M., Olsen, C.R., Solomon, D.K. and Larsen, I.L., (1991). Stable isotopes of oxygen and natural and fallout radionuclides used for tracing runoff during snowmelt in an Arctic watershed. *Water Resources Research*, **27**, 2171–2179.

Copland, L., Harbor, J., Gordon, S. and Sharp, M., (1997a). The use of borehole video in investigating the hydrology of a temperate glacier. *Hydrological Processes*, **11**, 211–224.

Copland, L., Harbor, J. and Sharp, M., (1997b). Borehole video observation of englacial and basal ice conditions in a temperate valley glacier. *Annals of Glaciology*, **24**, 277–282.

Criss, R.E., (1995). *Stable isotope distribution: variations from temperature, organic and water–rock interactions.* In: T.J. Ahrens (Ed.), *A Handbook of Physical Constants: Global Earth Physics (Vol. 1)*. American Geophysical Union, Washington, DC, 292–307.

Cuffey, K. and Alley, R.B., (1996). Is erosion by deforming subglacial sediments significant? (Toward till continuity). *Annals of Glaciology*, **22**, 17–24.

Dal Piaz, G.V., de Vecci, G.P. and Hunzker, J., (1977). The Austroalpine layered gabbros of the Matterhorn and Mont Collon-Dents de Bertol. *Schweizerische Mineralogische Und Petrographische Mitteilungen*, **57**, 59–81.

de Boer, G.B.J., de Weerd, C. and Goossens, H.W.J., (1987). Laser diffraction spectrometry: Fraunhofer versus Mie scattering. *Particle Characteristation*, **4**, 14–19.

Denner, J.C., Lawson, D.E., Larson, G.J., Evenson, E.B., Alley, A.B., Strasser, J.C. and Kopczynski, S., (1999). Seasonal variability in hydrologic-system response to intense rain events, Matanuska Glacier, Alaska, USA. *Annals of Glaciology*, **28**, 267–271.

Dreimanis, A. and Vagners, U.J., (1971). *Bimodal distribution of rock and mineral fragments in basal tills.* In: R.P. Goldthwaite (Ed.), *Till – a symposium.* Ohio State University Press, Columbira, Ohio, 237–250.

Droppo, I.G. and Ongley, E.D., (1989). *Flocculation of suspended solids in southern Ontaria rivers: Sediment and the Environment.* IAHS Publication No. 184, 95–103.

Droppo, I.G. and Stone, M., (1994). In-channel surficial fine-grained laminae. Part I: physical characteristics and formational processes. *Hydrological Processes*, **8**, 101–111.

Edwards, T.K. and Glysson, G.D., (1988). *Field methods for measurement of fluvial sediment.* U.S. Geological Survey Open-File Report 86–531.

Eisma, D., (1993). *Suspended matter in the aquatic environment.* Berlin, Heidelberg, New York.

Elliston, G.R., 1973. *Water movement through the Gornergletscher.* , Symposium on the hydrology of glaciers, Cambridge, 7–13 September, 1969. Glaciological Society, 79–84.

Elverhøi, A., Hooke, R.L. and Solheim, A., (1998). Late cenozoic erosion and sediment yield from the Svalbard-Barents sea region: Implications for understanding erosion of glacierized basins. *Quaternary Science Reviews*, **17**, 209–241.

Ensminger, S.L., Evenson, E.B., Larson, G.J., Lawson, D.E., Alley, R.B. and Strasser, J.C., (1999). Preliminary study of laminated, silt–rich debris bands: Matanuska Glacier, Alaska, USA. *Annals of Glaciology*, **28**, 261–266.

Evenson, E.B. and Clinch, J.M., (1987). *Debris transfer mechanisms of active Alpine glaciers: Alaskan case studies.* In: K. Kugansuu and M. Saarnisto (Eds.), *INQUA Till Symposium, Finland 1985.* Geological Survey of Finland Special Paper, 3, 111–136.

Eyles, N.S., Slatt, R.M. and Rogerson, R.J., (1982). Geochemical denudation rates and solute transport mechanisms in a maritime temperate glacier basin. *Canadian Journal of Earth Sciences*, **19**, 1570–1581.

Fahnestock, R.K., (1963). *Morphology and hydrology of a glacial stream, White River, Mount Rainier, Washington*, 422–A. United States Geological Survey Professional Paper.

Fenn, C.R., (1987). *Sediment transfer processes in alpine glacier basins.* In: A.M. Gurnell and M.J. Clark (Eds.), *Glacio–fluvial sediment transfer: An Alpine perspective.* Wiley, Chichester, 59–85.

Fenn, C.R. and Gomez, B., (1989). Particle size analysis of suspended sediment in a proglacial stream: Glacier d'Tsidjiore Nouve, Switzerland. *Hydrological Processes*, **3**, 123–135.

Ferguson, R.I., (1984). *Sediment load of the Hunza River.* In: K.J. Miller (Ed.), *The International Karakoram Project, Vol 2.* Cambridge University Press, Cambridge, 581–598.

Ferguson, R.I., (1986). River loads underestimated by rating curves. *Water Resources Research*, **22**, 74–76.

Ferguson, R.I., (1987a). Accuracy and precision of methods for estimating river loads. *Earth Surface Processes and Landforms*, **12**, 95–104.

Ferguson, R.I., (1987b). *Discussion of "Conceptual models of sediment transport in streams" by Beschta, R. L.* In: C.R. Thorne, J.C. Bathurst and R.D. Hey (Eds.), *Sediment Transport in Gravel Bed Rivers.* Wiley, Chichester, 305–354.

Fischer, U.H., Clarke, G.K.C. and Blatter, H., (1999). Evidence for temporally varying sticky spots at the base of Trapridge Glacier, Yukon Territory, Canada. *Journal of Glaciology*, **45**, 352–360.

Fischer, U.H. and Hubbard, B., (1999). Subglacial sediment textures: character and evolution at Haut Glacier d'Arolla, Switzerland. *Annals of Glaciology*, **28**, 241–246.

Flint, R.F., (1971). *Glacial and Quaternary Geology.* Wiley, Chichester.

Foster, I.D.L., Gurnell, A.M. and Walling, D.E., (2000). *Sediment delivery to a proglacial river: mineral magnetic, geochemical and the potential for radionuclide fingerprinting.* In: I. Foster (Ed.), *Tracers in Geomorphology.* Wiley, Chichester, 233–343.

Fountain, A.G., (1994). Borehole water level variations and implications for the subglacial hydraulics of South Cascade Glacier, Washington State, USA. *Jornal of Glaciology*, **40**, 293–304.

Fountain, A.G., (1996). Effect of snow and firn hydrology on the physical and chemical characteristics of glacial runoff. *Hydrological Processes*, **10**, 509–521.

Fountain, A.G. and Walder, J.S., (1998). Water flow through temperate glaciers. *Reviews of Geophysics*, **36**, 299–328.

Gaudin, A.M., (1926). An investigation of crushing phenomena. *Transactions of the American Institute of Mining Engineers*, **73**, 253–316.

Gemmell, A.M.D., (1988). Zeroing of the TL in sediment undergoing glaciofluvial transport, an example from Austerdalen, western Norway. *Quaternary Science Reviews*, **7**, 339–345.

Gemmell, A.M.D., (1994). Thermoluminescence in Suspended Sediment of Glacier Meltwater Streams. *Journal of Glaciology*, **40**, 158–166.

Gemmell, A.M.D., (1997). Fluctuations in the thermoluminescence signal of suspended sediment in an alpine glacial meltwater stream. *Quaternary Science Reviews*, **16**, 281–290.

Gibbs, M.T. and Kump, L.R., (1994). Global chemical erosion during the last glacial maximum and the present: sensitivity to changes in lithology and hydrology. *Paleoceanography*, **9**, 529–543.

Gippel, C.G., (1989). The use of turbidity instruments to measure stream water suspended sediment concentration. *Hydrobiologia*, **176/177**, 465–480.

Gippel, C.G., (1995). Potential of turbidity monitoring for measuring the transport of suspended solids in streams. *Hydrological Processes*, **9**, 83–97.

Gomez, B., (1987). *Bedload.* In: A.M. Gurnell and M.J. Clark (Eds.), *Glacio–fluvial sediment transfer: An Alpine perspective.* Wiley, Chichester, 355–376.

Goodsell, B., (1999). *The formation of a medial moraine on an alpine glacier: Haut Glacier d'Arolla.* Unpublished Undergraduate Dissertation, University of Aberystwyth.

Gordon, S., Sharp, M., Hubbard, B., Smart, C., Ketterling, B. and Willis, I., (1998). Seasonal reorganisation of subglacial drainage inferred from measurements in boreholes. *Hydrological Processes*, **12**, 105–133.

Gurnell, A., Hannah, D. and Lawler, D., (1996). *Suspended sediment yield from glacier basins.* In: D.E. Walling and B.E. Webb (Eds.), *Erosion and sediment yield: global and regional perspectives.* IAHS Publication No. 236, 97–104.

Gurnell, A.M., (1982). *The dynamics of suspended sediment concentration in a proglacial stream system.* In: J.W. Glen (Ed.), *Hydrological aspects of Alpine and high–mountain areas.* Wiley, Chichester, 59–85.

Gurnell, A.M., (1987a). *Fluvial sediment yield from Alpine, glacierized catchments.* In: A.M. Gurnell and M.J. Clark (Eds.), *Glacio-fluvial sediment transfer: An Alpine perspective.* Wiley, Chichester, 415–420.

Gurnell, A.M., (1987b). *Suspended sediment.* In: A.M. Gurnell and M.J. Clark (Eds.), *Glacio-fluvial sediment transfer: An Alpine perspective.* Wiley, Chichester, 305–354.

Gurnell, A.M., (1993). How many reservoirs? An analysis of flow recessions from a glacier basin. *Journal of Glaciology*, **39**, 409–414.

Gurnell, A.M., (1995). *Sediment yield from Alpine glacier basins.* In: I.D.L. Foster, A.M. Gurnell and B.W. Webb (Eds.), *Sediment and water quality in river catchments.* Wiley, Chichester, 407–435.

Gurnell, A.M., Clark, M.J. and Hill, C.T., (1992a). Analysis and interpretaion of patterns within and between hydroclimatological time series in an Alpine glacier basin. *Earth Surface Processes and Landforms*, **17**, 821–839.

Gurnell, A.M., Clark, M.J., Hill, C.T. and Greenhalgh, J., (1992b). *Reliability and representativeness of suspended sediment concentration monitoring programme for a remote alpine proglacial river.* In: J. Bogen, D.E. Walling and T. Day (Eds.), *Erosion and Sediment Transport Monitoring Programmes in River Basins.* IAHS Publication No. 210, 191–208.

Gurnell, A.M., Clark, M.J., Tranter, M., Brown, G.H. and Hill, C.T., (1991). Alpine glacier hydrology inferred from a proglacial river monitoring programme. *Proceedings of the British Hydrological Society National Symposium*, 5.9–5.16.

Gurnell, A.M. and Fenn, C.R., (1984a). Box–Jenkins transfer function models applied to suspended sediment concentration–discharge relationships in a proglacial stream. *Arctic and Alpine Research*, **16**, 93–106.

Gurnell, A.M. and Fenn, C.R., (1984b). Flow separation, sediment source areas and suspended sediment transport in a proglacial stream. *Catena*, **5**, 109–119.

Gurnell, A.M. and Warburton, J., (1990). *The significance of suspended sediment pulses for estimating suspended sediment load and identifying suspended sediment sources in Alpine glacier basins.* In: H. Lang and A. Musy (Eds.), *Hydrology in Mountainous Regions. 1: Hydrological Measurements; the Water Cycle.* IAHS Publication No. 193, 463–470.

Gustavson, T.C. and Boothroyd, J.C., (1987). A depositional model for outwash, sediment sources and hydrologic characteristics, Malaspina Glacier, Alaska: a modern analogue fo the south–eastern margin of the Laurentide Ice Sheet. *Geological Society of America Bulletin*, **99**, 187–200.

Guymon, G.L., (1974). Regional sediment analysis of Alaska Streams. *American Society of Civil Engineers, Journal of Hydraulics Division*, **100**, 41–51.

Hagen, J.O., Wold, B., Liestøl, O., Ostrem, G. and Sollid, J.L., (1983). Subglacial processes at Bondhusbreen. *Annals of Glaciology*, **4**, 91–98.

Haldorsen, S., (1981). Grain–size distribution of till and its relation to glacial crushing and abrasion. *Boreas*, **10**, 95–105.

Hallet, B., (1979a). Subglacial regelation water film. *Journal of Glaciology*, **23**, 321–323.

Hallet, B., (1979b). A theoretical model of glacial abrasion. *Journal of Glaciology*, **23**, 39–50.

Hallet, B., (1996). Glacial quarrying: A simple theoretical model. *Annals of Glaciology*, **22**, 1–8.

Hallet, B., Hunter, L. and Bogen, J., (1996). Rates of erosion and sediment evacuation by glaciers: A review of field data and their implications. *Global and Planetary Change*, **12**, 213–235.

Hammer, K.M. and Smith, N.D., (1983). Sediment production and transport in a proglacial stream, Hilda Glacier, Alberta, Canada. *Boreas*, **12**, 91–106.

Hannah, D.M., Gurnell, A.M. and McGregor, G.R., (1999). A methodology for investigation of the seasonal evolution in proglacial hydrograph form. *Hydrological Processes*, **13**, 2603–2621.

Hannah, D.M., Smith, B.P.G., Gurnell, A.M. and McGregor, G.R., (2000). An approach to hydrograph classification. *Hydrological Processes*, **14**, 317–338.

Harbor, J., Sharp, M., Copland, L., Hubbard, B., Nienow, P. and Mair, D., (1997). Influence of subglacial drainage conditions on the velocity distribution within a glacier cross section. *Geology*, **25**, 739–742.

Harbor, J. and Warburton, J., (1993). Relative rates of glacial and nonglacial erosion in alpine environments. *Arctic and Alpine Research*, **25**, 1–7.

Hasholt, B. and Walling, D.E., (1992). *Use of caesium–137 to investigate sediment sources and sediment delivery in a small glacierised mountain drainage basin in eastern Greenland.* In: D. Walling, T. Davies and B. Hasholt (Eds.), *Erosion, debris flows and environment in mountainous regions.* IAHS Publication No. 209, 87–100.

Hay, W.W., (1998). Detrital sediment fluxes from continents to oceans. *Chemical Geology*, **145**, 287–323.

Hay, W.W., Shaw, C.A. and Wold, C.N., (1989). Mass-balanced paleographic reconstructions. *Geologische Rundschau*, **78**, 207–242.

He, Q. and Owens, P., (1995). *Determination of suspended sediment provenance using Caesium–137, unsupported Lead–210 and Radium–226: A numerical mixing model approach.* In: I.D.L. Foster, A.M. Gurnell and B.W. Webb (Eds.), *Sediment and water quality in river catchements.* Wiley, Chichester, 207–227.

Head, K.H., (1980). *Manual of Soil Laboratory Testing, Volume 1: Soil Classification and Compaction Tests.* Pentech Press, London.

Hicks, D.M., McSaveney, M.J. and Chinn, T.J.H., (1990). Sedimentation in proglacial Ivory Lake, Southern Alps, New Zealand. *Arctic and Alpine Research*, **22**, 26–42.

Higgit, D.L., (1995). *The development and application of caesium–137 measurements in erosion investigations.* In: I.D.L. Foster, A.M. Gurnell and B.W. Webb (Eds.), *Sediment and water quality in river catchments.* Wiley, Chichester, 287–305.

Hillier, S., (2001). Particle composition and origin of suspended sediment in the R. Don, Aberdeenshire, UK. *The Science of the Total Environment*, **265**, 281–293.

Hock, R. and Hooke, R.L., (1993). Evolution of the internal drainage system in the lower part of the ablation area of Storglaciären, Sweden. *Geological Society of America Bulletin*, **105**, 537–546.

Hodgkins, R., (1996). Seasonal trends in suspended sediment transport from and Arctic glacier, and implications for drainage system structure. *Annals of Glaciology*, **22**, 147–151.

Hodgkins, R., (1999). Controls on suspended sediment transfer at a high–Arctic glacier, determined from statistical modelling. *Earth Surface Processes and Landforms*, **24**, 1–21.

Hodson, A., Gurnell, A., Tranter, M., Bogen, J., Hagen, J.O. and Clark, M., (1998a). Suspended sediment yield and transfer processes in a small High-Arctic glacier basin, Svalbard. *Hydrological Processes*, **12**, 73–86.

Hodson, A.J., Tranter, M., Dowdeswell, J.A., Gurnell, A.M. and Hagen, J.O., (1997). Glacier thermal regime and suspended sediment yield: a comparison of two high-Arctic glaciers. *Annals of Glaciology*, **24**, 32–37.

Hodson, A.J. and Ferguson, R.I., (1999). Fluvial suspended sediment transport from cold and warm–based glaciers in Svalbard. *Earth Surface Processes and Landforms*, **24**, 957–974.

Hodson, A.J., Gurnell, A.M., Washington, R., Tranter, M., Clark, M.J. and Hagen, J.O., (1998b). Meteorological and runoff time series characteristics in a small, high-Arctic glaciated basin, Svalbard. *Hydrological Processes*, **12**, 509–526.

Hoff, E.V. and Bott, S., (1990). *Optical theory and refractive index: Why it is important to particle size analysis*, Coulter Technical Bulletin LS Series 1010.

Holmlund, P., (1988). Internal geometry and the evolution of moulins, Storglaciären, Sweden. *Journal of Glaciology*, **34**, 242–248.

Hooke, R.L., (1984). On the role of mechanical energy in maintaining subglacial water conduits at atmospheric pressure. *Journal of Glaciology*, **30**, 180–187.

Hooke, R.L., (1989). Englacial and subglacial hydrology: A qualitative review. *Arctic and Alpine Research*, **21**, 221–233.

Hooke, R.L., Calla, P., Holmlund, P., Nilsson, M. and Stroeven, A., (1989). A three–year record of seasonal variations in surface velocity, Storglaciären, Sweden. *Journal of Glaciology*, **35**, 235–247.

Hooke, R.L., Laumann, T. and Kohler, J., (1990). Subglacial water pressures and the shape of subglacial conduits. *Journal of Glaciology*, **36**, 67–71.

Hooke, R.L. and Pohjola, V.A., (1994). Hydrology of a segment of a glacier situated in an overdeepening. *Journal of Glaciology*, **40**, 140–148.

Hooke, R.L., Wold, B. and Hagen, J.O., (1985). Subglacial hydrology and sediment transport at Bondhusbreen, southwest Norway. *Geological Society of America Bulletin*, **96**, 388–397.

Howard, A.D., Dietrich, W.E. and Siedl, M.A., (1994). Modeling fluvial erosion on regional to continental scales. *Journal of Geophysical Research*, **99**, 13971–13986.

Hubbard, B., (1992). *Basal ice facies and their formation in the western Alps.* Unpublished PhD Thesis, University of Cambridge.

Hubbard, B. and Nienow, P., (1997). Alpine subglacial hydrology. *Quaternary Science Reviews*, **16**, 939–955.

Hubbard, B.P., Sharp, M.J., Willis, I.C., Nielsen, M.K. and Smart, C.C., (1995). Borehole water level variations and the structure of the subglacial hydrological system of Haut Glacier d'Arolla, Valais, Switzerland. *Journal of Glaciology*, **41**, 572–583.

Humphrey, N., Raymond, C. and Harrison, W., (1986). Discharges of trubid water during mini-surges of Variegated Glacier, Alaska, U.S.A. *Journal of Glaciology*, **32**, 195–207.

Humphrey, N.F. and Raymond, C.F., (1994). Hydrology, Erosion and Sediment Production in a Surging Glacier – Variegated Glacier, Alaska, 1982–83. *Journal of Glaciology*, **40**, 539–552.

Iken, A., (1974). *Velocity fluctuations of an arctic valley glacier, a study of the White Glacier, Axel Heiberg Island, Canadian Arctic Archipelago*, McGill University, Montreal.

Iken, A., (1981). The effect of subglacial water pressure on the sliding velocity of a glacier in an idealized numerical model. *Journal of Glaciology*, **27**, 407–421.

Iken, A. and Bindschadler, R.A., (1986). Combined measurements of subglacial water pressure and surface velocity of Findelengletscher, Switzerland: Conclusions about drainage system and sliding mechanism. *Journal of Glaciology*, **32**, 101–118.

Iken, A., Röthlisberger, H., Flotron, A. and Haeberli, W., (1983). The uplift of Unteraargletscher at the beginning of the melt season – a consequence of water storage at the bed? *Journal of Glaciology*, **29**, 28–47.

Isacks, B.L., (1992). *'Long–term' land surface processes: erosion, tectonics and climate history in mountain belts.* In: P.M. Mather (Ed.), *TERRA–1: understanding the terrestrial environment.* Taylor & Francis, London, 21–36.

Iverson, N., (1990). Laboratory simulations of glacier abrasion: comparison with theory. *Journal of Glaciology*, **36**, 304–314.

Iverson, N., (1991). Potential effects of subglacial water pressure fluctuations on quarrying. *Journal of Glaciology*, **37**, 27–36.

Iverson, N.R., (1995). *Processes of erosion.* In: J. Menzies (Ed.), *Modern Glacial Environments: Processes, Dynamics and Sediments.* Butterworth–Heinemann, Oxford, 241–259.

Iverson, N.R., Hanson, B., Hooke, R.L.B. and Jansson, P., (1995). Flow mechanism of glacier on soft beds. *Science*, **267**, 80–81.

Kalkstein, L.S., Tan, G. and Skindlov, J.A., (1987). An evaluation of three clustering procedures for use in synoptic climatological classifications. *Journal of Climate and Applied Meteorology*, **26**, 717–730.

Kamb, B., (1987). Glacier surge mechanism based on linked cavity configuration of the basal water conduit system. *Journal of Geophysical Research*, **92**, 9083–9100.

Kamb, B. and Engelhardt, H., (1987). Waves of accelerated motion in a glacier approaching surge: the mini–surges of Variegated Glacier, Alaska, USA. *Journal of Glaciology*, **33**, 27–46.

Kamb, B. and La Chapelle, E., (1964). Direct observation of the mechanism of glacier sliding over bedrock. *Journal of Glaciology*, **5**, 159–172.

Karlsen, E., (1991). Variations in grain size distribution of suspended sediment in a glacial meltwater stream, Austre Okstindbreen, Norway. *Journal of Glaciology*, **37**, 113–119.

Kirkbride, M.P., (1995). *Processes of transportation.* In: J. Menzies (Ed.), *Modern Glacial Environments: Processes, Dynamics and Sediments.* Butterworth–Heinemann, Oxford, 261–292.

Kirkbride, M.P. and Spedding, N., (1996). The influence of englacial drainage on sediment transport pathways and till texture of temperate valley glaciers. *Annals of Glaciology*, **22**, 160–166.

Klovan, J.E., (1966). The use of factor analysis in determining depositional environments from grain–size distributions. *Journal of Sedimentary Petrology*, **36**, 115–125.

Kump, L.B. and Alley, R.B., (1994). *Global chemical weathering on glacial time scales.* In: W.W. Hay (Ed.), *Material fluxes on the surface of the Earth.* National Academy Press, Washington, 46–60.

Kurashige, Y. and Fusejima, Y., (1997). Source identification of suspended sediment from grain–size distributions: I. Application of nonparametric statistical tests. *Catena*, **31**, 39–52.

Laine, E.P., (1980). New evidence from beneath the western North Atlantic for the depth of glacial erosion in Greenland and North America. *Quaternary Research*, **14**, 1–11.

Lamb, H.R., (1997). *Chemical weathering in Alpine subglacial environments.* Unpublished PhD Thesis, University of Bristol.

Lang, H., (1973). *Variations in the relation between glacier discharge and meteorological elements.* IASH Publication No. 95, 85–94.

Lang, H., Leibundhut, C. and Festel, E., (1979). Results from tracer experiments on the water flow through the Aletschgletscher. *Zeitschrift für Gletscherkunde und Glazialgeologie*, **15**, 209–218.

Lawson, D.E., (1993). *Glaciohydrologic and glaciohydraulic effects on runoff and sediment yield in glacierized basins.* US Army Cold Regions Research and Engineering Laboratory, Monograph 93–2, Hanover, NH, USA.

Lawson, D.E., Strasser, J.C., Evenson, E.B., Alley, R.B., Larson, G.J. and Arcone, S.A., (1998). Glaciohydraulic supercooling: a freeze–on mechanism to create stratified, debris–rich basal ice: I. Field evidence. *Journal of Glaciology*, **44**, 216–226.

Liestøl, O., (1967). *Storbreen glacier in Jotunheimen, Norway.* Norsk Polarinstitutt Skrifter, 141.

Lliboutry, L., (1968). General theory of subglacial cavitation and sliding of temperate glaciers. *Journal of Glaciology*, **7**, 21–58.

Lliboutry, L.A., (1994). Monolithic erosion of hard beds by temperate glaciers. *Journal of Glaciology*, **40**, 433–450.

Loizeau, J.L., Arbouille, D., Santiago, S. and Vernet, J.P., (1994). Evaluation of a Wide-Range Laser Diffraction Grain-Size Analyzer For Use With Sediments. *Sedimentology*, **41**, 353–361.

Mair, D., Nienow, P., Sharp, M., Wohlleben, T. and Willis, I., (in press). Influence of subglacial drainage system evolution on glacier surface motion: Haut Glacier d'Arolla, Switzerland. *Journal of Geophysical Research.*

Mair, D., Nienow, P., Willis, I. and Sharp, M., (2001). Spatial patterns of glacier dynamics during a high-velocity event: Haut Glacier d'Arolla, Switzerland. *Journal of Glaciology*, **47**, 9–20.

Maisch, M., Haeberli, W., Hoelze, M. and Wenzel, J., (1999). Occurrence of rocky and sedimentary glacier beds in the Swiss Alps as estimated from glacier-inventory data. *Annals of Glaciology*, **28**, 231–235.

Matthews, M.D., (1991). *The effect of grain shape and density on size measurement.* In: J.P.M. Syvitski (Ed.), *Principles, methods, and application of particle size analysis.* Cambridge University Press, Cambridge, 22–33.

Matthews, W.H., (1963). Discharge of a glacial stream. *IASH Publication No. 163*, 290–300.

McCave, I.N. and Syvitski, J.P.M., (1991). *Principles and methods of geological particle size analysis.* In: J.P.M. Syvitski (Ed.), *Principles, methods, and application of particle size analysis.* Cambridge University Press, Cambridge, 3–21.

Meier, M.F. and Tangborn, W.V., (1961). Distinctive characteristics of glacier runoff. *United States Geological Survey Professional Paper*, **424B**, 14–16.

Mojena, R., (1988). Ward's clustering algorithm. In: S. Kotz, N.L. Johnson and C.B. Read (Eds.), *Encyclopedia of Statistical Sciences*. Wiley, Chichester, 529–532.

Molnar, P. and England, P., (1990). Late Cenozoic uplift of mountain ranges and global climat change: chicken or egg. *Nature*, **366**, 29–34.

Muggler, C.C., Pape, T. and Buurman, P., (1997). Laser grain–size determination in soil genetic studies: 2. Clay content, clay formation, and aggregation in some Brazilian oxisols. *Soil Science*, **162**, 219–228.

Munt, S., (1995). *Sizing up: Laser diffraction vs Coulter Principle*, Laboratory equipment/application note, Laboratory Products Technology, September, 1995.

Murdock, C., Zhang, H., Kelly, M., Chang, L.–Y. and Davison, W., (2001). DGT as an in situ tool for measuring radioceasium in natural waters. *Environmental Science and Technology*, **35**, 4530–4535.

Murray, T., (1997). Assessing the paradigm shift: deformable glacier beds. *Quaternary Science Reviews*, **16**, 995–1016.

Muste, M. and Patel, V.C., (1997). Velocity profiles for particles and liquid in open–channel flow with suspended sediment. *Journal of Hydraulic Engineering–Asce*, **123**, 742–751.

Nielsen, M.K., (1995). *Instrumentation for the monitoring of subglacial hydrology.* Unpublished M.Res. Thesis, University of Bristol.

Nienow, P., Sharp, M. and Willis, I., (1998). Seasonal changes in the morphology of the subglacial drainage system, Haut Glacier d'Arolla, Switzerland. *Earth Surface Processes and Landforms*, **23**, 825–843.

Nienow, P.W., Sharp, M.J., Boon, S., Heppenstall, K. and Bingham, R., (submitted). Supraglacial drainage processes on high Arctic glaciers: implications for subglacial hydrology and glacier flow dynamics. *Journal of Geophysical Research.*

Nijampurkar, V.N., Bhandari, N., Borole, D.V. and Bhattacharya, U., (1985). Radiometric chronology of Ghangme-Khangpu glacier, Sikim. *Journal of Glaciology*, **31**, 28–33.

Olive, L.J. and Rieger, W.A., (1988). *An examination of the role of sampling strategies in the study of suspended sediment transport.* In: M.P. Bordas and D.E. Walling (Eds.), *Sediment Budgets*. IAHS Publication No. 174, 259–267.

Østrem, G., (1975). *Sediment transport in glacial meltwater streams.* In: A.V. Jopling and B.C. McDonald (Eds.), *Glaciofluvial and glaciolacustrine sedimentation.* Society of Economic Paleontologists and Mineralologists, Special Publication No. 23, Tusla, USA, 101–122.

Paterson, W.S.B., (1994). *The physics of glaciers*. Pergamon, Oxford.

Phillips, J.M., (1996). *The effective particle–size characteristics of fluvial suspended sediment*. Unpublished PhD Thesis, University of Exeter.

Phillips, J.M. and Walling, D.E., (1995). Measurement in situ of the effective particle–size characteristics of fluvial suspended sediment by means of a portable laser back–scatter probe: some preliminary results. *Marine and Freshwater Research*, **46**, 349–357.

Phillips, J.M. and Walling, D.E., (1998). Calibration of a Par–Tec 200 laser back–scatter probe for in situ sizing of fluvial suspended sediment. *Hydrological Processes*, **12**, 221–232.

Picciotto, E. and Crozaz, G., (1967). Lead–210 and strontium–90 in an Alpine glacier. *Earth and Planetary Science Letters*, **3**, 237–242.

Pinglot, J.F. and Pourchet, M., (1995). Radioactivity measurements applied to glaciers and lake sediments. *The Science of the Total Environment*, **173/174**, 211–223.

Pourchet , M., Pinglot, J.F., Reynaud, L. and Holdsworth, G., (1988). Identification of Chernobyl fallout as a new reference level in Northern Hemisphere Glaciers. *Journal of Glaciology*, **34**, 183–187.

Federal Interagency Sedimentation Project (no date). *Sampling with the USDH48 depth–integrating suspended sediment sampler*. http://fisp.wes.army.mil/.

Rainwater, F.H. and Guy, H.P., (1961). *Some observations on the hydrochemistry and sedimentation of the Chamberlain glacier area, Alaska*. United States Geological Survey Professional Paper, 414–C.

Raymo, M.E. and Ruddiman, W.F., (1992). Tectonic forcing of late Cenozoic climate. *Nature*, **359**, 117–122.

Raymo, M.E., Ruddiman, W.F. and Froelich, P.N., (1988). Influence of late Cenozoic mountain building on ocean geochemical cycles. *Geology*, **16**, 649–653.

Raymond, C.F., (1987). How do glaciers surge? A review. *Journal of Geophysical Research*, **92**, 9121–9134.

Raymond, C.F., Benedict, R.J., Harrison, W.D., Echelmeyer, K.A. and Sturn, M., (1995). Hydrological discharges and motion of Fels and Black Rapids Glaciers, Alaska, USA: implications for the structure of their drainage systems. *Journal of Glaciology*, **41**, 290–304.

Raymond, C.F. and Malone, S.D., (1981). *Relationship of directly observed sliding rate and conditions to variations in surface velocity, strain rates, and seismic activity*, 34. Progress Report for National Science Foundation Grant no. DPP–7903942.

Rea, B.R., (1996). A note on the experimental production of a mechanically polished surface within striations. *Glacial Geology and Geomorphology*, http://boris.qub.ac.uk/ggg.

Repp, K., (1988). The hydrology of Bayelva, Spitsbergen. *Nord. Hydrol.*, **19**, 259–268.

Reynolds, R.C. and Johnson, N.M., (1972). Chemical weathering inn the temperate glacial environment of the North Cascade Mountains. *Geochimica et Cosmochimica Acta*, **36**, 537–554.

Rice, S. and Church, M., (1998). Grain size along two gravel–bed rivers: Statistical variation, spatial pattern and sedimentary links. *Earth Surface Processes and Landforms*, **23**, 345–363.

Richards, K., (1982). *Rivers: Form and Process in Alluvial Channels.* Methuen, London.

Richards, K., (1984). Some process observations on suspended sediment dynamics in Storbregrova, Jotunheim. *Earth Surface Processes and Landforms*, **9**, 101–112.

Richards, K., Sharp, M., Arnold, N., Gurnell, A., Clark, M., Tranter, M., Nienow, P., Brown, G., Willis, I. and Lawson, W., (1996). An integrated approach to modelling hydrology and water quality in glacierized catchments. *Hydrological processes*, **10**, 479–508.

Riley, N.W., (1982). *Rock wear by sliding ice.* Unpublished PhD Thesis, University of Newcastle upon Tyne.

Robin, G.d.Q., (1976). Is the basal ice of a temperate glacier at the pressure melting point? *Journal of Glaciology*, **2**, 523–532.

Rogerson, P.A., (2001). *Statistical methods for geography.* Sage, London.

Rooseboom, A. and Annandale, G.W., (1981). *Techniques applied in determining sediment loads in South African rivers.* Erosion and Sediment Transport Measurement, IAHS Publication No. 133, 219–224.

Röthlisberger, H., (1972). Water pressure in intra– and subglacial channels. *Journal of Glaciology*, **11**, 177–203.

Röthlisberger, H. and Iken, A., (1981). Plucking as an effect of water pressure variations at the glacier bed. *Annals of Glaciology*, **2**, 57–62.

Röthlisberger, H. and Lang, H., (1987). *Glacial hydrology.* In: A.M. Gurnell and M.J. Clark (Eds.), *Glacio-fluvial sediment transfer: An Alpine perspective.* Wiley, Chichester, 207–284.

Rubey, W.W., (1933). Settling velocities of gravel, sand and silt particles. *American Journal of Science*, **25**, 325–338.

Sambrook Smith, G.H., Nicholas, A.P. and Ferguson, R.I., (1997). Measuring and defining bimodal sediments: problems and implications. *Water Resources Research*, **33**, 1179–1185.

Santiago, S., Thomas, R.L. and McCarty, E.A., (1992). Particle size characteristics of suspended and bed sediments in the Rhone River. *Hydrological Processes*, **6**, 227–240.

SAS Institute (1990). *SAS/STAT Users Guide, Version 6*. SAS Publishing.

Schallenberg, M. and Kalef, J., (1993). The ecology of sediment bacteria in lakes and comparisons with other aquatic ecosystems. *Ecology*, **74**, 919–934.

Schneider, T. and Bronge, C., (1993). *Suspended sediment transport and discharge of Tarfalajåkk, the proglacial stream of Storglaciären, Northern Sweden, 1980–1990*. Research reports. University of Stokholm, Department of Physical Geography, Stockholm.

Schneider, T. and Bronge, C., (1996). Suspended sediment transport in the Storglaciären drainage basin. *Geografiska Annaler*, **78 A**, 155–161.

Scientific, C., (1994–1996). *247 Conductivity and Temperature Probes*, Campbell Scientific Inc., Loughborough.

Seaberg, S.Z., Seaberg, J.Z., Hooke, R.L. and Wieberg, D.W., (1988). Character of the englacial and subglacial drainage system in the lower part of the ablation area of Storglaciären, Sweden, as revealed by dye-trace studies. *Journal of Glaciology*, **34**, 217–227.

Sharp, M., Lamb, H., Tranter, M., Parkes, J., Cragg, B. and Fairchild, I.J., (1999). Widespread bacterial populations at glacier beds and their relationship to rock weathering and carbon cycling. *Geology*, **27**, 107–110.

Sharp, M., Richards, K., Willis, I., Arnold, N., Nienow, P., Lawson, W. and Tison, J.–L., (1993). Geometry, bed topography and drainage system structure of the Haut Glacier d'Arolla, Switzerland. *Earth Surface Processes and Landforms*, **18**, 557–571.

Sharp, M., Tranter, M., Brown, G.H. and Skidmore, M., (1995). Rates of Chemical Denudation and CO_2 Drawdown in a Glacier-Covered Alpine Catchment. *Geology*, **23**, 61–64.

Sharp, M.J., 1991. *Hydrological inferences from meltwater quality data, the unfulfilled potential*. Proceedings of the British Hydrological Society 3rd National Symposium, Southampton, 16–18 September 1991, 5.2–5.8.

Shreve, R.L., (1972). Movement of water in glaciers. *Journal of Glaciology*, **11**, 205–214.

Shreve, R.L., (1985). Esker characteristics in terms of glacier physics, Katahdin esker system, Maine. *Geological Society of America Bulletin*, **96**, 639–646.

Skidmore, M.L. and Sharp, M.J., (1999). Drainage system behaviour of a High–Arctic polythermal glacier. *Annals of Glaciology*, **28**, 209–215.

Small, R.J., (1987). *Moraine sediment budgets.* In: A.M. Gurnell and M.J. Clark (Eds.), *Glacio-fluvial sediment transfer: An Alpine perspective.* Wiley, Chichester, 165–197.

Souchez, R.A. and Lemmens, M.M., (1987). *Solutes.* In: A.M. Gurnell and M.J. Clark (Eds.), *Glacio-fluvial sediment transfer: An Alpine perspective.* Wiley, Chichester, 285–303.

Spedding, N., (1997). *Meltwater controls on ice-marginal sedimentation.* Unpublished PhD Thesis, University of Edinburgh.

Spedding, N., (2000). *Hydrological controls on sediment transport pathways: Implications for debris–covered glaciers.* In: M. Nakawo, C.F. Raymond and A. Fountain (Eds.), *Debris Covered Glaciers.* IAHS Publication No. 264, 133–142.

StatSoft, (1995). *Statistica: Statistics II.* StatSoft, Tusla.

Stenborg, T., (1969). Studies of the internal drainage of glaciers. *Geografiska Annaler,* **51 A**, 13–41.

Stenborg, T., (1970). Delay of runoff from a glacier basin. *Geografiska Annaler,* **52A**, 1–30.

Stone, D.B. and Clarke, G.K.C., (1996). In situ measurements of basal water quality and pressure as an indicator of the character of subglacial drainage systems. *Hydrological Processes,* **10**, 615–628.

Strasser, J.C., Lawson, D.E., Larson, G.J., Evenson, E.B. and Alley, R.B., (1996). Preliminary results of tritium analyses in basal ice, Matanuska Glacier, Alaska, USA: evidence for subglacial ice accretion. *Annals of Glaciology,* **22**, 126–133.

Sugden, D.E. and John, B.S., (1976). *Glaciers and Landscape: A Geomorphological Approach.* Wiley, Chichester.

Swift, D.A., Nienow, P.W., Spedding, N. and Hoey, T.B., (2002). Geomorphic implications of subglacial drainage system configuration: rates of basal sediment evacuation controlled by seasonal drainage system evolution. *Sedimentary Geology.*

Taylor, H.P., (1978). Oxygen and hydrogen isotope studies of plutonic granitic rocks. *Earth and Planetary Science Letters,* **38**, 177–210.

Thayyen, R.J., Gergan, J.T. and Dobhal, D.P., (1999). Particle size characteristics of suspended sediments and subglacial hydrology of Dokriani Glacier, Garhwal Himalaya, India. *Hydrological Sciences Journal,* **44**, 47–61.

Tranter, M., Brown, G., Raiswell, R., Sharp, M. and Gurnell, A., (1993). A conceptual model of solute acquisition by Alpine glacial meltwaters. *Journal of Glaciology,* **39**, 573–581.

Tyler, A.N., (2000). Monitoring anthropogenic radioactivity in salt marsh environments through in situ gamma-ray spectroscopy. *Journal of Environmental Radioactivity*, **45**, 235–252.

Udelhoven, T., Nagel, A. and Gasparini, F., (1997). Sediment and suspended particle interactions during low water flow in a small heterogeneous catchment. *Catena*, **30**, 135–147.

Vagners, U.J., (1969). *Mineral distribution in tills, south-central Ontario*. Unpublished PhD Thesis, University of Western Ontario, London, Canada.

Vatne, G., Etzelmuller, B., Ødegård, R.S. and Sollid, J.L., (1992). Glaciofluvial sediment transfer of a subpolar glacier, Erikbreen, Svalbard. *Stuttgarter Geographishe Studien*, **117**, 253–266.

Vatne, G., Etzelmuller, B., Sollid, J.L. and Ødegård, R.S., (1995). Hydrology of a polythermal glacier, Erikbreen, northern Spitsbergen. *Nordic Hydrology*, **26**, 169–190.

Vivian, R., (1975). *Les Glaciers des Alpes Occidentales*. Imprimerie Allier, Grenoble.

Wadell, H., (1932). Volume, shape and roundness of rock particles. *Journal of Geology*, **40**, 443–451.

Walder, J.S., (1986). Hydraulics of subglacial cavities. *Journal of Glaciology*, **32**, 439–445.

Walder, J.S. and Costa, J.E., (1996). Outburst floods from glacier-dammed lakes: The effect of mode of lake drainage on flood magnitude. *Earth Surface Processes and Landforms*, **21**, 701–723.

Walder, J.S. and Fowler, A., (1994). Channelised subglacial drainage over a deformable bed. *Journal of Glaciology*, **40**, 3–15.

Walling, D.E. and Kloe, A.H.A., (1979). *Sediment yield of rivers in areas of low precipitation: a review, The Hydrology of Areas of Low Precipitation*. IAHS Publication No., 479–493.

Walling, D.E. and Moorhead, P.W., (1987). Spatial and temporal variations in the particle size characteristics of suspended sediment. *Geografiska Annaler*, **69A**, 47–59.

Walling, D.E. and Moorhead, P.W., (1989). The particle size characteristics of fluvial sediment: an overview. *Hydrobiologia*, **176/177**, 125–149.

Walling, D.E. and Quine, T.A., (1992). *The use of ceasium–137 measurements in soil erosion surveys*. In: J. Bogen, D.E. Walling and T. Day (Eds.), *Erosion and sediment transport monitoring programmes in river basins*. IAHS Publication No. 210, 143–152.

Warburton, J., (1990). An Alpine proglacial fluvial sediment budget. *Geografiska Annaler*, **72 A**, 261–272.

Warburton, J. and Fenn, C.R., (1994). Unusual flood events from an Alpine glacier: Observations and deductions on generating mechanisms. *Journal of Glaciology*, **40**, 176–186.

Weertman, J., (1961). Mechanism for the formation of inner moraines found near the edge of cold ice caps and ice sheets. *Journal of Glaciology*, **3**, 965–978.

Weertman, J., (1972). General theory of water flow at the base of a glacier or ice sheet. *Reviews of Geophysics and Space Physics*, **10**, 287–333.

Weertman, J., (1986). Basal water and high–pressure basal ice. *Journal of Glaciology*, **32**, 455–463.

White, W.A., (1972). Deep erosion by continental ice sheets. *Geological Society of America Bulletin*, **83**, 1037–1056.

Willis, I., Hubbard, B., Nienow, P., Mair, D., Fischer, U. and Hubbard, A., (1999). *3–D patterns of stress and velocity in glaciers.*

Willis, I.C., (1995). Intra–annual variations in glacier motion: a review. *Progress in Physical Geography*, **19**, 61–106.

Willis, I.C., Richards, K.S. and Sharp, M.J., (1996). Links Between Proglacial Stream Suspended Sediment Dynamics, Glacier Hydrology and Glacier Motion At Midtdalsbreen, Norway. *Hydrological Processes*, **10**, 629–648.

Willis, I.C., Sharp, M.J. and Richards, K.S., (1990). Configuration of the drainage system of Midtdalsbreen, Norway, as indicated by dye-tracing experiments. *Journal of Glaciology*, **36**, 89–101.

Zhang, X. and Zhang, Y., (1995). *Use of caesium–137 to investigate sediment sources in the Hekouzhen–Longmen Basin of the Middle Yellow River, China.* In: I.D.L. Foster, A.M. Gurnell and B.W. Webb (Eds.), *Sediment and water quality in river catchments.* Wiley, Chichester, 353–362.

Zussman, J., (1977). *X-ray Diffraction.* In: J. Zussman (Ed.), *Physical Methods in Determinative Mineralogy.* Academic Press, London, 391–474.